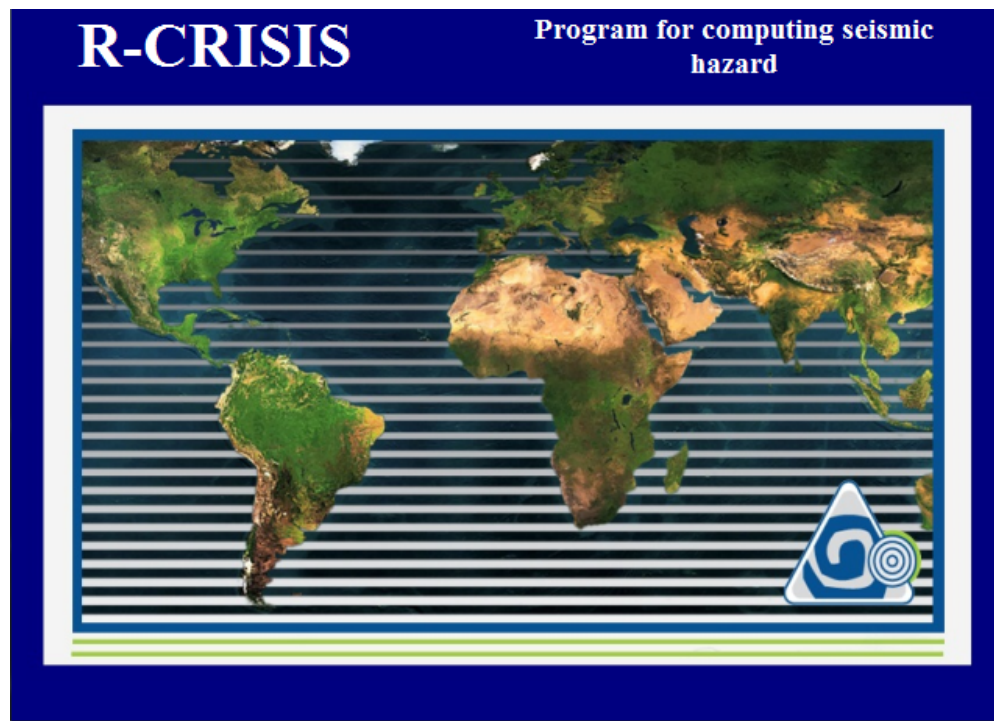


R-CRISIS Validation and Verification Document

Program for Probabilistic Seismic Hazard Analysis



Implemented methodologies
User manual
Validation and verification tests

Mexico City, 2020

Citation

Please cite this document as:

Ordaz M. and Salgado-Gálvez M.A. (2020). R-CRISIS v20 Validation and Verification Document. ERN Technical Report. Mexico City, Mexico.

Copyright © 2020 Instituto de Ingeniería – Universidad Nacional Autónoma de México & Evaluación de Riesgos Naturales - ERN

Table of Contents

1	Introduction.....	1
1.1	Description of R-CRISIS	1
1.2	Hardware and software requirements	2
1.3	Installing R-CRISIS.....	3
1.4	Launching R-CRISIS	5
2	Theoretical background of the methodologies and models implemented in R-CRISIS...7	
2.1	Seismicity models	7
2.1.1	Modified Gutenberg-Richter model.....	7
2.1.2	Characteristic earthquake model	13
2.1.3	Generalized non-Poissonian model	14
2.1.4	Generalized Poissonian model	16
2.2	Geometry models	19
2.2.1	Area sources.....	20
2.2.2	Area plane sources.....	28
2.2.3	Volume sources.....	29
2.2.4	Line sources	30
2.2.5	Point sources	33
2.2.6	Gridded sources.....	34
2.2.7	Rectangular faults.....	37
2.2.8	Slab geometries	39
2.2.9	Ruptures	40
2.3	Measuring distances in R-CRISIS.....	41
2.4	Strong ground motion attenuation models	42
2.4.1	GMPE tables	43
2.4.2	Probabilistic interpretation of attenuation relations.....	48
2.4.3	Built-in GMPEs.....	51
2.4.4	Generalized GMPE	53
2.4.5	Hybrid attenuation models	56
2.4.6	Special attenuation models	57
2.4.7	Point source (ω^2) attenuation model	58
2.5	Site effects.....	59
2.5.1	CAPRA Type (ERN.SiteEffects.MallaEfectosSitioSismoRAM)	60
2.5.2	Chiou and Youngs, 2014 (ERN.SiteEffects.MallaVs30CY14).....	63
2.5.3	V_{s30} (ERN.SiteEffects.MallaVs30).....	63
2.6	Spatial integration procedure	64
2.6.1	Area sources.....	64

2.6.2	Line sources	66
2.7	Use of a digital elevation model (DEM).....	67
2.8	Combination of seismicity, geometric and attenuation models.....	69
2.8.1	Normal attenuation models	70
2.8.2	Generalized attenuation models	72
2.9	Hazard computation algorithm	74
2.10	Hazard disaggregation.....	78
2.10.1	Magnitude-distance disaggregation.....	78
2.10.2	Epsilon disaggregation	79
2.10.3	Interpretation of ϵ for other probability distributions	82
2.11	Cumulative Absolute Velocity filter	82
2.12	Logic trees	84
2.13	Optimum spectra	85
2.14	Stochastic catalogue generator	87
2.14.1	Validation of location of events.....	88
2.14.2	Validation of magnitude and number of events	92
2.15	Conditional mean spectrum	93
2.16	Probabilistic liquefaction hazard analysis.....	95
3	Creating a PSHA project in R-CRISIS.....	98
3.1	Introduction	98
3.2	File administration.....	101
3.2.1	Opening existing project	101
3.2.2	Logic-tree calculations	102
3.2.3	Saving a project	103
3.3	Data assignment.....	104
3.3.1	Map data (optional).....	105
3.3.2	Data of computation sites.....	106
3.3.3	Source geometry data	109
3.3.4	Data on spectral ordinates	121
3.3.5	Seismicity data.....	123
3.3.6	Attenuation data.....	126
3.3.7	GMPE analyzer	132
3.3.8	Site-effects grids (optional).....	133
3.3.9	Digital elevation models (optional).....	134
3.3.10	Global parameters	135
3.3.11	Setting output files	136
3.3.12	Saving the project on disk	138

3.3.13	Validate data and start execution.....	138
3.4	Results visualization and post-processing tools	140
3.4.1	See hazard maps	141
3.4.2	Show disaggregation chart	144
3.4.3	Batch disaggregation parameters.....	146
3.4.4	CAPRA seismic scenario generator	147
3.4.5	Compute the event-set for a site and generation of stochastic catalogues.....	151
3.4.6	Show event-set characteristics	153
3.4.7	Tools.....	153
3.4.8	Optimum spectra	157
3.4.9	Probabilistic liquefaction hazard analysis	158
3.4.10	Conditional Mean Spectrum	161
3.4.11	Export source data to shape	164
3.5	Results and output files.....	166
3.5.1	Results file *.res	166
3.5.2	Graphics file *.gra	167
3.5.3	Source by source file *.fue	167
3.5.4	Map file *.map	167
3.5.5	M-R disaggregation file *.des.....	168
3.5.6	Maximum earthquakes file *.smx	168
4	Validation tests	169
4.1	PEER validation tests (set 1)	169
4.1.1	Geometry of the earthquake sources.....	169
4.1.2	Rupture areas	171
4.1.3	Description of ground motion attenuation	172
4.1.4	Other instructions from PEER.....	172
4.1.5	Set 1 case1	172
4.1.6	Set 1 case 2	182
4.1.7	Set 1 case 3	187
4.1.8	Set 1 case 4	187
4.1.9	Set 1 case 5	193
4.1.10	Set 1 case 6	199
4.1.11	Set 1 case 7	204
4.1.12	Set 1 case 8a	210
4.1.13	Set 1 case 8b.....	215
4.1.14	Set 1 case 8c	219
4.1.15	Set 1 case 9	223

4.1.16	Set 1 case 10	223
4.1.17	Set 1 case 11.....	226
4.1.18	Comments about the computation of distances	230
4.2	PEER validation tests (set 2).....	230
4.2.1	Set 2 case 1	230
4.2.2	Set 2 case 2.....	235
4.2.3	Set 2 case 3.....	240
4.2.4	Set 2 case 4a.....	245
4.2.5	Set 2 case 5a.....	247
4.2.6	Set 2 case 5b.....	249
4.3	PEER validation tests (set 3).....	250
4.4	Validation against some analytical solutions.....	250
4.4.1	Case 1: Point source with deterministic GMPM	251
4.4.2	Case 2: Point source with probabilistic GMPM	252
4.4.3	Case 3: Area source with probabilistic GMPM	254
4.5	GMPM validation tests.....	255
4.5.1	Comparison against published raw data.....	255
4.5.2	Graphical comparisons.....	261
4.5.3	GMPM where R-CRISIS developers are authors	288
4.5.4	GMPM data provided directly by the authors.....	288
4.6	Additional validation tests	288
4.6.1	Hybrid GMPM vs. Logic trees calculations.....	288
4.6.2	Verification of the handling of the non-Poissonian occurrence probabilities	289
5	References	292
	Annex 1: Triangulation algorithm (for sub-sources division).....	300
	Annex 2: Supplementary information and datasets	308

List of Figures

Figure 1-1 Launching the setup.exe of R-CRISIS	3
Figure 1-2 Initial screen of the R-CRISIS setup wizard	4
Figure 1-3 Storage path and access restrictions of R-CRISIS	4
Figure 1-4 Welcome of R-CRISIS	5
Figure 1-5 Main screen of R-CRISIS	6
Figure 2-1 Probability density function of the M_U value	13
Figure 2-2 Area plane with 8 vertexes	20
Figure 2-3 Area plane with 8 vertexes and 6 sub-sources	21
Figure 2-4 Example of in-plane circular fault ruptures in one sub-source of the area source of Figure 2-2	24
Figure 2-5 Definition of an area source with the treat as fault behavior option	26
Figure 2-6 Schematic representation or the leaky boundary behavior	27
Figure 2-7 Schematic representation or the strict boundary behavior	27
Figure 2-8 Example of dip values to orientate the rupture planes in R-CRISIS	28
Figure 2-9 Illustration of oriented circular ruptures in an horizontal area source	29
Figure 2-10 Volume sources in R-CRISIS	30
Figure 2-11 Example of a fault area with varying depth and 4 vertexes	30
Figure 2-12 Example of fault ruptures in a line source	32
Figure 2-13 Basic grid parameters	35
Figure 2-14 Seismicity parameters structure for the gridded geometric model	36
Figure 2-15 Schematic representation of a delimitation polygon	36
Figure 2-16 Structure of input data to define the orientation of ruptures in the gridded model	37
Figure 2-17 Example of a rectangular fault with dip equal to 90°	38
Figure 2-18 Illustration of slab geometry model in R-CRISIS	39
Figure 2-19 Distance measures implemented in R-CRISIS	42
Figure 2-20 Effect of different truncation schemes on GMPM	50
Figure 2-21 Example of a hybrid GMPE	56
Figure 2-22 Detail of the end tail of the example hybrid GMPE	57
Figure 2-23 Source subdivision with minimum triangle size=11km, minimum distance/triangle size ratio=3	65
Figure 2-24 Source subdivision with minimum triangle size=5km, minimum distance/triangle size ratio=3	65
Figure 2-25 Source subdivision with minimum triangle size=11km, minimum distance/triangle size ratio=4	66
Figure 2-26 Source subdivision with minimum triangle size=0.5km, minimum distance/triangle size ratio=4	66
Figure 2-27 Measurement of distances when using DEM	68
Figure 2-28 Top view of R_{JB} and R_{RUP} distances	68
Figure 2-29 DEM v.s. no DEM seismic hazard results	69
Figure 2-30 Differences due to the number of intensity levels in the hazard plot	77
Figure 2-31 Differences due to the distance scaling in the hazard plot	78
Figure 2-32 Estimation of the non-exceedance probability for given median and standard deviation of the natural logarithm	80
Figure 2-33 Estimation of A_{eps}	81
Figure 2-34 Optimum design framework	86
Figure 2-35 Validation of the location for the stochastic catalogue generated for line faults.	88

Figure 2-36 Validation of the location for the stochastic catalogue generated in a rectangular fault	89
Figure 2-37 Validation of the location for the stochastic catalogue generated in an area-plane	89
Figure 2-38 Validation of the location for the stochastic catalogue generated in point sources (SSG)	90
Figure 2-39 Validation of the location for the stochastic catalogue generated in area sources. Left: normal behavior. Right: treat as fault behavior	90
Figure 2-40 Validation of the location for the stochastic catalogue generated in slab sources	91
Figure 2-41 Validation of the location for the stochastic catalogue generated in gridded sources.....	91
Figure 2-42 Comparison of theoretical G-R recurrence plots for theoretical values and a stochastic catalogue with 100 years duration	92
Figure 2-43 Comparison of theoretical G-R recurrence plots for theoretical values and a stochastic catalogue with 10000 years duration.....	93
Figure 2-44 Conditional Spectrum for $T^*=2.0s$ and Jaimes and Candia (2019) inter-period correlation model.....	95
Figure 2-45 PLHA results in terms of annual exceedance rates (a), return periods (b) and occurrence probability in the next 50 years (c).....	97
Figure 3-1 Access to menus and tools from the main screen of R-CRISIS.....	99
Figure 3-2 File administration buttons in R-CRISIS.....	101
Figure 3-3 Opening a existing project in R-CRISIS.....	102
Figure 3-4 Logic-tree calculations screen in R-CRISIS	103
Figure 3-5 Successfully stored R-CRISIS project.....	104
Figure 3-6 Data assignment buttons in R-CRISIS	105
Figure 3-7 Reference map data screen in R-CRISIS	106
Figure 3-8 Defining the title of the run in a R-CRISIS project.....	107
Figure 3-9 Definition of a grid of computation sites in R-CRISIS.....	108
Figure 3-10 Grid reduction polygon in R-CRISIS.....	108
Figure 3-11 Definition of a list of computation sites	109
Figure 3-12 Source geometry data screen in R-CRISIS	110
Figure 3-13 Area source geometry data screen in R-CRISIS	111
Figure 3-14 Assignment of rupture size parameters to area sources in R-CRISIS.....	112
Figure 3-15 List of built-in K 's for area sources in R-CRISIS	112
Figure 3-16 Behavior type selection for area sources in R-CRISIS.....	113
Figure 3-17 Definition of the aspect ratio for area sources in R-CRISIS.....	113
Figure 3-18 Volume sources in R-CRISIS	114
Figure 3-19 Area plane source geometry data screen in R-CRISIS	115
Figure 3-20 Line source geometry data screen in R-CRISIS	116
Figure 3-21 Grid sources in R-CRISIS.....	117
Figure 3-22 Point (SSG) sources in R-CRISIS	118
Figure 3-23 Visualization of several seismic sources in R-CRISIS.....	119
Figure 3-24 Verification of sub-sources slenderness in R-CRISIS (1 of 2).....	120
Figure 3-25 Verification of sub-sources slenderness in R-CRISIS (2 of 2)	120
Figure 3-26 Definition of spectral ordinates and associated parameters in R-CRISIS	122
Figure 3-27 Modified G-R seismicity model screen in R-CRISIS.....	123
Figure 3-28 Characteristic earthquake model screen in R-CRISIS	124
Figure 3-29 Gridded seismicity model in R-CRISIS	126
Figure 3-30 Attenuation data screen in R-CRISIS.....	127
Figure 3-31 Adding a built-in GMPM to a R-CRISIS project.....	127

Figure 3-32 Adding an attenuation table to a R-CRISIS project	128
Figure 3-33 Visualization of active GMPM in R-CRISIS	129
Figure 3-34 Adding hybrid GMPM to R-CRISIS.....	130
Figure 3-35 Hybrid GMPM constructor of R-CRISIS.....	130
Figure 3-36 Assignment of GMPM to the seismic sources	131
Figure 3-37 GMPM analyzer screen of R-CRISIS	132
Figure 3-38 Site-effects screen of R-CRISIS	133
Figure 3-39 Visualization of added site-effects grids to R-CRISIS project	134
Figure 3-40 DEM screen and visualization screen of R-CRISIS	135
Figure 3-41 Definition of global parameters for the seismic hazard analysis	136
Figure 3-42 Output file menu access in R-CRISIS.....	137
Figure 3-43 Selection of output files in R-CRISIS	138
Figure 3-44 Validation data screen of R-CRISIS	139
Figure 3-45 Hazard progress bar and remaining time screen	139
Figure 3-46 Successful computation and generated output files screen of R-CRISIS.....	140
Figure 3-47 Visualization and post-processing options of R-CRISIS.....	141
Figure 3-48 Hazard maps screen of R-CRISIS	142
Figure 3-49 Setting scale limits in the hazard maps screen.....	143
Figure 3-50 Visualization and export of hazard plots and UHS	143
Figure 3-51 Hazard map export options and formats in R-CRISIS	144
Figure 3-52 Hazard disaggregation screen of R-CRISIS.....	145
Figure 3-53 Batch disaggregation parameters screen of R-CRISIS.....	147
Figure 3-54 CAPRA seismic scenario (multiple) generator of R-CRISIS	148
Figure 3-55 *.AME metadata screen in R-CRISIS	149
Figure 3-56 Scenario generation progress in R-CRISIS	149
Figure 3-57 CAPRA seismic (single) scenario generator of R-CRISIS	150
Figure 3-58 Event set screen of R-CRISIS	151
Figure 3-59 Visualization of the event set characteristics for a seismic source	153
Figure 3-60 GMPM branch constructor tool of R-CRISIS	155
Figure 3-61 Map comparer tool of R-CRISIS.....	156
Figure 3-62 Optimum spectra screen of R-CRISIS.....	158
Figure 3-63 Liquefaction analysis screen of R-CRISIS.....	161
Figure 3-64 CMS screen of R-CRISIS	162
Figure 3-65 Example of a CMS calculation in R-CRISIS	163
Figure 3-66 CMS exported results.....	164
Figure 3-63 Export source data to shapefile in R-CRISIS	165
Figure 3-64 Confirmation of a successful shapefile export.....	166
Figure 4-1 Geometry of the fault sources (1 & 2) and location of the observation sites.....	170
Figure 4-2 Geometry of the area sources and location of the observation sites.....	171
Figure 4-3 Schematic representation of elliptical rupture areas in R-CRISIS	172
Figure 4-4 Geometry of the seismic source (rectangular fault) in R-CRISIS. Case 1, set 1..	174
Figure 4-5 Geometry of the seismic source (area fault) in R-CRISIS. Case 1, set 1.....	175
Figure 4-6 Seismicity data in R-CRISIS. Case 1, set 1.....	176
Figure 4-7 Attenuation model assignment in R-CRISIS for case 1, set 1.....	177
Figure 4-8 Comparison of the CRISIS and PEER-2015 results for Sites 1 to 7 (Set 1 Case 1)	180
.....	
Figure 4-9 Comparison of elliptical and rectangular rupture shapes for PEER-2015 Set 1 Case	181
1	
Figure 4-10 Seismicity values in R-CRISIS. Case 1, set 2.....	183
Figure 4-11 Comparison of the CRISIS and PEER-2015 results for Sites 1 to 7 (Set 1 Case 2)	185
.....	

Figure 4-12 Comparison of elliptical and rectangular rupture shapes for PEER-2015 Set 1 Case 2.....	186
Figure 4-13 Geometry data for Fault 2 in PEER-2015 validation tests	188
Figure 4-14 Seismicity parameters assigned in R-CRISIS for set 1, case 4	188
Figure 4-15 Comparison of the CRISIS and PEER-2015 results for Sites 1 to 7 (Set 1 Case 4)	191
Figure 4-16 Comparison of elliptical and rectangular rupture shapes for PEER-2015 Set 1 Case 4	192
Figure 4-17 Seismicity parameters assigned in R-CRISIS for set 1, case 5.....	194
Figure 4-18 Comparison of the CRISIS and PEER-2015 results for Sites 1 to 7 (Set 1 Case 5)	197
Figure 4-19 Comparison of elliptical and rectangular rupture shapes for PEER-2015 Set 1 Case 5	198
Figure 4-20 Seismicity parameters assigned in R-CRISIS for set 1, case 6.....	199
Figure 4-21 Comparison of the CRISIS and PEER-2015 results for Sites 1 to 7 (Set 1 Case 6)	202
Figure 4-22 Comparison of elliptical and rectangular rupture shapes for PEER-2015 Set 1 Case 6	203
Figure 4-23 Seismicity parameters assigned in R-CRISIS for set 1, case 7 (modified G-R model)	205
Figure 4-24 Seismicity parameters assigned in R-CRISIS for set 1, case 7 (characteristic earthquake model).....	206
Figure 4-25 Comparison of the CRISIS and PEER-2015 results for Sites 1 to 7 (Set 1 Case 7)	208
Figure 4-26 Comparison of elliptical and rectangular rupture shapes for PEER-2015 Set 1 Case 7	209
Figure 4-27 Untruncated sigma assignment for Set 1 case 8a of PEER-2015.....	210
Figure 4-28 Comparison of the CRISIS and PEER-2015 results for Sites 1 to 7 (Set 1 Case 8a)	213
Figure 4-29 Comparison of elliptical and rectangular rupture shapes for PEER-2015 Set 1 Case 8a	214
Figure 4-30 Comparison of the CRISIS and PEER-2015 results for Sites 1 to 7 (Set 1 Case 8b)	217
Figure 4-31 Comparison of elliptical and rectangular rupture shapes for PEER-2015 Set 1 Case 8b.....	218
Figure 4-32 Comparison of the CRISIS and PEER-2015 results for Sites 1 to 7 (Set 1 Case 8c)	221
Figure 4-33 Comparison of elliptical and rectangular rupture shapes for PEER-2015 Set 1 Case 8c	222
Figure 4-34 Geometry data for area source in set 1, case 10.....	224
Figure 4-35 Seismicity parameters assigned in R-CRISIS for set 1, case 10	224
Figure 4-36 Comparison of the CRISIS and PEER-2015 results for Sites 1 to 4 (Set 1 Case 10)	226
Figure 4-37 Geometry data for area source in set 1, case 11.....	227
Figure 4-38 Comparison of the CRISIS and PEER-2015 results for Sites 1 to 4 (Set 1 Case 11)	229
Figure 4-39 Geometry of the fault sources, the area source and the location of the observation size for Set 2, case 1.....	231
Figure 4-40 Comparison of the CRISIS and PEER results for site 1 (set 2 case 1).....	232
Figure 4-41 Comparison of the disaggregation results of CRISIS and PEER by distance (top left), magnitude (top right) and epsilon (bottom). PGA – 0.05g	233

Figure 4-42 Comparison of the disaggregation results of CRISIS and PEER by distance (top left), magnitude (top right) and epsilon (bottom). PGA corresponding to a hazard of 0.001	234
Figure 4-43 Comparison of the disaggregation results of CRISIS and PEER by distance (top left), magnitude (top right) and epsilon (bottom). PGA – 0.35g.....	234
Figure 4-44 Geometry of the fault source and the location of the observation size for set 2, case 2	235
Figure 4-45 Comparison of the CRISIS and PEER results for sites 1 to 6 (set 2 case 2a)...	237
Figure 4-46 Comparison of the CRISIS and PEER results for sites 1 to 6 (set 2 case 2b) ..	238
Figure 4-47 Comparison of the CRISIS and PEER results for sites 1 to 6 (set 2 case 2c) ...	239
Figure 4-48 Comparison of the CRISIS and PEER results for sites 1 to 6 (set 2 case 2d) ..	240
Figure 4-49 Geometry of the fault source and the location of the observation size for set 2, case 3	241
Figure 4-50 Comparison of the CRISIS and PEER results for sites 1 to 6 (set 2 case 3a)...	242
Figure 4-51 Comparison of the CRISIS and PEER results for sites 1 to 6 (set 2 case 3b) ...	243
Figure 4-52 Comparison of the CRISIS and PEER results for sites 1 to 6 (set 2 case 3c) ...	244
Figure 4-53 Comparison of the CRISIS and PEER results for sites 1 to 6 (set 2 case 3d)...	245
Figure 4-54 Geometry of the fault source and the location of the observation size for set 2, case 4a	246
Figure 4-55 Comparison of the CRISIS and PEER results for site 1 (set 2 case 4a).....	247
Figure 4-56 Geometry of the fault source and the location of the observation size for set 2, cases 5a-5b	248
Figure 4-57 Comparison of the CRISIS and PEER results for site 1 (set 2 case 5a).....	249
Figure 4-58 Comparison of the CRISIS and PEER results for site 1 (set 2 case 5b)	250
Figure 4-59 Comparison of analytical and numerical solutions for Case 1 of Ordaz (2004)	252
Figure 4-60 Comparison of analytical and numerical solutions for Case 2 of Ordaz (2004); $\sigma=0.3$	253
Figure 4-61 Comparison of analytical and numerical solutions for Case 2 of Ordaz (2004); $\sigma=0.5$	253
Figure 4-62 Comparison of analytical and numerical solutions for Case 2 of Ordaz (2004); $\sigma=0.7$	254
Figure 4-63 Comparison of analytical and numerical solutions for Case 3 of Ordaz (2004)	254
Figure 4-64 Comparison of median values between original and built-in Abrahamson et al. (2014) GMPM	256
Figure 4-65 Comparison of percentile 84 values between original and built-in Abrahamson et al. (2014) GMPM.....	256
Figure 4-66 Comparison of median values between original and built-in Chiou and Youngs (2014) GMPM with $R_x=1$ km.....	257
Figure 4-67 Comparison of median values between original and built-in Chiou and Youngs (2014) GMPM with $R_x=10$ km	258
Figure 4-68 Comparison of median values between original and built-in Campbell and Bozorgnia (2014) GMPM. Cases 1, 3 and 4	259
Figure 4-69 Comparison of median values between original and built-in Campbell and Bozorgnia (2014) GMPM. Case2	259
Figure 4-70 Comparison of median values between original and built-in Campbell and Bozorgnia (2014) GMPM. Case5	260
Figure 4-71 Comparison of distance scaling of the Akkar et al. (2014) model for different magnitudes and distances	260

Figure 4-72 Comparison of distance scaling of R_{JB} model for different spectral ordinates. Top left: PGA; top right: 0.2s; bottom left: 1.0s; bottom right: 4.0s261

Figure 4-73 Comparison of median estimations of the predicted spectra for strike-slip mechanism, $R_{JB}=30\text{km}$, $V_{s30}=800\text{m/s}$ and $M_w=5$ (left) and $M_w=7$ (right).....261

Figure 4-74 Comparison of median values between original and built-in Zhao et al. (2006) data. PGA and 4 magnitudes 262

Figure 4-75 Comparison of median values between original and built-in Zhao et al. (2006) data. Full spectral range and 4 site classes..... 263

Figure 4-76 Comparison of median values between original and built-in Zhao et al. (2006) data. Full spectral range and pseudo-velocity. Source distance=40 km 264

Figure 4-77 Comparison of median values between original and built-in Zhao et al. (2006) data. Full spectral range and pseudo-velocity. Source distance=60 km 265

Figure 4-78 Comparison of median values between original and built-in Abrahamson and Silva (1997) GMPM. $M=7$, PGA, rock and different mechanisms 266

Figure 4-79 Comparison of median values between original and built-in Abrahamson and Silva (1997) GMPM. Strike-slip earthquake at a rupture distance of 10km. Average horizontal component 266

Figure 4-80 Comparison of median values between original and built-in Chiou and Youngs (2008) GMPM. 0.01s and 3.0s 267

Figure 4-81 Comparison of pseudo spectral accelerations between original and built-in Akkar and Bommer (2010) GMPM 268

Figure 4-82 Comparison in terms of median PSA spectra at rock sites among the predictive equations of Cauzzi et al. (2017) for $M_w 6.5$ 269

Figure 4-83 Comparison in terms of median PSA spectra at rock sites among the predictive equations of Cauzzi et al. (2017) for $M_w 6.5$ 269

Figure 4-84 Comparison of response spectra for a fore-arc with $V_{s30}=300\text{ m/s}$ for intraplate earthquake with Montalva et al. 2017 GMPM. $M_w=6.5$ and 8.5; $R_{RUP}=25\text{km}$ 270

Figure 4-85 Comparison of response spectra for a fore-arc with $V_{s30}=300\text{ m/s}$ for intraplate earthquake with Montalva et al. 2017 GMPM. $M_w=6.5$ and 8.5; $R_{RUP}=50\text{km}$ 270

Figure 4-86 Comparison of response spectra for a fore-arc with $V_{s30}=300\text{ m/s}$ for intraplate earthquake with Montalva et al. 2017 GMPM. $M_w=6.5$ and 8.5; $R_{RUP}=100\text{km}$ 271

Figure 4-87 Comparison of response spectra for a fore-arc with $V_{s30}=300\text{ m/s}$ for intraplate earthquake with Montalva et al. 2017 GMPM. $M_w=6.5$ and 8.5; $R_{RUP}=150\text{km}$ 271

Figure 4-88 Comparison of response spectra for a fore-arc with $V_{s30}=300\text{ m/s}$ for in-slab earthquake with Montalva et al. 2017 GMPM. $M_w=6.5$ and 8.5; $R_F=75\text{km}$ 272

Figure 4-89 Comparison of response spectra for a fore-arc with $V_{s30}=300\text{ m/s}$ for in-slab earthquake with Montalva et al. 2017 GMPM. $M_w=6.5$ and 8.5; $R_F=100\text{km}$ 272

Figure 4-90 Comparison of response spectra for a fore-arc with $V_{s30}=300\text{ m/s}$ for in-slab earthquake with Montalva et al. 2017 GMPM. $M_w=6.5$ and 8.5; $R_F=150\text{km}$ 273

Figure 4-91 Comparison of response spectra for a fore-arc with $V_{s30}=300\text{ m/s}$ for in-slab earthquake with Montalva et al. 2017 GMPM. $M_w=6.5$ and 8.5; $R_F=200\text{km}$ 273

Figure 4-92 Within event standard deviation versus periods for Bindi et al. (2017) GMPM 274

Figure 4-93 Between event standard deviation versus periods for Bindi et al. (2017) GMPM 274

Figure 4-94 Total standard deviation versus periods for Bindi et al. (2017) GMPM.....275

Figure 4-95 Comparison of the period-dependence of median pseudo spectral accelerations derived from Derras et al. (2014) with those proposed in other European GMPEs. $M_w=5$, $V_{s30}=800\text{m/s}$275

Figure 4-96 Comparison of the period-dependence of median pseudo spectral accelerations derived from Derras et al. (2014) with those proposed in other European GMPEs. Mw=5, Vs30=300m/s..... 276

Figure 4-97 Comparison of the period-dependence of median pseudo spectral accelerations derived from Derras et al. (2014) with those proposed in other European GMPEs. Mw=6, Vs30=800m/s..... 276

Figure 4-98 Comparison of the period-dependence of median pseudo spectral accelerations derived from Derras et al. (2014) with those proposed in other European GMPEs. Mw=6, Vs30=300m/s.....277

Figure 4-99 Comparison of the period-dependence of median pseudo spectral accelerations derived from Derras et al. (2014) with those proposed in other European GMPEs. Mw=7, Vs30=800m/s.....277

Figure 4-100 Comparison of the period-dependence of median pseudo spectral accelerations derived from Derras et al. (2014) with those proposed in other European GMPEs. Mw=5, Vs30=300m/s..... 278

Figure 4-101 Validation of the predictions for peak horizontal velocities for Mw 5.0, 6.0 and 7.0. Left: rock; right: soil 278

Figure 4-102 Validation of the median spectra predicted for increasing magnitudes at stiff site and 30km distance 279

Figure 4-103 Validation of the total aleatory variability for two magnitudes (4.0 and 6.0) and soft and stiff soil conditions..... 280

Figure 4-104 Validation of the response spectra predicted by the Pezeshk et al. (2018) GMPM based on the stochastic-scaling approach281

Figure 4-105 Validation of the response spectra predicted by the Pezeshk et al. (2018) GMPM based on the empirical-scaling approach..... 282

Figure 4-106 Validation of the PGA and PSA for four spectral ordinates 283

Figure 4-107 Validation of the CENA-adjusted GMPM for T=0.1s (top left), T=0.5s (top right), T=1.0s (bottom left) and T=3.0s (bottom right) 284

Figure 4-108 Validation of the CENA and California adjusted response spectra for DRUP=10km (left) and DRUP=100km (right) 284

Figure 4-109 Validation of the PGA predictions of the Darzi et al. (2019) model for Mw 5.5 and 7.0..... 285

Figure 4-110 Validation of the T=1.0s predictions of the Darzi et al. (2019) model for Mw 5.5 and 7.0..... 285

Figure 4-111 Validation of predicted median pseudo-acceleration of the Darzi et al. (2019) model for different soil classes. RJB=5km 286

Figure 4-112 Validation of the T=1.0s predictions of the Lanzano et al. (2019) model for Mw 4.0 and 6.8, Vs30=600 m/s and normal faulting mechanism 287

Figure 4-113 Validation of the T=1.0s predictions of the Lanzano et al. (2019) model for Mw 4.0 and 6.8, Vs30=300 m/s and strike-slip faulting mechanism..... 287

Figure 4-114 Comparison of the results obtained with Poissonian and non-Poissonian sources for 20 years timeframe 290

Figure 4-115 Comparison of the results obtained with Poissonian and non-Poissonian sources for 50 years timeframe..... 290

Figure 4-116 Comparison of the results obtained with Poissonian and non-Poissonian sources for 100 years timeframe.....291

List of Tables

Table 2-1 Generalized seismicity file structure (part 1)	15
Table 2-2 Generalized seismicity file structure (part 2)	16
Table 2-3 Generalized Poissonian seismicity file structure	17
Table 2-4 Generalized Poissonian seismicity file example	18
Table 2-5 Wells and Coppersmith (1994) rupture area regression coefficients	22
Table 2-6 R-CRISIS rupture area coefficients for the Wells and Coppersmith (1994) model	23
Table 2-7 Equivalences between R-CRISIS and Wells and Coppersmith (1994) rupture area coefficients	23
Table 2-8 Built-in K_1 and K_2 constants	23
Table 2-9 Wells and Coppersmith (1994) SRL and SSRL rupture length regression coefficients	31
Table 2-10 R-CRISIS SRL and SSRL rupture length coefficients for the Wells and Coppersmith (1994) model	32
Table 2-11 Equivalences between Wells and Coppersmith (1994) and R-CRISIS coefficients for SLR and SSLR	32
Table 2-12 Point geometry file structure	33
Table 2-13 Geometry record file structure	33
Table 2-14 Point-source geometry file example	34
Table 2-15 Required parameters for the definition of a grid source	35
Table 2-16 Description of the header fields accepted by R-CRISIS for attenuation tables ..	44
Table 2-17 Description of magnitude range and number in attenuation tables	44
Table 2-18 Description of distance range, number and type in attenuation tables	45
Table 2-19 Codes for types of distances in attenuation tables	45
Table 2-20 Description of attenuation table data	46
Table 2-21 Example of a *.atn file (user defined attenuation table)	47
Table 2-22 Physical dimensions accepted by R-CRISIS	48
Table 2-23 Implemented methods for physical dimensions in R-CRISIS	48
Table 2-24 Acceptable probability distributions to describe hazard intensities in R-CRISIS	49
Table 2-25 Built-in GMPEs in R-CRISIS	52
Table 2-26 Description of the *.gaf file structure	54
Table 2-27 Description of the amplification factors file structure	61
Table 2-28 Example of site-effects file	62
Table 2-29 Feasibility of normal attenuation, geometric and seismicity models combination	70
Table 2-30 Feasibility of generalized attenuation, geometric and seismicity models combination	72
Table 3-1 Summary of spectral ordinates for the CAPRA Island example	122
Table 3-2 Example of a *.csv file for liquefaction analysis in R-CRISIS	160
Table 4-1 Summary of input data for Set 1, case 1	173
Table 4-2 Coordinates of the fault source 1	173
Table 4-3 Coordinates and comments of the computation sites for fault sources 1 and 2 ..	173
Table 4-4 Annual exceedance probabilities obtained in R-CRISIS for Case 1, set 1	178
Table 4-5 Annual exceedance probabilities reported as benchmarks by PEER project coordinators for Case 1, set 1	178
Table 4-6 Analytical annual exceedance probabilities obtained by PEER project coordinators for Case 1, set 1	179

Table 4-7 Summary of input data for Set 1, case 2.....	182
Table 4-8 Annual exceedance probabilities obtained in R-CRISIS for Case 1, set 2.....	183
Table 4-9 Annual exceedance probabilities reported as benchmarks by PEER project coordinators for Case 1, set 2.....	184
Table 4-10 Analytical annual exceedance probabilities obtained by PEER project coordinators for Case 1, set 2.....	184
Table 4-11 Summary of input data for Set 1, case 4.....	187
Table 4-12 Annual exceedance probabilities obtained in R-CRISIS for Case 1, set 4.....	189
Table 4-13 Annual exceedance probabilities reported as benchmarks by PEER project coordinators for Case 1, set 4.....	189
Table 4-14 Analytical annual exceedance probabilities obtained by PEER project coordinators for Case 1, set 4.....	190
Table 4-15 Summary of input data for Set 1, case 5.....	193
Table 4-16 Annual exceedance probabilities obtained in R-CRISIS for Case 1, set 5.....	195
Table 4-17 Annual exceedance probabilities reported as benchmarks by PEER project coordinators for Case 1, set 5.....	195
Table 4-18 Analytical annual exceedance probabilities obtained by PEER project coordinators for Case 1, set 5.....	196
Table 4-19 Summary of input data for Set 1, case 6.....	199
Table 4-20 Annual exceedance probabilities obtained in R-CRISIS for Case 1, set 6.....	200
Table 4-21 Annual exceedance probabilities reported as benchmarks by PEER project coordinators for Case 1, set 6.....	201
Table 4-22 Analytical annual exceedance probabilities obtained by PEER project coordinators for Case 1, set 6.....	201
Table 4-23 Summary of input data for Set 1, case 7.....	204
Table 4-24 Annual exceedance probabilities obtained in R-CRISIS for Case 1, set 7.....	206
Table 4-25 Annual exceedance probabilities reported as benchmarks by PEER project coordinators for Case 1, set 7.....	207
Table 4-26 Analytical annual exceedance probabilities obtained by PEER project coordinators for Case 1, set 7.....	207
Table 4-27 Summary of input data for Set 1, case 8a.....	210
Table 4-28 Annual exceedance probabilities obtained in R-CRISIS for Case 1, set 8a.....	211
Table 4-29 Annual exceedance probabilities reported as benchmarks by PEER project coordinators for Case 1, set 8a.....	212
Table 4-30 Summary of input data for Set 1, case 8b.....	215
Table 4-31 Annual exceedance probabilities obtained in R-CRISIS for Case 1, set 8b.....	216
Table 4-32 Annual exceedance probabilities reported as benchmarks by PEER project coordinators for Case 1, set 8b.....	216
Table 4-33 Summary of input data for Set 1, case 8c.....	219
Table 4-34 Annual exceedance probabilities obtained in R-CRISIS for Case 1, set 8c.....	220
Table 4-35 Annual exceedance probabilities reported as benchmarks by PEER project coordinators for Case 1, set 8c.....	220
Table 4-36 Summary of input data for Set 1, case 10.....	223
Table 4-37 Coordinates and comments of the computation sites for the area source.....	224
Table 4-38 Annual exceedance probabilities obtained in R-CRISIS for Case 1, set 10.....	225
Table 4-39 Summary of input data for Set 1, case 11.....	227
Table 4-40 Annual exceedance probabilities obtained in R-CRISIS for Case 1, set 11.....	228
Table 4-41 Annual exceedance probabilities reported as benchmarks by PEER project coordinators for Case 1, set 11.....	229
Table 4-42 Real distance computed by R-CRISIS with the PEER project coordinates.....	230
Table 4-43 Adjustment on coordinates to estimate the same real distance in R-CRISIS...	230

Table 4-44 Summary of input data for Set 2, case 1..... 231

Table 4-45 Coordinates of the fault source B 232

Table 4-46 Coordinates of the fault source C 232

Table 4-47 Coordinates and comments of the computation site for set 2 case 1..... 232

Table 4-48 Summary of input data for Set 2, case 2 (a,b,c,d)..... 235

Table 4-49 Coordinates of the fault source 3 236

Table 4-50 Coordinates and comments of the computation sites for set 2 case 2 236

Table 4-51 Summary of input data for set 2, case 3 (a,b,c,d)..... 241

Table 4-52 Coordinates of the fault source 4 241

Table 4-53 Coordinates and comments of the computation sites for set 2 case 3..... 242

Table 4-54 Summary of input data for Set 2, case 4a 246

Table 4-55 Coordinates of the fault source 5..... 246

Table 4-56 Coordinates and comments of the computation site for set 2 case 4a 246

Table 4-57 Summary of input data for Set 2, case 5a..... 248

Table 4-58 Coordinates of the fault source 6 248

Table 4-59 Coordinates and comments of the computation site for set 2 cases 5a-5b 248

Table 4-60 Summary of input data for Set 2, case 5b 249

Table 4-61 Seismicity parameters for the comparison against the analytical solution 251

Table 4-62 Characteristics of the 5 validation cases of the Campbell-Bozorgnia (2014) GMPM 258

Table 4-63 Comparison of annual exceedance probabilities with logic-trees and hybrid GMPM approaches 288

List of Acronyms

- CAPRA: Comprehensive Approach to Probabilistic Risk Assessment
- CAV: Cumulative Absolute Velocity
- CE model: Characteristic Earthquake seismicity model
- CoV: Coefficient of variation
- CMS: Conditional Mean Spectrum
- CS: Conditional Spectrum
- DEM: Digital Elevation Model
- GMPE: Ground Motion Prediction Equation
- GMPM: See GMPE
- G-R model: Gutenberg-Richter seismicity model
- GUI: Graphical User Interface
- MCE: Maximum Credible Earthquake
- M_o : Threshold magnitude
- M_U : Maximum magnitude
- M_w : Moment magnitude
- PEER: Pacific Earthquake Engineering Research Center
- PLHA: Probabilistic Liquefaction Hazard Analysis
- PSHA: Probabilistic Seismic Hazard Analysis
- R_{EPI} : Epicentral distance
- R_F : Focal distance
- R_{JB} : Joyner and Boore distance (closest distance to the projection of the fault plane on the Earth's surface)
- R_{RUP} : Closest distance to rupture area
- SEC: Stochastic event catalogue
- SLR: Surface Rupture Length
- SSLR: Subsurface Rupture Length
- V&V: Validation and Verification





1 Introduction

This document provides a complete description of the R-CRISIS program, which has been developed to perform probabilistic seismic hazard analyses with the possibility to the user of selecting different seismicity and geometrical models and with a friendly graphical user interface (GUI). The document is structured as follows: first an introduction and description of the program is made together with the list of minimum hardware and software requirements and a description of the installing process. Second, a full description of the theoretical background of all the methodologies implemented in the program is presented, accompanied by the illustration of some key procedures with the objective of helping the user understand what is done during the computation process of the seismic hazard in a probabilistic manner. Third, a hands-on guide of the program is included using a hypothetical example which explores the main tools, menus and options besides showing the required input data, its format and where to add it in the project. Finally, a comprehensive set of validation and verification (V&V) tests are included to provide full details on the capability, accuracy and usefulness of the program. This last section allows also concluding that R-CRISIS is fully suitable for performing a wide range of seismic hazard analyses with different complexities, from simple cases with analytical solutions, to the development of specific studies for critical facilities such as nuclear infrastructure.

The methodologies explained in this document together with the user manual have been developed for the latest available version of the R-CRISIS program (v20 at the time of writing this document). Although some of the features have been implemented in previous versions, the validation and verification results of this document are applicable only to the latest releases.

This document has been assembled using contributions from several people that have been involved in the development of CRISIS in its different versions and at different stages. Also, this V&V document uses texts previously written for the purposes of the validation of the R-CRISIS code within the framework of the PEER project (phases 1 and 2) by M. Villani, E. Faccioli, M. Ordaz and A. Aguilar, together with their results and findings.

1.1 Description of R-CRISIS

R-CRISIS is a Windows based software with the capability of performing probabilistic seismic hazard analysis (PSHA) using a fully probabilistic approach, allowing the calculation of results in terms of outputs with different characteristics (i.e. exceedance probability curves, stochastic event sets). The first version of the program was launched on 1986 and since then, more than thirty years ago, several and continuous updates and improvements have been included to keep the program as a state-of-the-art tool. Originally developed using FORTRAN as programming language (Ordaz, 1991) and without a GUI, it developed later into CRISIS99 (Ordaz, 1999) which was a tool that first introduced a GUI written in Visual Basic but with the computation engine using a FORTRAN dynamic link library. Since 2007 the program was upgraded in view of the advantages offered by the object-oriented technologies (i.e. Visual Basic.NET). In that version, called CRISIS2007, both the GUI and the computation engine were written in the same programming language.



Different experts with multidisciplinary backgrounds (from civil engineers to seismologists) have worked in its development and today it is a worldwide well-known tool which has been used in the development of different projects at different scales and the seismic zonation for the definition of seismic design coefficients in more than 10 countries in the Latin America and the Caribbean region. R-CRISIS has been mainly written and developed by PSHA practitioners and therefore, the development loop has been relatively short where most of the modifications, improvements and upgrades have been made to satisfy the needs of the developers themselves.

R-CRISIS provides a friendly environment to perform seismic hazard calculations within a fully probabilistic framework. The program computes seismic hazard by considering earthquake occurrence probabilities, attenuation characteristics and the geographical distribution of earthquakes.

Seismic hazard results are mainly obtained, for each computation site, in terms of probabilities of exceeding a given intensity value within different time frames, whereas it is also possible to obtain the results in terms of both, non-exceedance probabilities and equivalent annual exceedance rates.

1.2 Hardware and software requirements

The minimum hardware requirements for the installation and use of R-CRISIS are fulfilled by almost any personal computer in the market today. These are:

- PC with a Pentium IV (or higher) and processor speed higher than 2.0 GHz
- A free hard drive capacity of 5.0 GB
- 512 MB of Extended Memory (RAM)
- 16 MB video card
- Internet connection

To ensure optimum system operation with high processing speed, it is recommended that the computer where R-CRISIS is being installed meets the following hardware requirements:

- PC with a Pentium IV (or higher) and processor speed higher than 3.5 GHz
- A free hard disk capacity of 10.0 GB
- 1GB of Extended Memory (RAM)

Since the latest versions of R-CRISIS include optimization procedures based on parallelization, computers with larger RAM memory and available processors can have a faster performance.

The software requirements for installing and running R-CRISIS are:

- *Windows operating system*: all software packages used in this document were designed to operate on Microsoft Windows 7, but newer versions can run without requiring any additional changes and without restrictions¹.
- *.NET Framework 4.0*: all software packages used in this document use Microsoft .NET Framework².

1.3 Installing R-CRISIS

To install R-CRISIS the user needs to double click on the executer (Setup.exe³) as shown in Figure 1-1.

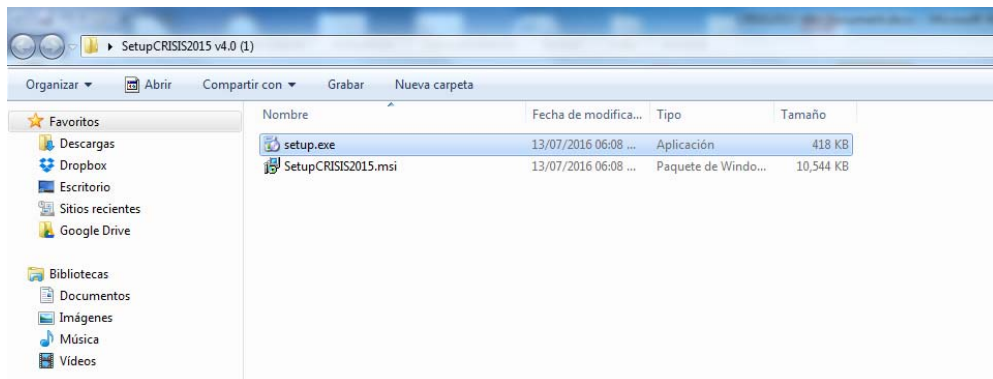


Figure 1-1 Launching the setup.exe of R-CRISIS

The *.exe file will start the R-CRISIS setup wizard (see Figure 1-2) which instructions are to be followed.

¹ R-CRISIS has been tested in Windows 8 and Windows 10 environments

² <http://www.microsoft.com/es-es/download/details.aspx?id=17851>

³ Available at: www.r-crisis.com

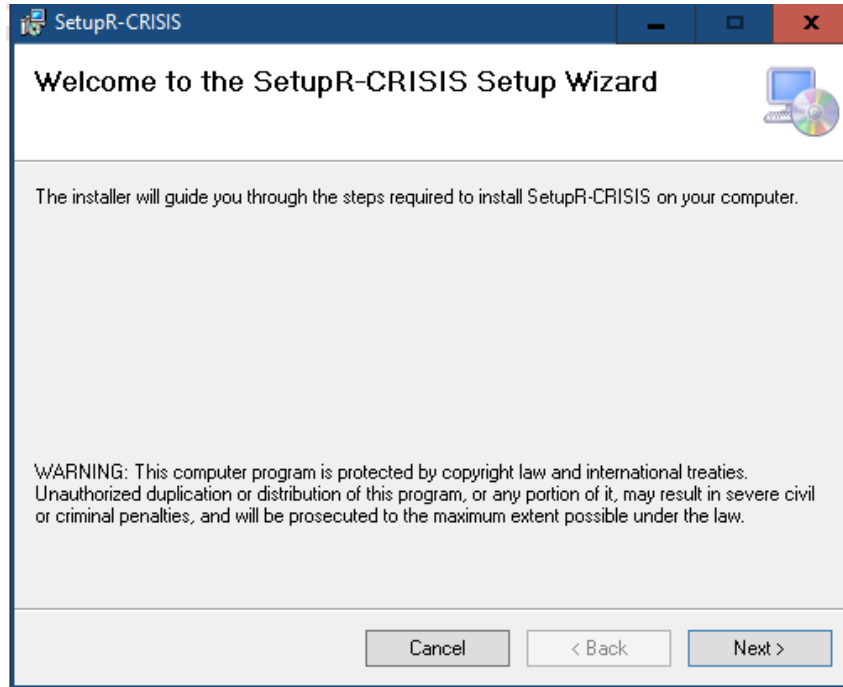


Figure 1-2 Initial screen of the R-CRISIS setup wizard

The user can modify the path where the program files will be stored as shown in Figure 1-3. By default, it is set to “C:\Program Files\ERN\R-CRISIS”. From this screen the user can grant permission on the installation of the program for only themselves and/or for other users of the same PC.

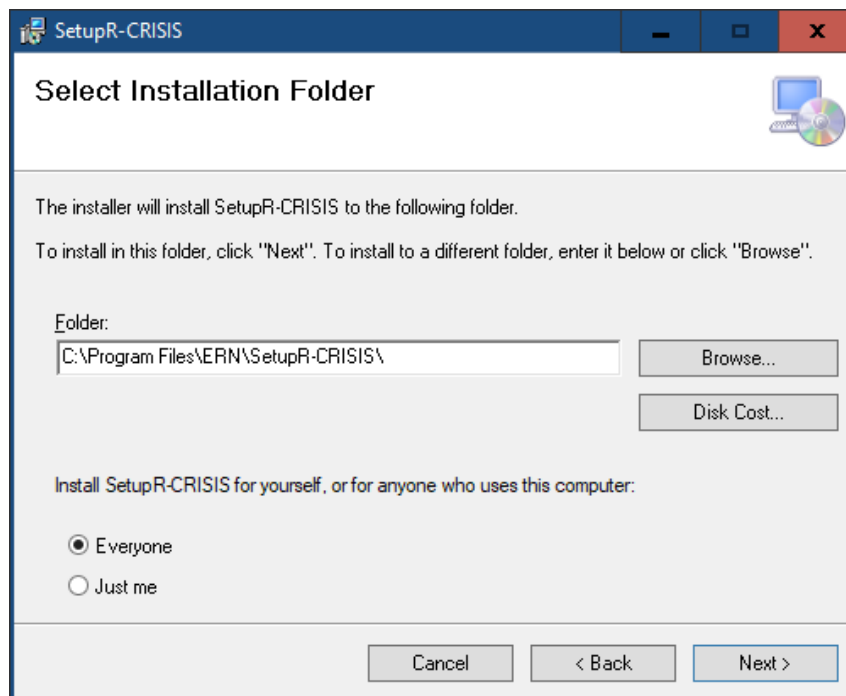


Figure 1-3 Storage path and access restrictions of R-CRISIS

Once all the steps of the setup wizard have been completed, the program will be installed, and a shortcut will be available in the desktop⁴.

Note: for a correct functioning of the program, it is mandatory that the decimal symbol is set to period “.” and that negative values are preceded by a minus “-” sign. These changes can be made in the control panel of windows in the regional setting options. This change must be done before launching the program accessing the control panel and making the appropriate selection at the regional settings.

1.4 Launching R-CRISIS

Once the program has been installed, by double clicking in the shortcut available at the desktop, R-CRISIS can be launched and the initial screen, as the one shown in Figure 1-4, will appear showing the version of the program as well as the developers’ team. To move forward to the main screen of the program click once on the “OK” button (bottom right).

Note: this screen will be displayed every time that the user launches the program.



Figure 1-4 Welcome of R-CRISIS

After this, the main screen of R-CRISIS will be displayed, as shown in Figure 1-5. This screen allows selecting the different options as well as using the different tools available in the program. For more details on how to create a seismic hazard project in R-CRISIS, see Chapter 3 of this V&V document.

⁴ If the desktop shortcut does not automatically appear, look for the *.exe file at the installation path

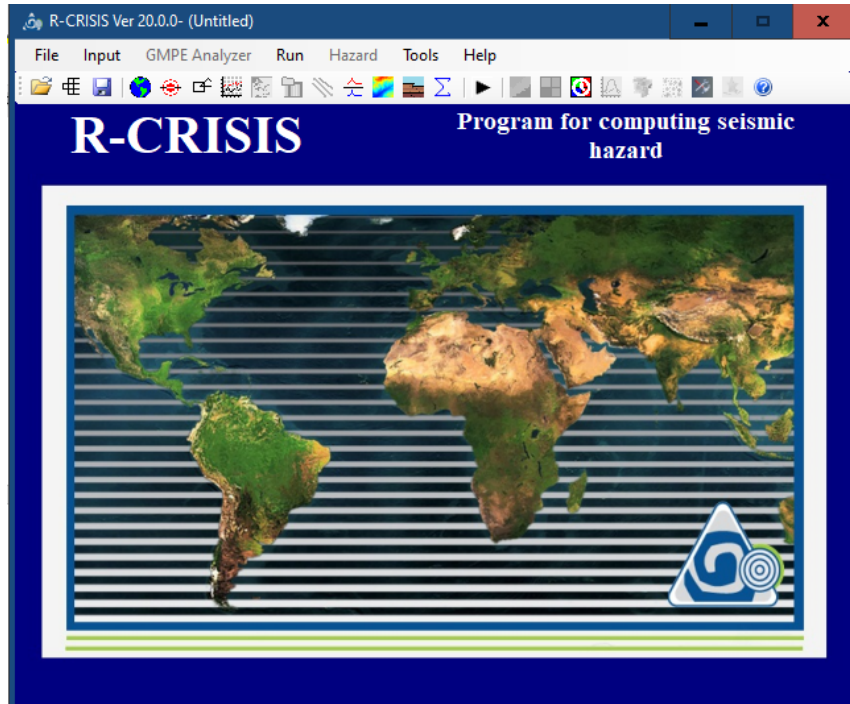


Figure 1-5 Main screen of R-CRISIS

2 Theoretical background of the methodologies and models implemented in R-CRISIS

2.1 Seismicity models

Generally speaking, R-CRISIS expects to have the seismicity described by means of the probabilities of having 1, 2, ..., N earthquakes of given magnitudes, at a given location, during the next T_f years. As can be noted by the reader, this is the most general description of seismicity that can possibly be given.

To get this information, R-CRISIS admits three different types of seismicity models. The first two are related to Poissonian occurrences, although they differ in the way in which the earthquake magnitude exceedance rates are defined, whereas the third model corresponds to a generalized non-Poissonian model where the required probabilities are explicitly provided by the user to the program. A complete description of each seismicity model implemented in R-CRISIS is provided next.

2.1.1 Modified Gutenberg-Richter model

This model is associated to Poissonian occurrences and so, the probability of exceeding the intensity level a in the next T_f years, given that an earthquake with magnitude M occurred at a distance R from the site of interest, is described by:

$$Pe(a, T | M, R) = 1 - \exp[-\Delta\lambda(M)T \cdot p_1(a | M, R)] \quad \text{Eq. (2-1)}$$

where $Pe(a | M, R)$ is the exceedance probability of the hazard intensity level a , given that an event with magnitude M occurred at a distance R from the site of interest, and $\Delta\lambda(M)$ is the Poissonian magnitude exceedance rate associated to the magnitude range (also denoted herein as magnitude bin) characterized by magnitude M . Note that $Pe(a | M, R)$ depends only on the magnitude and the site-to-hypocenter distance and therefore, this probability does not depend on earthquake occurrence probabilities.

On the other hand, $\Delta\lambda(M)$ can be computed as

$$\Delta\lambda(M) = \lambda\left(\frac{M - \Delta M}{2}\right) - \lambda\left(\frac{M + \Delta M}{2}\right) \quad \text{Eq. (2-2)}$$

where it is implicit that the magnitude bin characterized by magnitude M covers the range between $M - \Delta M/2$ and $M + \Delta M/2$. For the modified Gutenberg-Richter model (Cornell and Vanmarke, 1969), the earthquake magnitude exceedance rate is given by:

$$\lambda(M) = \lambda_0 \frac{\exp(-\beta M) - \exp(-\beta M_U)}{\exp(-\beta M_o) - \exp(-\beta M_U)}, M_o \leq M \leq M_U \quad \text{Eq. (2-3)}$$

where λ_o is the exceedance rate of the threshold magnitude, M_o ; β is a parameter equivalent to the "b-value" for the source (except that it is given in terms of its natural logarithm) and M_U is the maximum magnitude associated to the seismic source.

R-CRISIS can account for uncertainties in both β and M_U . On the one hand and to handle the uncertainty in the β parameter, the user must provide its expected value and its coefficient of variation (CoV); on the other hand, and in order to handle the uncertainty in the M_U value, its expected value and standard deviations are needed. More details about the treatment of those uncertainties are explained next.

Uncertainty in β value

Using a Bayesian framework, R-CRISIS treats λ_o and β parameters as independent random (and unknown) variables. Moreover, it assumes that uncertainty in β is correctly described by means of a Gamma probability distribution and, for the reasons described later, it disregards uncertainty in λ_o .

To explain the soundness of this treatment, the following commonly accepted hypotheses are assumed:

1. Occurrences are Poissonian
2. The probability distribution of magnitudes follows a Gutenberg-Richter (G-R) relation that is unbounded at the right-hand side. This is to say that the maximum possible magnitude, M_U , is much larger than M_o .

A consequence of the first assumption is that the times between earthquakes with magnitude $M \geq M_o$, τ , are independent, equally distributed random variables that follow an exponential distribution. Thus, its associated probability density function is:

$$p_T(\tau) = \lambda_o e^{-\lambda_o \tau} \quad \text{Eq. (2-4)}$$

where λ_o is an unknown parameter. Also, it follows from hypothesis 1 that the times of earthquake occurrences, and their corresponding magnitudes, are independent from each other. From hypothesis 2 it is implied that magnitudes are independent too and are represented by means of equally distributed random variables with a shifted exponential distribution. Therefore, their probability density function is:

$$p_M(M) = \beta e^{-\beta(M-M_o)} \quad \text{Eq. (2-5)}$$

where β is also an unknown parameter. It can be verified that equation 2-4 integrates to unity in the range of $\tau \geq 0$ while equation 2-5 integrates to 1.0 in the range $M \geq M_o$ (remember that, until now, M is unbounded).

Now, consider the observation of an event consisting in the occurrence of N earthquakes, with inter-event times, τ_i , and magnitudes M_i , $i=1..N$. According to the assumptions mentioned before, the likelihood of this event, given unknown parameters $\theta=(\lambda_o, \beta)$ can be written as:

$$l(\varepsilon | \theta) = \prod_{i=1}^N \lambda_o e^{-\lambda_o \tau_i} \beta e^{-\beta(M_i - M_o)} \quad \text{Eq. (2-6)}$$

Or, in other words,

$$l(\varepsilon | \theta) = \lambda_o^N e^{-\lambda_o \sum_i \tau_i} \beta^N e^{-\sum_i \beta(M_i - M_o)} \quad \text{Eq. (2-7)}$$

From equation 2-7, the classic maximum likelihood estimators for λ_o and β can be estimated:

$$\hat{\lambda}_o = \frac{N}{\sum_i \tau_i} = \frac{N}{T} \quad \text{Eq. (2-8)}$$

$$\hat{\beta} = \frac{N}{\sum_i \beta(M_i - M_o)} \quad \text{Eq. (2-9)}$$

where $T = \sum_i \tau_i$ is the total observation time in the catalog for the selected threshold magnitude, M_o .

Continuing with the use of a Bayesian approach, λ_o and β are regarded as random variables whose probability distributions are fixed *a priori* and then updated in the light of the earthquake observations (Newmark and Rosenblueth, 1971).

A common approach is to use as prior distributions the natural conjugates of the process. In this case, an examination of the likelihood function in equation 2-7 shows that the following likelihood (the kernel of the probability function) is the natural conjugate of the process:

$$l(\theta) = \lambda_o^{r-1} e^{-u\lambda_o} \beta^{k-1} e^{-s\beta} \quad \text{Eq. (2-10)}$$

where, under the *a priori* Bayesian approach, the expected value of β is k/s and its *CoV* is equal to $1/\sqrt{s}$. On the other hand, the expected value of λ_o is r/u and its *CoV* equal to $1/\sqrt{r}$.

The selected prior is the product of two Gamma distributions. Then, applying Bayes' theorem, the posterior distribution of the unknown parameters is found.

$$l(\theta | \varepsilon) = l(\varepsilon | \theta)l(\theta) = \lambda_o^{N+r-1} e^{-\lambda_o(u + \sum_i \tau_i)} \beta^{N+k-1} e^{-\beta(s + \sum_i (M_i - M_o))} \quad \text{Eq. (2-11)}$$

It is evident that, *a posteriori*, both λ_o and β are Gamma distributed but, more relevant for this explanation, it can be observed that, *a posteriori*, they are independent from each other since the joint posterior likelihood of θ is simply the product of the likelihoods of λ_o and β .

The result is perhaps unexpected for those not familiar with the use of Bayesian methods (now the user can see that the maximum likelihood approach is a particular case of the more general Bayesian method), but it is intuitively correct. It is correct to say that one is estimating λ_o and β with the maximum likelihood method (equations 2-8 and 2-9). Now say that after a first estimation round, one discovers that one of the magnitudes in the sample was wrong. This new information, as can be seen from equations 2-8 and 2-9, would change the estimation of β , but it would not change the estimation of λ_o , which is basically a rate.

Equation 2-11 justifies two important features of R-CRISIS:

1. Treating λ_o and β as independent (provided, of course, that they have been estimated by Bayesian methods or, at least, with the maximum likelihood method);
2. Treating the uncertainty in β assuming that this variable follows a Gamma distribution.

Equation 2-11, by the way, also provides information about the size of the uncertainty in β : *a posteriori*, since its *CoV* is:

$$CoV(\beta) = \frac{1}{\sqrt{(N + k - 1)}} \quad \text{Eq. (2-12)}$$

so, if the prior information is not very large (that is, if $r \ll N$, meaning that the sample size is reasonably large) then its coefficient of variation is of the order of $1/N^{1/2}$.

Now, we will remove the restriction that $M_U \gg M_o$. R-CRISIS estimates the magnitude exceedance rate following a modified G-R relationship, provided by equation 2-3 and for this case, the probability density function of M is the following:

$$p_M(M) = \beta \frac{e^{-\beta(M-M_o)}}{1 - e^{-\beta(M_U-M_o)}} \quad \text{Eq. (2-13)}$$

Replacing equation 2-13 into equation 2-7 and considering that nothing has changed related to the occurrence times, it can be found that:

$$l(\varepsilon | \theta) = \lambda_o^N e^{-\lambda_o \sum_i \tau_i} \beta^N \frac{e^{-\sum_i \beta(M_i - M_o)}}{(1 - e^{-\sum_i \beta(M_U - M_o)})^N} \quad \text{Eq. (2-14)}$$

Now, the maximum likelihood estimators cannot be determined analytically (although, in general, they do not differ by much from those obtained with equations 2-8 and 2-9). But, if

we continue with the Bayesian process, we can find that, although β is not Gamma distributed anymore (although its distribution is not far from a Gamma if M_o and M_U are not close enough), λ_o and β remain independent, *a posteriori*, due to the fact that λ_o is not present in the β -related term of the event likelihood. Because of this, the posterior joint likelihood of θ is again, simply the product of the likelihoods of λ_o and β .

The reason why R-CRISIS disregards uncertainty in λ_o is the following: consider that the basic seismic hazard equation, expressed in terms of intensity exceedance rates (even if a similar analysis could be performed for exceedance probabilities in given time frames), for a single point-source located at distance R from the site of analysis is:

$$\nu(a | \lambda_o, \beta) = \lambda_o \int_{M_o}^{M_U} p_M(M) \cdot \Pr(A > a | M, R) dM \quad \text{Eq. (2-15)}$$

where $\nu(a | \lambda_o, \beta)$ is the exceedance rate of the hazard intensity a given that λ_o and β are known. Replacing equation 2-13 into equation 2-15 we find that:

$$\nu(a | \lambda_o, \beta) = \lambda_o \int_{M_o}^{M_U} \beta \frac{e^{-\beta(M-M_o)}}{1 - e^{-\beta(M_U-M_o)}} \cdot \Pr(A > a | M, R) dM \quad \text{Eq. (2-16)}$$

To remove the conditionality in $\nu(a)$ we integrate with respect to the joint probability density function of the unknown parameters (λ_o and β in this case), which amounts to computing its expected value with respect to them:

$$\nu(a) = \iint \nu(a | \lambda_o, \beta) p_{\beta, \lambda_o}(\beta, \lambda_o) d\beta d\lambda_o \quad \text{Eq. (2-17)}$$

Since it was already established that λ_o and β are independent random variables, it can be said that:

$$\nu(a) = \iint \nu(a | \lambda_o, \beta) p_{\beta}(\beta) p_{\lambda_o}(\lambda_o) d\beta d\lambda_o \quad \text{Eq. (2-18)}$$

and, since the distribution of β does not depend on λ_o , $\nu(a)$ is:

$$\nu(a) = \int \lambda_o p_{\lambda_o}(\lambda_o) d\lambda_o \int_{M_o}^{M_U} \frac{e^{-\beta(M-M_o)}}{1 - e^{-\beta(M_U-M_o)}} \Pr(A > a | M, R) p_{\beta}(\beta) dM d\beta \quad \text{Eq. (2-19)}$$

Therefore,

$$\nu(a) = E(\lambda_o) E_{\beta} \left\{ \int_{M_o}^{M_U} \frac{e^{-\beta(M-M_o)}}{1 - e^{-\beta(M_U-M_o)}} \Pr(A > a | M, R) dM \right\} \quad \text{Eq. (2-20)}$$

where $E_{\beta}(\cdot)$ denotes the expected value with respect to β . It is clear from equation 2-20 that the first probability moment of the exceedance rate (the quantity usually reported as “the” exceedance rate) is insensitive to uncertainty in λ_o but, since $\nu(a)$ depends on the probability distribution assigned to β (we need this distribution to compute the expected value with respect to β), it definitively depends on the uncertainty of β .

In summary, to compute the expected value of the exceedance rates, R-CRISIS solves equation 2-20 for point-sources, generated from the subdivision of the sources originally given by the user (see Section 2.2.1), using a Gamma distribution to describe the uncertainty in β . Since exceedance rates are additive, so are their expected values. Hence, disregarding uncertainty in λ_o for computing the first probability moment of the intensity exceedance rate is rigorously justified.

Note from equation 2-20 that disregarding uncertainty in β would be equivalent to replacing the probability density function assigned to this parameter with the following Dirac’s delta function:

$$p_{\beta}(\beta) = \delta[\beta - E(\beta)] \quad \text{Eq. (2-21)}$$

In that case, equation 2-20 would take the following form:

$$\nu(a) = E(\lambda_o) \int_{M_o}^{M_U} \frac{e^{-E(\beta)(M-M_o)}}{1 - e^{-E(\beta)(M_U-M_o)}} \Pr(A > a | M, R) dM \quad \text{Eq. (2-22)}$$

which is evidently, the classic seismic hazard equation (compare against equation 2-16) when parameters λ_o and β are deterministically equal to their respective expected values. In general, however, equation 2-20 must be considered only a first-order approximation to the true value of the seismic hazard intensity exceedance rate.

Clearly, if higher-order moments of $\nu(a)$ are required, a correct answer could only be obtained by accounting for the uncertainty in λ_o . Anyhow, since R-CRISIS reports only the expected value of the intensity exceedance rates, there is no need to know how uncertain λ_o is.

Note: From R-CRISIS v20, the same methodology to consider uncertainty of the β -value has been maintained but its incorporation into synthetic catalogues has been optimized.

Uncertainty in the maximum magnitude

R-CRISIS regards the maximum magnitude, M_U , as an unknown quantity. It is possible to assign to this variable a uniform probability distribution between M_{U1} and M_{U2} (see Figure 2-

1), which are informed to R-CRISIS in terms of two values: the expected value of M_U , $E(M_U)$, and σM . If $\sigma M < 0.5$, M_U is treated in a deterministic way with a weight concentration equal to 1.0 at $M_U = E(M_U)$. But, if $\sigma M \geq 0.5$, R-CRISIS generates five probability concentrations centered at $E(M_U)$ with a uniform density between M_{U1} and M_{U2} that correspond to the values indicated by equations 2-23 and 2-24.

$$M_{U1} = E(M_U) - \sigma M \tag{Eq. (2-23)}$$

$$M_{U2} = E(M_U) + \sigma M \tag{Eq. (2-24)}$$

Thus, maximum magnitude is considered equally likely for all values between M_{U1} and M_{U2} .

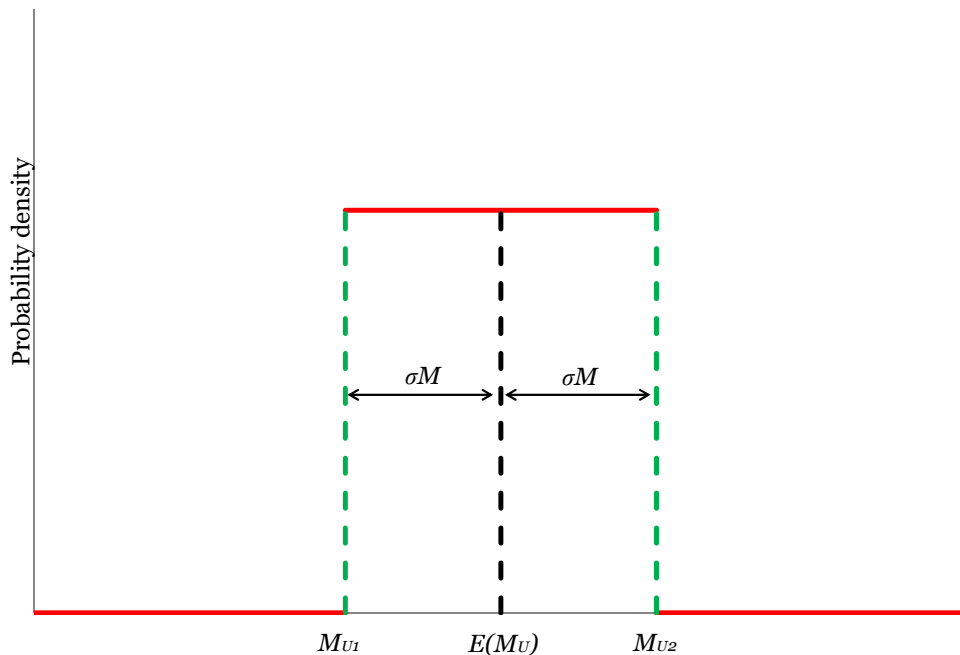


Figure 2-1 Probability density function of the M_U value

2.1.2 Characteristic earthquake model

This seismicity model is also associated to Poissonian occurrences and therefore, the probability of exceeding the intensity level, a , in the next T_f years, given that an earthquake with magnitude M occurred at a distance R from the site, is again given by equation 2-1 with the same considerations and assumptions explained before.

For the Characteristic Earthquake model (Youngs and Coppersmith, 1985) implemented in R-CRISIS, the earthquake magnitude exceedance rate is given by:

$$\lambda(M) = \lambda_o \frac{\Phi\left[\frac{M_U - EM}{s}\right] - \Phi\left[\frac{M - EM}{s}\right]}{\Phi\left[\frac{M_U - EM}{s}\right] - \Phi\left[\frac{M_o - EM}{s}\right]}, M_o \leq M \leq M_U \quad \text{Eq. (2-25)}$$

where $\Phi[\cdot]$ is the standard normal cumulative function and M_o and M_U are the threshold and maximum characteristic magnitudes, respectively; EM and s are, on the other hand, parameters that define the distribution of M .

EM can be interpreted as the expected value of the characteristic earthquake and s as its standard deviation. λ_o is the exceedance rate of magnitude M_o . In addition, a slip-predictable behavior can be modeled assuming that EM grows with the time elapsed since the last characteristic event, T_{oo} , in the following way:

$$E(M) = D + F \ln(T_{oo}) \quad \text{Eq. (2-26)}$$

Note: if F is set to zero, then EM is equal to D , independently of the time elapsed.

2.1.3 Generalized non-Poissonian model

This type of seismicity description allows specifying directly the required probabilities, that is, the probabilities of having 1, 2, ..., N_s earthquakes of given magnitudes, at a given location, during the next T_f years.

This information is provided by the user to R-CRISIS by means of a binary file, with *.nps⁵ extension, which has the structure explained in Tables 2-1 and 2-2.

⁵ Non-Poissonian Seismicity

Table 2-1 Generalized seismicity file structure (part 1)

Generalized seismicity file				
Description	Variable	Type	Length	Comments
Number of point sources	TotSrc	Integer	4	-
Number of magnitude bins	Nbin	Integer	4	-
Number of time frames	Nt	Integer	4	-
Maximum number of events for which Prob(i,j) is given	Ns	Integer	4	-
Magnitude representative of bin 1	M(1)	Double	8	Magnitude values are useful only if parametric attenuation models are used. They are not used in generalized attenuation models
...	
Magnitude representative of bin Nbin	M(Nbin)	Double	8	
Time frame 1	Tf(1)	Double	8	-
...	-
Time frame Nt	Tf(Nt)	Double	8	-
Seismicity record for source 1	Seis(1)	Seismicity record	8+8*Ns*Nt*Nbin	-
Seismicity record for source 2	Seis(2)	Seismicity record	8+8*Ns*Nt*Nbin	-
...	-
Seismicity record for	Seis(TotSrc)	Seismicity record	8+8*Ns*Nt*Nbin	-
source TotSrc				

Table 2-2 Generalized seismicity file structure (part 2)

Seismicity record					
	Variable	Type	Length	Description	
Probability of having 1, 2,...,Ns events of magnitude 1 in time frame 1	Prob(1,1,1)	Double	8	Block associated to Magnitude 1	
	Prob(1,1,2)	Double	8		
	...	-	-		
	Prob(1,1,Ns)	Double	8		
Probability of having 1, 2,...,Ns events of magnitude 1 in time frame 2	Prob(1,2,1)	Double	8		
	Prob(1,2,2)	Double	8		
	...	-	-		
	Prob(1,2,Ns)	Double	8		
...
Probability of having 1, 2,...,Ns events of magnitude 1 in time frame Nt	Prob(1,Nt,1)	Double	8		
	Prob(1,Nt,2)	Double	8		
	...	-	-		
	Prob(1,Nt,Ns)	Double	8		
...	
Probability of having 1, 2,...,Ns events of magnitude Nbin in time frame 1	Prob(Nbin,1,1)	Double	8	Block associated to Magnitude Nbin	
	Prob(Nbin,1,2)	Double	8		
		
	Prob(Nbin,1,Ns)	Double	8		
Probability of having 1, 2,...,Ns events of magnitude Nbin in time frame 2	Prob(Nbin,2,1)	Double	8		
	Prob(Nbin,2,2)	Double	8		
		
	Prob(Nbin,2,Ns)	Double	8		
...
Probability of having 1, 2,...,Ns events of magnitude Nbin in time frame Nt	Prob(Nbin,Nt,1)	Double	8		
	Prob(Nbin,Nt,2)	Double	8		
		
	Prob(Nbin,Nt,Ns)	Double	8		

2.1.4 Generalized Poissonian model

In this option, included in R-CRISIS by suggestion of Dr. Ramón Secanell, seismicity is described by means of a non-parametric characterization of the activity (or occurrence) rates of earthquakes of given magnitudes at one or several seismic sources.

Seismicity information is provided by the user to R-CRISIS in a text file, with *.gps⁶ extension, which has the structure shown in Table 2-3

⁶ Generalized Poissonian Seismicity

Table 2-3 Generalized Poissonian seismicity file structure

Description	Comments
ID Header	A line of text used for identification purposes
NumSources	Number of different sources whose seismicity is described in the file
NumBins	Number of magnitude bins in which the seismicity curve is discretized
Magnitude 1	Central point of magnitude bin 1
Magnitude 2	Central point of magnitude bin 2
....	...
Magnitude NumBins	Central point of magnitude bin NumBins
$\Delta\lambda(1,1)$	Occurrence rate of earthquakes with magnitude 1 in source 1
$\Delta\lambda(2,1)$	Occurrence rate of earthquakes with magnitude 2 in source 1
...	...
$\Delta\lambda(\text{NumBins},1)$	Occurrence rate of earthquakes with magnitude NumBins in source 1
$\Delta\lambda(1,2)$	Occurrence rate of earthquakes with magnitude 1 in source 2
....	...
$\Delta\lambda(\text{NumBins},2)$	Occurrence rate of earthquakes with magnitude NumBins in source 2
...	...
$\Delta\lambda(\text{NumBins},\text{NumSources})$	Occurrence rate of earthquakes with magnitude NumBins in source NumSources

The format of the *.gps file allows for the use of ":" as a separator (i.e. everything written before the separator is ignored by R-CRISIS). Table 2-4 shows an example of a *.gps file, describing the seismicity of four sources using 9 magnitude bins (please recall that everything written before ":" is ignored by R-CRISIS):

Table 2-4 Generalized Poissonian seismicity file example

Example of *.gps file
Four ModifiedGR sources with $M_0=4$, $\mu=8$, $\beta=1$, $\lambda_{d0}=1$
NumSources: 4
NumBins: 9
Magnitude 1: 4.2222
Magnitude 2: 4.6667
Magnitude 3: 5.1111
Magnitude 4: 5.5556
Magnitude 5: 6.0000
Magnitude 6: 6.4444
Magnitude 7: 6.8889
Magnitude 8: 7.3333
Magnitude 9: 7.7778
Source 1 M=4.222222 : 0.5891
Source 1 M=4.666667 : 0.2422
Source 1 M=5.111111 : 0.0996
Source 1 M=5.555555 : 0.0409
Source 1 M=6.000000 : 0.0168
Source 1 M=6.444444 : 0.0069
Source 1 M=6.888888 : 0.0028
Source 1 M=7.333333 : 0.0012
Source 1 M=7.777777 : 0.0004
Source 2 M=4.222222 : 0.5891
Source 2 M=4.666667 : 0.2422
Source 2 M=5.111111 : 0.0996
Source 2 M=5.555555 : 0.0409
Source 2 M=6.000000 : 0.0168
Source 2 M=6.444444 : 0.0069
Source 2 M=6.888888 : 0.0028
Source 2 M=7.333333 : 0.0012
Source 2 M=7.777777 : 0.0004
Source 3 M=4.222222 : 0.5891
Source 3 M=4.666667 : 0.2422
Source 3 M=5.111111 : 0.0996
Source 3 M=5.555555 : 0.0409
Source 3 M=6.000000 : 0.0168
Source 3 M=6.444444 : 0.0069
Source 3 M=6.888888 : 0.0028
Source 3 M=7.333333 : 0.0012
Source 3 M=7.777777 : 0.0004
Source 4 M=4.222222 : 0.5891
Source 4 M=4.666667 : 0.2422
Source 4 M=5.111111 : 0.0996
Source 4 M=5.555555 : 0.0409
Source 4 M=6.000000 : 0.0168
Source 4 M=6.444444 : 0.0069
Source 4 M=6.888888 : 0.0028
Source 4 M=7.333333 : 0.0012
Source 4 M=7.777777 : 0.0004

Note that the values provided by this file are the occurrence rates of earthquakes with magnitudes contained within a magnitude bin. In other words, R-CRISIS expects, for a magnitude bin between M_1 and M_2 , with $M_2 > M_1$, the number of earthquakes, per unit time, that this source generates with magnitudes between M_1 and M_2 . For instance, if these occurrence rates were to be computed from a usual exceedance rate plot, $\lambda(M)$, the occurrence rate of earthquakes in the mentioned magnitude bin corresponds to $\lambda(M_1) - \lambda(M_2)$.

For seismic hazard computation purposes, earthquakes generated in this source will have only the magnitudes given in the file as the central points of the various bins. Therefore, it is the responsibility of the user to give a magnitude discretization that is dense enough (which is a parameter that is user-defined in R-CRISIS).

This option was originally created specifically to be applied with the smoothed seismicity method developed by Woo (1996). Therefore, this option is frequently used to describe the seismicity of numerous point sources whose geometrical properties (e.g., location, rupture planes) are given by means of an *.ssg⁷ file (see Section 2.2.5). In this case, R-CRISIS interprets that each source described in this seismicity file corresponds to a point source described in the *.ssg file.

However, this Generalized Poisson model can be used to describe, in a non-parametric manner, the seismicity of area and/or line sources. For these cases, R-CRISIS will interpret that the occurrence rates provided in the *.gps file are associated to the whole source (area or line), and then, R-CRISIS will uniformly distribute the occurrence rate across or along it, depending if the geometry is described by means of an area or a line.

2.2 Geometry models

R-CRISIS has implemented different geometry models to describe the characteristics of the seismic sources. The available geometry models in R-CRISIS are:

- a) Area sources (where area planes and volumes correspond to particular cases) that are modelled as planes by means of a set of vertexes that account for a three-dimensional representation.
- b) Line sources that are modeled as polylines with constant or variable depths.
- c) Point sources (where grid sources are a particular case).

The following sections provide a complete description of the geometry models implemented in R-CRISIS together with an explanation about how they are treated within the PSHA framework.

Note: within the same seismic hazard project, R-CRISIS allows the combination of different geometry models for different sources.

⁷ SSG stands for: smoothed seismicity geometry

2.2.1 Area sources

When this geometry model is chosen, the seismic sources are modelled as polygons defined by the 3D coordinates for each of their vertexes. Figure 2-2 shows an example consisting of a 3D polygon with 8 vertexes representing a dipping plate, which also has a varying dip angle.

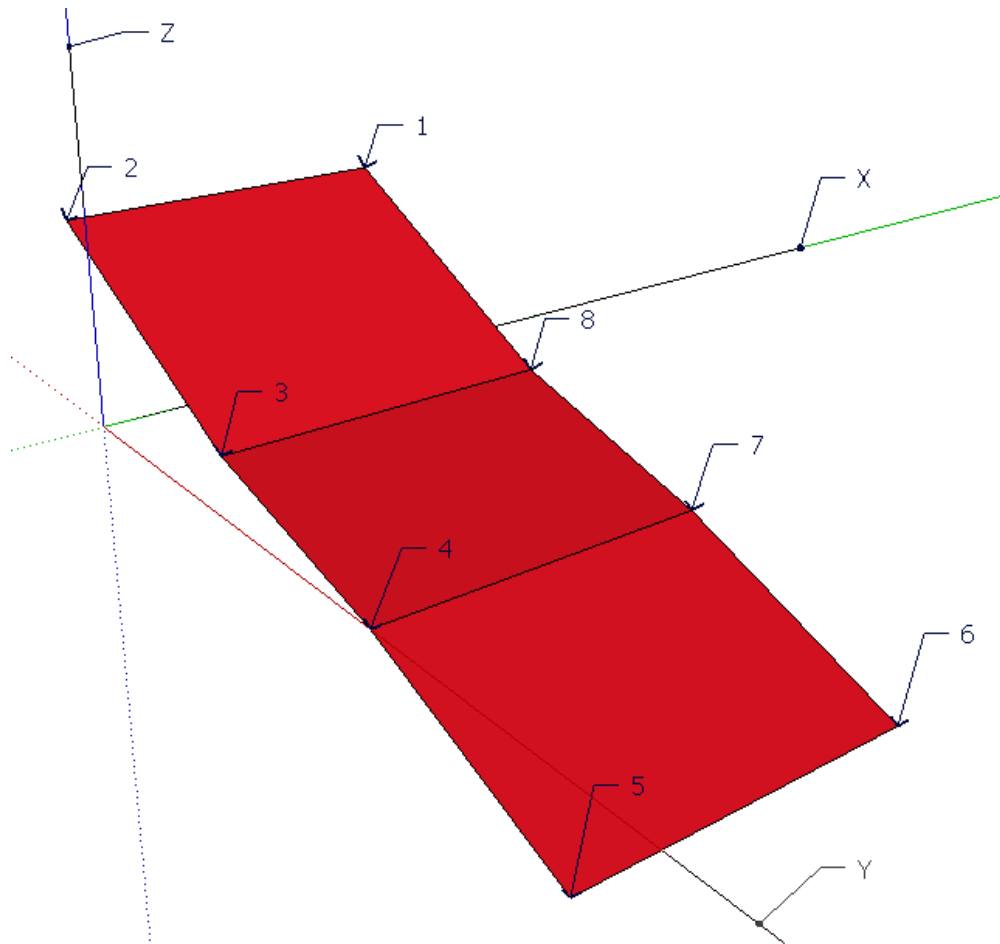


Figure 2-2 Area plane with 8 vertexes

Note: vertical planes are allowed in R-CRISIS.

In the case of area sources, and to perform the spatial integration (see Section 2.6), R-CRISIS divides the polygon into triangles using the routine explained with detail in Annex 1. In summary, R-CRISIS first checks if the triangulation can be made in the XY plane as shown in Figure 2-3 in terms of six triangles of different colors.

Note: the numbering of the vertexes of the area source must be provided in counter-clockwise order when this plane is seen from above the Earth's surface.

In the cases of vertical planes, R-CRISIS will try to triangulate the area in the XZ plane, so for these cases, the numbering of the vertexes must be done counter-clockwise in said plane.

Finally, R-CRISIS will try to perform the triangulation in the YZ plane. It is important to bear in mind that there are some particularly complicated source geometries that cannot be well triangulated by R-CRISIS (e.g. an L-shaped vertical plane) and then for these cases, an error will be reported.

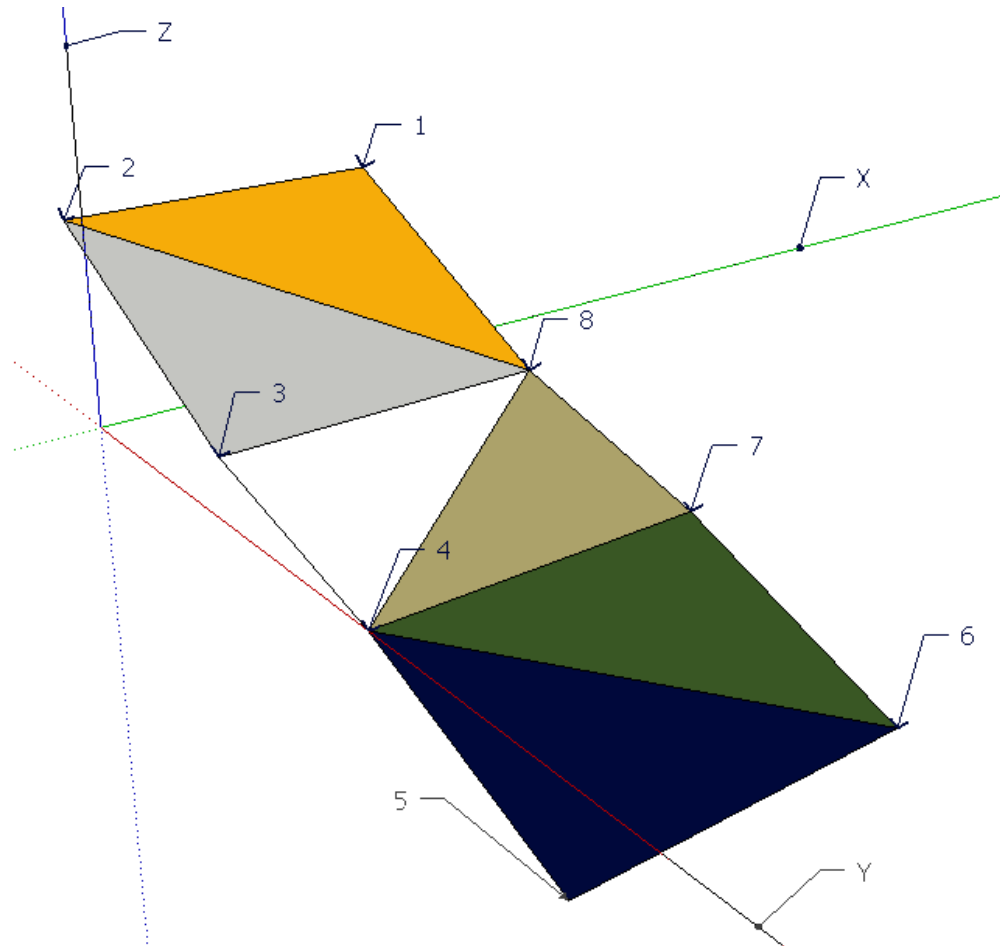


Figure 2-3 Area plane with 8 vertexes and 6 sub-sources

Note: to guarantee a good triangulation process, vertexes used to define the same seismic source cannot be closer than the perimeter of the source/1000000 (in m).

Relation between magnitude and rupture area

In R-CRISIS, attenuation relations (or ground motion prediction equations GMPE) can be specified in terms of 4 different distance measures (see Section 2.3). If R_{RUP} or R_{JB} distances are used, R-CRISIS requires means to know the rupture area (or length), as a function of magnitude, to compute the appropriate values for the distances.

For area and smoothed seismicity (gridded) sources, R-CRISIS initially assumes a circular rupture which radius R (in km) relates with the magnitude M in the following manner:

$$A = \pi R^2 \quad \text{Eq. (2-27)}$$

where:

$$R = K_1 \cdot e^{K_2 M} \quad \text{Eq. (2-28)}$$

and K_1 and K_2 are constants of the relationship between the magnitude and the rupture area.

Equation 2-27 can be rewritten thus as:

$$A = \pi K_1^2 \cdot e^{2K_2 M} \quad \text{Eq. (2-29)}$$

Several regression analyses performed to study the relationship between magnitude and rupture area (i.e. Wells and Coppersmith, 1994) adopt the following regression form:

$$\log A = a + bM \quad \text{Eq. (2-30)}$$

where A is the rupture area, M is the magnitude and a and b are the regression coefficients. If Eq. 2-30 is rewritten as:

$$A = 10^a \cdot 10^{bM} \quad \text{Eq. (2-31)}$$

equations 2-29 and 2-31 end with a similar structure with the following equivalences:

$$\pi K_1^2 = 10^a \quad \text{Eq. (2-32)}$$

$$e^{2K_2} = 10^b \quad \text{Eq. (2-33)}$$

To verify the correctness of the equivalences shown in equations 2-32 and 2-33, in Tables 2-5 to 2-7 the regression coefficients, the R-CRISIS coefficients and the equivalences are shown.

Table 2-5 Wells and Coppersmith (1994) rupture area regression coefficients

Model	a	b
Strike-slip	-3.42	0.90
Reverse	-3.99	0.98
Normal	-2.87	0.82
All	-3.49	0.91

Table 2-6 R-CRISIS rupture area coefficients for the Wells and Coppersmith (1994) model

Model	K_1	K_2
Strike-slip	0.01100	1.03616
Reverse	0.00571	1.12827
Normal	0.02072	0.94406
All	0.01015	1.04768

Table 2-7 Equivalences between R-CRISIS and Wells and Coppersmith (1994) rupture area coefficients

Model	Eq 2-32		Eq 2-33	
	10^a	πK_1^2	10^b	e^{2K_2}
Strike-slip	3.80E-04	3.80E-04	7.943	7.943
Reverse	1.02E-04	1.02E-04	9.550	9.550
Normal	1.35E-03	1.35E-03	6.607	6.607
All	3.24E-04	3.24E-04	8.128	8.128

R-CRISIS has the built-in sets of constants, proposed by well-known authors (Brune, 1970; Singh et al., 1980; Wells and Coppersmith, 1994), as shown in Table 2-8.

Table 2-8 Built-in K_1 and K_2 constants

Model	K_1	K_2
Brune (1970)	0.00381	1.15130
Singh et al. (1980)	0.00564	1.15300
Wells and Coppersmith (1994) - Strike-slip	0.01100	1.03616
Wells and Coppersmith (1994) - Reverse	0.00571	1.12827
Wells and Coppersmith (1994) - Normal	0.02072	0.94406
Wells and Coppersmith (1994) - All	0.01015	1.04768

As shown in Figure 2-4 and considering that at each location earthquakes with different magnitudes are likely to occur, depending on the magnitude the area rupture will change. Each circle in Figure 2-4 corresponds to the area rupture associated to earthquakes, occurring at the same location but with different M .

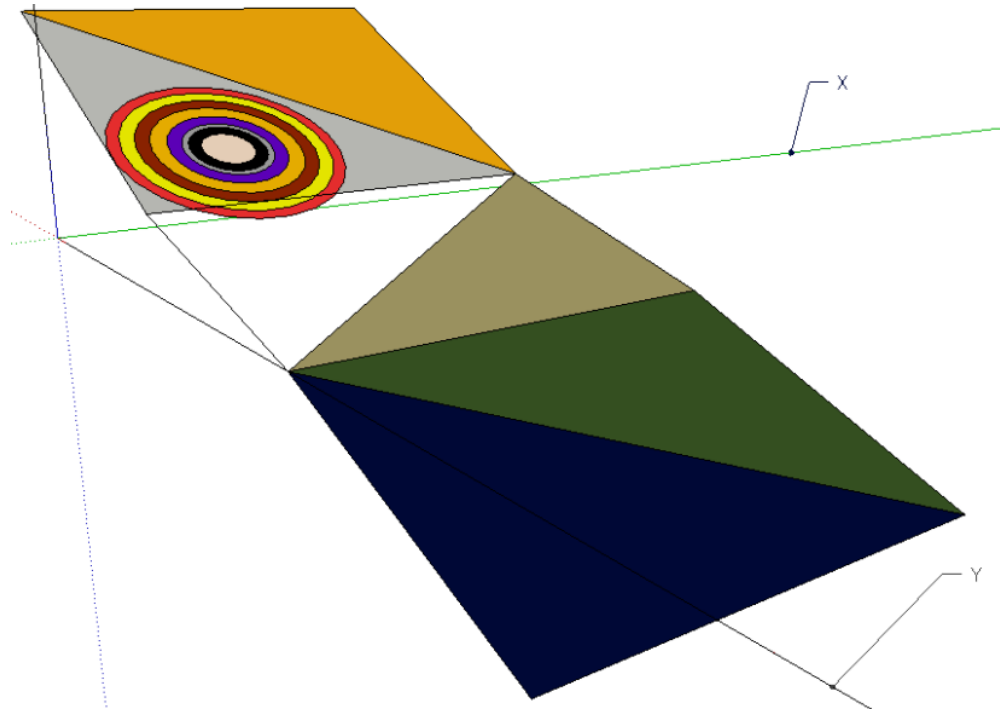


Figure 2-4 Example of in-plane circular fault ruptures in one sub-source of the area source of Figure 2-2

Orientation of the rupture plane

The orientation of the ruptures of the area sources are assigned by means of the values provided to R-CRISIS by the user in the strike field of the GUI. That value is to be provided in degrees. By default, R-CRISIS estimates an initial strike using the angle between vertexes 1 and 2 but this value can be changed by the user at any time.

Behavior options

R-CRISIS implements different models in which the rupture areas are modelled with differences ranging from the aspect ratio to the extent in which the fault can break. The different available options are explained with detail herein.

Normal

This is the default behavior in R-CRISIS for area sources. In general, the rupture areas are circular (i.e. ellipses with aspect ratio equal to 1.0), whose area is related to magnitude through parameters $K1$ and $K2$ as described in equation 2-27. For these cases, the rupture areas are contained in the plane of the source area itself and then, if the source area is a horizontal plane (that is, all its vertexes have the same depth) then the rupture planes will be horizontal whereas if the area source is a vertical plane, then the circles that represent the ruptures will be contained in a vertical plane. If the area geometry is complex (that is, it is a non-planar area), then the rupture plane will be that of the triangle in which the corresponding hypocenter is contained (see Figure 2-4). When this option is selected, it is important to bear in mind that R-CRISIS allows the rupture area to expand outside of the

source area geometry (*leaky boundary*). If this behavior is not considered correct for the modelling purposes, then the behavior option “**treat as fault**” is suggested to be selected.

Treat as fault

The difference between area sources with normal or treat as fault behavior is that, for the latter case, R-CRISIS does not allow rupture areas to extend outside the limits defined by the geometry of the source (*strict boundary*). This difference is relevant only in the cases in which R_{RUP} or R_{JB} are used as distance measures and rupture areas are larger than 0 (i.e. parameters $K1$ and $K2 > 0$).

To be possible in R-CRISIS than an area source is assigned the treat as fault behavior the following conditions must be met:

1. It must have 4 vertexes.
2. All vertexes must roughly be in the same plane (there are tolerances).
3. All internal angles of the polygon must be roughly straight (there are tolerances).

The tolerances for the verification about the vertexes being in the same plane is done by calculating a unit vector of vertex 1 by generating a triangle whose vertexes correspond to number 1, 2 and 4 of Figure 2-5 and then repeating the same calculation now for vertex 3 now generating a triangular plane by using vertexes 2, 3 and 4. The angle is estimated between the two normal vectors and if its difference is smaller than 1.146° , the source is considered as acceptable for the use of this behavior option.

The tolerances for the verification process about straight internal angles are the following; R-CRISIS calculates the values of the four internal angles using the geometry data provided by the user. If all the four internal angles are between 84.26° and 95.74° , the source is considered as acceptable for the use of this behavior option.

In this case the rupture areas will be elliptical with aspect ratio equal to the value provided to R-CRISIS by the user with an area related to magnitude through parameters $K1$ and $K2$. The aspect ratio, Ar is defined as:

$$Ar = \frac{Dx}{Dy} \tag{Eq. (2-34)}$$

where Dx is the dimension of the fault in the X direction and Dy is the dimension of the fault in the Y direction. It must be recalled that, when the treat as fault behavior option is selected, the area source must have exactly four vertexes that form a rectangle that lies in a single plane. By definition, the X direction is the one that joins vertexes 1 and 2 of the area source, while the Y direction is the one that joins vertexes 2 and 3 as shown in Figure 2-5.

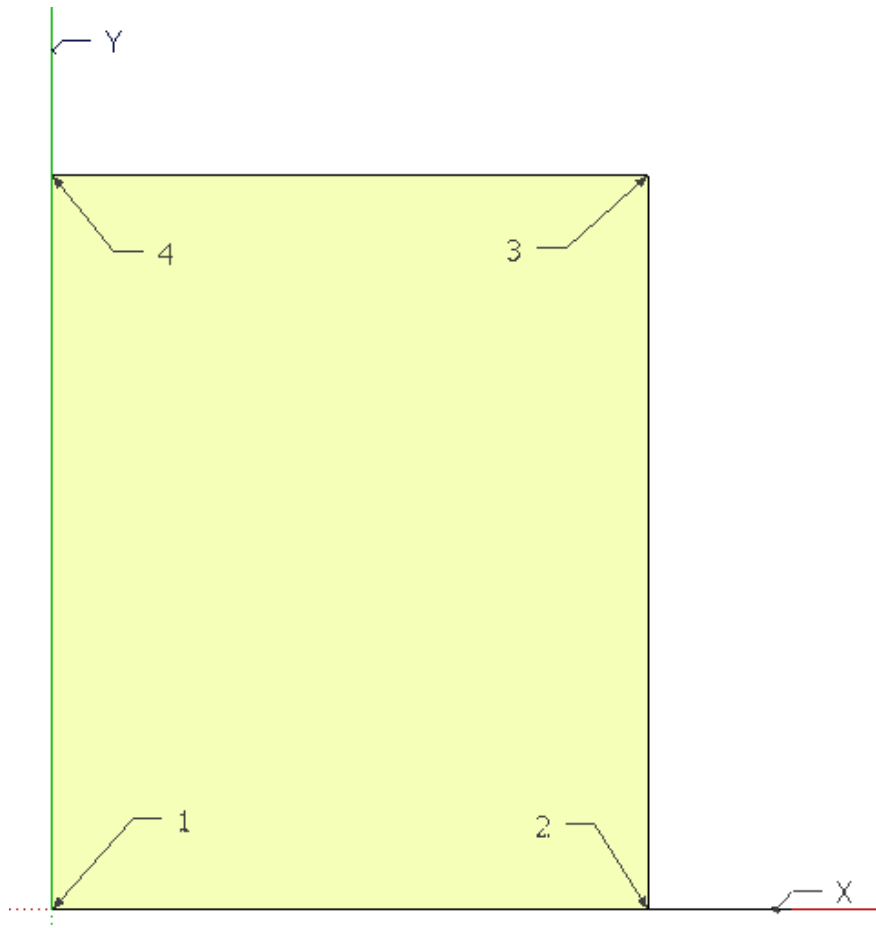


Figure 2-5 Definition of an area source with the treat as fault behavior option

Elliptical ruptures are constructed with the aspect ratio indicated by the user until they do not fit in the rectangular area of the source with that aspect ratio to accommodate the largest possible rupture area. When this situation is reached, R-CRISIS has a smooth transition between the aspect ratio given by the user and the rectangular area source aspect ratio (i.e. width/length). In other words, for small magnitudes, rectangular ruptures start having the aspect ratio indicated by the user, but the aspect ratio might change as magnitude increases, approaching smoothly the rectangular area aspect ratio width/length. Note that this issue slightly can affect the estimation of R_{RUP} and R_{JB} distances for relatively large earthquakes.

Note: An area source with treat as fault behavior is equivalent to a source modelled as a rectangular fault.

Breaks always

When this behavior option is selected, at the source, regardless of the magnitude, the area will break completely for each earthquake. This option is normally used for earthquakes which, by hypothesis, will completely fill up the rupture area, regardless their magnitudes. In view of this, there is only one hypocenter associated to the area. This hypocenter is the point

within the source closest to the computation site. Again, this is only relevant when R_{RUP} or R_{JB} are being used as distance measures.

Note: in this case, the values of $K1$ and $K2$ coefficients provided to R-CRISIS become irrelevant.

Leaky and strict boundaries

As mentioned before, depending on the selection of the behavior for the seismic sources, it is possible to allow the ruptures to extend beyond its boundaries or be always within the plane. The first case is known as leaky boundary and epicenters can occur at the edges of the sources as shown in Figure 2-6. In this case, L corresponds to Dx whereas W corresponds to Dy .

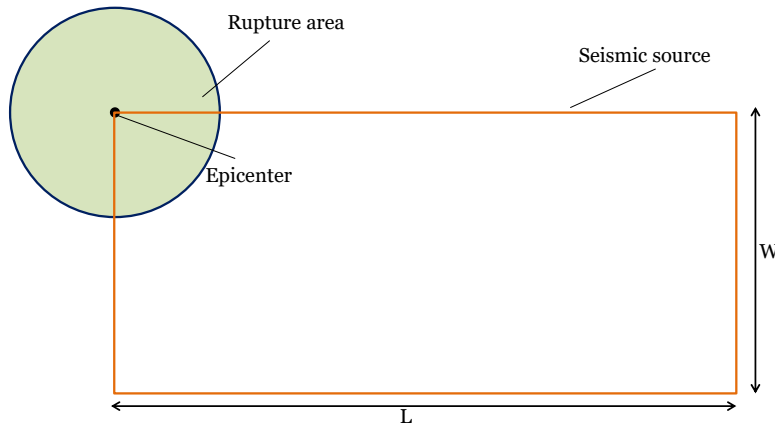


Figure 2-6 Schematic representation of the leaky boundary behavior

In the second case, known as strict boundary, the geometry of the rupture is not allowed to extend beyond the geometric limits of the source and then, depending on the size of the rupture, the location of the epicenter is adjusted so that the totality of the rupture can be accommodated within the plane as shown in Figure 2-7. In this case, L corresponds to Dx whereas W corresponds to Dy .

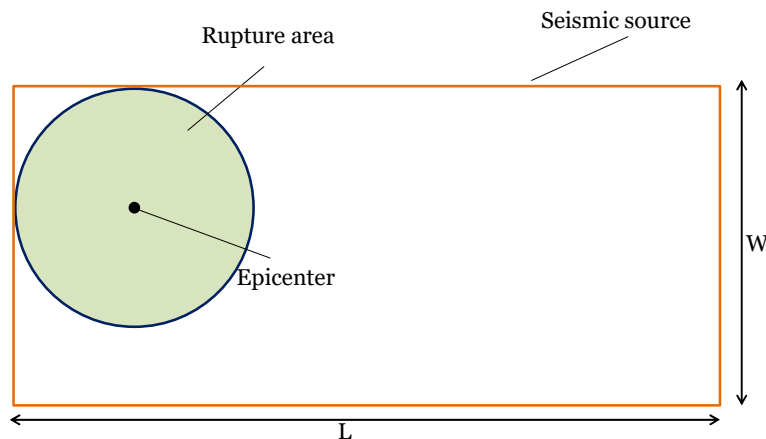


Figure 2-7 Schematic representation of the strict boundary behavior

2.2.2 Area plane sources

This geometry model considers the active source in the same way as an area source, explained before, with the differences that for this case the rupture planes can have an orientation defined by the user. They are different from the common area sources because in said geometry model the ruptures are planes formed by the area itself, whereas in this geometry model, the rupture planes have a constant orientation provided to R-CRISIS by the user. The geometry of the source (plane coordinates and depth) is defined in the same way as in the area case.

Orientation of the rupture plane

The orientation of the rupture planes of the area plane sources are assigned by means of the values provided to R-CRISIS by the user for the strike (in degrees) and the dip (in degrees). Figure 2-8 shows three examples with the same strike and different dip values, as understood by R-CRISIS (values in parenthesis indicate the normal vectors associated to the different orientations).

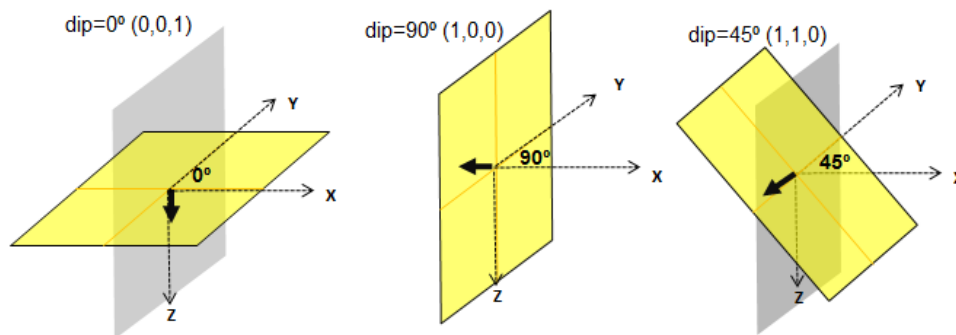


Figure 2-8 Example of dip values to orientate the rupture planes in R-CRISIS

Size of the rupture

A magnitude-dependent size of the rupture plane can be assigned using parameters $K1$ and $K2$. This choice is, again, relevant only in the cases in which R_{RUP} or R_{JB} are used as distance measures. The way in which R-CRISIS recognizes those values associated to the size of the rupture is the same as explained for the case of the area sources. Figure 2-9 shows schematically how, at one sub-source, rupture areas associated to different M values are considered when this geometry model is used. The grey plane corresponds to the area source whereas the yellow plane corresponds to the orientation of the rupture provided by the user by means of the unit vector.

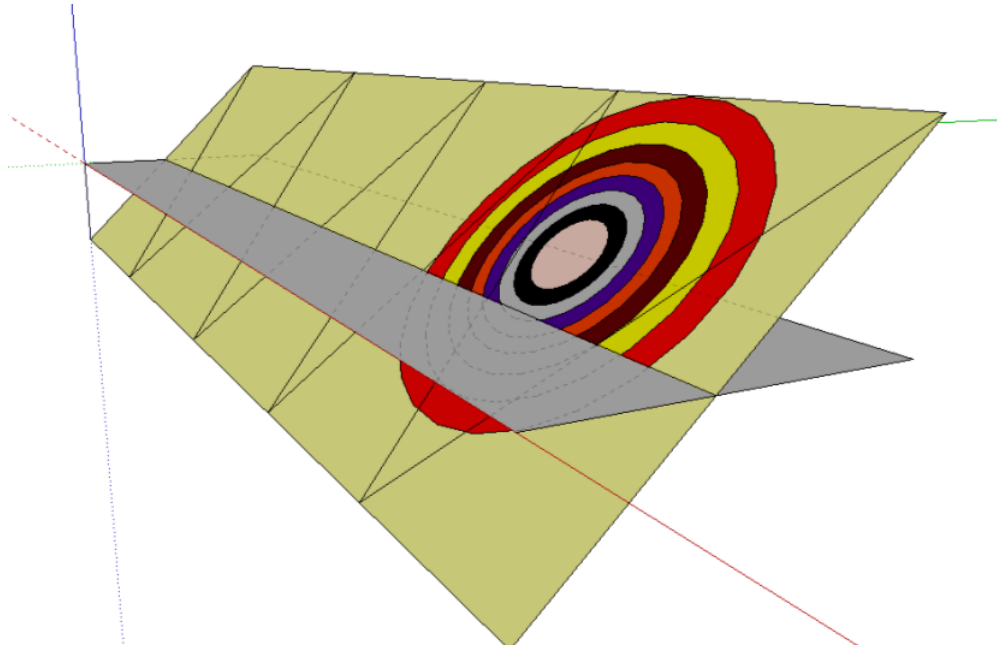


Figure 2-9 Illustration of oriented circular ruptures in an horizontal area source

Aspect ratio

The same approach as in the case of area sources is followed. Dx is understood by R-CRISIS in the direction of the strike whereas Dy in the direction of the dip.

2.2.3 Volume sources

In R-CRISIS the seismic sources can be treated as volumes by first defining the geometry of an area source and then setting the thickness of the volume and the number of slices in which the seismicity is to be distributed. This means that the volume source is modelled by N area sources (slices), all with the same coordinates but located at different depths as shown in Figure 2-10. The yellow polygon represents the original area source and the grey polygons represent the additional slices that comprise the volume area. In this case, the seismicity is evenly divided among the N slices (4 in the case of Figure 2-10). The option is intended to simulate an even distribution of seismicity with depth.

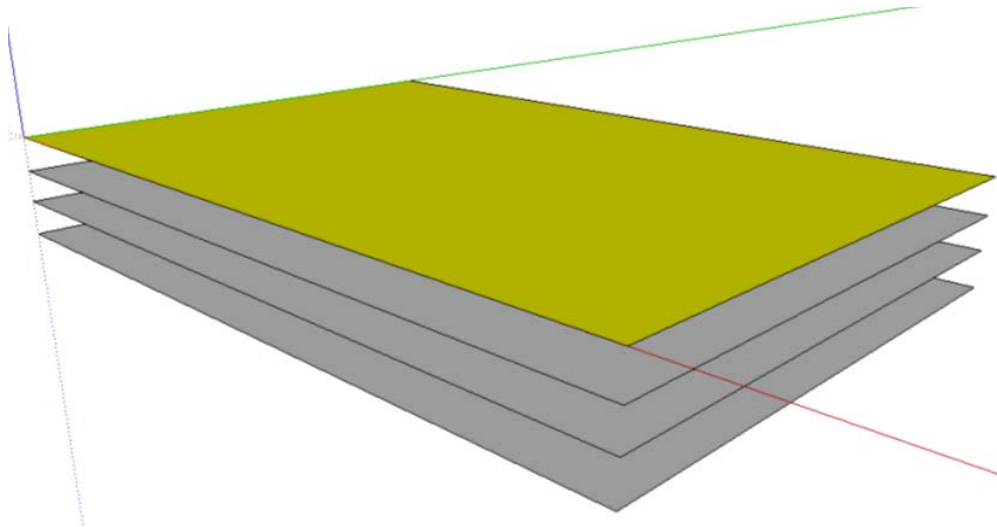


Figure 2-10 Volume sources in R-CRISIS

The seismicity models to be used when this geometric representation is chosen are the modified G-R, the characteristic earthquake, the generalized Poisson and the generalized non-Poisson. In all cases, the seismicity rates (λ) are uniformly distributed into the N slices. That is, each slice has a seismicity rate equal to λ/N but located at a different depth.

Note: if $N=1$, the source will be considered by R-CRISIS as an area source.

2.2.4 Line sources

This geometry model allows defining the active source as a fault (line) source. Line sources are, in general, polylines defined by the 3D coordinates of their vertexes. Figure 2-11 shows a fault source of 4 vertexes, located in the XZ plane with varying depth.

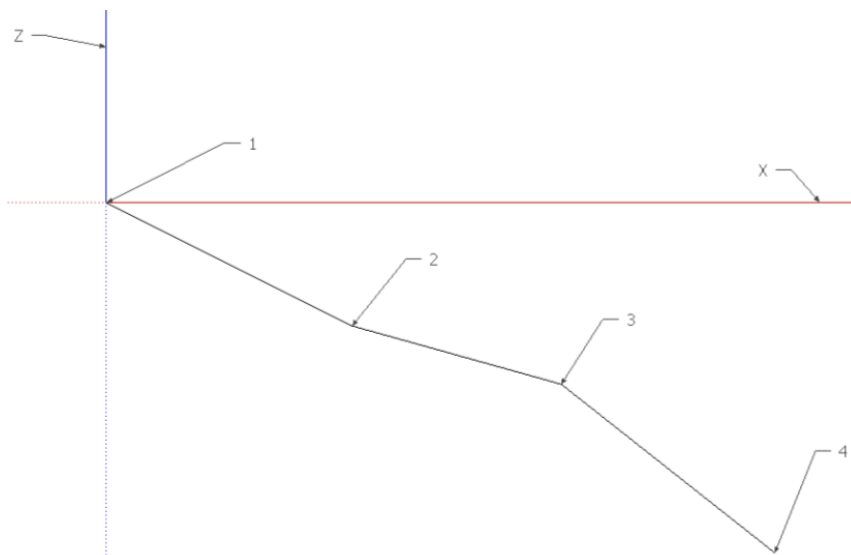


Figure 2-11 Example of a fault area with varying depth and 4 vertexes



Note: the “break always” behavior option for line sources works exactly in the same way as in the case of area sources.

Relation between magnitude and rupture length

For line sources, R-CRISIS relates the rupture length, L , to the magnitude M , for surface rupture length (SLR) and subsurface rupture length (SSLR) by means of:

$$L = K_3 \cdot e^{K_4 M} \tag{Eq. (2-35)}$$

where L is in km and K_3 and K_4 are coefficients that relate the magnitude with the length of the rupture. For instance, the regression form proposed by Wells and Coppersmith (1994) has the following form:

$$\log L = a + bM \tag{Eq. (2-36)}$$

Equation 2-36 can be rewritten as:

$$L = 10^a \cdot 10^{bM} \tag{Eq. (2-37)}$$

As in the case of the area sources, equations 2-35 and 2-37 have a similar structure that allows the following equivalences:

$$K_3 = 10^a \tag{Eq. (2-38)}$$

$$e^{K_4} = 10^b \tag{Eq. (2-39)}$$

Tables 2-9 to 2-11 show the regression coefficients, the R-CRISIS coefficients and the equivalences for the Wells and Coppersmith (1994) model.

Table 2-9 Wells and Coppersmith (1994) SRL and SSLR rupture length regression coefficients

Model	a	b
Strike-slip (SLR)	-3.55	0.74
Reverse (SLR)	-2.86	0.63
Normal (SLR)	-2.01	0.50
All (SLR)	-3.22	0.69
Strike-slip (SSLR)	-2.57	0.62
Reverse (SSLR)	-2.42	0.58
Normal (SSLR)	-1.88	0.50
All (SSLR)	-2.44	0.59

Table 2-10 R-CRISIS SRL and SSRL rupture length coefficients for the Wells and Coppersmith (1994) model

Model	K_3	K_4
Surface Rupture Length (SLR) - Strike-slip	0.00028	1.70391
Surface Rupture Length (SLR) - Reverse	0.00138	1.45063
Surface Rupture Length (SLR) - Normal	0.00977	1.15129
Surface Rupture Length (SLR) - All	0.00060	1.58878
Subsurface Rupture Length (SSLR) - Strike-slip	0.00269	1.42760
Subsurface Rupture Length (SSLR) - Reverse	0.00380	1.33550
Subsurface Rupture Length (SSLR) - Normal	0.01318	1.15129

Table 2-11 Equivalences between Wells and Coppersmith (1994) and R-CRISIS coefficients for SLR and SSLR

Model	Eq 2-38		Eq 2-39	
	10^a	K_3	10^b	e^{K_4}
Strike-slip (SLR)	2.82E-04	2.80E-04	5.495	5.495
Reverse (SLR)	1.38E-03	1.38E-03	4.266	4.266
Normal (SLR)	9.77E-03	9.77E-03	3.162	3.162
All (SLR)	6.03E-04	6.00E-04	4.898	4.898
Strike-slip (SSLR)	2.69E-03	2.69E-03	4.169	4.169
Reverse (SSLR)	3.80E-03	3.80E-03	3.802	3.802
Normal (SSLR)	1.32E-02	1.32E-02	3.162	3.162
All (SSLR)	3.63E-03	3.63E-03	3.890	3.890

In the case of line sources, R-CRISIS assumes that the earthquakes occur along a line defined by the source geometry, and that the rupture length will be centered at the hypocenter as shown in Figure 2-12.

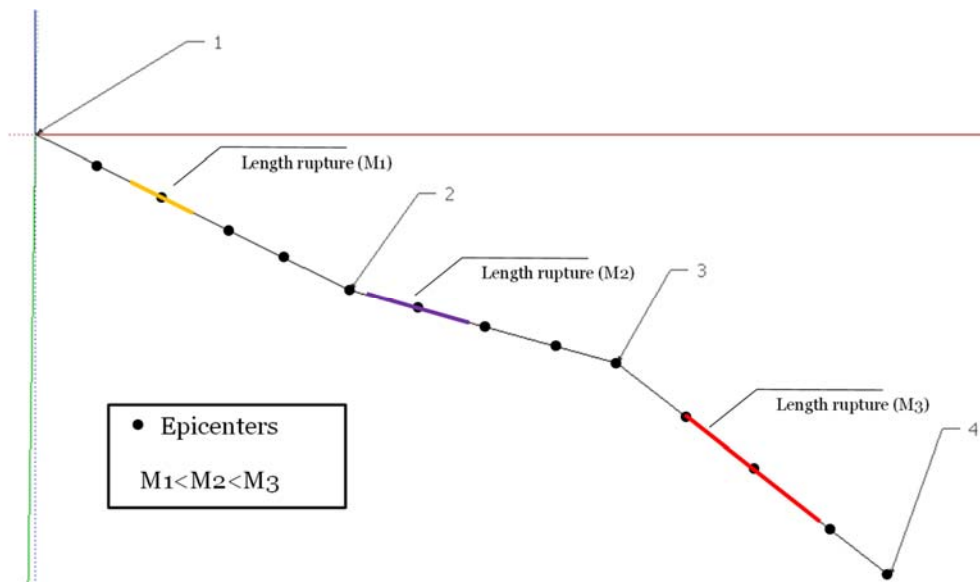


Figure 2-12 Example of fault ruptures in a line source

2.2.5 Point sources

This option defines the active source as a collection of point sources, in which each vertex is assumed to be in R-CRISIS an individual point source. Each point is a potential earthquake hypocenter and is defined by means of the following parameters:

1. Longitude, latitude and depth (in km) of the point.
2. A unit vector normal to the rupture plane associated to each point source. This unit vector is relevant only when the GMPE associated to this source uses distance measures for which the rupture areas are relevant (i.e. R_{RUP} or R_{JB}).

Since point sources are generally used to geometrically describe potentially thousands of focal locations, information about this type of source is provided by the user to R-CRISIS by means of an ASCII file with extension *.ssg, with the structure shown in Table 2-12.

Table 2-12 Point geometry file structure

Point geometry file		
Description	Variable	Type
ID Header	Header	String
Number of point sources	TotSrc	Integer
Geometry record for source 1	Geom(1)	Geometry record
Geometry record for source 2	Geom(2)	Geometry record
....
Geometry record for source TotSrc	Geom(TotSrc)	Geometry record

Table 2-13 on the other hand describes the structure of a geometry record.

Table 2-13 Geometry record file structure

Geometry record		
Description	Variable	Type
Hypocentral location	h.X	in degrees
	h.Y	in degrees
	h.Z	in km (positive)
Unit vector describing the orientation of the fault plane	e1.x	These three values describe a unit vector normal to the fault plane. X is longitude, Y is latitude and Z is depth
	e1.y	
	e1.z	

Finally, Table 2-14 shows an example of a point-source geometry file, where N point sources are geometrically described:

Table 2-14 Point-source geometry file example

Line in file	Comment
Header	Header line for identification purposes
N	Number of points described
Long1 Lat1 Dep1 0 0 0	Each line provides the longitude, latitude and depth for the N point sources. In tis case the coordinates of the unit vector normal to the fault plane is 0,0,0 which means that they are unknown or irrelevant. Those are relevant for instance if an attenuation model based on focal distance is to be used. If the unit vector normal to the fault plane is described with (0,0,0) a horizontal plane will be default
Long2 Lat2 Dep2 0 0 0	
....	
....	
....	
....	
....	
....	
LongN LatN DepN 0 0 0	

As explained in the case of area sources, the relation between the magnitude and the rupture area size depends on M and the $K1$ and $K2$ parameters and for this geometry model is treated in the same way than for the area sources in R-CRISIS.

One special case of point sources corresponds to the use of a stochastic event catalogue (SEC) that is to be arranged in *.csv format with the following fields:

- ID (string value)
- Rupture area (in km²)
- Annual probability
- Magnitude
- Strike
- Dip
- Rake
- Longitude
- Latitude
- Depth
- Aspect ratio

The strike angle is measured in the same way as the azimuth; the dip angle is measured in clockwise order with reference to the strike angle. The dip angle is always \leq than 90° (if a higher angle is required, it needs to be modified by 180°). The length of the rupture, L , is measured in the strike direction whereas its width, W , is measured in the dip (down-dip) direction. Aspect ratio is therefore, equal to L/W .

Note: each SEC is treated in R-CRISIS as a source so the same GMPE will be used for all events included in it.

2.2.6 Gridded sources

This option defines the active source as a collection of point sources located at the nodes of a rectangular grid that is parallel to the surface of the Earth (i.e. a grid in which all the nodes have the same depth). Each one of the nodes is considered in R-CRISIS as a potential

hypocenter. The nodes of the grid are the only hypocenters that R-CRISIS will consider in the calculations as point sources. If the grid is not sufficiently dense, the modelled sources may be too far apart and may not be suitable for performing a good PSHA.

The grid is defined by the parameters shown in Table 2-15 which construct it in the way the grid shown in Figure 2-13.

Table 2-15 Required parameters for the definition of a grid source

Description	Longitude	Latitude
Origin (Usually the SW corner)	Xmin	Ymin
End (Usually the NE corner)	Xmax	Ymax
Number of lines in each orthogonal direction	N	M

After this, the total number of nodes in the grid is equal to $N * M$.

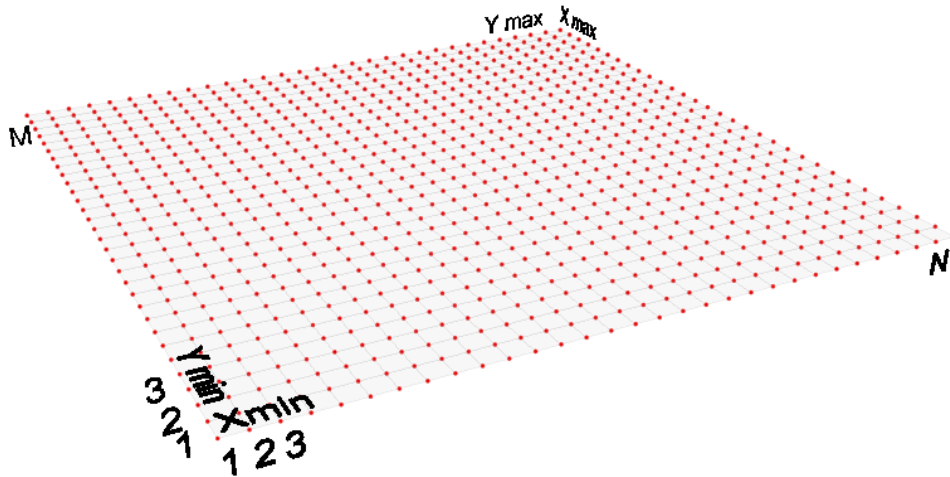


Figure 2-13 Basic grid parameters

The seismicity model that can be used together with this geometry model is the modified G-R where it is considered that M_o is constant across the seismic province but λ_o , β and M_U can have geographical variations defined by means of separate grids, one for each of these parameters. The values of those parameters are provided to R-CRISIS through 3 different files with *.grd format (Surfer 6 ASCII or binary). Figure 2-14 shows a schematic representation of the structure of this model. Those denoted as Lo.grd, EB.grd and MU.grd correspond to the λ_o , β and M_U grids.

Note: the uniform depth of the seismicity grid is provided to R-CRISIS in kilometers.

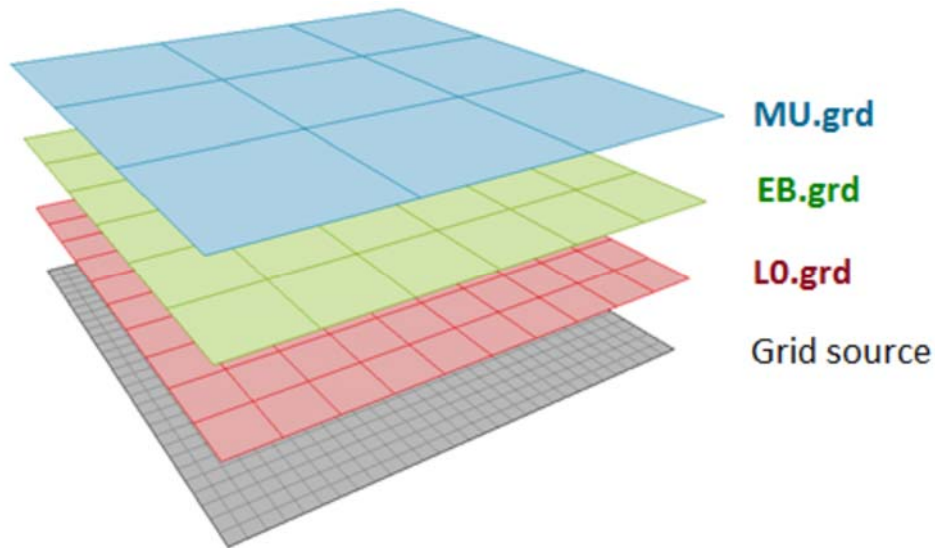


Figure 2-14 Seismicity parameters structure for the gridded geometric model

Note: the limits (Xmin, Xmax, Ymin and Ymax) of each seismicity parameters' grid must coincide with the ones of the source geometry grid but the number of rows and columns in them can be equal or smaller than those of the seismicity grid. Even more, the number of rows and columns may be different for the three seismicity parameters.

The relation between the magnitude and the rupture area size again depends on M and the $K1$ and $K2$ parameters. For the gridded geometry model, those are treated in the same way than for the area sources in R-CRISIS.

Delimitation polygon (optional)

The grid can be delimited by a polygon or group of polygons provided in Shapefile *.shp format as schematically shown in Figure 2-15. Only the grid nodes that lie within at least one of the polygons will be considered active point sources.

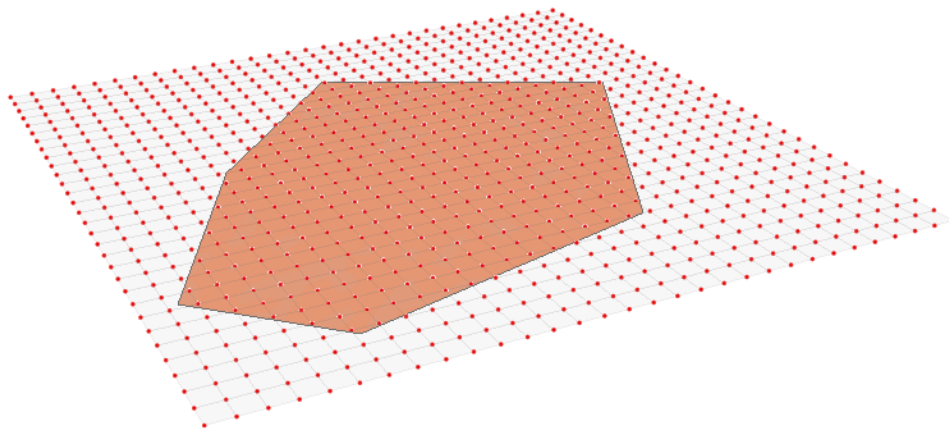


Figure 2-15 Schematic representation of a delimitation polygon

Orientation of rupture plane (optional)

The orientation of the rupture planes can be provided for the grid sources to R-CRISIS by defining normal vectors as schematically shown in Figure 2-16. For this geometry model, these vectors are provided to R-CRISIS by means of three grids that contain the X, Y and Z values, respectively, of the unit vectors that define the plane orientations. These files must be in *.grd format (either Surfer 6 ASCII or Surfer 6 Binary formats) and have the same resolution for the X, Y and Z values than the gridded seismic source.

The names of these files are fixed and are as follows:

- NormalVector_X.grd
- NormalVector_Y.grd
- NormalVector_Z.grd

The path of the folder containing these files must be provided to R-CRISIS. If normal vector grids are not provided to R-CRISIS, horizontal rupture planes (dip=0°) are assumed. Normal vector grids must have the same origin, end and spacing than the main source grid:

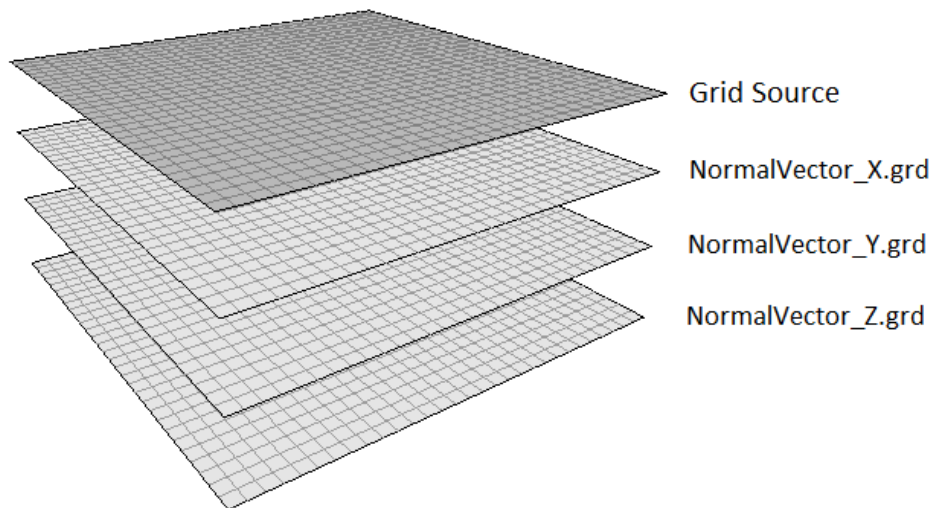


Figure 2-16 Structure of input data to define the orientation of ruptures in the gridded model

The inclusion of normal vector grids is relevant only in the cases in which R_{RUP} or R_{JB} are used as distance measures in the attenuation relations and also in those cases where rupture areas are different from 0 (i.e. parameters $K1$ and $K2 > 0$).

2.2.7 Rectangular faults

This geometry defines a rectangle in which hypocenters can take place, without allowing rupture areas to be partially out of the rectangle (*strict boundary*). This rectangle is a common model for an earthquake fault and it is defined by the following parameters:

Upper lip or fault trace

This line, defined by at least two points, describes the projection of trace of the fault on the Earth's surface. The distance between the two points that form the strike line is the length of the fault, and the angle they form defines its strike. Both points of the strike line must have the same depth, which marks the beginning of the seismogenic zone as shown in Figure 2-17.

Width

This parameter defines the dimension of the fault in the direction perpendicular to the strike line, as shown in Figure 2-17.

Dip

This value defines the dip angle (in degrees) of the fault. This angle must be between 0° (horizontal fault) and 90° (a vertical fault as in Figure 2-17). Negative dip values are not accepted by R-CRISIS and therefore, if required, the strike must be modified by 180° .

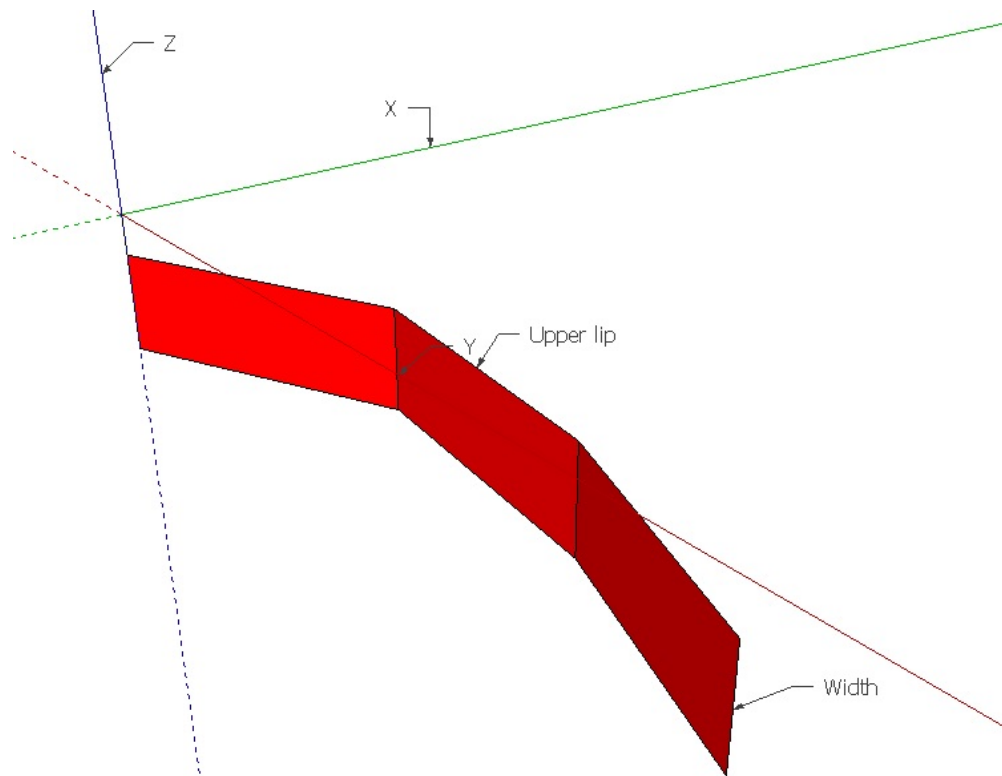


Figure 2-17 Example of a rectangular fault with dip equal to 90°

Note: $K1$ and $K2$ parameters as well as the fault aspect ratio are defined in the same way as in the case of area sources described before.

Stirling fault

There are several possibilities to resolve the geometry of the lower lip of a bending fault. If this option is selected, then the fault will be considered an Stirling fault, in which the upper lip and the average dip are used to create a corrugated surface by translating the upper lip down dip, perpendicular to the average fault strike. If this option is not selected, then the fault is treated as a Frankel fault, where the dip direction of each rectangle is perpendicular to the strike of its local segment. For relatively smooth bending, there is little difference between both types of fault.

2.2.8 Slab geometries

This geometry model can be used to represent in-slab sources where, instead of using the area geometry model and assuming that the ruptures are points occurring within the plane defined by the user, using the geometry of the top end of the slab a set of rectangular faults are generated and ruptures therefore occur on them.

This geometry generates a seismogenetic source from a polygon that needs to have the nodes defined in the way shown in grey in Figure 2-18. Segment 1-2 corresponds to the upper lip of the slab whereas segment 3-4 corresponds to its lower lip. The depth (in km) of nodes 1 and 2 needs to be equal and the same condition holds for the depth of nodes 3 and 4. With these input data, a set of rectangular faults (blue) is generated, as shown in Figure 2-18 after defining 3 slices (rectangular faults).

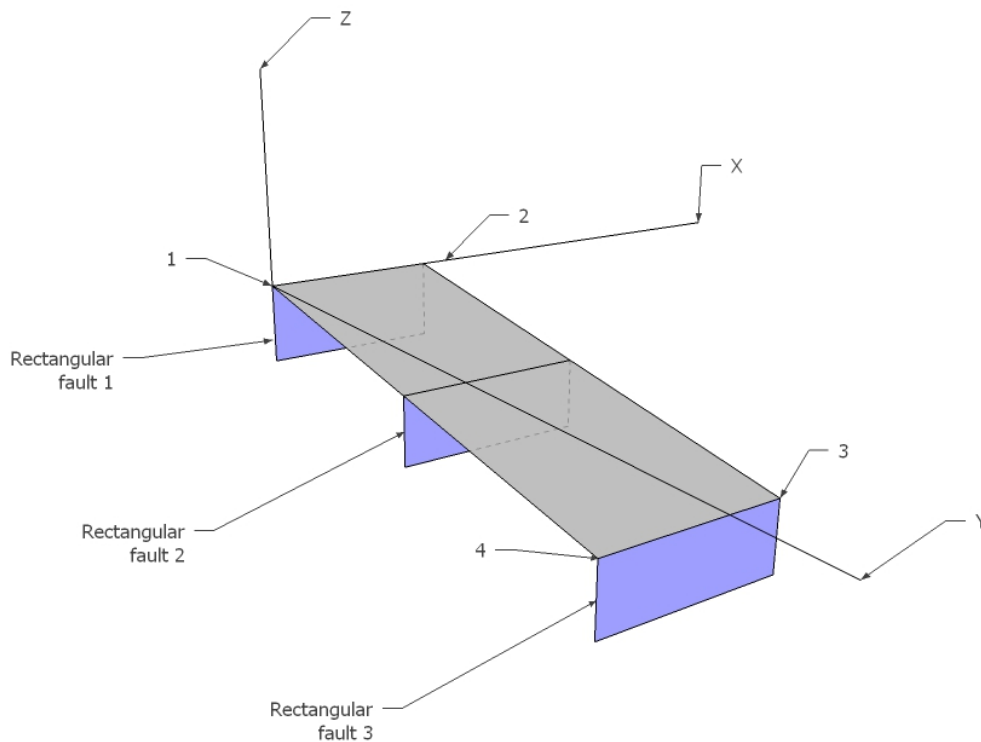


Figure 2-18 Illustration of slab geometry model in R-CRISIS

Additionally, the following parameters need to be defined by the user:

Dip

This line, defined by two points, describes the projection of trace of the fault on the Earth's surface. The distance between the two points that form the strike line is the length of the fault, and the angle they form defines its strike. The same dip applies to all rectangular faults in which the slab is divided.

Width

This parameter defines the dimension of the fault in the direction perpendicular to the strike line. The same width applies to all rectangular faults in which the slab is divided.

Note: If the dip is set to 90° , the width would correspond then to the thickness of the slab.

Rectangular ruptures

This parameter indicates if the ruptures will be considered as rectangular (true) or elliptical (false). The same choice applies to all rectangular faults in which the slab is divided.

Note: $K1$ and $K2$ parameters as well as the fault aspect ratio are defined in the same way as in the case of area sources described before.

2.2.9 Ruptures

In R-CRISIS it is also possible to describe the occurrence of future earthquakes by means of ruptures for which several characteristics, as explained herein, are defined. This is an approach that can be also used for validation purposes if only a historical catalogue is used.

Each rupture needs to have assigned information about the following parameters:

- Date (DD/MM/YY)
- Area (Km²)
- Annual occurrence probability
- Magnitude
- Strike
- Dip
- Rake
- Longitude (Decimal degrees)
- Latitude (Decimal degrees)
- Depth (Km)
- Aspect ratio



The information for each set of ruptures needs to be provided in terms of a *.csv file. Each *.csv file is considered by R-CRISIS as a seismic source for which a GMPE needs to be assigned.

2.3 Measuring distances in R-CRISIS

Distances in R-CRISIS are estimated using the coordinate system known as World Geodetic System 84 (WGS84) that allows locating any site within the Globe by means of three values. To facilitate the use of R-CRISIS in different locations, this coordinates system has been selected since it is the only one that is used and valid at global level. The geometry of the sources as well as the location of the computation sites are provided to R-CRISIS using decimal degrees and those distances are converted to kilometers using by assuming that the Earth is a sphere with radius equal to 6366.707 km. This distance corresponds to the average value of the major and semi-minor axis of the WGS84 datum (Department of Defense, 1997).

In R-CRISIS, there are four ways of measuring site-to-source distances:

1. Focal distance (R_F)
2. Epicentral distance (R_{EPI})
3. Joyner and Boore distance (closest distance to the projection of the fault plane on the Earth's surface; R_{JB})
4. Closest distance to rupture area (R_{RUP})

Figure 2-19 illustrates the differences between the measure distances recognized by R-CRISIS considering that H corresponds to the focal depth.

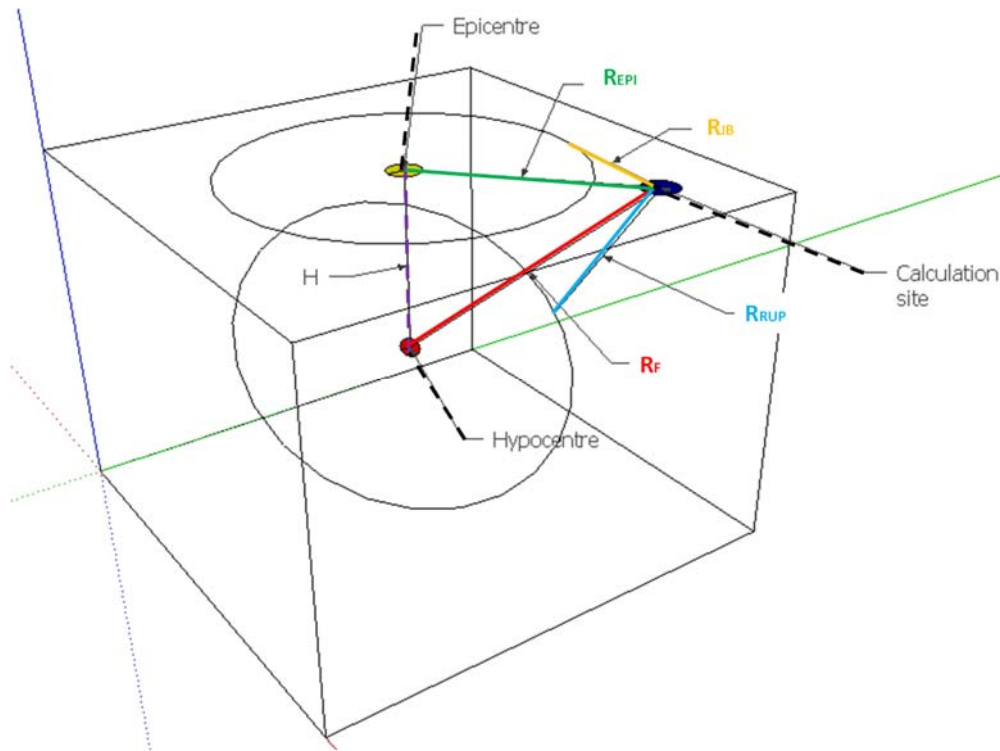


Figure 2-19 Distance measures implemented in R-CRISIS

Computation of R_F and R_{EPI} deserves no further comments but, computation of R_{RUP} and R_{JB} , however, requires the specification of a rupture area (or length). In R-CRISIS, as explained before, the area is assumed to be circular, with radius r , which depends on magnitude M together with the $K1$ and $K2$ parameters. The circular rupture is contained in the plane defined by the triangle resulting from source subdivision (see Section 2.6.1), whose centroid is assumed to be the hypocentral location (see Figure 2-4).

Note: if the site is within the projection of the fault in the Earth’s surface, $R_{JB}=0$ and $R_{RUP}=H$.

The user must indicate R-CRISIS what type of distance is to be used within the PSHA, which in most cases depends on the characteristics of the GMPE being used. For elliptical and rectangular ruptures, R_{RUP} and R_{JB} are computed in an exact and rigorous manner within the distances of interest between the rupture and each calculation site. When the ratio between the rupture radius and R_F or R_{JB} is smaller than 0.025, R-CRISIS performs the following approximation: $R_{RUP}=R_F$ or $R_{JB}=R_{EPI}$. This approximation has little, if any implications, in the final results, even for large magnitudes.

2.4 Strong ground motion attenuation models

In general, ground motion prediction equations (GMPE), also referred to as attenuation relations, establish probabilistic relations between earthquake characteristics, intensities and distances at the computation sites. These relations are probabilistic since, for given earthquake characteristics, the intensities are regarded as random variables whose probability distribution is completely fixed by the GMPE. In most of the cases this means that



at least the first two probability moments (e.g. the median and the standard deviation of the natural logarithm in the lognormal case) of the probability distribution must be defined for the GMPE. R-CRISIS recognizes three different "families" of GMPE (i.e. the way in which those are included in the seismic hazard analysis project):

1. **GMPE tables:** In these tables, relations between earthquake characteristics and intensities at a site are given in terms of the following parameters: magnitude, structural period, source to site distance and depth. For the first probability moment (usually the median of a lognormal distribution), the attenuation relations are matrices in which the rows account for the magnitudes and the columns account for the distances. Note that when using attenuation tables, the relations between magnitude, distance and intensity do not need to be of parametric nature, since the intensity medians are given, point by point, for the different magnitude-distance combinations.
2. **Built-in GMPE:** These are popular models, published in the literature and developed by well-known authors, in which magnitudes, distances and intensities are probabilistically related by, usually, a set of formulas or parametric equations. There is a set of built-in models ready to use in R-CRISIS and there is also the possibility of adding new models. See Table 2-17 for the list of built-in GMPM available in R-CRISIS.
3. **Generalized models:** Generalized attenuation models are non-parametric probabilistic descriptions of the ground motions produced by an earthquake. In the framework of R-CRISIS, a generalized attenuation model is a collection of probabilistic footprints, one for each of the events considered in the analysis. Each footprint provides, in probabilistic terms, the geographical distribution of the intensities produced by this specific event.
4. **Hybrid models:** Hybrid models, sometimes known also as "composite" models, are lineal combinations of other types of GMPE, either user given or built-in. Sometimes, and for some applications, they can be used to replace, to some extent, logic trees.

A detailed description of each of these families is presented next.

2.4.1 GMPE tables

These tables provide R-CRISIS the probabilistic relations between magnitude, source-site distance and intensities. Each attenuation table must be saved in a different file and must have the structure explained next.

Attenuation table header

All the lines of this portion of the file are optional. The user, however, must be aware of the default values that are used for the parameters that are described herein. The header can contain up to 4 lines that provide different characteristics of the attenuation table and lines can be given in any order. Field names (including capital letters) are fixed. Table 2-16 describes the four possible header fields recognized by R-CRISIS.

Table 2-16 Description of the header fields accepted by R-CRISIS for attenuation tables

Field name	Field value	Comments	Default value
Description	A string providing a brief description of the attenuation table (e.g. author, date of publication, suitable tectonic environment, etc.)	This information is for displaying on the "Attenuation data" screen	"Not available"
Units	A string providing the units for which the model was developed for	The original units are displayed for information purposes and will guide the user to define if a units coefficient is needed	"Not available"
Distribution	An integer number indicating the probability distribution assigned to the residuals of the attenuation model	Supported values are: Normal = 1, Lognormal = 2, Beta = 3, Gamma = 4	2 (Lognormal)
Dimension	A string value providing the physical dimension of the intensities described in the attenuation table	See Table 2.16	"Acceleration"

Parameters defining the magnitude limits (1 line)

The values defining the magnitude limits are provided in one line and denoted as: *MINF*, *MSUP*, *NMAG* as described in Table 2-17.

Table 2-17 Description of magnitude range and number in attenuation tables

Variable	Description
<i>MINF</i>	Lower limit of magnitude given in the table
<i>MSUP</i>	Upper limit of magnitude given in the table
<i>NMAG</i>	Number of magnitudes for which intensity is given

R-CRISIS assumes that intensities are given for magnitudes $M(K)$, where

$$M(K) = MINF + (K - 1) * DMAG \tag{Eq. (2-40)}$$

and,

$$DMAG = \frac{(MSUP - MINF)}{(NMAG - 1)} \tag{Eq. (2-41)}$$

Parameters defining the distance limits and type (1 line)

The values defining the distance limits (and type) are provided in one line and denoted as: *RINF*, *RSUP*, *NRAD*, *TYPE* and described in Table 2-18.

Table 2-18 Description of distance range, number and type in attenuation tables

Variable	Description
<i>RINF</i>	Lower limit of distance given in the table
<i>RSUP</i>	Upper limit of distance given in the table
<i>NRAD</i>	Number of distances for which intensity is given
<i>TYPE</i>	An integer indicating the type of distance used by the attenuation table

R-CRISIS assumes that intensities are given for distances $R(K)$, where

$$\text{Log}(R(K)) = \text{Log}(RINF) + (K - 1) * DLRAD \tag{Eq. (2-42)}$$

and

$$DLRAD = \frac{(\text{Log}(RSUP) - \text{Log}(RINF))}{(NRAD - 1)} \tag{Eq. (2-43)}$$

which means that distances are logarithmically spaced.

The *TYPE* field can have any of the values shown in Table 2-19⁸, depending on the type of distance for which the GMPE has been developed.

Table 2-19 Codes for types of distances in attenuation tables

Value	Type of distance
1 (or blank)	Focal (R_F)
2	Epicentral (R_{EPI})
3	Joyner and Boore (R_{JB})
4	Closest to rupture area (R_{RUP})

⁸ Colors indicate the distance type in Figure 2-15

Parameters defining the spectral ordinate, standard deviation, hazard intensity and depth coefficient

Once the magnitude and distance ranges and limits have been defined in each attenuation table, the following values are required for each spectral ordinate in the same line. For notation purposes, the main data of these lines (one for each spectral ordinate) are referred to as: $T(J)$, $SLA(J,o)$, $AMAX(J)$, $COEFH$ which complete description is provided in Table 2-20.

Table 2-20 Description of attenuation table data

Variable	Description
$T(J)$	Structural period of the j th spectral ordinate. It is used only for identification purposes and to plot the uniform hazard spectra, so in the cases in which structural period has no meaning, it can be a sequential number
$SLA(J,o)$	Standard deviation of the natural logarithm of the j th measure of intensity. A value of $SLA(J,o) \leq 0$ implies that the user will provide standard deviations that vary with magnitude. In this case, the corresponding σ values (one for each of the $NMAG$ magnitudes) has to be given after the table of $SA()$ values
$AMAX(J)$	See Section 2.4.2 for the definition of this value
$COEFH$	Depth coefficient (see below)

Some recent GMPE include a coefficient to make the intensity explicitly dependent on the focal depth. This information can be provided by the user to R-CRISIS by means of the $COEFH$ coefficient, so that:

$$MED(A | M, R) = Sa(M, R) \cdot \exp(COEFH * H) \tag{Eq. (2-44)}$$

where $MED(A|M,R)$ is the (depth-dependent) median value of intensity for given values of magnitude M and distance R and $Sa(M,R)$ corresponds to the median intensity given in the attenuation table for the same values of magnitude and distance, and H is focal depth.

Matrix of median intensities, associated to a magnitude (row) and a distance (column)

For each spectral ordinate the attenuation table includes a matrix that contains the median intensities associated to the magnitudes (rows) and to the distances (columns). For notation purposes those are referred to as: $Sa(1,1,1)$, $Sa(1,1,2)$, ..., $Sa(J,K,L)$, ..., $Sa(NT,NMAG,NRAD)$ where $Sa(J,K,M)$ corresponds to the median value of the intensity, for the J^{th} spectral ordinate, the K^{th} magnitude and the L^{th} distance.

Only if $SLA(J) \leq 0$:

$SLA(J,1)$
 $SLA(J,2)$
 ...
 $SLA(J,NMAG)$

Note: the attenuation tables to be used in R-CRISIS are to be saved in ASCII format and with *.atn extension.

Example of a *.atn file

Table 2-21 shows an example of an attenuation table that includes $NT=2$ periods (or intensity measures). Values shown in black are those to be included in the table whereas those shown in red provide only a description of the meaning of the values used in this example.

Table 2-21 Example of a *.atn file (user defined attenuation table)

#	: Description	Example of attenuation table (CRISIS2015 manual)						
#	: Units	gal						
#	: Distribution	2						
#	: Dimension	Spectral acceleration						
4.5	8.5	5		5 magnitudes between 4.5 and 8.5				
5.0	500.0	10	1	10 distances between 5 and 500 km (log-spaced); focal distance				
0.0	0.7	0.0	0.0	Period 0; $\sigma=0.7$, $A_{max}=0$ (no truncation), $CoeffH=0$				
119.3	97.5	70.5	45.3	14.7	7.6	3.4	1.2	0.3
202.5	165.0	120.1	76.9	24.3	12.6	5.8	1.8	0.5
344.0	251.2	201.5	130.6	43.5	22.3	9.8	3.0	0.8
584.1	477.4	354.3	221.8	72.5	36.4	16.5	5.6	1.3
992.0	811.2	585.6	376.7	122.5	60.1	27.5	9.6	2.4
0.5	-1.0	0.0	0.0035	Period 0.5; σ variable with M, $A_{max}=0$ (no truncation), $CoeffH=0.0$				
239.4	217.6	190.6	165.4	134.8	127.7	123.5	121.3	120.4
322.6	285.1	240.2	197.0	144.4	132.7	125.9	121.9	120.6
464.1	371.3	321.6	250.7	163.6	142.4	129.9	123.1	120.9
704.2	597.5	474.4	341.9	192.6	156.5	136.6	125.7	121.4
1112.1	931.3	705.7	496.8	242.6	180.2	147.6	129.7	122.5
0.83				5 values of magnitude-dependent σ (one for each magnitude)				
0.78								
0.62								
0.63								
0.51								

Physical dimensions of the hazard intensities

To have stricter checks of the compatibility among different GMPE when performing logic-tree computations (see Section 2.12), each GMPM must be assigned a physical dimension of the measures of hazard intensity that the model is describing. The physical dimension of most GMPE is spectral acceleration (because they are usually constructed for PGA and the response spectral ordinates at selected fundamental periods), but other physical dimensions are also accepted and can be used. R-CRISIS accepts the physical dimensions shown in Table 2-22, which correspond to classes defined for this purpose.

Table 2-22 Physical dimensions accepted by R-CRISIS

Physical dimension	Assembly name
Acceleration	Crisis2008.NewAttenuation.dll
Velocity	Crisis2008.NewAttenuation.dll
Displacement	Crisis2008.NewAttenuation.dll
MMI	Crisis2008.NewAttenuation.dll
MCSI	Crisis2008.NewAttenuation.dll
DuctilityDemand	ExtraDimensions.dll
ISDrift	ExtraDimensions.dll

Although only these physical dimensions are recognized by R-CRISIS, it is relatively simple to construct additional classes associated to other intensity measures. To do so, the constructed class must implement the methods shown in Table 2-23.

Table 2-23 Implemented methods for physical dimensions in R-CRISIS

Method	Purpose
Public ReadOnly Property distancePow() As Integer	Returns an integer indicating the distance power of this dimension
Public ReadOnly Property forcePow() As Integer	Returns an integer indicating the force power of this dimension
Public ReadOnly Property timePow() As Integer	Returns an integer indicating the time power of this dimension
Public ReadOnly Property chargePow() As Integer	Returns an integer indicating the charge power of this dimension
Public MustOverride ReadOnly Property name() As String	Provides a number specific to the class
Public Overrides Function Equals(ByVal obj As Object) As Boolean	Checks if the types have same power for MKSA elements describing dimensions

Classes constructed that implement these methods must be compiled in the form of a *.dll, which must be saved in the R-CRISIS application directory. In addition, the file “CRISISDimensions.ini”⁹ must be edited to add the new classes. The general format of the lines of this file is the following:

Full class name, Assembly name

2.4.2 Probabilistic interpretation of attenuation relations

In general, given a magnitude and a distance, intensity A is assumed to be a random variable with a given probability distribution (usually lognormal). GMPE provide the first two probability moments of A given a magnitude and a distance, that is, $A|M,R$. These two moments usually describe the mean or median value of $A|M,R$ and a measure of its uncertainty.

R-CRISIS supports three probability distributions that can be used to describe hazard intensities. These distributions are presented in Table 2-24, together with the two probability moments that have to be given in order to correctly describe $A|M,R$ as a random variable.

⁹ Stored at the installation path

Table 2-24 Acceptable probability distributions to describe hazard intensities in R-CRISIS

Distribution	1st moment (μ_1)	2nd moment (μ_2)	Lower limit	A_{max}
Lognormal	Median	Standard deviation of the natural logarithm	0	$\mu_1 \exp(K \mu_2)$
Gamma	Mean	Standard deviation	0	$\mu_1 + K \mu_2$
Normal	Mean	Standard deviation	-infinity	$\mu_1 + K \mu_2$

As part of the hazard computations, R-CRISIS requires to compute the probability that intensity A at a given site exceeds a known value, a , given that at some hypocentral location, H , an earthquake of magnitude M occurred, that is, $\Pr(A > a | M, H)$.

If no truncation is applied to the hazard intensity values, this probability is computed by means of:

$$\Pr(A > a | M, H) = 1 - F_A [a; \mu_1(M, H), \mu_2(M, H)] \quad \text{Eq. (2-45)}$$

where $\mu_1(M, H)$ and $\mu_2(M, H)$ are the first and second probability moments, respectively, of intensity A , given that at hypocentral location H an earthquake of magnitude M occurred. Depending on the probability distribution assigned to A , the first and second probability moments have the interpretation presented in Table 2-24. $F_A[a; \mu_1(M, H), \mu_2(M, H)]$ is the probability distribution of A (also called the cumulative probability function) whose form depends on the type of distribution chosen for the analysis.

The probability moments of $A|M, R$, that is, $\mu_1(M, H)$ and $\mu_2(M, H)$ are provided by the user by means of the GMPE. In many cases, truncation is specified in the GMPE through a parameter denoted as "Sigma truncation", T_c . This means that the integration across the attenuation relation uncertainty implied in the previous equations is not carried out up to infinity, but up to a certain value, T_c .

Depending on the value of the truncation coefficient given in the GMPE, the following considerations are made:

$T_c=0$

In this case, no truncation is applied, so equation 2-45 is used.

$T_c>0$

In this case, a truncated distribution between the lower limit of A and T_c is assumed, regardless of magnitude and distance. Hence,

$$\Pr(A > a | M, H) = \begin{cases} \frac{1 - F_A [a; \mu_1(M, H), \mu_2(M, H)]}{1 - F_A [Tc; \mu_1(M, H), \mu_2(M, H)]}, & a < Tc \\ 0, & a > Tc \end{cases} \quad \text{Eq. (2-46)}$$

Note: when truncating intensities, the original units of the attenuation model should be used regardless any unit factor has been included in the R-CRISIS project.

Tc < 0

In this case, $ABS(Tc)=K$, is interpreted as the number of standard deviations, for which integration will be performed. Hence, the integration will be performed between the lower limit and A_{max} , both explained in Table 2-24. Therefore,

$$\Pr(A > a | M, H) = \begin{cases} \frac{1 - F_A [a; \mu_1(M, H), \mu_2(M, H)]}{1 - F_A [A_{max}; \mu_1(M, H), \mu_2(M, H)]}, & a < A_{max} \\ 0, & a > A_{max} \end{cases} \quad \text{Eq. (2-47)}$$

Depending on the distribution chosen, A_{max} takes the values indicated in Table 2-24. Note that in this case, the actual truncation value for A depends on magnitude and distance. Figure 2-20 shows the effect of the different truncation schemes.

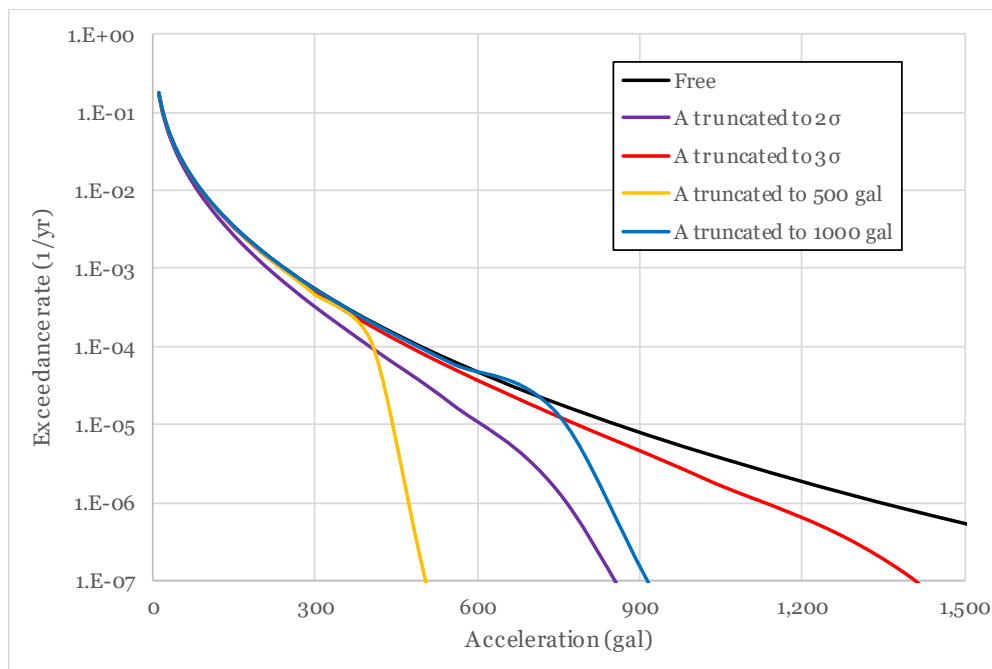


Figure 2-20 Effect of different truncation schemes on GMPM



2.4.3 Built-in GMPEs

As mentioned before, the built-in GMPEs correspond to well-known models published in the literature, that the user can use as attenuation relationships for the R-CRISIS projects. These models, as the user defined attenuation tables, relate in probabilistic terms, earthquake magnitudes and a certain distance measure with the intensity at a computation site. Also, many of these attenuation equations require specification of additional parameters that the user must select, such as style of faulting and soil type.

Table 2-25 includes the list of the available built-in GMPM to date in R-CRISIS and show whereas those have been verified or not. More details about this process are included in Section 4.3 of this document.

The number available built-in models in R-CRISIS expands with time depending on the publication of new models and/or updates of existing ones. Although most of the available built-in GMPEs in R-CRISIS have been included by the developers, users can also provide their inputs through the contact channels available at www.r-crisis.com.

Table 2-25 Built-in GMPEs in R-CRISIS

Reference	Magnitude range	Distance range	Spectral period range
Abrahamson and Silva (1997)	4.0-7.5	0.1-200 km	0.01-5.00 s
Abrahamson et al. (2014) NGA-West2	3.0-8.5	0-300 km	0.0-10.0 s
Abrahamson et al. (2016) BCHydro	5.0-8.4	1-300 km	0.0-3.0 s
Akkar and Bommer (2007)	5.0-7.6	1-100 km	0.0-4.0 s
Akkar and Bommer (2010)	5.0-7.6	1-100 km	0.0-3.0 s
Akkar et al. (2014)	4.0-8.0	0-200 km	0.005-4.0 s
Arroyo et al. (2010)	5.0-8.5	16-400 km	0.001-5.0 s
Atkinson and Boore (2003)	5.0-8.5	1-300 km	0.0-3.0 s
Atkinson and Boore (2006)	3.5-8.0	1-1000 km	0.01-5.0 s
Atkinson (2008)	4.3-7.6	10-1000 km	0.0-5.0 s
Bindi et al. (2011)	4.0-6.9	0.1-200 km	0.0-4.0 s
Bindi et al. (2017)	3.0-8.0	0.1-300 km	0.0-4.0 s
Boore and Atkinson (2008) NGA	5.0-8.0	1-200 km	0.0-10.0 s
Boore et al. (2014) NGA-West2	3.0-8.5	0-400 km	0.01-10.0 s
Campbell (2003)	5.0-8.2	1-1000 km	0.01 - 4.0 s
Campbell and Bozorgnia (2003)	5.0-7.5	1-60 km	0.03-4.0 s
Campbell and Bozorgnia (2008) NGA	4.0-8.5	0-200 km	0.0-10.0 s
Campbell and Bozorgnia (2014) NGA-West2	3.0-8.5	0-300 km	0.0-10.0 s
Cauzzi and Faccioli (2008)	5.0-7.2	6-150 km	0.01-20.0 s
Cauzzi et al. (2015)	4.5-8.0	0-150 km	0.0-10.0 s
Chávez (2006)	4.0-8.5	10-500 km	0.0-5.0 s
Chiou and Youngs (2008) NGA	4.0-8.5	0-200 km	0.0-10.0 s
Chiou and Youngs (2014) NGA-West2	3.5-8.0	0-300 km	0.0-10.0 s
Climent et al. (1994)	4.0-8.0	1-500 km	0.0-5.0 s
Contreras and Boroschek (2012)	5.0-9.0	20-600 km	0.0-2.0 s
Darzi et al. (2019)	4.5-7.4	0-200 km	0.01-10.0 s
Derras et al. (2014)	4.0-7.0	5-200 km	0.0-4.0 s
Derras et al. (2016)	3.5-7.3	3-300 km	0.0-4.0 s
Faccioli et al. (2010)	5.0-7.2	6-150 km	0-20 s
García et al. (2005)	5.0-8.0	0.1-400 km	0.0-5.0 s
Gómez (2017)	3.8-7.1	0.11-634 km	PGA
Idriss (2008)	5.0-8.5	0-200 km	0.01-10.0 s
Idriss (2014) NGA-West2	5.0-8.0	0-150 km	0.01-10.0 s
Jaimes et al. (2006)	5.0-8.4	150-500 km	0.01-6.0 s
Jaimes et al. (2015)	5.2-7.5	103-464 km	0.0-5.0 s
Kanno et al. (2006)	5.5-8.0	1-400 km	0.0-5.0 s
Lanzano et al. (2019)	4.0-8.0	0-200 km	0.04-10.0 s
Lin and Lee (2008)	4.0-8.0	20-250 km	0.0-5.0 s
McVerry et al. (2006)	5.25-8.0	0-400 km	0.0-3.0 s
Montalva et al. (2017)	5.0-9.0	0-300 km	0.01-10.0 s
Pankow and Pechmann (2004)	5.0-7.7	0-100 km	0.01-2.0 s
Pasolini et al. (2008)	4.0-7.0	0-140 km	PGA
Pezeshk and Zandieh (2011)	5.0-8.0	0.1-1000 km	0.0-10.0 s
Pezeshk et al. (2018)	4.0-8.0	0.1-1000 km	0.0-10.0 s
Reyes (1998)	5.0-8.6	150-450 km	0.0-6.0 s
Sabetta and Pugliese (1996)	4.6-6.8	1-100 km	0.1-4.0 s
Sadigh et al. (1997)	4.0-8.0	0.01-200 km	0.0-4.0 s
Sharma et al. (2009)	5.0-7.0	0-100 km	0.0-2.5 s
Spudich et al. (1999) SEA99	5.0-7.5	0.01-100 km	0.0-2.0 s
Tavakoli and Pezeshk (2005)	5.0-8.2	0-1000 km	0.0-4.0 s
Toro et al. (1997)	5.0-8.0	1-500 km	0.0-2.0 s
Yenier and Atkinson (2015)	3.0-8.0	0-600 km	0.0 - 10.0 s
Youngs et al. (1997)	5.0-8.5	10-500 km	0.0-3.0 s
Zhao et al. (2006)	5.0-9.0	0.4-300 km	0.0-5.0 s

Note that in R-CRISIS, besides the parameters that each GMPE uses (e.g. soil type or style of faulting), all built-in GMPEs contain two extra parameters, called "Units coefficient" and

"Sigma truncation". The first one is used to change the original units of the model while the second one is used to truncate the probability distribution of the residuals as explained before.

2.4.4 Generalized GMPE

Generalized attenuation models are non-parametric probabilistic descriptions of the ground motions produced by an earthquake. Ground motions descriptions obtained when using traditional GMPE are generally functions of earthquake magnitude and source-to-site distance as explained in sections 2.4.1 and 2.4.2 but, generalized attenuation models are not explicit functions of magnitude and distance. In the framework of R-CRISIS, a generalized attenuation model is a collection of probabilistic footprints, one for each of the events considered in the analysis. Each footprint provides, in a probabilistic manner, the geographical distribution of the intensities produced by that particular event.

For a given event, the footprint consists of several pairs of grids of values. Each pair of grids is associated to one of the intensity measures for which hazard is being computed. R-CRISIS requires two grids for each intensity measure because, as with other ground motion prediction models, the intensity caused by the earthquake is considered probabilistic and then, to fix a probability density function of the intensity caused by an earthquake at a particular location.

For instance, assume that one generalized attenuation model will be used to describe the intensities caused by 10 different earthquakes. Also, assume that the hazard analysis is being made for seven intensity measures (for instance, the response spectral ordinates for seven different periods). For this example, each event will be described by 14 different grids, two for each intensity measure, the first one providing the geographical distribution of the median intensity and the second one providing the geographical distribution of the standard deviation of the natural logarithm of the intensity. Hence, a total of 140 grids will form the generalized attenuation model of this example. It would be natural that all the 140 grids cover the same geographical extension; however, there are no restrictions at this respect.

From this description, it would be extremely difficult to perform a hazard study of regional (or higher) extension using generalized attenuation models. Usually, a hazard model of regional size contains thousands of events, and the task of geographically describing the intensities caused by each of them in a non-parametric form would be titanic.

Rather, generalized attenuation models are very likely to be used in local studies, for which the relevant earthquakes are few and can be clearly identified. In this case, the grids of required values (geographical distribution of statistical moments of one or more intensity measures for each event) can be constructed using, for instance, advanced ground-motion simulation techniques (Villani et al., 2014).

Generalized attenuation models are provided to R-CRISIS in the form of binary generalized attenuation files (*.gaf extension¹⁰). The reason for requiring those files to be in binary format

¹⁰ Generalized Attenuation Files

is the computational need of having random access to individual intensity values, something that is basically dictated by computational speed issues.

Table 2-26 shows in detail the format and structure of the *.gaf files.

Table 2-26 Description of the *.gaf file structure

Description	Type	Length	Comments
Custom file description	String	Variable	Provides a brief description of the main features of the GAF
Original units	String	Variable	
Data type (short, integer, single, double, long)	Integer	4	
Probability distribution assigned to intensity (normal, lognormal, beta, gamma)	Integer	4	
Number of intensity measures (e.g. number of fundamental periods)	Integer	4	
Number of sources (locations)	Integer	4	
Number of magnitudes per location	Integer	4	
Number of probability moments of the intensity stored	Integer	4	
Period 1	Double	8	Period values are required since the user may want to compute hazard for arbitrary periods
Period 2	Double	8	
...	
Period number of intensity measures	Double	8	
Representative magnitude of bin 1	Double	8	Magnitude values are required to compute occurrence rates when G-R or characteristic earthquake models are used. When non-Poissonian seismicity files are used, these magnitudes are irrelevant
Representative magnitude of bin 2			
...	
Representative magnitude of last bin	Double	8	
Scenario name	Char	40	Magnitude values are required to compute occurrence rates when G-R or characteristic earthquake models are used. When non-Poissonian seismicity files are used, these magnitudes are irrelevant
Grid for intensit measure 1, probability moment 1	ModGRN	56+Nbytes*Nx1*Ny1	
Grid for intensit measure 1, probability moment 2	ModGRN	56+Nbytes*Nx1*Ny1	
...	

Grid for intensit measure 1, probability moment NumMoments	ModGRN	56+Nbytes*Nx1*Ny1	
Grid for intensit measure 2, probability moment 1	ModGRN	56+Nbytes*Nx1*Ny1	
Grid for intensit measure 2, probability moment 2	ModGRN	56+Nbytes*Nx1*Ny1	
...	
Grid for intensit measure 2, probability moment NumMoments	ModGRN	56+Nbytes*Nx1*Ny1	
...	
Grid for intensity measure NumInt, probability moment 1	ModGRN	56+Nbytes*Nx1*Ny1	Then, the actual georeferenced probabilistic intensity values follow
Grid for intensity measure NumInt, probability moment 2	ModGRN	56+Nbytes*Nx1*Ny1	
...	
Grid for intensity measure NumInt, probability moment NumMoments	ModGRN	56+Nbytes*Nx1*Ny1	
Scenario name	Char	40	Magnitude values are required to compute occurrence rates when G-R or characteristic earthquake models are used. When non-Poissonian seismicity files are used, these magnitudes are irrelevant
Grid for intensit measure 1, probability moment 1	ModGRN	56+Nbytes*Nx2*Ny2	
Grid for intensit measure 1, probability moment 2	ModGRN	56+Nbytes*Nx2*Ny2	
...	
Grid for intensit measure 1, probability moment NumMoments	ModGRN	56+Nbytes*Nx2*Ny2	
Grid for intensit measure 2, probability moment 1	ModGRN	56+Nbytes*Nx2*Ny2	
Grid for intensit measure 2, probability moment 2	ModGRN	56+Nbytes*Nx2*Ny2	
...	
Grid for intensit measure 2, probability moment NumMoments	ModGRN	56+Nbytes*Nx2*Ny2	
...	
Grid for intensity measure NumInt, probability moment 1	ModGRN	56+Nbytes*Nx2*Ny2	
Grid for intensity measure NumInt, probability moment 2	ModGRN	56+Nbytes*Nx2*Ny2	
...	
Grid for intensity measure NumInt, probability moment NumMoments	ModGRN	56+Nbytes*Nx2*Ny2	
Similar blocks continue for all remaining scenarios			

2.4.5 Hybrid attenuation models

A hybrid (or composite) GMPE is the result of the weighted combination of two or more distributions (usually normal ones) that can have different mean values and standard deviations (Scherbaum et al., 2005). In its most general form, the conditional probability of exceeding an intensity measure A is calculated by means of:

$$P(A > a) = \sum_{i=1}^N w_i \left\{ 1 - \Phi \left[\frac{a - \mu_i}{\sigma_i} \right] \right\} \tag{Eq. 2-48}$$

where w_i is the weight assigned to the i^{th} base GMPE, $\Phi[\cdot]$ is the normal distribution and μ_i and σ_i are the mean values and standard deviations respectively of the i^{th} base GMPE. Figure 2-21 shows a schematic representation for the resulting probability function of a hybrid GMPE generated using three base GMPE as well as their weighted probability densities.

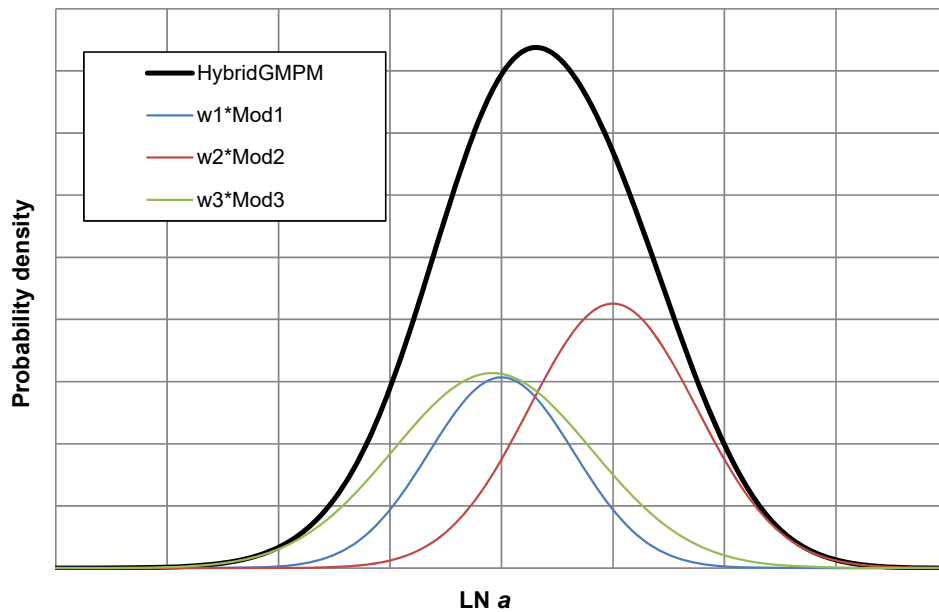


Figure 2-21 Example of a hybrid GMPE

These hybrid GMPE are useful for cases where the normal distributions do not fit well with the recorded earthquake data (i.e. observations show that there are higher probabilities of extremes than those provided by the normal distributions). This issue is more evident, when using normal distributions, at high epsilons and, the development of hybrid GMPE generally allow considering heavier tails as shown in Figure 2-22, which zooms the end tail of Figure 2-21.

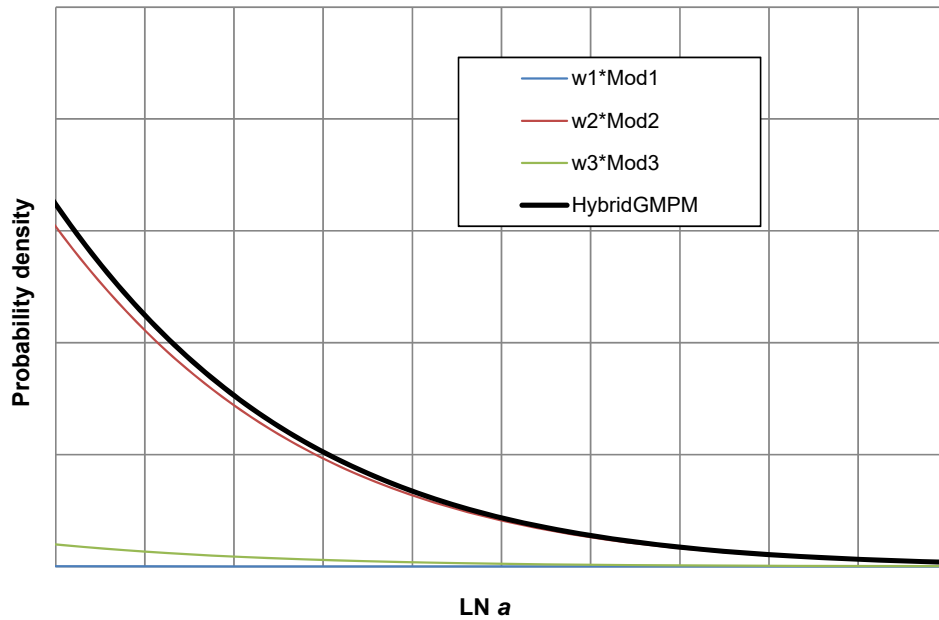


Figure 2-22 Detail of the end tail of the example hybrid GMPE

Note: editing of hybrid GMPEs is restricted in R-CRISIS. In case the user wants to make any change, those must be implemented directly in the base models and, after that, the existing hybrid model must be deleted and created again. Also, care must be taken so that the updated one is properly assigned to the sources in the R-CRISIS project.

Hybrid GMPE vs. logic trees

Hybrid GMPE can be used instead of logic trees when differences in the R-CRISIS models only have to do with the GMPE assignation. Instead of assigning weights to the branches, those are assigned to the base GMPE for the generation of a hybrid attenuation model. Although both approaches produce the same results in terms of expected values because the way in which uncertainties are considered is different (epistemic in the logic trees and random in the hybrid GMPE), the estimations of variances do differ (see Ordaz and Arroyo, 2016).

Note: when hybrid GMPE are used, the seismic hazard intensity is treated as a hybrid random variable and not a lognormal one anymore. Therefore, the second probability moment does not correspond to the standard deviation of the logarithm but to the standard deviation itself.

2.4.6 Special attenuation models

In the most frequent cases, only one attenuation model is assigned to a seismic source. However, there is the possibility to assign one or more special attenuation models to a source, which will be effective only for sites located inside corresponding polygons, called “special



attenuation regions” provided by the user. If special attenuation models are given, then R-CRISIS will proceed in the following way:

When computing hazard from a source, R-CRISIS will check if this source has assigned a special attenuation model. If it does not, then it will use the general GMPE assigned to the source. If the source on the other hand has assigned a special attenuation model, then R-CRISIS checks if the site of computation is inside one of the user-provided polygons. If affirmative, R-CRISIS will use the model assigned to this source-site combination. If the site is not inside any of the special polygons, then R-CRISIS will use the general attenuation model assigned to the source.

It must be noted that if site-effects grids are used (see Section 2.5), the amplification factors will be applied on top of the intensities computed either with the general attenuation model assigned to the source or with attenuation models assigned to special attenuation regions. This is of importance to avoid double counting or omission of the site-effects.

2.4.7 Point source (ω^2) attenuation model

R-CRISIS allows developing a GMPE using a point source, ω^2 model based on the following parameters:

- Beta: S-wave velocity in km/s
- C1: first constant required to compute duration
- C2: second constant required to compute duration
- Epsilon
- FFMAX: cut-off frequency, in Hz
- Fmax: maximum frequency for which the GMPM will be calculated
- Fmin: minimum frequency for which the GMPM will be calculated
- FS: free surface amplification factor, usually taken as 2
- t*: near-surface attenuation factor, in s
- Nf: number of frequencies, between Fmin and Fmax for which intensities will be calculated
- NPoles: Number of poles of Butterworth filter
- Qo: where $Q(f)=Q_o \cdot f^e$
- Rho: density, in gr/cm³
- Stress drop: in bar
- Sigma truncation: following the R-CRISIS notation

The units of this GMPE will be always cm/s² for accelerations, cm/s for velocities and cm for displacements, although the unit factor field is available. For the case of accelerations, R-CRISIS will automatically estimate the Sa(T) for all the values of the spectral ordinates defined in the seismic hazard project.

Note: the user should review that the frequency range defined for the GMPE covers well enough the spectral ordinates range. Special care must be taken for long period (low frequency) values which can be adjusted through the f_{min} field.

2.5 Site effects

R-CRISIS allows including local site effects in the seismic hazard computations. Site effects are included to the R-CRISIS project in terms of amplification/de-amplification factors that depend on the site location, structural period and ground-motion level (to account for the soil non-linearity).

Amplification factors are interpreted by R-CRISIS in the following way: during the hazard computations, R-CRISIS requires to compute the hazard intensity at structural period T that would take place at site S due to the occurrence of an earthquake of magnitude M originating at distance R . We will denote this intensity as $I(S,T,M,R)$.

Normally, $I(S,T,M,R)$ is computed using the attenuation relationship that the user has selected for the source (either from an attenuation table, a built-in model or a special attenuation model).

The value computed is interpreted by R-CRISIS as the median intensity without site effects but, if site effects data are provided, then the median intensity that R-CRISIS will use for the hazard computations, I_s , is the product of $I(S,T,M,R)$ and the amplification factor defined by the user which as expected, depends on the site location, the structural period and the ground motion level, I_o . This amplification factor is denoted as $A(S,T,I_o)$.

In other words:

$$I_s = (S, T, M, R) = I(S, T, M, R) \cdot A(S, T, I_o) \quad (\text{Eq. 2-49})$$

Uncertainty in the hazard intensities after site effects are included can be accounted for in R-CRISIS. If the user has provided not only amplifications factors but also an optional file with the sigma values, the uncertainty measure will be extracted from the latter. If no sigma file has been provided by the user, the standard deviation of the acceleration after site-effects will have the same value than the one it had before site-effects (i.e. that of the GMPE for each spectral ordinate).

The user has to provide R-CRISIS the means to obtain the amplification factors $A(S,T,I_o)$ and, optionally, the uncertainty values $\sigma(S,T,I_o)$. These factors are provided to R-CRISIS by means of two (or three¹¹) binary files that are described in the following paragraphs. These files must have the same base name, but different extensions.

Note: if no site-effects are included, $A(S,T,I_o)=1.0$

There are three different ways implemented in R-CRISIS to consider the local site effects and those are denoted as:

- CAPRA Type

¹¹ If the sigma file is provided

- Chiou and Youngs 2014
- V_{s30}

The complete explanation for each case is presented next from where the structure of the required files can be better understood by the user.

2.5.1 CAPRA Type (ERN.SiteEffects.MallaEfectosSitioSismoRAM)

This approach to consider the local site effects requires providing R-CRISIS a set of files which are used to construct the spectral transfer functions at different locations. The first two are mandatory whereas the third one is optional.

Fundamental period file

This file corresponds to a binary grid file *.grd (in Surfer 6 binary format). The main purpose of this file is to provide a geographical reference for the grid for which the amplification factors are given, as well as to account for the grid's resolution. This grid contains as "z-values" the predominant ground periods associated to each point of the grid. Points with positive periods are interpreted as part of the area for which site effects are known. Points with negative periods are interpreted as outside the area for which site effects are known. Hence, for these points, the amplification factor will always be 1.0 regardless of period and ground motion level. For these points, the uncertainty will be that of the acceleration computed without site-effects.

Extension *.grd is required for this file (e.g. SiteEffects.grd).

Amplification factors file

This file contains the amplification factors themselves. As indicated before, the amplification factors depend on the site location, the structural period and the ground-motion level (if soil non-linearity is considered). In view of this, amplification factors are provided to R-CRISIS by means of a 4-index matrix.

The first two indexes are used to sweep through the geographical extension (i.e. rows and columns of a grid). The size, spacing and extension of the grid containing the amplification factors needs to be the same as for the grid with the predominant periods. The third index sweeps through structural periods, while the fourth index sweeps through ground motion levels.

In principle, amplification factors for a given site and period can be different depending on the size of the ground motion. R-CRISIS uses as an indicator of this size the intensity for the shortest period available for the GMPE that is used to compute the intensity without site effects. It is common practice that for most of the cases (but not always) this intensity corresponds to peak ground acceleration (PGA).

The format in which the amplification factors must be provided to the R-CRISIS project is described in Table 2-27.

Table 2-27 Description of the amplification factors file structure

Block	Variable	Size	Comments
Header	A number 1	Integer	This field is reserved for future use
	Number of ground motion levels, NL	Integer	If NL=1, elastic behavior is assumed
	Number of periods, NT	Integer	
	Ground motion level 1	Double	
	Ground motion level 2	Double	
	
	Ground motion level NL	Double	
	Period 1	Double	
	Period 2	Double	
...	...		
Period NT	Double		
For site 1,1	Amplification function for ground-motion level 1	NT doubles	The amplification function for a give site and ground-motion level is a collection of NT numbers, one for each structural period. The first number is associated to Period 1 and so on
	Amplification function for ground-motion level 2	NT doubles	
	
	Amplification function for ground-motion level NL	NT doubles	
For site 1,2	Amplification function for ground-motion level 1	NT doubles	The order of the sites is the same as the associated fundamental period grid, starting from the lowest-left cornert and the counter advancing for the columns (i.e. sites are described following the order of cross sections of constant y)
	Amplification function for ground-motion level 2	NT doubles	
	
	Amplification function for ground-motion level NL	NT doubles	
For site Nx,Ny	Amplification function for ground-motion level 1	NT doubles	Nx and Ny are the number of grid lines along the X axis (columns) and the number of grid lines along the Y axis (rows) provided in the associated period grid file
	Amplification function for ground-motion level 2	NT doubles	
	
	Amplification function for ground-motion level NL	NT doubles	

The first column of Table 2-28 shows an example of the contents of a site-effects file with extension *.ft; the second column includes some comments about each field.

Table 2-28 Example of site-effects file¹²

Value	Comments
1	A number 1 reserved for future use
3	3 ground motion levels
5	5 different fundamental periods
20	First ground motion level
100	Second ground motion level
300	Third ground motion level
0.0	First period for which amplification factors are provided
0.2	Second period for which amplification factors are provided
0.5	Third period for which amplification factors are provided
1.0	Fourth period for which amplification factors are provided
2.0	Fifth period for which amplification factors are provided
1.3 1.5 2.3 1.0 0.9	Five amplification factors, one for each fundamental period for ground-motion level 1
1.2 1.8 2.6 0.9 0.7	Five amplification factors, one for each fundamental period for ground-motion level 2
1.1 1.3 2.1 0.6 0.6	Five amplification factors, one for each fundamental period for ground-motion level 3
2.3 2.6 3.0 2.2 1.8	Five amplification factors, one for each fundamental period for ground-motion level 1
2.2 2.4 3.1 1.9 1.6	Five amplification factors, one for each fundamental period for ground-motion level 2
2.1 2.3 3.1 1.7 1.4	Five amplification factors, one for each fundamental period for ground-motion level 3
...	...
2.4 2.6 3.4 2.0 1.9	Five amplification factors, one for each fundamental period for ground-motion level 1
2.2 2.4 3.1 1.7 1.6	Five amplification factors, one for each fundamental period for ground-motion level 2
2.0 2.2 2.9 1.5 1.4	Five amplification factors, one for each fundamental period for ground-motion level 3

This data is also provided to R-CRISIS by means of a binary file, with extension *.ft. (e.g. SiteEffects.ft).

Sigma file (optional)

This file contains the values of the uncertainty parameter that will be used instead of that provided by the GMPE if no site-effects are considered. Sigma values depend on the site location, the structural period and the ground-motion level. Dependence on ground-motion level is to account for non-linear soil behavior. In view of this, sigma values are given by means of a 4-index matrix which has the same structure as the matrix than contains the amplification factors (see Table 2-20). If this file is not provided, then the uncertainty after site effects will be the same as uncertainty without site-effects.

This data is also provided through an optional binary file, with extension *.sig. (e.g. SiteEffects.sig).

¹² This file must be in binary format and can be generated using a toolbox included in R-CRISIS

2.5.2 Chiou and Youngs, 2014 (ERN.SiteEffects.MallaVs30CY14)

This approach requires the definition of a fixed V_{s30} value (in m/s) at bedrock level for the area of analysis together with a grid (*.grd format) which contains the variable V_{s30} values, one for each node (again, in m/s). With this data, R-CRISIS calculates the amplification factors using the methodology proposed in the Chiou and Youngs (2014) GMPE.

The soil amplifications, both linear and non-linear, is considered in this case using the proposal by Chiou and Youngs (2014) through an amplification factor, AF .

$$AF = \phi_1 \cdot \min \left[\ln \left(\frac{V_{s30}}{1130} \right); 0 \right] + \phi_2 \left[e^{\phi_3 (\min(V_{s30}; 1130) - 360)} - e^{\phi_3 (1130 - 360)} \right] \ln \left(\frac{y_{ref} + \phi_4}{\phi_4} \right) \quad (\text{Eq. 2-50})$$

where $\phi_1, \phi_2, \phi_3, \phi_4$ are the coefficients of the site response model provided in Tables 3 and 4 of Chiou and Youngs (2014); V_{s30} is the travel-time averaged shear-wave velocity (in m/s) at the top 30m of soil and y_{ref} is the ground motion amplitude estimated at bedrock.

The ground motions including the amplification caused by the site effects, y_{se} , are obtained after using the amplification factors on top of the ground motion values obtained from the GMPE (at rock), provided a reference value by the user.

$$y_{se} = y_{ref} \cdot e^{AF} \quad (\text{Eq. 2-51})$$

where y_{ref} is the ground motion amplitude estimated by the GMPE at bedrock level and AF is the V_{s30} -dependent amplification factor obtained from Equation 2-41.

Units factor

The Chiou and Youngs (2014) AF is estimated in terms of g. If the R-CRISIS project uses different units (e.g. cm/s²), the user must indicate the factor for which the AF are to be multiplied for (e.g. if cm/s², the unit factor should be equal to 981).

2.5.3 V_{s30} (ERN.SiteEffects.MallaVs30)

This approach requires a grid (*.grd format) with the V_{s30} values (in m/s) at different locations. If the selected GMPE used in the R-CRISIS project accounts explicitly for a V_{s30} value in its formulation (e.g. Atkinson and Boore, 2006; Kanno et al., 2006; Atkinson and Boore, 2008; Boore and Atkinson, 2008; Campbell and Bozorgnia, 2008; 2014; Chiou and Youngs, 2008; 2014; Cauzzi and Faccioli, 2008; Idriss, 2008; Abrahamson et al. 2014; 2016) said input value will be read from the site effects grid and therefore, at each computation site a V_{s30} customized GMPE will be used.

2.6 Spatial integration procedure

R-CRISIS assumes that, within a source, seismicity is evenly distributed by unit area for the cases of area and volume sources or by unit length for the cases of line sources. For point and gridded sources, all seismicity is assumed to be concentrated at the points.

In order to correctly account for this modeling assumption, R-CRISIS performs a spatial integration by subdividing the sources originally defined by the user. Once the original source has been subdivided, R-CRISIS assigns to a single point all the seismicity associated to each sub-source, and then the spatial integration adopts a summation form.

The subdivision procedure is briefly described next, although more details about the implemented algorithm are shown in Annex 1.

2.6.1 Area sources

As explained in Section 2.2.1, the geometry of the 3D polygons that represent the seismic sources is described by the user through N vertexes for which coordinates (longitude, latitude and depth) are provided. After this, the area source is initially subdivided into $N-2$ triangles. These triangles are further subdivided until one of the following two conditions are met:

1. The size of the triangle is smaller than the value “minimum triangle size” provided to R-CRISIS by the user which means that this is a recursive process where the triangle is subdivided if it is still very big.
2. The ratio between the site-to-source distance and the triangle size is larger than the value “minimum distance/triangle size ratio” provided to R-CRISIS by the user. This is also a recursive process where the triangle is subdivided if the site is still not far enough.

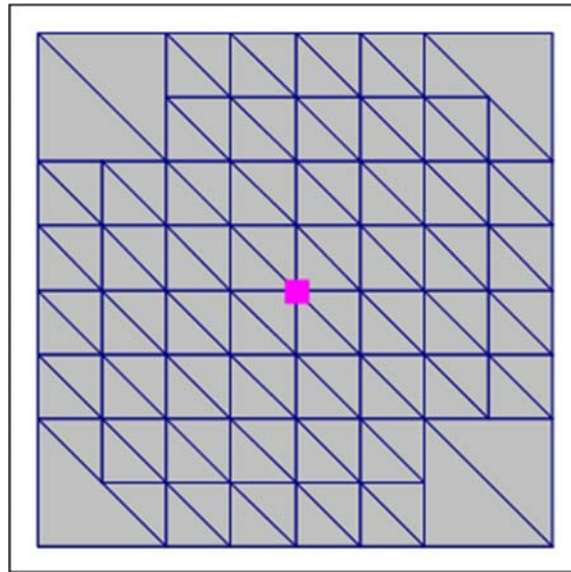
More details about the recursive function used for this purpose are shown in Annex 1. The site-to-source distance is measured from the computation site to the centroid of the triangle whose possible sub-division is being examined. The size of the triangle is simply the square root of its area. At this stage it is worth remembering that the seismicity associated to each centroid is proportional to the triangle’s area.

If based on the criterion provided by the user, R-CRISIS decides that a triangle has to be again sub-divided, this process is done by dividing the initial triangle into four new ones, whose vertexes are the mid-points of the three sides of the original triangle.

R-CRISIS uses the following as default parameters:

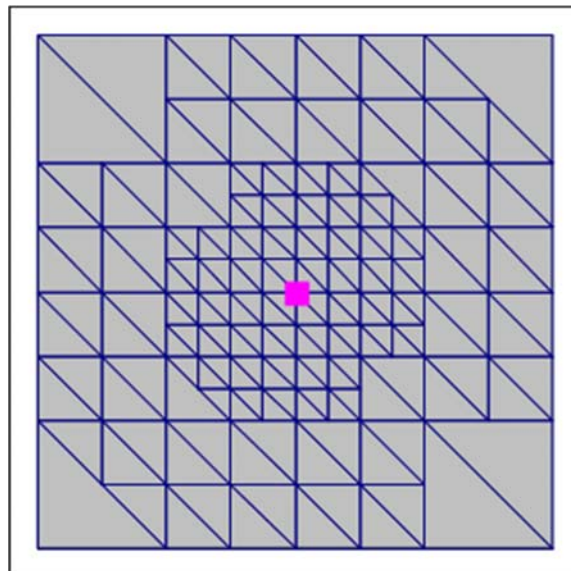
- Minimum triangle size=11 km.
- Minimum distance/triangle size ratio=3.

Figure 2-23 shows the resulting subdivision of a squared source of size $1^{\circ} \times 1^{\circ}$ when the computation site is located at the center of the source and using the default integration parameters.



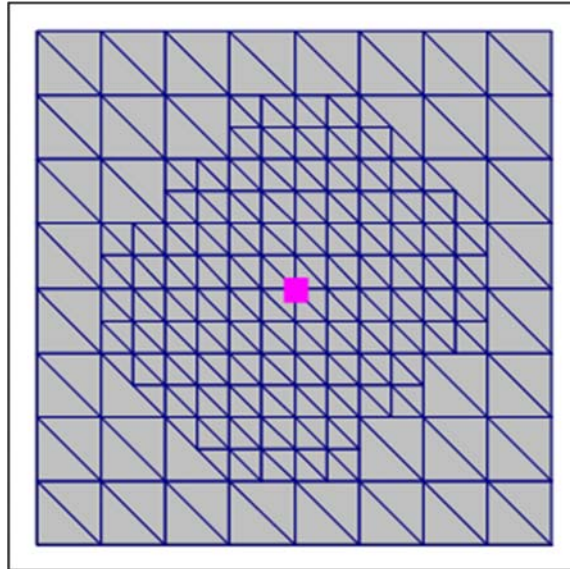
**Figure 2-23 Source subdivision with minimum triangle size=11km,
minimum distance/triangle size ratio=3**

Figure 2-24 shows the same sub-division process but with minimum triangle size=5 km, minimum distance/triangle size ratio=3. Note how, as expected, this sub-division yields smaller triangles in the neighborhood of the computation site.



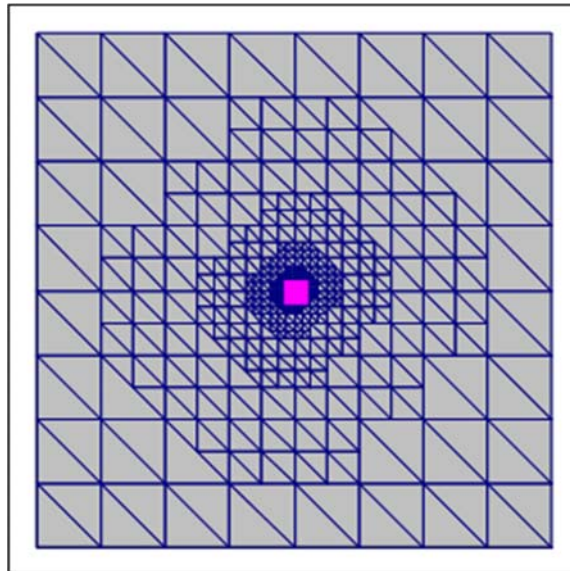
**Figure 2-24 Source subdivision with minimum triangle size=5km,
minimum distance/triangle size ratio=3**

Figure 2-25 shows the same sub-division process but now with minimum triangle size=5 km, minimum distance/triangle size ratio=4. Note that the smaller triangles cover now a wider area around the computation site.



**Figure 2-25 Source subdivision with minimum triangle size=11km,
minimum distance/triangle size ratio=4**

Finally, Figure 2-26 shows the resulting subdivision with minimum triangle size=0.5 km and minimum distance/triangle size ratio=4. Note how the density of triangles varies radially as one move away from the computation site.



**Figure 2-26 Source subdivision with minimum triangle size=0.5km,
minimum distance/triangle size ratio=4**

2.6.2 Line sources

For this case, the subdivision is performed by the bi-partition of a fault source segment, again until one of the following criteria are met:



1. The size of the line is smaller than the value “minimum triangle size” defined by the user.
2. The ratio between the site-to-source distance and the line size is larger than the value “minimum distance/triangle size ratio” defined by the user.

The site-to-source distance is measured from the computation site to the midpoint of the line whose possible subdivision is being examined. The size of the line corresponds simply to its length. In this case, the seismicity associated to each centroid is proportional to the line’s length.

2.7 Use of a digital elevation model (DEM)

R-CRISIS allows including of a digital elevation model (DEM) to be used in the seismic hazard computations. The DEM is provided to R-CRISIS in terms of elevation values (in km) for each location.

The elevation values are interpreted by R-CRISIS in the following way: during the hazard computations, R-CRISIS requires to compute the ground motion intensity due to an earthquake of magnitude M , with focal depth H , at the distance R between the source from which it was originated and the computation site.

Originally, the distance and depth are estimated assuming that the computation site is located at altitude 0. However, if the user includes a DEM, the altitude of the computation site will be that given by the DEM, which will have an influence on the computation of both, distance and focal depth.

Figure 2-27 illustrates the way in which R-CRISIS calculates distance and depth when a DEM is provided whereas Figure 2-28 shows a top view in which the differences between R_{RUP} and R_{JB} can be better understood. For a practical case study on the use of this feature, see more details in Peruzza et al. (2017).

CROSS SECTION:

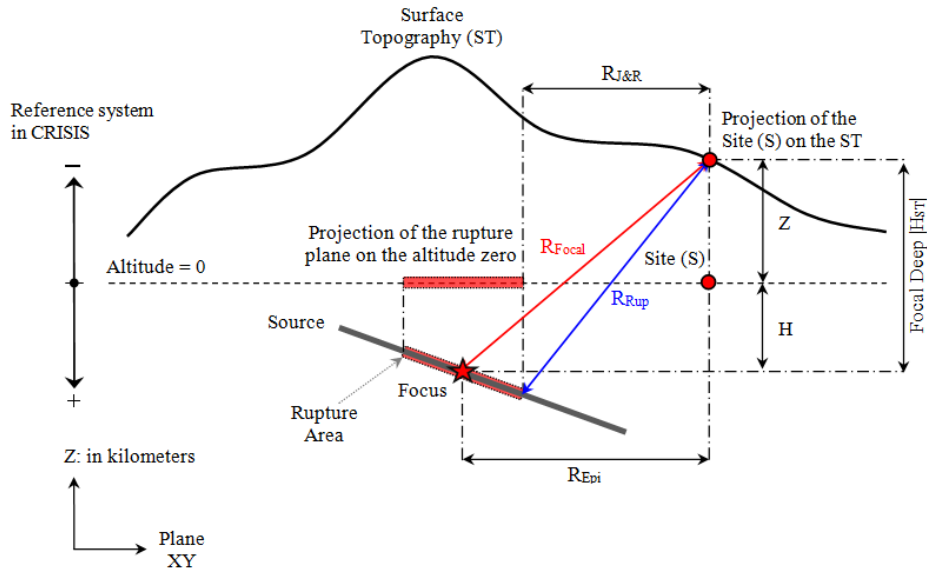


Figure 2-27 Measurement of distances when using DEM

where:

- Z: Elevation value at the computation site
- H: Focal depth relative to zero altitude
- H_{ST} : Focal depth measured from the surface topography to the hypocenter
- R_F : Focal distance
- R_{EPI} : Epicentral distance
- R_{JB} : Joyner and Boore distance (closest distance to the projection of the fault plane at altitude zero)
- R_{RUP} : Closest distance to rupture area

TOP VIEW XY PLANE:

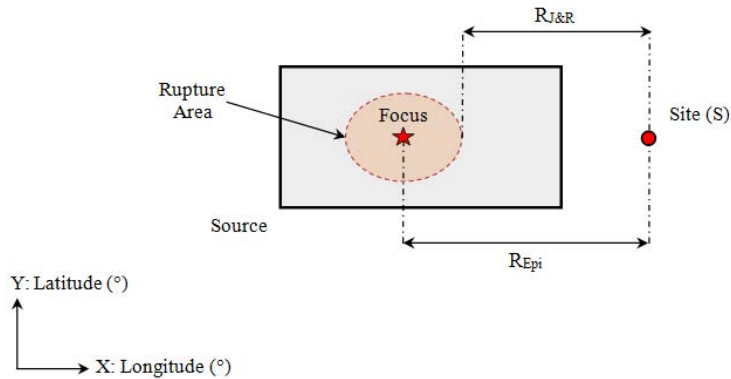


Figure 2-28 Top view of R_{JB} and R_{RUP} distances

In R-CRISIS, the DEM is provided by means of a Surfer grid file¹³ (either in Surfer 6 binary or Surfer 6 ASCII formats). The main purpose of this file is to locate in space the grid of altitude values, as well as to provide the grid's spatial resolution. This grid contains as z-values the ground altitude, in km, associated to each point of the grid. Points with positive values are interpreted as above sea level and points with negative values as sites below sea level.

Figure 2-29 shows schematically the difference of considering or not a DEM at a city located at high altitude with respect the mean sea level (e.g. Mexico City, Bogotá D.C., La Paz). It is evident that in the case where the DEM has been considered, since computation distances are larger, exceedance probabilities, mainly for higher intensities are lower; although this of course depends highly on the GMPE used in the PSHA.

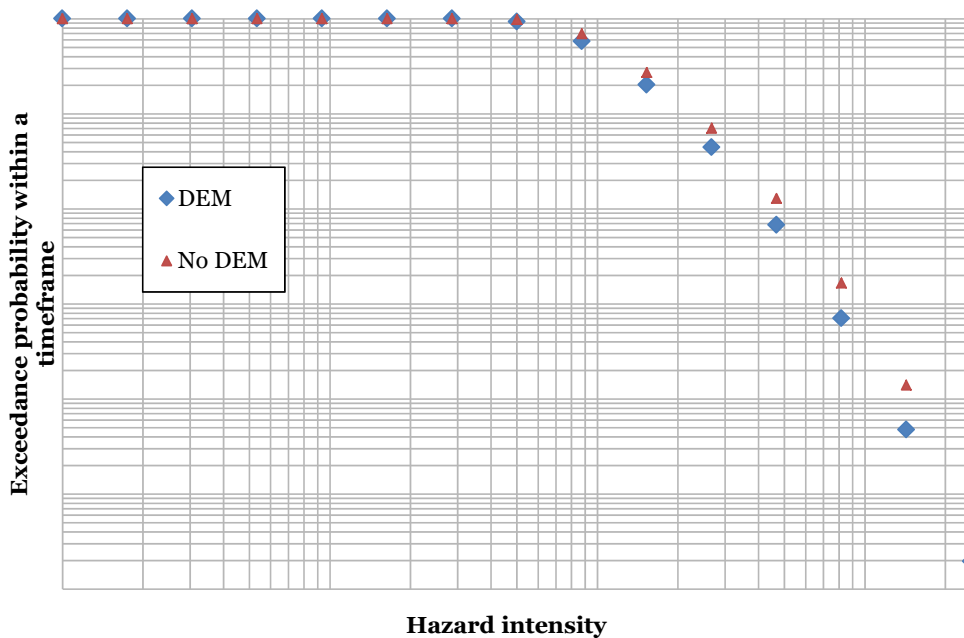


Figure 2-29 DEM v.s. no DEM seismic hazard results

2.8 Combination of seismicity, geometric and attenuation models

Different geometry, seismicity and attenuation models can be combined in R-CRISIS and this section shows which of those combinations are feasible to be used. Tables 2-24 and 2-25 show the validity of the combinations for different seismicity, geometric and attenuation models. In all of them, the color codes indicate the following:

- **Green:** Combination that is always valid regardless of the parameters values
- **Yellow:** Combination that is valid, or not, depending on the parameters values
- **Red:** Combination that is never valid
- **Blue:** Combination that is potentially valid but not yet implemented

¹³ *.grd extension

2.8.1 Normal attenuation models

Table 2-29 shows the validity of the combinations for normal attenuation models (i.e. attenuation tables and built-in GMPM).

Table 2-29 Feasibility of normal attenuation, geometric and seismicity models combination

Geometric model / Seismicity model	Modified G-R	Characteristic earthquake	Generalized non-Poissonian	Generalized Poissonian	Gridded seismicity
Area	A	A	B	B	E
Line	A	A	B	B	E
SSG	C	E	D	D	E
Area-planes	A	A	B	B	E
Grid	E	E	E	E	E

The codes on each field mean the following:

- A: These are options available since previous CRISIS versions that are always valid.
- B: In this option a source is represented by means of line or area geometry model which means that every point that belongs to the source has the same probability of being a hypocenter (the usual assumption when using these geometry models in R-CRISIS). Attenuation models, as in previous versions of CRISIS are constructed using a parametric description (normal GMPE). Anyhow, the new option allows considering the earthquake occurrence probabilities with a generalized Poissonian or non-Poissonian model and not by means of parametric frequency-magnitude relations (i.e. G-R or characteristic earthquake). The occurrence probabilities provided in the Poissonian or non-Poissonian seismicity files correspond to the whole seismic source, that is to be understood as having the probabilities of earthquakes of given magnitudes and within a timeframe anywhere within the source. Using the spatial integration algorithm, explained in Section 2.6, R-CRISIS will sample the source in order to compute hazard accounting for all possible locations of the earthquakes inside it. Not that however, when probabilities are specified for the whole source, those associated to segments of it or to the sub-sources are not univocally defined. The following approach is adopted by R-CRISIS in order to define the occurrence probabilities associated to sub-sources with known sizes.

Assuming that there is a conventional Poissonian source, the probability of having i events of magnitude M in the next T_f years and accounting for the participation of the whole fault, $P(i, M, T_f)$, is given by:

$$P(i, M, T_f) = \exp(-\Delta\lambda(M)T_f) \tag{Eq. 2-52}$$

where $\Delta\lambda(M)$ is the Poissonian magnitude occurrence rate of earthquakes with magnitudes in the vicinity of M , again for the whole source. This occurrence rate can be written as:

$$\Delta\lambda(M) = -\text{Ln} \left[\frac{P(i, M, T_f)}{T_f} \right] \quad (\text{Eq. 2-53})$$

In the case of Poissonian occurrences, it is well known that rates are additive and thus, the occurrence rate corresponding to a sub-source of relative size w_j is:

$$\Delta\lambda_j(M) = \Delta\lambda(M) \cdot w_j \quad (\text{Eq. 2-54})$$

When considering all sub-sources, it is evident that $\sum w_j = 1.0$. Knowing this, the occurrence probability associated to the sub-source j is:

$$P_j(i, M, T_f) = \exp(-\Delta\lambda_j(M)T_f) = \exp(-\Delta\lambda(M)T_f \cdot w_j) = \exp(\text{Ln} [P(i, M, T_f)] w_j) \quad (\text{Eq. 2-55})$$

From which it is evident that:

$$P_j(i, M, T_f) = P(i, M, T_f)^{w_j} \quad (\text{Eq. 2-56})$$

If only the occurrence probabilities for the whole source are specified, there is not a unique way to define the occurrence probabilities associated to the sub-sources. Anyhow, the approach followed by R-CRISIS is very reasonable, besides being exact for the case of the Poissonian sources.

The only compatibility restriction when using this option is that the file that contains the non-Poissonian occurrence probabilities must include (in the *.nps file) that the number of sources is equal to 1, which means that only a set of occurrence probabilities is provided. See section 2.1.4 to see where this parameter is to be included.

Note: within the CRISIS development team, this combination is known as *Peruzza type* since Prof. Laura Peruzza suggested its implementation and used it during the calculations made in the context of Project S2 (2008-2010) funded by the Italian Civil Protection Authority (Italian Research Project INGV-DPC S2).

- C: For this option, the point geometry model is used together with a normal attenuation model and a parametric seismicity description (either modified G-R or characteristic earthquake). This is an option available in previous versions of CRISIS and there are not compatibility restrictions.
- D: In this option, the point geometry model is used together with normal attenuation models and earthquake probabilities defined by means of generalized Poissonian and non-Poissonian models. This option is mainly used to model the so-called smoothed seismicity but now with probabilities obtained with spatially arbitrarily complex Poissonian or non-Poissonian models. The only compatibility restriction in this option is that the number of vertexes used in the description of the point-sources must be equal to the number of sources provided in the Poissonian or non-Poissonian seismicity files.

Note: within the CRISIS development team, this combination is known as *Warner-type* since Dr. Warner Marzocchi suggested its implementation and used it during the calculations made in the context of Project S2 (2008-2010) funded by the Italian Civil Protection Authority (Italian Research Project INGV-DPC S2).

- E: The gridded seismicity model only works currently together with grid sources are used as geometry model.

2.8.2 Generalized attenuation models

Table 2-30 shows the validity of the combinations for generalized attenuation models.

Table 2-30 Feasibility of generalized attenuation, geometric and seismicity models combination

Geometric model / Seismicity model	Modified G-R	Characteristic earthquake	Generalized non-Poissonian	Generalized Poissonian	Gridded seismicity
Area	AG	AG	BG	BG	EG
Line	AG	AG	BG	BG	EG
SSG	CG	CG	DG	DG	EG
Area-planes	AG	AG	BG	BG	EG
Grid	CG	CG	DG	DG	FG

The codes on each field in this case mean the following:

- **AG:** In this option, line or area geometry models are used and ground motion characteristics are described by means of a generalized attenuation model (see section 2.4.3). This option is not possible to use since generalized attenuation models are associated to known, fixed focal locations while line or area sources account, implicitly for uncertainty about the location of future hypocentres being then incompatible.

In addition, generalized attenuation models contain information about individual events with known (although in some cases irrelevant) magnitudes. Since each event is associated to a fixed value of magnitude, occurrence probabilities for each of the events included in the attenuation model cannot be computed for continuous, arbitrary values of magnitude with the information provided by parametric seismicity descriptions, such as earthquake magnitude exceedance rates. It is important to remember that, starting with magnitude exceedance rates, occurrence probabilities within given timeframes can only be computed for magnitude intervals (magnitude “bins”) and not for point values.

- **BG:** In this option, line or area geometry models are used, seismicity is described by means of a generalized non-Poissonian model and ground motion characteristics are provided through a generalized attenuation model. This is the only option in which generalized attenuation models can be used.

Note that when using this type of ground motion model, locations of earthquake hypocenters are, in principle, unknown and irrelevant. In consequence, specification

of a source location is also, in principle, irrelevant. However, there are two reasons that justify why a source location must be specified:

1. When developing a hazard model using the R-CRISIS interface, it is useful for the modeler to have a visual reference of the source location and,
2. For hazard disaggregation purposes (see Section 2.10), R-CRISIS must know the location to which the hazard coming from all events has to be assigned. For hazard disaggregation purposes, earthquake location is conventionally considered to be the geometrical center of the line or the area source.

On the other hand, since also earthquake magnitudes are fixed (and again, irrelevant) in generalized attenuation models, and each set of grids that represent individual events, it would be impossible to associate the seismicity parameters of the events using parametric descriptions. In view of this, the only possibility is that earthquake occurrence probabilities are assigned using non-Poissonian generalized models. The compatibility conditions for the use of this option are the following:

1. The number of sources in the generalized attenuation model file (*.gaf) must be the same that the number of sites in the generalized non-Poissonian seismicity file (*.nps).
2. The number of magnitudes in the generalized attenuation model file (*.gaf) must be the same that the number of sites in the generalized non-Poissonian seismicity file (*.nps).

Note: within the CRISIS development team, this combination is known as *Stupazzini-Villani type* since Marco Stupazzini and Manuela Villani were the two researches in charge of its development in the context of Project S2 (2008-2010) funded by the Italian Civil Protection Authority (Italian Research Project INGV-DPC S2).

- CG: In this option the geometry of the sources is described through a collection of points and ground motion characteristics using a generalized attenuation model. The use of this combination is considered as impossible since, generalized attenuation models, contain information about individual events with known (although irrelevant) magnitudes. Since each event is associated to a fixed value of magnitude, occurrence probabilities for each of the events contained in the attenuation model cannot be computed for continuous and arbitrary values of magnitude with the information provided by parametric seismicity descriptions (e.g. earthquake magnitude exceedance rates). It is important to remember that, starting with magnitude exceedance rates, occurrence probabilities within given timeframes can only be computed for magnitude intervals (magnitude “bins”) and not for point values.
- DG: Note that this option is like BG except that the source geometry in this case is of point-source type. In principle, this option could have been considered as valid since, when using generalized attenuation models, source geometry is irrelevant. However, the BG option (in which sources can be seen by the modeler) is considered more useful and this one has been inhibited in R-CRISIS to avoid any possible confusion.

- EG: Although methodologically possible, this combination has not yet been implemented.

2.9 Hazard computation algorithm

To compute seismic hazard, the territory under study is first divided into seismic sources according to geotectonic considerations (Cornell, 1968; Esteva, 1970). In most cases, it is assumed that, within a seismic source, an independent earthquake-occurrence process is taking place. For each seismic source, earthquake occurrence probabilities are estimated by means of statistical analysis of earthquake catalogues.

In the more general case, earthquake occurrence probabilities must stipulate the probability of having s events ($s=0, 1, \dots, N_s$) of magnitude M_i in the following T_j years at a given source k . We will denote these probabilities as $P_k(s, M_i, T_j)$ and they completely characterize the seismicity of source k .

Seismic hazard produced by an earthquake of magnitude M_i at a single point source, say the k^{th} source and for the next T_j years, can be computed as:

$$\Pr(A \geq a | M_i, T_j, k) = 1 - \sum_{s=0}^{N_s} P_k(s, M_i, T_j) [1 - \Pr(A \geq a | M_i, R_k)]^s \quad (\text{Eq. 2-57})$$

where $\Pr(A \geq a | M_i, R_k)$ is the probability that intensity a is exceeded given that an earthquake of magnitude M_i occurred at source k , that is separated from the site of interest by a distance R_k . Please note that this probability depends only on magnitude, M , and source-to-site distance, R , and it is normally computed using the probabilistic interpretation of intensities through the use of GMPM. We also note that implicit in equation 2-46 is the assumption that exceedances of intensity values at source k , given that an earthquake of magnitude M_i occurred, are independent from each other. This is the reason why the non-exceedance probability of a given s events of magnitude M_i occurred at source k can be computed as $[1 - \Pr(A \geq a | M_i, R_k)]^s$.

Seismic hazard, contained in equation 2-57, is more easily expressed in terms of non-exceedance probabilities in the following manner:

$$\Pr(A \leq a | M_i, T_j, k) = \sum_{s=0}^{N_s} P_k(s, M_i, T_j) [\Pr(A \leq a | M_i, R_k)]^s \quad (\text{Eq. 2-58})$$

Equation 2-58 gives the non-exceedance probability of intensity value a given that only earthquakes of magnitude M_i occurred. The non-exceedance probability of a , associated to the occurrence of earthquakes of all magnitudes at source k in the next T_j years can be computed as:

$$\Pr(A \leq a | T_j, k) = \prod_{i=1}^{Nm} \Pr(A \leq a | M_i, T_j, k) \quad (\text{Eq. 2-59})$$

where Nm is the number of magnitude bins into which the earthquake occurrence process has been discretized. Again, we have used the independence hypothesis among earthquakes of all magnitudes.

But seismic sources are usually points, lines, areas or volumes, so a spatial integration process must be carried out to account for all possible focal locations. We will assume that the spatial integration process leads to N sources. So finally, if earthquake occurrences at different sources are independent from each other, we obtain that the non-exceedance probability of intensity a in the next T_j years due to earthquakes of all magnitudes located at all sources, can be computed with:

$$\Pr(A \leq a | T_j) = \prod_{k=1}^N \Pr(A \leq a | T_j, k) \quad (\text{Eq. 2-60})$$

$$\Pr(A \leq a | T_j) = \prod_{k=1}^N \prod_{i=1}^{Nm} \Pr(A \leq a | M_i, T_j, k) \quad (\text{Eq. 2-61})$$

$$\Pr(A \leq a | T_j) = \prod_{k=1}^N \prod_{i=1}^{Nm} \sum_{s=0}^{Ns} P_k(s, M_i, T_j) [\Pr(A \leq a | M_i, R_k)]^s \quad (\text{Eq. 2-62})$$

Finally,

$$\Pr(A > a | T_j) = 1 - \prod_{k=1}^N \prod_{i=1}^{Nm} \sum_{s=0}^{Ns} P_k(s, M_i, T_j) [\Pr(A \leq a | M_i, R_k)]^s \quad (\text{Eq. 2-63})$$

Equation 2-63 is the one used by R-CRISIS to compute seismic hazard for situations in which the sources are spatially distributed ($k=1, \dots, N$), there are earthquakes of various magnitudes ($M_i, i=1, \dots, Nm$) and the earthquake occurrence probabilities in known time frames T_j at source k are defined by $P_k(s, M_i, T_j)$, that is, the probability of having s events of magnitude M_i in the next T_j years occurring at source k .

The equations presented herein are, in general, applicable to non-Poissonian occurrence processes. But they are also applicable to the Poissonian process. Let us see what results we obtain if we assume that the occurrence process is Poissonian. Let us assume that in all sources, a Poissonian occurrence process is taking place for earthquakes of all magnitudes. Under this assumption, $P_k(s, M_i, T_j)$ takes the form of, precisely, a Poisson probability distribution:

$$P_k(s, M_i, T_j) = \frac{[\Delta\lambda_k(M_i)T_j]^s \exp[-\Delta\lambda_k(M_i)T_j]}{s!}, s \geq 0 \quad (\text{Eq. 2-64})$$

where $\Delta\lambda_k(M_i)$ is the number of earthquakes of magnitude M_i that, per unit time, take place at source k . In other words, this quantity is the conventional exceedance rate of earthquakes in the range of magnitudes represented by M_i , that is,

$$\Delta\lambda_k(M_i) = \lambda_k \left(\frac{M_i - \Delta M}{2} \right) - \lambda_k \left(\frac{M_i + \Delta M}{2} \right) \quad (\text{Eq. 2-65})$$

Replacing equation 2-55 in equation 2-49 we obtain:

$$\Pr(A \leq a | M_i, T_j, k) = \sum_{s=0}^{\infty} \frac{[\Delta\lambda_k(M_i)T_j]^s \exp[-\Delta\lambda_k(M_i)T_j]}{s!} [\Pr(A \leq a | M_i, R_k)]^s \quad (\text{Eq. 2-66})$$

Note that now the sum extends to infinity since, in the Poisson process, the possible range of values of s ranges from zero (0.0) to infinity. The sum in equation 2-57 has an analytical solution:

$$\Pr(A \leq a | M_i, T_j, k) = \exp\{-\Delta\lambda_k(M_i)T_j [1 - \Pr(A \leq a | M_i, R_k)]\} \quad (\text{Eq. 2-67})$$

$$\Pr(A \leq a | M_i, T_j, k) = \exp\{-\Delta\lambda_k(M_i)T_j \Pr(A \geq a | M_i, R_k)\} \quad (\text{Eq. 2-68})$$

Hence, from equation 2-63 we get that

$$\Pr(A > a | T_j) = 1 - \prod_{k=1}^N \prod_{i=1}^{Nm} \exp\{-\Delta\lambda_k(M_i)T_j \Pr(A \geq a | M_i, R_k)\} \quad (\text{Eq. 2-69})$$

$$\Pr(A > a | T_j) = 1 - \exp\left\{-\sum_{k=1}^N \sum_{i=1}^{Nm} \Delta\lambda_k(M_i)T_j \Pr(A \geq a | M_i, R_k)\right\} \quad (\text{Eq. 2-70})$$

But, under the Poissonian assumption for the earthquake occurrences, the process of intensity exceedances follows also a Poissonian process, for which the exceedance probability of intensity a during the next T_j years is given by:

$$\Pr(A > a | T_j) = 1 - \exp\{-\nu(a)T_j\} \quad (\text{Eq. 2-71})$$

where $\nu(a)$ is the exceedance rate of intensity a . Comparing equations 2-70 and 2-71 we obtain that

$$\nu(a) = \sum_{k=1}^N \sum_{i=1}^{Nm} \Delta\lambda_k(M_i) \Pr(A \geq a | M_i, R_k) \quad (\text{Eq. 2-72})$$

Note that $v(a)$, the well-known Poissonian intensity exceedance rate, does not depend anymore on T_j . In the limit, the inner sum of equation 2-61 can readily be recognized as the integral with respect to magnitude that is present in the conventional Esteva-Cornell approach (Cornell, 1968; Esteva, 1970) to compute Poissonian seismic hazard. The outer sum in equation 2-72 is simply the aggregation of intensity exceedance rates due to all sources. In other words:

$$v(a) = \sum_{k=1}^N \sum_{i=1}^{Nm} \frac{\Delta\lambda_k(M_i)}{\Delta M} \Pr(A \geq a | M_i, R_k) \Delta M \tag{Eq. 2-73}$$

$$v(a) = \sum_{k=1}^N \int_M -\frac{d\lambda_k(M)}{dM} \Pr(A \geq a | M, R_k) dM \tag{Eq. 2-74}$$

Note that, due to the definition we used for $\Delta\lambda_k(M_i)$ in equation 2-73, its sign changed when we converted it to its differential form. We have then shown that equation 2-63, derived for the general non-Poissonian case, is also valid for the Poissonian case, leading to the well-known Esteva-Cornell expression to compute seismic hazard.

The maximum integration distance is a value provided by the user to the R-CRISIS project and also, the way it is spaced between the lower and upper limits of the hazard intensities for each spectral ordinate can be defined. This last refers to the number of points for which the hazard curve is constructed as well as its spacing. Linear and logarithmic scales can be selected. Figure 2-30 schematically shows the results for the same computation site in terms of annual exceedance probabilities with hazard curves constructed by 5 and 15 points, respectively.

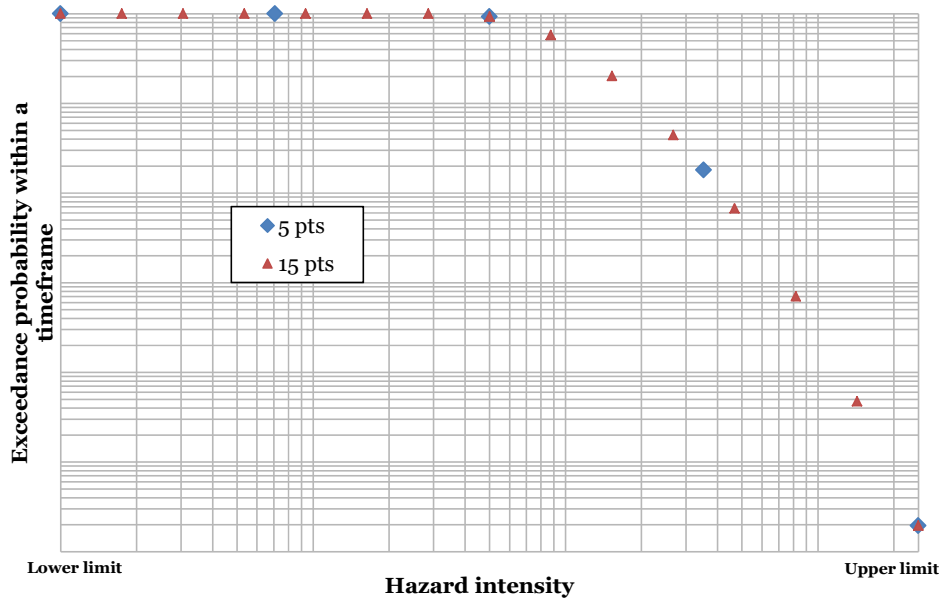


Figure 2-30 Differences due to the number of intensity levels in the hazard plot

Figure 2-31 shows the difference when again, for the same calculation site and using 15 intensity levels, linear and logarithm spacing scales are used.

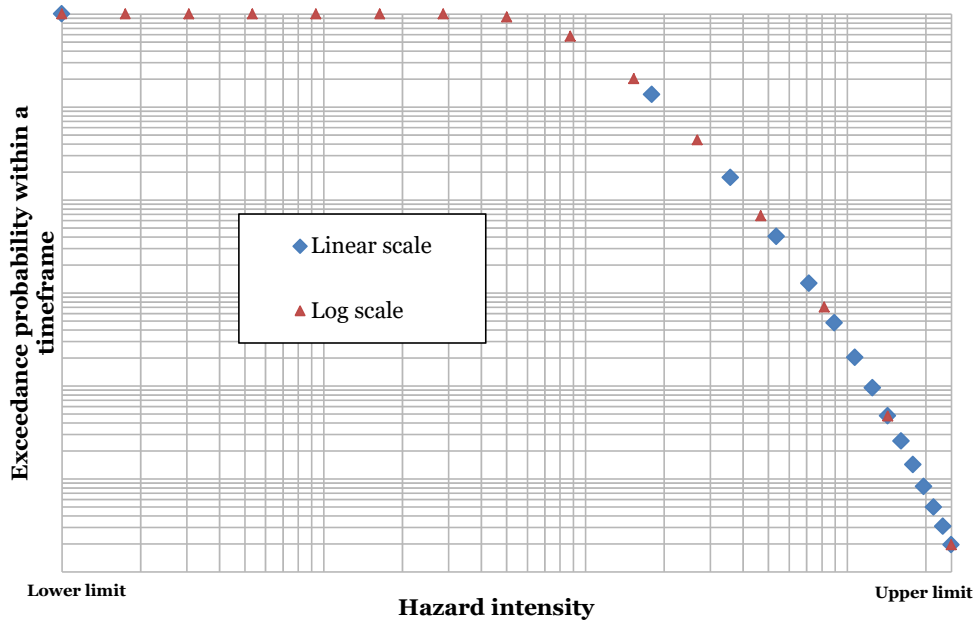


Figure 2-31 Differences due to the distance scaling in the hazard plot

Note: starting with CRISIS2008, the code does not work anymore with intensity exceedance rates as measures of seismic hazard. The more recent versions estimate seismic hazard in terms of probabilities of exceedance of intensity values in given time frames. For instance, a valid measure of seismic hazard in the newer versions is the probability of experiencing peak ground acceleration greater or equal than 0.20g in the next 50 years at a given location. This change was made in order to allow users to introduce in the computations probabilities of earthquake occurrences derived from non-Poissonian models. Poissonian computations, however, are still possible since one can regard this case as a particular case of the non-Poisson computations.

2.10 Hazard disaggregation

2.10.1 Magnitude-distance disaggregation

Consider the basic hazard computation equation (same as equation 2-61 but repeated herein for convenience of the reader)

$$\Pr(A \leq a | T_j) = \prod_{k=1}^N \prod_{i=1}^{Nm} \Pr(A \leq a | M_i, T_j, k) \tag{Eq. (2-61*)}$$

where $\Pr(A < a | T_j)$ is the probability of not exceeding intensity a at a site in the next T_j years, when subjected to a seismic regime composed by N point sources, each of which produces earthquakes of magnitudes M_1, M_2, \dots, M_{Nm} . It can be noted that the product in equation 2-

61* is composed by many terms, each of which corresponds to a particular magnitude value, M_i , and to a specific source-to-site distance, which is the one from source k to the site for which hazard is being computed.

In view of this, the contributions to $\Pr(A < a | T_j)$ or to $\Pr(A > a | T_j)$ could be grouped for a range of magnitudes (i.e. from M_1 to M_2) and a range of distances. This is the magnitude-distance disaggregation. These results indicate which combinations of magnitude and distance contribute more to the seismic hazard at a site, for a given intensity measure, for a given time frame and at certain level of intensity, a in this case.

Let's say that hazard has been disaggregated, leading to a matrix of N_g rows (one for each magnitude range) and N_r columns (one for each distance range). The contents of each cell must be such that the following relation is satisfied:

$$\Pr(A \leq a | T_j) = \prod_{l=1}^{N_r} \prod_{m=1}^{N_m} p_{lm} \quad \text{Eq. (2-75)}$$

In other words, the original non-exceedance probability must be equal to the product of the non-exceedance probabilities disaggregated for each magnitude-distance bin. This means that, opposite to what happens with intensity exceedance rates, which are additive, non-exceedance probabilities (or exceedance probabilities) are not additive but multiplicative, in the sense expressed by equation 2-75. In view of this, when interpreting R-CRISIS disaggregation results, the user must not expect that the exceedance probabilities associated to each cell used for the disaggregation add up to the total exceedance probability computed for the same site, intensity value and time frame.

Note: arithmetic of exceedance probabilities is more complex to that of intensity exceedance rates used in conventional hazard studies.

2.10.2 Epsilon disaggregation

In occasions, it is interesting to know which portions of the intensity probability density function contribute most to the seismic hazard at a given site. Consider the following equation, which is equation 2-61* but written in terms of exceedance probabilities:

$$\Pr(A > a | T_j) = 1 - \prod_{k=1}^N \prod_{i=1}^{N_m} [1 - \Pr(A > a | M_i, T_j, k)] \quad \text{Eq. (2-76)}$$

For a given magnitude, time frame and source location, the term $\Pr(A > a | M_i, T_j, k)$ will be computed by calculating the area shown in green in Figure 2-32.

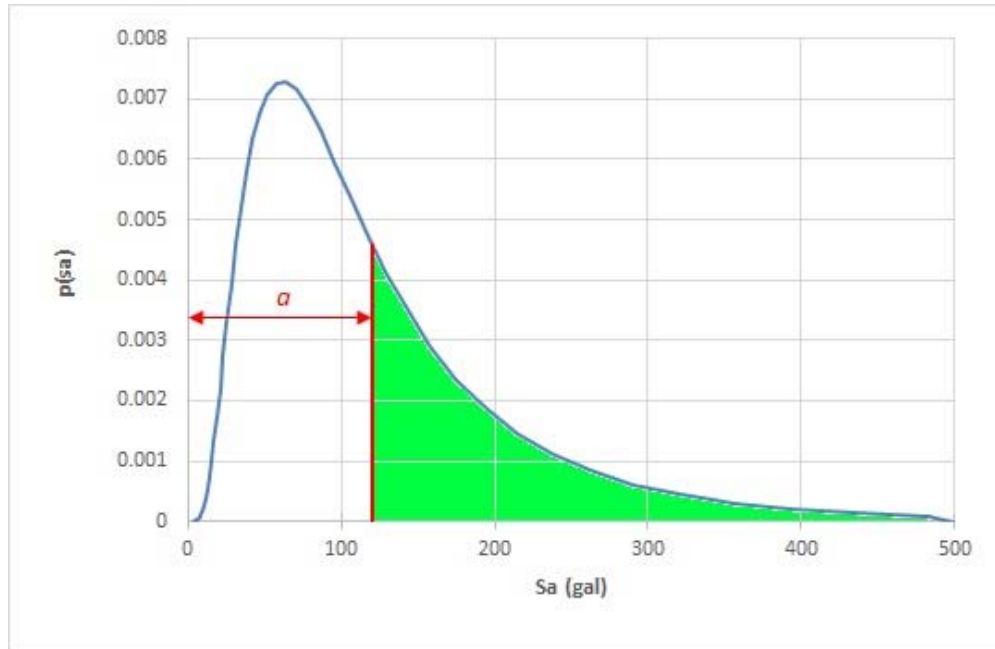


Figure 2-32 Estimation of the non-exceedance probability for given median and standard deviation of the natural logarithm

The example in Figure 2-32 corresponds to a case in which acceleration has a lognormal distribution with median, $MED(A|M1,Tj,k)$ equal to 120 cm/s² and standard deviation of the natural logarithm, σ_{LN} , equal to 0.7.

The shape of the probability density function of Sa depends on magnitude, distance, and GMPM employed, while a is an arbitrarily fixed value: the one for which seismic hazard is being computed.

However, it is sometimes of interest to know how much of the probability marked in green in Figure 2-32 comes from the high percentiles of the distribution. For instance, how much of the green probability comes from the area to the left of value A_{eps} shown in orange in Figure 2-33.

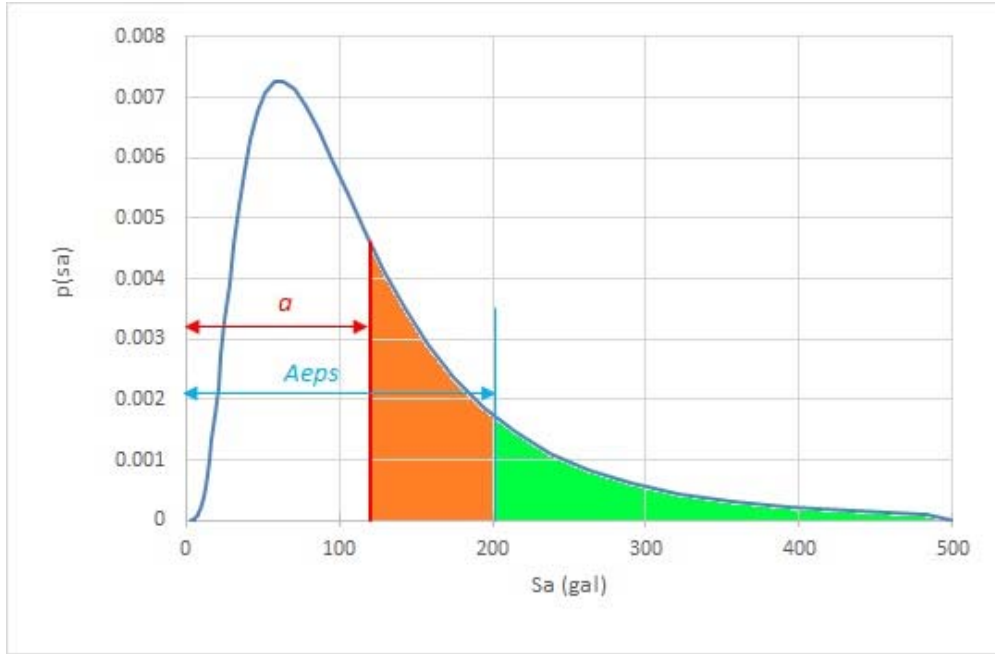


Figure 2-33 Estimation of A_{eps}

Normally, A_{eps} is indexed to an "epsilon" (ϵ) value, such that:

$$A_{eps} = MED(A | M_i, T_j, k) \exp[\epsilon \sigma_{LN}(A | M_i, T_j, k)] \quad \text{Eq. (2-77)}$$

where $MED(A | M_i, T_j, k)$ and $\sigma_{LN}(A | M_i, T_j, k)$ are, respectively, the median and the logarithmic standard deviation of A given the occurrence of an earthquake with magnitude M_i at source k ; the value of ϵ is kept fixed for the whole analysis. In the case of Figure 2-29, $\epsilon=2$ and therefore, $A_{eps}=120 \cdot \exp(2 \cdot 0.7)=201.37$. In view of this, when an epsilon disaggregation is required, exceedance probabilities required to evaluate equation 2-77 are computed with:

$$\Pr(A > a | M_i, T_j, k) = \int_{A_{eps \max}}^{\infty} p_{A|M_i, T_j, k}(u) du \quad \text{Eq. (2-78)}$$

where $p_{A|M_i, T_j, k}(\cdot)$ is the probability density function of A given magnitude M_i at source k , and:

$$A_{eps \max} = \max(A_{eps}, a) \quad \text{Eq. (2-79)}$$

R-CRISIS allows performing the epsilon disaggregation with two different approaches:

1. With an accumulated epsilon where the user defines the value of ϵ_1 and the procedure is done between $-\infty$ and ϵ_1 .
2. Between two predefined epsilon values, where the user defines the values for ϵ_0 and ϵ_1 . $\epsilon_0 < \epsilon_1$.

2.10.3 Interpretation of ε for other probability distributions

Usually, intensity A is assigned a lognormal probability distribution, so equation 2-75 can be used to compute the lower integration limit, A_{eps} . However, it admits the possibility of using four different types of probability distributions, being them: Lognormal, Gamma, Normal and Beta. In the three last cases, the meaning of ε is not unambiguously defined. In R-CRISIS, the following interpretations of ε are adopted:

For the Gamma distribution

$$A_{eps} = E(A | M_i, T_j, k) + \varepsilon \sigma(A | M_i, T_j, k), L \geq 0 \quad \text{Eq. (2-80)}$$

For the Normal distribution

$$A_{eps} = E(A | M_i, T_j, k) + \varepsilon \sigma(A | M_i, T_j, k) \quad \text{Eq. (2-81)}$$

For the Beta distribution

$$A_{eps} = E(A | M_i, T_j, k) + \varepsilon \sigma(A | M_i, T_j, k), 0 \leq L \leq 1 \quad \text{Eq. (2-82)}$$

In the three cases, $E(A | M_i, T_j, k)$ and $\sigma(A | M_i, T_j, k)$ are, the expected value and the standard deviation of A given magnitude M_i at source k , respectively.

2.11 Cumulative Absolute Velocity filter

It is common practice in PSHA to define a threshold magnitude, M_o , to determine from what magnitude on, earthquakes can produce damages in the structures and components of a dwelling in order to only consider those while performing the hazard analyses. Nevertheless, EPRI (2006) proposed that as an alternative to using M_o the Cumulative Absolute Velocity (CAV) can be used. Its value is given by the integral of the absolute value of a strong ground motion recording. There is some agreement that damaging events are those with $CAV > 0.16$ g-sec and for that, the CAV filtering method states that the exceeding probabilities of given values of intensity, a , should be filtered by the probability that $CAV > C_o$ given that a ground motion, with that level of intensity, has occurred. That probability is computed by means of a special type of attenuation relationship that relates the CAV with magnitude, M , and distance, R , (IRSN, 2005; Kostov, 2005).

For a single source, when the hazard integral is formulated in terms of exceedance rates of accelerations, a , this minimum magnitude is included in the following way:

$$\nu(a) = \lambda_0 \int_{M_0}^{M_U} \int_{R_{min}}^{R_{max}} f_m(M) f_R(R) \Pr(A > a | M, R) dR dM \quad \text{Eq. (2-83)}$$

where $\nu(a)$ is the exceedance rate of acceleration a , $f_m(\cdot)$ and $f_R(\cdot)$ are the density of magnitude, M , and distance, R , respectively, and λ_o is the exceedance rate of earthquakes with $M > M_o$ in the seismic source.

A typical value for M_o adopted in seismic hazard studies is $M_w=5.0$. But, as indicated in EPRI (2006), as an alternative to using earthquake magnitude to determine non-damaging earthquakes, it is proposed to use the ground motion measure denoted as Cumulative Absolute Velocity (CAV), given by the integral of the absolute value of a ground motion acceleration recording. To make the CAV value representative of strong ground shaking rather than coda waves the definition of CAV was later restricted to computing CAV for 1-second time windows that have amplitudes of at least 0.025g.

Although the logic behind using CAV filtering is relatively complex (see EPRI, 2006), the general idea in a few words is that the only ground motions that should contribute to the hazard estimations are those with the capability of producing damage to structures; furthermore, there is some agreement in the fact that damaging motions are those with $CAV > 0.16$ g-sec. In view of this, the CAV filtering method states that the exceeding probabilities of given values of intensity a should be weighted (filtered) by the probability that $CAV > C_o$ given that a ground motion with that level of intensity, a , took place.

Although there are other possible approaches, in R-CRISIS the following CAV filtering strategy is used:

$$\nu_F(a) = \lambda_o \int_{M_o}^{M_U} \int_{R_{min}}^{R_{max}} f_m(M) f_R(R) \Pr(A > a | M, R) \Pr(CAV > C_o | M, R) dR dM \quad \text{Eq. (2-84)}$$

where $\nu_F(a)$ is the filtered exceedance rate and $\Pr(CAV > C_o | M, R)$ is the probability that CAV is greater than the threshold value (taken as 0.16g-sec) given that an earthquake with magnitude M took place at distance R . In other words, the probability of having a damaging ground motion given that an earthquake of these characteristics took place.

This probability is computed by means of a special kind of attenuation relations that relate CAV with M and R . This is the case, for example, of the equation defined by the IRSN (2005) using the seismic data of the RFS 2001-01. It is also the case of the equation proposed by Kostov (2006), using the European ground motion database (Ambraseys et al., 2004).

Currently, R-CRISIS uses the following two filtering formulas:

For surface-wave magnitude, M_s

$$\Pr(CAV > C_o | M, R) = \begin{cases} 1 & \text{if } M \leq 5.5 \\ 1 - \Phi(z) & \text{if } M > 5.5 \end{cases} \quad \text{Eq. (2-85)}$$

where:

$$z = \frac{\text{Log}(C_0) - \text{Log}(C | M, R)}{\sigma} \quad \text{Eq. (2-86)}$$

$$\text{Log}(C | M, R) = 0.4354M + 0.0018R - \text{Log}(R) - 0.901 \quad \text{Eq. (2-87)}$$

where $C_0=1.6$ m/s and $\sigma=0.302$

In the above formulas, $M=M_s$ and R is the focal distance, while $F(.)$ is the standard Gaussian probability distribution. This equation was fitted using the RFS-2001.01 (Berge-Thierry et al., 2004) database.

For moment magnitude, M_w

Make (as proposed by Scordilis (2006)):

$$M = \frac{M_w - 2.07}{0.67} \quad \text{Eq. (2-88)}$$

And use the above-mentioned formulas.

2.12 Logic trees

In the context of R-CRISIS, each branch of a logic tree is formed by one data file together with a measure of the degree of belief that the user has on each of the branches of being the "true" one. Results from the different branches, along with the weights assigned to each branch, are computed using the combination rule described next.

Assume that the probability of exceeding level a of intensity measure A at a computation site, in the i^{th} time frame, according to the j^{th} branch of a logic tree is $P_{ij}(A > a)$. Assume also that the probability of being the true one assigned to the j^{th} branch is $w_j, j=1, \dots, N$.

Then, the expected value of $P_{ij}(A > a)$ once all branches have been accounted for, $P_i(A > a)$, is given by:

$$P_i(A > a) = \sum_{j=1}^N P_{ij}(A > a) \cdot w_j \quad \text{Eq. (2-89)}$$

Results of the logic-tree combination will be given in the form of a new hazard model, with an associated *.dat file that will have the base name of the logic-tree file that described the combination but with the extension *.dat.

Note: it is required that the N weights add up to 1.0.

This resulting hazard model can be loaded into R-CRISIS and the corresponding hazard results can be analyzed with it (in order to obtain hazard maps, exceedance probability curves, uniform hazard spectra) as if they were the results of a regular *.dat file. Disaggregation results, however, cannot be obtained for the hazard resulting from the logic-tree combination.

Note: for a better understanding of the underlying framework of logic trees in R-CRISIS, a careful reading of the paper published by Bommer et al. (2005) is suggested.

2.13 Optimum spectra

Although establishing the design coefficient values associated to a fixed return period by means of probabilistic methodologies is a remarkable step towards the achievement of seismic safety, they do not necessarily lead to optimum design coefficients, which, as proposed by Esteva (1970) are optimal if they minimize the sum of the expected cost associated to the decision of having used that value in the design of the structure. This said in other words, means that an optimum design is that one which minimizes the sum of the initial construction cost and the net present value of the future losses because of earthquakes.

Following the methodology proposed by Rosenblueth (1976) and Whitman and Cornell (1976), to estimate the optimum earthquake design coefficients, a PSHA is first needed to be performed in R-CRISIS to obtain the hazard intensity rates $v(a)$ at the locations where the design coefficients are to be established. Then, after establishing a set of descriptors that account for the cost of the structures as a function of the design coefficient and by selecting an appropriate discount rate to consider the value of money in the future, it is possible to obtain optimum values for those design coefficients.

The methodology implemented in R-CRISIS follows the next assumptions:

1. The earthquake occurrence in the future is characterized by means of a Poissonian process
2. The initial cost of the building as well as the cost of future losses because of earthquakes depend only on one parameter, c , which is the nominal design resistance quantified in terms of the base shear
3. Time starts for every building once its construction phase has finished, and,
4. Every time the seismic demand exceeds the capacity, there is a total loss of the building.

The optimum design approach explicitly accounts for the economic factors involved during the construction and life-service time of a building; this is done by selecting the coefficient value that minimizes the initial construction cost, C_I as well as the one associated to the future losses because of earthquakes, C_{FL} . The total cost of the structure C_T is thus the sum of both.

$$C_T = C_I + C_{FL} \quad \text{Eq. (2-90)}$$

Since all the costs are function of the design coefficient, c , they are denoted as $C_I(c)$, $C_{FL}(c)$ and $C_T(c)$ and then, equation 2-81 can be rewritten as

$$C_T(c) = C_I(c) + C_{FL}(c) \tag{Eq. (2-91)}$$

Figure 2-34 explains schematically the optimum coefficient approach where the red line, representing C_I , increases as c does whereas the blue line, representing C_{FL} , decreases as c increases. Finally, the green plot represents the utility function to be optimized and from where the optimum value of c is obtained.

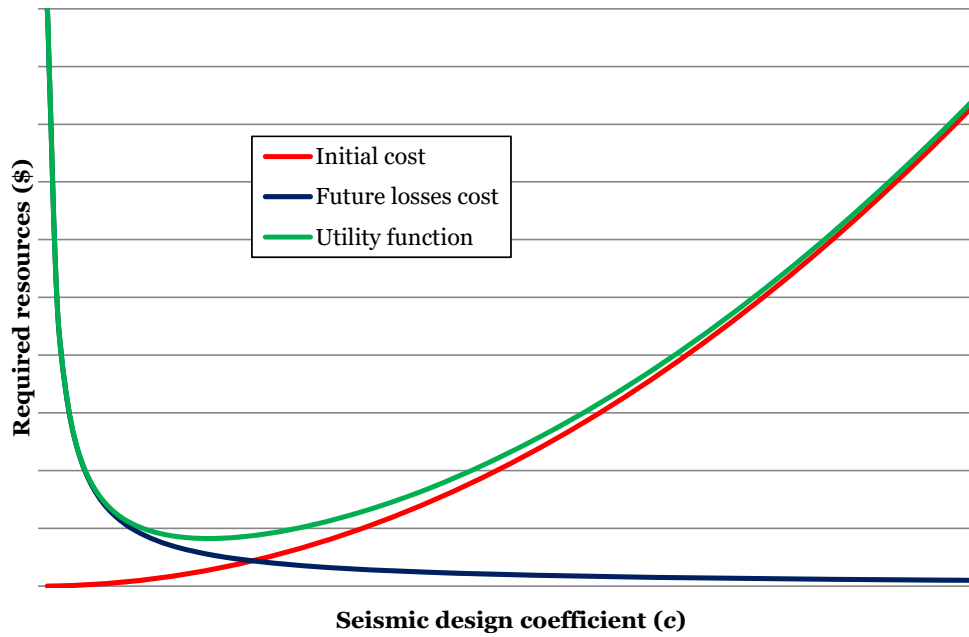


Figure 2-34 Optimum design framework

If the building was to be designed only by considering the gravitational loads, there would still be a cost associated to it, here forth referred to as C_0 . That same building will also have an implicit lateral resistance, which under this framework is considered as free of charge and denoted as c_0 . The initial cost of the structure can be then calculated as

$$C_I(c) = C_0 + C_{Res} (c - c_0)^\alpha \tag{Eq. (2-92)}$$

where C_{Res} is the cost of the planned and paid lateral resistance and α is a parameter that considers the cost increase of the structure with increasing design coefficient. If equation 2-92 is normalized by C_0 , it can be rewritten as

$$\frac{C_I(c)}{C_0} = 1 + \frac{C_{Res}}{C_0} (c - c_0)^\alpha \tag{Eq. (2-93)}$$

and, if the ratio between C_{Res} and C_0 is denoted as ϵ , equation 2-81 finally transforms into

$$\frac{C_I(c)}{C_o} = 1 + \varepsilon(c - c_o)^\alpha \quad \text{Eq. (2-94)}$$

Within this methodology, it is assumed that $c \geq c_o$ since the latter is generally very low.

The net present value of the future losses of the building because of earthquakes needs to be calculated and it is also a function of the design coefficient. $NPV_{FL}(c)$ is then calculated as

$$NPV_{FL}(c) = C_I(c) \cdot (1 + S_L) \cdot \frac{\nu(c)}{\mu} \quad \text{Eq. (2-95)}$$

where S_L accounts for secondary losses and those that occur due to human losses, $\nu(c)$ is the exceedance rate of the seismic demand and μ is the discount rate that considers the value of money in the future.

Once the optimum value of c has been established, its associated mean return period is obtained from the hazard plot at each location. This leads to seismic hazard maps which values have variable mean return periods that are reflected in a smoother transition between adjacent zones.

Finally, the mean return period variable is truncated to a minimum and maximum value, T_{Min} and T_{Max} . The first one to follow the building code philosophy of establishing minimum requirements while the second one is used to avoid the appearance of accelerations associated to not feasible earthquakes in zones of very low seismic activity.

2.14 Stochastic catalogue generator

Based on the geometry and seismicity parameters assigned to each of the sources, and when Poissonian occurrence models have been assigned to them, it is possible in R-CRISIS to generate stochastic catalogues. These catalogues represent a possible realization of a random occurrence in space and time within a defined duration (in years) specified by the user.

The generation of the stochastic catalogues is available when using any Poissonian seismicity model in combination with any of the following geometric models:

- Line fault
- Rectangular fault
- Area-planes
- Point
- Area
- Slabs
- Grids

One relevant aspect when generating stochastic catalogues is guaranteeing that the events are compatible with the base information in the sense that, for instance, those events occur only

within the boundaries of the seismic sources and that the magnitudes and number of events in each observation timeframe, are in line with the recurrence models that were used to characterize the earthquake occurrence at each source. Next, a description of the validation processes for the location, magnitude and number of events followed when implementing this feature in R-CRISIS is presented.

2.14.1 Validation of location of events

The validation of the location of generated events using this feature in R-CRISIS was validated for all the possible geometry models. In all cases a duration of 100 years was used and different shapes, including complex geometries, were used. First, Figure 2-35 shows the validation for the case of a line-fault where the geometry of the source is displayed as the red line whereas the epicenters correspond to the blue dots.

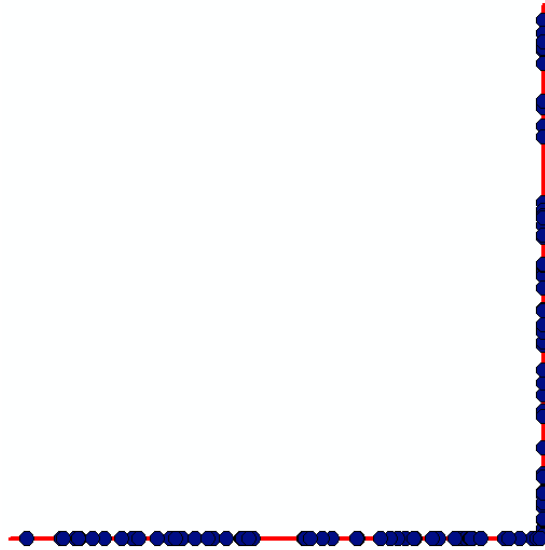


Figure 2-35 Validation of the location for the stochastic catalogue generated for line faults.

Figure 2-36 shows the validation for the case of a rectangular fault, with the upper lip as indicated in the red line, with dip of 45° and width of 20km; the epicenters in this case correspond again to the blue dots. The depth of the events varies in accordance to the inclined plane formed by this rectangular fault.

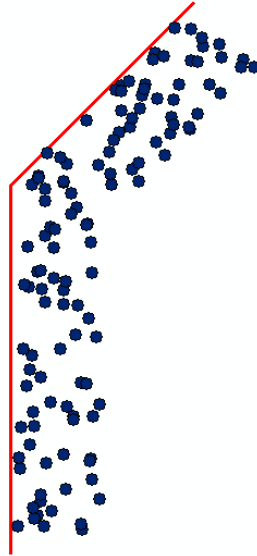


Figure 2-36 Validation of the location for the stochastic catalogue generated in a rectangular fault

Figure 2-37 shows the validation for the case of an area-plane with complex geometry. The boundaries of the source are depicted by the red polygon whereas the epicenters correspond to the blue dots.

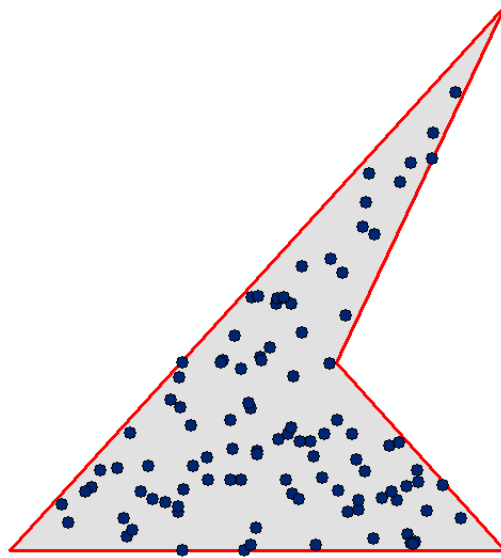


Figure 2-37 Validation of the location for the stochastic catalogue generated in an area-plane

Figure 2-38 shows the validation for the case of point sources (SSG) where the location of the sources is depicted by the red squares whereas the epicenters associated to the stochastic catalogue by the blue dots.



Figure 2-38 Validation of the location for the stochastic catalogue generated in point sources (SSG)

Figure 2-39 (left) shows the validation for the case of area sources where behavior is set as normal (ruptures can go beyond the boundaries of the source). The boundaries of the source are depicted by the red polygon whereas the epicenters by the orange dots. Figure 2-39 (right) shows the validation for the case of again, area sources, but now with the behavior set as treat as fault. In the second case, it is evident that epicenters (depicted by blue dots) are not that close to the boundaries of the polygon if compared to the normal behavior case.

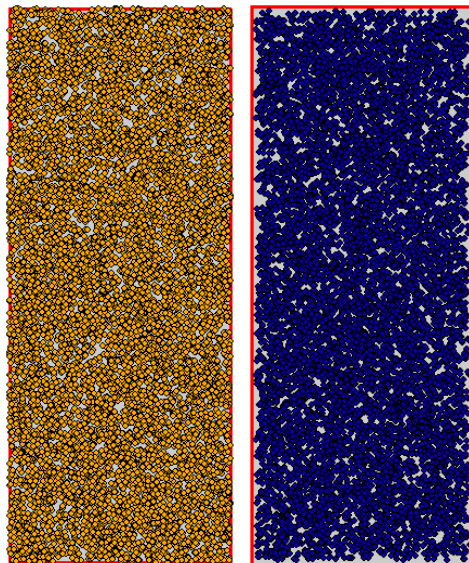


Figure 2-39 Validation of the location for the stochastic catalogue generated in area sources.
Left: normal behavior. Right: treat as fault behavior

Figure 2-40 shows the validation for the case of a slab source comprised by three slices which dip is equal to 80° and have all an equal width of 15km. The upper part of the slab is depicted

by the red polygon whereas the blue dots correspond to the epicenters. From the latter it is possible to visualize the geometry and alignment of the three slices that are part of this source.

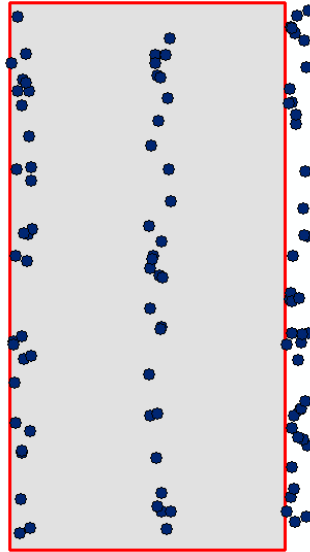


Figure 2-40 Validation of the location for the stochastic catalogue generated in slab sources

Figure 2-41 shows the validation for the case of a grid source which boundaries are depicted by the red polygon. Epicenters (shown as blue dots) occur only at the location of the nodes of the grid, in this case with equal spacing in both orthogonal directions. Depths are the same (as of the grid) for all the events.

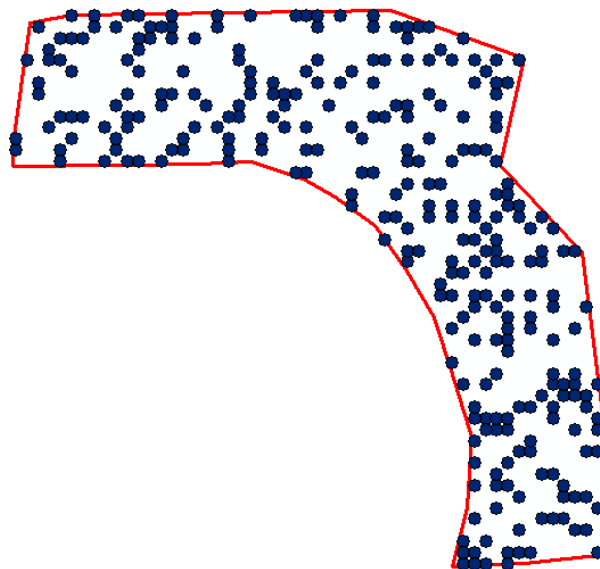


Figure 2-41 Validation of the location for the stochastic catalogue generated in gridded sources

2.14.2 Validation of magnitude and number of events

Figure 2-42 shows the comparison of the modified G-R recurrence relationships for a source which seismic parameters λ_0 , β and M_U are 1.0, 2.0 and 8.0 respectively, and those estimated using the maximum likelihood methodology (McGuire, 2004) for a stochastic catalogue of 100 years duration. Knowing that 100 years is not a long enough observation window, it should not be a surprise that moderate to large earthquakes, although feasible of occurring at that source, are not part of the events included in the stochastic catalogue. λ_0 and β for the stochastic catalogue with 100 years duration are in this case equal to 1.02 and 2.17, respectively.

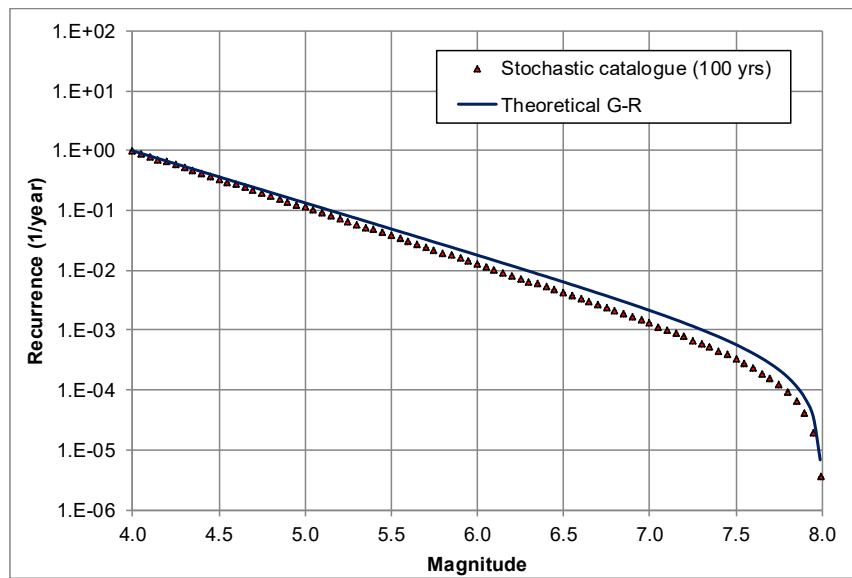


Figure 2-42 Comparison of theoretical G-R recurrence plots for theoretical values and a stochastic catalogue with 100 years duration

If the duration of the catalogue is increased to a long enough timeframe (e.g. 10000 years), the same comparison yields the results shown in Figure 2-43, matching almost exactly the theoretical values. λ_0 and β for the stochastic catalogue with 10000 years duration are in this case equal to 1.01 and 2.02, respectively.

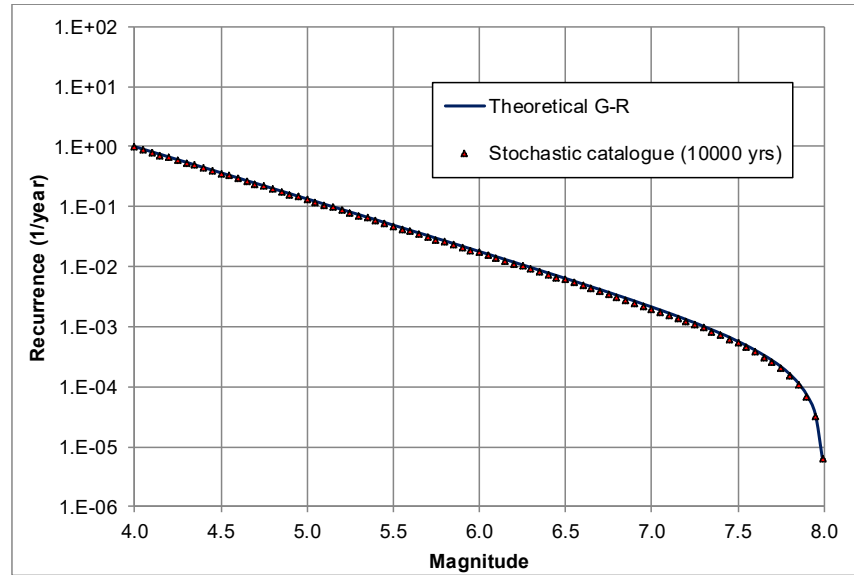


Figure 2-43 Comparison of theoretical G-R recurrence plots for theoretical values and a stochastic catalogue with 10000 years duration

2.15 Conditional mean spectrum

The conditional mean spectrum (CMS) is a spectrum that incorporates correlations across periods to estimate the expected pseudo acceleration values, S_a , at all periods T , given the target S_a value at the period of interest T^* , $S_a(T^*)$. R-CRISIS implements a procedure to calculate the “exact” conditional spectrum (CS) instead of the CMS, which uses mean values of M , R and other parameters related to the GMPEs.

R-CRISIS calculates the exact CS following the aggregation approach method proposed by Lin et al. (2013), which uses the same event set used in the PSHA computation to aggregate the hazard. To calculate the CS, it is necessary to:

- Define the calculation site. R-CRISIS will set the calculation site as the city or grid point that lies closest to the click point.
- Define the period of interest: choose the period of interest, T^* , for which the CS will be calculated. The periods for which the CS calculation are available are those defined for the PSHA in R-CRISIS.
- Set either the target intensity, $S_a(T^*)$, or the exceedance probability, P_e . Choose the intensity value for which CS results will be presented or choose the desired exceedance probability (R-CRISIS will compute the exceedance probability if the intensity is given, or the intensity if the exceedance probability is provided).
- Choose the inter-period correlation model: in the calculation model, it is necessary to establish the inter-period correlation model $\rho(T^*, T)$. Two models are available for this in R-CRISIS, the one by Baker and Jayaram (2008) and the model by Jaimes and Candia (2019).

Once these parameters are defined, R-CRISIS will calculate the CS, given a target value at the period of interest, $Sa(T^*)$, using the following equation.

$$\mu \ln Sa(T_i) | \ln Sa(T^*) = \sum_k \sum_j p_{j,k}^d \times \mu \ln Sa_{j,k}(T_i) | \ln Sa(T^*) \quad \text{Eq. (2-96)}$$

where $p_{j,k}^d$ is the mean annual exceedance frequency of the j^{th} event (earthquake) and k^{th} logic-tree branch, normalized by the total aggregated hazard and,

$$\mu \ln Sa(T_i) | \ln Sa(T^*) = \mu \ln Sa_k(M_j, R_j, \theta_j, T_i) + \rho(T^*, T_i) \cdot \varepsilon_j(T^*) \cdot \sigma \ln Sa_k(M_j, \theta_j, T_i) \quad \text{Eq. (2-97)}$$

where $\mu \ln Sa_k$ is the natural logarithm of the intensity Sa associated to event j given a magnitude M_j , distance R_j , other parameters θ_j and spectral period T_i . $\rho(T^*, T_i)$ is the correlation between the period of interest, T^* , and the spectral period T_i , $\varepsilon_j(T^*)$ is the number of standard deviations b which $\ln Sa(T_i)$ differs from the mean spectral ordinate predicted by a given GMPE, $\mu \ln Sa(M, R, \theta, T_i)$, at T_i .

$$\varepsilon(T_i) = \frac{\ln Sa(T_i) - \mu \ln Sa(M, R, \theta, T_i)}{\sigma \ln Sa(M, \theta, T_i)} \quad \text{Eq. (2-98)}$$

$\sigma \ln Sa_k(M_j, \theta_j, T_i)$ is the standard deviation of $\mu \ln Sa_k(M_j, R_j, \theta_j, T_i)$. Finally, the standard deviation associated to the CS is also calculated as:

$$\sigma \ln Sa | \ln Sa(T^*) = \sqrt{\sum_k \sum_j p_{j,k}^d \left[\sigma_{\ln Sa_{j,k}(T_i) | \ln Sa(T^*)}^2 + (\mu \ln Sa_{j,k}(T_i) | \ln Sa(T^*) - \mu \ln Sa(T_i) | \ln Sa(T^*))^2 \right]} \quad \text{Eq. (2-99)}$$

where,

$$\sigma \ln Sa_{j,k}(T_i) | \ln Sa(T^*) = \sigma \ln Sa_k(M_j, \theta_j, T_i) \times \sqrt{1 - \rho^2(T_i, T^*)} \quad \text{Eq. (2-100)}$$

As the reader might have noted, all the calculation process has been done in terms of the natural logarithm; this happens because it is assumed that the GMPEs involved follow a lognormal probability distribution. Therefore, when using GMPEs that are not lognormally distributed (e.g., truncated, gamma, hybrid, etc.), the CS will only be computed approximately.

Figure 2-44 shows an example of CS calculation for 2.0s spectral period, 143 cm/s² target intensity and Jaimes and Candia (2019) inter-period correlation model. Curves of CS \pm one standard deviation are also plotted.

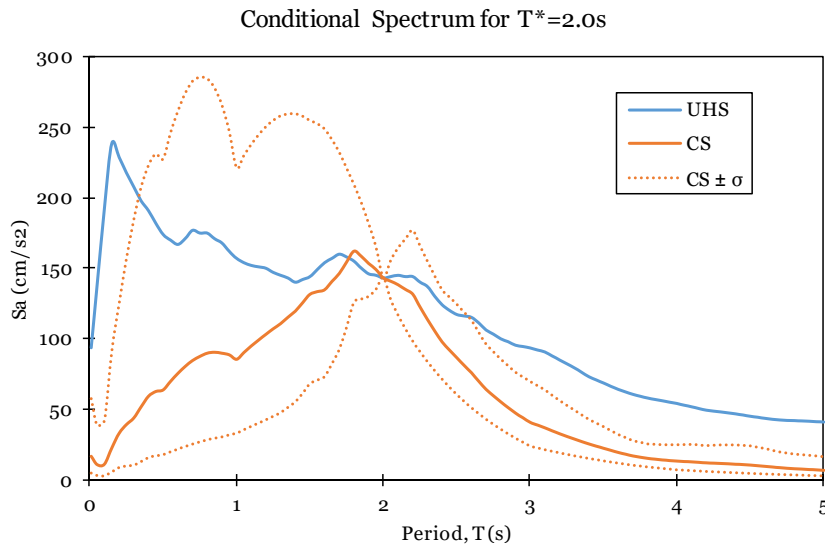


Figure 2-44 Conditional Spectrum for $T^*=2.0s$ and Jaimes and Candia (2019) inter-period correlation model

2.16 Probabilistic liquefaction hazard analysis

Most of the methods commonly used to assess the susceptibility to liquefaction aim to estimate the safety factor (F_s) against liquefaction, or the probability of liquefaction occurrence triggered by an earthquake with known parameters, once the relevant characteristics of a soil profile are available. This approach usually considers only one event, usually referred to as the Maximum Credible Earthquake (MCE) and therefore, it is impossible to know how frequently liquefaction can occur since there is just a vague link between the MCE and its frequency of occurrence.

The safety factor against liquefaction, F_s , is estimated as:

$$F_s = \frac{CRR}{CSR} \tag{Eq. (2-101)}$$

where CRR is the Cyclic Resistance Ratio and CSR the Cyclic Stress Ratio.

Since there are many other earthquakes besides the MCE that can contribute, with a non-negligible share, to the liquefaction probability, R-CRISIS allows a rigorous probabilistic liquefaction hazard analysis (PLHA) that is performed within a framework mostly taken from PSHA and using an event-based approach. On this approach, the effects of multiple (generally thousands of) earthquakes with different magnitudes, locations and occurrence frequencies are considered, knowing also that the ground motions of these earthquakes can be only predicted with large uncertainties and that site effects can modify seismic waves.

Several authors have proposed ways to adapt the deterministic models to probabilistic frameworks and proposed empirical expressions to estimate the liquefaction probability for

a given event. For instance, Ku et al. (2012) have proposed the following expression, which is the probabilistic version of the Robertson and Wride method for liquefaction evaluation:

$$P_L = \frac{1}{1 + \left(\frac{F_s}{0.9}\right)^{6.3}} \quad \text{Eq. (2-102)}$$

Where P_L is the probability of experiencing liquefaction given that the earthquake characterized by the a_{max} and M values has occurred.

In this methodology, the same framework of PSHA is followed but for a better understanding, the hazard analysis is performed by summing individual events rather than in terms of integrals. Then, the annual frequency of occurrence of liquefaction, at a given depth, z , $\nu_L(z)$, can be estimated as:

$$\nu_L(z) = \sum_{i=1}^N \Pr(\text{Liquefaction at depth } z | \text{Event } i) \cdot F_{ai} \quad \text{Eq. (2-103)}$$

where N is the total number of events that are part of the stochastic catalogue, $\Pr(\text{Liquefaction at depth } z | \text{Event } i)$ is the probability of experiencing liquefaction at depth z given that the i^{th} event occurred and F_{ai} is the annual occurrence frequency of the i^{th} event.

An individual earthquake is characterized by several parameters, θ , such as its magnitude, hypocentral location, rupture area and orientation of the fault plane, among others. Therefore, the term $\Pr(\text{Liquefaction at depth } z | \text{Event } i)$ requires calculating the liquefaction probability for an event with given θ parameters and not only by an event defined by its a_{max} and M values. Within a PSHA framework, a_{max} is usually modelled as a random variable to account for uncertainties in the GMPM, in view of which, $\Pr(\text{Liquefaction at depth } z | \text{Event } i)$ is computed as:

$$\Pr(\text{Liquefaction at depth } z | \text{Event } i) = \int_0^{\infty} \Pr(\text{Liquefaction at depth } z | a_{max}, M) \cdot p(a_{max} | \theta_i) da_{max} \quad \text{Eq. (2-104)}$$

where $p(a_{max} | \theta_i)$ is the probability density function of a_{max} given the parameters θ_i that characterize this event. This PDF is usually furnished by the GMPM (or combination of GMPMs) that is being used and, very importantly, by a soil response analysis since a_{max} is the PGA at the surface of the soil deposit whose liquefaction potential is being assessed. On the other hand, Eq. 2-102, 2-103 and 2-104 illustrate the linkage between conventional liquefaction analysis methods and PSHA. These equations are useful to estimate the annual occurrence frequency of liquefaction, not triggered by a single event but in a complex seismic environment characterized by a stochastic earthquake catalogue and one or more GMPMs.

In the current version, R-CRISIS has implemented the liquefaction probability estimation after Robertson and Wride, but any other approach that allows estimating liquefaction probabilities can be implemented within the above explained framework.

Typical results of a PLHA are shown in Figure 2-45. where, for different depths, the annual occurrence rate of liquefaction, the return period of the liquefaction occurrence and the probability of liquefaction occurring within a timeframe of 50 years are shown.

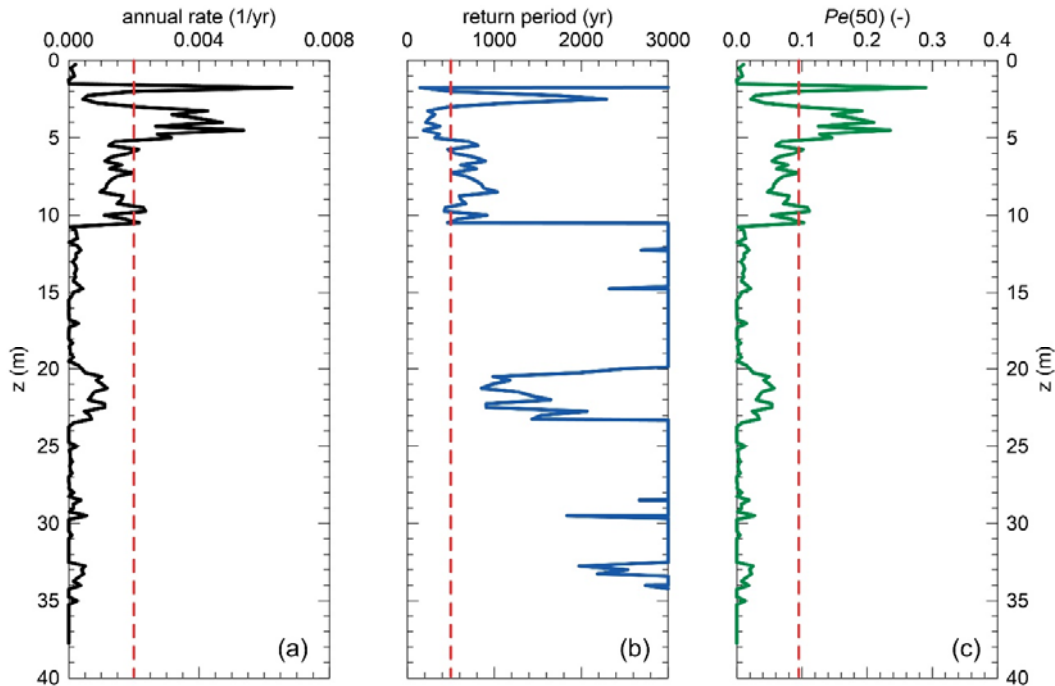


Figure 2-45 PLHA results in terms of annual exceedance rates (a), return periods (b) and occurrence probability in the next 50 years (c)

3 Creating a PSHA project in R-CRISIS

3.1 Introduction

This section shows a description of the different menus, options and input parameters available on R-CRISIS that are to be used for the creation of a R-CRISIS project through the GUI. Those are explained using a hands-on example, which dataset accompanies this user manual with the objective that it can be easily replicated by the user at any moment.

The geometry and seismicity data for each seismic source of this example is included in the accompanying Excel files denoted as: `Sources_geometry.xlsx` and `Seismicity_parameters.xlsx`. Also, the fundamental periods associated to the 10 spectral ordinates used in the example are included in the `Spectral_ordinates.xlsx` file.

The hypothetical example used herein corresponds to a fictitious location referred to as *CAPRA Island* and uses different geometry models for the sources (area, area plane, volume and grids) together with different seismicity models (modified G-R and characteristic earthquake) and different attenuation models (built-in and hybrid GMPM) for them.

In R-CRISIS the projects (*.dat or *.xml files¹⁴) are created by means of the GUI which has several screens and menu items. Those are available from the main screen of R-CRISIS once the program has been launched and the welcome screen has been closed.

The access to the different screens and options can be done by either selecting them from the different menus (those inside the red rectangle in Figure 3-1) or directly from the buttons (those inside the green rectangle in Figure 3-1) located at the main screen of the program.

¹⁴ From v20 onwards, the default saving format has been set to *.xml. However, the user also has the possibility to save the new files in the classic *.dat format

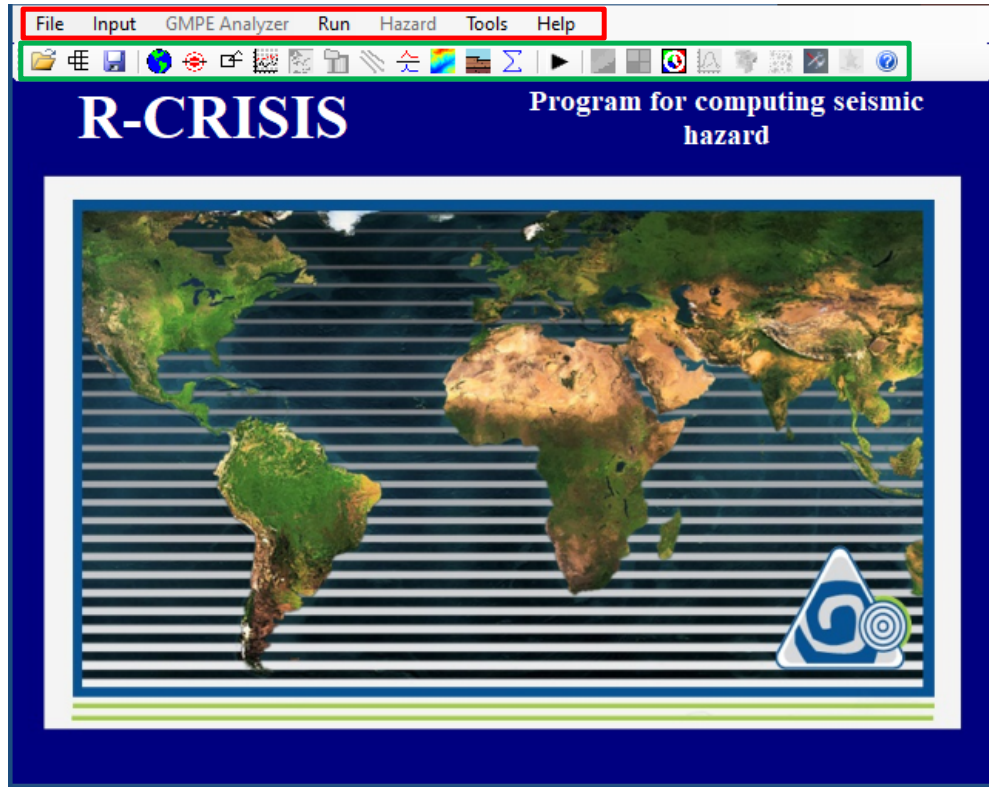







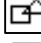

Figure 3-1 Access to menus and tools from the main screen of R-CRISIS



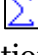

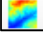

The screens and/or options of R-CRISIS are classified in the seven menus as explained next. For more details about each option, it is indicated in brackets the section of this V&V document where the complete explanation of its use is included.

File

- New
- Open  (see Section 3.2.1)
- Open logic-tree  (see Section 3.2.2)
- Save as...  (see Section 3.3.12)
- Add source data from shape
- Export source data to shape
- Exit

Input


- Maps (optional)  (see Section 3.3.1)
- Grid of sites  (see Section 3.3.2)
- Source geometry  (see Section 3.3.3)
- Source seismicity  (see Section 3.3.5)

- Attenuation data  (see Section 3.3.6)
- Spectral ordinates  (see Section 3.3.4)
- Global parameters  (see Section 3.3.10)
- Set output files (optional) (see Section 3.3.11)
- Site-effects (optional)  (see Section 3.3.8)
- Digital elevation model (optional) 
- Liquefaction analysis  (see Section 3.4.9)






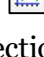

GMPE Analyzer

- GMPE Analyzer  (see Section 3.3.7)

Run

- Validate and run  (see Section 3.3.13)

Hazard

- See hazard maps  (see Section 3.4.1)
- Disaggregation charts  (see Section 3.4.2)
- Batch disaggregation  (see Section 3.4.3)
- CAPRA scenario generation  (see Section 3.4.4)
- Event-set generation  (see Section 3.4.5)
- Conditional Mean Spectrum  (see Section 3.4.10)
- Optimum spectra  (see Section 3.4.8)

Tools

- GMPE branch construction (see Section 3.4.6)
- Map comparer (see Section 3.4.6)
- Site-effects file conversion
- Non-Poisson file conversion

Help

- Index
- About CRISIS
- Supported GMPE
- Supported dimensions

An explanation of each screen is provided next showing, in all cases, the input data required and the different options that the user can choose during the development of a PSHA project in R-CRISIS.

3.2 File administration

The menus and buttons that have to do with the storage (saving and opening) of the R-CRISIS projects together with the management and development of logic-tree analyses are included in the “file administration” category. Those can be accessed by selecting the buttons inside the red rectangle in Figure 3-2.

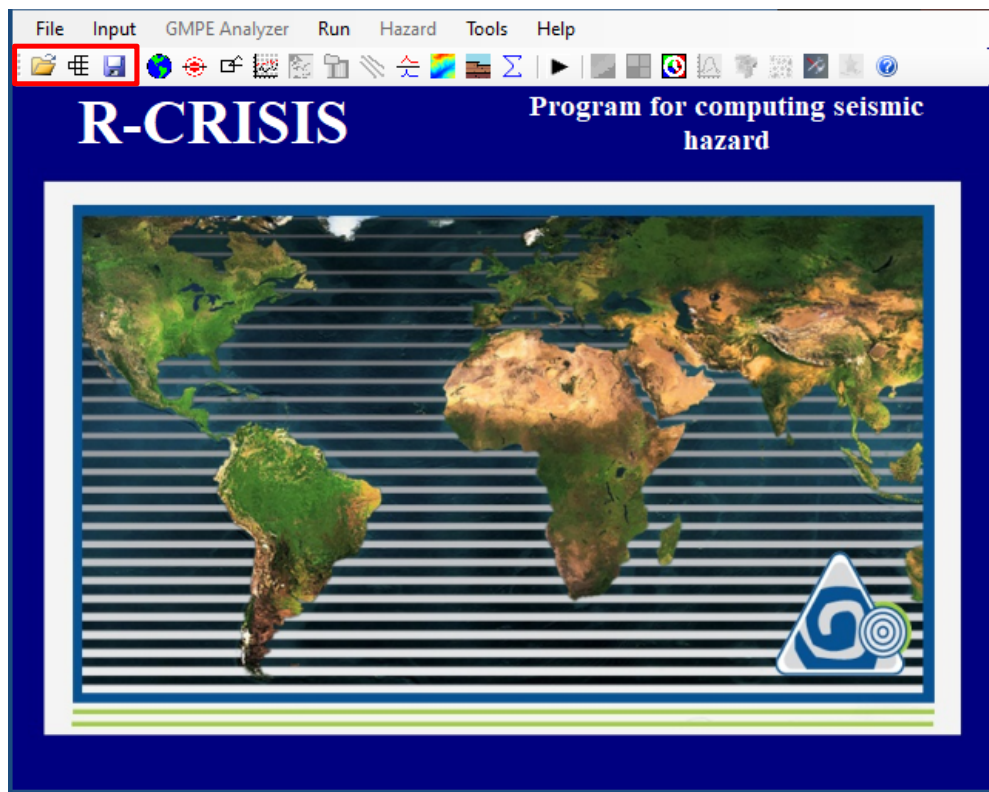



Figure 3-2 File administration buttons in R-CRISIS

3.2.1 Opening existing project

To open an existing R-CRISIS project (*.dat or *.xml file) the  button in the main screen of R-CRISIS needs to be selected. After clicking on it, the explorer window will be displayed as shown in Figure 3-3 where the user first needs to indicate the path where the *.dat or *.xml file is stored and then double click on its name to open the file. Note that at the bottom right (red rectangle) the user can define the extension of the files that are displayed when accessing this screen.

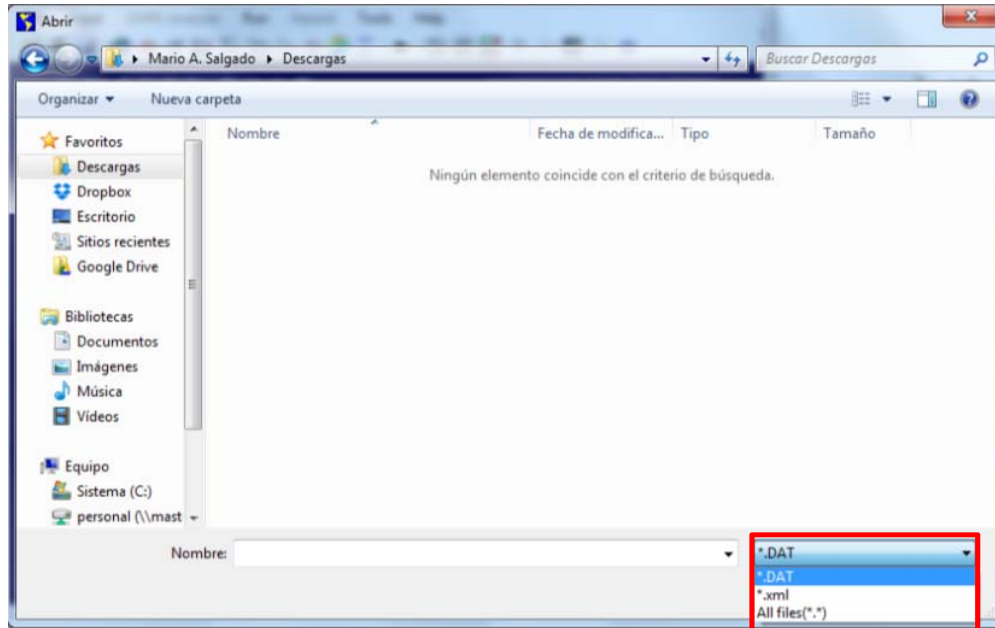




Figure 3-3 Opening a existing project in R-CRISIS

3.2.2 Logic-tree calculations

The logic tree button, , opens a window as the one shown in Figure 3-4 where the user can add different R-CRISIS projects (*.dat files) and assign to each of them their relative weights in order to be considered in a subsequent logic-tree calculation.

To add a branch, the user must click on the “add branch” button, , in the main screen of R-CRISIS and load the corresponding *.dat files. This process is to be repeated as many times as branches to be included. Note that a minimum of two different *.dat files must be considered in order to perform a PSHA with the logic-tree approach. The available branches are displayed with full name and path as shown in Figure 3-4 and then, the relative weights are defined by the user in the fields shown within the red rectangle; with this, their associated probabilities are calculated automatically as shown in the green rectangle.

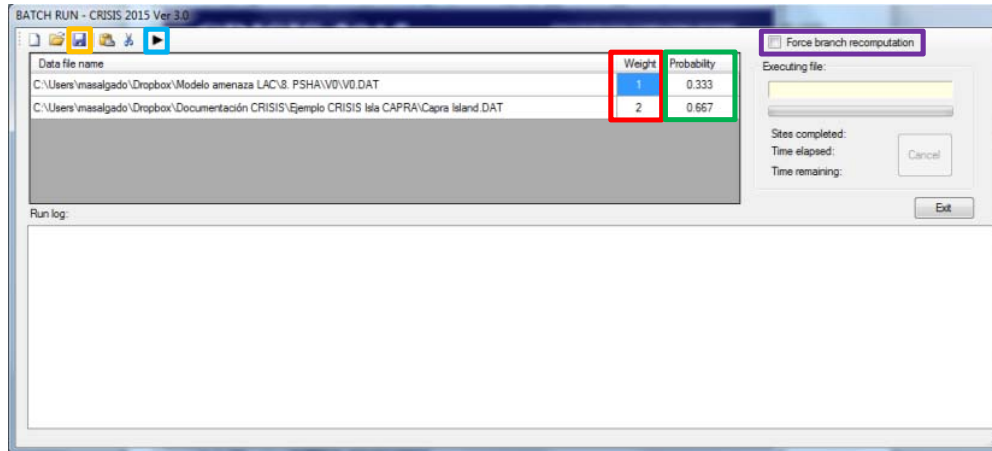



Figure 3-4 Logic-tree calculations screen in R-CRISIS

Before performing any computation, the logic tree must be saved onto disk using the “save LTC file” button (orange rectangle shown in Figure 3-3) and defining the path of the logic tree project (*.ltc¹⁵ extension). After this, the PSHA that uses the logic-tree approach can be started by clicking on the “compute LTC combination” button (blue rectangle in Figure 3-3). Results are saved at the same path where the *.ltc file has been stored.

The force branch recomputation option (purple rectangle in Figure 3-4) can be used to guarantee that for each PSHA that uses the logic-tree approach, all the R-CRISIS projects involved in the project are recalculated.

3.2.3 Saving a project

To save the seismic hazard project on disk, the user must click on the “save data file” button, , on the main screen of R-CRISIS. This will display an explorer window where the storage path is to be indicated by the user. Once the project has been successfully stored on disk, the name specified by the user is displayed at the top of the main window of CRISIS as shown in the red rectangle of Figure 3-5.

Note: in this example, the *.dat file is called *Capra Island*.

¹⁵ Logic Tree Calculation

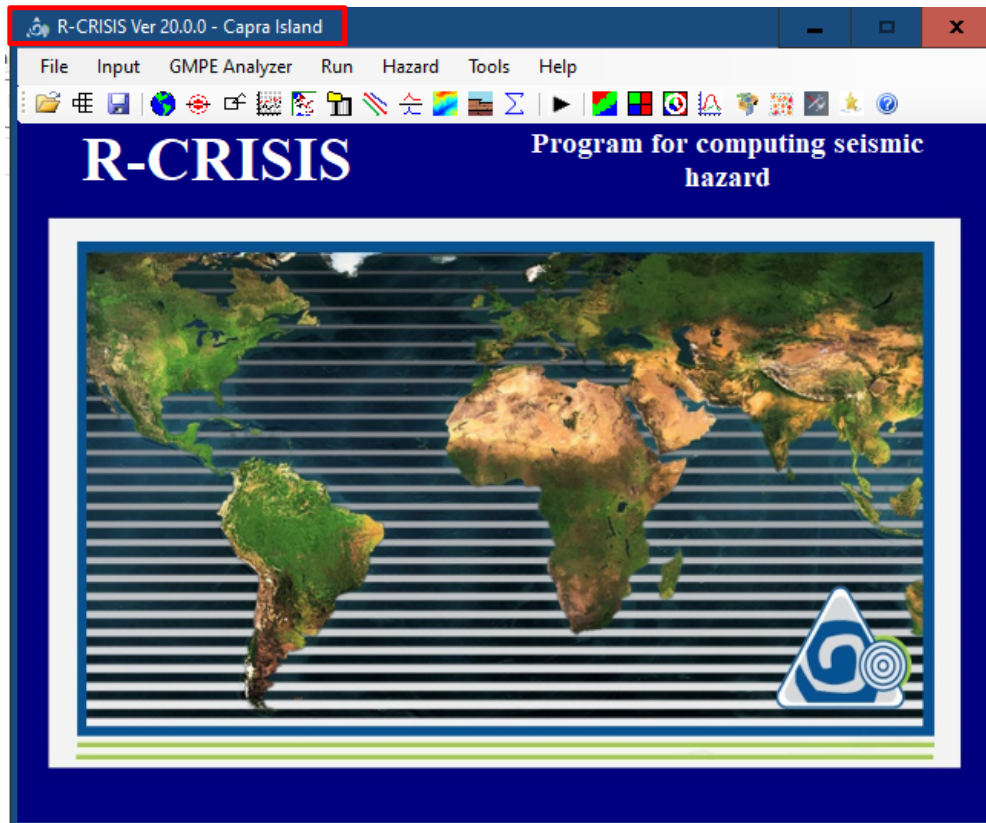


Figure 3-5 Successfully stored R-CRISIS project

3.3 Data assignment

The following menus and buttons have to do with the assignment of data related to seismicity, geometry and GMPM as well as with adding reference maps and locations that can help the verification of the input data to the user. Those can be accessed by selecting the buttons inside the red rectangle in Figure 3-6.




Figure 3-6 Data assignment buttons in R-CRISIS

3.3.1 Map data (optional)

In order to facilitate the verification of the location of the seismic sources of the PSHA project, the user can add reference maps that will be later displayed in other screens of R-CRISIS. R-CRISIS works with coordinates in decimal degrees on the *WGS-84 projection system* as explained in Section 2.3 and therefore, the maps added herein must have that same projection for a proper functioning¹⁶.

R-CRISIS supports two types of formats to be used as reference maps:

- ESRI shapefiles (*.shp)
- ASCII files (*.asc) with the structure explained below:
 - Number of cities as a header
 - Name of the state, name of the city, longitude, latitude (1 line for each city with this data separated by commas).

By clicking the “map data” button, , a screen like the one shown in Figure 3-7 will be displayed. On said screen, by double clicking in the map data field (red rectangle), a new

¹⁶ R-CRISIS does not make any changes of coordinates projection systems. The fact that all maps in shapefile format are displayed is not a guarantee of the fulfillment of this requirement. It is strongly suggested that the user verifies that all reference data is provided using said coordinates system.

explorer window will appear and the user must indicate the storage location of the *.shp file (in this example the map file is called: Island contour.shp) whereas to assign the city data, by double clicking in the area inside the green rectangle the procedure explained before is to be repeated (in this example the cities' file is called: cities.asc).

Note: when adding the reference maps or cities, verify that at the right bottom of the explorer window the appropriate extension (i.e. *.shp or *.asc) is selected.

Once those files have been added to the R-CRISIS project, they will be available in the visualization window of the map data screen (orange rectangle in Figure 3-7). Map data will be displayed with a solid grey background whereas the cities are displayed by means of green points.

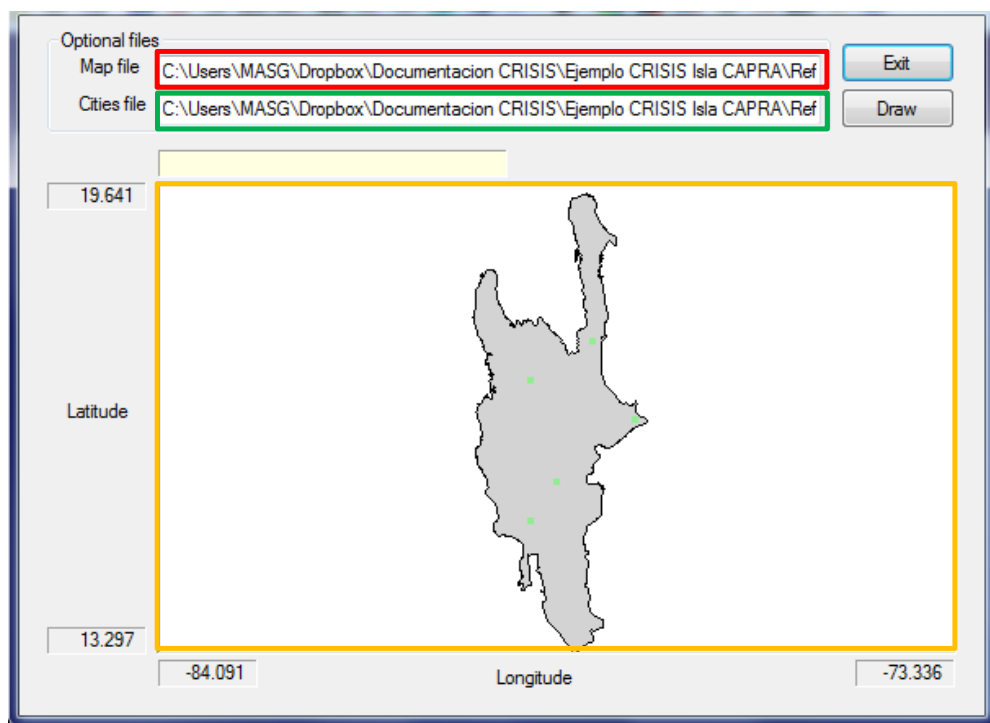



Figure 3-7 Reference map data screen in R-CRISIS

To return to the main screen of R-CRISIS, click on the “Exit” button (top right).

3.3.2 Data of computation sites

To define the site(s) where seismic hazard is to be computed, by selecting the “Data of computation sites” button, , from the main screen of R-CRISIS, a screen like the one shown in Figure 3-8 will be displayed. From it, the user can choose from two different categories: grid calculation or site calculation. The first one allows the calculation of seismic hazard maps whereas the second one allows obtaining the different seismic hazard results only for some points of interest that do not need to be equally spaced in the orthogonal directions. Its use for both cases is explained next. Regardless the type of computation sites

arrangement, what is needed to be defined by the user is the name of the run which can have any alphanumerical combination and is to be included in the field indicated inside the red rectangle of Figure 3-8 (in this case, the run has been named “*Capra Island Example*”).

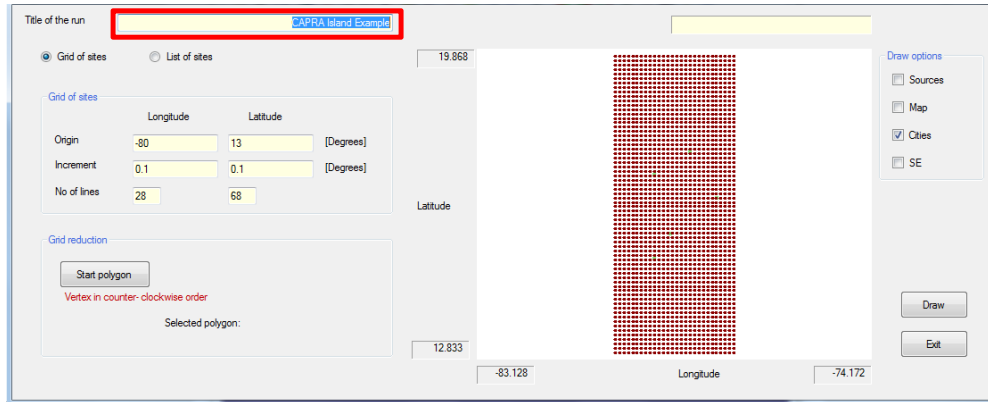


Figure 3-8 Defining the title of the run in a R-CRISIS project

Grid of sites

When hazard maps are required as outputs of the PSHA, the computation sites need to be defined by the user in terms of a grid, which origin, increment (spacing) and number of lines in the two orthogonal directions are specified by the modeler. First, the option of grid of sites needs to be selected as indicated in the red rectangle of Figure 3-9 and then, using the fields shown inside the green rectangle of Figure 3-9 the characteristics of the grid in terms of origin, spacing and number of lines, in the two orthogonal directions, are provided to the program. Note that for the origin and spacing, values are to be included in decimal degrees, again using the WGS-84 coordinate projection system.

For this example the following values are used for the construction of the grid:

- Origin: longitude=-80°; latitude=13° (minus values indicates western hemisphere)
- Increment: 0.1° in both orthogonal directions
- No of lines: 28 for longitude and 68 for latitude

If any map and/or city reference files have been added to the R-CRISIS project, they can be activated/deactivated for visualization purposes at any stage without interfering in any of the PSHA calculations.

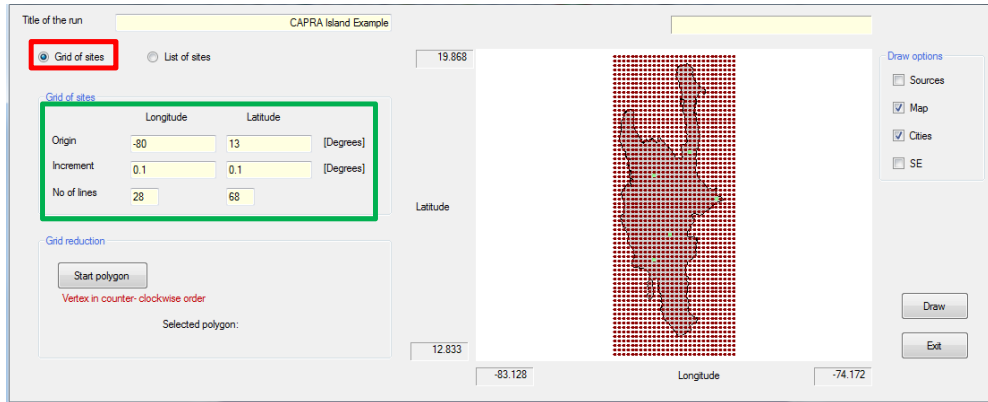


Figure 3-9 Definition of a grid of computation sites in R-CRISIS

A grid reduction polygon can be defined by clicking on the “Start polygon” button, shown in the red rectangle of Figure 3-10. Said polygon is to be drawn by the user in the visualization window (green rectangle in Figure 3-10) with the only condition of doing so in counter-clockwise order. Once all vertexes are defined, by clicking on the “End polygon” button, it will be closed and will be shown in the list inside the orange rectangle of Figure 3-10.

Note: the grid reduction polygons can be deleted by first selecting it from the list and then clicking on the “Delete selected polygon” button (blue rectangle in Figure 3-10).



Figure 3-10 Grid reduction polygon in R-CRISIS

To return to the main screen of R-CRISIS, click on the “Exit” button (right bottom).

Note: the hazard map computations of the CAPRA Island for this example will not make use of the reduction polygon.

List of sites

When only some sites are of interest for performing the PSHA and output is required in terms of hazard curves and/or uniform hazard spectra, for a faster computation process it is suggested that the list of sites options is chosen by selecting the corresponding field, as indicated in the red rectangle of Figure 3-11. Once this option has been selected, the list of computation sites is to be indicated by double clicking in the field inside the green rectangle

of Figure 3-11. For this case the list of computation sites is to be included in the same *.asc format previously explained.

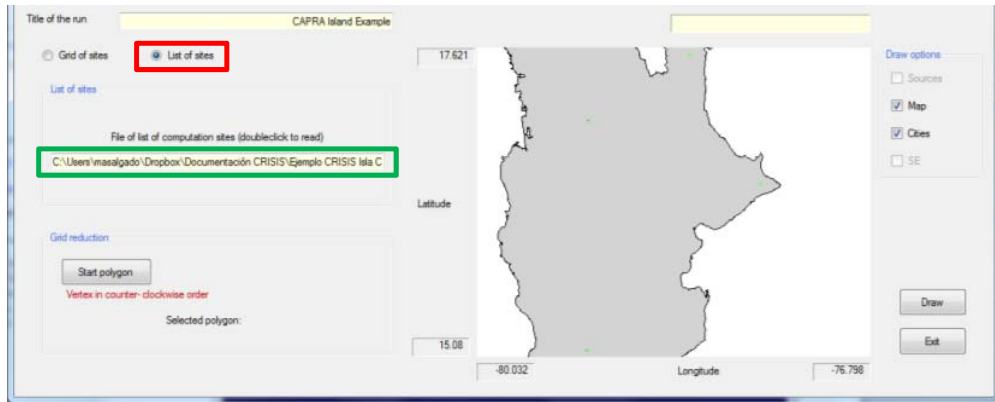



Figure 3-11 Definition of a list of computation sites

To return to the main menu of R-CRISIS, click on the “Exit” button (right bottom).

Note: the list of sites option is used in this example for the hazard disaggregation and the review of the hazard contribution by seismic source at specific locations.

3.3.3 Source geometry data

To define the geometry of the seismic sources to be considered in the R-CRISIS project, the user must click on the “Source geometry data” button, , in the main screen of R-CRISIS and a new screen like the one shown in Figure 3-12 will be displayed. Since there are different geometrical models implemented in R-CRISIS (see Section 2.2) and also in the same R-CRISIS project there can be combinations of them, the user must select first the geometry model for each case from the expanding menu (see red rectangle in Figure 3-12) and afterwards click on the “Add new source” button (green rectangle in Figure 3-12). For each source, in the space inside the orange rectangle of Figure 3-12, the different parameters and options to be specified and/or selected for each geometry model will be displayed.

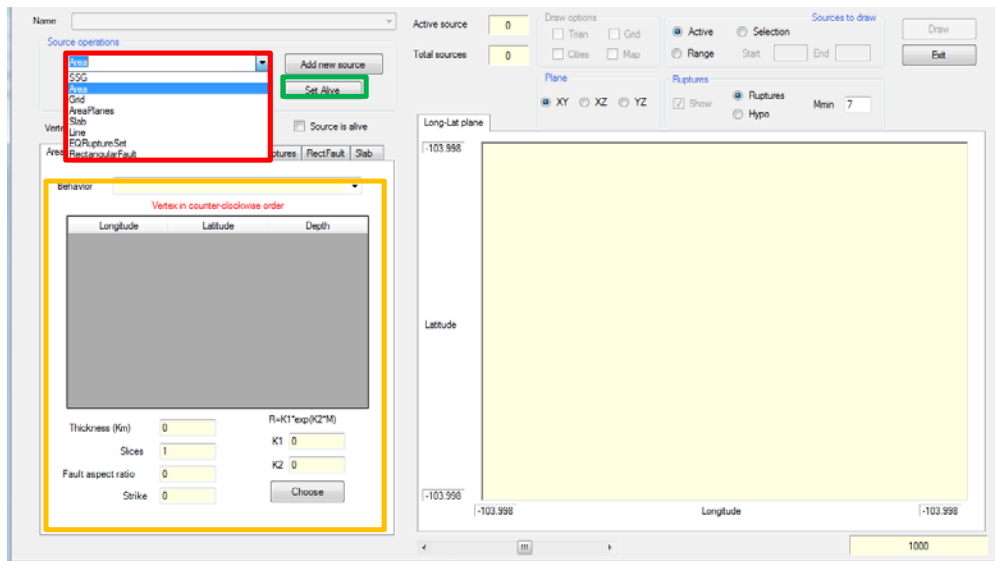


Figure 3-12 Source geometry data screen in R-CRISIS

The CAPRA Island example considers nine (9) seismic sources and a combination of geometry models is used. Area, area-plane, volume and gridded sources are modeled in this example and next, the instructions for defining each case are presented.

Area sources (Sources 1 and 2)

After having selected the area source model and added it to the R-CRISIS project by following the procedure explained above, by default three vertexes are displayed for the initial definition of the geometry. Since it is normal than more than three vertexes are used, the user can add as many as needed by first right clicking on the vertex window (red rectangle in Figure 3-13) and then selecting the “Insert row” option as shown in the green rectangle in Figure 3-13 (if on the contrary, a vertex is to be deleted, select it from the list and then click on the “Delete row” option). A vertex counter is available to guide the user and it is automatically updated every time a vertex is added or deleted as shown in the orange rectangle of Figure 3-13.

The coordinates (in decimal degrees and WGS-84 coordinate system projection) and depth (in km) of each vertex needs to be provided for each vertex in the corresponding fields bearing in mind that those must be introduced in counter-clockwise order. In this example, Sources 1 and 2 are defined by means of four vertexes each with the parameters specified in the accompanying source geometry Excel file (Sources_geometry.xlsx). Once those values have been included in the R-CRISIS project, by clicking “Draw” (top right) the source will be displayed. Note again that if reference maps and cities files have been included, those will also be displayed. If the source is to be renamed, it can be done using any alphanumeric combination by selecting the “Rename” button (blue rectangle in Figure 3-13).

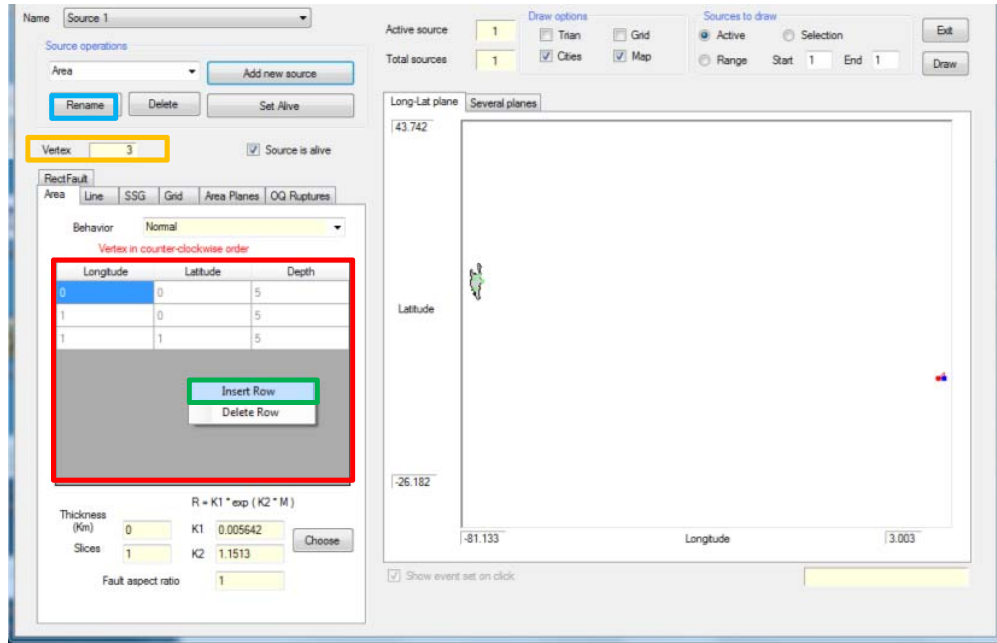


Figure 3-13 Area source geometry data screen in R-CRISIS

Together with the geometry, a set of parameters such as the rupture size, behavior type and fault aspect ratio are to be defined by the user and are explained next.

Rupture parameters (K 's)

The K parameters that define the size of the rupture area can be specified by the user or selected from the built-in models. If the first option is desired it can be done by directly typing the values on the $K1$ and $K2$ fields inside the red rectangle of Figure 3-14. If on the contrary, one of the built-in K values is to be used, click on the “Choose” button (green rectangle in Figure 3-14) and a screen like the one shown in Figure 3-15 will be displayed showing the available values. From the list the user must select the model of interest. The displayed $K1$ and $K2$ values will automatically be updated.

For the CAPRA Island example, the built-in model of “Singh et al.” is selected for Sources 1 and 2.

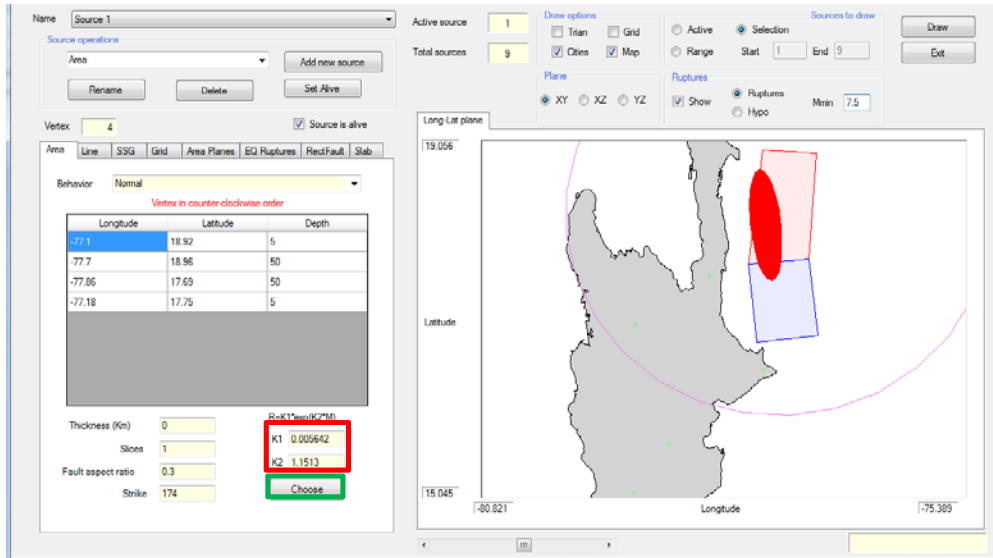


Figure 3-14 Assignment of rupture size parameters to area sources in R-CRISIS

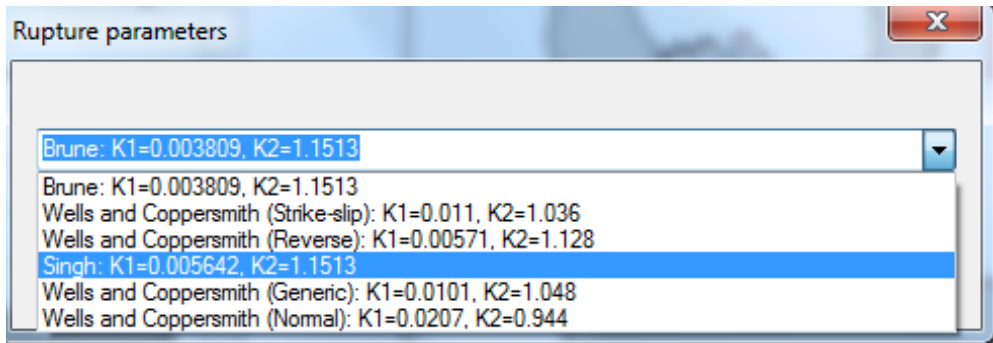


Figure 3-15 List of built-in K's for area sources in R-CRISIS

Behavior

The behavior type that will define the way in which ruptures are considered in R-CRISIS can be selected from the list available inside the red rectangle of Figure 3-16. In the CAPRA Island example the normal behavior is assigned to sources 1 and 2.

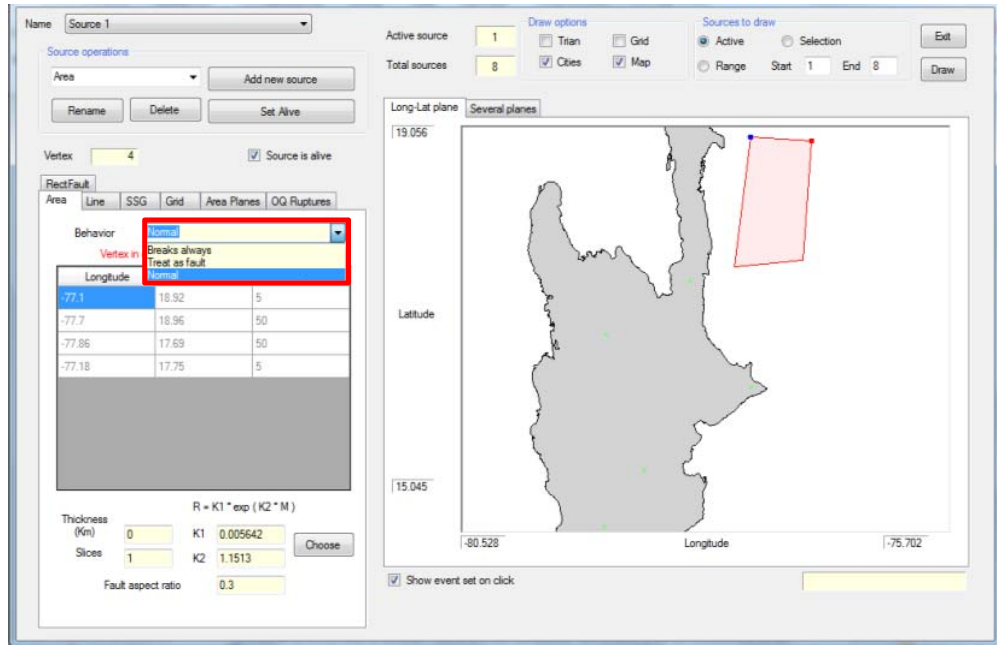


Figure 3-16 Behavior type selection for area sources in R-CRISIS

Fault aspect ratio

The fault aspect ratio can be defined by modifying the parameter shown inside the red rectangle of Figure 3-17. Values different than 1.0 mean that elliptical ruptures are used whereas values equal to 1.0 represent circular ones. In the CAPRA Island example, aspect ratios equal to 0.3 are used for Sources 1 and 2.

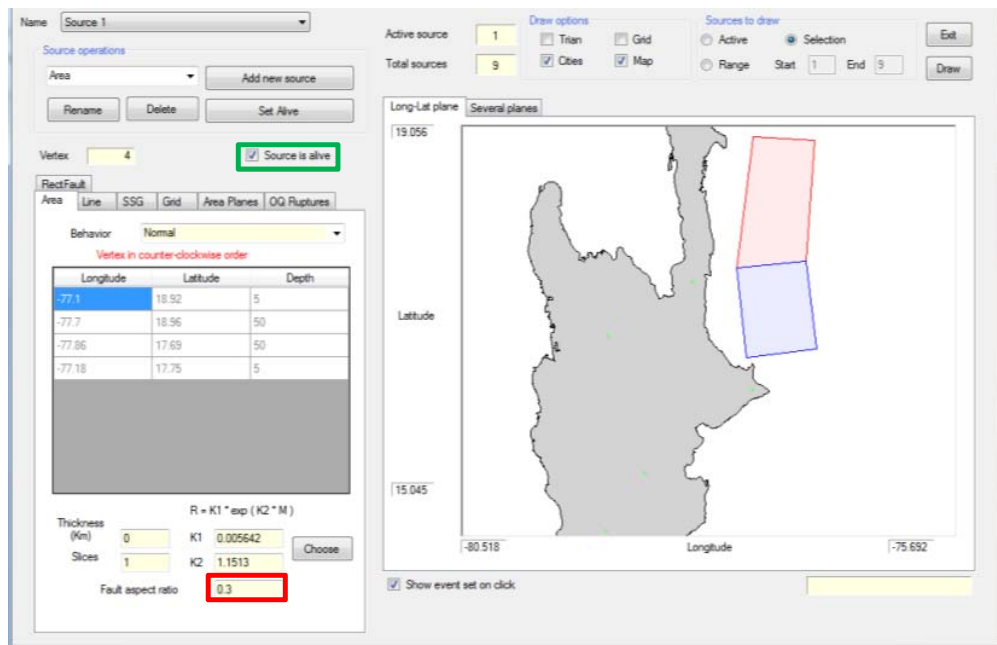


Figure 3-17 Definition of the aspect ratio for area sources in R-CRISIS

Note: for the seismic source to be considered in the PSHA, the “Source is alive” option must be activated (green rectangle in Figure 3-17). This applies for all type of sources in R-CRISIS.

Volume sources (Sources 3 and 4)

Sources in R-CRISIS can be considered as volumes where the seismicity is distributed uniformly at different depths in a set of slices defined by the user. For the case of sources 3 and 4 of the CAPRA Island example, the area model needs to be selected and the geometry of each source included in the R-CRISIS project following the same procedure explained above and using the values provided in the accompanying Excel file (Sources_geometry.xlsx).

After this, the thickness of the volume and the number of slices into which the seismic activity is to be distributed needs to be specified in the fields inside the red rectangle of Figure 3-18. For sources 3 and 4, a thickness equal to 30km and 6 slices are used to represent the volume source.

Note: the geometry provided will be the top of the volume and the slices will be distributed downwards until reaching the thickness depth.

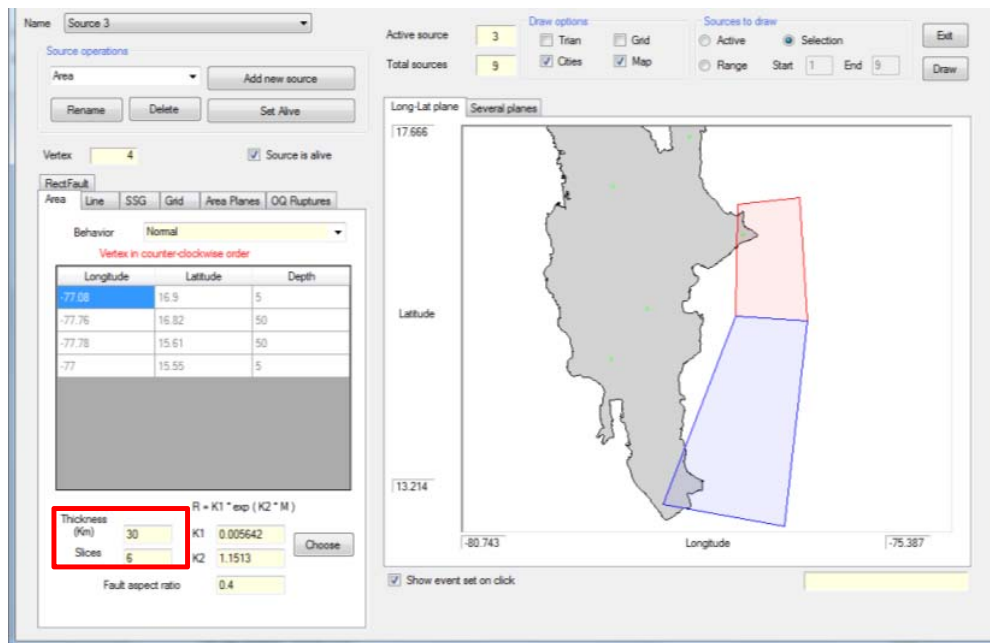


Figure 3-18 Volume sources in R-CRISIS

In these cases, the rupture parameters (*K*'s) and fault aspect ratios need also to be defined. For this example, source 3 and 4 have assigned the Singh et al. built-in *K*'s and a fault aspect ratio equal to 0.4.

Note: if the default values are not modified (Thickness=0, Slices=1), the source will be considered by R-CRISIS as an area and not as a volume.

Area-plane sources (Sources 5 and 6)

After adding an area-plane source by selecting the corresponding option in the list available from the geometry data screen, it can be seen that the required data in terms of geometry and vertexes is exactly the same as in the case of area sources with the difference that, in this case, the orientation of the rupture plane can be provided to R-CRISIS by means of the strike and dip characteristics. These values are to be introduced in the fields inside the red rectangle of Figure 3-19 and for the CAPRA Island example, sources 5 and 6 are modelled as horizontal planes where the orientation of the rupture is assumed to be vertical (dip=90°) and with N-S orientation (strike=0°).

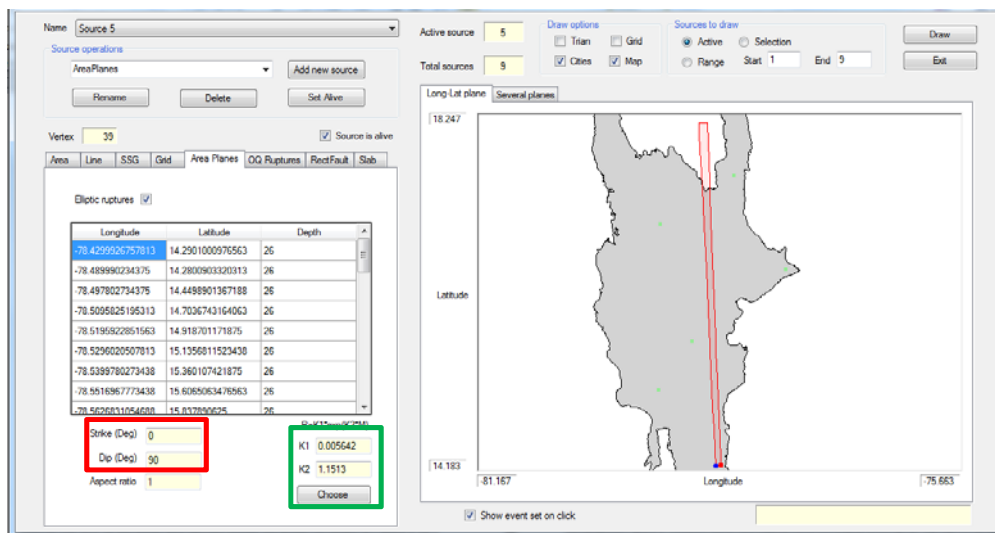


Figure 3-19 Area plane source geometry data screen in R-CRISIS

Rupture parameters (K 's) are to be defined and the procedure is the same as in the area sources but now in the fields and options inside the green rectangle of Figure 3-19.

Note: As in the case of area sources, aspect ratios can be defined. In this case D_x is understood by CRISIS to be in the same direction of the strike whereas D_y is in the same direction of the dip. This example uses an aspect ratio of 1.0 (circular ruptures).

Line sources (Source 7)

After the line source option has been selected from the list and the seismic source has been added to the R-CRISIS project, the coordinates of the vertex of the line source are to be included in a similar way as explained for the area, volume and area-plane cases. In the CAPRA Island example, Source 7 is represented by means of a line source that corresponds to a polyline with varying depth as shown in Figure 3-20.

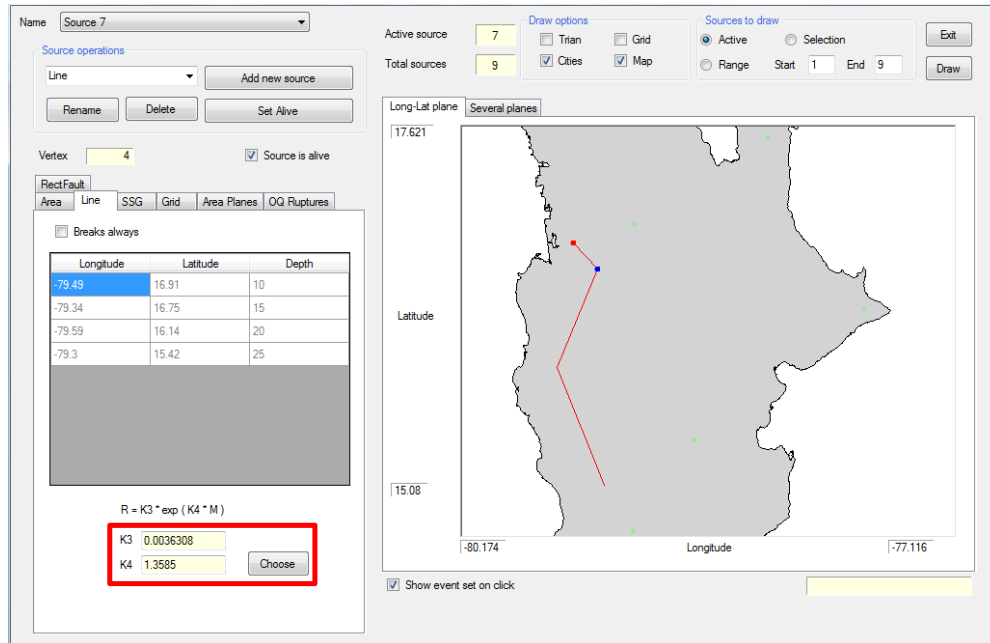


Figure 3-20 Line source geometry data screen in R-CRISIS

Rupture parameters (K 's)

For the case of line sources, the rupture length parameters need also to be defined. As in the case of area and area-planes those can be either user defined or selected from the built-in values. Those are to be assigned using the fields and/or options inside the red rectangle of Figure 3-20.

Grid sources (Source 8)

When a grid source is added to the R-CRISIS project, some differences with the previous geometric models used are evident. First, what needs to be defined is the grid extension in terms of origin, end and number of lines in both orthogonal directions as shown in the red rectangle of Figure 3-21 followed by the definition of the depth of the grid¹⁷ (green rectangle of Figure 3-21).

For the CAPRA Island example, source 8 is represented by means of a grid source which parameters are:

- Origin: Longitude=-80; Latitude=16.6
- End: Longitude=-79.35; Latitude=18.25
- No. of lines: Longitude=14; Latitude=34
- Depth: 20km

¹⁷ Only a uniform depth can be used for the grid sources

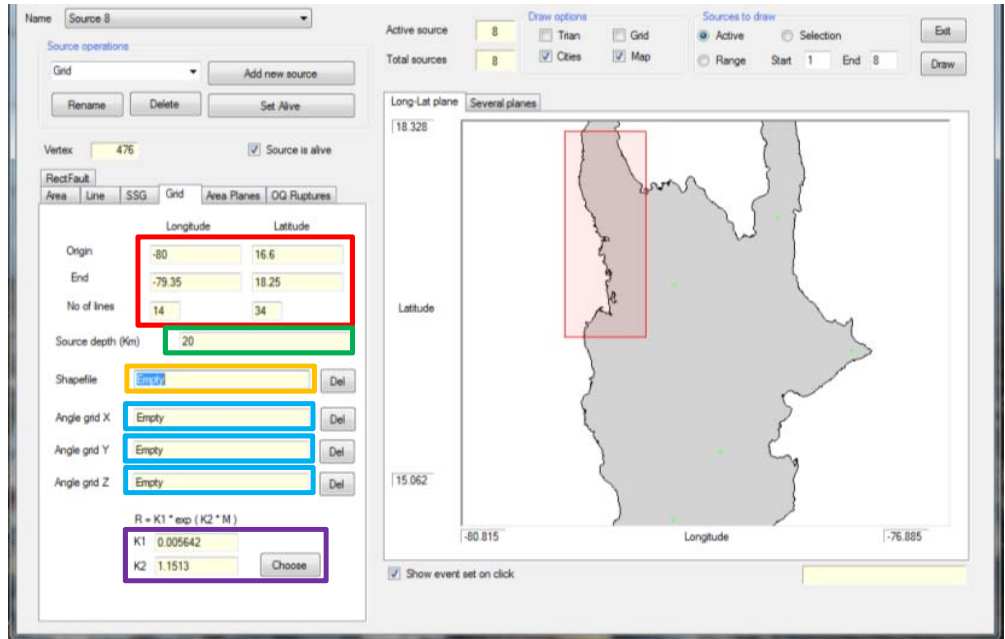


Figure 3-21 Grid sources in R-CRISIS

Delimitation polygon (optional)

A delimitation polygon can be included to only make estimations within it in terms of a shapefile. It can be added to the R-CRISIS project by double clicking on the field inside the orange rectangle of Figure 3-21.

Orientation of the rupture areas (optional)

The grids that define the unit vectors in X, Y and Z directions are to be loaded in the R-CRISIS project by double clicking on the fields inside the blue rectangles in Figure 3-21.

Rupture parameters (K's)

As in the previously explained geometry models, the *K* parameters, that define the characteristics of the rupture extent, need to be specified. The procedure is the same as explained before (i.e. those can be user defined or selected from the built-in values) and is to be performed on the fields and/or options inside the purple rectangle of Figure 3-21.

Point sources (Source 9)

The last geometric model used in the CAPRA Island example corresponds to the point source (SSG) and is used to model source 9 which in the island is assumed to be a volcano. After the SSG model has been chosen and the seismic source has been added to the R-CRISIS project, the *.ssg file¹⁸ (Volcano.ssg in the example) is added to the project by double clicking in the

¹⁸ There can be different point sources in the same *.ssg file but in this example only one source is included

area inside the red rectangle of Figure 3-22. Since each point in the *.sbg file has assigned a reference name, it will be displayed in the list inside the green rectangle of Figure 3-22.

As in the other geometry models, the rupture parameters can be defined and to do so, the user must select the corresponding fields and/or button inside the orange rectangle of Figure 3-22.

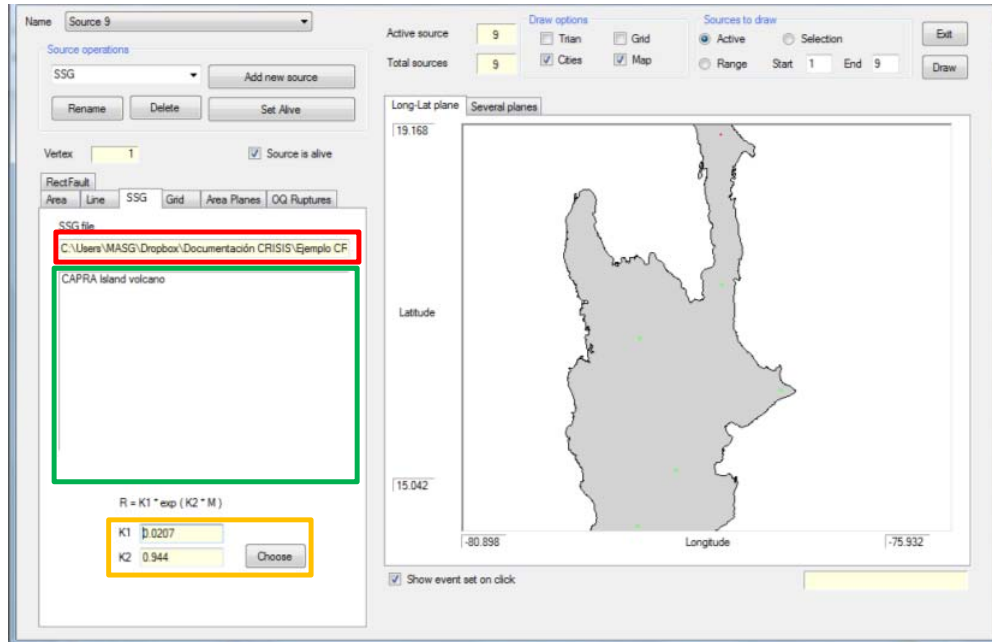


Figure 3-22 Point (SSG) sources in R-CRISIS

Note: To add a SEC the *.csv file needs to be added as a new source of the OQ ruptures tipe.

Visualization of several sources at the same time

Once the geometries of two or more sources have been defined, they can be visualized at the same time by selecting the “Range” option on the “Sources to draw” menu as shown in the red rectangle of Figure 3-23. If only some sources are of interest to be displayed, they can be chosen by clicking on “Selection” (green rectangle of Figure 3-23) and activating only the ones of interest. To refresh the screen, click on the “Draw” button (orange rectangle in Figure 3-23). The selected source will always show in red and it can be changed from the list that expands by clicking in the area within the blue rectangle in Figure 3-23.

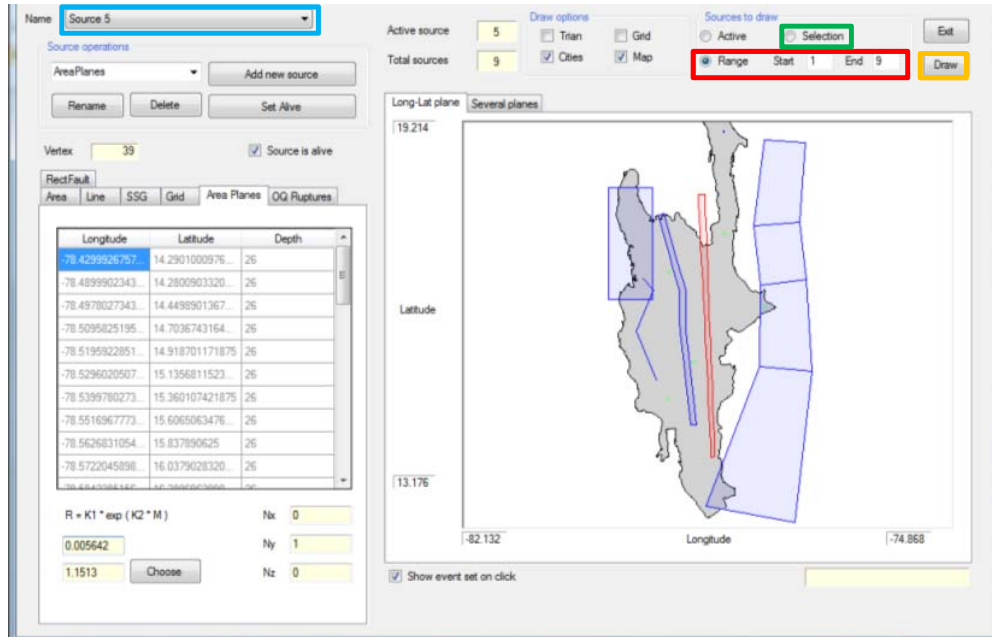


Figure 3-23 Visualization of several seismic sources in R-CRISIS

Review of the slenderness of the sub-sources (for area and area-plane sources)

Since R-CRISIS performs a subdivision of each seismic source into simpler geometries (triangles), a verification of their slenderness can be performed by activating the “Trian” option in the “Draw options” menu as shown inside the red rectangle of Figure 3-24. If triangles are shown in either red or blue, it means that they are considered as appropriate for performing the PSHA. If on the other hand they are shown in green (see green ellipse in Figure 3-24 for sources 5 and 6 of the CAPRA Island example), it means that they are very slender and additional vertexes should be included so that R-CRISIS can perform a better recursive subdivision of the source.

Note: the slenderness verification process is considered as a warning in R-CRISIS and the PSHA can be performed even if slender (green) triangles exist. Anyhow, it is strongly suggested in those cases to refine the subdivision by adding more vertexes as shown in the green ellipse of Figure 3-25.

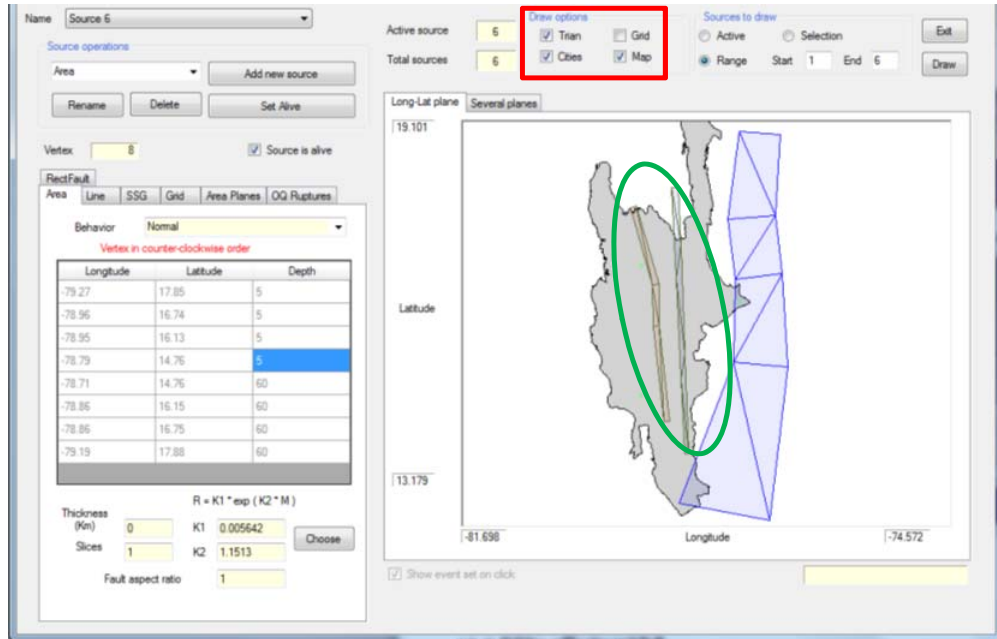


Figure 3-24 Verification of sub-sources slenderness in R-CRISIS (1 of 2)

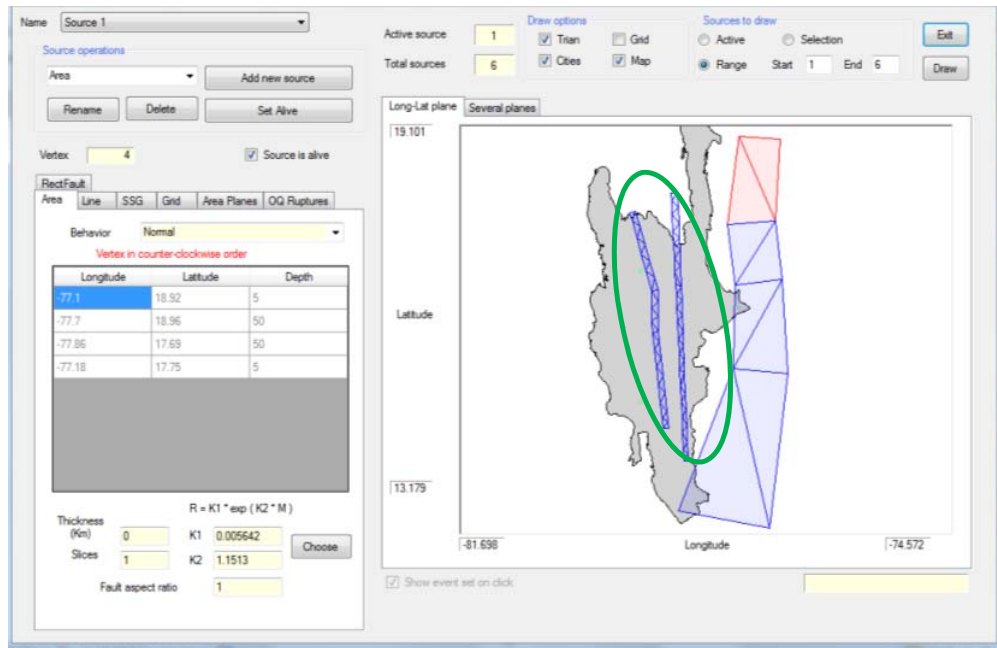
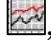


Figure 3-25 Verification of sub-sources slenderness in R-CRISIS (2 of 2)

To return to the main screen of R-CRISIS click on the “Exit” button (top right).

3.3.4 Data on spectral ordinates

To define the number of spectral ordinates and their associated fundamental periods the user can access the corresponding screen by clicking once on the “Data on spectral ordinates” button, , in the main screen of R-CRISIS. A screen like the one shown in Figure 3-26 will be displayed and the different parameters that need to be assigned are explained herein:

- Total number of spectral ordinates: in this field (red rectangle in Figure 3-26), the total number of spectral ordinates for the analysis is defined. For the CAPRA Island example 10 spectral acceleration ordinates are used.
- Actual spectral ordinate: with this counter the user can change between the spectral ordinates to define the parameters of the active one.
- Structural period of actual spectral ordinate: in this field (green rectangle in Figure 3-26), the fundamental period (in seconds) is assigned to each spectral ordinate. The 10 fundamental periods of the CAPRA Island example can be found in the accompanying spectral ordinates Excel file (Spectral_ordinates.xlsx).
- Lower and upper limit of the intensity level: in these fields (orange rectangle in Figure 3-26) the minimum and maximum intensity values for the computation of the exceedance probabilities within a defined timeframe are defined. (Note that these values are closely related to the units of the GMPM). The lower and upper intensity limits for each spectral ordinates of the CAPRA Island example can be found in the accompanying spectral ordinates Excel file (Spectral_ordinates.xlsx).
- Spacing: The user can define the spacing type of the exceedance probability plot at each location. Four different options are available that can be selected from the menu shown in the blue rectangle in Figure 3-26. (A logarithmic spacing is chosen for the CAPRA Island example)
 - Log: logarithmic spacing between intensity points
 - Linear: constant (arithmetic) spacing between intensity points
 - PEER and Large PEER: Used for PEER validation tests (see Chapter 4 of this document)
- Units: The user can include, only as a reference, the units for each spectral ordinate in the field shown with the purple rectangle in Figure 3-26. (All spectral ordinates in the CAPRA Island example are defined in terms of cm/s^2)
- Number of levels of intensity for which seismic hazard will be computed: Exceedance probabilities will be computed for the number of levels defined in this field (black rectangle in Figure 3-26) and between the lower and upper limits of the intensity level using the spacing type previously defined.

The values used in this example for all the parameters explained above are summarized in Table 3-1.

Table 3-1 Summary of spectral ordinates for the CAPRA Island example

Period index	T (s)	Lower limit	Upper limit	Units
1	0.01	1	2500	gal
2	0.05	1	2500	gal
3	0.15	1	2500	gal
4	0.30	1	2500	gal
5	0.50	1	2500	gal
6	0.75	1	1500	gal
7	1.00	1	1500	gal
8	1.50	1	1500	gal
9	2.00	1	1000	gal
10	3.00	1	1000	gal

There is always a compromise between speed and precision: the larger the number of points used to define the curve or the larger the intensity range, the longer the computation time. Generally speaking, no more than 20 points are required to accurately define the exceedance probability curve. For the CAPRA Island example the exceedance probability curves are defined by means of 15 points.

Note: the value defined for number of intensity for which seismic hazard will be computed applies for all the spectral ordinates.

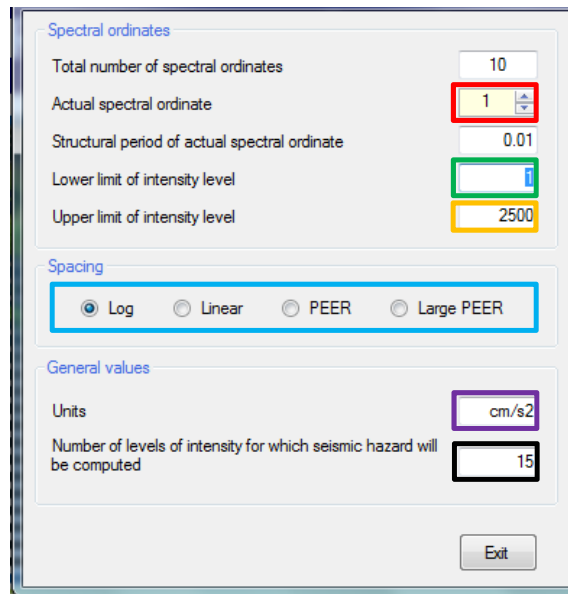



Figure 3-26 Definition of spectral ordinates and associated parameters in R-CRISIS

To return to the main window of CRISIS click on the “Exit” button (bottom right).

3.3.5 Seismicity data

To select and define the seismicity parameters for each seismic source, the corresponding menu is accessed by clicking on the “Seismicity data” button, , on the main screen of R-CRISIS and then, a screen like the one shown in Figure 3-27 will be displayed.

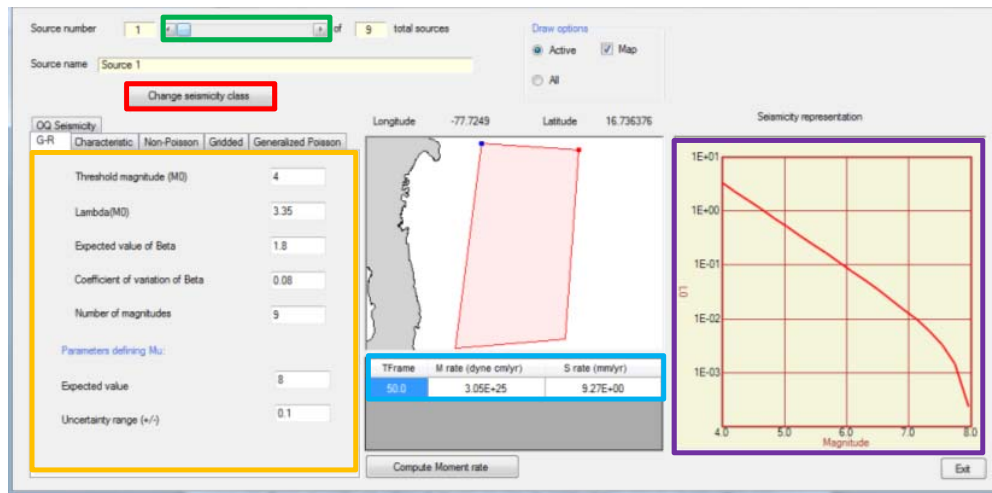


Figure 3-27 Modified G-R seismicity model screen in R-CRISIS

All seismic sources in the R-CRISIS project need to have assigned seismicity parameters and to change from one source to another in order to set them, the sliding bar shown within the green rectangle in Figure 3-27 can be moved either to the left or to the right. The number and name of the source will be automatically updated.

Modified Gutenberg-Richter seismicity model (Sources 1, 2, 3, 5, 6, 7 and 9)

By default, the modified G-R seismicity model is assigned to each source but if it is to be changed, by clicking on the “Change seismicity class” button (red rectangle in Figure 3-27), the other seismicity models available in R-CRISIS are displayed. This section explains the different values that need to be included when the modified G-R model is selected.

For each seismic source that uses this model, the following parameters need to be assigned in the fields inside the orange rectangle of Figure 3-27. For the 7 sources of the CAPRA Island example that use this seismicity model, the values of the corresponding parameters can be found in the accompanying seismicity parameters Excel file (Seismicity_parameters.xlsx).

- Threshold magnitude (M_0): Threshold magnitude for the selected source.
- Lambda(M_0): Average annual number of earthquakes with equal or higher magnitude than M_0 . (Units are 1/year).
- Expected value of Beta: Expectation of the b -value for the source, defined in terms of its natural logarithm.
- Coefficient of variation of beta: Coefficient of variation of the b -value for the source, defined in terms of the natural logarithm. This value is to consider the uncertainty in β .

- Number of magnitudes: Number of magnitudes used in the hazard integration process. Usually 9 magnitudes are enough and smaller numbers for this parameter are rarely used. 9 corresponds to the default value of this parameter.
- Expected value of M_U : Expected value of the maximum magnitude for the source.
- Uncertainty range (+/-): Number that indicates that the maximum magnitude will have a uniform probability density function, centered at its expected value, plus and minus this value.

Seismic moments and slip rates are automatically computed based on the seismicity parameters and timeframes and are displayed in the fields shown inside the blue rectangle of Figure 3-27. Also, the G-R plot is constructed based on the input data for each source and displayed in the area inside the purple rectangle of Figure 3-27.

To return to the main screen of R-CRISIS click the “Exit” button (bottom right).

Characteristic earthquake seismicity model (Source 4)

When this seismicity model is assigned to a seismic source (as it is the case for source 4 of the CAPRA Island example), a screen like the one shown in Figure 3-28 will be displayed. For each seismic source that uses this model, the required data is to be introduced in the fields inside the red rectangle of Figure 3-28.

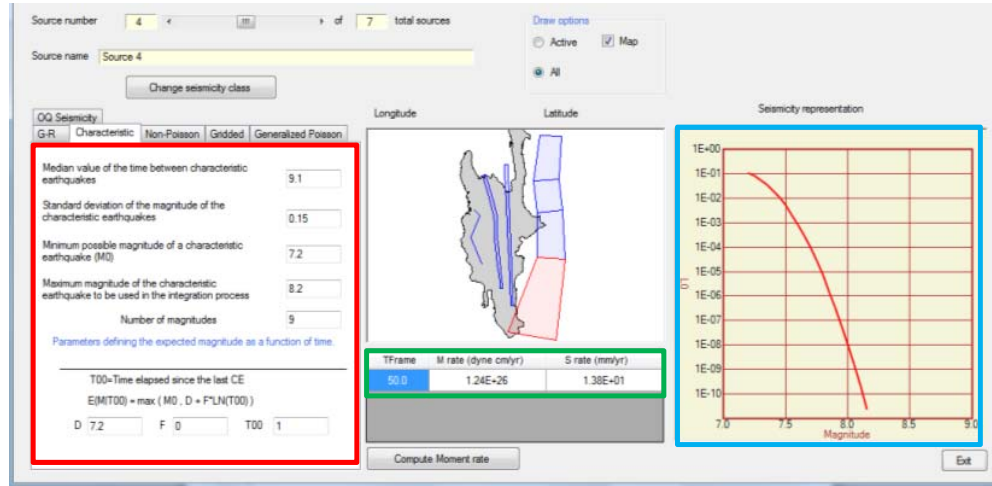


Figure 3-28 Characteristic earthquake model screen in R-CRISIS

The following parameters are needed for the description of the characteristic earthquake seismicity model. The values of the parameters that define the characteristic earthquake for source 4 of the CAPRA Island example can be found in the accompanying seismicity parameters Excel file (Seismicity_parameters.xlsx).

- Median value of the time between characteristic earthquakes.
- Standard deviation of the magnitude of the characteristic earthquakes.
- Minimum possible magnitude of a characteristic earthquake (M_0).

- Maximum magnitude of the characteristic earthquake to be used in the integration process.
- Number of magnitudes: number of magnitudes used in the integration of hazard. Usually 9 magnitudes are enough and smaller numbers for this parameter are rarely used. 9 corresponds to the default value of this parameter.
- Parameters D and F define the expected magnitude as a function of time, as in the slip-predictable model. It is assumed that:

$$E(M|T_{oo}) = \max(M_o, D + F * LN(T_{oo})) \quad \text{Eq. (3-1)}$$

where T_{oo} is the elapsed time since the last characteristic event. If F is set to zero, the D becomes the expected time-independent magnitude of the characteristic earthquake.

Seismic moments and slip rates are automatically computed based on the seismicity parameters and timeframes and are displayed in the fields shown inside the green rectangle of Figure 3-27. Seismicity rates are shown in the visualization window inside the blue rectangle of Figure 3-27.

To return to the main screen of R-CRISIS click the “Exit” button (bottom right).

Note: point sources allow the use of modified G-R, characteristic earthquake, generalized Poissonian and non-Poissonian seismicity models. To assign any of those, follow the same instructions presented before to the corresponding sources.

Gridded seismicity model

When a grid geometric model has been used, it needs to be accompanied by the gridded seismicity parameter data in order to construct at each location within the grid the magnitude recurrence information using the modified G-R seismicity model. If this seismicity model is selected a screen like the one shown in Figure 3-29 will be shown.

The following parameters need to be added to the R-CRISIS project and for the source 8 of the CAPRA Island example those can be found in the accompanying seismicity parameters Excel file (Seismicity_parameters.xlsx) as well as with the L_o , E_B and M_u grids.

- Threshold magnitude (M_o): Threshold magnitude for the whole extension of the grid (red rectangle in Figure 3-29).
- Number of magnitudes: number of magnitudes used in the hazard integration process. Usually 9 magnitudes are enough and smaller numbers for this parameter are rarely used (green rectangle in Figure 3-29). 9 corresponds to the default value of this parameter.
- L_o Grid: Grid with the average annual number of earthquakes with equal or higher magnitude than M_o for all nodes. (Units are 1/year).
- E_B Grid: Grid with the expectation of the b -value for the source, defined in terms of its natural logarithm for all nodes.

- M_U Grid: Grid with the expected value of the maximum magnitude for all nodes

The L_0 , E_B and M_U grids are to be assigned by clicking in the corresponding field (orange rectangles in Figure 3-29) and providing their storage path.

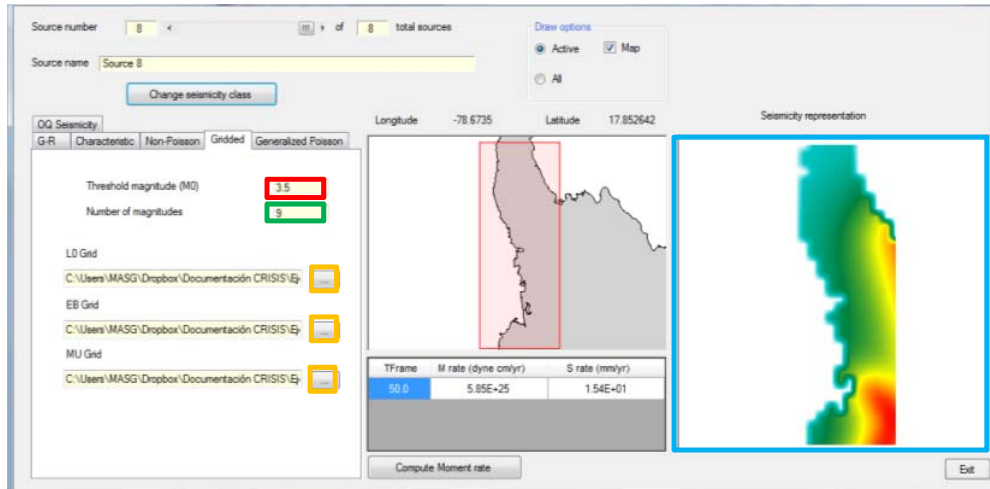



Figure 3-29 Gridded seismicity model in R-CRISIS

To return to the main screen of R-CRISIS click the “Exit” button (bottom right).

3.3.6 Attenuation data

To add GMPM to the R-CRISIS project and assign them to the seismic sources, click the “Attenuation data” button, , in the main screen of R-CRISIS. After this, a screen with empty parameters, as the one shown in Figure 3-30 will be displayed.

Adding built-in and user defined attenuation models

There are two different ways of adding GMPM to the R-CRISIS project:

1. Use any of the available built-in models (for the full list see Section 2.4.2)
2. Add a user-defined attenuation table (through *.atn files).

As many GMPM as needed can be added to the R-CRISIS project and combinations between user defined and built-in models are allowed. To add a GMPM to the R-CRISIS project click once on the “Add model” button (red rectangle in Figure 3-30) that will display a new screen, as the one shown in Figure 3-31.

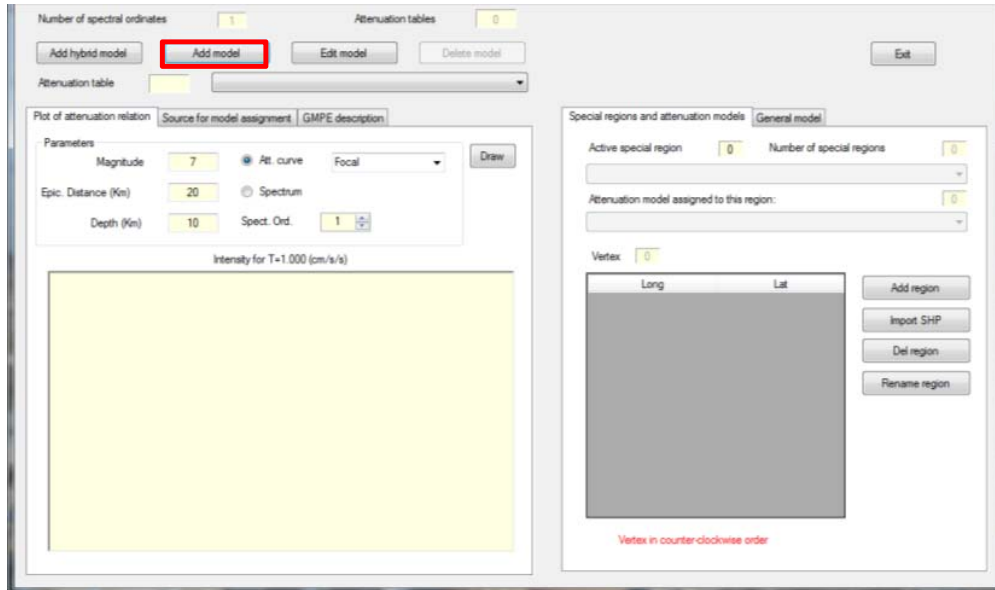


Figure 3-30 Attenuation data screen in R-CRISIS

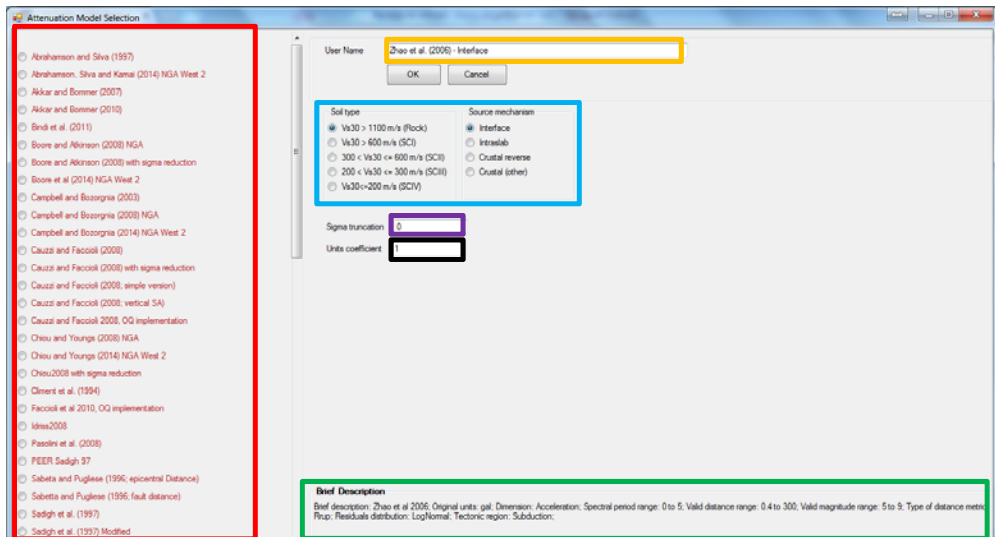


Figure 3-31 Adding a built-in GMPM to a R-CRISIS project

For the case when built-in GMPM are to be added to the R-CRISIS project, the model needs to be selected from the list shown inside the red rectangle of Figure 3-31. A brief description of the selected model will be displayed at the bottom of the GMPM screen (green rectangle in Figure 3-31) and then, the user can define a name for the model in the field inside the orange rectangle of Figure 3-31. After this and for each GMPM, the user can select the different options regarding specific parameters of each built-in model (e.g. fault and soil types) in the fields and options inside the blue rectangle in Figure 3-31. Finally, the user can define if the GMPM is to be truncated to sigma (and how) by setting the corresponding value in the field shown inside the purple rectangle of Figure 3-31 and finally, if the original units differ from the one of the defined by the user in the CRISIS project (information provided in the brief description of each GMPM), a unit coefficient can be introduced in the field shown within the

black rectangle in Figure 3-31. Once all these values have been set, by clicking on the “OK” button (below the user defined name for the model) the GMPM will be added to the R-CRISIS project.

For the CAPRA Island example, the following built-in GMPM are to be added to the project:

- Sadigh et al. (1997) – modified. Fault type: strike-slip/normal; soil type: rock; sigma truncation: 0; units coefficient: 1.
- Zhao et al. (2006). Soil type: rock; source mechanism: interface; sigma truncation: 0; units coefficient: 1.
- Lin and Lee (2008). Fault mechanism: interface; soil type: rock; sigma truncation: 0; units coefficient: 0.0010197 (to convert from g’s to cm/s²).

To add a user defined GMPM (attenuation table), the process is the same with the difference that in the GMPM list, the “Attenuation table” option must be selected. On it, by double clicking on the field shown in the red rectangle of Figure 3-32, the explorer window will be displayed and on it the user must provide the path to the *.atn file. As in the case of the built-in GMPM, a name and a unit’s coefficient can be defined. By clicking on the “OK” button (below the user defined name for the model) the GMPM will be added to the R-CRISIS project.

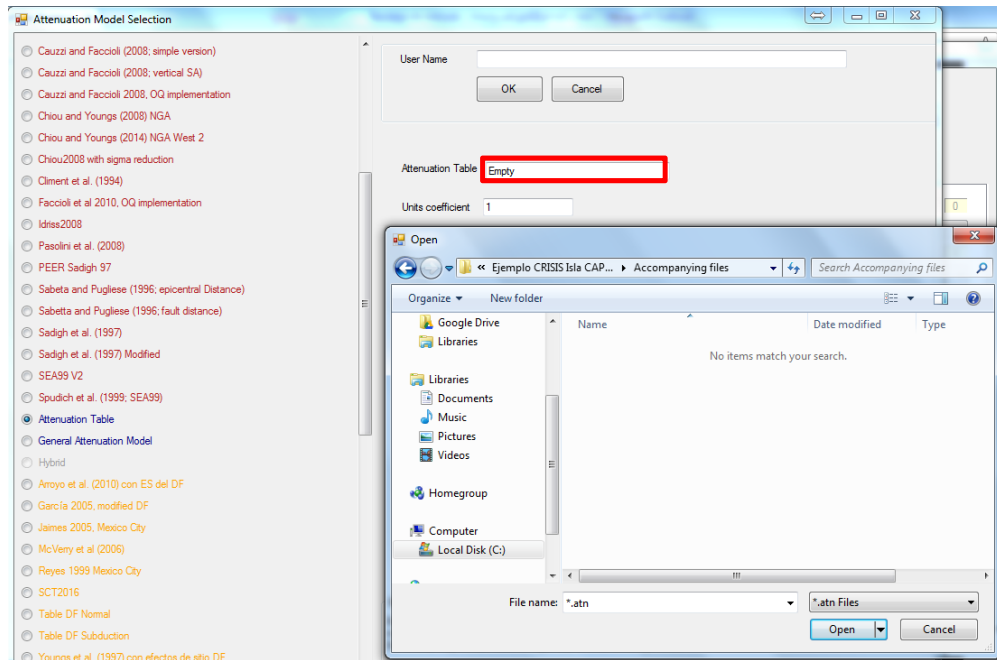


Figure 3-32 Adding an attenuation table to a R-CRISIS project

This process is to be repeated as many times as GMPM to be provided to the R-CRISIS PSHA project.

Once all the GMPM of interest have been added to the R-CRISIS project, some useful data for each added model are available on the main GMPM screen as shown in Figure 3-33. When

the “Plot of attenuation relation” tab is selected, the magnitude/distance plot is displayed (red rectangle in Figure 3-33) for the combination of values provided in the fields inside the green rectangles of Figure 3-33. To refresh the view the user must click the “Draw” button (orange rectangle in Figure 3-33).

Also, since different distance measures can be used (i.e. R_F , R_{EPI} , R_{JB} , R_{RUP}) the one of interest for the user can be chosen from the list shown with the blue rectangle in Figure 3-33. The GMPM plots can be displayed in terms of the attenuation curve for the selected spectral ordinate (which can be changed using the list) and the other magnitude, distance and depth parameters or also in terms of the spectrum (constructed for all the previously defined spectral ordinates) and fixed magnitude, distance and depth values.

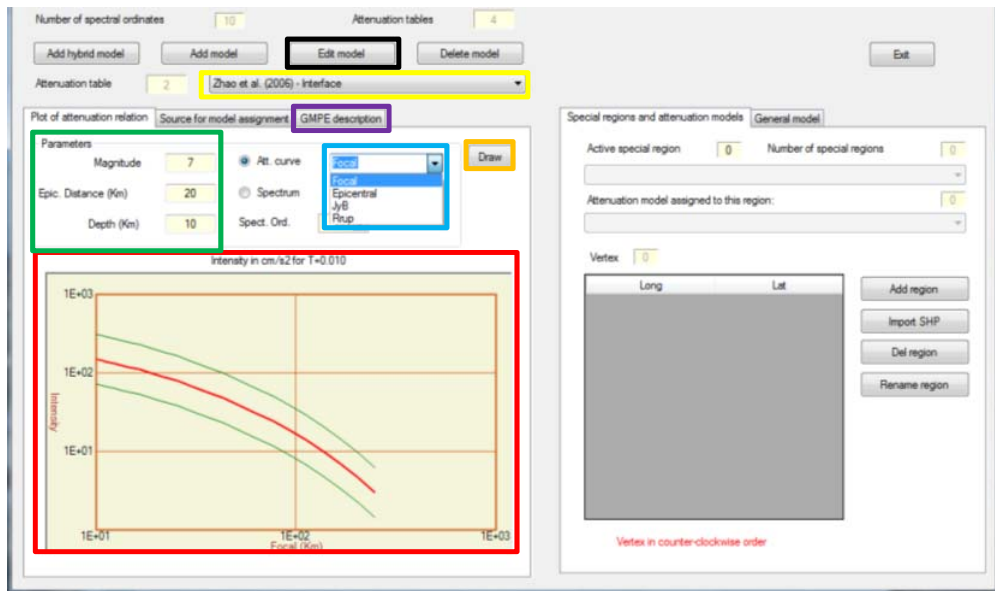


Figure 3-33 Visualization of active GMPM in R-CRISIS

To edit a GMPM, by selecting the one of interest from the list shown in the yellow rectangle of Figure 3-33 and then on the “Edit model” button (black rectangle of Figure 3-33), the same screen as shown in Figure 3-31 will be displayed and the changes can be made.

Note: if the GMPM description is required after it has been added to the R-CRISIS project, it can be accessed directly choosing the GMPM of interest from the list and then by selecting the “GMPM description” tab shown inside the purple rectangle of Figure 3-33.

Adding hybrid GMPM

In R-CRISIS it is also possible to create and assign hybrid GMPM (see Section 2.4.4). To do so, in the main GMPM screen click on the “Add hybrid model” (red rectangle in Figure 3-34) and a screen like the one shown in Figure 3-35 will be displayed.

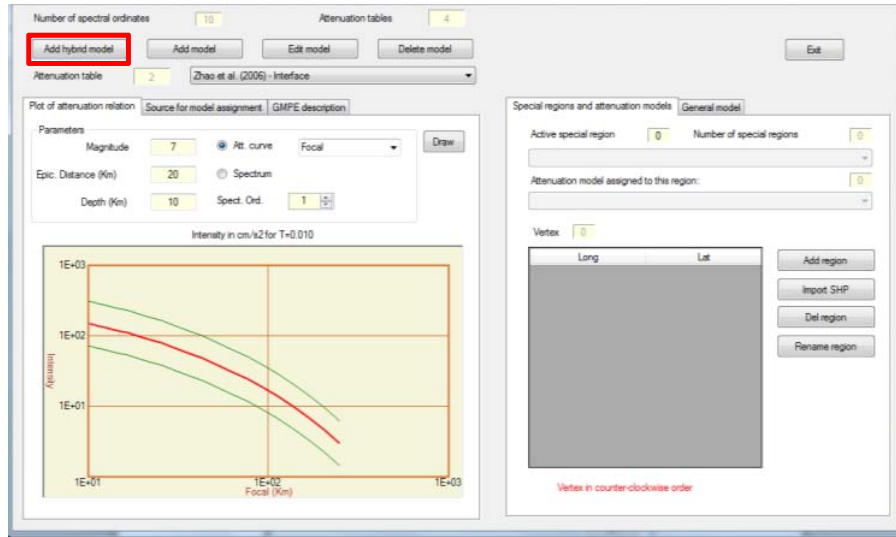


Figure 3-34 Adding hybrid GMPM to R-CRISIS

On the hybrid GMPM constructor, all the GMPM added to the CRISIS project (either built-in or user defined models) will be displayed in the area inside the red rectangle of Figure 3-35 and they can be added and removed from the hybrid model by clicking on the buttons shown in the green and orange rectangles of Figure 3-35. A relative weight needs to be assigned in the fields inside the purple rectangle of Figure 3-35 to each of the models and those values will correspond to the equivalent probabilities.

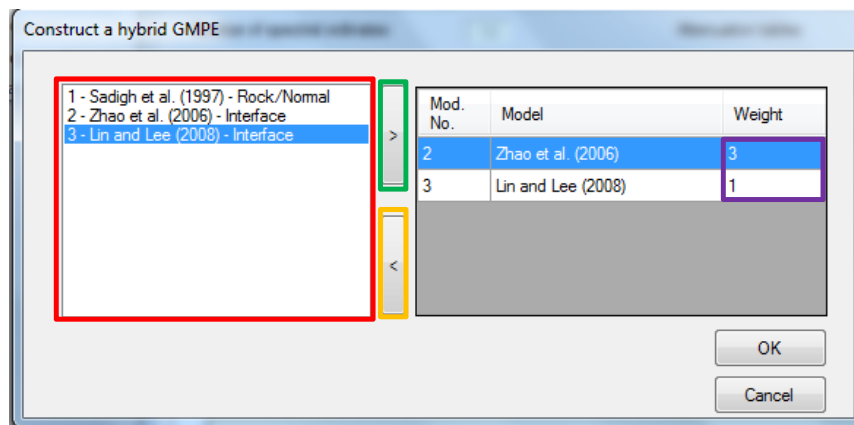


Figure 3-35 Hybrid GMPM constructor of R-CRISIS

After all GMPM and weights have been set, by clicking on the “OK” button (bottom right), the model will be added and will be available for display in the main GMPM screen. The hybrid model by default will be named “Hybrid of models 1/2/....N”.

For the CAPRA Island example, an hybrid GMPM is used considering as base models the Zhao et al. (2006) and Lin and Lee (2008) GMPM. The relative weights for those are 3 and 1 respectively (which would correspond to weights of 0.75 and 0.25 respectively).

Note: hybrid GMPM cannot be edited in CRISIS. If changes are needed, the model needs to be deleted and created again.

Assigning GMPM to the seismic sources

So far, GMPM have been added to the project but not yet assigned to the seismic sources. To proceed to that stage, on the “Attenuation data” screen the user needs to select the “Source for model assignment” and “General model” tabs as shown in the red and green rectangles in Figure 3-36. For each seismic source a GMPM needs to be assigned from the list shown in the orange rectangle of Figure 3-36. This process is to be repeated for each source. To change the active source, click on the button inside the blue rectangle of Figure 3-36.

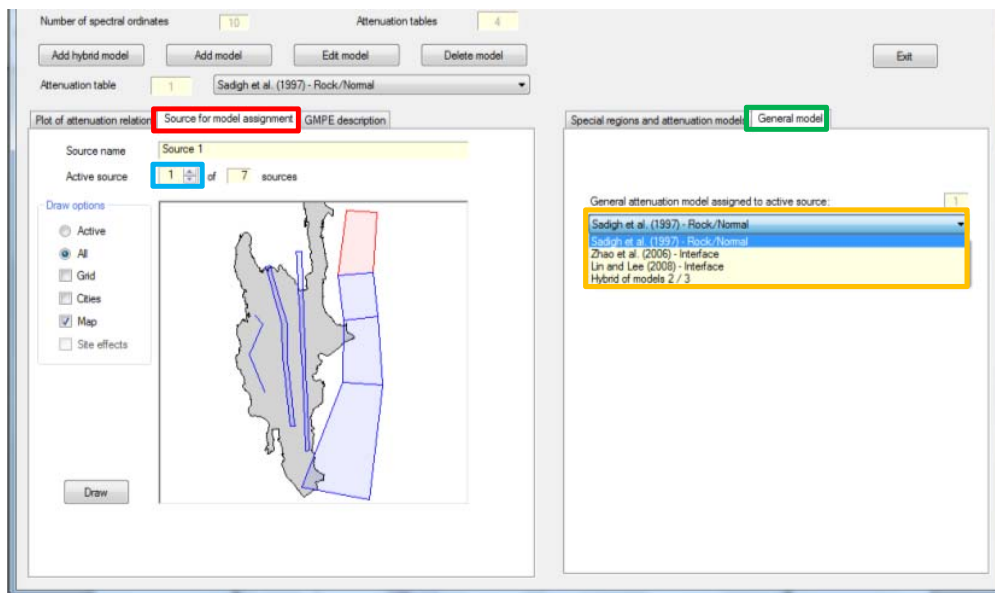



Figure 3-36 Assignment of GMPM to the seismic sources

For the CAPRA Island example, the GMPM assigned to each seismic source is as follows:

- Source 1: Hybrid of models 2/3
- Source 2: Hybrid of models 2/3
- Source 3: Hybrid of models 2/3
- Source 4: Hybrid of models 2/3
- Source 5: Sadigh et al. (1997)
- Source 6: Sadigh et al. (1997)
- Source 7: Sadigh et al. (1997)
- Source 8: Sadigh et al. (1997)
- Source 9: Sadigh et al. (1997)

Once all seismic sources have assigned a GMPM, click on the “Exit” button (top right) to return to the main screen of R-CRISIS.

3.3.7 GMPE analyzer

R-CRISIS provides the capability of comparing, in a graphical way, the different GMPM that have been added to the PSHA project. To access this tool, click on the “GMPE analyzer” button, , in the main screen of R-CRISIS and afterwards, a screen like the one shown in Figure 3-37 will be displayed. On it, all the GMPM that have been previously added to the R-CRISIS project are displayed and their visualization can be activated and/or deactivated with the “draw” option (tick boxes) shown in the red rectangle of Figure 3-37. GMPM are displayed either in terms of spectra (for the previously defined spectral ordinate range) or attenuation curves. For the latter, any of the four distances accepted by R-CRISIS can be selected from the display list inside the green rectangle of Figure 3-37. Magnitude, spectral ordinate and percentile values can be set from the fields inside the orange rectangle in Figure 3-37 and the plot refreshed with the “Draw” button (top right). The tick boxes in the horizontal and vertical axes when are activated set logarithmic scales. The data of the GMPM that is being displayed can be copied to the clipboard (in ASCII format) by clicking the “Copy” button (blue rectangle in Figure 3-37). It can be later copied in any spreadsheet (e.g. Microsoft Excel) for further analysis.

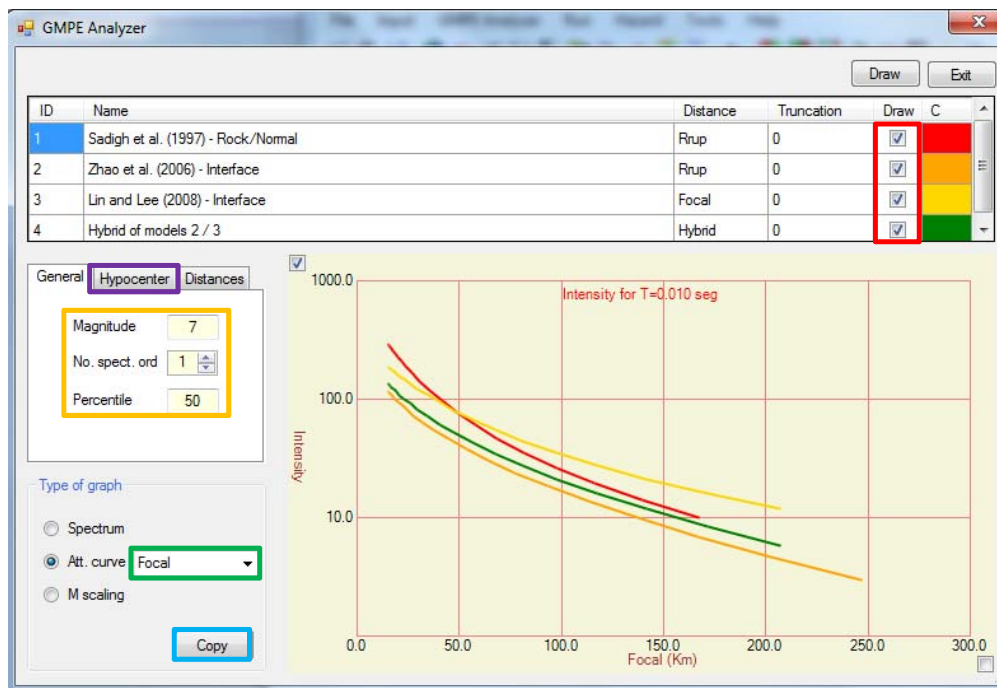



Figure 3-37 GMPM analyzer screen of R-CRISIS

In the “Hypocenter” tab (purple rectangle), the user can also define some of the characteristics of the rupture that can influence the intensities provided by the GMPM when R_{RUP} and/or R_{JB} distances are used, such as the strike and dip.

To return to the main screen of R-CRISIS, click on the “Exit” button (top right).

3.3.8 Site-effects grids (optional)

Site-effects can be considered in the PSHA project of R-CRISIS by means of spectral transfer functions (CAPRA-type), or special attenuation models (CY2014 or V_{s30} models) – See Section 2-5 for more details. To add the site-effects to the R-CRISIS project, click on the “Site-effects grids” button, , in the main screen of R-CRISIS and a screen like the one shown in Figure 3-38 will be displayed from where the corresponding option in which the site-effects are to be included needs to be selected (red rectangle in Figure 3-38). The available options in that list are explained next:

- ERN.SiteEffects.MallaVs30: Vs30 grid to be used directly in the GMPMs of the R-CRISIS project
- ERN.SiteEffects.MallaEfectosSitioSismoRAM: CAPRA-type format
- ERN.SiteEffects.MallaVs30CY14: Vs30 grid to be used in the estimation of the amplification factors by Chiou and Youngs (2014).

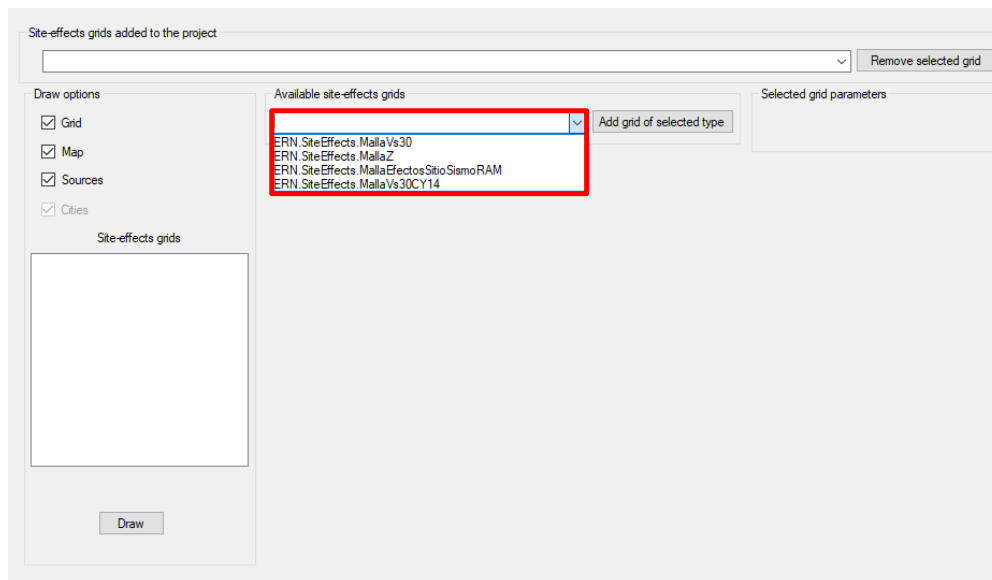


Figure 3-38 Site-effects screen of R-CRISIS

For the CAPRA Island example the site effects will be included in the CAPRA-type format (accompanying microzonation *.grd and *.ft files) that have associated the spectral transfer functions for three homogeneous soil zones for a location within the CAPRA Island. When said button is clicked, an explorer window will be displayed from where the user needs to specify the path where the *.grd file is stored¹⁹.

¹⁹ When the CAPRA-type site-effects format is selected, the *.grd file needs to be stored at the same path with an accompanying *.ft file that has the same name

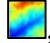
Once the *.grd file has been added, the name of the grid file will appear in the site-effects grid list (red rectangle in Figure 3-39) and the different homogeneous soil zones will be displayed in the area shown inside the green rectangle of Figure 3-39. All computation points inside the site-effects grid will have the hazard intensities modified by the values defined in the spectral transfer functions and therefore, within that area, results are to be understood as at ground level instead of at bedrock one.



Figure 3-39 Visualization of added site-effects grids to R-CRISIS project

To return to the main screen of R-CRISIS, click the “close” button (top right).

3.3.9 Digital elevation models (optional)

To add a digital elevation model (DEM) to the R-CRISIS project, click on the “Give a DEM” button, , in the main screen of R-CRISIS and a screen like the one shown in Figure 3-40 will be displayed. By double clicking on the button just to the right of the path field (see red rectangle of Figure 3-40), on the explorer window the DEM, in *.grd format, can be added to the R-CRISIS project.

For the CAPRA Island example, the grid named “CAPRA Island DEM” corresponds to the DEM (in km) to be used.

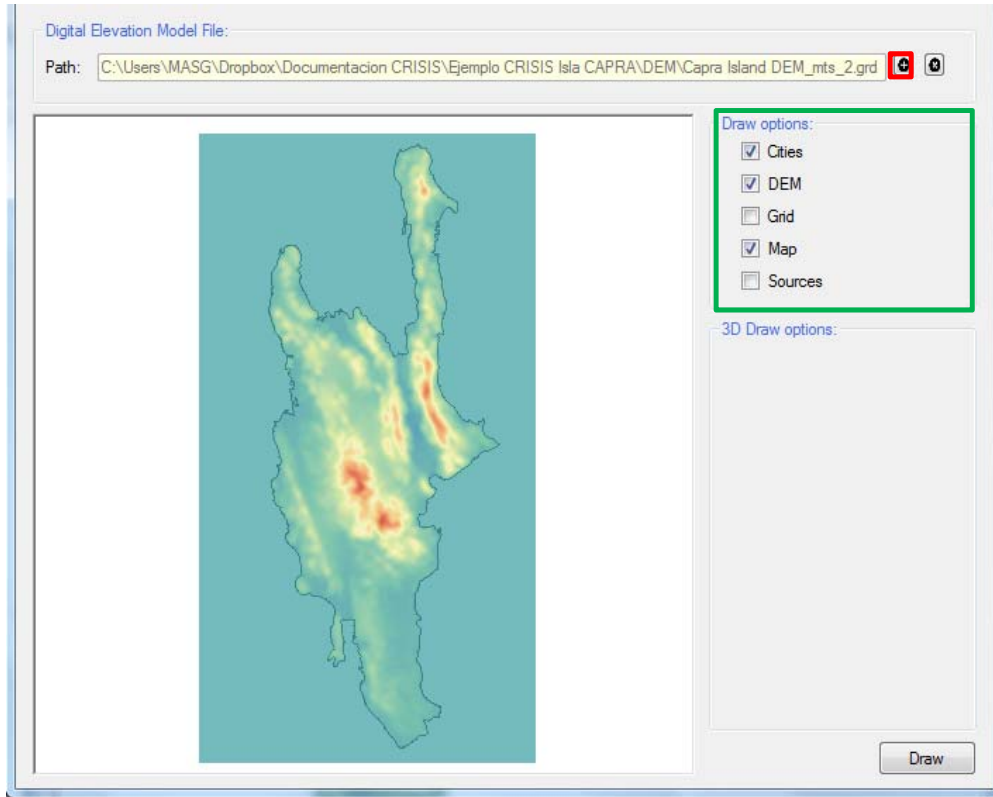



Figure 3-40 DEM screen and visualization screen of R-CRISIS

Once a DEM has been added to the R-CRISIS project, all hazard calculations for sites that are within the extent of the grid will consider the distance to the surface.

To return to the main screen of R-CRISIS, click the “close” button (top right).

3.3.10 Global parameters

To either review or setup some parameters of the R-CRISIS project that will be used during the computation process such as the maximum integration distance, timeframes (for the exceedance probabilities) and mean return periods for the hazard maps and uniform hazard spectra, by clicking in the “Global parameters” button, , in the main screen of R-CRISIS, a screen like the one shown in Figure 3-41 will be displayed.

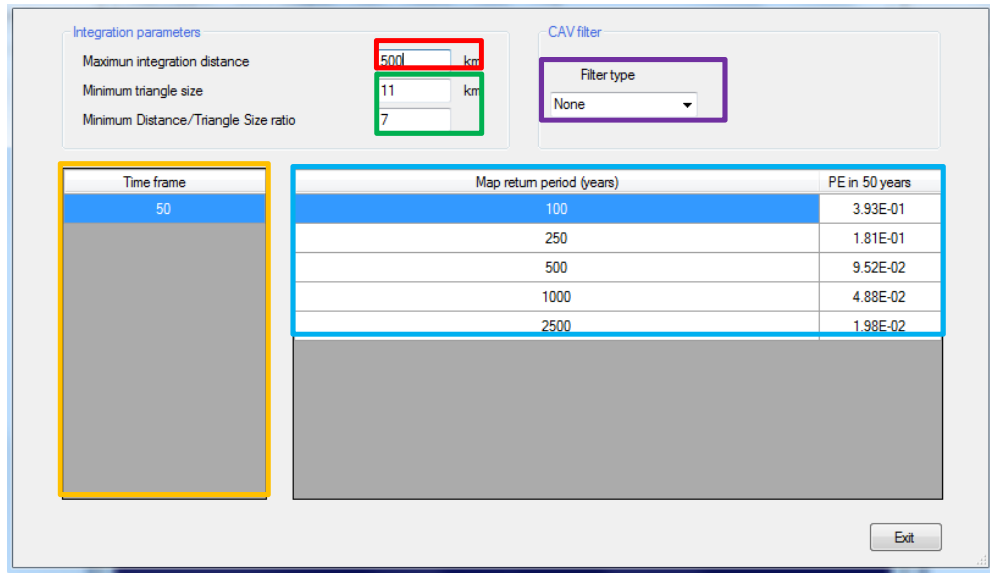


Figure 3-41 Definition of global parameters for the seismic hazard analysis

The maximum integration distance (in km) is to be set in the field inside the red rectangle in Figure 3-41, whereas the parameters for the recursive subdivision of the sources into triangles are to be provided in the fields inside the green rectangles of Figure 3-41. By default, only one timeframe is included in the R-CRISIS project (50 years) but additional ones can be added or deleted by right clicking on the area inside the orange rectangle in Figure 3-41 and choosing the “Insert row” or “Delete row” options respectively. Five different mean return periods can be set by typing their value in years in the fields shown inside the blue rectangle in Figure 3-41. Automatically, for each timeframe, the exceedance probability for each of these values will be calculated. CAV filters (see Section 2.11) for M_s and M_w can be selected from the list inside the purple rectangle of Figure 3-41.

For the CAPRA Island example, the maximum integration distance is set to 250km whereas the default values for the sub-sources data are used. Also, only one timeframe equal to 50 years is used and no CAV filter is applied.

To return to the main screen of the program, click once on the “Exit” button (bottom right).

Note: maximum integration distance is closely related to the distance range of the selected GMPM in the PSHA project.

3.3.11 Setting output files

The different possible output files can be activated and/or deactivated by accessing screen available in the Input – “Set output files (optional)” menu as shown in Figure 3-42. After this, a screen like the one shown in Figure 3-43 will be displayed from where the different output files can be activated (see a full description of each one in Section 3.3). Note that depending on the project geographical extension and the type of outputs, the resulting files can require large available disk space (e.g. hazard disaggregation for a dense grid). It is suggested that for

the uniform hazard spectra, hazard disaggregation and contribution by source data, instead of a computation grid, a list of sites is provided.

For the CAPRA Island example, when the computation sites are defined by means of a grid, only the *.gra output files are selected. For the case when the computation sites are specified by means of a list of sites, the *.fue, *.map and *.des output files are chosen.

Also, from this menu, three hazard measure types can be chosen:

1. Exceedance probabilities
2. Non-exceedance probabilities
3. Equivalent exceedance rates (annual)

For the CAPRA Island example the hazard intensity measure type corresponds to exceedance probabilities.

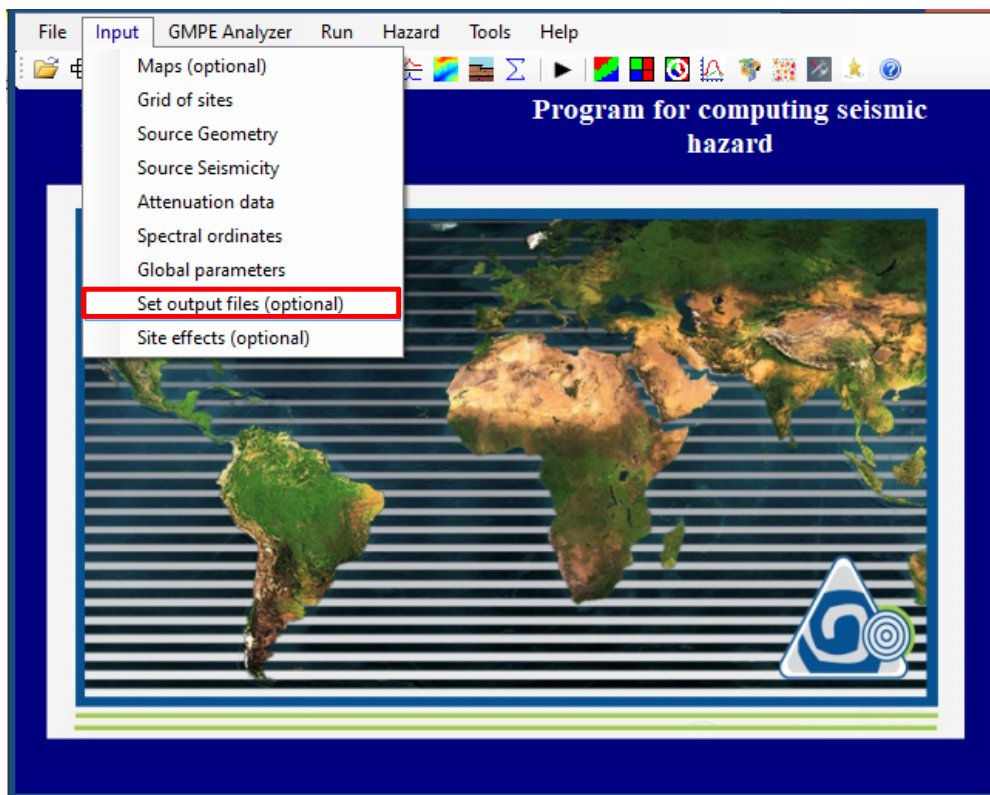


Figure 3-42 Output file menu access in R-CRISIS

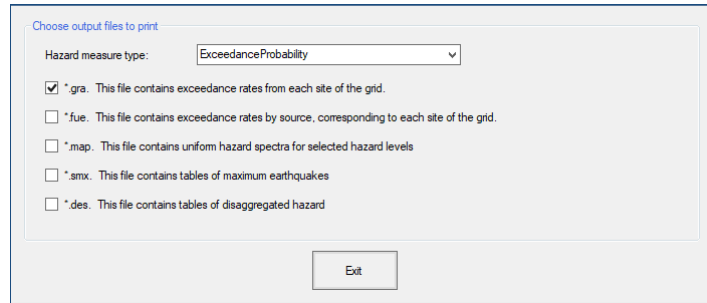




Figure 3-43 Selection of output files in R-CRISIS

To return to the main screen of CRISIS click the “Exit” button at the bottom of the screen shown in Figure 3-43.

3.3.12 Saving the project on disk

The R-CRISIS project can be saved at any stage by clicking once on the “Save data file” button, , in the main screen of R-CRISIS from where using the explorer window, the user can indicate the path where the *.dat or *.xml file will be stored. At this same location, all selected output files will be also stored keeping the same name of the CRISIS project but changing the extension.

3.3.13 Validate data and start execution

To make a final validation of the data associated to the project, by clicking on the “Validate data and start execution” button, , in the main screen of R-CRISIS, a screen like the one shown in Figure 3-44 will be displayed. As a result of the validation process two different of messages can be displayed: warnings and errors. The first are suggestions made by the program after performing verifications mostly on the GMPM regarding the covered magnitude and distance ranges. The second category shows the list of errors (if any) that cover other aspects such as open polygons, sources without assigned GMPM and others.

There is a difference in which R-CRISIS handles those alerts since in the first case (warnings), even if no changes are made by the user to the PSHA project, the computation process can be started; whereas for the second case (errors), changes that solve them are needed before allowing the start of the computation process.

Once the review of the data validation process has been performed by R-CRISIS, the analysis can be executed by clicking on the “Run” button, shown inside the red rectangle of Figure 3-44.

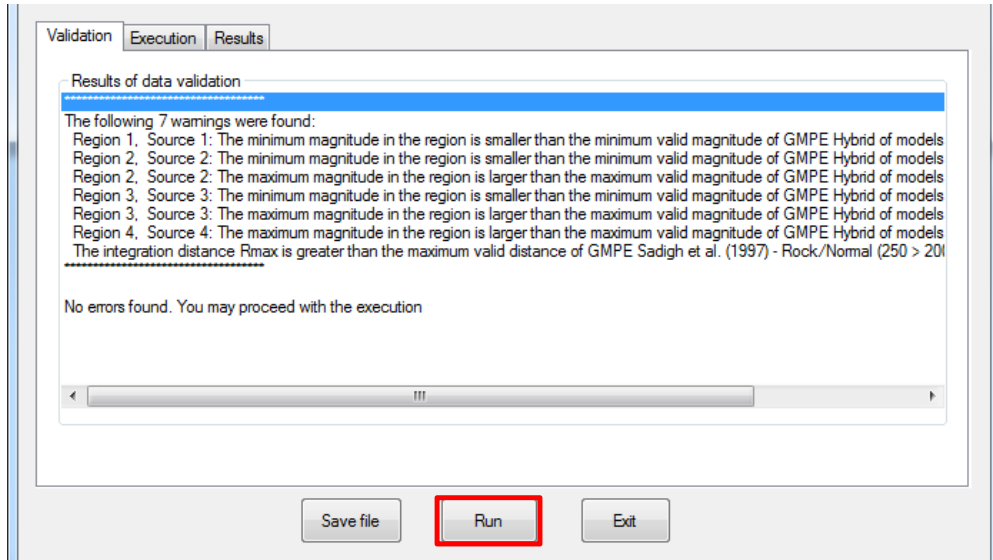


Figure 3-44 Validation data screen of R-CRISIS

While the PSHA is being performed, a screen like the one shown in Figure 3-45 is displayed from where the progress of the analysis can be monitored in both, progress percentage and remaining time. The PSHA can be cancelled at any stage by clicking on the “Cancel” button (red rectangle in Figure 3-45).

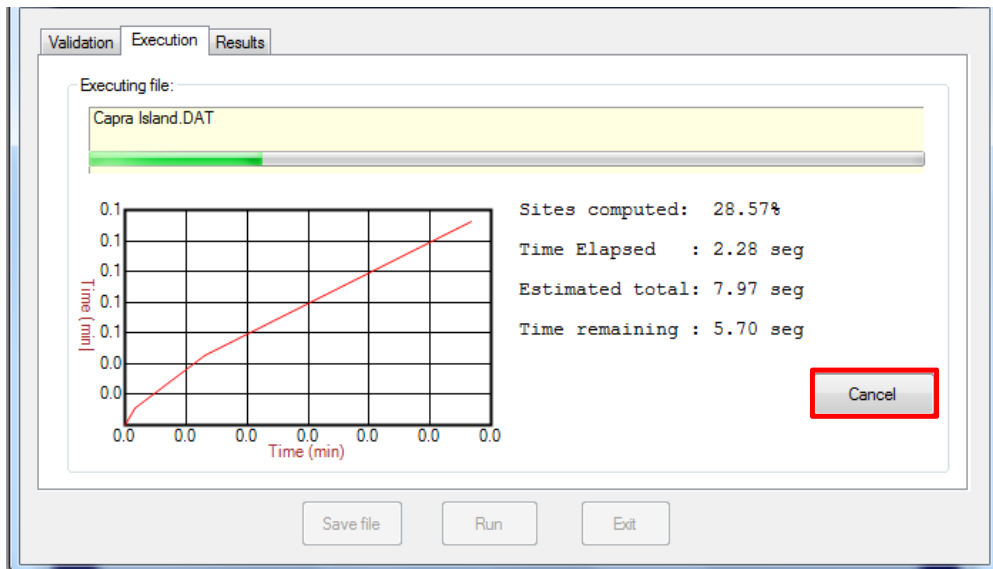


Figure 3-45 Hazard progress bar and remaining time screen

Once the calculation is finished, a screen like the one shown in Figure 3-46 will be displayed from where it can be seen the elapsed time of the calculation process together with the output files that were generated. To return to the main screen of CRISIS, click on the “Exit” button (red rectangle in Figure 3-46).

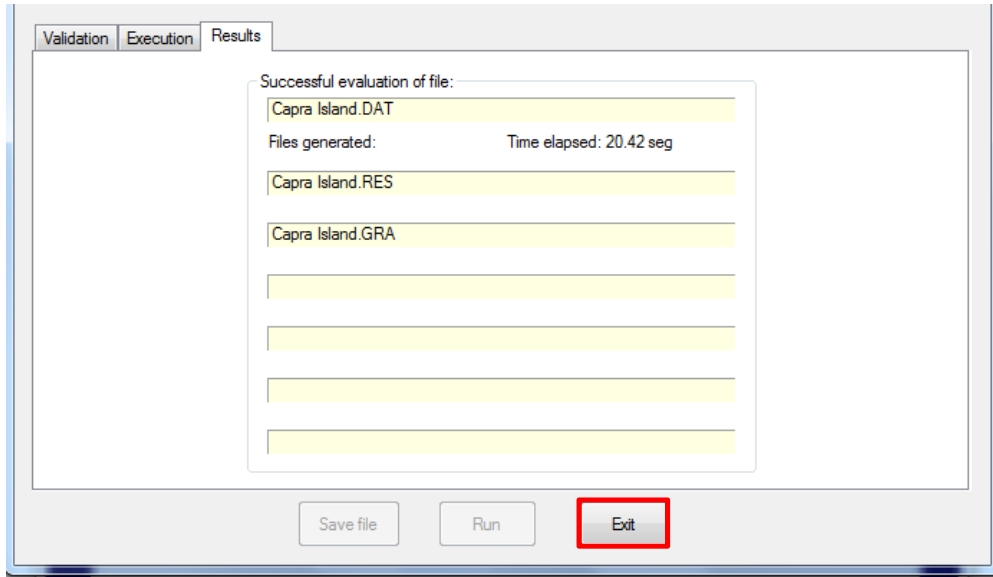


Figure 3-46 Successful computation and generated output files screen of R-CRISIS

Note: regardless the output file(s) selected, a *.res file (see Section 3.5.1 for its complete description) will always be generated for each R-CRISIS project.

3.4 Results visualization and post-processing tools

The following sections describe the different options and tools that R-CRISIS have incorporated to visualize, explore and make comparisons of the results performed on it. To access these tools, the R-CRISIS project needs to be complete (i.e. geometry, seismicity and attenuation data fully assigned) and the PSHA performed. Those can be accessed by selecting the buttons inside the red rectangle in Figure 3-47.

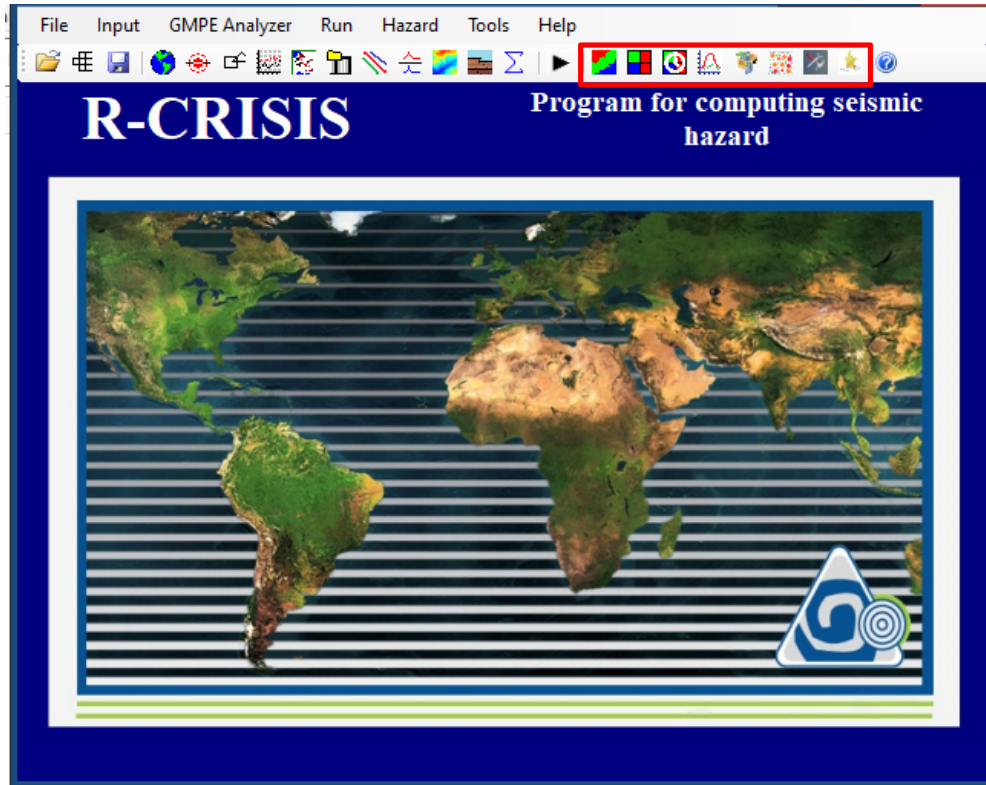
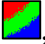


Figure 3-47 Visualization and post-processing options of R-CRISIS

3.4.1 See hazard maps

Once the PSHA has been performed (and it has been done over a grid of computation sites and *.gra output files have been activated), by clicking on the “See hazard maps” button, , in the main screen of R-CRISIS, a screen like the one shown in Figure 3-48 will be displayed from where hazard maps can be generated, drawn and exported.

General settings for the hazard maps

On this screen, the spectral ordinate of interest to obtain the seismic hazard map can be chosen from the available ones in the list within the red rectangle of Figure 3-48. If more than one timeframe has been included in the global parameters, it can be selected from the list inside the green rectangle of Figure 3-48. The exceedance probability of interest is to be set by the user in the field inside the orange rectangle of Figure 3-48.

Different zoom options (in, out and window) can be selected from the buttons inside the blue rectangle of Figure 3-48 whereas the display of additional layers such as the computation grid, the reference map, the seismic sources, reference cities and site effects can be activated by selecting the corresponding choices in the tick boxes inside the purple rectangle of Figure 3-48.

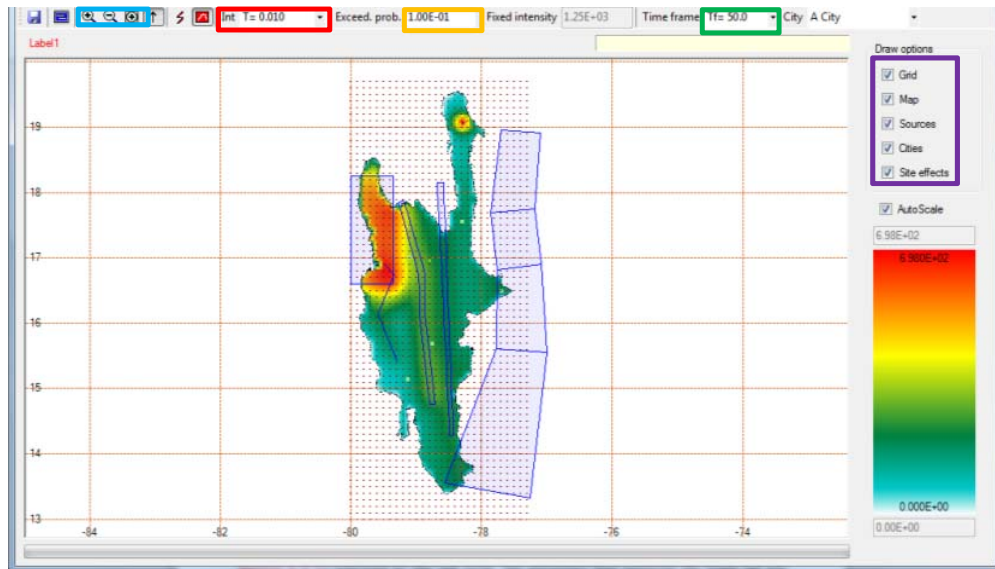


Figure 3-48 Hazard maps screen of R-CRISIS

Additional options for the hazard maps

The intensity scales are initially set by default but those can be later defined by the user by deactivating the “Auto Scale” tick box (red rectangle in Figure 3-49). If this option is selected, the minimum and maximum values of the scale specified by the user are to be included in the fields inside the green rectangles of Figure 3-49. To refresh the view and set it to the new scale, click on the “Draw map with selected options” button (orange rectangle in Figure 3-49).

By clicking at any location within the calculation grid or by choosing a city from the list (blue rectangle of Figure 3-49) if reference cities have been added to the R-CRISIS project, the hazard curve (for the active spectral ordinate and the selected hazard intensity measure in the global parameters) and the uniform hazard spectra (for the corresponding mean return period based on the timeframe and exceedance probability) will be displayed in a screen like the one shown in Figure 3-50.

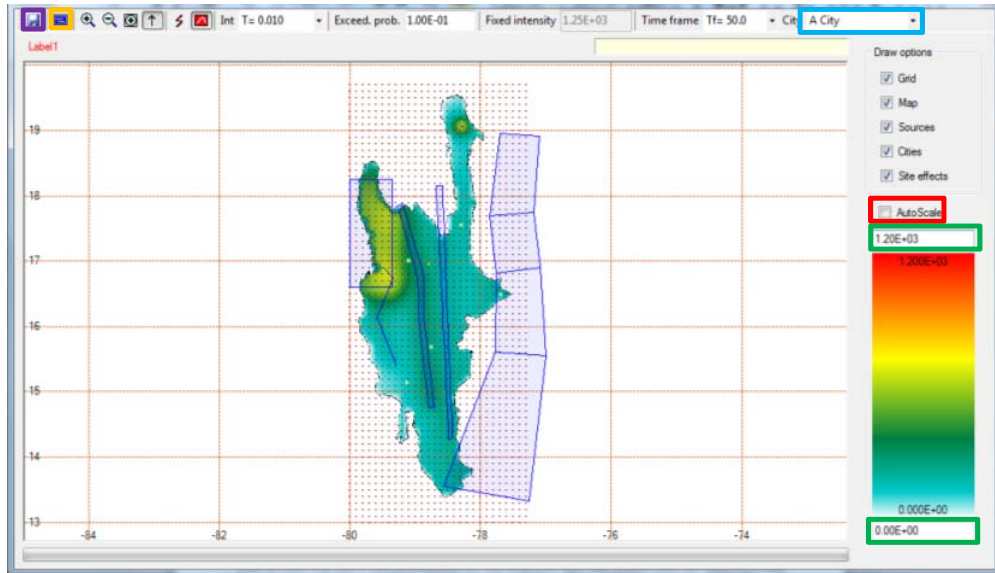


Figure 3-49 Setting scale limits in the hazard maps screen

This screen will show the coordinates of the location that was clicked and the data on it can be either saved (in a text file) or copied (to the clipboard) by using the buttons inside the red rectangles in Figure 3-50.

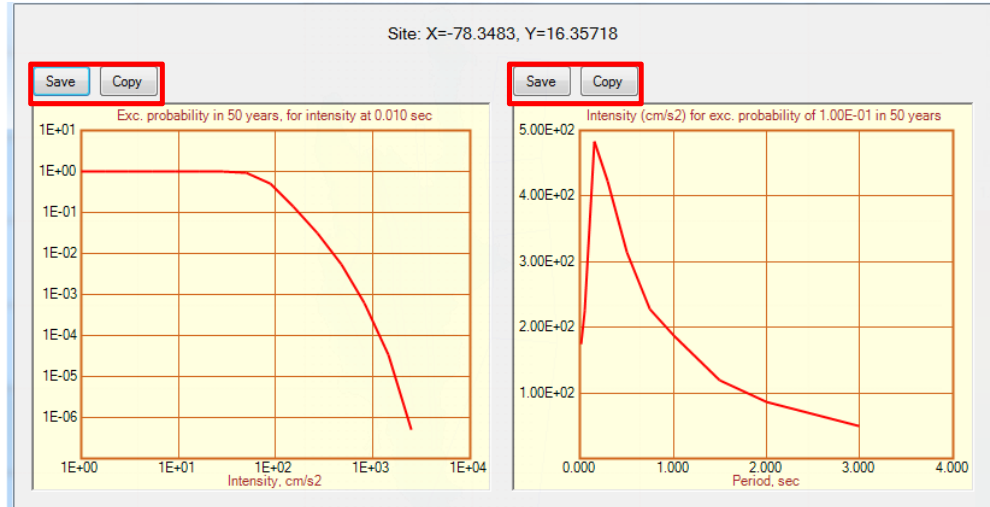


Figure 3-50 Visualization and export of hazard plots and UHS

R-CRISIS allows exporting the hazard maps in different formats and to access these options click on the “Save maps in different formats” button (purple rectangle in Figure 3-49). From the list inside the red rectangle in Figure 3-51, the following output formats for the hazard maps can be chosen:

- Bitmap
- *.xyz file
- Bing maps

- Surfer 6.0 DSBB

If more than one time frame has been included in the global parameters, it needs to be selected from the list (green rectangle in Figure 3-51) and depending on it, the correspondent exceedance probabilities within that timeframe are to be included in the list inside the orange rectangle. To add more exceedance probabilities, right click once on the area inside the orange rectangle of Figure 3-51 and click the “Insert row” option. For each mean return period, hazard maps will be generated for the structural periods that have the tick box activated in the list inside the blue rectangle of Figure 3-51. Once all the options of interest have been selected by the user, by clicking on the “Search output folder” button (purple rectangle in Figure 3-51), the explorer window will be displayed and the path to save the files can be selected by the user. To return to the hazard map screen, click on the “OK” button (bottom right). After this the user will be redirected to the main hazard maps screen of R-CRISIS (Figure 3-49).

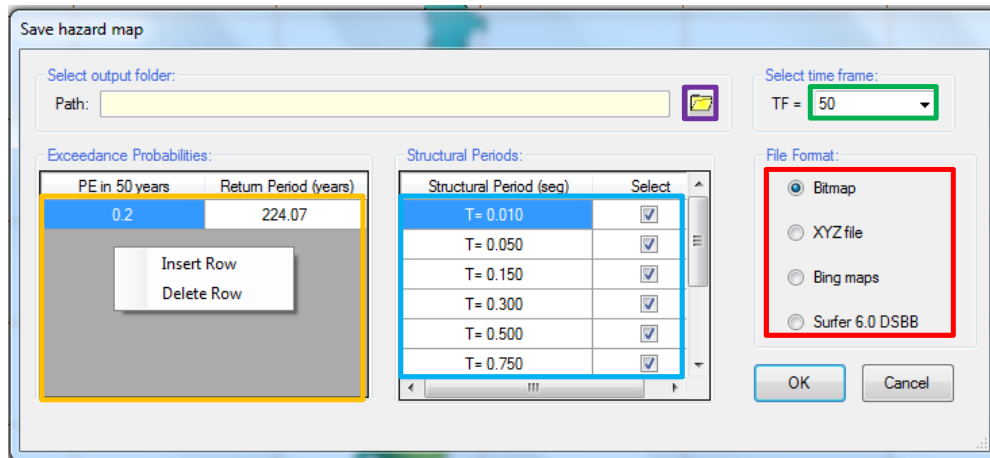



Figure 3-51 Hazard map export options and formats in R-CRISIS

To return from the hazard maps screen to the CRISIS main screen, click on the close button (top right).

3.4.2 Show disaggregation chart

R-CRISIS can generate the exceedance rates disaggregated by magnitude, distance and epsilon (ϵ) value if the *.des output file has been activated. Those results are presented graphically and the corresponding screen can be accessed by clicking once the “Show disaggregation chart” button,  in the main screen of R-CRISIS. After this, a screen like the one shown in Figure 3-52 is displayed and first, the location for which the hazard disaggregation process is required must be defined. By clicking on the map (red rectangle of Figure 3-52) the coordinates are set (those will correspond to the grid node or computation site closest to the point clicked by the user) and displayed in the fields inside the green rectangle of Figure 3-52. Then, the values for the intensity measure (e.g. spectral ordinate), timeframe and epsilon value are to be set by the user from the lists inside the orange rectangle in Figure 3-52. Next, the selection of the intensity or the exceedance probability for which disaggregation results are required is needed; the selection and the values are to be defined

by the user in the fields inside the blue rectangle of Figure 3-52. Finally, in the grid options frame (purple rectangle in Figure 3-52), the user needs to define the extent of the disaggregation chart by setting the lower and upper limits for the magnitude and distance as well as the number of points for which the disaggregation process will be performed. After the parameters have been defined, the disaggregation chart (black rectangle in Figure 3-52) will be updated.

The value at each cell corresponds to the probability that the selected intensity level is exceeded within a given timeframe if only earthquakes with magnitudes and distances within its considered range are accounted for. The color scale is automatically adjusted but, following the same procedure of the seismic hazard maps display, can be customized by the user.

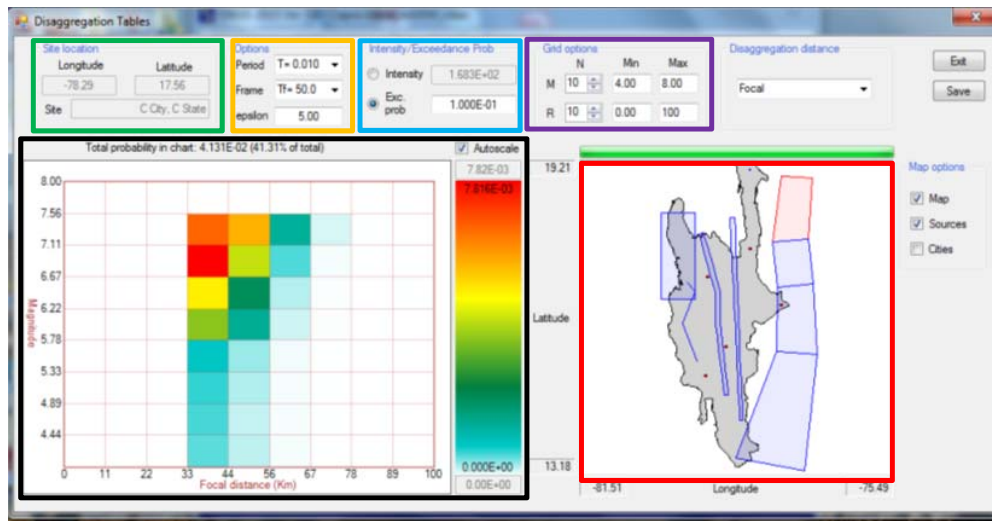


Figure 3-52 Hazard disaggregation screen of R-CRISIS


Disaggregation charts can be saved by clicking the “Save” button that will store a text file with the matrix of disaggregated hazard values.

Note: on the top of the disaggregation chart, the following legend is displayed:

“Total probability in chart: X.XXXE-XX (XX.XX% of total)”

It indicates that with the current grid settings (magnitude and distance ranges) together with the ϵ value provided by the user, the total probability of exceedance is a certain percentage of the total exceedance probability (for all magnitudes and distances and epsilon equal to minus infinity). However, the total probability is computed by interpolation of the previously computed hazard curve for the site and errors in the integration process can be positive or negative. If that hazard curve was calculated using a small number of intensity levels, the interpolation cannot be exact and percentages shown in the legend can be misleading. This problem can be solved by simply considering a larger number of intensity levels in the R-CRISIS project (please refer to the spectral ordinates screen).

3.4.3 Batch disaggregation parameters

Disaggregation files can be generated in R-CRISIS upon user request by clicking once the “Batch disaggregation parameters” button, , in the main screen. After this, a screen like the one shown in Figure 3-53 will be displayed. In the values shown inside the green rectangle in Figure 3-53, the user needs to provide the characteristics of the magnitude-distance grids that will be generated in terms of minimum and maximum values together with the number of bins for each case in each orthogonal direction. In this example, disaggregation will be performed for 10 magnitude bins between 5.0 and 8.0 and for 10 distance bins between 0.0 and 200.0 km. From the list shown inside the orange rectangle in Figure 3-53 the user needs to select the type of used for the disaggregation process (available distances are: R_F , R_{EPI} , R_{JB} and R_{RUP}). From the list shown inside the blue rectangle in Figure 3-53 the user needs to specify the hazard measure in terms of which the disaggregated values will be obtained (available hazard measures are: exceedance probabilities, non-exceedance probabilities and equivalent exceedance rates). In the field inside the red rectangle of Figure 3-53 the user needs to indicate for which periods the disaggregation process will be performed; in case that there is more than one period of interest, values need to be separated by commas. These values correspond for the period indexes, not the actual values of the spectral ordinates. For this example, the indexes 1, 2 and 5 correspond to 0.01, 0.05 and 0.50 s (see Table 3-1). In the field inside the purple rectangle of Figure 3-53 the indexes for the time frames are to be provided; if more than one timeframe is of interest, values need to be separated by commas. From the list inside the black rectangle of Figure 3-53, the user can define if disaggregation is performed for fixed mean return periods (in years) or intensity values; in either case, after selecting the corresponding option, in the fields next to the label the values of interest are to be provided; again, if more than one is of interest, values need to be separated by commas. Finally, in the field inside the yellow rectangle of Figure 3-53, the epsilon values for which the disaggregation charts will be constructed are to be provided; epsilon values are separated by commas and in this example, the values provided indicate that disaggregation charts will be generated for epsilon values of 1, 2 and 5. By default, R-CRISIS performs the hazard disaggregation in a cumulative manner. If the user wants to perform it between two values of ε in the batch disaggregation tool, the tick box in the brown rectangle of Figure 3-53 must be deactivated and the epsilon values must be provided in the field inside the yellow rectangle. The first value of epsilon will be the first upper limit (i.e. hazard disaggregation will be performed from $-\infty$ to that value and for the second batch, that value will ε_0 correspond to ε_1). Using the example of Figure 3-53 and assuming that no cumulative calculations are indicated to be done, the ranges for the disaggregation would be:

- $-\infty$ to 1
- 1 to 2
- 2 to 5

Note: to generate a *.des file, the tick-box in the screen needs to be activated; those files will be stored in the same path as the seismic hazard project (*.dat or *.xml).

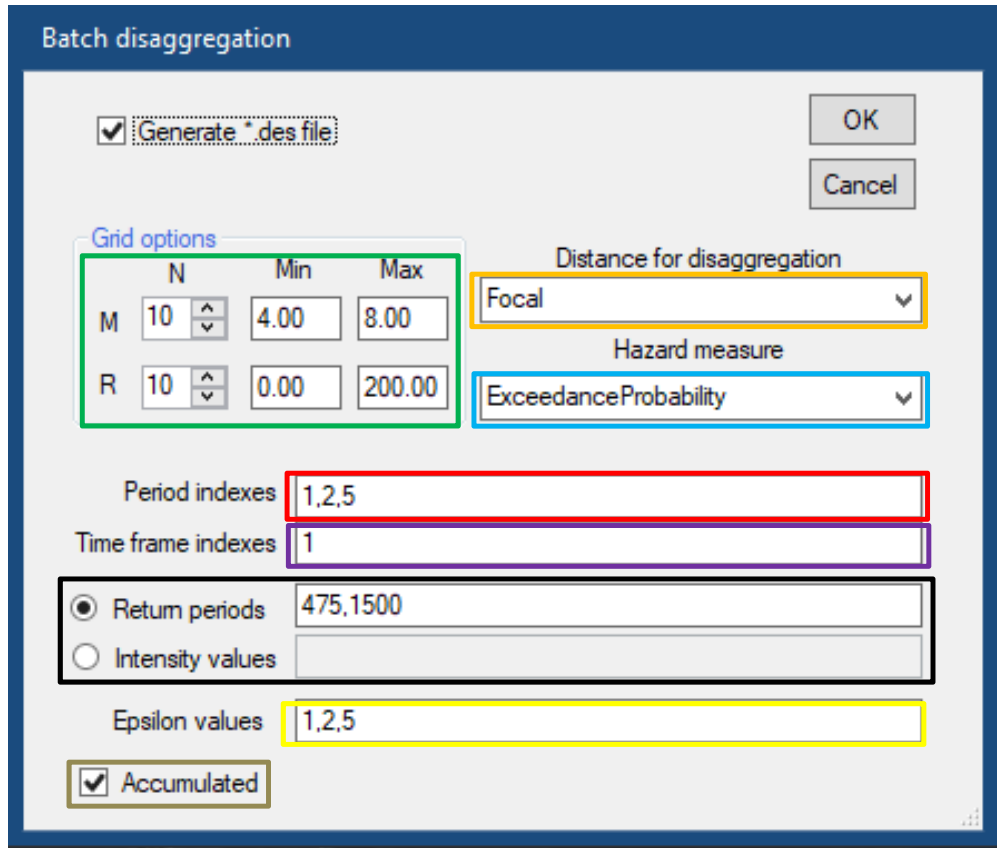



Figure 3-53 Batch disaggregation parameters screen of R-CRISIS

3.4.4 CAPRA seismic scenario generator

3.4.4.1 Multiple scenarios

There are some cases where the PSHA is being developed as an input for a subsequent probabilistic seismic risk analysis. When the last is performed using state-of-the-art methodologies, it is required that the hazard representation corresponds to a set of stochastic events, in this case, all the possible earthquakes that can occur within the analysis area.

In R-CRISIS it is possible to generate said stochastic event set in *.AME format which is compatible with open source and proprietary tools. To do so, by clicking on the “Capra seismic scenario generation” button, , in the main screen of R-CRISIS, a new screen as the one shown in Figure 3-54 will be displayed. On it, the path and name of the resulting *.AME file can be specified by the user in the field inside the red rectangle of Figure 3-54 whereas in the fields inside the green rectangle of Figure 3-54 the parameters which description is included herein is to be defined by the user. Those values will apply for all seismic sources in the R-CRISIS project.

- **Minimum magnitude:** corresponds to the minimum value of magnitudes for which events are to be generated from the seismic sources in the R-CRISIS project. This value needs to be equal or higher than the minimum threshold magnitude (M_o) assigned in the seismicity parameters of all the sources.
- **Number of magnitudes:** This is the number of magnitudes for which at each source stochastic events are to be generated. The values of the magnitudes will depend on the value of this parameter as well as in the minimum magnitude of the *.AME file and the M_U of each seismic source.
- **Sub-source size:** This value, in km, will indicate the resolution level of the stochastic set event.
- **Amin:** This value defines the lower limit of the hazard intensity that will be associated to each event in the stochastic set. This is used in order to avoid large grids with zero or almost zero values.

Default values are provided by R-CRISIS and those, in most of the typical cases are confirmed to work fine. After these values have been set, by clicking on the “Compute AME” button (orange rectangle in Figure 3-54), a metadata screen as the one shown in Figure 3-55 will be displayed.

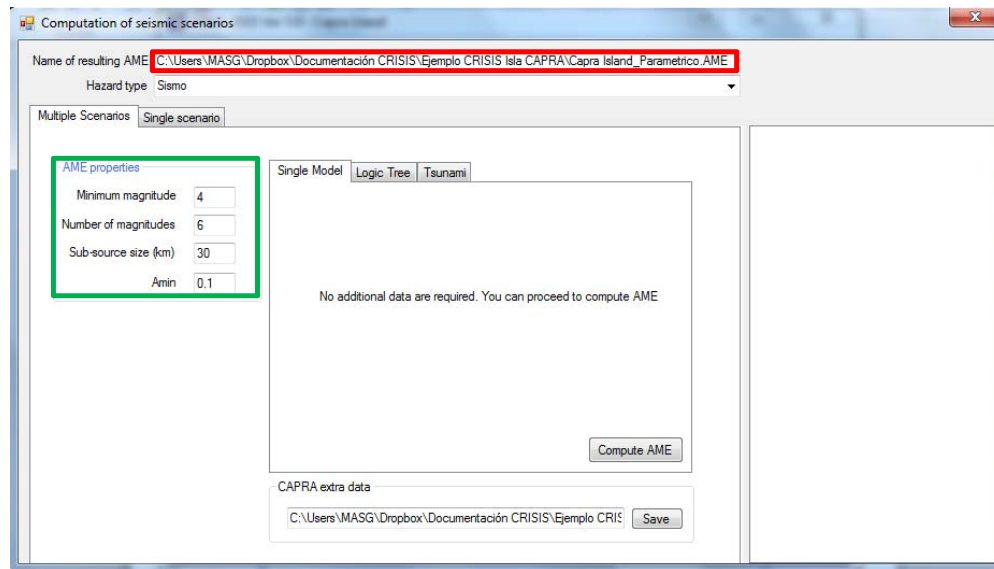


Figure 3-54 CAPRA seismic scenario (multiple) generator of R-CRISIS

The *.AME metadata screen has several tabs which are strongly suggested to be completed by the modeler to keep a tidy record of what is being generated. The metadata will have records about the base R-CRISIS project, the spectral ordinates included, the *.AME properties defined by the user and some contact detail about the individual and/or organization that was in charge of developing the PSHA. Once the details have been completed, by clicking on the “Accept” button (red rectangle in Figure 3-55) the metadata screen will disappear, and the scenario generation process will begin.

The stochastic scenario generation process can be tracked in the list inside the red rectangle of Figure 3-56.

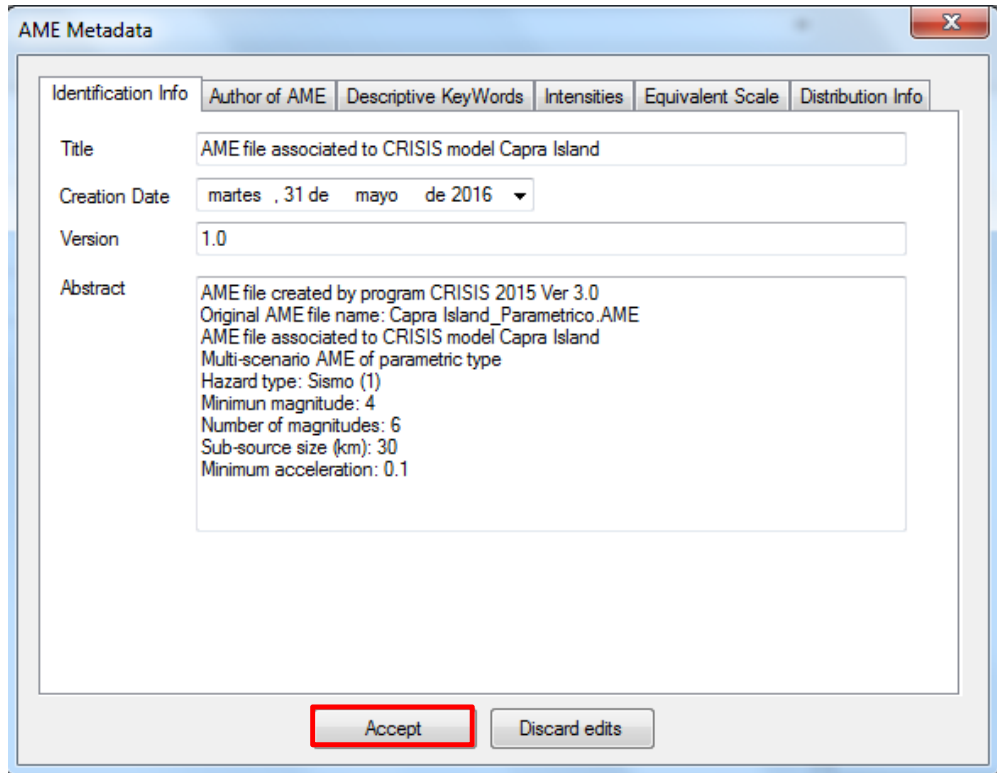


Figure 3-55 *.AME metadata screen in R-CRISIS

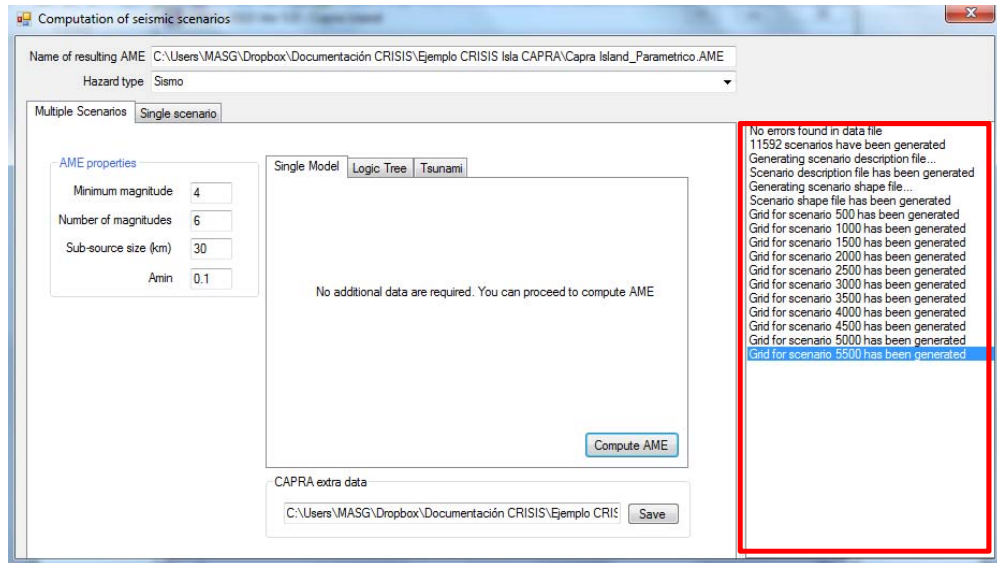


Figure 3-56 Scenario generation progress in R-CRISIS

To return to the main screen of R-CRISIS, click the “close” button (top right).

3.4.4.2 Single scenario

It is also possible to generate an *.AME file that contains information about only one earthquake. In this case, in the “Computation of seismic scenarios” window, the “Single scenario” tab must be selected as shown in the red rectangle of Figure 3-56. On this screen the user can define several parameters such as magnitude, longitude, latitude, depth, strike and depth in the fields shown inside the green rectangle of Figure 3-57. The aspect ratio and the shape of the rupture (elliptical or rectangular) can be defined using the fields inside the orange rectangle in Figure 3-57. *W* is defined in the same direction as the strike whereas *L* is defined in the same direction as the dip. Finally, the user must indicate to which of the seismic sources the single scenario is associated in the top field inside the blue rectangle in Figure 3-58; this is done to assign the GMPM. To estimate the rupture area, if the value is left blank R-CRISIS will calculate it from the *K1* and *K2* values associated to the source but if needed, the user can provide the area (in km²) and that value will be used. After all the fields are completed, the user must click on the “Generate AME” button (black rectangle in Figure 3-57) and the event will be displayed in the area inside the purple rectangle of Figure 3-57.

The single-scenario generator has the option to create hazard footprints only for the median values of the hazard intensity measures used in the R-CRISIS project. If the tick-box is activated a *.grd file will be created with the corresponding information. The user must define the extension of the grid (R value) and the spacing of the grid. Both values are to be indicated in decimal degrees. The *.AME file will be stored in the location defined by the user in the same way as in the multiple scenarios option.

As in the case of the multiple scenarios, R-CRISIS will display a window where the user is expected to fill key metadata. By default, R-CRISIS stores in that metadata the rupture characteristics defined by the user, such as the strike, dip, shape and aspect ratio.

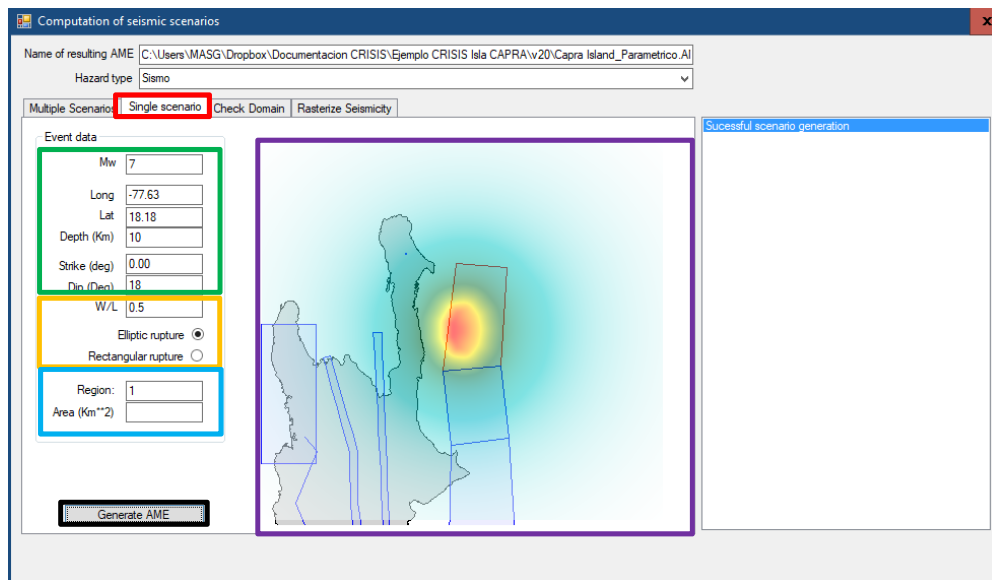



Figure 3-57 CAPRA seismic (single) scenario generator of R-CRISIS

To return to the main screen of R-CRISIS, click the “close” button (top right).

3.4.5 Compute the event-set for a site and generation of stochastic catalogues

This screen will display the event set (i.e. the set of earthquakes that will be used to compute seismic hazard) for a given computation site. To access this tool, click on the “Compute event set for site” button, , in the main screen of R-CRISIS and a screen like the one shown in Figure 3-58 will be displayed.

To calculate the event set, click on the desired computation site (or provide the coordinates in the field inside the red rectangle of Figure 3-58) and, based on the integration distance (see Section 3.3.10) indicated by the red circle, the epicenters that comprise the event set are displayed in the visualization window (green rectangle of Figure 3-58). The colors of the epicenters are different depending on the seismic sources they are associated with.

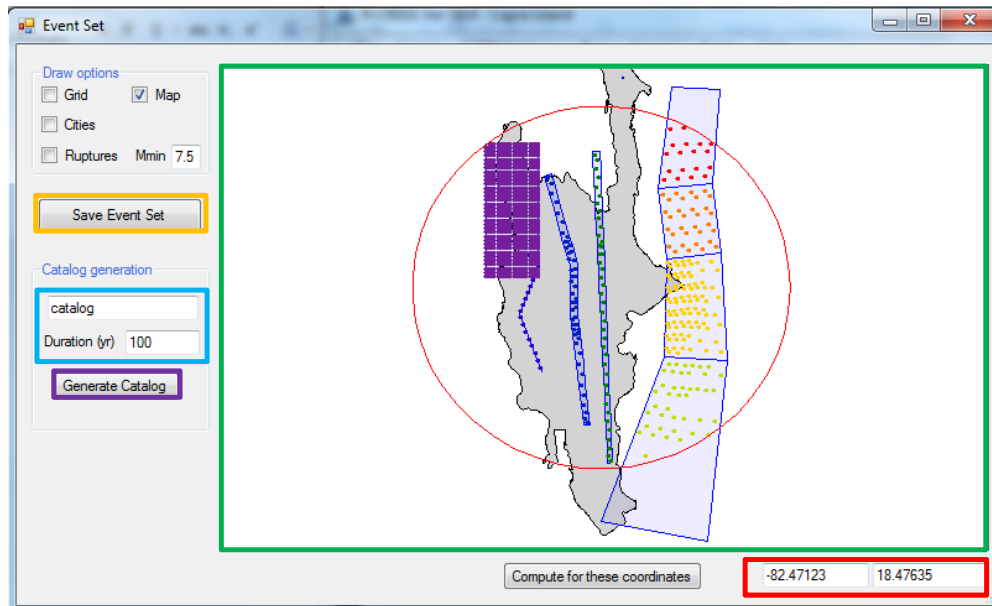


Figure 3-58 Event set screen of R-CRISIS

By clicking on the “Save event set” button (orange rectangle in Figure 3-58), a text file is stored in the path indicated by the user with the following information in columns for each event:

- Kx, Ky and Kz: Hypocentral coordinates (in km), measured with respect to the reference point (usually the first vertex) of the corresponding seismic source.
- X and Y: Epicentral location in geographical coordinates (longitude and latitude in decimal degrees).
- Z: Hypocentral depth in km
- Rfoc: Focal distance from the hypocenter to the computation site
- Rrup: Closest distance to the rupture from the computation site
- RJyB: Joyner and Boore distance from the computation site

- REpi: Epicentral distance to the computation site
- Mag: Event's magnitude
- MED(Sa): Median value of the acceleration, for the first structural period, caused by the event at the computation site.
- SD(LnSa): Standard deviation of the logarithm of acceleration, for the first structural period, caused by the event at the computation site.
- NR: Index of the seismic source to which the event belongs to.
- ZToR: Depth (in km) to the shallowest point of the event's rupture surface.
- Rx: Shortest horizontal distance from the site to a line defined by extending the fault trace (or the top edge of the rupture) to infinity in both directions. Values on the hanging-wall are positive and those in the foot-wall are negative.
- Rate: Annual occurrence rate for the event
- Strike: Strike in degrees for the event
- Dip: Dip in degrees for the event
- RupSize: Rupture size in km²
- Fault aspect ratio: Rupture aspect ratio for the event

From R-CRISIS v20 onwards, the MED(Sa) and SD(LnSa) values can be obtained for all the spectral ordinates defined in the R-CRISIS project. Previous versions of the program only reported the value for the first spectral ordinate of the R-CRISIS project (typically set to PGA).

In R-CRISIS, on the event set generator tool, the user has the possibility to generate a stochastic catalog, for all the active sources in the R-CRISIS project, for a predefined time frame. For this, in the event set generator screen, a name and duration (in years) of the stochastic catalog is to be provided (in the fields inside the blue rectangle of Figure 3-58) followed by a click in the "Generate catalog" button (purple rectangle of Figure 3-58). This tool will generate, in accordance to the seismicity parameters and geometry characteristics of the sources, a possible realization of earthquakes within the indicated duration. In case a large enough time frame is chosen, in all cases a full sample will be generated for small, moderate and large magnitudes, whereas in cases that short time frames are used (e.g. 25, 50 years), the observation of earthquakes with moderate and large magnitudes can be rare.


A shapefile (*.shp) will be stored at the same location as the R-CRISIS project with the following attributes:

- Date: a random date assuming as day 0 the moment of generation of the catalogue
- Magnitude: magnitude of each event
- Long: longitude (in decimal degrees) of each event
- Lat: latitude (in decimal degrees) of each event
- Depth: depth (in km) of each event
- Region: ID of the source to which each event is associated to

Note: this option is only available to seismic sources where earthquake occurrence is characterized by means of Poissonian seismicity models.

To return to the main screen of R-CRISIS, click the "close" button (top right).

3.4.6 Show event-set characteristics

A new feature implemented in R-CRISIS has to do with the possibility of visualizing the characteristics, in terms of rupture (shape, size and aspect ratio, among others) of each event associated to the seismic sources. To see these features, the user must click on the “Source geometry data” button, , in the main screen of R-CRISIS and the geometry screen of R-CRISIS (see Figure 3-12) will be displayed. If, for instance, the characteristics of the event set associated to Source 1 in this example want to be seen, the user must activate the tick-box associated to showing the event set (as shown inside the red rectangle in Figure by clicking in the button inside the red rectangle in Figure 3-59). After that, the user can click at any location within the boundaries of the seismic source and the all the events will be displayed in the window inside the green rectangle in Figure 3-59. The speed of the visualization process can be controlled by the user by changing the location of the button shown inside the yellow rectangle in Figure 3-59. The more it is placed to the left, the faster it will move between events. Once the visualization of all the events is finished (the last one will remain visible and still in the visualization screen), the user can return to the main screen of CRISIS by clicking on the exit button (top right).

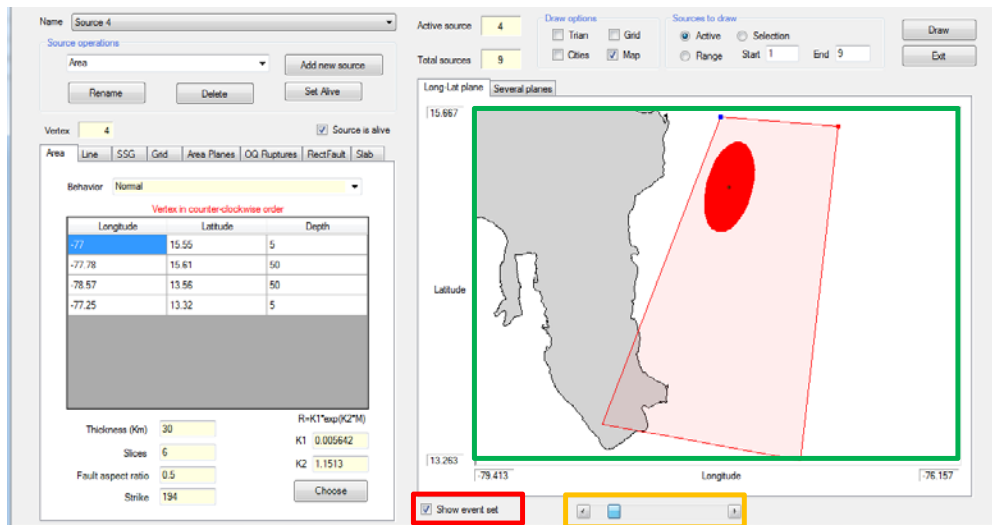

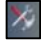


Figure 3-59 Visualization of the event set characteristics for a seismic source

3.4.7 Tools

R-CRISIS has implemented a set of tools that can be useful for both, file preparation and results comparison purposes. This manual provides an explanation of the “GMPM branch constructor” and “Map comparer tools” that can be accessed by clicking on the “Tools” button, , in the main screen of R-CRISIS and by selecting the corresponding tab on the displayed screen.

GMPM branch constructor

This screen allows constructing the different branches for a PSHA that uses the logic-tree approach when only changes related to the GMPM exist. To activate this screen, click on the “Tools” button, , in the main screen of R-CRISIS and select the corresponding tab as shown in Figure 3-60. With this approach, each *.dat file corresponds to one of the branches of the logic-tree. To build the logic-tree using this tool the following information needs to be provided to R-CRISIS. First, by clicking on the button inside the green rectangle of Figure 3-60, the base hazard model is provided; this corresponds to the *.dat file that serves as the basis for the construction of all the branches. This file must be a valid R-CRISIS model from which seismicity, geometry and general information (e.g. spectral ordinates, number of calculation points, etc.) will be read. The GMPM branch constructor will also read from the base model the number of GMPM, *NMOD*, as well as the seismic sources to which each GMPM is assigned. Each row of the data grid represents one of the GMPM provided in the base hazard model. The first row corresponds to GMPM 1 and so on. For instance, if the base hazard model was constructed using four different GMPM, these data grids will have four rows.

Note: the user cannot change the number of rows.

For the i^{th} row, each non-empty column indicates the possible values that the i^{th} GMPM in the base hazard model can take; for example, if for row 1 there are three non-empty columns, this means that GMPM 1 can take three possible values. The user can click in any cell of the data grids to change the selected GMPM and/or the assigned weight.

By clicking in the buttons inside the red rectangle of Figure 3-60, columns are added or deleted from the data grids, whereas by clicking in the button inside the blue rectangle of Figure 3-60, the selected cell’s content is cleared. Each column represents an option for GMPM and their associated weights can be included directly by selecting the tab inside the black rectangle in Figure 3-60. Finally, after the user has provided all the required information about the GMPM and their corresponding weights, by clicking in the purple rectangle of Figure 3-60 all the *.dat files that represent the logic-tree branches are created. By clicking this button, a *.ltc file, which contains the names of the *.dat files corresponding to each branch together with their associated names will be created. This *.ltc file needs to be loaded in the logic-tree calculations screen (see Section 3.2.2) in order to make the PSHA for each branch and the logic-tree combination.

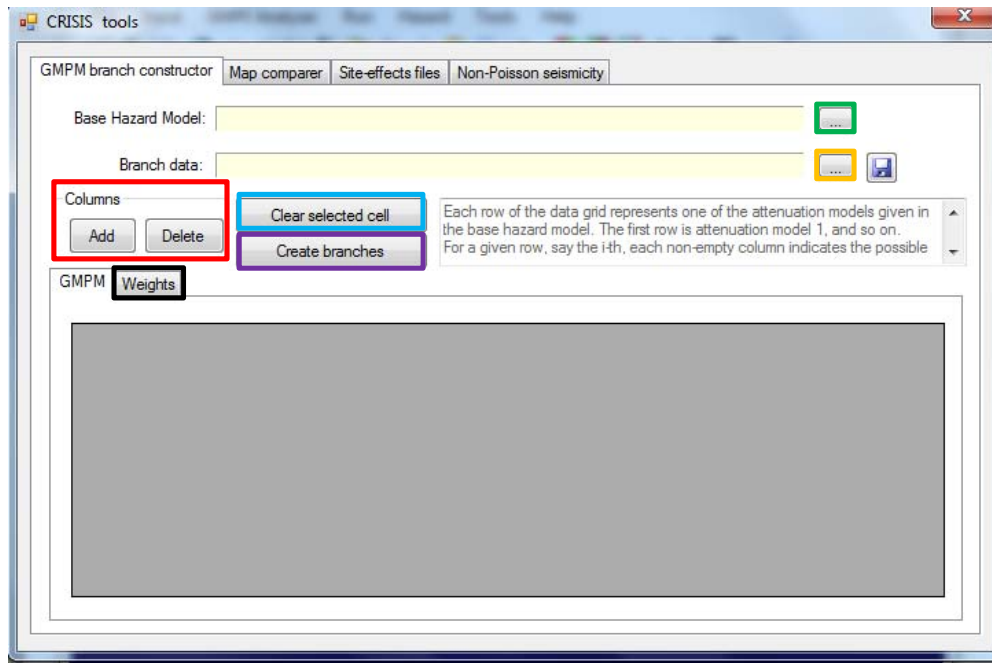


Figure 3-60 GMPM branch constructor tool of R-CRISIS

Note: the logic-tree that can be constructed with this tool is the one in which the geometry and the seismicity characteristics are fixed (i.e. are the same for all the branches) but each branch of the tree represents a different combination of GMPM.

To return to the main screen of R-CRISIS, click the “close” button (top right).

Map comparer

This tool has the capability of comparing in a graphical way the hazard results of two different R-CRISIS projects or the differences between different spectral ordinates for the same R-CRISIS project. To use this tool, it is mandatory that the PSHA has been previously performed and all the output files stored onto disk. Also, it is mandatory that the PSHA in the models that are being compared has been performed at exactly the same computation sites.

In the screen like the one shown in Figure 3-61, the two R-CRISIS models are to be loaded by clicking once in the buttons shown in the red rectangle of Figure 3-61. Once those have been loaded, the fixed probability or intensity levels and options are to be defined in the options and fields inside the green rectangle of Figure 3-61. After this, it is possible then to select, for Model 1 and Model 2 the period (spectral ordinate) and timeframe for which the comparison is desired in the fields indicated inside the orange rectangles in Figure 3-61.

The comparison can be done in absolute (default) or relative values. If the last is desired, the tick box inside the blue rectangle of Figure 3-61 needs to be activated. To refresh the view every time that a change in the parameters has occurred, click on the “Draw” button (purple rectangle in Figure 3-61) and the results together with the scale value will be displayed in the area inside the black rectangle of Figure 3-61.

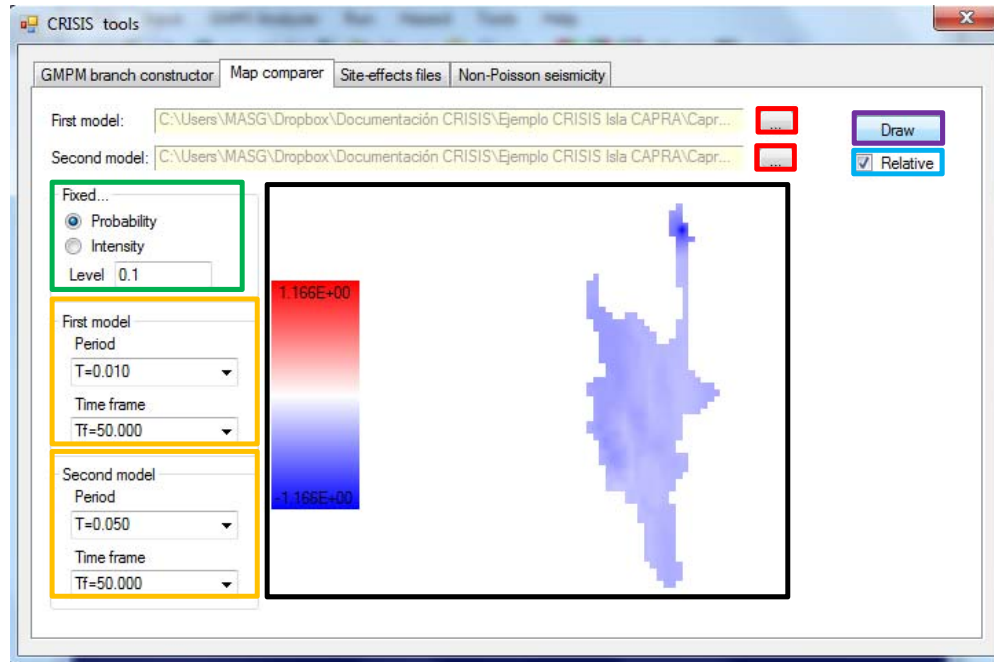


Figure 3-61 Map comparer tool of R-CRISIS

To return to the main screen of R-CRISIS, click the “close” button (top right).

Smoothed seismicity grids from an earthquake catalogue

R-CRISIS includes a tool to generate smoothed seismicity grids from an earthquake catalogue using the approach by Woo (1996). This procedure allows estimating the λ_0 values for each node of the grid after defining a maximum and minimum smoothing radius.

R-CRISIS does not perform any validation of the data on the catalogue. This means that the user should do, beforehand, all the required pre-processing of the information such as, aftershock and foreshock removal, magnitude homogenization and definition of completeness windows.

The catalogue needs to be arranged in either *.shp or *.csv format. In the case of the shapefiles, the user must indicate R-CRISIS from the menu which are the attributes that include the information about the depth and the magnitude of the events. Latitude and longitude are read directly from the shapefile. In the case of the *.csv values, the user should arrange a file with the following format:

Header (eg., long, lat, depth, M)

For each event, separated by comma, the user must provide the following data:

- Longitude (in decimal degrees)
- Latitude (in decimal degrees)
- Depth (in km)


- Magnitude (user defined)

Once the catalogue is loaded in R-CRISIS, the user can define the following parameters to generate the smoothed seismicity grid.

- MaxDepth: maximum depth (in km) to be considered from the catalogue
- MinDepth: minimum depth (in km) to be considered from the catalogue
- Nx: number of points in the X direction
- Ny: number of points in the Y direction
- Xmax: maximum latitude (in decimal degrees) for the grid
- Xmin: minimum latitude (in decimal degrees) for the grid
- Ymax: maximum longitude (in decimal degrees) for the grid
- Ymin: minimum longitude (in decimal degrees) for the grid
- Mmin: threshold magnitude for which the λ is calculated
- t: completeness window in years
- Rmax: minimum smoothing radius (in decimal degrees)
- Rmin: maximum smoothing radius (in decimal degrees)

The smoothed grid will be stored in the same path as the earthquake catalogue in the format required by R-CRISIS to be used as input data for the λ value in the gridded seismicity geometric model. If the gridded seismicity has been calculated from a catalogue in *.csv format, R-CRISIS also generates a *.shp file with the longitude, latitude, depth and magnitude data in form of attributes.

3.4.8 Optimum spectra

If the “Optimum spectra” button, , is selected from the main screen of R-CRISIS, a screen like the one shown in Figure 3-62 will be displayed from where, using the methodological approach proposed by Whitman and Cornell, 1976 and Rosenblueth (1976) which combines the PSHA results with the required capital investment for the construction of buildings, the optimal solution at the societal level can be obtained for the earthquake resistant design coefficients. Based on a set of parameters, as described next, the optimum hazard intensities (and/or the optimum exceedance rates) can be obtained. For the use of this tool, the PSHA needs to be performed first in R-CRISIS and the values for the following parameters provided within the fields inside the red rectangle of Figure 3-62:

- Epsilon and alpha: cost parameters
- Phi: Value of the secondary losses
- Gamma: Discount rate
- T_{min} and T_{max} : Lower and upper limits for the definition of the optimum rates
- Co: lateral resistance of the building when only gravitational loads has been considered.

Note: Units for Co must be the same as the ones selected for the hazard intensity measures in the original R-CRISIS project.

Once those values have been set, by selecting either the optimum intensities or rates from the buttons inside the green rectangle of Figure 3-62, the values indicated in the map inside the orange rectangle of Figure 3-62 correspond to the optimal solution. The same options for export, setting limits of the scale and zooming the results explained for the hazard maps apply in this tool.

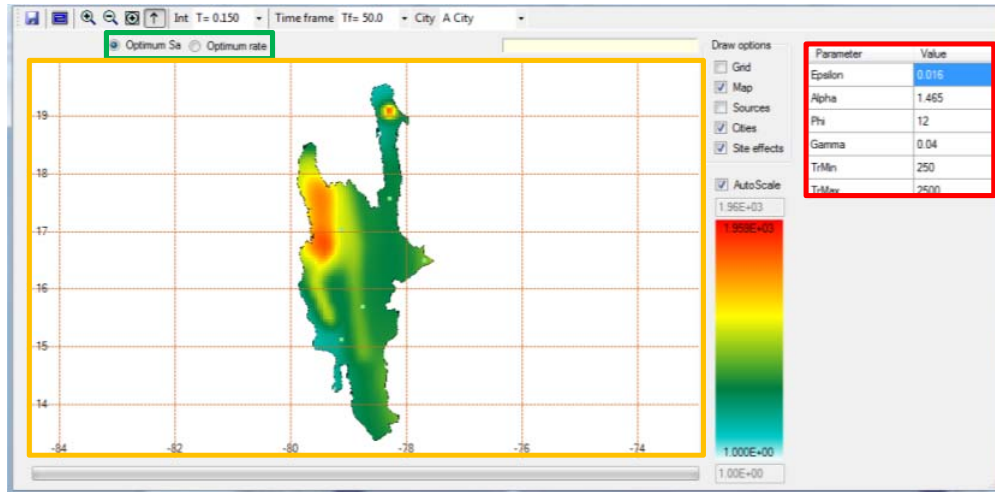



Figure 3-62 Optimum spectra screen of R-CRISIS

To return to the main screen of R-CRISIS, click the “close” button (top right).

3.4.9 Probabilistic liquefaction hazard analysis

When the “Liquefaction analysis” button, , is selected from the main screen of R-CRISIS, a screen like the one shown in Figure 3-63 will be displayed, from where the method to estimate the liquefaction probability can be chosen (red rectangle in Figure 3-63). To date, R-CRISIS implements the model by Ku et al. (2012) although any other that allow estimating the probability of liquefaction can be added seamlessly to the code.

By clicking on the button inside the green rectangle of Figure 3-63, the user can provide R-CRISIS with the soil stratigraphy data in *.csv format with the following structure: a header with the values of $\Delta\sigma$, Nrd and G values. The first one indicates the existence or not of overweight in the soil at the site under analysis. Values larger than zero indicate overweight. Nrd indicates the number of functions for the stress reduction coefficients and G is a unit factor to convert values to g.

The file continues with the Amax values, in the same units as the R-CRISIS project. There can be as much Amax values as needed. Finally, the file contains the soil profile data where for each soil layer, the following information needs to be provided, from top to bottom:

- z: depth in meters
- σ_{vo} : total stress (in MPa)



- σ'_{vo} : effective stress (in MPa)
- $CRR_{7.5}$: cyclic resistance ratio for M7.5. Values equal to -1 indicate depths above the water table level
- r_{d1} : stress reduction coefficient for Amax 1
- r_{d2} : stress reduction coefficient for Amax 2
- ...
- ...
- r_{dN} : stress reduction coefficient for the Nth Amax

Table 3-2 shows an example of a *.csv file to be used in a PLHA in R-CRISIS. Values shown in black are those that need to be included in the *.csv file whereas values shown in red are description of the data included in those particular rows.

Table 3-2 Example of a *.csv file for liquefaction analysis in R-CRISIS

$\Delta\sigma$	Nrd	G						
0	4	981	No overweight stress, 4 stress reduction coefficient functions, GMPEs in cm/s2					
Amax1	Amax2	Amax3	Amax4					
74	143	183	256	4 Amax values (in cm/s2)				
Z	σ_v	σ'_{v0}	CRR75	rd1	rd2	rd3	rd4	
0.02	0.33	0.33	-1	0.9998	0.9994	0.9996	0.9997	
0.04	0.66	0.66	-1	0.9997	0.9978	0.9982	0.9988	
0.08	1.32	1.32	-1	0.9994	0.9972	0.9978	0.9986	
0.1	1.65	1.65	-1	0.9992	0.9967	0.9974	0.9983	
0.12	1.80	1.80	0.3574	0.9991	0.9961	0.9969	0.9980	
0.14	2.10	2.10	0.3697	0.9989	0.9956	0.9965	0.9977	
0.16	2.40	2.40	0.4215	0.9988	0.9950	0.9961	0.9974	
0.18	2.70	2.70	0.3744	0.9986	0.9944	0.9956	0.9971	
0.20	3.00	3.00	0.3747	0.9985	0.9939	0.9952	0.9968	
0.22	3.30	3.30	0.3833	0.9983	0.9933	0.9947	0.9965	
0.24	3.60	3.60	0.4178	0.9982	0.9928	0.9943	0.9962	
0.26	3.90	3.90	0.4414	0.9980	0.9922	0.9939	0.9960	
0.28	4.20	4.20	0.4609	0.9979	0.9917	0.9934	0.9957	
0.30	4.51	4.51	0.4609	0.9977	0.9911	0.9930	0.9954	
0.32	4.81	4.81	0.4609	0.9976	0.9906	0.9925	0.9951	
.....	
.....	
.....	
2.40	38.63	38.43	0.1158	0.9816	0.9883	0.9908	0.9939	
2.42	38.95	38.55	0.1160	0.9815	0.9878	0.9903	0.9936	
2.44	39.27	38.68	0.1188	0.9813	0.9872	0.9899	0.9934	
2.46	39.59	38.80	0.1247	0.9812	0.9867	0.9895	0.9931	
2.48	39.91	38.93	0.1292	0.9810	0.9861	0.9890	0.9928	
2.50	40.23	39.05	0.1322	0.9809	0.9856	0.9886	0.9925	
2.52	40.55	39.17	0.1308	0.9807	0.9850	0.9882	0.9922	
2.54	40.87	39.30	0.1256	0.9806	0.9845	0.9877	0.9919	
2.56	41.19	39.42	0.1227	0.9804	0.9839	0.9873	0.9916	
2.58	41.51	39.55	0.1222	0.9803	0.9833	0.9868	0.9913	
2.60	41.83	39.67	0.1238	0.9801	0.9828	0.9864	0.9910	
2.62	42.15	39.79	0.1291	0.9800	0.9822	0.9860	0.9907	
2.64	42.47	39.92	0.1326	0.9798	0.9814	0.9852	0.9902	
2.66	42.79	40.04	0.1302	0.9797	0.9801	0.9842	0.9895	

Next, the user must define the values for the parameters indicated in the yellow rectangle of Figure 3-63, which correspond to:

- maxCRR_{7.5}: Maximum relative CRR_{7.5} value
- minCRR_{7.5}: Minimum relative CRR_{7.5} value
- NCR_{7.5}: Number of relative CRR_{7.5} values
- NDepths: Number of depth intervals
- Zmax: Maximum depth in m
- Zmin: Minimum depth in m

The first three parameters are aimed to answering a design question about the soil strength needed to have a given liquefaction probability at each depth. The minimum and maximum values for the CRR_{7.5} are defined together with the spacing which is logarithmic and remain fixed for all depths in the analysis. The last three parameters define the depth of interest (from top to bottom) on which the PLHA is performed. Zmin and Zmax values do not have to coincide with those of the soil profile described through the *.csv file, although must be within the valid range. NDepths define the number of depth points within the defined limits. If those

values do not coincide with the z values of the *.csv file, R-CRISIS will interpolate. To return to the main screen of R-CRISIS, click on the OK button (blue rectangle in Figure 3-63).




Figure 3-63 Liquefaction analysis screen of R-CRISIS

The output files of the PLHA are saved in the same path of the R-CRISIS project. In this case two types of files are generated:

- *.gra file including for each location and depth the corresponding exceedance probability, non-exceedance probability or equivalent annual exceedance rate, as selected by the user.
- *.map file including for each location and depth the required soil strength associated to each return period defined in the R-CRISIS project.

Note: it is not possible to perform in a simultaneous manner a PSHA and a PLHA. Once the data for the PLHA is provided to R-CRISIS, it will automatically perform that type of analyses. It is suggested that if a PSHA and a PLHA is performed for the same site(s), a different name is given to separate R-CRISIS projects since if saved at the same path, there will be an overwriting of the *.gra and *.map output files.

3.4.10 Conditional Mean Spectrum

To perform the conditional mean spectrum (CMS) analysis, the R-CRISIS project needs to be run first. After clicking click on the “Conditional mean spectrum” button, , in the main screen of R-CRISIS, a screen as the shown in Figure 3-64 will be displayed. By default, R-CRISIS will calculate the CMS for an arbitrary point within the calculation grid. However, this location can be changed. The R-CRISIS CMS screen displays the site location for which the analysis is performed (red rectangle in Figure 3-64). If a cities’ file has been added to the R-CRISIS project, the user can select a particular location. The vibration period and the timeframe for which the CMS analysis is performed can be selected from the fields inside the green rectangle in Figure 3-64. These values are the ones defined for the R-CRISIS project and if different ones are needed, those must be defined in their corresponding menus. The CMS analysis can be performed by setting an intensity value or an exceedance probability (see orange rectangle in Figure 3-64), so that R-CRISIS estimates the corresponding exceedance probability if the intensity value is provided or vice versa. Finally, the user can choose the correlation model to be used for the CMS analysis.

The CMS results will be displayed in the area inside the purple rectangle of Figure 3-64, where the target spectrum, the calculated CMS and the +/- standard deviation plots are displayed. To save the results (in a *.csv file), the user must click on the save button (brown rectangle in Figure 3-64).

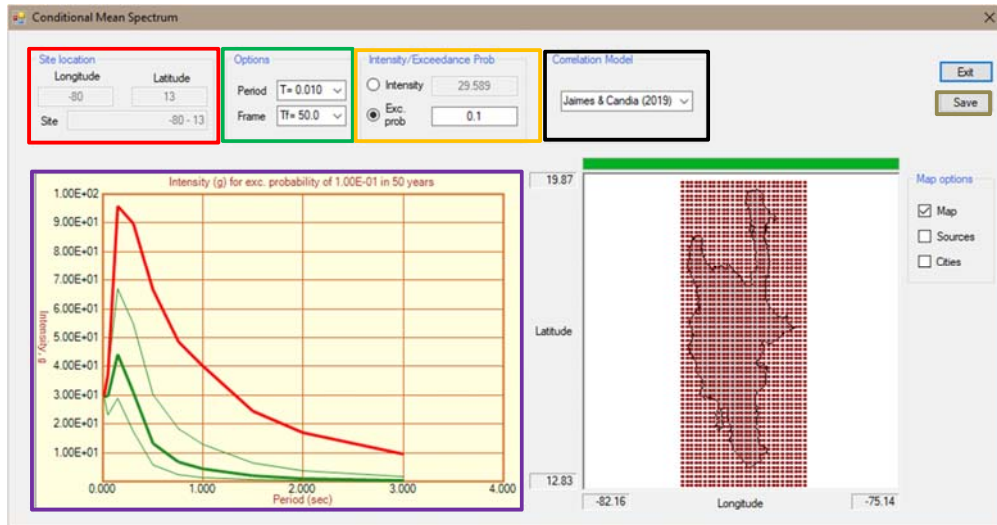


Figure 3-64 CMS screen of R-CRISIS

As an example, a CMS will be calculated for a point within the grid calculation considering the following characteristics:

- Spectral period, $T=0.75s$
- Time frame, $T_f=50$ years
- Exceedance probability, $P_e=0.1$ (which corresponds to a return period of 475)
- Correlation model: Jaimes and Candia (2019)

The selected calculation point is located -78.8° , 15.1° . Calculation parameters and CMS results are shown in Figure 3-65. It can be observed that the thick green curve matches the target intensity at $T=0.75$. The red curve represents the UHS associated to 0.1 exceedance probability in 50 years of time frame (475 years of return period) and the thin green plots depict plus/minus one standard deviation CMS.

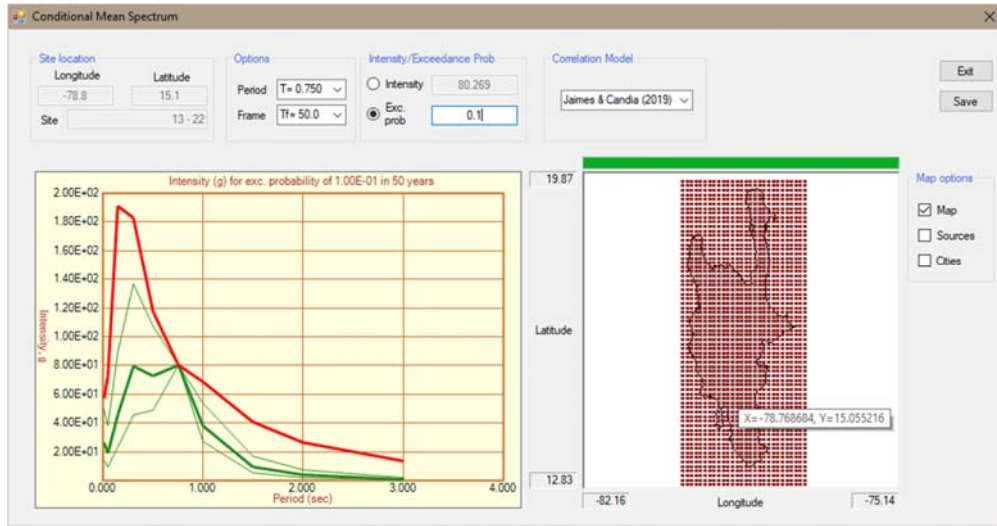


Figure 3-65 Example of a CMS calculation in R-CRISIS

After clicking on save button, results are exported to a *.csv file which contains the information of CMS, the standard deviation of CMS and the target spectrum as shown in Figure 3-66.

The calculation point is displayed at the header²⁰ and then, each column has the following information:

- First column: vibration periods for which the analysis has been performed. These are the same of the R-CRISIS project.
- Second column: CMS median values
- Third column: Standard deviation of the natural logarithm of the calculated CMS
- Fourth column: UHS associated to the return period that corresponds to the defined exceedance probability and timeframe.

The CMS sigma is provided in terms of its natural logarithm. Therefore, the +/- standard deviation of the CMS corresponds to:

$$CMS \pm \sigma_{\ln(CMS)} = e^{\ln(CMS \text{ Median}) \pm \sigma_{\ln(CMS)}} \tag{Eq. 3-1}$$

²⁰ The calculation point is not expressed in longitude and latitude coordinates, but in terms of row and column of grid calculation. In this case, -78.8°W 15.1°N coordinates correspond to row 13 and column 22, respectively.

13 - 22

Period (sec)	CMS Median	CMS SigmaLN _i	UHS
0.01	26.611	0.62653	56.991
0.05	18.827	0.69986	72.997
0.15	45.338	0.67876	191.43
0.3	79.321	0.54678	182.72
0.5	72.763	0.38944	117.66
0.75	80.269	2.2302E-07	80.269
1	38.066	0.34765	68.85
1.5	9.6626	0.5573	40.512
2	3.9135	0.67046	26.522
3	0.88567	0.82056	13.487

Figure 3-66 CMS exported results

Note: The use of hybrid GMPMs may bring problems when calculating CMS in R-CRISIS. It is strongly suggested that the user substitutes this approach by the classic logic-tree when performing these types of analyses in the program.

3.4.11 Export source data to shape

In R-CRISIS it is possible to export the source data to shapefile format. To do so, from the main screen of R-CRISIS access the “File” menu and select the “Export source data to shape” option as shown in Figure 3-63. After clicking on it, the shapefile will be exported to the same path where the *.dat or *.xml file is saved and a confirmation screen like the one shown in Figure 3-64 will be displayed.

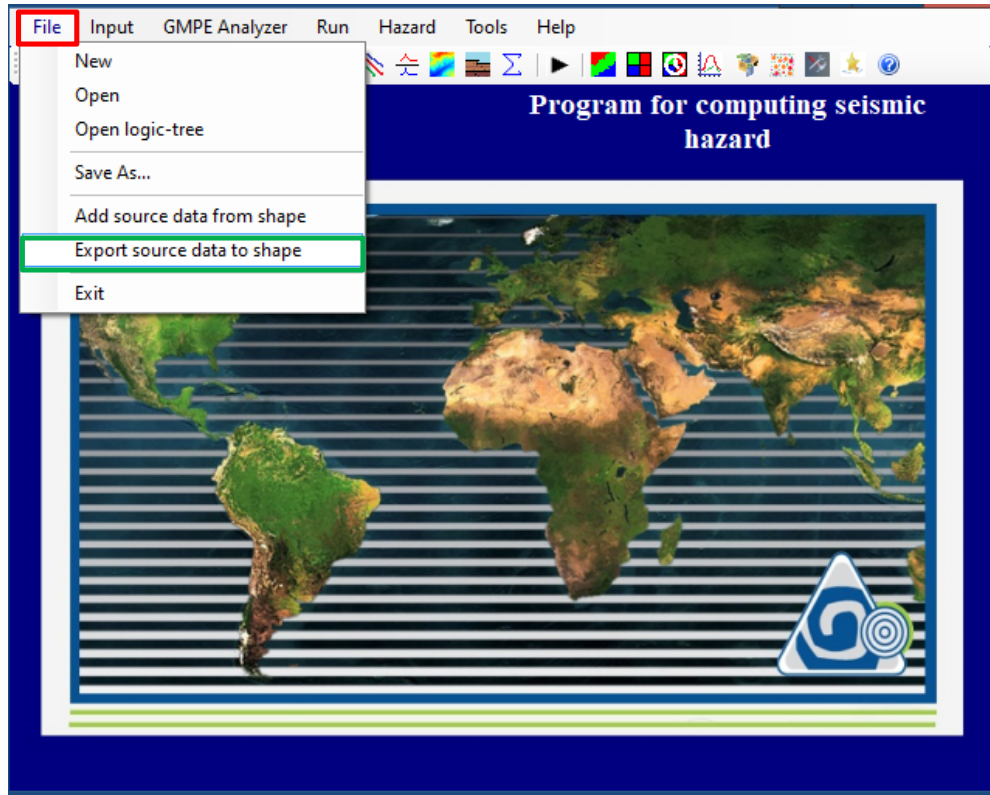


Figure 3-67 Export source data to shapefile in R-CRISIS

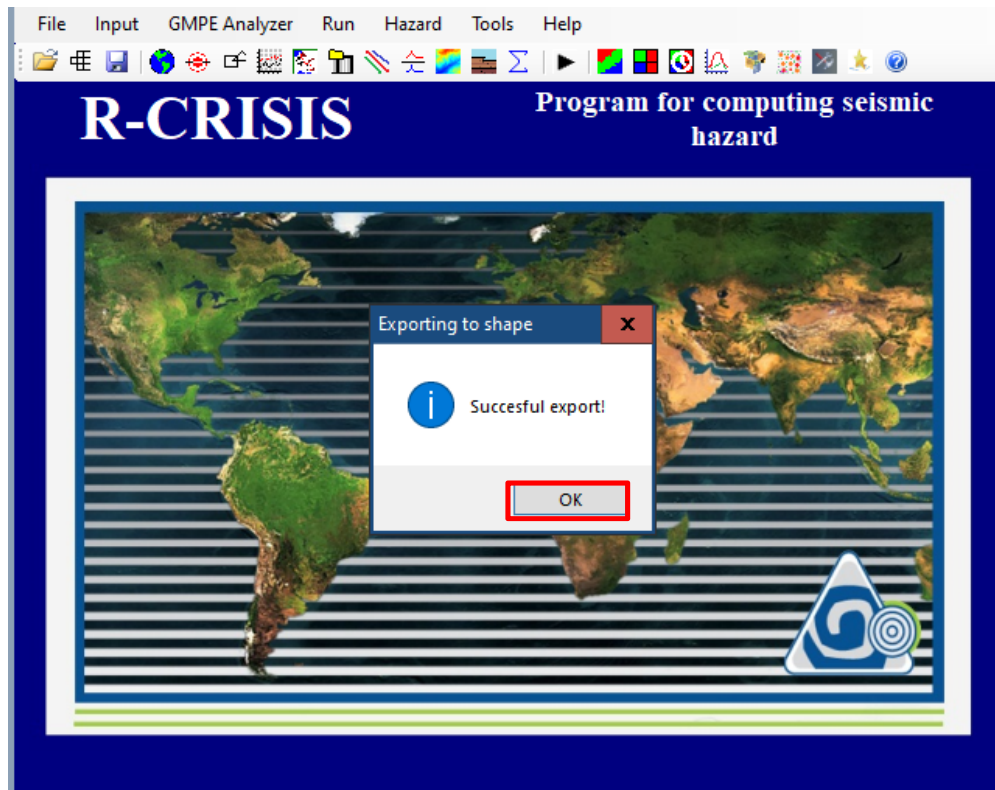


Figure 3-68 Confirmation of a successful shapefile export

To return to the main screen of R-CRISIS, click the “OK” button (right rectangle in Figure 3-64).

Note: a separate shapefile will be created for each geometry model used in the R-CRISIS project (i.e. in the CAPRA Island example, a separate shapefile will be created for the Area, area planes, grid and line sources).

3.5 Results and output files

Upon the user’s selection, CRISIS can generate several output files. The possible output files of R-CRISIS are:

3.5.1 Results file *.res

This file starts with a printout of the name of the run, the date and time of the calculation. It is followed with a summary of the values assigned to the seismicity and geometry models together with the characteristics of the attenuation models. Also it includes a block that summarizes some of the data used for the definition of the computation grid. It also gives a summary of the computations for each site, indicating which sources are of interest the site and which sources were skipped. The computing times are also written at the end of the file.



The *.res file is generated for every R-CRISIS project regardless of the other output files that have been selected.

Note: see the accompanying CAPRA Island.res file for more details

3.5.2 Graphics file *.gra

This file starts with a brief identification header where the version of the CRISIS, date, time, hazard measure and also includes the name of the run. This is followed by data, for each computation site and each spectral ordinate, about the hazard levels and exceedance measures (in terms of exceedance probabilities, non-exceedance probabilities or equivalent exceedance rates). Results are arranged by columns where at least, if only one timeframe has been defined has in the first column the intensity levels (using the spacing scale defined in the spectral ordinates screen) and in the second column the selected hazard measure. If more timeframes have been included, additional columns will be stored in the *.gra file.

This file contains the information required to plot intensity versus exceedance probability within a given timeframe curves.

Note: see the accompanying CAPRA Island.gra file for more details.

3.5.3 Source by source file *.fue

This file starts with a brief identification header where the version of the CRISIS, date, time, hazard measure and also includes the name of the run. This is followed by matrixes, one for each computation site, for each timeframe and for each spectral ordinate that has the exceedance probabilities (or the selected hazard measure) by source. This file contains the information required to plot intensity versus exceedance probability within a given timeframe curves by source to better understand the contribution of each of them to the overall seismic hazard results.

Additionally, CRISIS will generate binary files (one for each intensity measure used in the analysis) to be able to generate its own maps.

Note: see the accompanying CAPRA Island.fue file for more details

3.5.4 Map file *.map

This file starts with a brief identification header where the version of the CRISIS, date, time, hazard measure and also includes the name of the run. Then, for each timeframe and for each computation site, the results for fixed mean return periods, previously specified in the global parameters are written for each spectral ordinate. This file can be used to plot the uniform hazard spectra at different locations for fixed mean return periods; also it is useful to generate contour or 3D maps of intensity levels associated to constant exceedance rates.

Note: see the accompanying CAPRA Island.map file for more details



3.5.5 M-R disaggregation file *.des

This file starts with a brief identification header where the version of the CRISIS, date, time, hazard measure and also includes the name of the run. Then, this file contains results of seismic hazard disaggregation, as a function of magnitude and distance, for given intensity levels, mean return periods, timeframes and epsilon values. These disaggregated results indicate which combinations of magnitude and distance contribute more to the seismic hazard at a specific site, for a given intensity measure, timeframe, and mean return period.

3.5.6 Maximum earthquakes file *.smx

This file starts with a brief identification header where the version of the CRISIS, date, time, hazard measure and also includes the name of the run. Then, this file contains information about the maximum possible intensity values at each computation site. For a given site, these values are computed using the worst combination of distance to a source and expected value of M_U . The highest intensity computed for all sources is reported in this file, for different values of epsilon.

4 Validation tests

The verification of a seismic hazard computer code is crucial for ensuring the user that the calculations performed with it are reliable. The numerical verification process of R-CRISIS has been carried out considering a set of tests developed in a project sponsored by the Pacific Earthquake Engineering Research Center (PEER) documented by Thomas et al. (2010) for the first phase and by Thomas et al. (2014) in the second phase. The results presented herein correspond to the work developed by Villani et al. (2010) and by Ordaz and Aguilar (2015) and explains with detail the procedures, assumptions and options used for each particular case.

Finally, additional validation tests of geometrical, rupture, seismicity and attenuation parameters are included in this section in order to show that R-CRISIS performs well under the framework of the selected methodologies and is suitable for the development of probabilistic seismic hazard analyses.

4.1 PEER validation tests (set 1)

For these validation and verification exercises, two sets of test problems were used for testing some fundamental aspects of the R-CRISIS code such as the treatment of fault sources, recurrence models and rates, strong ground motion attenuation relationships and their associated uncertainties. For the simplest cases analytical solutions were also provided by the PEER project coordinators.

4.1.1 Geometry of the earthquake sources

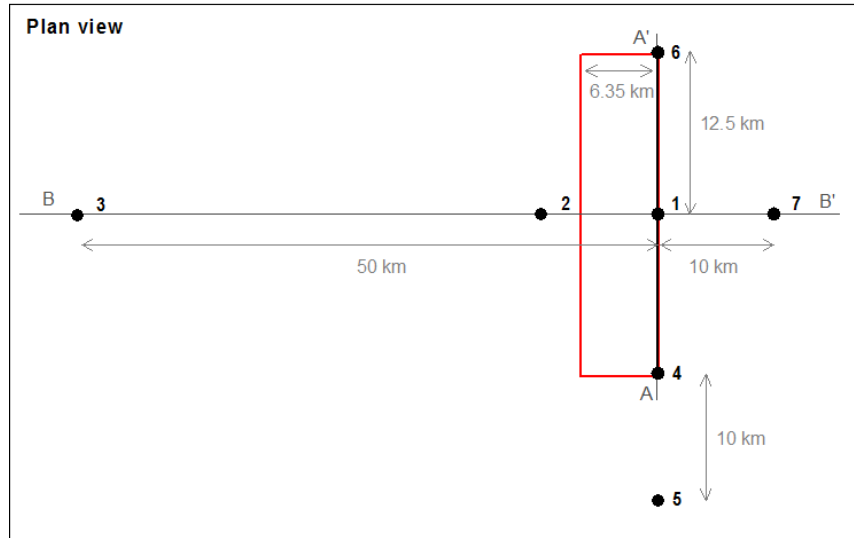
Three different types of earthquake sources were adopted for the tests:

- Two (2) fault sources and,
- One (1) area source with constant depth.

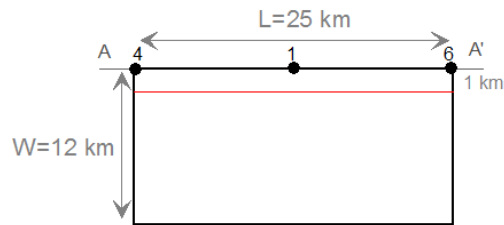
The two fault sources are shown in Figure 4-1 where the thick black line in the plan view corresponds to the trace of the two faults on the surface. Fault 1 (black line) corresponds to a strike-slip vertical source with depth between 0 and 12km, whereas fault 2 (red line) corresponds to a reverse fault with dip of 60° and with depth between 1 and 11km.

The area source is illustrated in Figure 4-2 and corresponds to a circular area with radius of 100km at a constant depth of 5km and with uniform seismicity. The black points identified with numbers in Figures 4-1 and 4-2 show the location of the sites (or observation sites) where the computation of the seismic hazard was made.

Geometry of fault 1 and 2



Cross-sectional view (AA')



Cross-sectional view (BB')



Figure 4-1 Geometry of the fault sources (1 & 2) and location of the observation sites

Geometry of area source

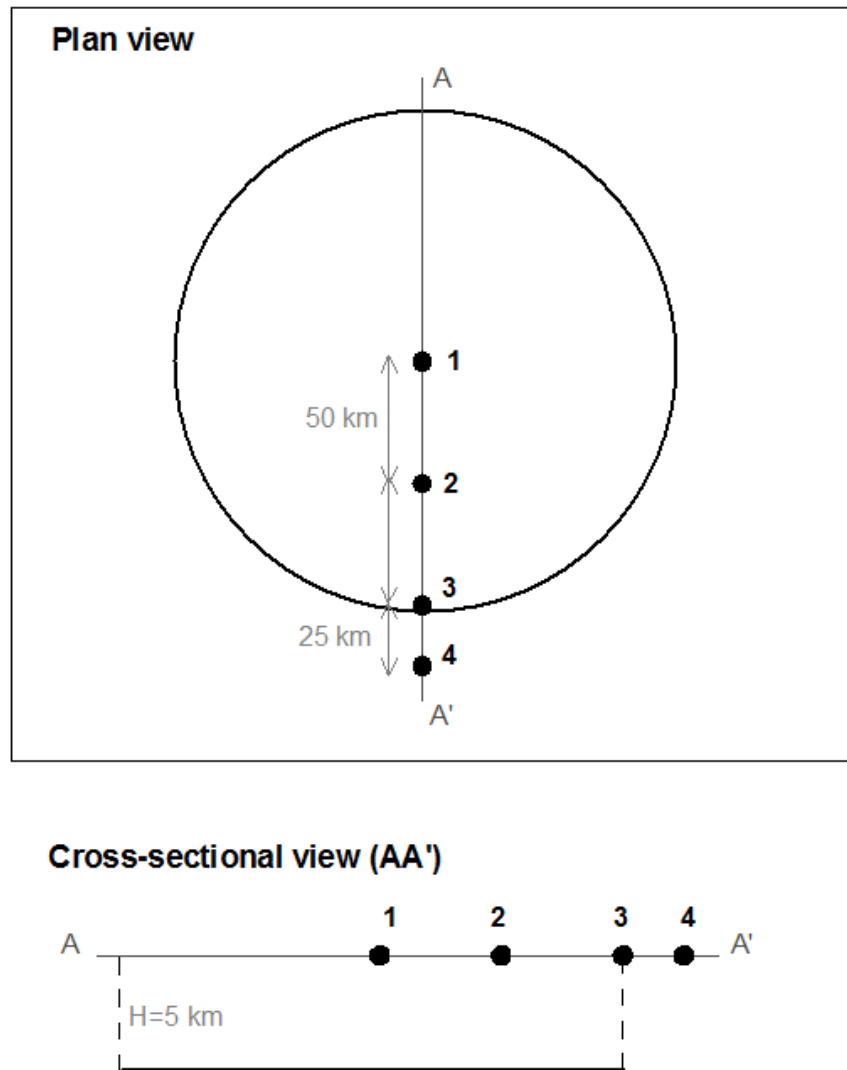


Figure 4-2 Geometry of the area sources and location of the observation sites

4.1.2 Rupture areas

Considering that since R-CRISIS the rectangular fault type was introduced and bearing in mind that for R-CRISIS the definition of the geometry also implies the definition of the shape of the rupture area. Comparisons of the results obtained between different rupture shapes (elliptical and rectangular) are included in this section with the aim of presenting, in a transparent way, the implications the selection of this parameter has in the final hazard results. It is anyhow important to highlight that, from a theoretical point of view, the rupture areas can be rectangular or elliptical (Villani et al., 2010).

Figure 4-3 shows the schematic representation of the elliptical rupture areas, using the strict boundary behavior which, from the theoretical point of view are considered as valid. Anyhow, the inconvenient with them, for locations such as computation sites 4 and 6 (for the cases

when the fault type sources are used) is that when elliptical ruptures exist, regions near the corners of the source do not have sub-sources included and then, the seismic hazard intensities are lower than in the case where rectangular shapes are used.

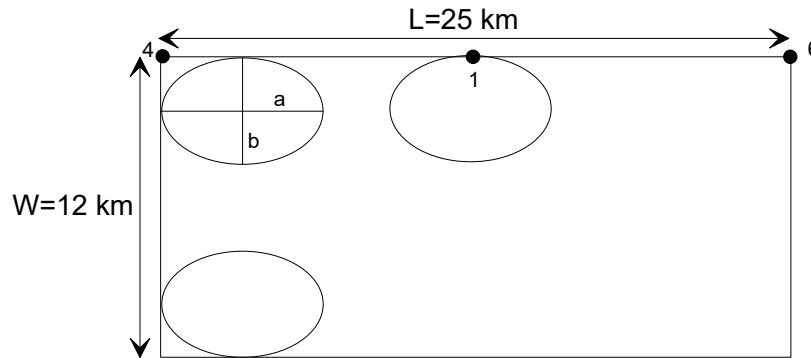


Figure 4-3 Schematic representation of elliptical rupture areas in R-CRISIS

4.1.3 Description of ground motion attenuation

In the PEER tests, the ground motion attenuation is described by means of the strong ground motion attenuation relationship proposed by Sadigh et al. (1997). In R-CRISIS, the Sadigh et al. (1997) model is using the built-in GMPM that accounts for magnitudes between 4.0 and 7.5 (with $\Delta M=0.1$) and for distances (R_{rup}) between 0.01 and 150km.

Note: in most cases the associated ground motion variability (σ) is assumed to be null. Hence, in the attenuation table a sigma value equal to 0.0001 was used (this because a null value is not accepted by the R-CRISIS code).

4.1.4 Other instructions from PEER

PEER provided some additional instructions to the developers of the tests, such as:

- The rupture area, A , should depend on magnitude in the form of $Log(A)=M_w-4$ with $\sigma_A=0.25$. In all tests, except in case #3, this variability is not included.
- For all faults the slip rate is 2mm/yr and the Gutenberg-Richter b -value is 0.9.
- The results should provide the mean probability of exceedance for peak horizontal acceleration between 0.001 and 1g.

4.1.5 Set 1 case1

Input parameters

The source adopted corresponds to fault 1 (see Figure 4-1). In Thomas et al. (2010; 2014) the seismicity input is specified through a b -value of 0.9, a slip rate of 2mm/yr and a magnitude density function in the form of a delta-function centered at 6.5.

Table 4-1 summarizes the input data whereas Table 4-2 shows the data associated to the geometry of the fault source. Table 4-3 includes the coordinates of the computation sites together with an explanation about its relevance for validation and verification purposes.

Table 4-1 Summary of input data for Set 1, case 1

Name	Description	Source	Mag-Density Function	Ground Motion Model ^{1,2}	Rupture Dimension Relationships ^{3,4,5,6}
Set 1 Case 1	Single rupture of entire fault plane. Tests distance, rate, and ground motion calculations.	Fault 1 (vertical SS) b-value=0.9 Slip rate=2mm/yr. The geometry and other characteristics of the source are shown in Figure 4-1	Delta function at M6.5	Sadigh et al. (1997), rock. $\sigma = 0$	$Log(A) = M - 4; \sigma_A = 0$ $Log(W) = 0.5 * M - 2.15; \sigma_W = 0$ $Log(L) = 0.5 * M - 1.85; \sigma_L = 0$

¹ Integration over magnitude zero.

² Use magnitude integration step size as small as necessary to model the magnitude density function.

³ For all cases, uniform slip with tapered slip at edges.

⁴ No ruptures are to extend beyond the edge of the fault plane.

⁵ Aspect ratio to be maintained until maximum width is reached, then increase length (maintain area at the expense of aspect ratio).

⁶ Down-dip and along strike integration step size should be as small as necessary for uniform rupture location.

Note: For all cases where the validation tests are performed using rupture dimension characteristics shown in Table 4-1, the following considerations are made. $Log(A)=M-4$ corresponds to the value proposed by Singh et al. (1980) and that is implemented as a built-in model in R-CRISIS. Instructions about $Log(W)$ and $Log(L)$ are handled by estimating the aspect ratio of L/W equal to 2.0 which correspond to elliptical ruptures.

Table 4-2 Coordinates of the fault source 1

Latitude	Longitude	Comment
38.0000	-122.0000	South end of fault
38.2248	-122.0000	North end of fault

Table 4-3 Coordinates and comments of the computation sites for fault sources 1 and 2

Site	Latitude	Longitude	Comment
1	38.113	-122.000	On fault, at midpoint along strike
2	38.113	-122.114	10 km west of fault, at midpoint along strike
3	38.111	-122.570	50 km west of fault, at midpoint along strike
4	38.000	-122.000	On fault, at southern end
5	37.910	-122.000	10 km south of fault along strike
6	38.225	-122.000	On fault, at northern end
7	38.113	-121.886	10 km east of fault, at midpoint along strike

In the R-CRISIS screen shown in Figures 4-4 and 4-5 (geometry of the seismic sources for rectangular and area sources), it is possible to assign the parameters that define the rupture dimensions. Particularly, in the case of sources with a surface, the rupture area is defined by means of equation 4-1 (which is the same as Eq. 2-27 but repeated herein for convenience of the reader). K_1 and K_2 parameters are user defined.

$$A = K_1 \cdot e^{K_2 M} \tag{Eq. 4-1}$$

where A is the source area (in km^2), M stands for magnitude and K_1 and K_2 are constants given by the user or chosen from a set of constants.

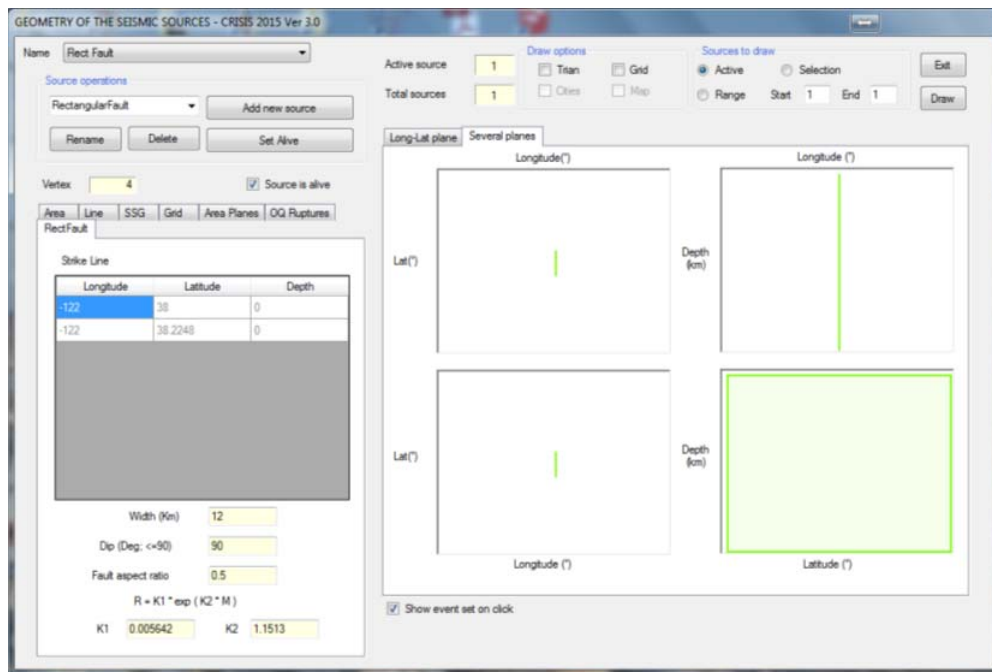


Figure 4-4 Geometry of the seismic source (rectangular fault) in R-CRISIS. Case 1, set 1

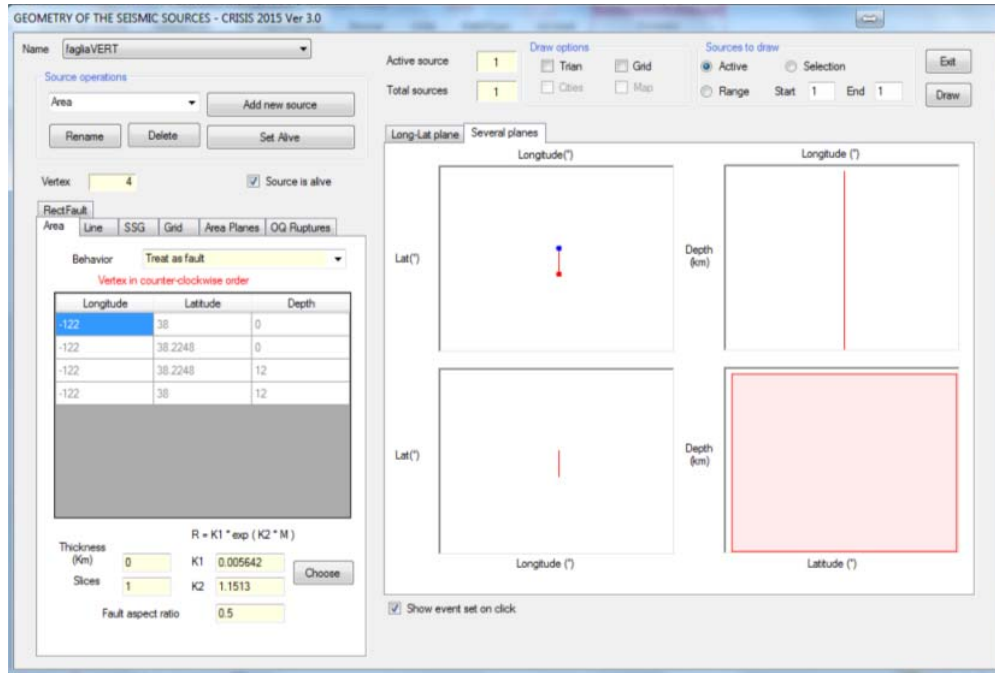


Figure 4-5 Geometry of the seismic source (area fault) in R-CRISIS. Case 1, set 1

In R-CRISIS, this input was described through a modified Gutenberg-Richter relation with minimum magnitude, $M_{min}=6.49$, and a maximum magnitude, $M_{max}=6.51$. The two parameters for the full description of the G-R relation are the slope b (equal to 0.9 as per the PEER instructions²¹) and the annual rate λ (i.e. the number of earthquakes with magnitude $M \geq M_{min}$). The latter can be computed from the slip rate using the scalar seismic moment, M_o as:

$$M_o = \mu A s \quad (\text{Eq. 4-2})$$

where:

- $M=3 \times 10^{11}$ (dyne/cm²)
- A = source area (cm²)
- s = average slip on the fault (cm)

Moreover, according to the definition of moment magnitude (M_w) by Hanks and Kanamori (1979):

$$M_w = \frac{2}{3} \log M_o [\text{dyne} \cdot \text{cm}] - 16.05 \quad (\text{Eq. 4-3})$$

From which it can be seen that:

²¹ Since in this case only one magnitude is considered, the b -value is irrelevant

$$M_o [dyne \cdot cm] = 10^{1.5M+16.05} \tag{Eq. 4-4}$$

The seismic moment rate (i.e. the seismic moment released by the source in one year, can be obtained by replacing the average slip on the fault (s) with the slip rate. since only one magnitude value (m) is possible, the seismic moment rate is λ (the number of earthquakes of magnitude equal to m in one year) times the seismic moment related to such magnitude m :

$$\dot{M}_o = \mu A \dot{s} = \lambda(10^{1.5m+16.05}) \tag{Eq. 4-5}$$

where s correspond to the slip rate on the source (cm/yr).

From equation 4-5, for $m=6.5$, $\lambda_{6.5}=0.002853$. Figure 4-6 shows the seismicity screen of R-CRISIS and how these values were set for this case.

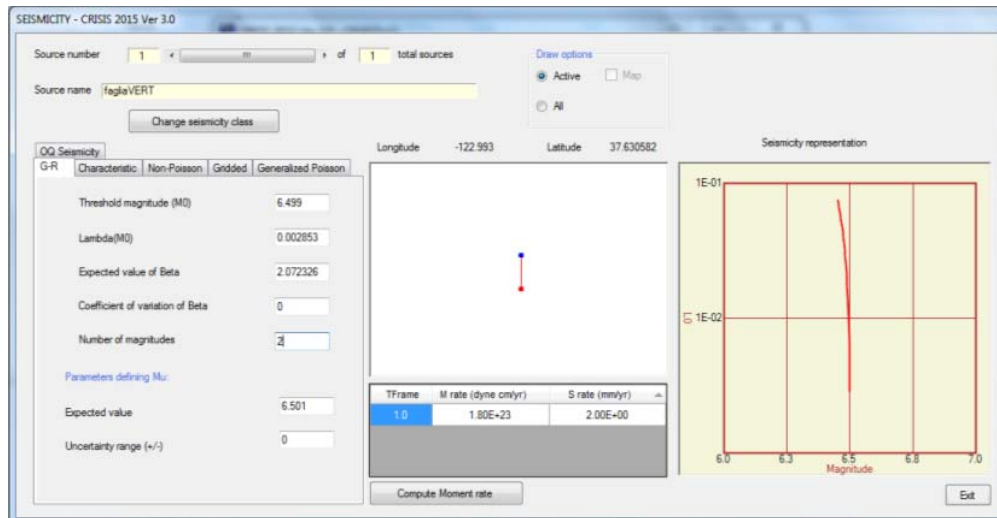


Figure 4-6 Seismicity data in R-CRISIS. Case 1, set 1

Finally, Figure 4-7 shows the attenuation data screen of R-CRISIS from where the Sadigh et al. (1997) GMPM has been assigned to the fault source.

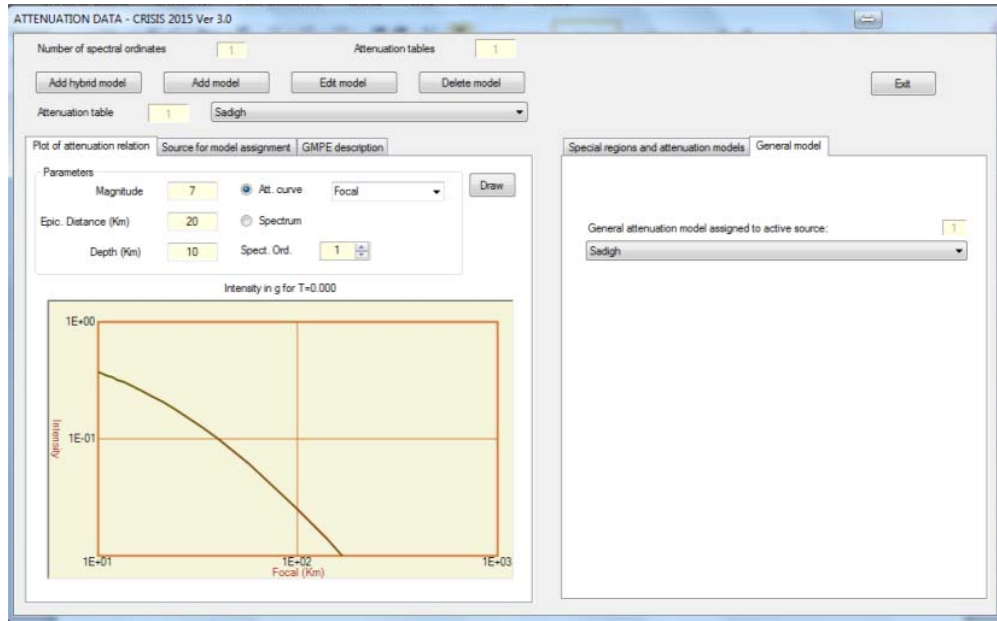


Figure 4-7 Attenuation model assignment in R-CRISIS for case 1, set 1

Results

Results obtained in R-CRISIS are summarized in Table 4-4. Additionally, in Table 4-5 it is possible to observe the results reported by PEER-2015 as benchmarks. Table 4-6 shows the results obtained analytically for the same case by the coordinators of the PEER-2015 project.

Figure 4-8 shows the plots of the seismic hazard results obtained by R-CRISIS and those considered as valid by the PEER-2015 project. In all the plots, it is seen a complete agreement between the results obtained by CRISIS and those provided by PEER-2015 and therefore, it is possible to conclude that CRISIS fulfills all the requirements evaluated by the PEER-2015 project in Set 1-Case 1.

Finally, for comparison purposes, Figure 4-9 shows the hazard plots comparing the results obtained with R-CRISIS (elliptical and rectangular options) and the ones provided by the PEER-2015 project. As expected, the differences occur in computation sites 4 and 6 for the reasons explained in Section 4.1.2.

Table 4-4 Annual exceedance probabilities obtained in R-CRISIS for Case 1, set 1

Peak Ground Acceleration (g)	Annual Exceedance Probability						
	Site 1	Site 2	Site 3	Site 4	Site 5	Site 6	Site 7
0.001	2.85E-03	2.85E-03	2.85E-03	2.85E-03	2.85E-03	2.85E-03	2.85E-03
0.01	2.85E-03	2.85E-03	2.85E-03	2.85E-03	2.85E-03	2.85E-03	2.85E-03
0.05	2.85E-03	2.85E-03	0.00E+00	2.85E-03	2.85E-03	2.85E-03	2.85E-03
0.10	2.85E-03	2.85E-03	0.00E+00	2.85E-03	2.85E-03	2.85E-03	2.85E-03
0.15	2.85E-03	2.85E-03	0.00E+00	2.85E-03	2.85E-03	2.85E-03	2.85E-03
0.20	2.85E-03	2.85E-03	0.00E+00	2.85E-03	2.85E-03	2.85E-03	2.85E-03
0.25	2.85E-03	2.85E-03	0.00E+00	2.85E-03	2.85E-03	2.85E-03	2.85E-03
0.30	2.85E-03	2.85E-03	0.00E+00	2.85E-03	2.85E-03	2.85E-03	2.85E-03
0.35	2.85E-03	0.00E+00	0.00E+00	2.85E-03	0.00E+00	2.85E-03	0.00E+00
0.40	2.85E-03	0.00E+00	0.00E+00	2.85E-03	0.00E+00	2.85E-03	0.00E+00
0.45	2.85E-03	0.00E+00	0.00E+00	2.85E-03	0.00E+00	2.85E-03	0.00E+00
0.50	2.85E-03	0.00E+00	0.00E+00	2.85E-03	0.00E+00	2.85E-03	0.00E+00
0.55	2.85E-03	0.00E+00	0.00E+00	2.85E-03	0.00E+00	2.85E-03	0.00E+00
0.60	2.85E-03	0.00E+00	0.00E+00	2.85E-03	0.00E+00	2.85E-03	0.00E+00
0.70	2.85E-03	0.00E+00	0.00E+00	2.85E-03	0.00E+00	2.85E-03	0.00E+00
0.80	0.00E+00	0.00E+00	0.00E+00	0.00E+00	0.00E+00	0.00E+00	0.00E+00
0.90	0.00E+00	0.00E+00	0.00E+00	0.00E+00	0.00E+00	0.00E+00	0.00E+00
1.00	0.00E+00	0.00E+00	0.00E+00	0.00E+00	0.00E+00	0.00E+00	0.00E+00

Table 4-5 Annual exceedance probabilities reported as benchmarks by PEER project coordinators for Case 1, set 1

Peak Ground Acceleration (g)	Annual Exceedance Probability						
	Site 1	Site 2	Site 3	Site 4	Site 5	Site 6	Site 7
0.001	2.85E-03	2.85E-03	2.85E-03	2.85E-03	2.85E-03	2.85E-03	2.85E-03
0.01	2.85E-03	2.85E-03	2.85E-03	2.85E-03	2.85E-03	2.85E-03	2.85E-03
0.05	2.85E-03	2.85E-03	0.00E+00	2.85E-03	2.85E-03	2.85E-03	2.85E-03
0.10	2.85E-03	2.85E-03	0.00E+00	2.85E-03	2.85E-03	2.85E-03	2.85E-03
0.15	2.85E-03	2.85E-03	0.00E+00	2.85E-03	2.85E-03	2.85E-03	2.85E-03
0.20	2.85E-03	2.85E-03	0.00E+00	2.85E-03	2.85E-03	2.85E-03	2.85E-03
0.25	2.85E-03	2.85E-03	0.00E+00	2.85E-03	2.85E-03	2.85E-03	2.85E-03
0.30	2.85E-03	2.85E-03	0.00E+00	2.85E-03	2.85E-03	2.85E-03	2.85E-03
0.35	2.85E-03	0.00E+00	0.00E+00	2.85E-03	0.00E+00	2.85E-03	0.00E+00
0.40	2.85E-03	0.00E+00	0.00E+00	2.85E-03	0.00E+00	2.85E-03	0.00E+00
0.45	2.85E-03	0.00E+00	0.00E+00	2.85E-03	0.00E+00	2.85E-03	0.00E+00
0.50	2.85E-03	0.00E+00	0.00E+00	2.85E-03	0.00E+00	2.85E-03	0.00E+00
0.55	2.85E-03	0.00E+00	0.00E+00	2.85E-03	0.00E+00	2.85E-03	0.00E+00
0.60	2.85E-03	0.00E+00	0.00E+00	2.85E-03	0.00E+00	2.85E-03	0.00E+00
0.70	2.85E-03	0.00E+00	0.00E+00	2.85E-03	0.00E+00	2.85E-03	0.00E+00
0.80	0.00E+00	0.00E+00	0.00E+00	0.00E+00	0.00E+00	0.00E+00	0.00E+00
0.90	0.00E+00	0.00E+00	0.00E+00	0.00E+00	0.00E+00	0.00E+00	0.00E+00
1.00	0.00E+00	0.00E+00	0.00E+00	0.00E+00	0.00E+00	0.00E+00	0.00E+00

Table 4-6 Analytical annual exceedance probabilities obtained by PEER project coordinators for Case 1, set 1

Peak Ground Acceleration (g)	Annual Exceedance Probability						
	Site 1	Site 2	Site 3	Site 4	Site 5	Site 6	Site 7
0.001	2.85E-03	2.85E-03	2.85E-03	2.85E-03	2.85E-03	2.85E-03	2.85E-03
0.01	2.85E-03	2.85E-03	2.85E-03	2.85E-03	2.85E-03	2.85E-03	2.85E-03
0.05	2.85E-03	2.85E-03	0.00E+00	2.85E-03	2.85E-03	2.85E-03	2.85E-03
0.10	2.85E-03	2.85E-03	0.00E+00	2.85E-03	2.85E-03	2.85E-03	2.85E-03
0.15	2.85E-03	2.85E-03	0.00E+00	2.85E-03	2.85E-03	2.85E-03	2.85E-03
0.20	2.85E-03	2.85E-03	0.00E+00	2.85E-03	2.85E-03	2.85E-03	2.85E-03
0.25	2.85E-03	2.85E-03	0.00E+00	2.85E-03	2.85E-03	2.85E-03	2.85E-03
0.30	2.85E-03	2.85E-03	0.00E+00	2.85E-03	2.85E-03	2.85E-03	2.85E-03
0.35	2.85E-03	0.00E+00	0.00E+00	2.85E-03	0.00E+00	2.85E-03	0.00E+00
0.40	2.85E-03	0.00E+00	0.00E+00	2.85E-03	0.00E+00	2.85E-03	0.00E+00
0.45	2.85E-03	0.00E+00	0.00E+00	2.85E-03	0.00E+00	2.85E-03	0.00E+00
0.50	2.85E-03	0.00E+00	0.00E+00	2.85E-03	0.00E+00	2.85E-03	0.00E+00
0.55	2.85E-03	0.00E+00	0.00E+00	2.85E-03	0.00E+00	2.85E-03	0.00E+00
0.60	2.85E-03	0.00E+00	0.00E+00	2.85E-03	0.00E+00	2.85E-03	0.00E+00
0.70	2.85E-03	0.00E+00	0.00E+00	2.85E-03	0.00E+00	2.85E-03	0.00E+00
0.80	0.00E+00	0.00E+00	0.00E+00	0.00E+00	0.00E+00	0.00E+00	0.00E+00
0.90	0.00E+00	0.00E+00	0.00E+00	0.00E+00	0.00E+00	0.00E+00	0.00E+00
1.00	0.00E+00	0.00E+00	0.00E+00	0.00E+00	0.00E+00	0.00E+00	0.00E+00

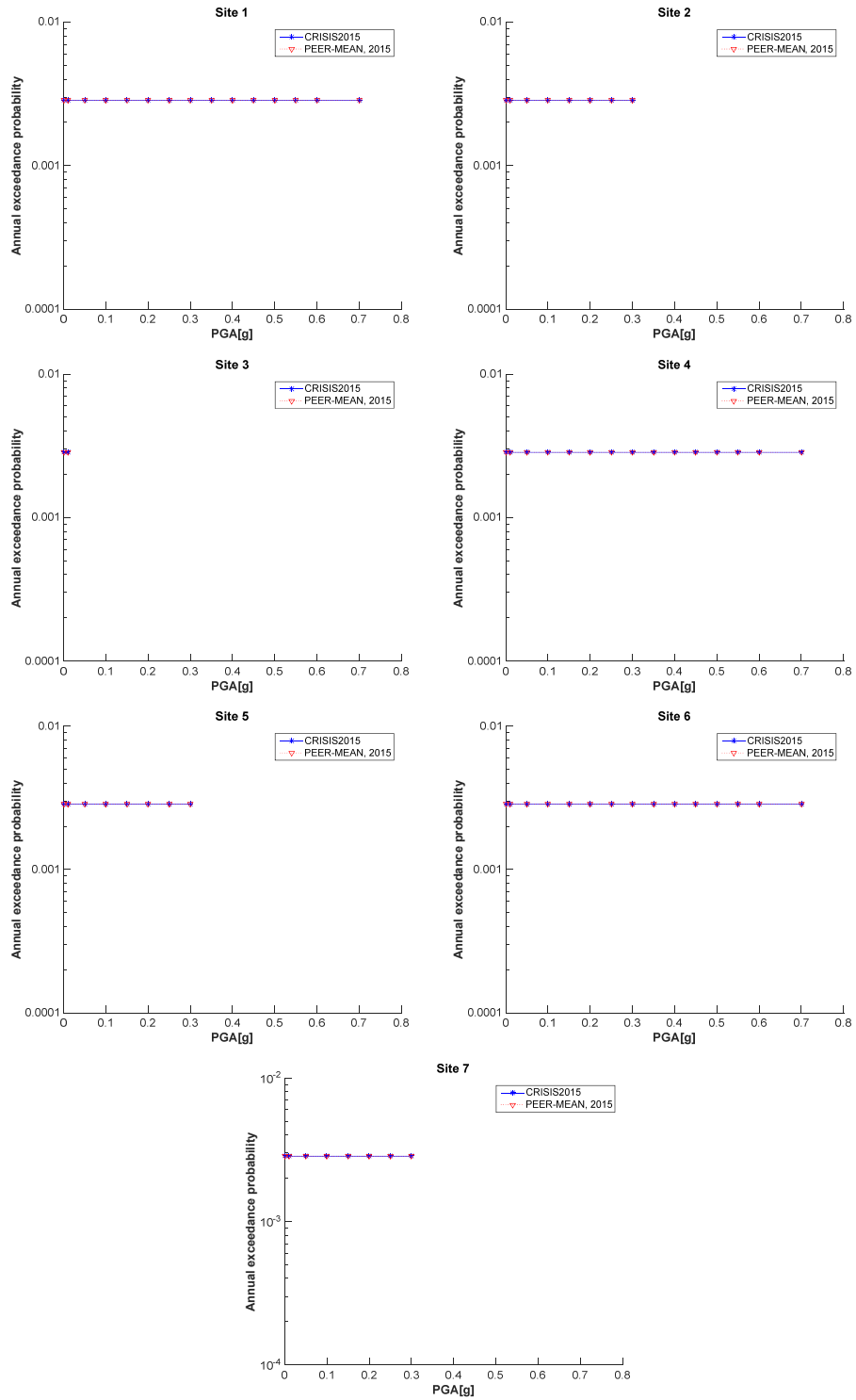


Figure 4-8 Comparison of the CRISIS and PEER-2015 results for Sites 1 to 7 (Set 1 Case 1)

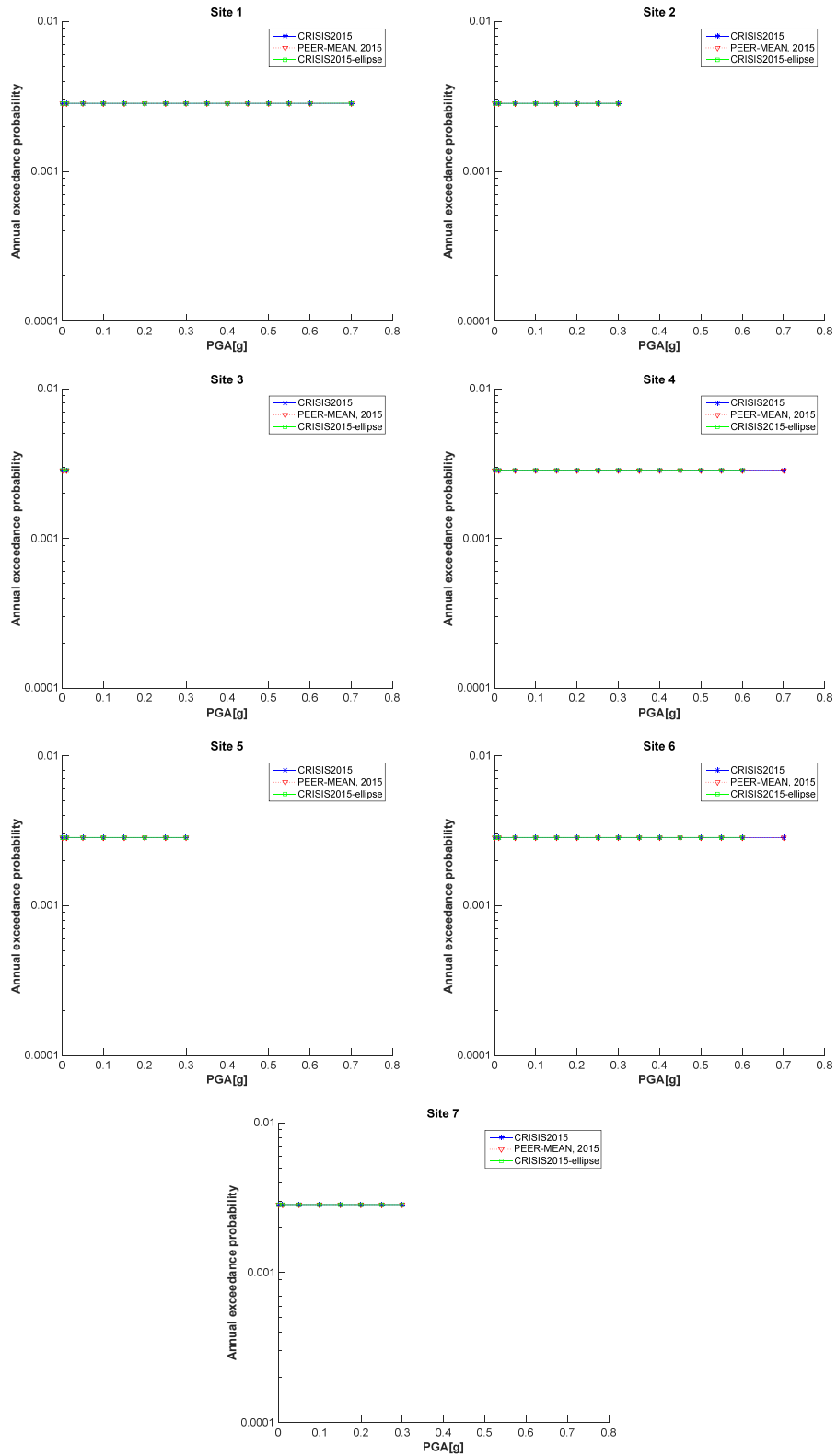


Figure 4-9 Comparison of elliptical and rectangular rupture shapes for PEER-2015 Set 1 Case 1

4.1.6 Set 1 case 2

Input parameters

The source adopted for this case corresponds to Fault 1. In Thomas et al. (2010; 2014) the seismicity input is specified by a b -value=0.9 a slip rate of 2mm/yr and a magnitude density function in the form of a delta-function centered at 6.0 as shown in Table 4-7.

Table 4-7 Summary of input data for Set 1, case 2

Name	Description	Source	Mag-Density Function	Ground Motion Model ^{1,2}	Rupture Dimension Relationships ^{3,4,5,6}
Set 1 Case 2	Single rupture of entire fault plane. Tests distance, rate, and ground motion calculations.	Fault 1 (vertical SS) b -value=0.9 Slip rate=2mm/yr. The geometry and other characteristics of the source are shown in Figure 4-1	Delta function at M6.0	Sadigh et al. (1997), rock. $\sigma = 0$	$Log(A) = M - 4; \sigma_A = 0$ $Log(W) = 0.5 * M - 2.15; \sigma_W = 0$ $Log(L) = 0.5 * M - 1.85; \sigma_L = 0$

¹ Integration over magnitude zero.

² Use magnitude integration step size as small as necessary to model the magnitude density function.

³ For all cases, uniform slip with tapered slip at edges.

⁴ No ruptures are to extend beyond the edge of the fault plane.

⁵ Aspect ratio to be maintained until maximum width is reached, then increase length (maintain area at the expense of aspect ratio).

⁶ Down-dip and along strike integration step size should be as small as necessary for uniform rupture location.

As in case 1, set 1, a modified G-R relation was used in R-CRISIS with minimum magnitude, $M_{min}=5.99$, maximum magnitude, $M_{max}=6.01$ and $\lambda=0.016043$, obtained from equation 4-5 now with $m=6$. Figure 4-10 shows the seismicity data included in the R-CRISIS screen which is the only difference if compared to the geometry and attenuation screens shown before for case 1, set 1 of the PEER project tests.

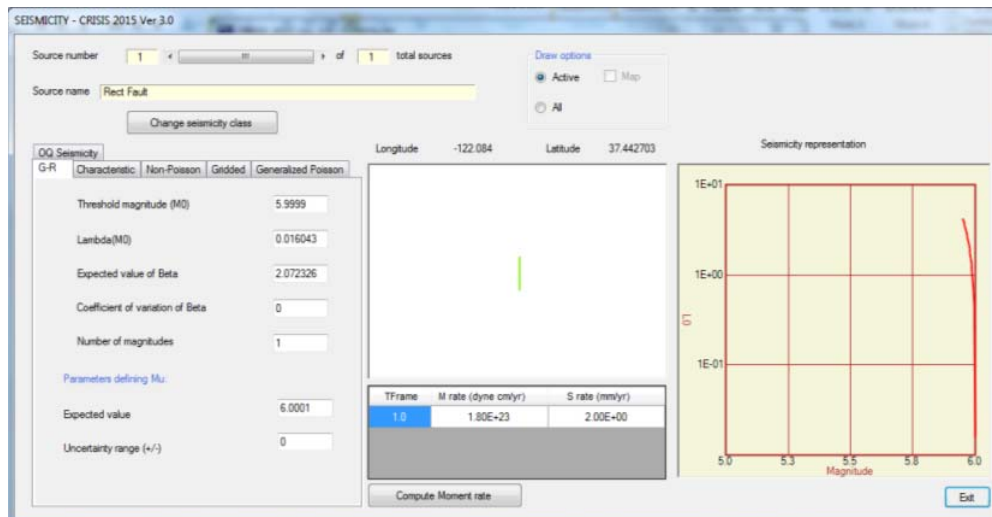


Figure 4-10 Seismicity values in R-CRISIS. Case 1, set 2

Results

Table 4-8 shows the results obtained in R-CRISIS for case 1, set 2. Additionally, Table 4-9 shows the mean values provided by PEER-2015 and finally Table 4-10 includes the analytical solution provided by the coordinators of the PEER-2015 project.

Figure 4-11 shows the comparison of the seismic hazard plots obtained by R-CRISIS and provided by PEER-2015. In all cases there is a full agreement between the results and therefore, it is possible to conclude that R-CRISIS fulfills all the requirements evaluated by the PEER project validation test in case 1, set 2.

Finally, Figure 4-12 shows the hazard plots comparing the results obtained with R-CRISIS (elliptical and rectangular options) and the ones provided by the PEER-2015 project. In this case differences exist at computation sites 1, 4, 5 and 6. The reason for these differences is the same explained before but it is worth noting that, as expected, it is much bigger at those computation sites in the corners than in other locations.

Table 4-8 Annual exceedance probabilities obtained in R-CRISIS for Case 1, set 2

Peak Ground Acceleration (g)	Annual Exceedance Probability						
	Site 1	Site 2	Site 3	Site 4	Site 5	Site 6	Site 7
0.001	1.59E-02	1.59E-02	1.59E-02	1.59E-02	1.59E-02	1.59E-02	1.59E-02
0.01	1.59E-02	1.59E-02	1.59E-02	1.59E-02	1.59E-02	1.59E-02	1.59E-02
0.05	1.59E-02	1.59E-02	0.00E+00	1.59E-02	1.59E-02	1.59E-02	1.59E-02
0.10	1.59E-02	1.59E-02	0.00E+00	1.59E-02	1.59E-02	1.59E-02	1.59E-02
0.15	1.59E-02	1.59E-02	0.00E+00	1.59E-02	7.78E-03	1.59E-02	1.59E-02
0.20	1.59E-02	1.59E-02	0.00E+00	1.58E-02	1.60E-03	1.58E-02	1.59E-02
0.25	1.59E-02	0.00E+00	0.00E+00	1.20E-02	0.00E+00	1.20E-02	0.00E+00
0.30	1.59E-02	0.00E+00	0.00E+00	8.68E-03	0.00E+00	8.63E-03	0.00E+00
0.35	1.59E-02	0.00E+00	0.00E+00	5.74E-03	0.00E+00	5.70E-03	0.00E+00
0.40	1.17E-02	0.00E+00	0.00E+00	3.10E-03	0.00E+00	3.07E-03	0.00E+00
0.45	8.24E-03	0.00E+00	0.00E+00	1.52E-03	0.00E+00	1.50E-03	0.00E+00
0.50	5.25E-03	0.00E+00	0.00E+00	6.09E-04	0.00E+00	6.00E-04	0.00E+00
0.55	2.63E-03	0.00E+00	0.00E+00	*	0.00E+00	*	0.00E+00
0.60	*	0.00E+00	0.00E+00	*	0.00E+00	*	0.00E+00
0.70	0.00E+00	0.00E+00	0.00E+00	0.00E+00	0.00E+00	0.00E+00	0.00E+00
0.80	0.00E+00	0.00E+00	0.00E+00	0.00E+00	0.00E+00	0.00E+00	0.00E+00
0.90	0.00E+00	0.00E+00	0.00E+00	0.00E+00	0.00E+00	0.00E+00	0.00E+00
1.00	0.00E+00	0.00E+00	0.00E+00	0.00E+00	0.00E+00	0.00E+00	0.00E+00

* for these cases a value different than zero was computed, however, it was considered by the PEER coordinators as inappropriate for comparative purposes since there are significant differences between the values obtained by the 5 reference codes used to estimate the mean value.

Table 4-9 Annual exceedance probabilities reported as benchmarks by PEER project coordinators for Case 1, set 2

Peak Ground Acceleration (g)	Annual Exceedance Probability						
	Site 1	Site 2	Site 3	Site 4	Site 5	Site 6	Site 7
0.001	1.59E-02	1.59E-02	1.59E-02	1.59E-02	1.59E-02	1.59E-02	1.59E-02
0.01	1.59E-02	1.59E-02	1.59E-02	1.59E-02	1.59E-02	1.59E-02	1.59E-02
0.05	1.59E-02	1.59E-02	0.00E+00	1.59E-02	1.59E-02	1.59E-02	1.59E-02
0.10	1.59E-02	1.59E-02	0.00E+00	1.59E-02	1.59E-02	1.59E-02	1.59E-02
0.15	1.59E-02	1.59E-02	0.00E+00	1.59E-02	7.78E-03	1.59E-02	1.59E-02
0.20	1.59E-02	1.59E-02	0.00E+00	1.58E-02	1.60E-03	1.58E-02	1.59E-02
0.25	1.59E-02	0.00E+00	0.00E+00	1.20E-02	0.00E+00	1.20E-02	0.00E+00
0.30	1.59E-02	0.00E+00	0.00E+00	8.68E-03	0.00E+00	8.63E-03	0.00E+00
0.35	1.59E-02	0.00E+00	0.00E+00	5.74E-03	0.00E+00	5.70E-03	0.00E+00
0.40	1.17E-02	0.00E+00	0.00E+00	3.10E-03	0.00E+00	3.07E-03	0.00E+00
0.45	8.24E-03	0.00E+00	0.00E+00	1.52E-03	0.00E+00	1.50E-03	0.00E+00
0.50	5.25E-03	0.00E+00	0.00E+00	6.09E-04	0.00E+00	6.00E-04	0.00E+00
0.55	2.63E-03	0.00E+00	0.00E+00	*	0.00E+00	*	0.00E+00
0.60	*	0.00E+00	0.00E+00	*	0.00E+00	*	0.00E+00
0.70	0.00E+00	0.00E+00	0.00E+00	0.00E+00	0.00E+00	0.00E+00	0.00E+00
0.80	0.00E+00	0.00E+00	0.00E+00	0.00E+00	0.00E+00	0.00E+00	0.00E+00
0.90	0.00E+00	0.00E+00	0.00E+00	0.00E+00	0.00E+00	0.00E+00	0.00E+00
1.00	0.00E+00	0.00E+00	0.00E+00	0.00E+00	0.00E+00	0.00E+00	0.00E+00

* for these cases a value different than zero was computed, however, it was considered by the PEER coordinators as inappropriate for comparative purposes since there are significant differences between the values obtained by the 5 reference codes used to estimate the mean value.

Table 4-10 Analytical annual exceedance probabilities obtained by PEER project coordinators for Case 1, set 2

Peak Ground Acceleration (g)	Annual Exceedance Probability						
	Site 1	Site 2	Site 3	Site 4	Site 5	Site 6	Site 7
0.001	1.59E-02	1.59E-02	1.59E-02	1.59E-02	1.59E-02	1.59E-02	1.59E-02
0.01	1.59E-02	1.59E-02	1.59E-02	1.59E-02	1.59E-02	1.59E-02	1.59E-02
0.05	1.59E-02	1.59E-02	0.00E+00	1.59E-02	1.59E-02	1.59E-02	1.59E-02
0.10	1.59E-02	1.59E-02	0.00E+00	1.59E-02	1.59E-02	1.59E-02	1.59E-02
0.15	1.59E-02	1.59E-02	0.00E+00	1.59E-02	7.75E-03	1.59E-02	1.59E-02
0.20	1.59E-02	1.59E-02	0.00E+00	1.58E-02	1.60E-03	1.58E-02	1.59E-02
0.25	1.59E-02	0.00E+00	0.00E+00	1.20E-02	0.00E+00	1.20E-02	0.00E+00
0.30	1.59E-02	0.00E+00	0.00E+00	8.64E-03	0.00E+00	8.64E-03	0.00E+00
0.35	1.59E-02	0.00E+00	0.00E+00	5.73E-03	0.00E+00	5.73E-03	0.00E+00
0.40	1.17E-02	0.00E+00	0.00E+00	3.09E-03	0.00E+00	3.09E-03	0.00E+00
0.45	8.23E-03	0.00E+00	0.00E+00	1.51E-03	0.00E+00	1.51E-03	0.00E+00
0.50	5.23E-03	0.00E+00	0.00E+00	6.09E-04	0.00E+00	6.08E-04	0.00E+00
0.55	2.64E-03	0.00E+00	0.00E+00	*	0.00E+00	*	0.00E+00
0.60	*	0.00E+00	0.00E+00	*	0.00E+00	*	0.00E+00
0.70	0.00E+00	0.00E+00	0.00E+00	0.00E+00	0.00E+00	0.00E+00	0.00E+00
0.80	0.00E+00	0.00E+00	0.00E+00	0.00E+00	0.00E+00	0.00E+00	0.00E+00
0.90	0.00E+00	0.00E+00	0.00E+00	0.00E+00	0.00E+00	0.00E+00	0.00E+00
1.00	0.00E+00	0.00E+00	0.00E+00	0.00E+00	0.00E+00	0.00E+00	0.00E+00

* for these cases a value different than zero was computed, however, it was considered by the PEER coordinators as inappropriate for comparative purposes since there are significant differences between the values obtained by the 5 reference codes used to estimate the mean value.

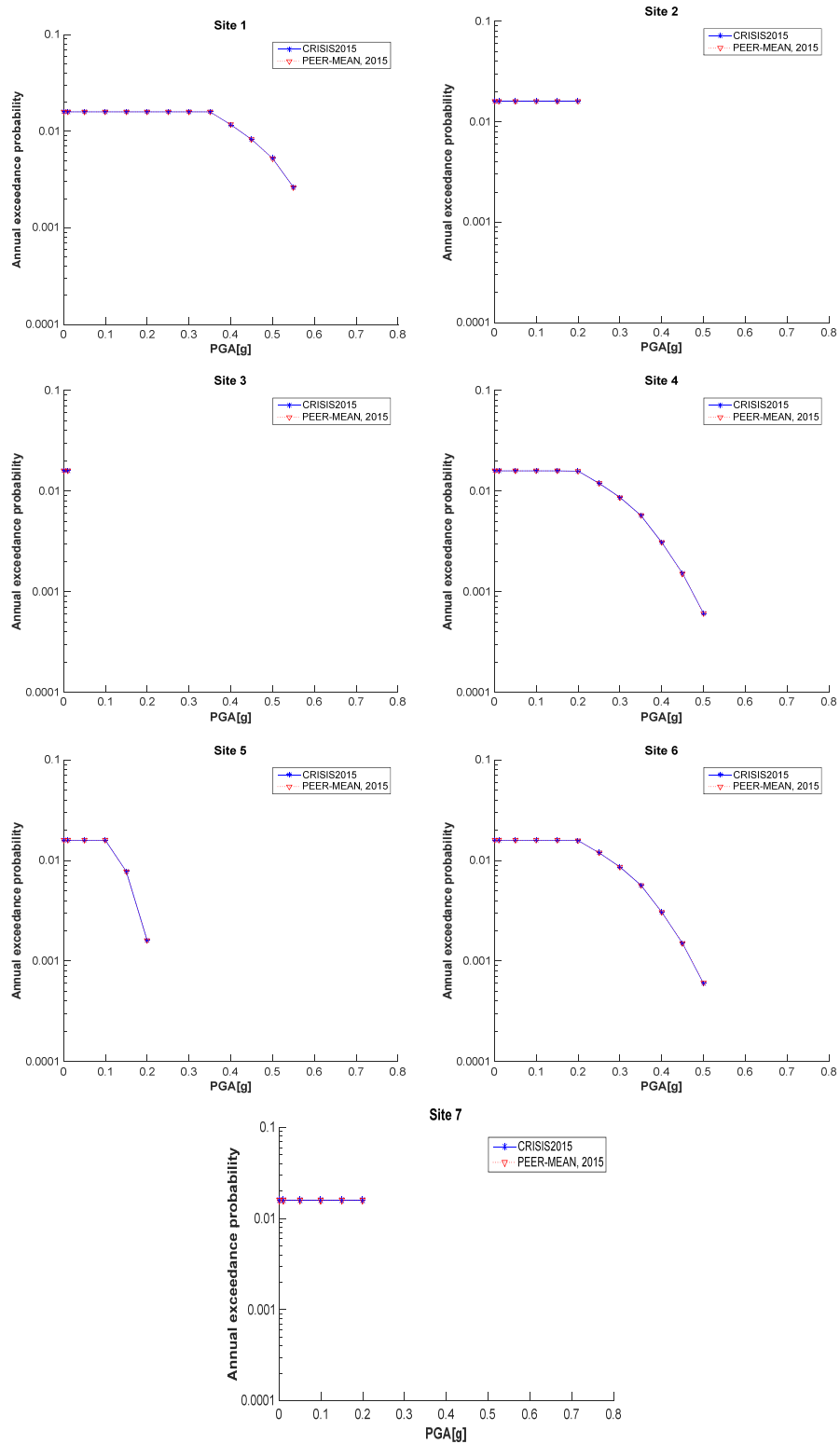


Figure 4-11 Comparison of the CRISIS and PEER-2015 results for Sites 1 to 7 (Set 1 Case 2)

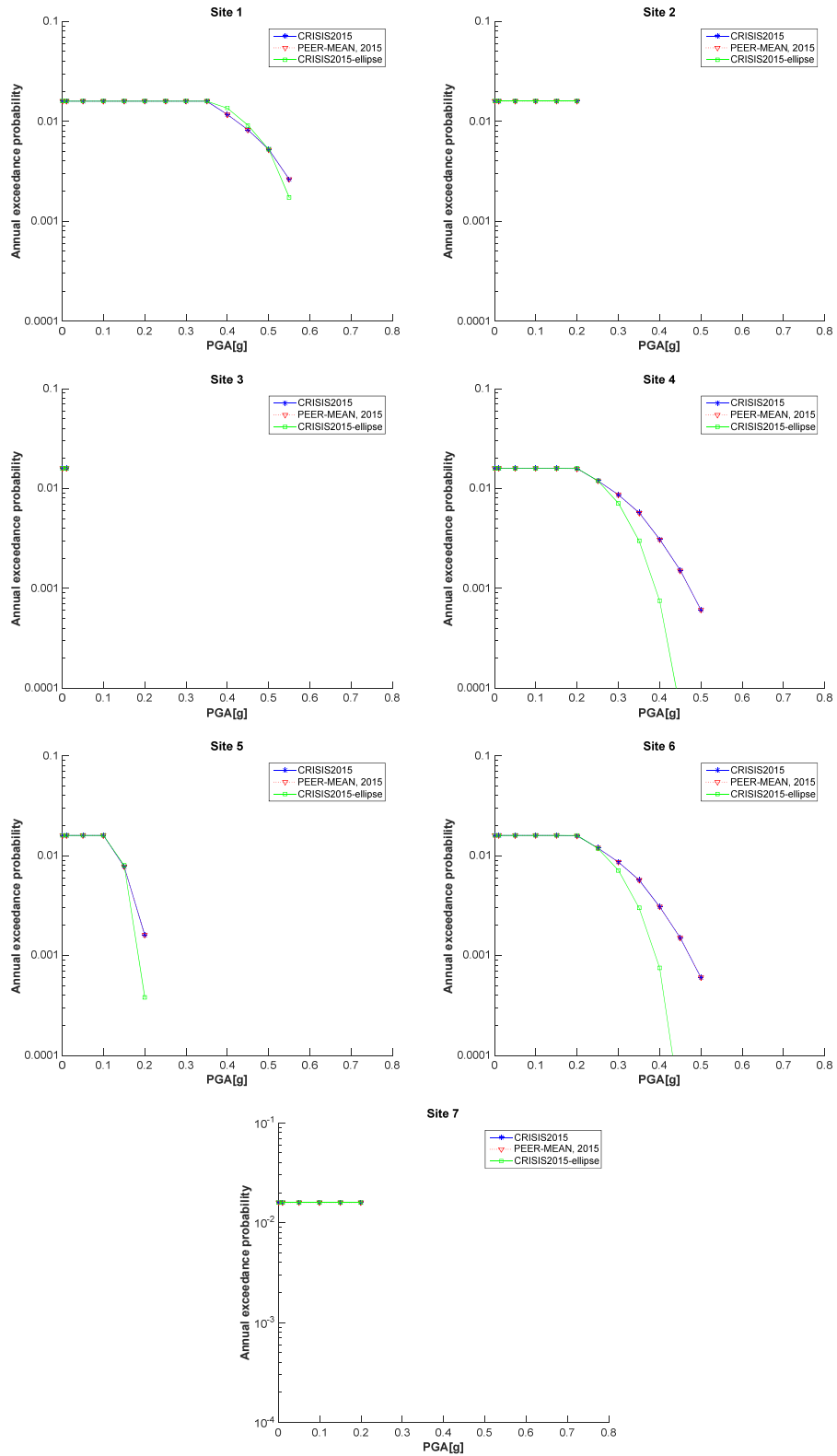


Figure 4-12 Comparison of elliptical and rectangular rupture shapes for PEER-2015 Set 1 Case 2

4.1.7 Set 1 case 3

The tests differ from case 2 due to the introduction of the variability of the rupture planes. A “sigma” is assigned to the rupture areas. This option is not yet available in R-CRISIS and thus, this test could not be carried out.

4.1.8 Set 1 case 4

Input parameters

The source used for this model corresponds to Fault 2 with a width $W=12.7\text{km} [=H/\sin(60^\circ)]$. The seismicity is similar to the set 1, case 2 except for the λ value that is in this case equal to 0.01698 (the area of the source is slightly different due to the depth and thus also the seismic moment rate). Table 4-11 summarizes the input data.

Table 4-11 Summary of input data for Set 1, case 4

Name	Description	Source	Mag-Density Function	Ground Motion Model ^{1,2}	Rupture Dimension Relationships ^{3,4,5,6}
Set 1 Case 4	Single rupture smaller than fault plane on dipping fault	Fault 2(reverse 60°) b-value=0.9 Slip rate=2mm/yr. The geometry and other characteristics of the source are shown in Figure 4-1	Delta function at M6.0	Sadigh et al. (1997), rock. $\sigma = 0$	$\text{Log}(A) = M - 4; \sigma_A = 0$ $\text{Log}(W) = 0.5 * M - 2.15; \sigma_W = 0$ $\text{Log}(L) = 0.5 * M - 1.85; \sigma_L = 0$

¹ Integration over magnitude zero.

² Use magnitude integration step size as small as necessary to model the magnitude density function.

³ For all cases, uniform slip with tapered slip at edges.

⁴ No ruptures are to extend beyond the edge of the fault plane.

⁵ Aspect ratio to be maintained until maximum width is reached, then increase length (maintain area at the expense of aspect ratio).

⁶ Down-dip and along strike integration step size should be as small as necessary for uniform rupture location.

Figure 4-13 shows the geometry data screen of R-CRISIS with the parameters that were used herein, whereas, Figure 4-14 shows the seismicity data screen of R-CRISIS with the assigned parameters for this particular case.

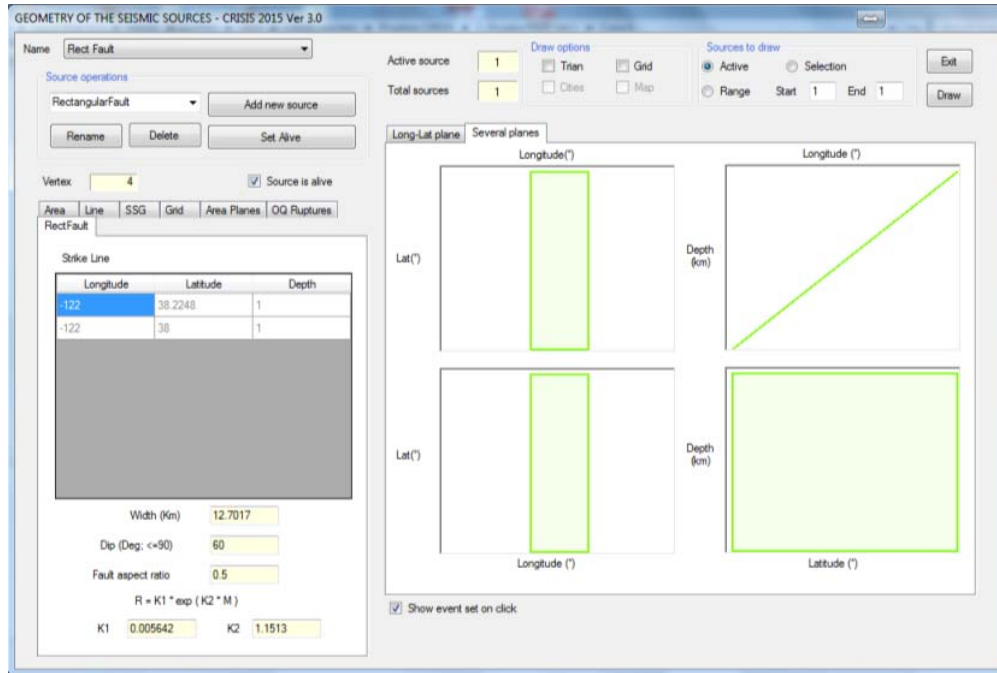


Figure 4-13 Geometry data for Fault 2 in PEER-2015 validation tests

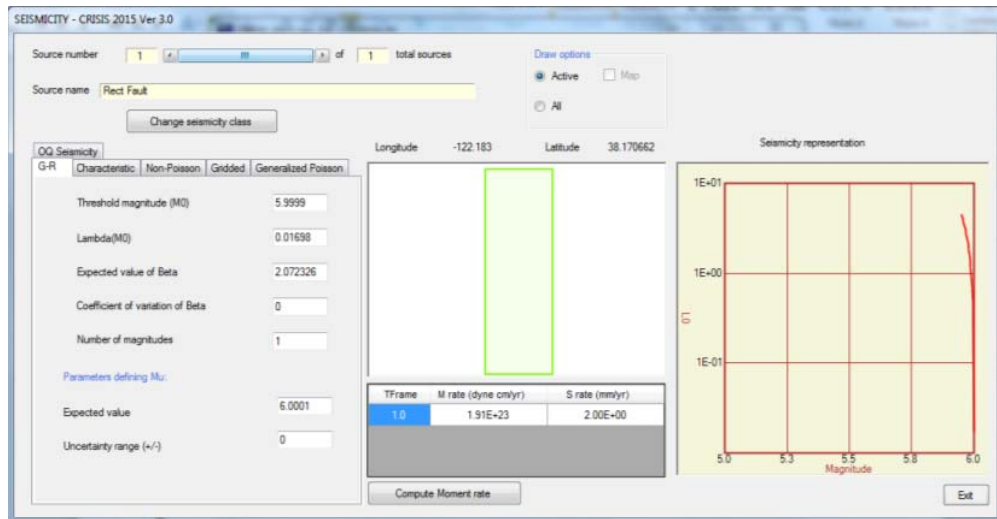


Figure 4-14 Seismicity parameters assigned in R-CRISIS for set 1, case 4

Results

Results computed in R-CRISIS for set 1, case 4 are shown in Table 4-12. Table 4-13 shows the results provided by the PEER-2015 project whereas Table 4-14 shows the analytical solution also provided by the coordinators of the PEER-2015 project. Figure 4-15 shows the hazard plots for the 7 computation sites. In all cases there is a full agreement between the results and therefore, it is possible to conclude that CRISIS fulfills all the requirements evaluated by the PEER-2015 project in Set 1-Case 4.

Figure 4-16 shows the hazard plots comparing the results obtained with R-CRISIS (elliptical and rectangular options) and the ones provided by the PEER-2015 project. Differences at computation sites 1, 4, 5 and 6 exist for exactly the same reasons explained in section 4.1.2.

Table 4-12 Annual exceedance probabilities obtained in R-CRISIS for Case 1, set 4

Peak Ground Acceleration (g)	Annual Exceedance Probability						
	Site 1	Site 2	Site 3	Site 4	Site 5	Site 6	Site 7
0.001	1.68E-02	1.68E-02	1.68E-02	1.68E-02	1.68E-02	1.68E-02	1.68E-02
0.01	1.68E-02	1.68E-02	1.68E-02	1.68E-02	1.68E-02	1.68E-02	1.68E-02
0.05	1.68E-02	1.68E-02	0.00E+00	1.68E-02	1.68E-02	1.68E-02	1.68E-02
0.10	1.68E-02	1.68E-02	0.00E+00	1.68E-02	1.68E-02	1.68E-02	1.68E-02
0.15	1.68E-02	1.68E-02	0.00E+00	1.68E-02	1.24E-02	1.68E-02	1.68E-02
0.20	1.68E-02	1.68E-02	0.00E+00	1.68E-02	5.26E-03	1.68E-02	1.66E-02
0.25	1.68E-02	1.68E-02	0.00E+00	1.57E-02	*	1.57E-02	4.37E-03
0.30	1.68E-02	0.00E+00	0.00E+00	1.18E-02	0.00E+00	1.18E-02	0.00E+00
0.35	1.68E-02	0.00E+00	0.00E+00	8.44E-03	0.00E+00	8.41E-03	0.00E+00
0.40	1.36E-02	0.00E+00	0.00E+00	5.10E-03	0.00E+00	5.07E-03	0.00E+00
0.45	1.01E-02	0.00E+00	0.00E+00	2.88E-03	0.00E+00	2.86E-03	0.00E+00
0.50	7.01E-03	0.00E+00	0.00E+00	1.48E-03	0.00E+00	1.46E-03	0.00E+00
0.55	4.37E-03	0.00E+00	0.00E+00	*	0.00E+00	6.17E-04	0.00E+00
0.60	*	0.00E+00	0.00E+00	*	0.00E+00	*	0.00E+00
0.70	0.00E+00	0.00E+00	0.00E+00	0.00E+00	0.00E+00	0.00E+00	0.00E+00
0.80	0.00E+00	0.00E+00	0.00E+00	0.00E+00	0.00E+00	0.00E+00	0.00E+00
0.90	0.00E+00	0.00E+00	0.00E+00	0.00E+00	0.00E+00	0.00E+00	0.00E+00
1.00	0.00E+00	0.00E+00	0.00E+00	0.00E+00	0.00E+00	0.00E+00	0.00E+00

* for these cases a value different than zero was computed, however, it was considered by the PEER coordinators as inappropriate for comparative purposes since there are significant differences between the values obtained by the 5 reference codes used to estimate the mean value.

Table 4-13 Annual exceedance probabilities reported as benchmarks by PEER project coordinators for Case 1, set 4

Peak Ground Acceleration (g)	Annual Exceedance Probability						
	Site 1	Site 2	Site 3	Site 4	Site 5	Site 6	Site 7
0.001	1.68E-02	1.68E-02	1.68E-02	1.68E-02	1.68E-02	1.68E-02	1.68E-02
0.01	1.68E-02	1.68E-02	1.68E-02	1.68E-02	1.68E-02	1.68E-02	1.68E-02
0.05	1.68E-02	1.68E-02	0.00E+00	1.68E-02	1.68E-02	1.68E-02	1.68E-02
0.10	1.68E-02	1.68E-02	0.00E+00	1.68E-02	1.68E-02	1.68E-02	1.68E-02
0.15	1.68E-02	1.68E-02	0.00E+00	1.68E-02	1.24E-02	1.68E-02	1.68E-02
0.20	1.68E-02	1.68E-02	0.00E+00	1.68E-02	5.24E-03	1.68E-02	1.63E-02
0.25	1.68E-02	1.68E-02	0.00E+00	1.57E-02	*	1.57E-02	4.18E-03
0.30	1.68E-02	0.00E+00	0.00E+00	1.18E-02	0.00E+00	1.18E-02	0.00E+00
0.35	1.68E-02	0.00E+00	0.00E+00	8.42E-03	0.00E+00	8.39E-03	0.00E+00
0.40	1.36E-02	0.00E+00	0.00E+00	5.09E-03	0.00E+00	5.07E-03	0.00E+00
0.45	1.01E-02	0.00E+00	0.00E+00	2.87E-03	0.00E+00	2.86E-03	0.00E+00
0.50	7.02E-03	0.00E+00	0.00E+00	1.47E-03	0.00E+00	1.47E-03	0.00E+00
0.55	4.37E-03	0.00E+00	0.00E+00	*	0.00E+00	6.25E-04	0.00E+00
0.60	*	0.00E+00	0.00E+00	*	0.00E+00	*	0.00E+00
0.70	0.00E+00	0.00E+00	0.00E+00	0.00E+00	0.00E+00	0.00E+00	0.00E+00
0.80	0.00E+00	0.00E+00	0.00E+00	0.00E+00	0.00E+00	0.00E+00	0.00E+00
0.90	0.00E+00	0.00E+00	0.00E+00	0.00E+00	0.00E+00	0.00E+00	0.00E+00
1.00	0.00E+00	0.00E+00	0.00E+00	0.00E+00	0.00E+00	0.00E+00	0.00E+00

* for these cases a value different than zero was computed, however, it was considered by the PEER coordinators as inappropriate for comparative purposes since there are significant differences between the values obtained by the 5 reference codes used to estimate the mean value.

Table 4-14 Analytical annual exceedance probabilities obtained by PEER project coordinators for Case 1, set 4

Peak Ground Acceleration (g)	Annual Exceedance Probability						
	Site 1	Site 2	Site 3	Site 4	Site 5	Site 6	Site 7
0.001	1.68E-02	1.68E-02	1.68E-02	1.68E-02	1.68E-02	1.68E-02	1.68E-02
0.01	1.68E-02	1.68E-02	1.68E-02	1.68E-02	1.68E-02	1.68E-02	1.68E-02
0.05	1.68E-02	1.68E-02	0.00E+00	1.68E-02	1.68E-02	1.68E-02	1.68E-02
0.10	1.68E-02	1.68E-02	0.00E+00	1.68E-02	1.68E-02	1.68E-02	1.68E-02
0.15	1.68E-02	1.68E-02	0.00E+00	1.68E-02	1.24E-02	1.68E-02	1.68E-02
0.20	1.68E-02	1.68E-02	0.00E+00	1.68E-02	5.25E-03	1.68E-02	1.64E-02
0.25	1.68E-02	1.68E-02	0.00E+00	1.57E-02	*	1.57E-02	4.17E-03
0.30	1.68E-02	0.00E+00	0.00E+00	1.18E-02	0.00E+00	1.18E-02	0.00E+00
0.35	1.68E-02	0.00E+00	0.00E+00	8.42E-03	0.00E+00	8.42E-03	0.00E+00
0.40	1.36E-02	0.00E+00	0.00E+00	5.09E-03	0.00E+00	5.09E-03	0.00E+00
0.45	1.01E-02	0.00E+00	0.00E+00	2.87E-03	0.00E+00	2.87E-03	0.00E+00
0.50	7.03E-03	0.00E+00	0.00E+00	1.47E-03	0.00E+00	1.47E-03	0.00E+00
0.55	4.37E-03	0.00E+00	0.00E+00	*	0.00E+00	6.26E-04	0.00E+00
0.60	*	0.00E+00	0.00E+00	*	0.00E+00	*	0.00E+00
0.70	0.00E+00	0.00E+00	0.00E+00	0.00E+00	0.00E+00	0.00E+00	0.00E+00
0.80	0.00E+00	0.00E+00	0.00E+00	0.00E+00	0.00E+00	0.00E+00	0.00E+00
0.90	0.00E+00	0.00E+00	0.00E+00	0.00E+00	0.00E+00	0.00E+00	0.00E+00
1.00	0.00E+00	0.00E+00	0.00E+00	0.00E+00	0.00E+00	0.00E+00	0.00E+00

* for these cases a value different than zero was computed, however, it was considered by the PEER coordinators as inappropriate for comparative purposes since there are significant differences between the values obtained by the 5 reference codes used to estimate the mean value.

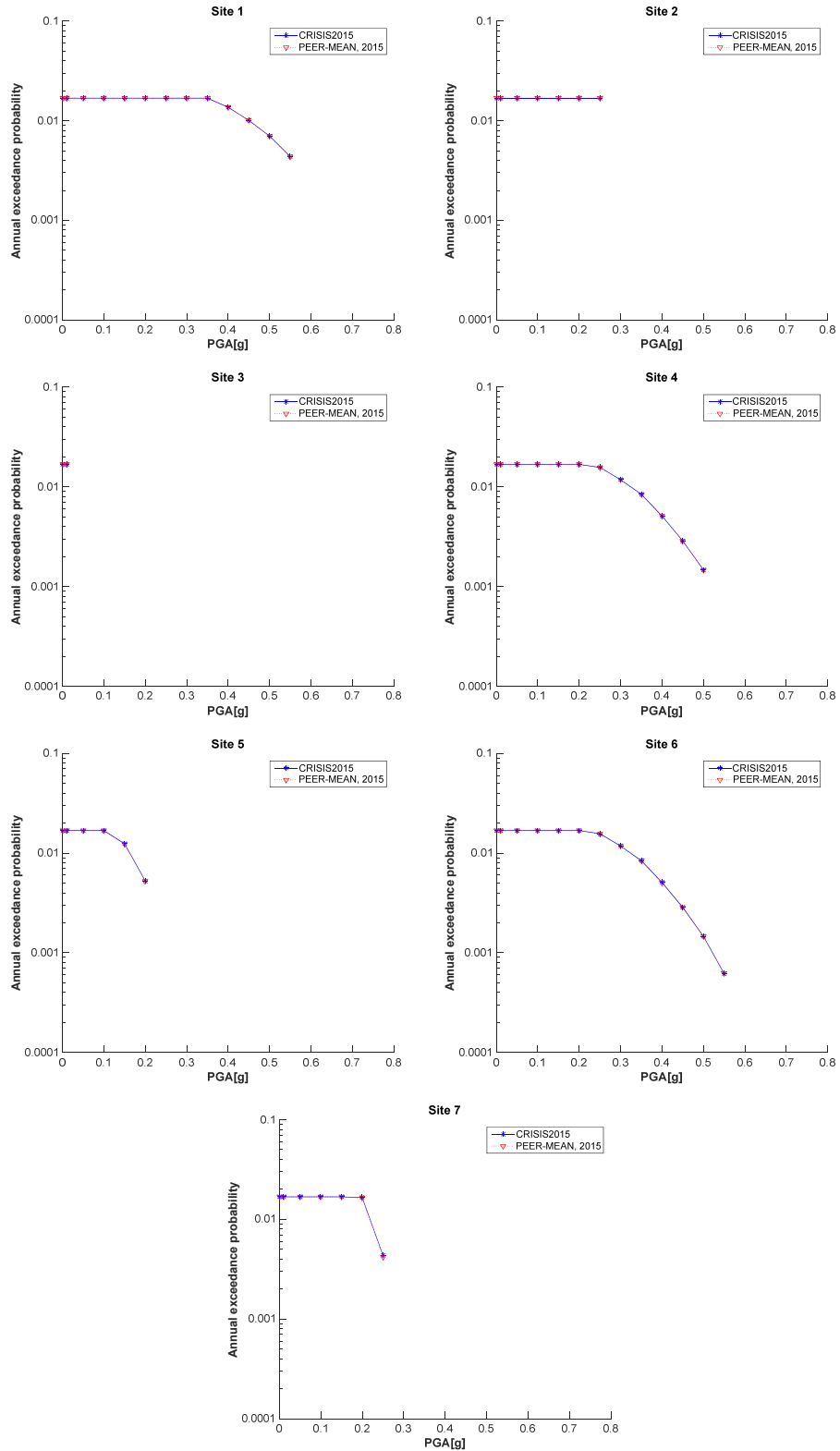


Figure 4-15 Comparison of the CRISIS and PEER-2015 results for Sites 1 to 7 (Set 1 Case 4)

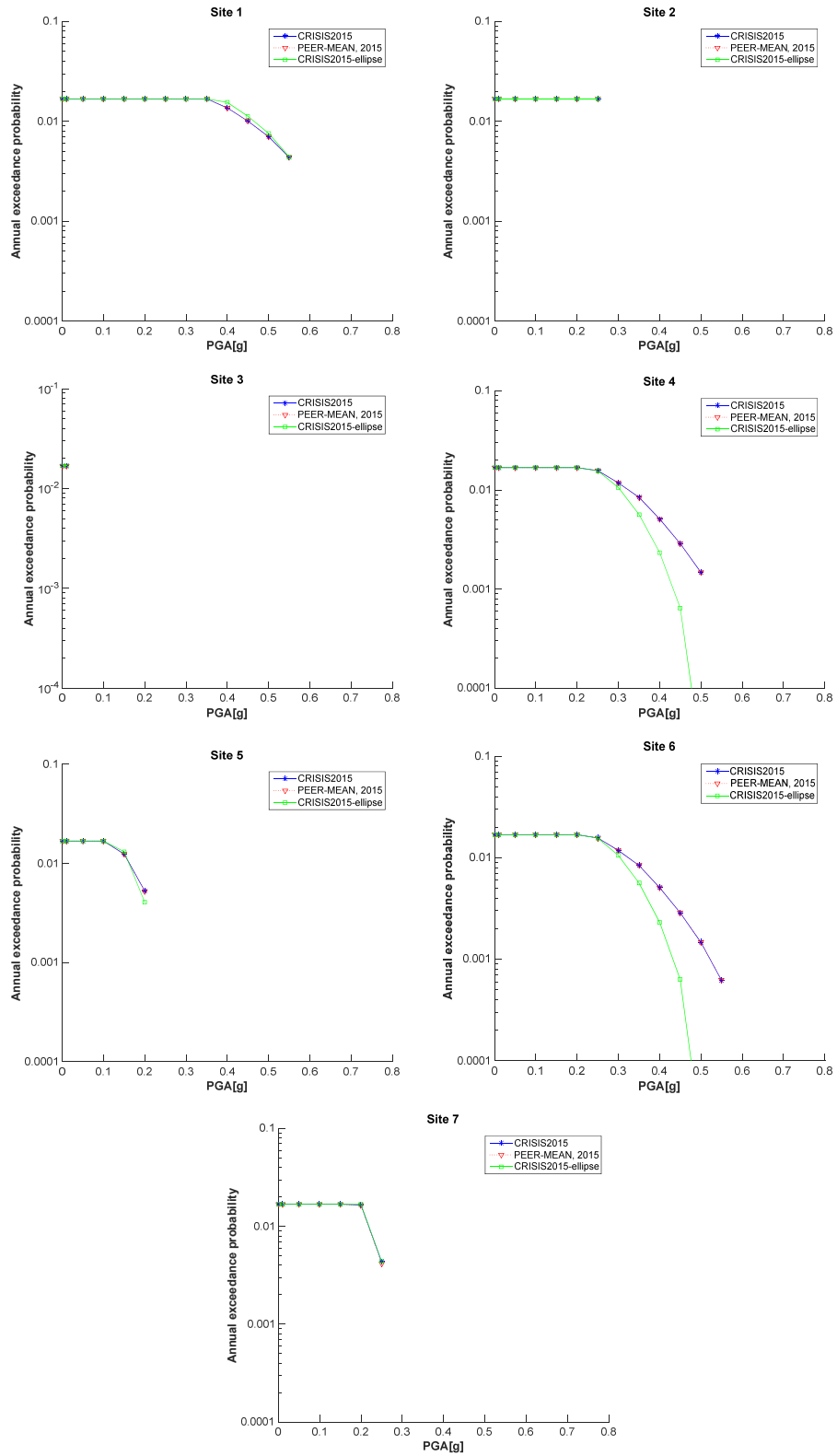


Figure 4-16 Comparison of elliptical and rectangular rupture shapes for PEER-2015 Set 1 Case 4

4.1.9 Set 1 case 5

Input parameters

The source adopted is fault 1. The seismic activity (magnitude distribution) is described by a truncated exponential model with a b -value=0.9, a slip rate of 2mm/yr, minimum magnitude $M_{min}=5$ and maximum magnitude $M_{max}=6.5$ as summarized in Table 4-15.

Table 4-15 Summary of input data for Set 1, case 5

Name	Description	Source	Mag-Density Function	Ground Motion Model ^{1,2}	Rupture Dimension Relationships ^{3,4,5,6}
Set 1 Case 5	Truncated exponential model	Fault 1(vertical SS) b-value=0.9 Slip rate=2mm/yr.	Truncated exponential model, Mmax=6.5, Mmin=5.0	Sadigh et al. (1997), rock. $\sigma = 0$	$Log(A) = M - 4; \sigma_A = 0$ $Log(W) = 0.5 * M - 2.15; \sigma_W = 0$ $Log(L) = 0.5 * M - 1.85; \sigma_L = 0$

¹ Integration over magnitude zero.

² Use magnitude integration step size as small as necessary to model the magnitude density function.

³ For all cases, uniform slip with tapered slip at edges.

⁴ No ruptures are to extend beyond the edge of the fault plane.

⁵ Aspect ratio to be maintained until maximum width is reached, then increase length (maintain area at the expense of aspect ratio).

⁶ Down-dip and along strike integration step size should be as small as necessary for uniform rupture location.

For this case, a modified G-R relation was adopted in R-CRISIS. Therefore, the seismicity rate, λ , is in this case the number of earthquakes with $M \geq 5$. The logic behind is the same as in set 1, case 1 but now, in this context, all the magnitudes between 5.0 and 6.5 are possible.

Following Youngs and Coppersmith (1985), the moment rate can be written as:

$$M_o = \mu A s = \int_{-\infty}^{M_{max}} M_o(m) f(m) dm \quad (\text{Eq. 4-6})$$

where:

- $M_o(m)$ is given by equation 4-4.
- $f(m)$ is the probability density function of magnitude, that in the case of a truncated exponential is:

$$f(m) = \frac{\lambda \beta \exp(-\beta(m - M_{min}))}{1 - \exp(-\beta(M_{max} - M_{min}))} \quad (\text{Eq. 4-7})$$

where $\beta = \ln(10) * b$

Hence, equation 4-6 becomes:

$$M_o = \mu A s = \frac{\lambda \beta \exp(-\beta(m - M_{min})) \times M_o(M_{max})}{[1 - \exp(-\beta(M_{max} - M_{min}))](1.5 - b)} \quad (\text{Eq. 4-8})$$

Solving equation 4-8 with respect to the unknown λ , gives $\lambda_5=0.0407$. Figure 4-17 shows the seismicity data screen of R-CRISIS for this case.

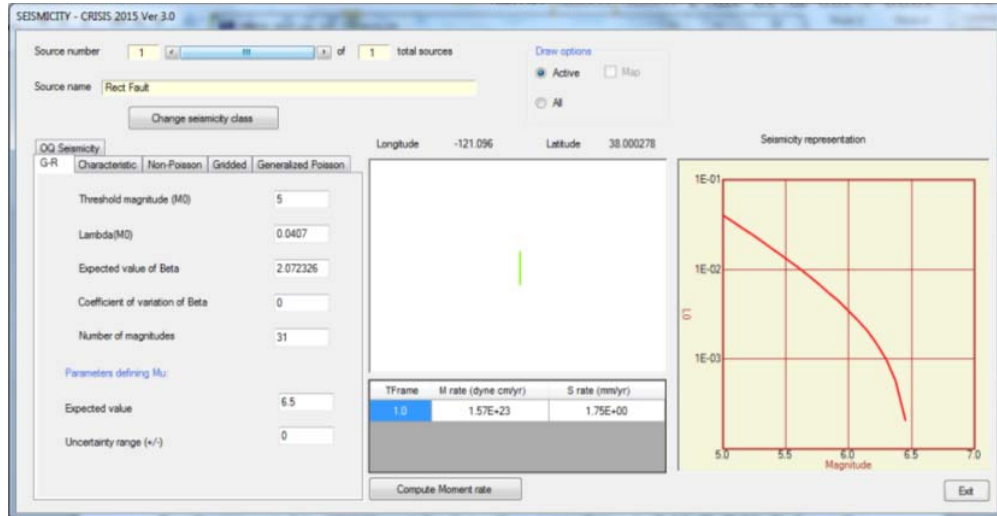


Figure 4-17 Seismicity parameters assigned in R-CRISIS for set 1, case 5

Results

Results computed in R-CRISIS for case 1, set 5 are shown in Table 4-16. Table 4-17 shows the results provided by the PEER-2015 project whereas Table 4-18 shows the analytical solution also provided by the coordinators of the PEER-2015 project. Figure 4.18 shows the hazard plots for the 7 computation sites. In all cases there is a full agreement between the results and therefore, it is possible to conclude that CRISIS fulfills all the requirements evaluated by the PEER-2015 project in Set 1-Case 5.

Figure X shows the hazard plots comparing the results obtained with R-CRISIS (elliptical and rectangular options) and the ones provided by the PEER-2015 project. Differences at computation sites 1, 4, 5 and 6 exist for exactly the same reasons explained before.

Table 4-16 Annual exceedance probabilities obtained in R-CRISIS for Case 1, set 5

Peak Ground Acceleration (g)	Annual Exceedance Probability						
	Site 1	Site 2	Site 3	Site 4	Site 5	Site 6	Site 7
0.001	3.99E-02	3.99E-02	3.99E-02	3.99E-02	3.99E-02	3.99E-02	3.99E-02
0.01	3.99E-02	3.99E-02	3.99E-02	3.99E-02	3.99E-02	3.99E-02	3.99E-02
0.05	3.99E-02	3.99E-02	0.00E+00	3.98E-02	3.14E-02	3.98E-02	3.99E-02
0.10	3.98E-02	3.35E-02	0.00E+00	2.99E-02	1.21E-02	2.99E-02	3.35E-02
0.15	3.49E-02	1.23E-02	0.00E+00	2.00E-02	4.41E-03	2.00E-02	1.23E-02
0.20	2.62E-02	4.90E-03	0.00E+00	1.30E-02	1.89E-03	1.30E-02	4.90E-03
0.25	1.91E-02	1.80E-03	0.00E+00	8.59E-03	7.53E-04	8.56E-03	1.80E-03
0.30	1.38E-02	*	0.00E+00	5.74E-03	*	5.71E-03	*
0.35	9.78E-03	0.00E+00	0.00E+00	3.89E-03	0.00E+00	3.87E-03	0.00E+00
0.40	6.80E-03	0.00E+00	0.00E+00	2.69E-03	0.00E+00	2.68E-03	0.00E+00
0.45	4.74E-03	0.00E+00	0.00E+00	1.92E-03	0.00E+00	1.91E-03	0.00E+00
0.50	3.29E-03	0.00E+00	0.00E+00	1.37E-03	0.00E+00	1.37E-03	0.00E+00
0.55	2.24E-03	0.00E+00	0.00E+00	9.72E-04	0.00E+00	9.65E-04	0.00E+00
0.60	1.47E-03	0.00E+00	0.00E+00	6.84E-04	0.00E+00	6.75E-04	0.00E+00
0.70	*	0.00E+00	0.00E+00	*	0.00E+00	*	0.00E+00
0.80	0.00E+00	0.00E+00	0.00E+00	0.00E+00	0.00E+00	0.00E+00	0.00E+00
0.90	0.00E+00	0.00E+00	0.00E+00	0.00E+00	0.00E+00	0.00E+00	0.00E+00
1.00	0.00E+00	0.00E+00	0.00E+00	0.00E+00	0.00E+00	0.00E+00	0.00E+00

* for these cases a value different than zero was computed, however, it was considered by the PEER coordinators as inappropriate for comparative purposes since there are significant differences between the values obtained by the 5 reference codes used to estimate the mean value.

Table 4-17 Annual exceedance probabilities reported as benchmarks by PEER project coordinators for Case 1, set 5

Peak Ground Acceleration (g)	Annual Exceedance Probability						
	Site 1	Site 2	Site 3	Site 4	Site 5	Site 6	Site 7
0.001	3.99E-02	3.99E-02	3.99E-02	3.99E-02	3.99E-02	3.99E-02	3.99E-02
0.01	3.99E-02	3.99E-02	3.99E-02	3.99E-02	3.99E-02	3.99E-02	3.99E-02
0.05	3.99E-02	3.99E-02	0.00E+00	3.98E-02	3.14E-02	3.98E-02	3.99E-02
0.10	3.98E-02	3.34E-02	0.00E+00	2.98E-02	1.21E-02	2.99E-02	3.34E-02
0.15	3.48E-02	1.23E-02	0.00E+00	2.00E-02	4.41E-03	2.00E-02	1.23E-02
0.20	2.62E-02	4.87E-03	0.00E+00	1.30E-02	1.89E-03	1.30E-02	4.87E-03
0.25	1.91E-02	1.78E-03	0.00E+00	8.58E-03	7.53E-04	8.58E-03	1.78E-03
0.30	1.37E-02	*	0.00E+00	5.73E-03	*	5.73E-03	*
0.35	9.77E-03	0.00E+00	0.00E+00	3.88E-03	0.00E+00	3.88E-03	0.00E+00
0.40	6.80E-03	0.00E+00	0.00E+00	2.69E-03	0.00E+00	2.69E-03	0.00E+00
0.45	4.74E-03	0.00E+00	0.00E+00	1.91E-03	0.00E+00	1.91E-03	0.00E+00
0.50	3.29E-03	0.00E+00	0.00E+00	1.36E-03	0.00E+00	1.37E-03	0.00E+00
0.55	2.24E-03	0.00E+00	0.00E+00	9.70E-04	0.00E+00	9.70E-04	0.00E+00
0.60	1.47E-03	0.00E+00	0.00E+00	6.71E-04	0.00E+00	6.73E-04	0.00E+00
0.70	*	0.00E+00	0.00E+00	*	0.00E+00	*	0.00E+00
0.80	0.00E+00	0.00E+00	0.00E+00	0.00E+00	0.00E+00	0.00E+00	0.00E+00
0.90	0.00E+00	0.00E+00	0.00E+00	0.00E+00	0.00E+00	0.00E+00	0.00E+00
1.00	0.00E+00	0.00E+00	0.00E+00	0.00E+00	0.00E+00	0.00E+00	0.00E+00

* for these cases a value different than zero was computed, however, it was considered by the PEER coordinators as inappropriate for comparative purposes since there are significant differences between the values obtained by the 5 reference codes used to estimate the mean value.

Table 4-18 Analytical annual exceedance probabilities obtained by PEER project coordinators for Case 1, set 5

Peak Ground Acceleration (g)	Annual Exceedance Probability						
	Site 1	Site 2	Site 3	Site 4	Site 5	Site 6	Site 7
0.001	3.99E-02	3.99E-02	3.99E-02	3.99E-02	3.99E-02	3.99E-02	3.99E-02
0.01	3.99E-02	3.99E-02	3.99E-02	3.99E-02	3.99E-02	3.99E-02	3.99E-02
0.05	3.99E-02	3.99E-02	0.00E+00	3.98E-02	3.14E-02	3.98E-02	3.99E-02
0.10	3.98E-02	3.33E-02	0.00E+00	2.99E-02	1.21E-02	2.99E-02	3.33E-02
0.15	3.49E-02	1.23E-02	0.00E+00	2.00E-02	4.41E-03	2.00E-02	1.23E-02
0.20	2.62E-02	4.85E-03	0.00E+00	1.30E-02	1.89E-03	1.30E-02	4.85E-03
0.25	1.91E-02	1.76E-03	0.00E+00	8.57E-03	7.52E-04	8.57E-03	1.76E-03
0.30	1.37E-02	*	0.00E+00	5.72E-03	*	5.72E-03	*
0.35	9.76E-03	0.00E+00	0.00E+00	3.88E-03	0.00E+00	3.87E-03	0.00E+00
0.40	6.79E-03	0.00E+00	0.00E+00	2.69E-03	0.00E+00	2.69E-03	0.00E+00
0.45	4.73E-03	0.00E+00	0.00E+00	1.91E-03	0.00E+00	1.91E-03	0.00E+00
0.50	3.28E-03	0.00E+00	0.00E+00	1.37E-03	0.00E+00	1.37E-03	0.00E+00
0.55	2.23E-03	0.00E+00	0.00E+00	9.72E-04	0.00E+00	9.72E-04	0.00E+00
0.60	1.47E-03	0.00E+00	0.00E+00	6.73E-04	0.00E+00	6.73E-04	0.00E+00
0.70	*	0.00E+00	0.00E+00	*	0.00E+00	*	0.00E+00
0.80	0.00E+00	0.00E+00	0.00E+00	0.00E+00	0.00E+00	0.00E+00	0.00E+00
0.90	0.00E+00	0.00E+00	0.00E+00	0.00E+00	0.00E+00	0.00E+00	0.00E+00
1.00	0.00E+00	0.00E+00	0.00E+00	0.00E+00	0.00E+00	0.00E+00	0.00E+00

* for these cases a value different than zero was computed, however, it was considered by the PEER coordinators as inappropriate for comparative purposes since there are significant differences between the values obtained by the 5 reference codes used to estimate the mean value.

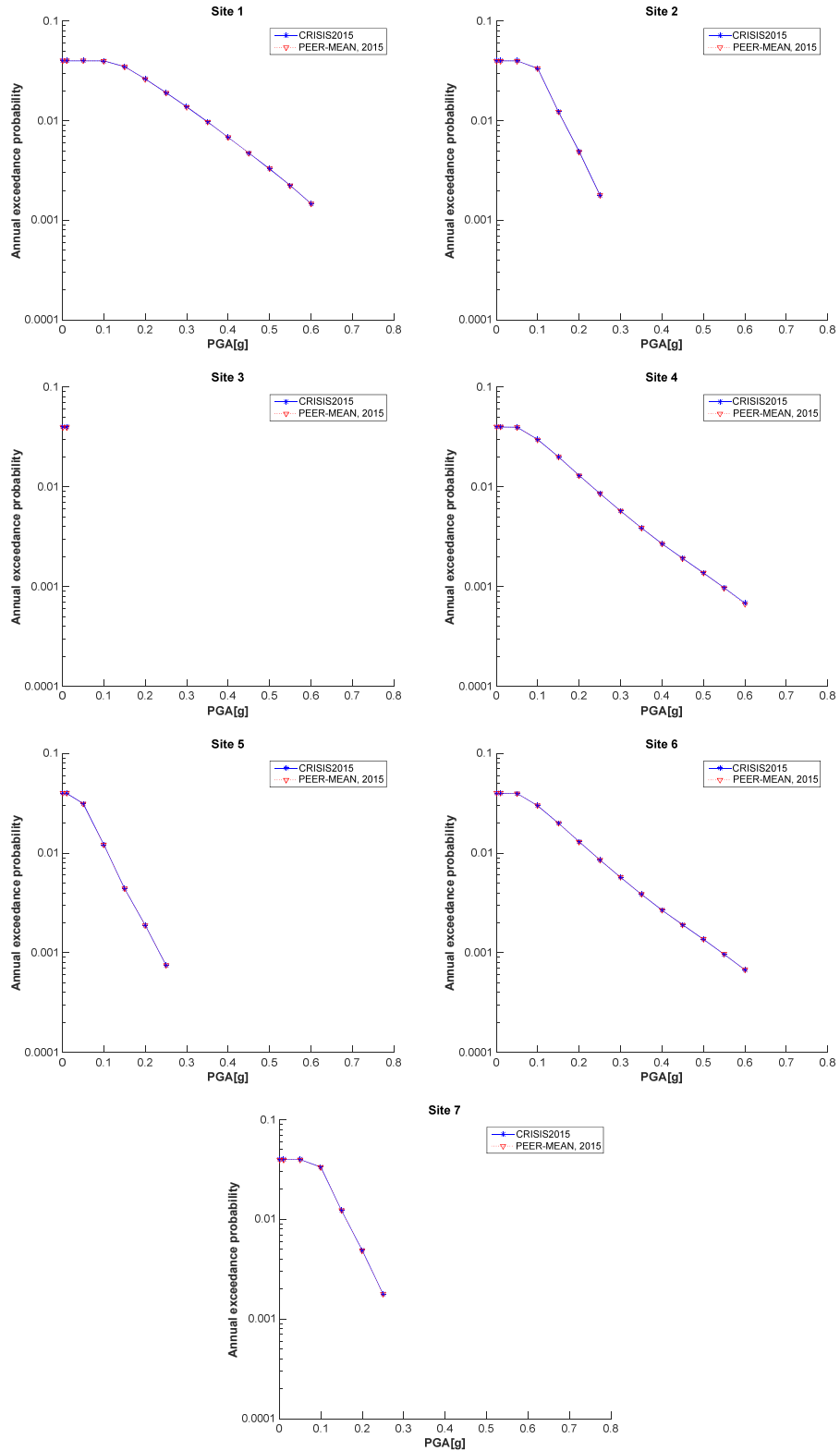


Figure 4-18 Comparison of the CRISIS and PEER-2015 results for Sites 1 to 7 (Set 1 Case 5)

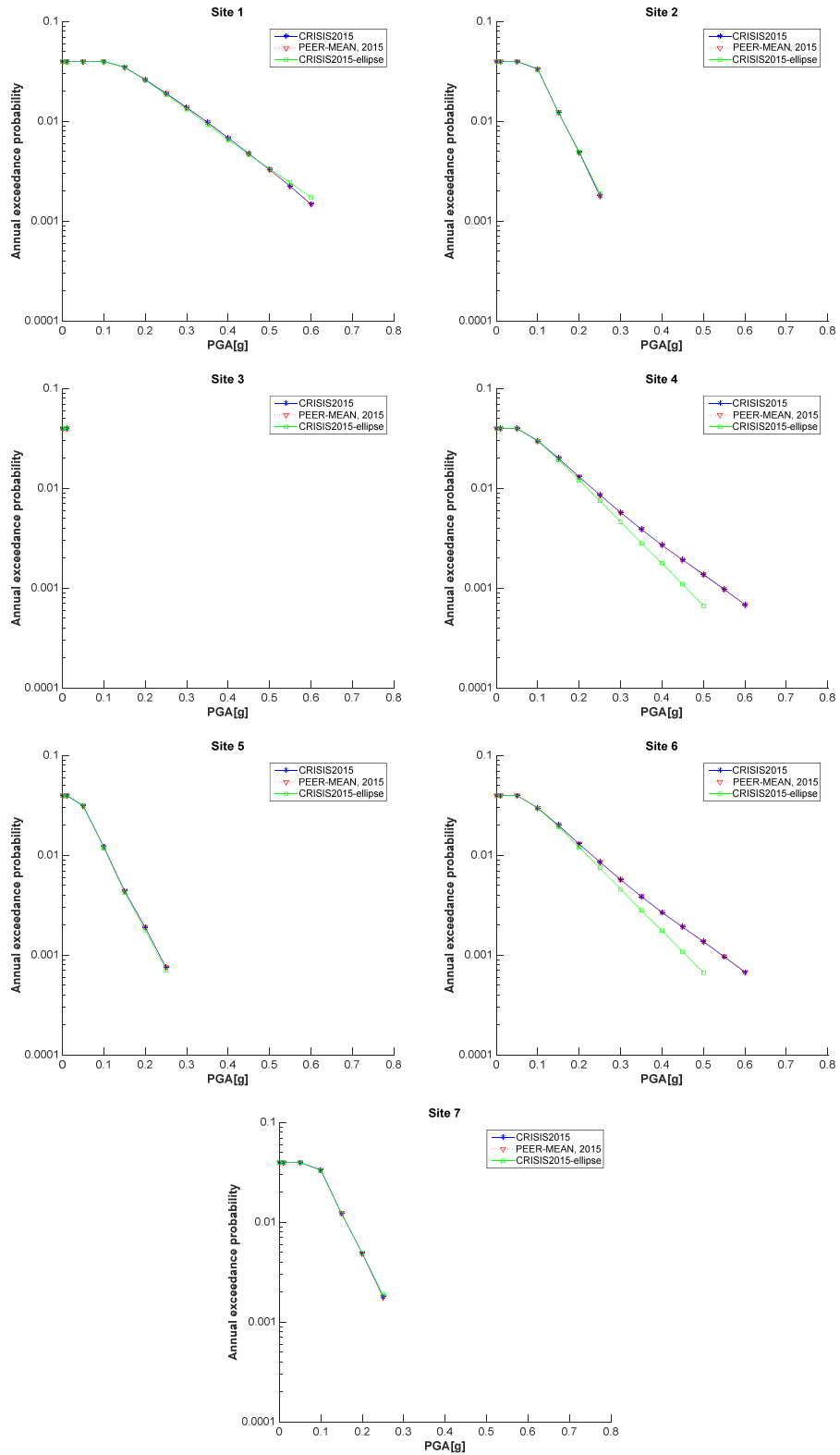


Figure 4-19 Comparison of elliptical and rectangular rupture shapes for PEER-2015 Set 1 Case 5

4.1.10 Set 1 case 6

Input parameters

The source adopted is Fault 1. The seismicity is described by a characteristic model with a truncated normal distribution with a b -value=0.9, a slip rate of 2mm/yr, $M_{min}=5$, $M_{max}=6.5$, a characteristic magnitude $M_{ch}=6.2$ and a sigma $\sigma_M=0.25$. Table 4-19 summarizes the input parameters.

Table 4-19 Summary of input data for Set 1, case 6

Name	Description	Source	Mag-Density Function	Ground Motion Model ^{1,2}	Rupture Dimension Relationships ^{3,4,5,6}
Set 1 Case 6	Truncated normal model	Fault 1 (vertical SS) b-value=0.9 Slip rate=2mm/yr.	Truncated normal model, $M_{max}=6.5$, $M_{min}=5.0$, $M_{char}=6.2$, $\sigma=0.25$	Sadigh et al. (1997), rock. $\sigma = 0$	$Log(A) = M - 4; \sigma_A = 0$ $Log(W) = 0.5 * M - 2.15; \sigma_W = 0$ $Log(L) = 0.5 * M - 1.85; \sigma_L = 0$

¹ Integration over magnitude zero.

² Use magnitude integration step size as small as necessary to model the magnitude density function.

³ For all cases, uniform slip with tapered slip at edges.

⁴ No ruptures are to extend beyond the edge of the fault plane.

⁵ Aspect ratio to be maintained until maximum width is reached, then increase length (maintain area at the expense of aspect ratio).

⁶ Down-dip and along strike integration step size should be as small as necessary for uniform rupture location.

Using the same approach as the one explained in set 1, case 7 with the provided data, the mean recurrence time between earthquakes was obtained and the characteristic earthquake seismicity model was used in R-CRISIS. According to the provided data, the mean recurrence time between characteristic earthquakes is 129 years. Figure 4-20 shows the seismicity data screen (now for the characteristic earthquake model) of R-CRISIS.

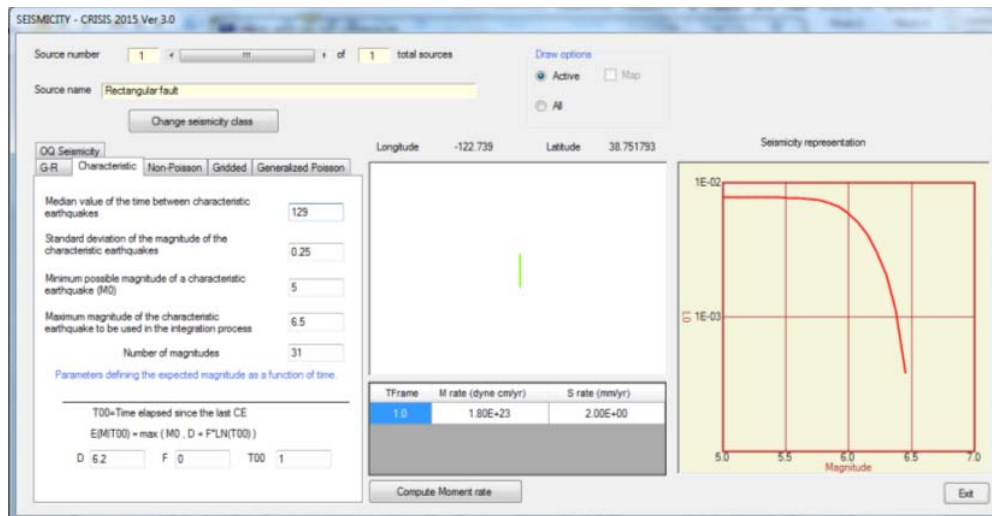


Figure 4-20 Seismicity parameters assigned in R-CRISIS for set 1, case 6

Results

Results computed in R-CRISIS for set 1, case 6 are shown in Table 4-20. Table 4-21 shows the results provided by the PEER-2015 project whereas Table 4-22 shows the analytical solution also provided by the coordinators of the PEER-2015 project. Figure 4-21 shows the hazard plots for the 7 computation sites. In all cases there is a full agreement between the results and therefore, it is possible to conclude that CRISIS fulfills all the requirements evaluated by the PEER-2015 project in Set 1-Case 6.

Figure 4-22 shows the hazard plots comparing the results obtained with R-CRISIS (elliptical and rectangular options) and the ones provided by the PEER-2015 project. Differences at computation sites 1, 4, 5 and 6 exist for exactly the same reasons explained in section 4.1.2.

Table 4-20 Annual exceedance probabilities obtained in R-CRISIS for Case 1, set 6

Peak Ground Acceleration (g)	Annual Exceedance Probability						
	Site 1	Site 2	Site 3	Site 4	Site 5	Site 6	Site 7
0.001	7.72E-03	7.72E-03	7.72E-03	7.72E-03	7.72E-03	7.72E-03	7.72E-03
0.01	7.72E-03	7.72E-03	7.72E-03	7.72E-03	7.72E-03	7.72E-03	7.72E-03
0.05	7.72E-03	7.72E-03	0.00E+00	7.72E-03	7.72E-03	7.72E-03	7.72E-03
0.10	7.72E-03	7.72E-03	0.00E+00	7.72E-03	7.35E-03	7.72E-03	7.72E-03
0.15	7.72E-03	7.67E-03	0.00E+00	7.62E-03	5.79E-03	7.62E-03	7.67E-03
0.20	7.72E-03	6.77E-03	0.00E+00	7.29E-03	3.54E-03	7.28E-03	6.77E-03
0.25	7.67E-03	3.65E-03	0.00E+00	6.72E-03	1.52E-03	6.71E-03	3.65E-03
0.30	7.52E-03	*	0.00E+00	5.98E-03	*	5.96E-03	*
0.35	7.20E-03	0.00E+00	0.00E+00	5.14E-03	0.00E+00	5.13E-03	0.00E+00
0.40	6.67E-03	0.00E+00	0.00E+00	4.27E-03	0.00E+00	4.25E-03	0.00E+00
0.45	5.92E-03	0.00E+00	0.00E+00	3.44E-03	0.00E+00	3.42E-03	0.00E+00
0.50	5.04E-03	0.00E+00	0.00E+00	2.64E-03	0.00E+00	2.63E-03	0.00E+00
0.55	3.99E-03	0.00E+00	0.00E+00	1.94E-03	0.00E+00	1.92E-03	0.00E+00
0.60	2.91E-03	0.00E+00	0.00E+00	1.37E-03	0.00E+00	1.35E-03	0.00E+00
0.70	*	0.00E+00	0.00E+00	*	0.00E+00	*	0.00E+00
0.80	0.00E+00	0.00E+00	0.00E+00	0.00E+00	0.00E+00	0.00E+00	0.00E+00
0.90	0.00E+00	0.00E+00	0.00E+00	0.00E+00	0.00E+00	0.00E+00	0.00E+00
1.00	0.00E+00	0.00E+00	0.00E+00	0.00E+00	0.00E+00	0.00E+00	0.00E+00

* for these cases a value different than zero was computed, however, it was considered by the PEER coordinators as inappropriate for comparative purposes since there are significant differences between the values obtained by the 5 reference codes used to estimate the mean value.

Table 4-21 Annual exceedance probabilities reported as benchmarks by PEER project coordinators for Case 1, set 6

Peak Ground Acceleration (g)	Annual Exceedance Probability						
	Site 1	Site 2	Site 3	Site 4	Site 5	Site 6	Site 7
0.001	7.73E-03	7.73E-03	7.73E-03	7.73E-03	7.73E-03	7.73E-03	7.73E-03
0.01	7.73E-03	7.73E-03	7.73E-03	7.73E-03	7.73E-03	7.73E-03	7.73E-03
0.05	7.73E-03	7.73E-03	0.00E+00	7.73E-03	7.73E-03	7.73E-03	7.73E-03
0.10	7.73E-03	7.73E-03	0.00E+00	7.72E-03	7.35E-03	7.72E-03	7.73E-03
0.15	7.73E-03	7.68E-03	0.00E+00	7.62E-03	5.79E-03	7.62E-03	7.68E-03
0.20	7.72E-03	6.77E-03	0.00E+00	7.28E-03	3.55E-03	7.28E-03	6.77E-03
0.25	7.68E-03	3.63E-03	0.00E+00	6.71E-03	1.52E-03	6.71E-03	3.65E-03
0.30	7.53E-03	*	0.00E+00	5.96E-03	*	5.96E-03	*
0.35	7.20E-03	0.00E+00	0.00E+00	5.12E-03	0.00E+00	5.12E-03	0.00E+00
0.40	6.66E-03	0.00E+00	0.00E+00	4.25E-03	0.00E+00	4.25E-03	0.00E+00
0.45	5.93E-03	0.00E+00	0.00E+00	3.41E-03	0.00E+00	3.41E-03	0.00E+00
0.50	5.03E-03	0.00E+00	0.00E+00	2.63E-03	0.00E+00	2.63E-03	0.00E+00
0.55	4.00E-03	0.00E+00	0.00E+00	1.93E-03	0.00E+00	1.93E-03	0.00E+00
0.60	2.92E-03	0.00E+00	0.00E+00	1.34E-03	0.00E+00	1.34E-03	0.00E+00
0.70	*	0.00E+00	0.00E+00	*	0.00E+00	*	0.00E+00
0.80	0.00E+00	0.00E+00	0.00E+00	0.00E+00	0.00E+00	0.00E+00	0.00E+00
0.90	0.00E+00	0.00E+00	0.00E+00	0.00E+00	0.00E+00	0.00E+00	0.00E+00
1.00	0.00E+00	0.00E+00	0.00E+00	0.00E+00	0.00E+00	0.00E+00	0.00E+00

* for these cases a value different than zero was computed, however, it was considered by the PEER coordinators as inappropriate for comparative purposes since there are significant differences between the values obtained by the 5 reference codes used to estimate the mean value.

Table 4-22 Analytical annual exceedance probabilities obtained by PEER project coordinators for Case 1, set 6

Peak Ground Acceleration (g)	Annual Exceedance Probability						
	Site 1	Site 2	Site 3	Site 4	Site 5	Site 6	Site 7
0.001	**	**	**	7.75E-03	7.75E-03	7.75E-03	**
0.01	**	**	**	7.75E-03	7.75E-03	7.75E-03	**
0.05	**	**	**	7.75E-03	7.75E-03	7.75E-03	**
0.10	**	**	**	7.74E-03	7.37E-03	7.74E-03	**
0.15	**	**	**	7.64E-03	5.81E-03	7.64E-03	**
0.20	**	**	**	7.31E-03	3.57E-03	7.31E-03	**
0.25	**	**	**	6.73E-03	1.52E-03	6.73E-03	**
0.30	**	**	**	5.99E-03	*	5.99E-03	**
0.35	**	**	**	**	**	**	**
0.40	**	**	**	4.27E-03	**	4.27E-03	**
0.45	**	**	**	**	**	**	**
0.50	**	**	**	2.64E-03	**	2.64E-03	**
0.55	**	**	**	**	**	**	**
0.60	**	**	**	1.35E-03	**	1.35E-03	**
0.70	**	**	**	*	**	*	**
0.80	**	**	**	**	**	**	**
0.90	**	**	**	**	**	**	**
1.00	**	**	**	**	**	**	**

* for these cases a value different than zero was computed, however, it was considered by the PEER coordinators as inappropriate for comparative purposes since there are significant differences between the values obtained by the 5 reference codes used to estimate the mean value.

** There are no data available for these cases

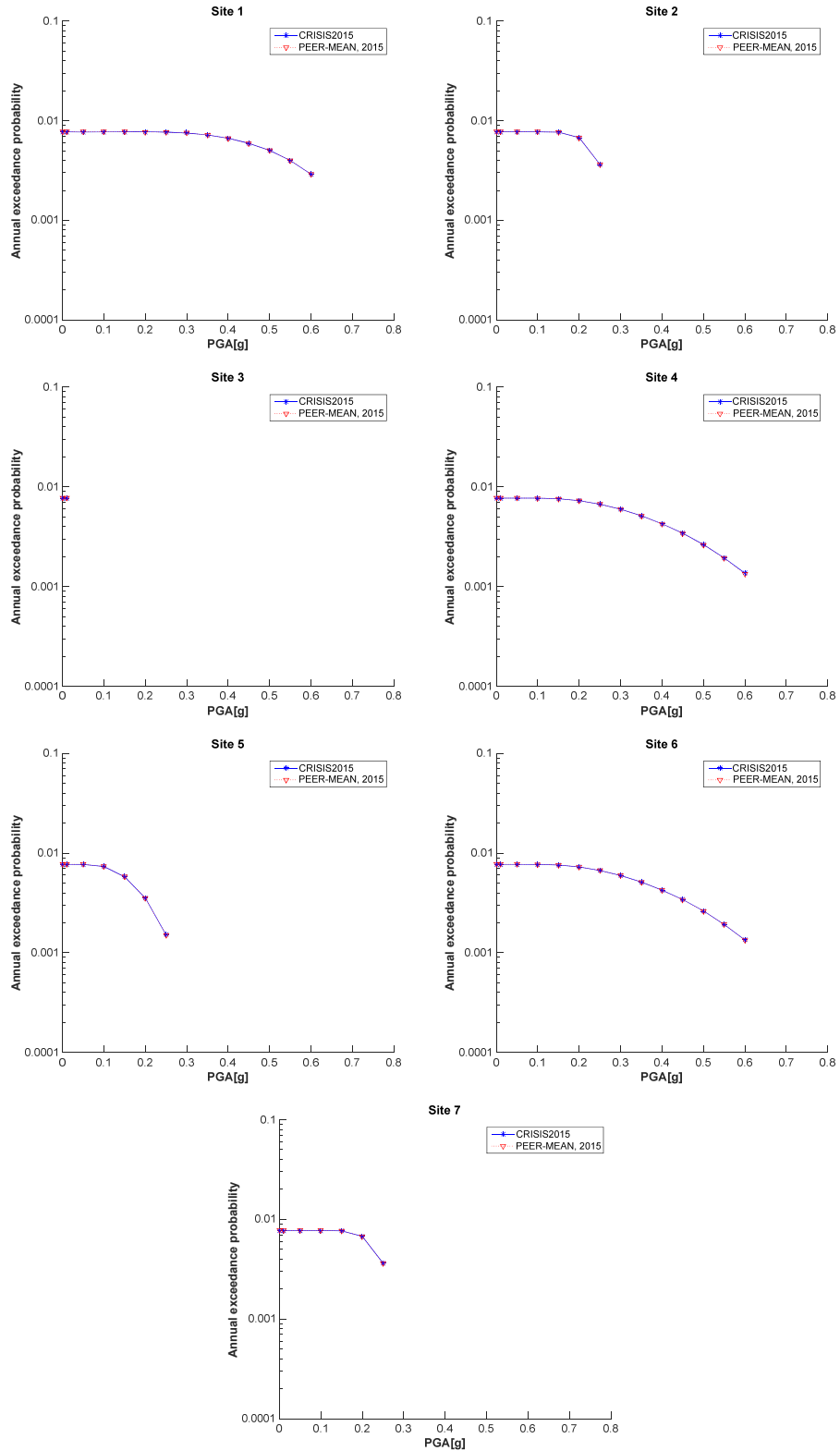


Figure 4-21 Comparison of the CRISIS and PEER-2015 results for Sites 1 to 7 (Set 1 Case 6)

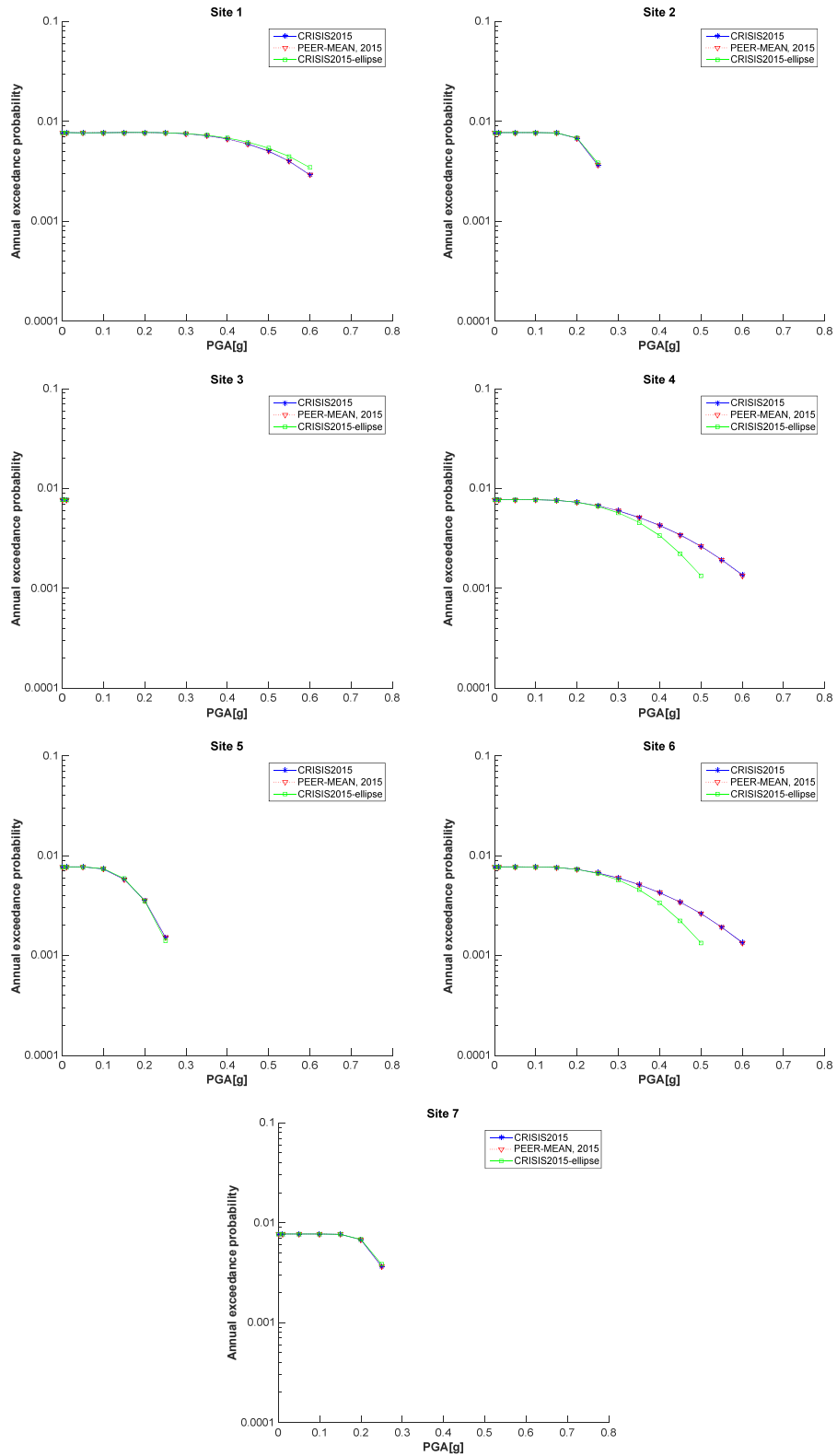


Figure 4-22 Comparison of elliptical and rectangular rupture shapes for PEER-2015 Set 1 Case 6

4.1.11 Set 1 case 7

Input parameters

The source adopted is fault 1 and Table 4-23 shows the seismicity input data provided for this case.

Table 4-23 Summary of input data for Set 1, case 7

Name	Description	Source	Mag-Density Function	Ground Motion Model ^{1,2}	Rupture Dimension Relationships ^{3,4,5,6}
Set 1 Case 7	Characteristic model (Youngs and Coppersmith, 1985)	Fault 1(vertical SS) b-value=0.9 Slip rate=2mm/yr.	Truncated normal model, Mmax=6.5, Mmin=5.0, Mchar=6.2, σ=0.25	Sadigh et al. (1997), rock. σ = 0	$Log(A) = M - 4; \sigma_A = 0$ $Log(W) = 0.5 * M - 2.15; \sigma_W = 0$ $Log(L) = 0.5 * M - 1.85; \sigma_L = 0$

¹ Integration over magnitude zero.

² Use magnitude integration step size as small as necessary to model the magnitude density function.

³ For all cases, uniform slip with tapered slip at edges.

⁴ No ruptures are to extend beyond the edge of the fault plane.

⁵ Aspect ratio to be maintained until maximum width is reached, then increase length (maintain area at the expense of aspect ratio).

⁶ Down-dip and along strike integration step size should be as small as necessary for uniform rupture location.

The seismicity for this case is described in R-CRISIS by means of the Youngs and Coppersmith (1985) characteristic model. That is:

- For low magnitude a G-R relation is assumed (between 5 and M_{max}^{GR})
- For higher magnitude a uniform density function describes the seismicity with the characteristic magnitude $M_{CH}=6.2$ and $\sigma M=0.25$.

The probability density function is:

$$f(m) = f_1(m) + f_2(m) \quad (\text{Eq. 4-9})$$

with:

$$f_1(m) = \frac{(\dot{N}(M_{min}) - \dot{N}(M_{ch})) \cdot \beta \exp(-\beta(m - M_{min}))}{1 - \exp(-\beta(M_{max}^{GR} - M_{min}))}, M_{min} \leq m \leq M_{max}^{GR} \quad (\text{Eq. 4-10})$$

$$f_2(m) = \dot{n}(M_{ch}), M_{ch} - \frac{\Delta M_{ch}}{2} \leq m \leq M_{ch} + \frac{\Delta M_{ch}}{2} \quad (\text{Eq. 4-11})$$

Where the term $\lambda^{GR} = (\dot{N}(M_{min}) - \dot{N}(M_{CH}))$ represents the rate of the non-characteristic, exponentially distributed earthquakes on the fault and $\dot{n}(M_{CH})$ is the rate density of the flat portion.

The two parameters needed for the description of the seismicity are the annual seismic rate λ and the mean recurrence time between characteristic earthquakes (T_{mean}). Following the original model of Youngs and Coppersmith (1985), we assume that:

1. Events of any magnitude are possible. this leads to $M_{max}^{GR} = M_{CH} - \Delta M_{ch} = 5.95$, where $M_{max} = 6.45$ (from PEER) and $\Delta M_{ch} = 0.25 \times 2 = 0.5$. Thus, a uniform distribution is adopted between 5.95 and 6.45.
2. $n(M_{CH}) \approx n(M_{max}^{GR} - 1)$

replacing equation 4-9 in equation 4-6 and solving the integral one obtains:

$$\dot{M}_o = \mu A \dot{s} = \frac{\lambda^{GR} b \exp(-\beta(M_{max}^{GR} - M_{min})) \times M_o(M_{max}^{GR})}{[1 - \exp(-\beta(M_{max}^{GR} - M_{min}))](1.5 - b)} + \frac{\dot{N}(M_{ch}) M_o(M_{max})(1 - 10^{-1.5 \Delta M_{ch}})}{c \ln(10) \Delta M_{ch}} \quad (\text{Eq. 4-12})$$

The input values are the b -value=0.9 and the slip rate of 2 mm/yr. Hence, with hypotheses 1 and 2, $\lambda^{GR} = 0.0048$ and $T_{mean} = 157$ yr. Figures 4-23 and 4-24 show the seismicity screens of R-CRISIS for the modified G-R and the characteristic earthquake seismicity models, respectively.

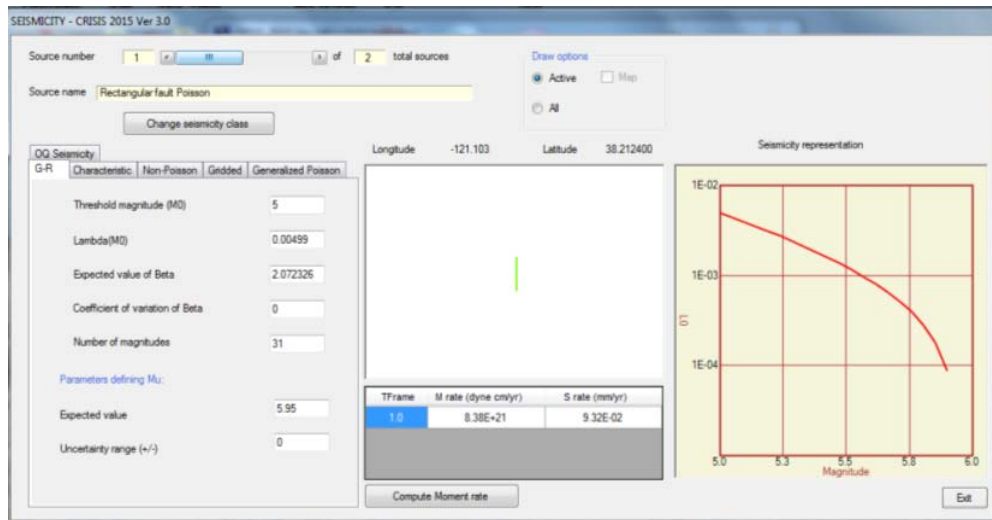


Figure 4-23 Seismicity parameters assigned in R-CRISIS for set 1, case 7 (modified G-R model)

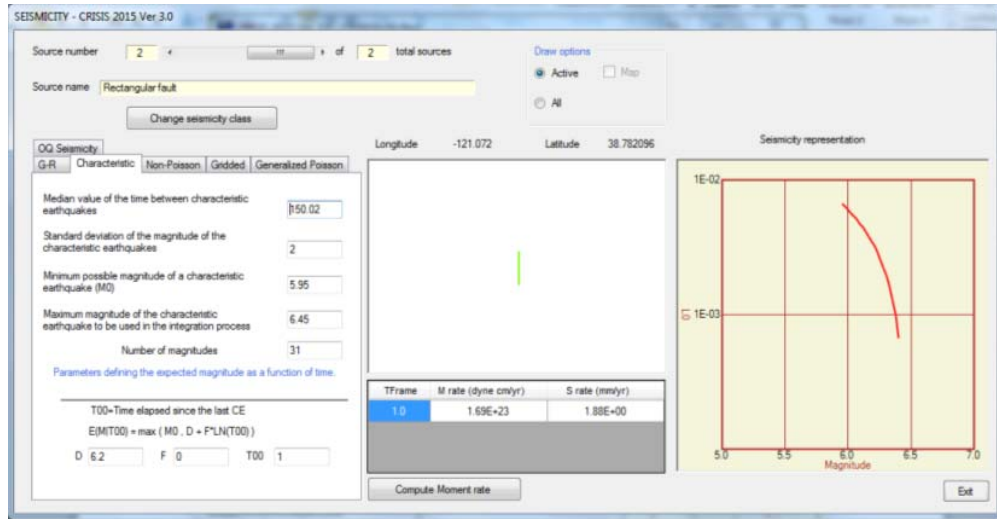


Figure 4-24 Seismicity parameters assigned in R-CRISIS for set 1, case 7 (characteristic earthquake model)

Results

Results computed in R-CRISIS for set 1, case 7 are shown in Table 4-24. Table 4-25 shows the results provided by the PEER-2015 project whereas Table 4-26 shows the analytical solution also provided by the coordinators of the PEER-2015 project. Figure 4-25 shows the hazard plots for the 7 computation sites. In all cases there is a full agreement between the results and therefore, it is possible to conclude that R-CRISIS fulfills all the requirements evaluated by the PEER-2015 project in set 1, case 7.

Figure 4-26 shows the hazard plots comparing the results obtained with R-CRISIS (elliptical and rectangular options) and the ones provided by the PEER-2015 project. Differences at computation sites 1, 4, 5 and 6 exist for exactly the same reasons explained in section 4.1.2.

Table 4-24 Annual exceedance probabilities obtained in R-CRISIS for Case 1, set 7

Peak Ground Acceleration (g)	Annual Exceedance Probability						
	Site 1	Site 2	Site 3	Site 4	Site 5	Site 6	Site 7
0.001	1.16E-02	1.16E-02	1.16E-02	1.16E-02	1.16E-02	1.16E-02	1.16E-02
0.01	1.16E-02	1.16E-02	1.16E-02	1.16E-02	1.16E-02	1.16E-02	1.16E-02
0.05	1.16E-02	1.16E-02	0.00E+00	1.16E-02	1.04E-02	1.16E-02	1.16E-02
0.10	1.16E-02	1.07E-02	0.00E+00	1.02E-02	7.74E-03	1.02E-02	1.07E-02
0.15	1.09E-02	7.77E-03	0.00E+00	8.83E-03	5.74E-03	8.82E-03	7.77E-03
0.20	9.68E-03	6.74E-03	0.00E+00	7.85E-03	3.56E-03	7.84E-03	6.74E-03
0.25	8.70E-03	3.58E-03	0.00E+00	6.94E-03	1.43E-03	6.93E-03	3.58E-03
0.30	7.97E-03	*	0.00E+00	6.03E-03	0.00E+00	6.02E-03	*
0.35	7.39E-03	0.00E+00	0.00E+00	5.14E-03	0.00E+00	5.13E-03	0.00E+00
0.40	6.68E-03	0.00E+00	0.00E+00	4.24E-03	0.00E+00	4.23E-03	0.00E+00
0.45	5.87E-03	0.00E+00	0.00E+00	3.40E-03	0.00E+00	3.38E-03	0.00E+00
0.50	4.98E-03	0.00E+00	0.00E+00	2.61E-03	0.00E+00	2.59E-03	0.00E+00
0.55	3.99E-03	0.00E+00	0.00E+00	1.89E-03	0.00E+00	1.86E-03	0.00E+00
0.60	2.88E-03	0.00E+00	0.00E+00	1.22E-03	0.00E+00	1.20E-03	0.00E+00
0.70	*	0.00E+00	0.00E+00	*	0.00E+00	*	0.00E+00
0.80	0.00E+00	0.00E+00	0.00E+00	0.00E+00	0.00E+00	0.00E+00	0.00E+00
0.90	0.00E+00	0.00E+00	0.00E+00	0.00E+00	0.00E+00	0.00E+00	0.00E+00
1.00	0.00E+00	0.00E+00	0.00E+00	0.00E+00	0.00E+00	0.00E+00	0.00E+00

* for these cases a value different than zero was computed, however, it was considered by the PEER coordinators as inappropriate for comparative purposes since there are significant differences between the values obtained by the 5 reference codes used to estimate the mean value.

Table 4-25 Annual exceedance probabilities reported as benchmarks by PEER project coordinators for Case 1, set 7

Peak Ground Acceleration (g)	Annual Exceedance Probability						
	Site 1	Site 2	Site 3	Site 4	Site 5	Site 6	Site 7
0.001	1.16E-02	1.16E-02	1.16E-02	1.16E-02	1.16E-02	1.16E-02	1.16E-02
0.01	1.16E-02	1.16E-02	1.16E-02	1.16E-02	1.16E-02	1.16E-02	1.16E-02
0.05	1.16E-02	1.16E-02	0.00E+00	1.16E-02	1.04E-02	1.16E-02	1.16E-02
0.10	1.16E-02	1.07E-02	0.00E+00	1.02E-02	7.74E-03	1.02E-02	1.07E-02
0.15	1.09E-02	7.76E-03	0.00E+00	8.83E-03	5.73E-03	8.83E-03	7.77E-03
0.20	9.67E-03	6.74E-03	0.00E+00	7.85E-03	3.55E-03	7.85E-03	6.75E-03
0.25	8.69E-03	3.57E-03	0.00E+00	6.93E-03	1.43E-03	6.93E-03	3.58E-03
0.30	7.97E-03	*	0.00E+00	6.02E-03	*	6.02E-03	*
0.35	7.38E-03	0.00E+00	0.00E+00	5.12E-03	0.00E+00	5.11E-03	0.00E+00
0.40	6.68E-03	0.00E+00	0.00E+00	4.23E-03	0.00E+00	4.22E-03	0.00E+00
0.45	5.87E-03	0.00E+00	0.00E+00	3.38E-03	0.00E+00	3.37E-03	0.00E+00
0.50	4.97E-03	0.00E+00	0.00E+00	2.59E-03	0.00E+00	2.59E-03	0.00E+00
0.55	3.98E-03	0.00E+00	0.00E+00	1.87E-03	0.00E+00	1.86E-03	0.00E+00
0.60	2.89E-03	0.00E+00	0.00E+00	1.21E-03	0.00E+00	1.21E-03	0.00E+00
0.70	*	0.00E+00	0.00E+00	*	0.00E+00	*	0.00E+00
0.80	0.00E+00	0.00E+00	0.00E+00	0.00E+00	0.00E+00	0.00E+00	0.00E+00
0.90	0.00E+00	0.00E+00	0.00E+00	0.00E+00	0.00E+00	0.00E+00	0.00E+00
1.00	0.00E+00	0.00E+00	0.00E+00	0.00E+00	0.00E+00	0.00E+00	0.00E+00

* for these cases a value different than zero was computed, however, it was considered by the PEER coordinators as inappropriate for comparative purposes since there are significant differences between the values obtained by the 5 reference codes used to estimate the mean value.

Table 4-26 Analytical annual exceedance probabilities obtained by PEER project coordinators for Case 1, set 7

Peak Ground Acceleration (g)	Annual Exceedance Probability						
	Site 1	Site 2	Site 3	Site 4	Site 5	Site 6	Site 7
0.001	**	**	**	1.14E-02	1.14E-02	1.14E-02	**
0.01	**	**	**	1.14E-02	1.14E-02	1.14E-02	**
0.05	**	**	**	1.14E-02	1.03E-02	1.14E-02	**
0.10	**	**	**	1.01E-02	7.65E-03	1.01E-02	**
0.15	**	**	**	8.72E-03	5.66E-03	8.72E-03	**
0.20	**	**	**	7.75E-03	3.50E-03	7.75E-03	**
0.25	**	**	**	6.84E-03	1.40E-03	6.84E-03	**
0.30	**	**	**	5.95E-03	**	5.95E-03	**
0.35	**	**	**	5.06E-03	**	5.06E-03	**
0.40	**	**	**	4.18E-03	**	4.18E-03	**
0.45	**	**	**	3.34E-03	**	3.34E-03	**
0.50	**	**	**	2.56E-03	**	2.56E-03	**
0.55	**	**	**	1.85E-03	**	1.85E-03	**
0.60	**	**	**	1.20E-03	**	1.20E-03	**
0.70	**	**	**	**	**	**	**
0.80	**	**	**	**	**	**	**
0.90	**	**	**	**	**	**	**
1.00	**	**	**	**	**	**	**

** There are no data available for these cases

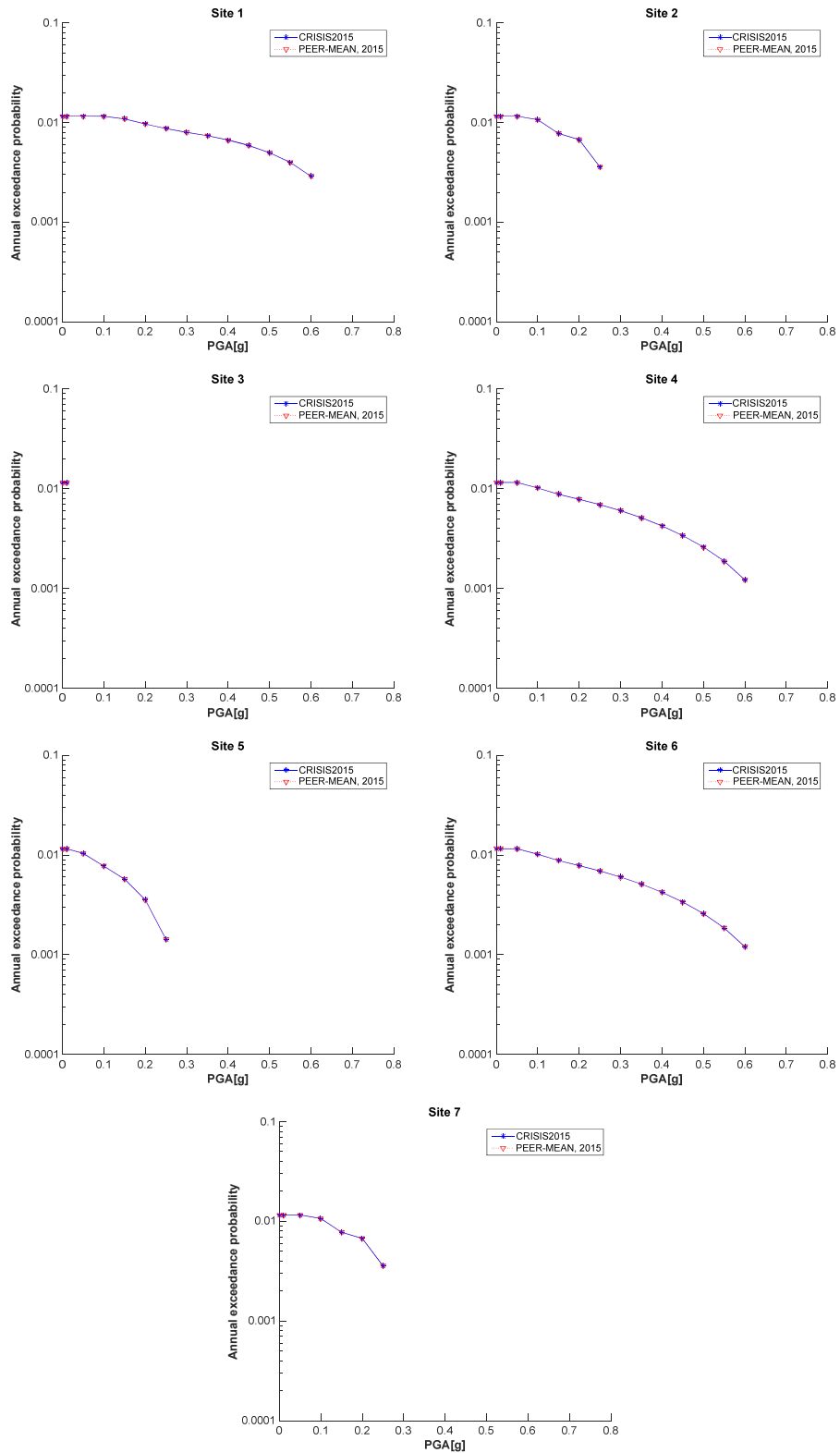


Figure 4-25 Comparison of the CRISIS and PEER-2015 results for Sites 1 to 7 (Set 1 Case 7)

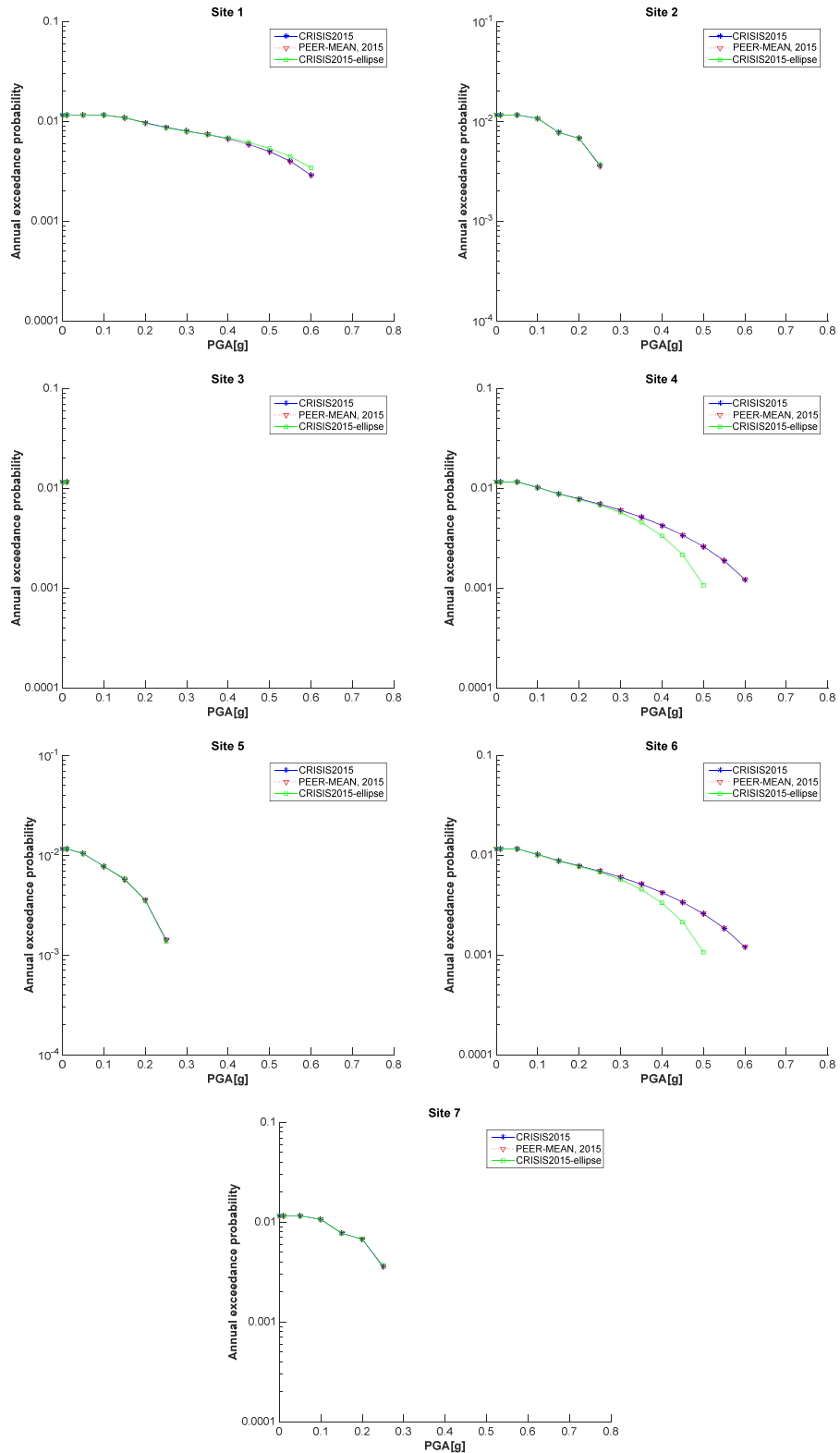


Figure 4-26 Comparison of elliptical and rectangular rupture shapes for PEER-2015 Set 1 Case 7

4.1.12 Set 1 case 8a

Input parameters

Table 4-27 summarizes the input data for case 8a. The computation sites are the same as in previous cases. Case 8a is similar to case 2 with the difference that the ground motion variability is considered as un-truncated herein.

Table 4-27 Summary of input data for Set 1, case 8a

Name	Description	Source	Mag-Density Function	Ground Motion Model ^{1,2}	Rupture Dimension Relationships ^{3,4,5,6}
Set 1 Case 8a	Single rupture smaller than fault plane. Untruncated ground motion variability	Fault 1 (vertical SS) b-value=0.9 Slip rate=2mm/yr.	Delta function at M 6.0	Sadigh et al. (1997), rock. No σ truncation	$Log(A) = M - 4; \sigma_A = 0$ $Log(W) = 0.5 * M - 2.15; \sigma_W = 0$ $Log(L) = 0.5 * M - 1.85; \sigma_L = 0$

¹ Integration over magnitude zero.

² Use magnitude integration step size as small as necessary to model the magnitude density function.

³ For all cases, uniform slip with tapered slip at edges.

⁴ No ruptures are to extend beyond the edge of the fault plane.

⁵ Aspect ratio to be maintained until maximum width is reached, then increase length (maintain area at the expense of aspect ratio).

⁶ Down-dip and along strike integration step size should be as small as necessary for uniform rupture location.

Figure 4-27 shows the R-CRISIS attenuation data screen where the corresponding option has been chosen.

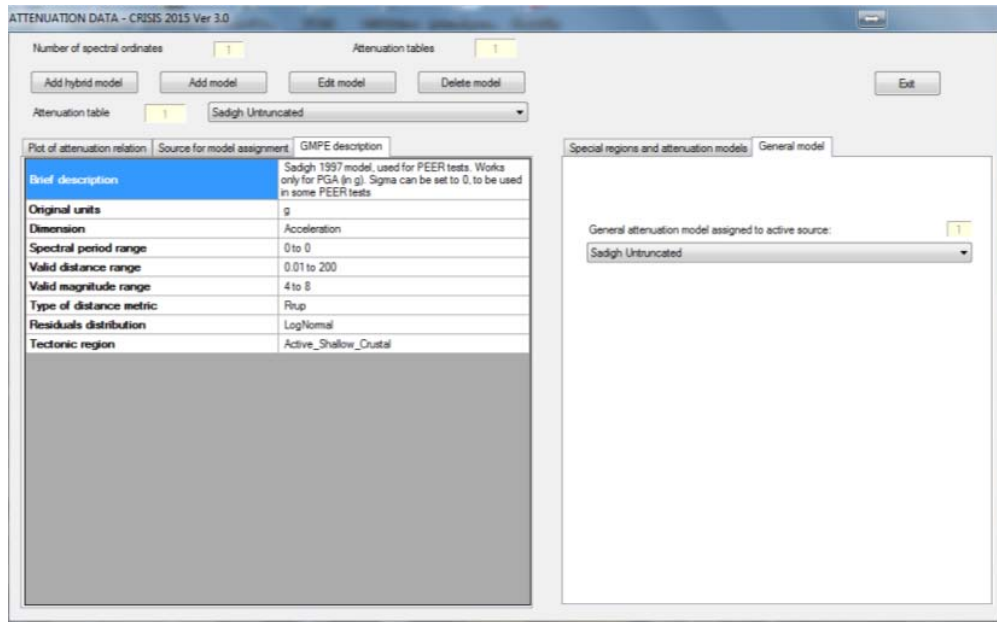


Figure 4-27 Untruncated sigma assignment for Set 1 case 8a of PEER-2015

Results

Results computed in R-CRISIS for set 1, case 8a are shown in Table 4-28 whereas Table 4-29 shows the results provided by the PEER-2015 project. Figure 4-28 shows the hazard plots for the 7 computation sites. In all cases there is a full agreement between the results and therefore, it is possible to conclude that R-CRISIS fulfills all the requirements evaluated by the PEER-2015 project in set 1, case 8a.

Figure 4-29 shows the hazard plots comparing the results obtained with R-CRISIS (elliptical and rectangular options) and the ones provided by the PEER-2015 project. Differences at computation sites 1, 4, 5 and 6 exist for exactly the same reasons explained in section 4.1.2.

Table 4-28 Annual exceedance probabilities obtained in R-CRISIS for Case 1, set 8a

Peak Ground Acceleration (g)	Annual Exceedance Probability						
	Site 1	Site 2	Site 3	Site 4	Site 5	Site 6	Site 7
0.001	1.59E-02	1.59E-02	1.59E-02	1.59E-02	1.59E-02	1.59E-02	1.59E-02
0.01	1.59E-02	1.57E-02	1.59E-02	1.59E-02	1.59E-02	1.59E-02	1.59E-02
0.05	1.59E-02	3.41E-03	1.59E-02	1.54E-02	1.59E-02	1.59E-02	1.59E-02
0.10	1.47E-02	3.18E-04	1.54E-02	1.20E-02	1.54E-02	1.47E-02	1.47E-02
0.15	1.20E-02	4.17E-05	1.41E-02	7.98E-03	1.41E-02	1.20E-02	1.20E-02
0.20	8.94E-03	7.28E-06	1.22E-02	4.99E-03	1.22E-02	8.94E-03	8.94E-03
0.25	6.39E-03	1.58E-06	1.02E-02	3.08E-03	1.02E-02	6.39E-03	6.39E-03
0.30	4.47E-03	4.02E-07	8.40E-03	1.91E-03	8.38E-03	4.47E-03	4.47E-03
0.35	3.10E-03	1.17E-07	6.81E-03	1.19E-03	6.79E-03	3.10E-03	3.10E-03
0.40	2.15E-03	3.77E-08	5.48E-03	7.59E-04	5.46E-03	2.15E-03	2.15E-03
0.45	1.49E-03	1.32E-08	4.40E-03	4.90E-04	4.39E-03	1.49E-03	1.49E-03
0.50	1.04E-03	*	3.53E-03	3.21E-04	3.52E-03	1.04E-03	1.04E-03
0.55	7.36E-04	*	2.84E-03	2.14E-04	2.83E-03	7.36E-04	7.36E-04
0.60	5.22E-04	*	2.29E-03	1.44E-04	2.28E-03	5.22E-04	5.22E-04
0.70	2.70E-04	*	1.50E-03	6.84E-05	1.49E-03	2.70E-04	2.70E-04
0.80	1.44E-04	*	9.91E-04	3.39E-05	9.86E-04	1.44E-04	1.44E-04
0.90	7.91E-05	*	6.66E-04	1.75E-05	6.62E-04	7.91E-05	7.91E-05
1.00	4.47E-05	*	4.54E-04	9.40E-06	4.51E-04	4.47E-05	4.47E-05

* for these cases a value different than zero was computed, however, it was considered by the PEER coordinators as inappropriate for comparative purposes since there are significant differences between the values obtained by the 5 reference codes used to estimate the mean value.

Table 4-29 Annual exceedance probabilities reported as benchmarks by PEER project coordinators for Case 1, set 8a

Peak Ground Acceleration (g)	Annual Exceedance Probability						
	Site 1	Site 2	Site 3	Site 4	Site 5	Site 6	Site 7
0.001	1.59E-02	1.59E-02	1.59E-02	1.59E-02	1.59E-02	1.59E-02	1.59E-02
0.01	1.59E-02	1.59E-02	1.57E-02	1.59E-02	1.59E-02	1.59E-02	1.59E-02
0.05	1.59E-02	1.59E-02	3.41E-03	1.59E-02	1.54E-02	1.59E-02	1.59E-02
0.10	1.59E-02	1.47E-02	3.20E-04	1.54E-02	1.20E-02	1.54E-02	1.47E-02
0.15	1.55E-02	1.20E-02	4.20E-05	1.41E-02	7.97E-03	1.41E-02	1.20E-02
0.20	1.47E-02	8.95E-03	7.34E-06	1.22E-02	4.98E-03	1.22E-02	8.95E-03
0.25	1.36E-02	6.40E-03	1.59E-06	1.02E-02	3.07E-03	1.02E-02	6.40E-03
0.30	1.22E-02	4.47E-03	4.07E-07	8.38E-03	1.90E-03	8.38E-03	4.47E-03
0.35	1.08E-02	3.10E-03	1.18E-07	6.79E-03	1.19E-03	6.79E-03	3.10E-03
0.40	9.43E-03	2.15E-03	3.82E-08	5.46E-03	7.57E-04	5.46E-03	2.15E-03
0.45	8.14E-03	1.50E-03	1.34E-08	4.39E-03	4.89E-04	4.39E-03	1.50E-03
0.50	6.97E-03	1.05E-03	*	3.52E-03	3.20E-04	3.52E-03	1.05E-03
0.55	5.95E-03	7.38E-04	*	2.83E-03	2.13E-04	2.83E-03	7.37E-04
0.60	5.06E-03	5.24E-04	*	2.28E-03	1.44E-04	2.28E-03	5.24E-04
0.70	3.64E-03	2.71E-04	*	1.49E-03	6.82E-05	1.49E-03	2.71E-04
0.80	2.62E-03	1.44E-04	*	9.89E-04	3.39E-05	9.87E-04	1.44E-04
0.90	1.89E-03	7.94E-05	*	6.65E-04	1.75E-05	6.63E-04	7.94E-05
1.00	1.37E-03	4.49E-05	*	4.53E-04	9.38E-06	4.52E-04	4.49E-05

* for these cases a value different than zero was computed, however, it was considered by the PEER coordinators as inappropriate for comparative purposes since there are significant differences between the values obtained by the 5 reference codes used to estimate the mean value.

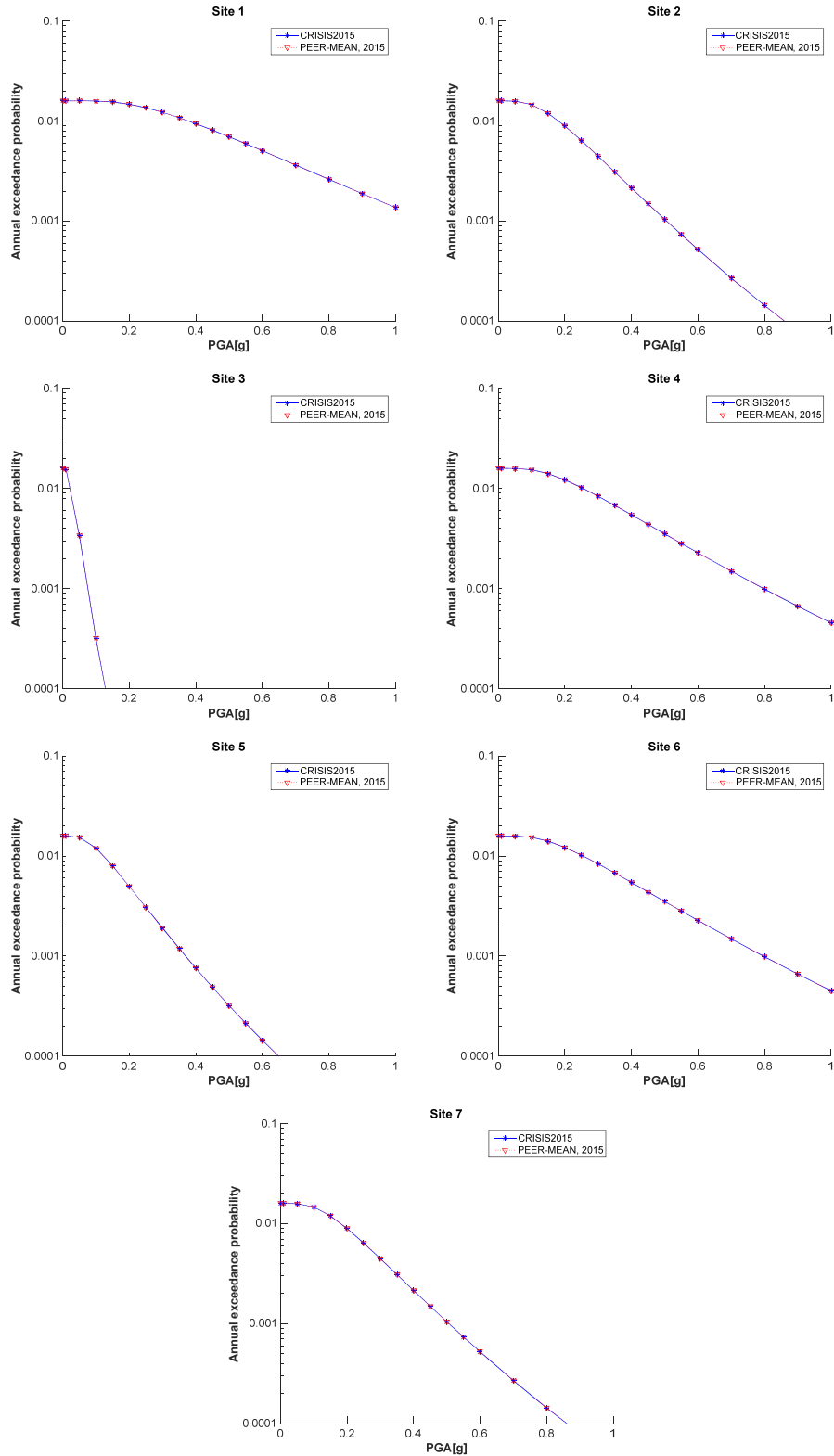


Figure 4-28 Comparison of the CRISIS and PEER-2015 results for Sites 1 to 7 (Set 1 Case 8a)

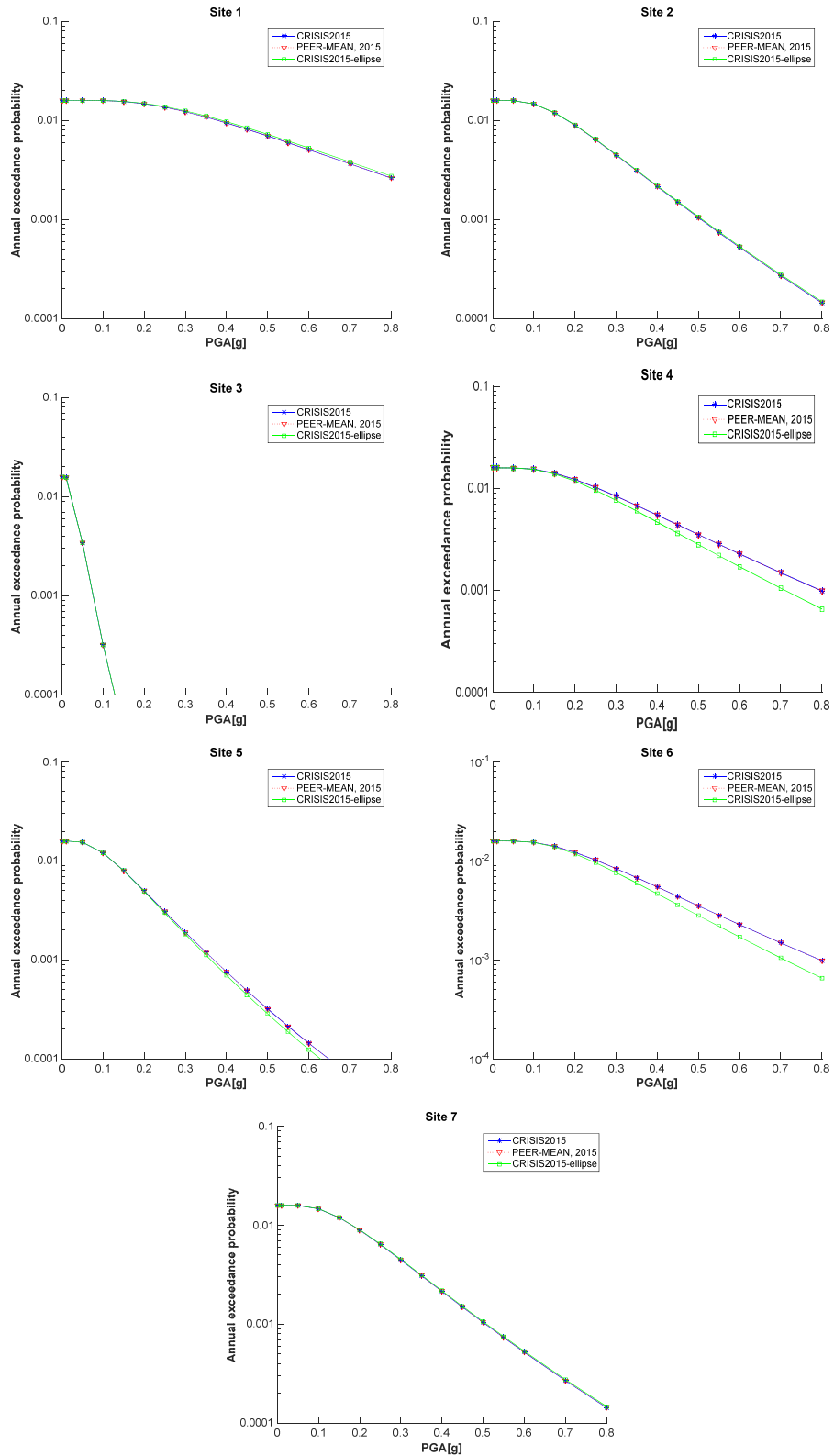


Figure 4-29 Comparison of elliptical and rectangular rupture shapes for PEER-2015 Set 1 Case 8a

4.1.13 Set 1 case 8b

Input parameters

Table 4.30 summarizes the input data for case 8b. The computation sites are the same as in previous cases. Case 8b is similar to case 2 with the difference that the ground motion variability is truncated to 2σ herein.

Table 4-30 Summary of input data for Set 1, case 8b

Name	Description	Source	Mag-Density Function	Ground Motion Model ^{1,2}	Rupture Dimension Relationships ^{3,4,5,6}
Set 1 Case 8b	Single rupture smaller than fault plane. Ground motion variability truncated at 2 sigma	Fault 1(vertical SS) b-value=0.9 Slip rate=2mm/yr.	Delta function at M 6.0	Sadigh et al. (1997), rock. Truncate σ at two standard deviations	$Log(A) = M - 4; \sigma_A = 0$ $Log(W) = 0.5 * M - 2.15; \sigma_W = 0$ $Log(L) = 0.5 * M - 1.85; \sigma_L = 0$

¹ Integration over magnitude zero.

² Use magnitude integration step size as small as necessary to model the magnitude density function.

³ For all cases, uniform slip with tapered slip at edges.

⁴ No ruptures are to extend beyond the edge of the fault plane.

⁵ Aspect ratio to be maintained until maximum width is reached, then increase length (maintain area at the expense of aspect ratio).

⁶ Down-dip and along strike integration step size should be as small as necessary for uniform rupture location.

Results

Results computed in R-CRISIS for set 1, case 8b are shown in Table 4-31 whereas Table 4-32 shows the results provided by the PEER-2015 project. Figure 4-30 shows the hazard plots for the 7 computation sites. In all cases there is a full agreement between the results and therefore, it is possible to conclude that R-CRISIS fulfills all the requirements evaluated by the PEER-2015 project in set 1, case 8b.

Figure 4-31 shows the hazard plots comparing the results obtained with R-CRISIS (elliptical and rectangular options) and the ones provided by the PEER-2015 project. Differences at computation sites 1, 4, 5 and 6 exist for the same reasons explained in section 4.1.2.

Table 4-31 Annual exceedance probabilities obtained in R-CRISIS for Case 1, set 8b

Peak Ground Acceleration (g)	Annual Exceedance Probability						
	Site 1	Site 2	Site 3	Site 4	Site 5	Site 6	Site 7
0.001	1.59E-02	1.59E-02	1.59E-02	1.59E-02	1.59E-02	1.59E-02	1.59E-02
0.01	1.59E-02	1.59E-02	1.56E-02	1.59E-02	1.59E-02	1.59E-02	1.59E-02
0.05	1.59E-02	1.59E-02	3.11E-03	1.59E-02	1.54E-02	1.59E-02	1.59E-02
0.10	1.59E-02	1.46E-02	0.00E+00	1.54E-02	1.19E-02	1.54E-02	1.46E-02
0.15	1.55E-02	1.19E-02	0.00E+00	1.41E-02	7.80E-03	1.41E-02	1.19E-02
0.20	1.47E-02	8.78E-03	0.00E+00	1.22E-02	4.74E-03	1.21E-02	8.78E-03
0.25	1.35E-02	6.17E-03	0.00E+00	1.01E-02	2.78E-03	1.01E-02	6.17E-03
0.30	1.22E-02	4.20E-03	0.00E+00	8.22E-03	1.58E-03	8.21E-03	4.20E-03
0.35	1.07E-02	2.80E-03	0.00E+00	6.59E-03	8.56E-04	6.58E-03	2.80E-03
0.40	9.28E-03	1.82E-03	0.00E+00	5.24E-03	4.49E-04	5.22E-03	1.82E-03
0.45	7.96E-03	1.15E-03	0.00E+00	4.13E-03	2.23E-04	4.12E-03	1.15E-03
0.50	6.77E-03	6.95E-04	0.00E+00	3.24E-03	9.99E-05	3.23E-03	6.95E-04
0.55	5.72E-03	3.79E-04	0.00E+00	2.53E-03	3.65E-05	2.52E-03	3.79E-04
0.60	4.81E-03	1.61E-04	0.00E+00	1.97E-03	8.29E-06	1.96E-03	1.61E-04
0.70	3.35E-03	0.00E+00	0.00E+00	1.17E-03	0.00E+00	1.17E-03	0.00E+00
0.80	2.31E-03	0.00E+00	0.00E+00	6.93E-04	0.00E+00	6.88E-04	0.00E+00
0.90	1.56E-03	0.00E+00	0.00E+00	4.00E-04	0.00E+00	3.97E-04	0.00E+00
1.00	1.03E-03	0.00E+00	0.00E+00	2.24E-04	0.00E+00	2.22E-04	0.00E+00

Table 4-32 Annual exceedance probabilities reported as benchmarks by PEER project coordinators for Case 1, set 8b

Peak Ground Acceleration (g)	Annual Exceedance Probability						
	Site 1	Site 2	Site 3	Site 4	Site 5	Site 6	Site 7
0.001	1.59E-02	1.59E-02	1.59E-02	1.59E-02	1.59E-02	1.59E-02	1.59E-02
0.01	1.59E-02	1.59E-02	1.58E-02	1.59E-02	1.59E-02	1.59E-02	1.59E-02
0.05	1.59E-02	1.59E-02	3.14E-03	1.59E-02	1.56E-02	1.59E-02	1.59E-02
0.10	1.59E-02	1.48E-02	0.00E+00	1.55E-02	1.21E-02	1.55E-02	1.48E-02
0.15	1.56E-02	1.20E-02	0.00E+00	1.42E-02	7.88E-03	1.42E-02	1.20E-02
0.20	1.49E-02	8.89E-03	0.00E+00	1.23E-02	4.78E-03	1.23E-02	8.88E-03
0.25	1.37E-02	6.24E-03	0.00E+00	1.02E-02	2.80E-03	1.02E-02	6.24E-03
0.30	1.23E-02	4.25E-03	0.00E+00	8.31E-03	1.59E-03	8.30E-03	4.25E-03
0.35	1.08E-02	2.83E-03	0.00E+00	6.66E-03	8.64E-04	6.65E-03	2.83E-03
0.40	9.40E-03	1.85E-03	0.00E+00	5.29E-03	4.54E-04	5.28E-03	1.84E-03
0.45	8.06E-03	1.17E-03	0.00E+00	4.17E-03	2.25E-04	4.17E-03	1.17E-03
0.50	6.85E-03	7.04E-04	0.00E+00	3.27E-03	1.01E-04	3.27E-03	7.02E-04
0.55	5.79E-03	3.85E-04	0.00E+00	2.56E-03	3.70E-05	2.55E-03	3.83E-04
0.60	4.87E-03	1.64E-04	0.00E+00	1.99E-03	*	1.98E-03	1.62E-04
0.70	3.40E-03	0.00E+00	0.00E+00	1.19E-03	0.00E+00	1.18E-03	0.00E+00
0.80	2.34E-03	0.00E+00	0.00E+00	7.00E-04	0.00E+00	6.99E-04	0.00E+00
0.90	1.58E-03	0.00E+00	0.00E+00	4.05E-04	0.00E+00	4.05E-04	0.00E+00
1.00	1.04E-03	0.00E+00	0.00E+00	2.27E-04	0.00E+00	2.26E-04	0.00E+00

* for these cases a value different than zero was computed, however, it was considered by the PEER coordinators as inappropriate for comparative purposes since there are significant differences between the values obtained by the 5 reference codes used to estimate the mean value.

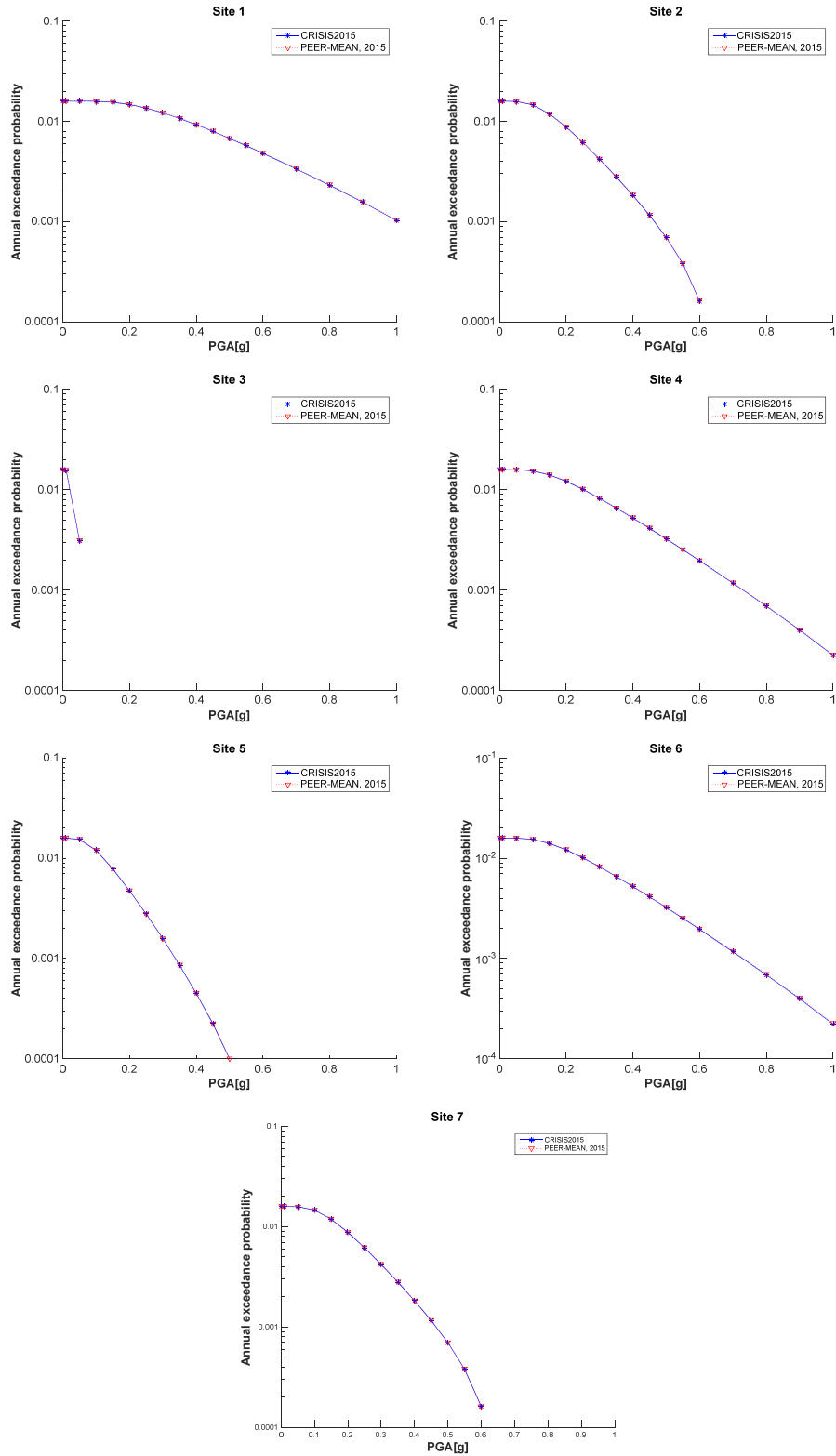


Figure 4-30 Comparison of the CRISIS and PEER-2015 results for Sites 1 to 7 (Set 1 Case 8b)

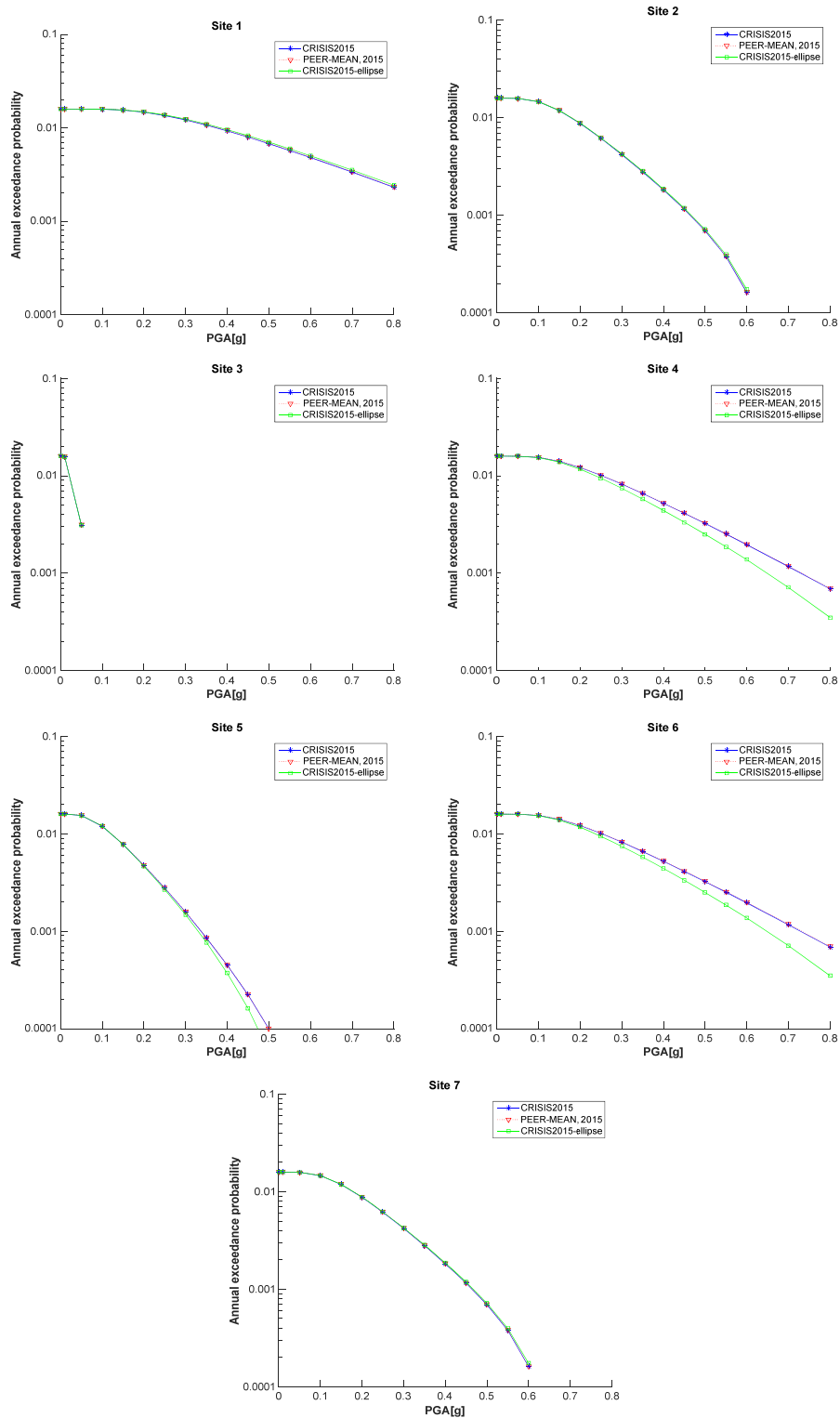


Figure 4-31 Comparison of elliptical and rectangular rupture shapes for PEER-2015 Set 1 Case 8b

4.1.14 Set 1 case 8c

Input parameters

Table 4-33 summarizes the input data for set 1, case 8c. The computation sites are the same as in previous cases. Case 8c is similar to case 2 with the difference that the ground motion variability is truncated to 3σ herein.

Table 4-33 Summary of input data for Set 1, case 8c

Name	Description	Source	Mag-Density Function	Ground Motion Model ^{1,2}	Rupture Dimension Relationships ^{3,4,5,6}
Set 1 Case 8c	Single rupture smaller than fault plane. Ground motion variability truncated at 3 sigma	Fault 1 (vertical SS) b-value=0.9 Slip rate=2mm/yr.	Delta function at M 6.0	Sadigh et al. (1997), rock. Truncate σ at three standard deviations	$Log(A) = M - 4; \sigma_A = 0$ $Log(W) = 0.5 * M - 2.15; \sigma_W = 0$ $Log(L) = 0.5 * M - 1.85; \sigma_L = 0$

¹ Integration over magnitude zero.

² Use magnitude integration step size as small as necessary to model the magnitude density function.

³ For all cases, uniform slip with tapered slip at edges.

⁴ No ruptures are to extend beyond the edge of the fault plane.

⁵ Aspect ratio to be maintained until maximum width is reached, then increase length (maintain area at the expense of aspect ratio).

⁶ Down-dip and along strike integration step size should be as small as necessary for uniform rupture location.

Results

Results computed in R-CRISIS for set 1, case 8c are shown in Table 4-34 whereas Table 4-35 shows the results provided by the PEER-2015 project. Figure 4-32 shows the hazard plots for the 7 computation sites. In all cases there is a full agreement between the results and therefore, it is possible to conclude that R-CRISIS fulfills all the requirements evaluated by the PEER-2015 project in set 1, case 8c.

Figure 4-33 shows the hazard plots comparing the results obtained with R-CRISIS (elliptical and rectangular options) and the ones provided by the PEER-2015 project. Differences at computation sites 1, 4, 5 and 6 exist for exactly the same reasons explained in section 4.1.2.

Table 4-34 Annual exceedance probabilities obtained in R-CRISIS for Case 1, set 8c

Peak Ground Acceleration (g)	Annual Exceedance Probability						
	Site 1	Site 2	Site 3	Site 4	Site 5	Site 6	Site 7
0.001	1.59E-02	1.59E-02	1.59E-02	1.59E-02	1.59E-02	1.59E-02	1.59E-02
0.01	1.59E-02	1.59E-02	1.57E-02	1.59E-02	1.59E-02	1.59E-02	1.59E-02
0.05	1.59E-02	1.59E-02	3.39E-03	1.59E-02	1.54E-02	1.59E-02	1.59E-02
0.10	1.59E-02	1.47E-02	2.97E-04	1.54E-02	1.20E-02	1.54E-02	1.47E-02
0.15	1.55E-02	1.19E-02	2.00E-05	1.41E-02	7.97E-03	1.41E-02	1.19E-02
0.20	1.47E-02	8.93E-03	0.00E+00	1.22E-02	4.98E-03	1.22E-02	8.93E-03
0.25	1.36E-02	6.38E-03	0.00E+00	1.02E-02	3.06E-03	1.02E-02	6.38E-03
0.30	1.22E-02	4.45E-03	0.00E+00	8.39E-03	1.89E-03	8.37E-03	4.45E-03
0.35	1.08E-02	3.08E-03	0.00E+00	6.79E-03	1.17E-03	6.78E-03	3.08E-03
0.40	9.42E-03	2.13E-03	0.00E+00	5.47E-03	7.38E-04	5.45E-03	2.13E-03
0.45	8.13E-03	1.47E-03	0.00E+00	4.38E-03	4.69E-04	4.37E-03	1.47E-03
0.50	6.96E-03	1.02E-03	0.00E+00	3.52E-03	3.00E-04	3.50E-03	1.02E-03
0.55	5.94E-03	7.15E-04	0.00E+00	2.82E-03	1.92E-04	2.81E-03	7.15E-04
0.60	5.05E-03	5.01E-04	0.00E+00	2.27E-03	1.23E-04	2.26E-03	5.01E-04
0.70	3.63E-03	2.49E-04	0.00E+00	1.48E-03	5.03E-05	1.47E-03	2.49E-04
0.80	2.60E-03	1.22E-04	0.00E+00	9.71E-04	1.96E-05	9.66E-04	1.22E-04
0.90	1.87E-03	5.75E-05	0.00E+00	6.45E-04	6.64E-06	6.42E-04	5.75E-05
1.00	1.35E-03	2.31E-05	0.00E+00	4.33E-04	1.58E-06	4.30E-04	2.31E-05

Table 4-35 Annual exceedance probabilities reported as benchmarks by PEER project coordinators for Case 1, set 8c

Peak Ground Acceleration (g)	Annual Exceedance Probability						
	Site 1	Site 2	Site 3	Site 4	Site 5	Site 6	Site 7
0.001	1.59E-02	1.59E-02	1.59E-02	1.59E-02	1.59E-02	1.59E-02	1.59E-02
0.01	1.59E-02	1.59E-02	1.57E-02	1.59E-02	1.59E-02	1.59E-02	1.59E-02
0.05	1.59E-02	1.59E-02	3.40E-03	1.59E-02	1.54E-02	1.59E-02	1.59E-02
0.10	1.59E-02	1.47E-02	2.99E-04	1.54E-02	1.20E-02	1.54E-02	1.47E-02
0.15	1.55E-02	1.20E-02	2.03E-05	1.41E-02	7.96E-03	1.41E-02	1.20E-02
0.20	1.47E-02	8.95E-03	0.00E+00	1.22E-02	4.97E-03	1.22E-02	8.95E-03
0.25	1.36E-02	6.39E-03	0.00E+00	1.02E-02	3.05E-03	1.02E-02	6.39E-03
0.30	1.22E-02	4.46E-03	0.00E+00	8.38E-03	1.88E-03	8.37E-03	4.46E-03
0.35	1.08E-02	3.09E-03	0.00E+00	6.78E-03	1.17E-03	6.78E-03	3.09E-03
0.40	9.43E-03	2.13E-03	0.00E+00	5.46E-03	7.37E-04	5.45E-03	2.13E-03
0.45	8.13E-03	1.48E-03	0.00E+00	4.38E-03	4.68E-04	4.37E-03	1.48E-03
0.50	6.97E-03	1.03E-03	0.00E+00	3.51E-03	2.99E-04	3.50E-03	1.03E-03
0.55	5.94E-03	7.17E-04	0.00E+00	2.82E-03	1.92E-04	2.81E-03	7.17E-04
0.60	5.05E-03	5.03E-04	0.00E+00	2.26E-03	1.23E-04	2.26E-03	5.03E-04
0.70	3.63E-03	2.50E-04	0.00E+00	1.47E-03	5.02E-05	1.47E-03	2.50E-04
0.80	2.60E-03	1.23E-04	0.00E+00	9.69E-04	1.95E-05	9.67E-04	1.23E-04
0.90	1.87E-03	5.78E-05	0.00E+00	6.44E-04	6.62E-06	6.43E-04	5.78E-05
1.00	1.35E-03	2.32E-05	0.00E+00	4.32E-04	1.58E-06	4.31E-04	2.32E-05

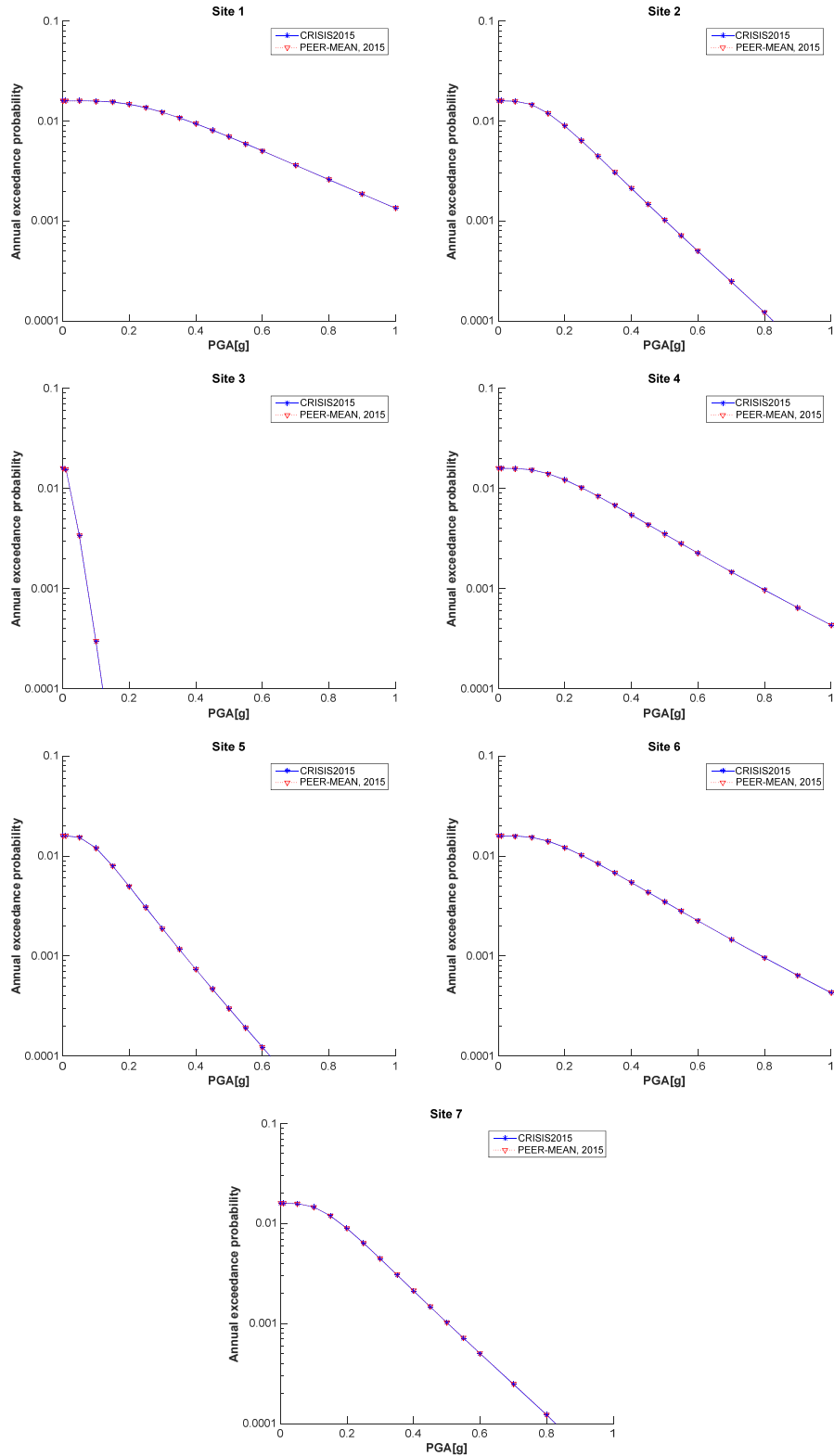


Figure 4-32 Comparison of the CRISIS and PEER-2015 results for Sites 1 to 7 (Set 1 Case 8c)

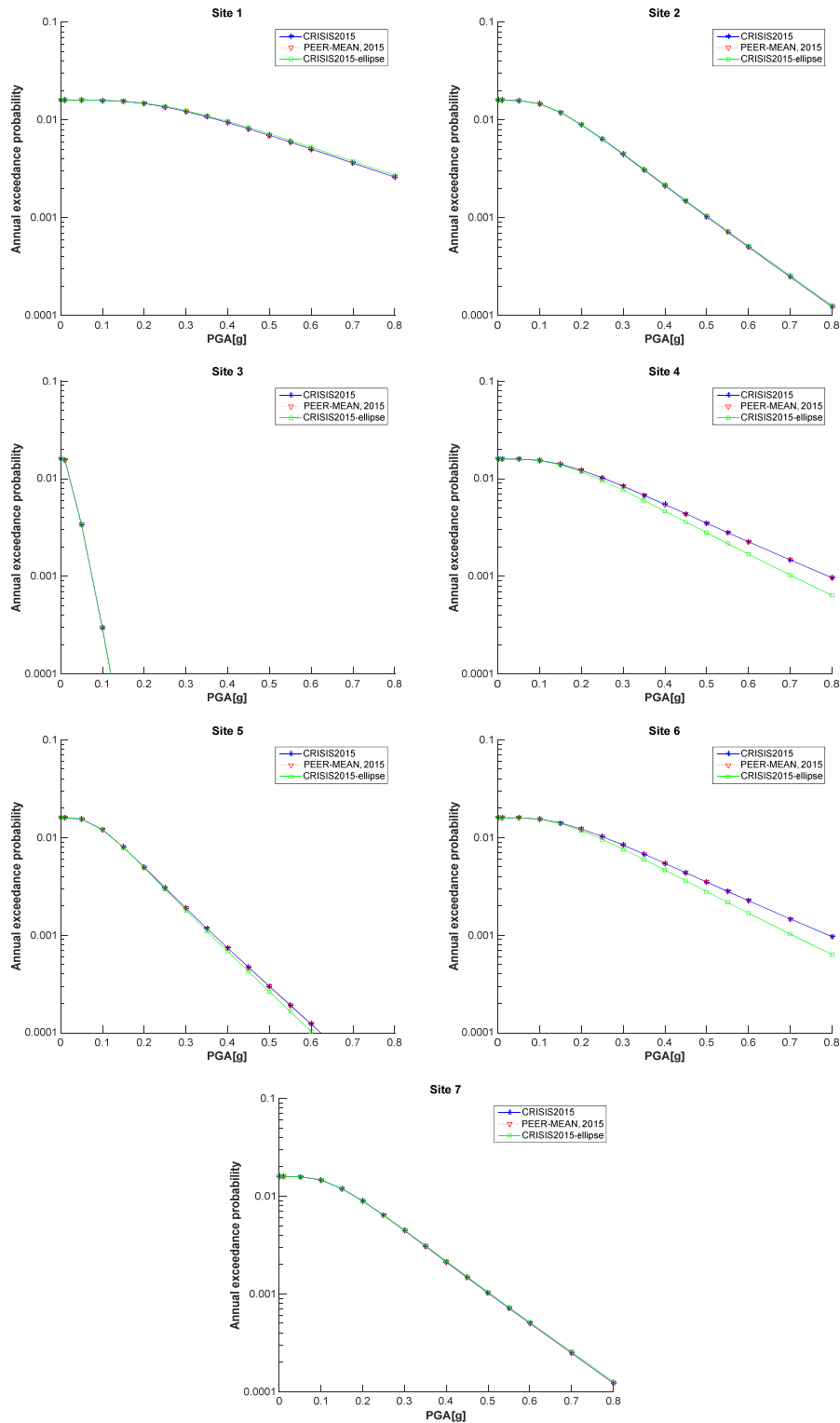


Figure 4-33 Comparison of elliptical and rectangular rupture shapes for PEER-2015 Set 1 Case 8c

4.1.15 Set 1 case 9

As for the three variations of case 8, the tests of case 9 aim at evaluating the computation of ground motion attenuation in the code. In these cases a dipping fault is used instead of a vertical fault and different GMPM are used. This test has not been performed since the handling of ground motion relations and their variability by the R-CRISIS code has already been shown to be satisfactory.

4.1.16 Set 1 case 10

Input parameters

The source adopted is the circular area source (Figure 4-2) with a constant depth of 5km. The seismicity was modeled assuming a b -value=0.9 and a seismicity rate, λ , (i.e. the annual number of earthquakes with magnitude $M \geq M_{min}$) of 0.0395. The magnitude density function is a truncated exponential with $M_{min}=5.0$ and $M_{max}=6.5$. For this test, PEER suggests adopting point sub-sources as shown in Table 4-36.

Figure 4-34 shows the geometry data screen of R-CRISIS with the parameters that were used herein, whereas, Figure 4-35 shows the seismicity data screen of R-CRISIS with the assigned parameters for this particular case.

Table 4-36 Summary of input data for Set 1, case 10

Name	Description	Source	Mag-Density Function	Ground Motion Model ^{1,2}	Rupture Dimension Relationships ^{3,4,5,6}
Set 1 Case 10	Area source with fixed depth of 5km	Area 1 $N(M \geq 5) = 0.0395$, b-value=0.9	Truncated exponential, $M_{max}=6.5$, $M_{min}=5.0$	Sadigh et al. (1997), rock	Use 1km grid spacing of point sources or small faults to simulate a uniform distribution

¹ Integration over magnitude zero.

² Use magnitude integration step size as small as necessary to model the magnitude density function.

³ For all cases, uniform slip with tapered slip at edges.

⁴ No ruptures are to extend beyond the edge of the fault plane.

⁵ Aspect ratio to be maintained until maximum width is reached, then increase length (maintain area at the expense of aspect ratio).

⁶ Down-dip and along strike integration step size should be as small as necessary for uniform rupture location.

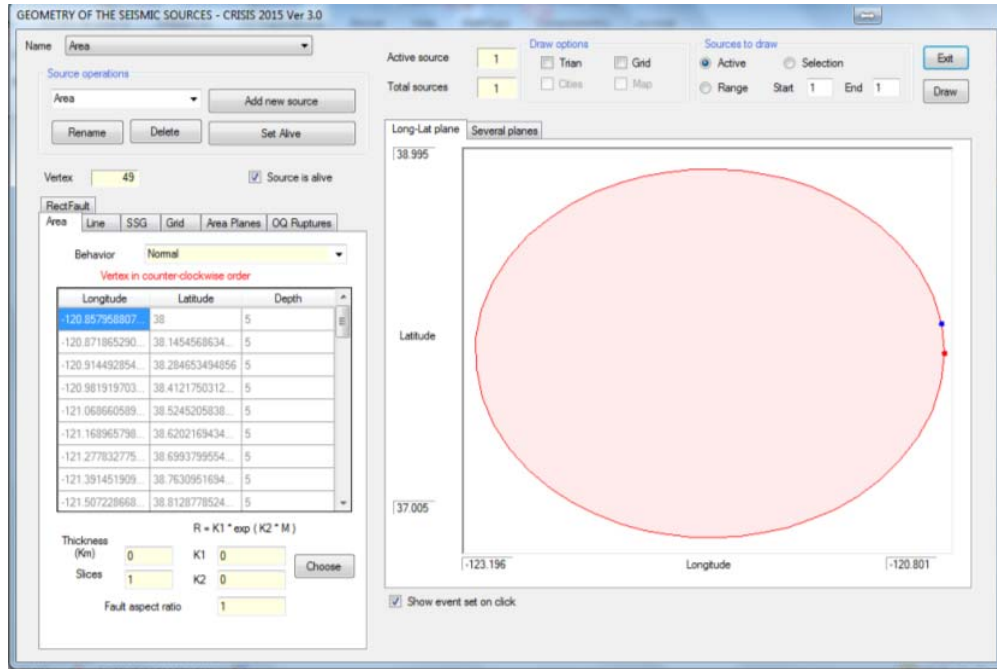


Figure 4-34 Geometry data for area source in set 1, case 10

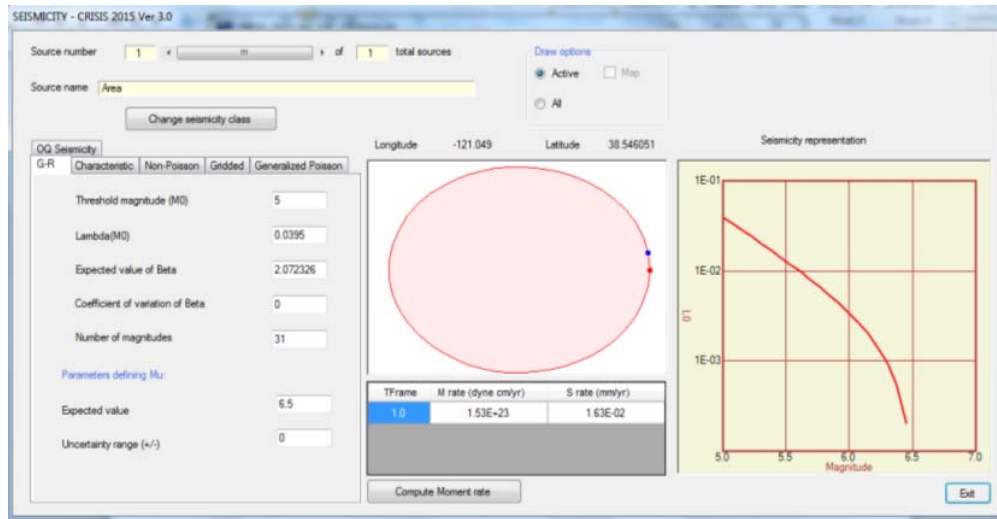


Figure 4-35 Seismicity parameters assigned in R-CRISIS for set 1, case 10

Note: the area source for this case is circular although, due to its location and the datum R-CRISIS uses, is displayed as elliptical.

The coordinates for the computation sites are shown in Table 4-37.

Table 4-37 Coordinates and comments of the computation sites for the area source



Site	Latitude	Longitude	Comment
1	38.000	-122.000	At center of area
2	37.550	-122.000	50 km from center (radially)
3	37.099	-122.000	On area boundary
4	36.874	-122.000	25 km from boundary

Results

Results computed in R-CRISIS for Set 1-Case 10 are shown in Table 4-38 whereas Table 4-39 shows the results provided by the PEER-2015 project. Figure 4-36 shows the hazard plots for the 4 computation sites. In all cases there is a full agreement between the results and therefore, it is possible to conclude that CRISIS fulfills all the requirements evaluated by the PEER-2015 project in Set 1-Case 10.

Table 4-38 Annual exceedance probabilities obtained in R-CRISIS for Case 1, set 10

Peak Ground Acceleration (g)	Annual Exceedance Probability			
	Site 1	Site 2	Site 3	Site 4
0.001	3.87E-02	3.87E-02	3.87E-02	3.82E-02
0.01	2.19E-02	1.82E-02	9.33E-03	5.33E-03
0.05	2.96E-03	2.96E-03	1.37E-03	1.21E-04
0.10	9.20E-04	9.20E-04	4.35E-04	1.40E-06
0.15	3.60E-04	3.60E-04	1.71E-04	0.00E+00
0.20	1.32E-04	1.32E-04	6.23E-05	0.00E+00
0.25	4.71E-05	4.71E-05	2.22E-05	0.00E+00
0.30	1.68E-05	1.69E-05	7.91E-06	0.00E+00
0.35	5.38E-06	5.38E-06	2.50E-06	0.00E+00
0.40	1.21E-06	1.21E-06	5.48E-07	0.00E+00
0.45	*	*	2.33E-08	0.00E+00
0.50	0.00E+00	0.00E+00	0.00E+00	0.00E+00
0.55	0.00E+00	0.00E+00	0.00E+00	0.00E+00
0.60	0.00E+00	0.00E+00	0.00E+00	0.00E+00
0.70	0.00E+00	0.00E+00	0.00E+00	0.00E+00
0.80	0.00E+00	0.00E+00	0.00E+00	0.00E+00
0.90	0.00E+00	0.00E+00	0.00E+00	0.00E+00
1.00	0.00E+00	0.00E+00	0.00E+00	0.00E+00

* for these cases a value different than zero was computed, however, it was considered by the PEER coordinators as inappropriate for comparative purposes since there are significant differences between the values obtained by the 5 reference codes used to estimate the mean value.

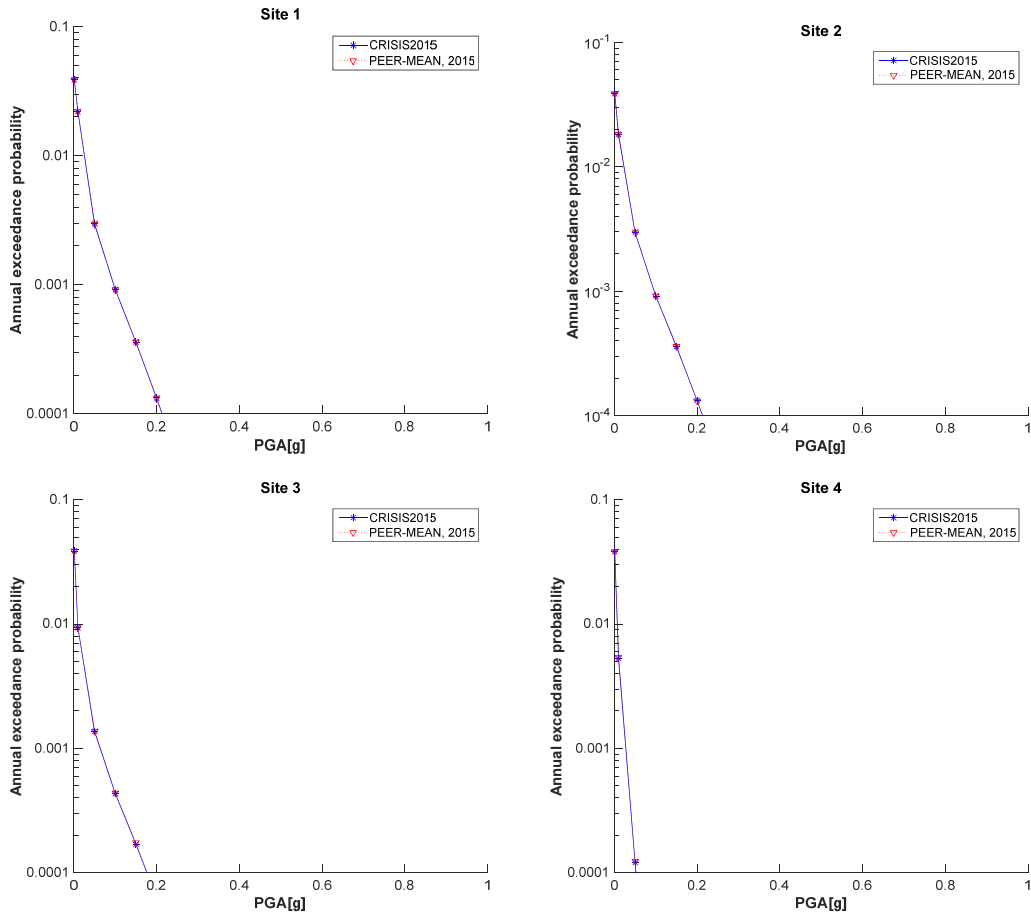


Figure 4-36 Comparison of the CRISIS and PEER-2015 results for Sites 1 to 4 (Set 1 Case 10)

4.1.17 Set 1 case 11

Input parameters

The source adopted is volume source with the shape of the area source of case 10 and a depth between 5 and 10km. In CRISIS the volume source was modelled by 6 area sources with the same coordinates of the original area source and at different depths (spaced at 1km, coherently with the prescriptions of PEER described in Table 4-39).

Figure 4-37 shows the geometry data screen of R-CRISIS with the parameters that were used herein (slices).

Table 4-39 Summary of input data for Set 1, case 11

Name	Description	Source	Mag-Density Function	Ground Motion Model ^{1,2}	Rupture Dimension Relationships ^{3,4,5,6}
Set 1 Case 11	Volume source with depth of 5km to 10km	Area 1 $N(M \geq 5) = 0.0395$, $b\text{-value} = 0.9$	Truncated exponential, $M_{max} = 6.5$, $M_{min} = 5.0$	Sadigh et al. (1997), rock	Use 1km grid spacing of point sources or small faults to simulate a uniform distribution. For the depth distribution a 1km spacing was used including 5 and 10km

¹ Integration over magnitude zero.

² Use magnitude integration step size as small as necessary to model the magnitude density function.

³ For all cases, uniform slip with tapered slip at edges.

⁴ No ruptures are to extend beyond the edge of the fault plane.

⁵ Aspect ratio to be maintained until maximum width is reached, then increase length (maintain area at the expense of aspect ratio).

⁶ Down-dip and along strike integration step size should be as small as necessary for uniform rupture location.

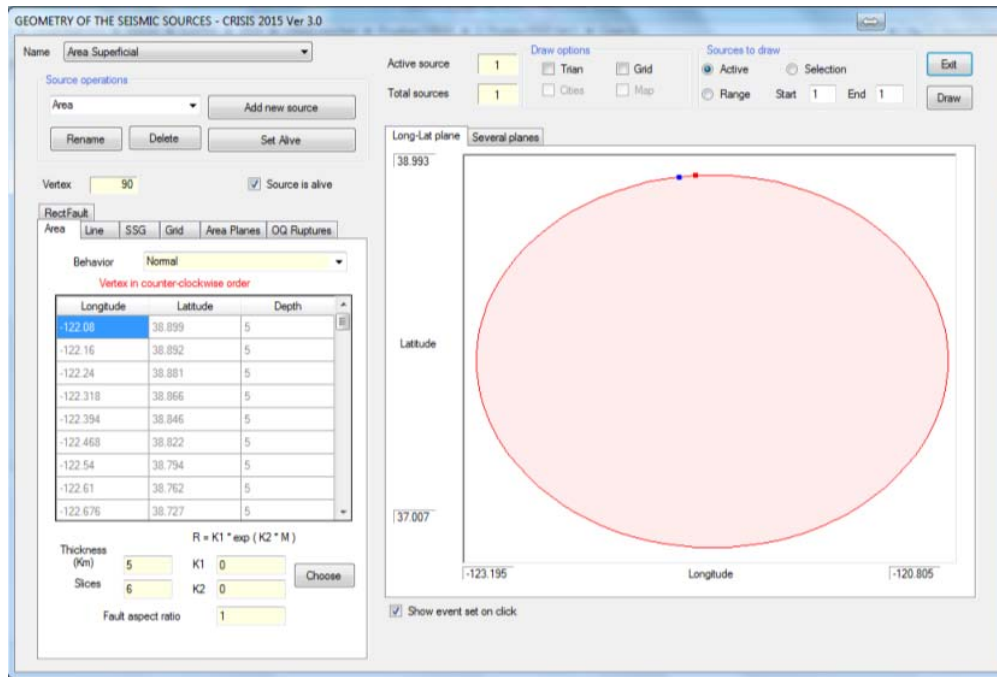


Figure 4-37 Geometry data for area source in set 1, case 11

Each slice is considered as an individual source and is modelled in R-CRISIS with a modified G-R seismicity model with $b\text{-value} = 0.9$ and a seismicity rate $\lambda = 0.0395/6$. As in set 1, case 10, the magnitude density function is a truncated exponential with $M_{min} = 5.0$ and $M_{max} = 6.5$.

Results

Results computed in R-CRISIS for Set 1-Case 11 are shown in Table 4-40 whereas Table 4-41 shows the results provided by the PEER-2015 project. Figure 4-38 shows the hazard plots for the 4 computation sites. In all cases there is a full agreement between the results and

therefore, it is possible to conclude that CRISIS fulfills all the requirements evaluated by the PEER-2015 project in set 1, case 11.

Table 4-40 Annual exceedance probabilities obtained in R-CRISIS for Case 1, set 11

Peak Ground Acceleration (g)	Annual Exceedance Probability			
	Site 1	Site 2	Site 3	Site 4
0.001	3.87E-02	3.83E-02	3.66E-02	3.50E-02
0.01	2.28E-02	1.91E-02	1.08E-02	6.81E-03
0.05	3.97E-03	3.86E-03	1.79E-03	4.50E-04
0.10	1.35E-03	1.35E-03	6.32E-04	6.44E-05
0.15	6.29E-04	6.29E-04	2.98E-04	1.44E-05
0.20	3.34E-04	3.34E-04	1.59E-04	4.04E-06
0.25	1.91E-04	1.91E-04	9.17E-05	1.33E-06
0.30	1.16E-04	1.16E-04	5.56E-05	4.90E-07
0.35	7.28E-05	7.28E-05	3.51E-05	1.98E-07
0.40	4.73E-05	4.73E-05	2.28E-05	8.59E-08
0.45	0.0000315	0.0000315	1.52E-05	3.97E-08
0.50	2.14E-05	2.14E-05	1.04E-05	1.93E-08
0.55	1.49E-05	1.49E-05	7.20E-06	9.83E-09
0.60	1.05E-05	1.05E-05	5.09E-06	5.20E-09
0.70	5.45E-06	5.45E-06	2.64E-06	1.61E-09
0.80	2.97E-06	2.97E-06	1.44E-06	5.58E-10
0.90	1.69E-06	1.69E-06	8.20E-07	2.10E-10
1.00	9.91E-07	9.91E-07	4.82E-07	8.54E-11

Table 4-41 Annual exceedance probabilities reported as benchmarks by PEER project coordinators for Case 1, set 11

Peak Ground Acceleration (g)	Annual Exceedance Probability			
	Site 1	Site 2	Site 3	Site 4
0.001	3.87E-02	3.83E-02	3.66E-02	3.49E-02
0.01	2.26E-02	1.90E-02	1.08E-02	6.79E-03
0.05	3.92E-03	3.82E-03	1.78E-03	4.49E-04
0.10	1.34E-03	1.33E-03	6.26E-04	6.46E-05
0.15	6.22E-04	6.21E-04	2.95E-04	1.44E-05
0.20	3.30E-04	3.30E-04	1.58E-04	4.08E-06
0.25	1.89E-04	1.89E-04	9.08E-05	1.35E-06
0.30	1.14E-04	1.14E-04	5.51E-05	4.98E-07
0.35	7.20E-05	7.20E-05	3.47E-05	2.02E-07
0.40	4.67E-05	4.67E-05	2.26E-05	8.79E-08
0.45	0.0000311	0.0000311	1.51E-05	4.07E-08
0.50	2.12E-05	2.12E-05	1.03E-05	1.98E-08
0.55	1.47E-05	1.47E-05	7.13E-06	1.01E-08
0.60	1.04E-05	1.04E-05	5.03E-06	5.36E-09
0.70	5.38E-06	5.38E-06	2.62E-06	1.66E-09
0.80	2.93E-06	2.93E-06	1.43E-06	5.74E-10
0.90	1.67E-06	1.67E-06	8.11E-07	2.15E-10
1.00	9.79E-07	9.79E-07	4.77E-07	8.56E-11

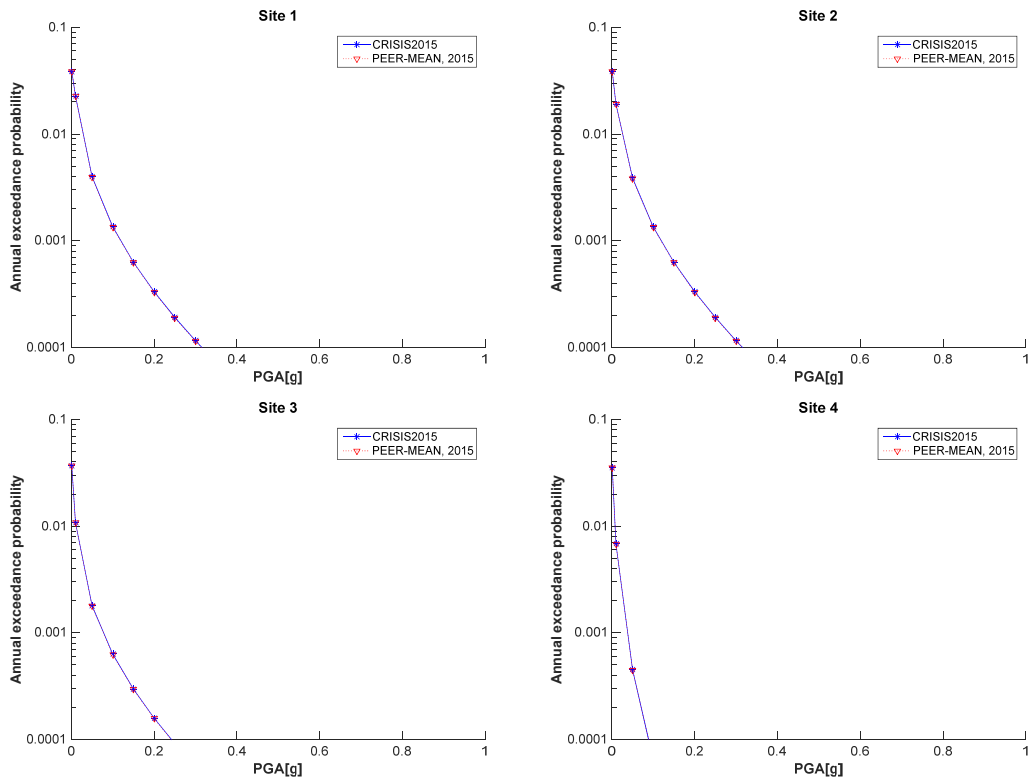


Figure 4-38 Comparison of the CRISIS and PEER-2015 results for Sites 1 to 4 (Set 1 Case 11)

4.1.18 Comments about the computation of distances

In the instructions provided by the PEER-2015 project the coordinates to generate each fault were included together with those of each computation site. Before showing the results of the validation and verification process, it is important to check the way in which R-CRISIS calculates the distance between two points and how it compares with the benchmark. Table 4-42 shows the distance computed by R-CRISIS for computation sites 1 and 2 of the Set 1 from where a slight difference can be seen.

Table 4-42 Real distance computed by R-CRISIS with the PEER project coordinates

Site	Latitude (degrees)	Longitude (degrees)	Distance between sites 1 and 2	
			Considered by PEER-2015 project	Computed by CRISIS2015
1	38.000*	-122.000*	25 km*	24.9798 km**
2	38.2248*	-122.000*		

To reach the same 25km distance between the two sites in R-CRISIS, small differences in the coordinates are needed as shown in Table 4-43.

Table 4-43 Adjustment on coordinates to estimate the same real distance in R-CRISIS

Site	Latitude (degrees)	Longitude (degrees)	Distance between sites 1 and 2
			Computed by CRISIS2015
1	38.000	-122.000	25.002 km
2	38.225	-122.000	

Seismic hazard calculations were made using both coordinates' values and no differences were obtained in the final results.

4.2 PEER validation tests (set 2)

A second phase of the PEER validation project was finished in 2018 (Hale et al., 2018). Among the PSHA tools, R-CRISIS was included. This second phase considered more complicated cases (e.g. multiple sources, the handling of state-of-the-art GMPMs – NGA West2 – and the modelling of complex intraslab sources) and again, the results obtained by R-CRISIS were compared against those provided as benchmark. As can be seen with detail in this section, the results obtained in R-CRISIS are highly satisfactory.

4.2.1 Set 2 case 1

Input parameters

Three different sources are used in this case, being two of them fault sources and the other an area source with constant depth as shown in Figure 4-39. The objective of this test is to review the estimation of hazard from multiple sources and to perform a disaggregation on the magnitude, distance and epsilon values. GMPE is set to Sadigh et al. (1997) for rock

conditions and untruncated σ . Details of the characteristics of the faults together with the magnitude density functions parameters are shown in Table 4-44.

Tables 4-45 and 4-46 show the geometry data associated to the fault sources whereas Table 4-47 includes the coordinates of the computation site together with the explanation of its relevance for the validation and verification purposes.

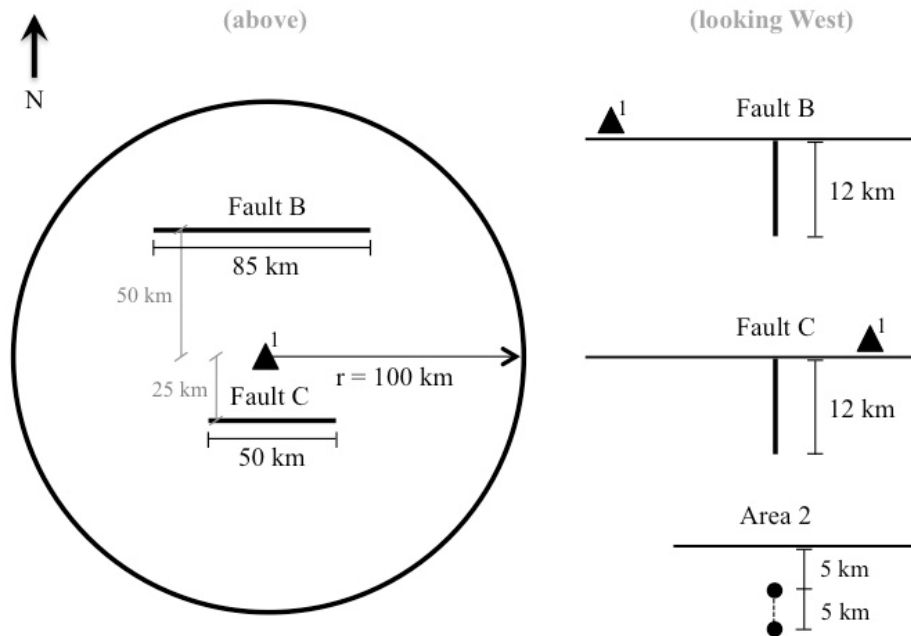


Figure 4-39 Geometry of the fault sources, the area source and the location of the observation size for Set 2, case 1

Table 4-44 Summary of input data for Set 2, case 1

Name	Description	Source	Mag-Density Function	Ground Motion Model	Rupture Dimension Relationships
Set 2 Case 1	Two faults and area source. Computation of hazard from multiple sources and M , R , ϵ disaggregation. Ground motion variability, untruncated σ	Area 2 b-value=0.9	Truncated exponential, $M_{max}=6.5$, $M_{min}=5.0$	Sadigh et al. (1997), rock, untruncated σ	$Log(A) = M - 4; \sigma_A = 0$ $Log(W) = 0.5 * M - 2.15; \sigma_W = 0$ $Log(L) = 0.5 * M - 1.85; \sigma_L = 0$
		Fault B (vertical SS) b-value=0.9 slip-rate 2mm/yr	Y&C Model. $M_{max}=7.0$, $M_{min}=5.0$, $M_{char}=6.75$		
		Fault C (vertical SS) b-value=0.9 slip-rate 1 mm/yr	Y&C Model. $M_{max}=6.75$, $M_{min}=5.0$, $M_{char}=6.5$		

Table 4-45 Coordinates of the fault source B

Latitude	Longitude	Comment
0.44966	-65.3822	West end of fault
0.44966	-64.6178	East end of fault

Table 4-46 Coordinates of the fault source C

Latitude	Longitude	Comment
-0.22483	-65.2248	West end of fault
-0.22483	-64.7752	East end of fault

Table 4-47 Coordinates and comments of the computation site for set 2 case 1

Site	Latitude	Longitude	Comment
1	0.00000	-65.00000	In center of area source

Results

Results obtained in R-CRISIS for the estimation of seismic hazard from multiple sources at Site 1 are shown in Figure 4-40 together with the comparison against the benchmark values provided by PEER. From the plot it can be seen a complete agreement between the results obtained by R-CRISIS and those provided by PEER. Because of that, it can be concluded that R-CRISIS fulfills all the requirements evaluated by the PEER project in Set2-Case1.

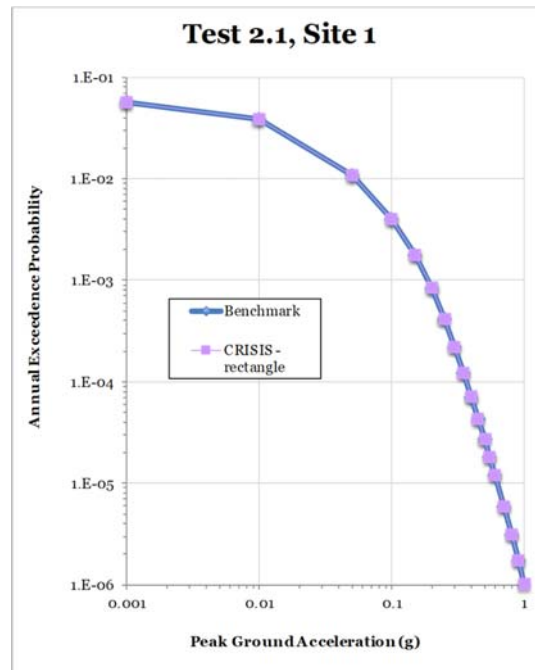


Figure 4-40 Comparison of the CRISIS and PEER results for site 1 (set 2 case 1)

In addition, Figures 4-41 to 4-43 show the comparison of the disaggregation results obtained by R-CRISIS and those provided as benchmark by PEER. The disaggregation was made for the following cases:

- a) PGA 0.05g
- b) PGA corresponding to a hazard of 0.001
- c) PGA 0.35g

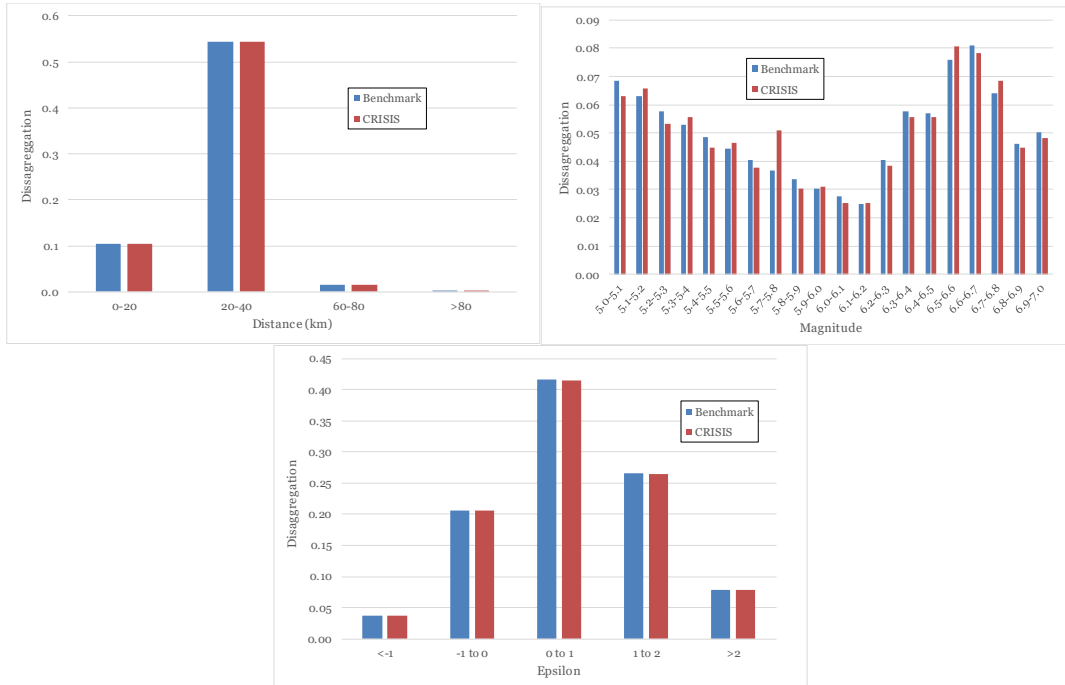


Figure 4-41 Comparison of the disaggregation results of CRISIS and PEER by distance (top left), magnitude (top right) and epsilon (bottom). PGA – 0.05g

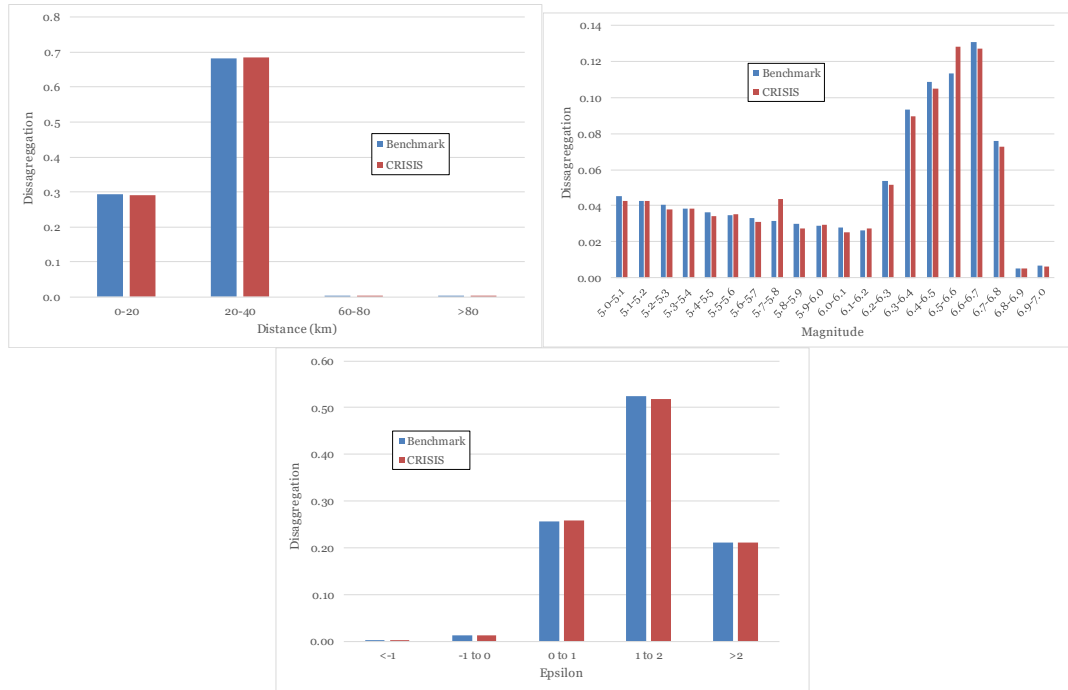


Figure 4-42 Comparison of the disaggregation results of CRISIS and PEER by distance (top left), magnitude (top right) and epsilon (bottom). PGA corresponding to a hazard of 0.001

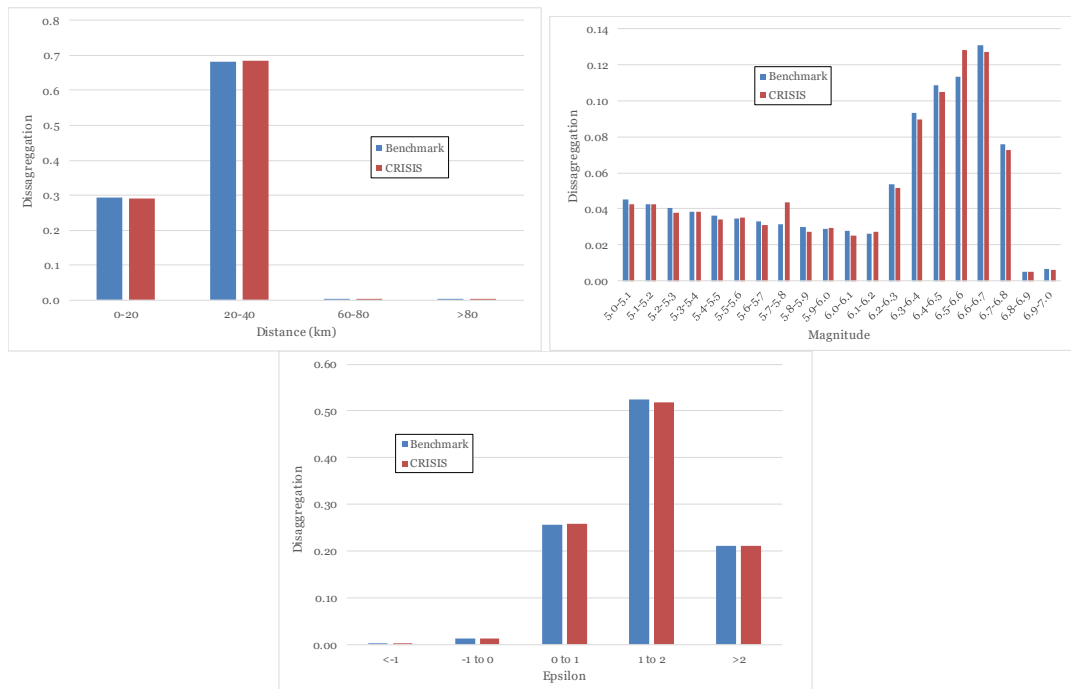


Figure 4-43 Comparison of the disaggregation results of CRISIS and PEER by distance (top left), magnitude (top right) and epsilon (bottom). PGA – 0.35g

4.2.2 Set 2 case 2

Input parameters

The source adopted for this case corresponds to fault 3 (see Figure 4-44). Seismicity input is specified through a b-value of 0.9, a slip rate of 2mm/yr and a magnitude density function in the form of a truncated exponential relationship with the minimum and magnitude values shown in Table 4-48. The objective of this test is to evaluate the handling of NGA-West2 ground-motion models (considering variability) for a source with strike-slip faulting mechanism.

Table 4-49 shows the data associated to the geometry of the fault source whereas Table 4-50 includes the coordinates of the computation sites together with an explanation about its relevance for validation and verification purposes.

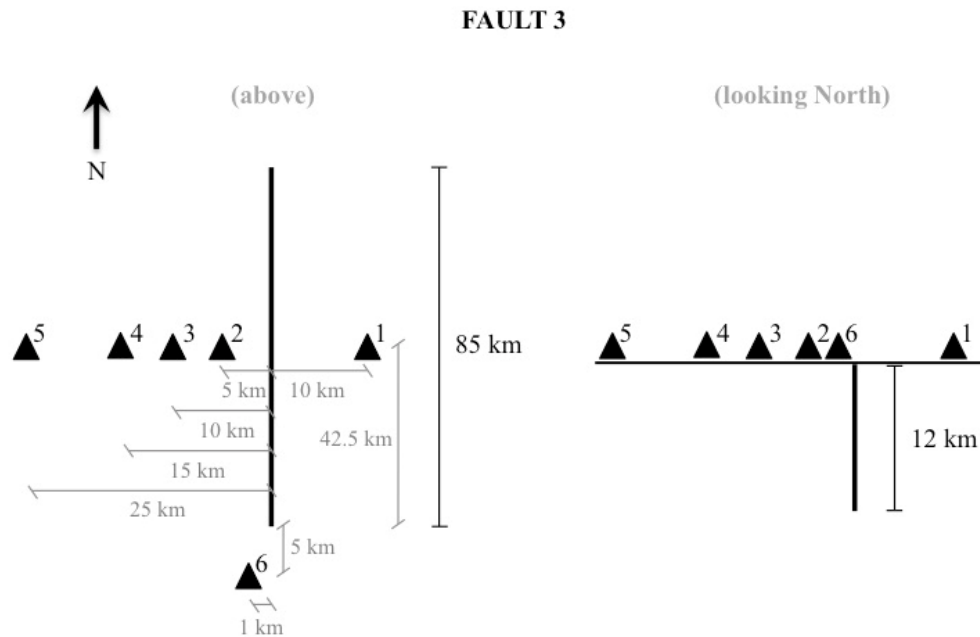


Figure 4-44 Geometry of the fault source and the location of the observation size for set 2, case 2

Table 4-48 Summary of input data for Set 2, case 2 (a,b,c,d)

Name	Description	Source	Mag-Density Function	Ground Motion Model ^{1,2,3,4}	Rupture Dimension Relationships
Set 2 Case 2	Single fault, NGA-West2 ground-motion models	Fault 3 (vertical SS) b-value=0.9 slip-rate 2mm/yr	Truncated exponential, Mmax=7.0, Mmin=5.0	NGA-West2; Damping ratio=5%; Vs30=760 m/s (measured); Z1.0=0.048 km; Z2.5=0.607 km; Region=California	$Log(A) = M - 4; \sigma_A = 0$ $Log(W) = 0.5 * M - 2.15; \sigma_W = 0$ $Log(L) = 0.5 * M - 1.85; \sigma_L = 0$

¹ Abrahamson et al. (2014) – σ untruncated

² Boore et al. (2014) – σ untruncated

³ Campbell and Bozorgnia (2014) – σ untruncated

⁴ Chiou and Youngs (2014) – σ untruncated

Note: These four GMPMs are included as built-in models in R-CRISIS

Table 4-49 Coordinates of the fault source 3

Latitude	Longitude	Comment
0.38221	-65.0000	North end of fault
-0.38221	-65.0000	South end of fault

Table 4-50 Coordinates and comments of the computation sites for set 2 case 2

Site	Latitude	Longitude	Comment
1	0.00000	-64.91005	10 km east of fault, at midpoint along strike
2	0.00000	-65.04497	5 km west of fault, at midpoint along strike
3	0.00000	-65.08995	10 km west of fault, at midpoint along strike
4	0.00000	-65.13490	15 km west of fault, at midpoint along strike
5	0.00000	-65.22483	25 km west of fault, at midpoint along strike
7	-0.42718	-65.00900	5 km south of southern end, 1 km west

Results for case 2a: Abrahamson et al. (2014)

Results obtained in R-CRISIS are shown in Figure 4-45 where the plots of the seismic hazard results obtained are compared against those provided as benchmark by PEER. In all the plots there is a complete agreement between the obtained results by R-CRISIS and the latter for the six computation sites.

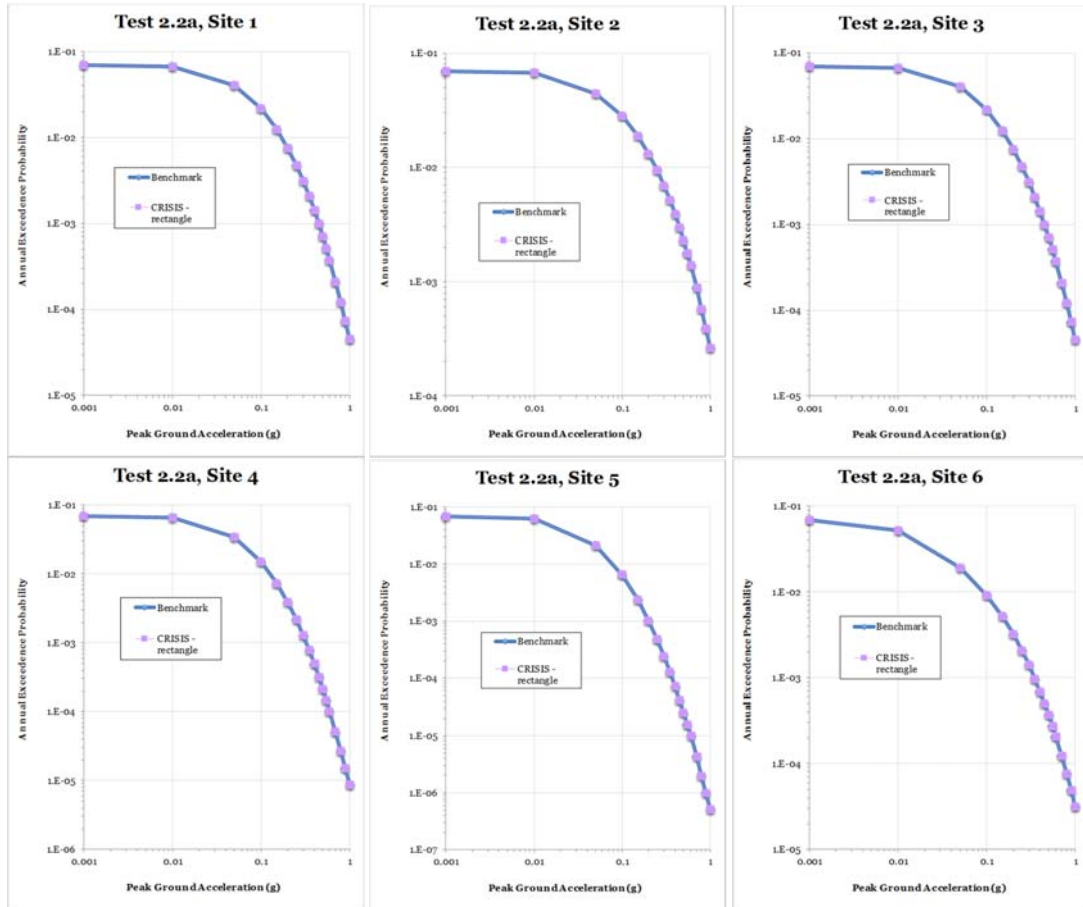


Figure 4-45 Comparison of the CRISIS and PEER results for sites 1 to 6 (set 2 case 2a)

Results for case 2b: Boore et al. (2014)

Results obtained in R-CRISIS are shown in Figure 4-46 where the plots of the seismic hazard results obtained are compared against those provided as benchmark by PEER. In all the plots there is a complete agreement between the obtained results by R-CRISIS and the latter for the six computation sites.

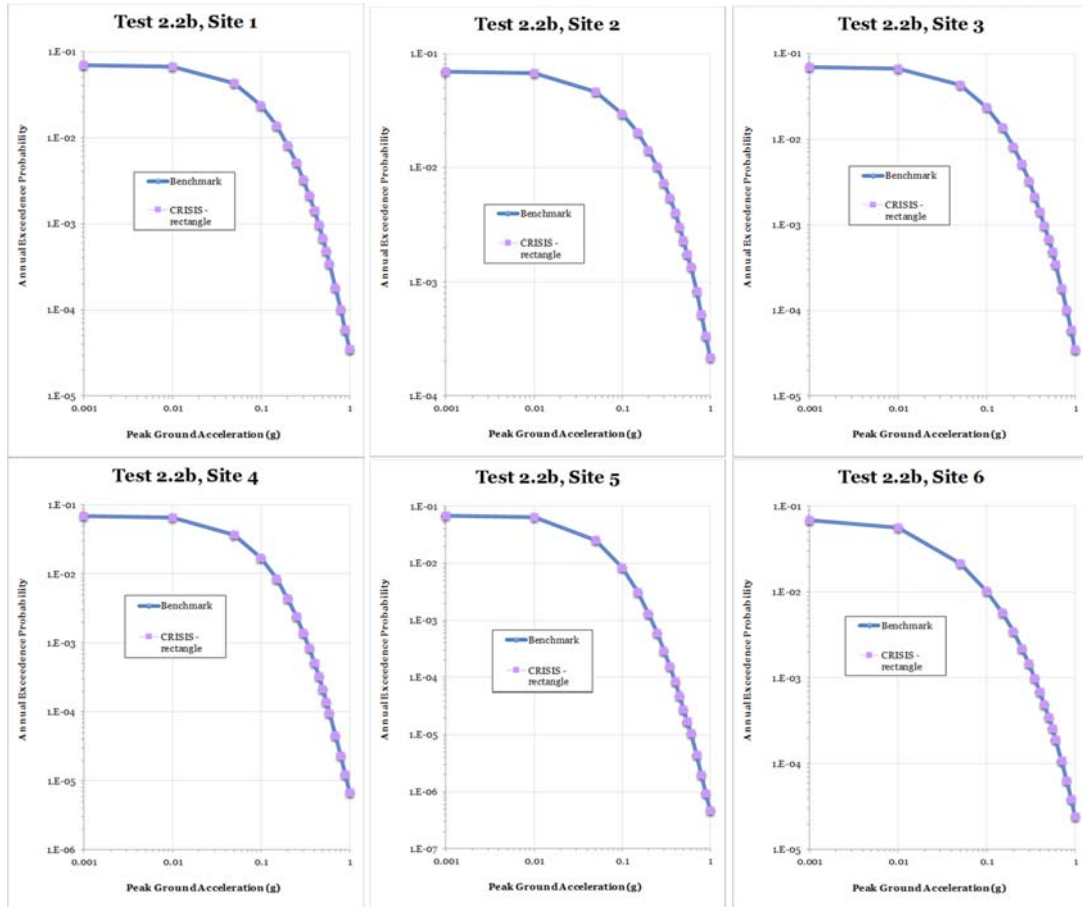


Figure 4-46 Comparison of the CRISIS and PEER results for sites 1 to 6 (set 2 case 2b)

Results for case 2c: Campbell and Bozorgnia (2014)

Results obtained in R-CRISIS are shown in Figure 4-47 where the plots of the seismic hazard results obtained are compared against those provided as benchmark by PEER. In all the plots there is a complete agreement between the obtained results by R-CRISIS and the latter for the six computation sites.

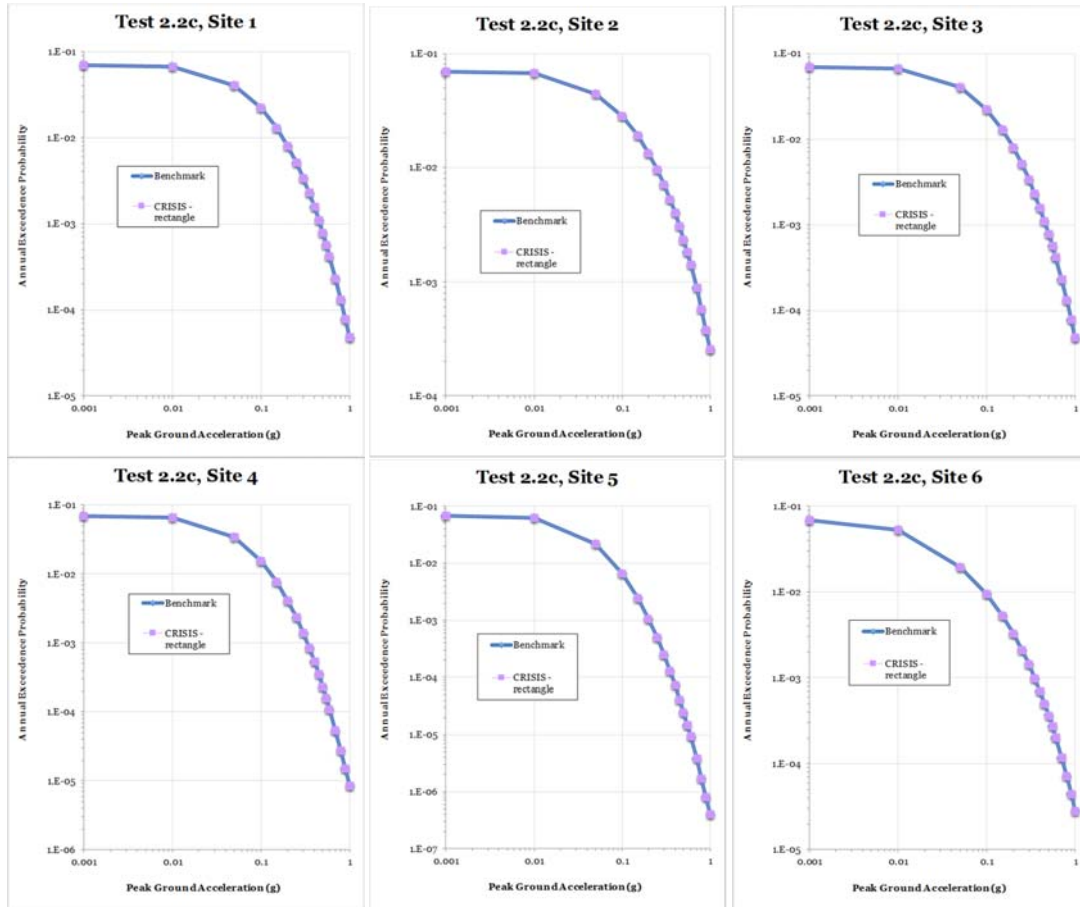


Figure 4-47 Comparison of the CRISIS and PEER results for sites 1 to 6 (set 2 case 2c)

Results for case 2d: Chiou and Youngs (2014)

Results obtained in R-CRISIS are shown in Figure 4-48 where the plots of the seismic hazard results obtained are compared against those provided as benchmark by PEER. In all the plots there is a complete agreement between the obtained results by R-CRISIS and the latter for the six computation sites.

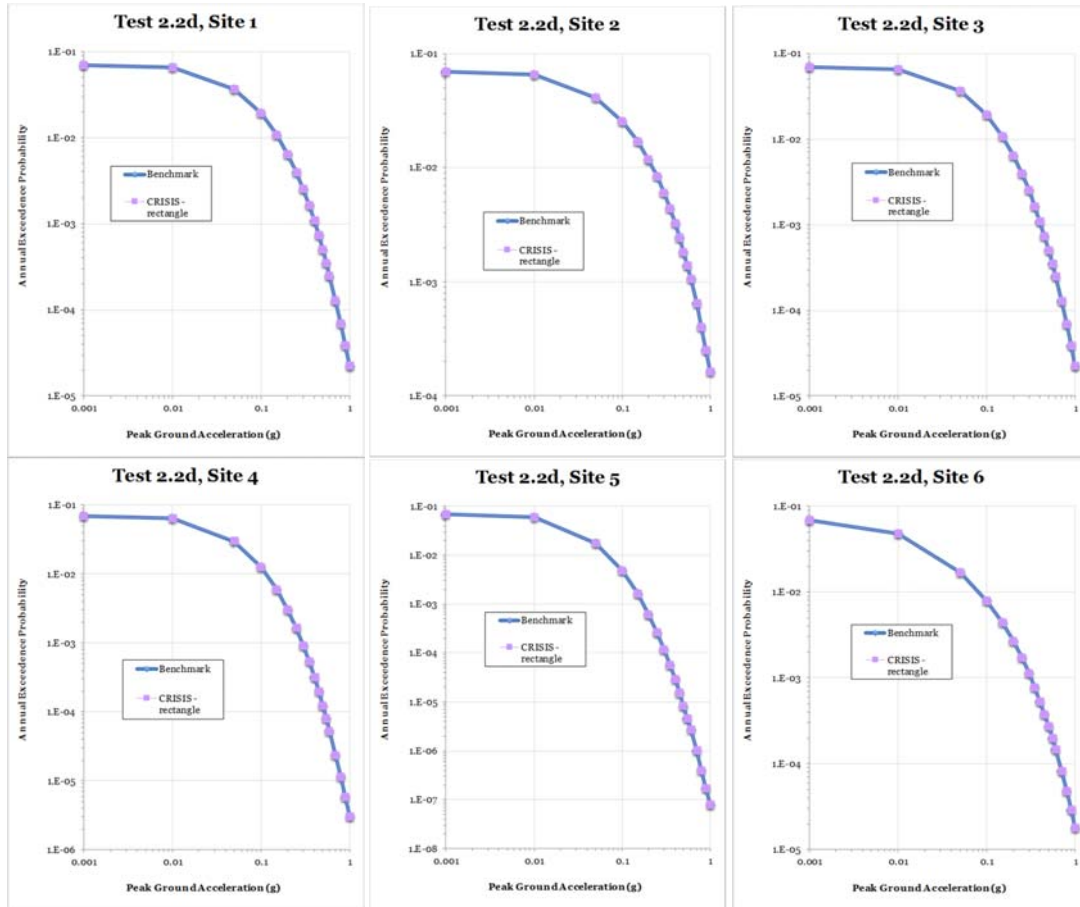


Figure 4-48 Comparison of the CRISIS and PEER results for sites 1 to 6 (set 2 case 2d)

4.2.3 Set 2 case 3

Input parameters

The source adopted for this case corresponds to fault 4 (see Figure 4-49), with reverse mechanism and 45° dip. Seismicity input is specified through a b-value of 0.9, a slip rate of 2mm/yr and a magnitude density function in the form of a delta function at M7.0 (see Table 4-51). The objective of this test is to evaluate the handling of NGA-West2 ground-motion models (considering variability) for a source with reverse faulting mechanism.

Table 4-52 shows the data associated to the geometry of the fault source whereas Table 4-53 includes the coordinates of the computation sites together with an explanation about its relevance for validation and verification purposes.

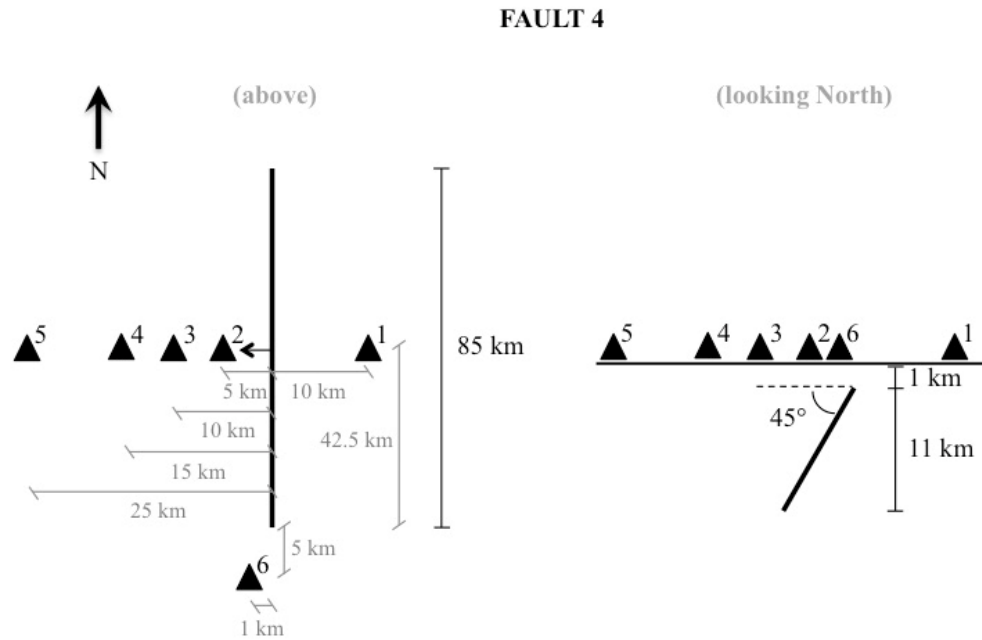


Figure 4-49 Geometry of the fault source and the location of the observation size for set 2, case 3

Table 4-51 Summary of input data for set 2, case 3 (a,b,c,d)

Name	Description	Source	Mag-Density Function	Ground Motion Model ^{1,2,3,4}	Rupture Dimension Relationships
Set 2 Case 3	Single fault, NGA-West2 ground-motion models	Fault 4 (reverse, 45° dip) b-value=0.9 slip-rate 2mm/yr	Delta function at M7.0	NGA-West2; Damping ratio=5%; Vs30=760 m/s (measured); Z1.0=0.048 km; Z2.5=0.607 km; Region=California	$Log(A) = M - 4; \sigma_A = 0$ $Log(W) = 0.5 * M - 2.15; \sigma_W = 0$ $Log(L) = 0.5 * M - 1.85; \sigma_L = 0$

¹ Abrahamson et al. (2014) – σ untruncated

² Boore et al. (2014) – σ untruncated

³ Campbell and Bozorgnia (2014) – σ untruncated

⁴ Chiou and Youngs (2014) – σ untruncated

Note: These four GMPMs are included as built-in models in R-CRISIS

Table 4-52 Coordinates of the fault source 4

Latitude	Longitude	Comment
0.38221	-65.0000	North end of fault
-0.38221	-65.0000	South end of fault

Table 4-53 Coordinates and comments of the computation sites for set 2 case 3

Site	Latitude	Longitude	Comment
1	0.00000	-64.91005	10 km east of fault, at midpoint along strike
2	0.00000	-65.04497	5 km west of fault, at midpoint along strike
3	0.00000	-65.08995	10 km west of fault, at midpoint along strike
4	0.00000	-65.13490	15 km west of fault, at midpoint along strike
5	0.00000	-65.22483	25 km west of fault, at midpoint along strike
7	-0.42718	-65.00900	5 km south of southern end, 1 km west

Results for case 3a: Abrahamson et al. (2014)

Results obtained in R-CRISIS are shown in Figure 4-50 where the plots of the seismic hazard results obtained are compared against those provided as benchmark by PEER. In all the plots there is a complete agreement between the obtained results by R-CRISIS and the latter for the six computation sites.

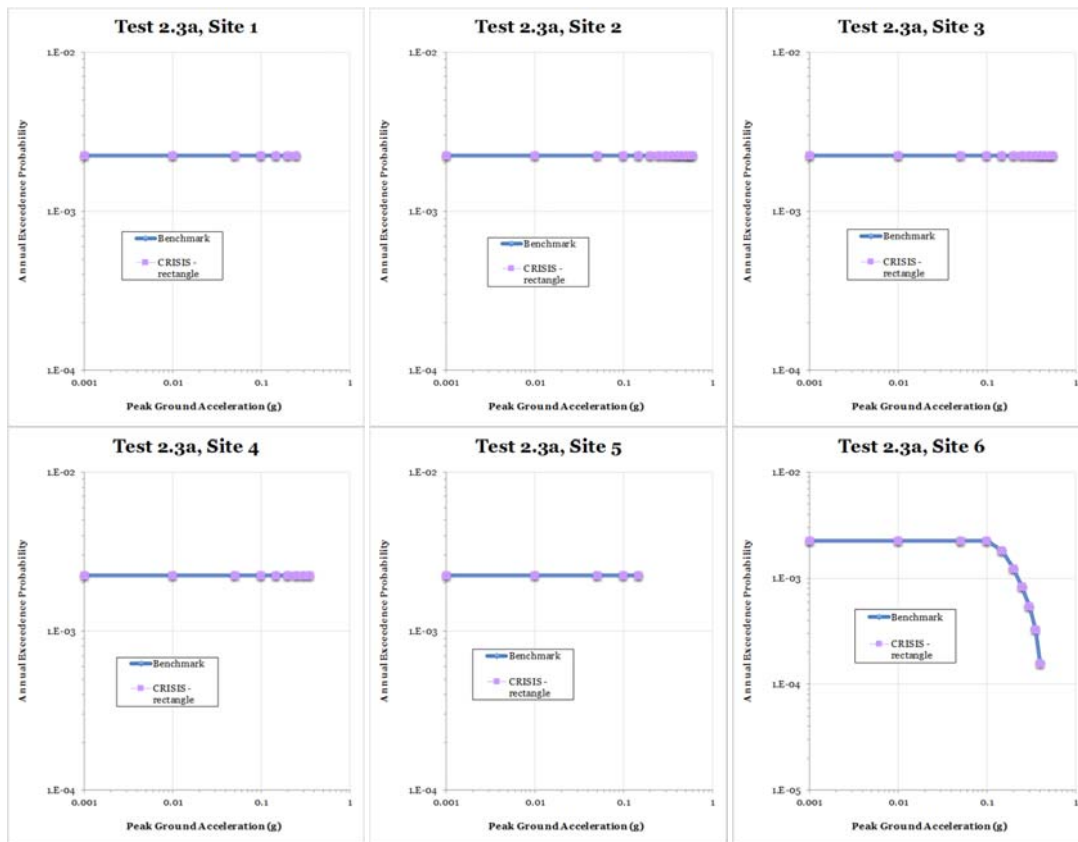


Figure 4-50 Comparison of the CRISIS and PEER results for sites 1 to 6 (set 2 case 3a)

Results for case 3b: Boore et al. (2014)

Results obtained in R-CRISIS are shown in Figure 4-51 where the plots of the seismic hazard results obtained are compared against those provided as benchmark by PEER. In all the plots

there is a complete agreement between the obtained results by R-CRISIS and the latter for the six computation sites.

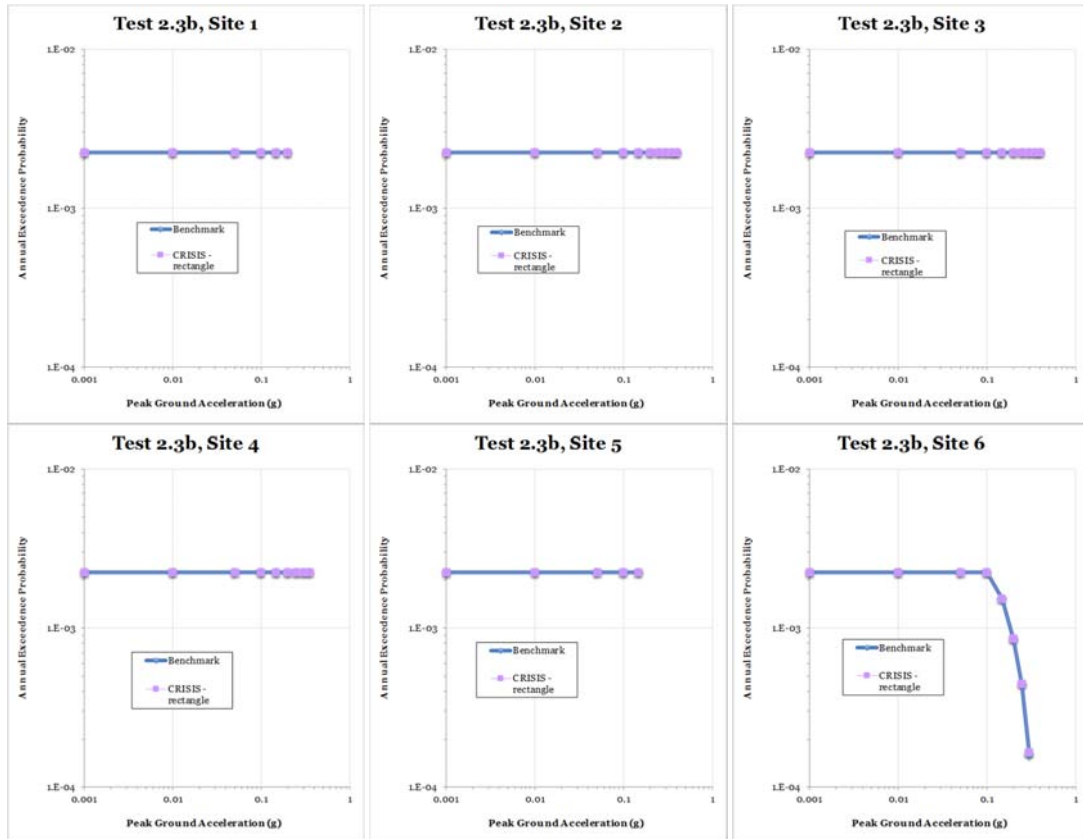


Figure 4-51 Comparison of the CRISIS and PEER results for sites 1 to 6 (set 2 case 3b)

Results for case 3c: Campbell and Bozorgnia (2014)

Results obtained in R-CRISIS are shown in Figure 4-52 where the plots of the seismic hazard results obtained are compared against those provided as benchmark by PEER. In all the plots there is a complete agreement between the obtained results by R-CRISIS and the latter for the six computation sites.

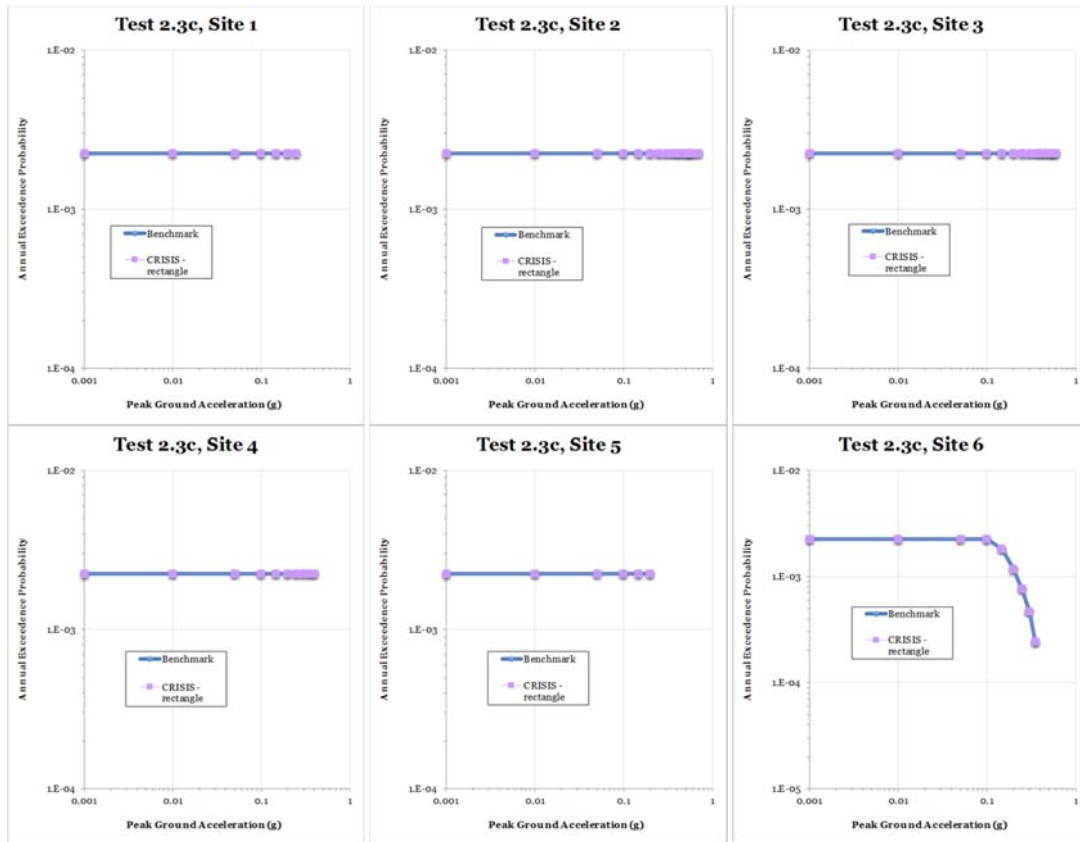


Figure 4-52 Comparison of the CRISIS and PEER results for sites 1 to 6 (set 2 case 3c)

Results for case 3d: Chiou and Youngs (2014)

Results obtained in R-CRISIS are shown in Figure 4-53 where the plots of the seismic hazard results obtained are compared against those provided as benchmark by PEER. In all the plots there is a complete agreement between the obtained results by R-CRISIS and the latter for the six computation sites.

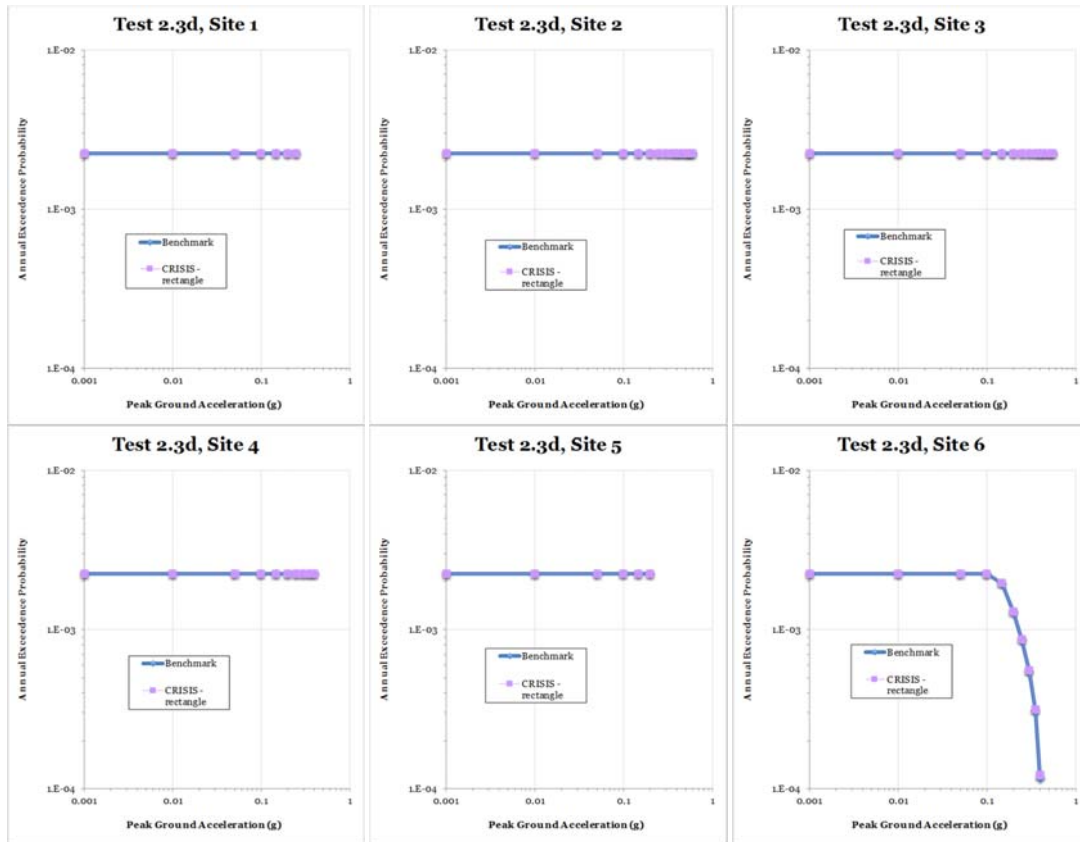


Figure 4-53 Comparison of the CRISIS and PEER results for sites 1 to 6 (set 2 case 3d)

4.2.4 Set 2 case 4a

Input parameters

The source adopted for this case corresponds to fault 5 (see Figure 4-54), with strike-slip mechanism and 90° dip. Seismicity input is specified through a b-value of 0.9, a slip rate of 2mm/yr and a magnitude density function in the form of a delta function at M6.0 (see Table 4-54). The objective of this test is to evaluate the results when using an uniform distribution down dip of the epicenters.

Table 4-55 shows the data associated to the geometry of the fault source whereas Table 4-56 includes the coordinates of the computation site together with an explanation about its relevance for validation and verification purposes.

FAULT 5

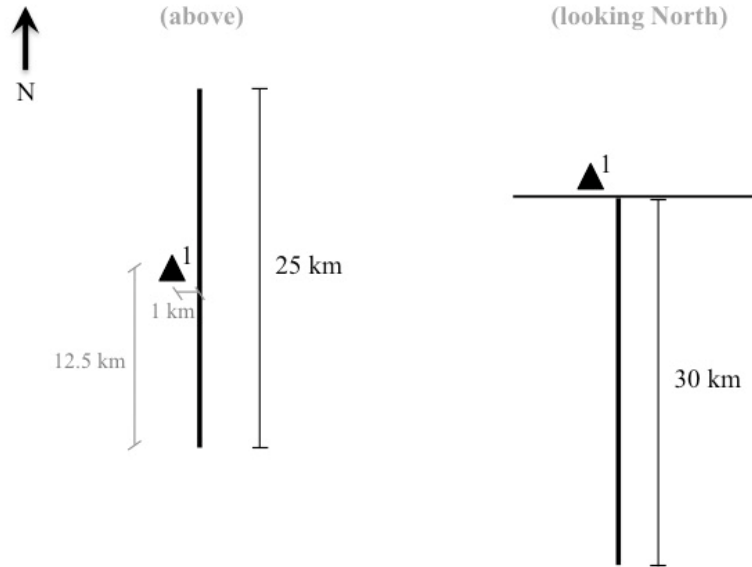


Figure 4-54 Geometry of the fault source and the location of the observation site for set 2, case 4a

Table 4-54 Summary of input data for Set 2, case 4a

Name	Description	Source	Mag-Density Function	Ground Motion Model	Rupture Dimension Relationships
Set 2 Case 4a	Single fault, NGA-West2 ground motion model, uniform distribution down dip	Fault 5 (vertical SS) b-value=0.9 slip-rate 2mm/yr	Delta function at M6.0	Chiou and Youngs (2014); $\sigma=0$; Damping ratio=5%; $V_{s30}=760$ m/s (measured); $Z_{1.0}=0.048$ km; $Z_{2.5}=0.607$ km; Region=California	$\text{Log}(A) = M - 4; \sigma_A = 0$ $\text{Log}(W) = 0.5 * M - 2.15; \sigma_W = 0$ $\text{Log}(L) = 0.5 * M - 1.85; \sigma_L = 0$

Table 4-55 Coordinates of the fault source 5

Latitude	Longitude	Comment
0.11240	-65.0000	North end of fault
-0.11240	-65.0000	South end of fault

Table 4-56 Coordinates and comments of the computation site for set 2 case 4a

Site	Latitude	Longitude	Comment
1	0.00000	-65.00900	1 km west of fault, at midpoint along strike

Results

Results obtained in R-CRISIS for the estimation of seismic hazard at Site 1 are shown in Figure 4-55 together with the comparison against the benchmark values provided by PEER. In all the plots, it can be seen a complete agreement between the results obtained by R-CRISIS and those provided by PEER. Because of that, it can be concluded that R-CRISIS fulfills all the requirements evaluated by the PEER project in Set2-Case4a.

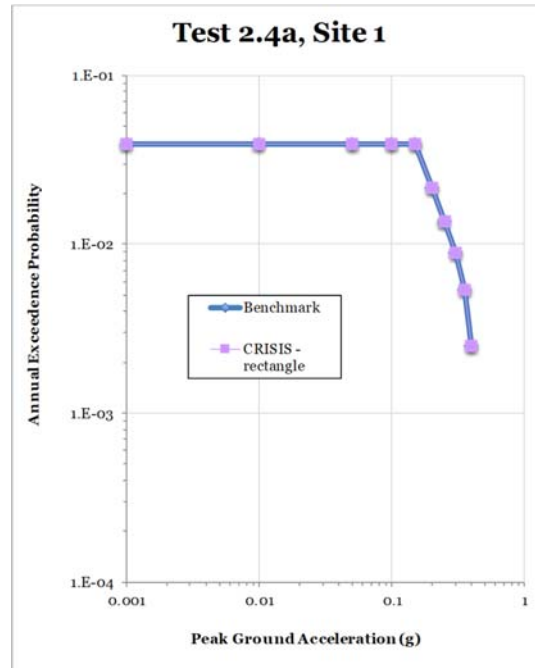


Figure 4-55 Comparison of the CRISIS and PEER results for site 1 (set 2 case 4a)

Note: The implementation of non-uniform hypocenter distributions (set 2 case 4b) is not yet implemented in R-CRISIS.

4.2.5 Set 2 case 5a

Input parameters

The source adopted for this case corresponds to fault 5 (see Figure 4-56), with strike-slip mechanism and 90° dip. Seismicity input is specified through a b-value of 0.9, a slip rate of 2mm/yr and a magnitude density function in the form of a delta function at M6.0 (see Table 4-57). The objective of this test is to evaluate the capability of R-CRISIS to model a normal distribution out to high epsilon values.

Table 4-58 shows the data associated to the geometry of the fault source whereas Table 4-59 includes the coordinates of the computation sites together with an explanation about its relevance for validation and verification purposes.

FAULT 6

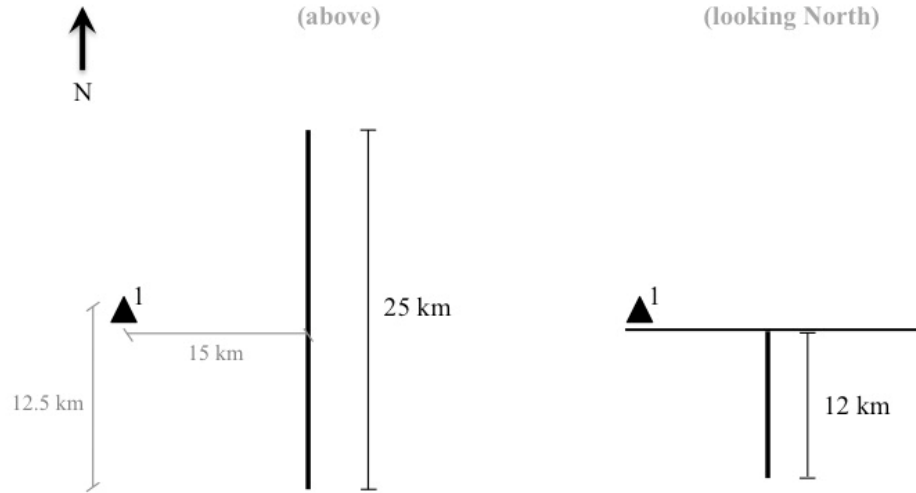


Figure 4-56 Geometry of the fault source and the location of the observation site for set 2, cases 5a-5b

Table 4-57 Summary of input data for Set 2, case 5a

Name	Description	Source	Mag-Density Function	Ground Motion Model	Rupture Dimension Relationships
Set 2 Case 5a	Single fault, NGA-West2 ground motion model, extreme tails	Fault 6 (vertical SS) b-value=0.9 slip-rate 2mm/yr	Delta function at M6.0	Chiou and Youngs (2014); $\sigma=0.65$ (untruncated); Damping ratio=5%; $V_{s30}=760$ m/s (measured); $Z_{1.0}=0.048$ km; $Z_{2.5}=0.607$ km; Region=California	$\text{Log}(A) = M - 4; \sigma_A = 0$ $\text{Log}(W) = 0.5 * M - 2.15; \sigma_W = 0$ $\text{Log}(L) = 0.5 * M - 1.85; \sigma_L = 0$

Table 4-58 Coordinates of the fault source 6

Latitude	Longitude	Comment
0.11240	-65.0000	North end of fault
-0.11240	-65.0000	South end of fault

Table 4-59 Coordinates and comments of the computation site for set 2 cases 5a-5b

Site	Latitude	Longitude	Comment
1	0.00000	-65.13490	15 km west of fault, at midpoint along strike

Results

Results obtained in R-CRISIS for the estimation of seismic hazard at Site 1 are shown in Figure 4-57 together with the comparison against the benchmark values provided by PEER. In all the plots, it can be seen a complete agreement between the results obtained by R-CRISIS

and those provided by PEER. Because of that, it can be concluded that R-CRISIS fulfills all the requirements evaluated by the PEER project in Set2-Case5a.

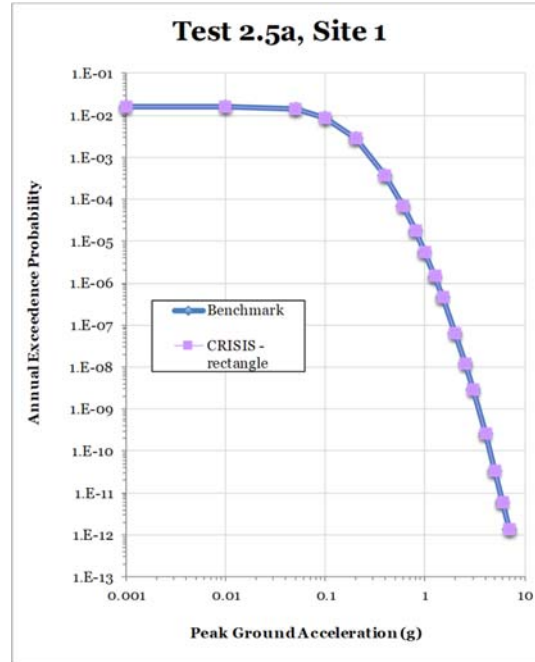


Figure 4-57 Comparison of the CRISIS and PEER results for site 1 (set 2 case 5a)

4.2.6 Set 2 case 5b

Input parameters

The source adopted for this case corresponds again to fault 6 (see Figure 4-56), with strike-slip mechanism and 90° dip. Seismicity input is specified through a b-value of 0.9, a slip rate of 2mm/yr and a magnitude density function in the form of a delta function at M6.0 (see Table 4-60). The objective of this test is to evaluate the consideration of mixture models (combination of two log-normal distribution).

The geometry of the source as well as the computation site are the same as in set 2 case 5a (Tables 4-58 and 4-59).

Table 4-60 Summary of input data for Set 2, case 5b

Name	Description	Source	Mag-Density Function	Ground Motion Model	Rupture Dimension Relationships
Set 2 Case 5b	Single fault, NGA-West2 ground motion model, mixture model, wmix1=0.5; wmix2=0.5; σmix1= 1.2σ; σmix2= 0.8σ	Fault 6 (vertical SS) b-value=0.9 slip-rate 2mm/yr	Delta function at M6.0	Chiou and Youngs (2014); σ=0.65 (untruncated); Damping ratio=5%; Vs30=760 m/s (measured); Z1.0=0.048 km; Z2.5=0.607 km; Region=California	$Log(A) = M - 4; \sigma_A = 0$ $Log(W) = 0.5 * M - 2.15; \sigma_W = 0$ $Log(L) = 0.5 * M - 1.85; \sigma_L = 0$

Results

Results obtained in R-CRISIS for the estimation of seismic hazard at Site 1 are shown in Figure 4-58 together with the comparison against the benchmark values provided by PEER. In all the plots, it can be seen a complete agreement between the results obtained by R-CRISIS and those provided by PEER. Because of that, it can be concluded that R-CRISIS fulfills all the requirements evaluated by the PEER project in Set2-Case5b.

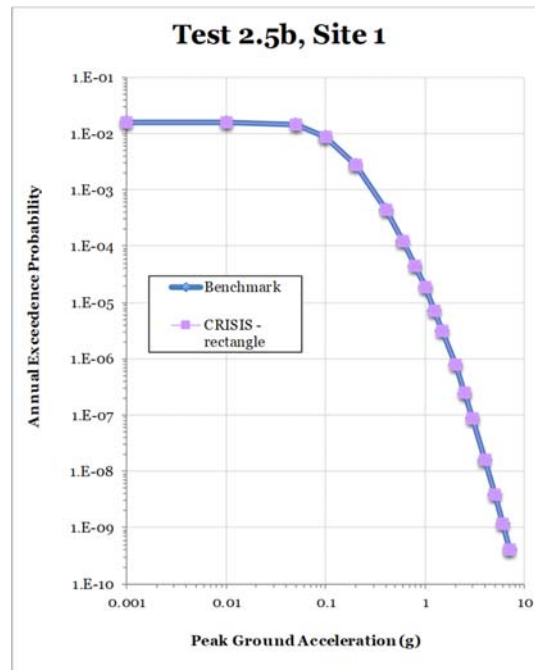


Figure 4-58 Comparison of the CRISIS and PEER results for site 1 (set 2 case 5b)

4.3 PEER validation tests (set 3)

Set 3 of the PEER validation tests aimed to verify the most complex elements of the PSHA codes. For example, the consideration of a bending fault, how the mean hazard and fractiles from logic trees, the modeling of intraslab sources at a subduction source and also the consideration of finite ruptures within area sources. Because there is not a single approach for the solution of any of these cases, no benchmark results were provided, reason why the reader is referred to the original reference (Hale et al., 2018) for reviewing the obtained results.

4.4 Validation against some analytical solutions

PSHA is, essentially, an integration process with respect to two variables, distance and magnitude. Said integration process is performed numerically by R-CRISIS, which is capable of solving general cases that involve geographic source layouts and GMPM. Since complex cases can only be solved numerically, the accuracy of the program can be tested by comparing the numerical solutions obtained in simple cases against their analytical solutions.

This section includes the comparison of the numerical and analytical solutions of the three cases proposed by Ordaz (2004) which although simple, are useful as canonical ones against which to calibrate the numerical code of R-CRISIS. The three cases have the following characteristics:

- Case 1: Point source with deterministic GMPM
- Case 2: Point source with probabilistic GMPM
- Case 3: Area source with probabilistic GMPM

In all cases the modified G-R seismicity model is used with the values of the parameters shown in Table 4-61.

Table 4-61 Seismicity parameters for the comparison against the analytical solution

M_o	4.0
λ_o	1.0
β	2.0
M_U	8.0

Also, a GMPM with the form:

$$E(\ln a) = a_1 + a_2 M + a_3 \ln R + a_4 R \quad (\text{Eq. 4-13})$$

with the coefficients proposed by Ordaz et al. (1989) is used.

4.4.1 Case 1: Point source with deterministic GMPM

This is the simplest case that considers a point source located at $R=30$ km from the computation site which seismicity is characterized by means of a modified G-R model with the parameters shown in Table 4-61. The GMPM shown in equation 4-13 with $\sigma=0$ is used. Figure 4-59 shows the comparison between the analytical and the numerical solutions for the simplest of the three cases.

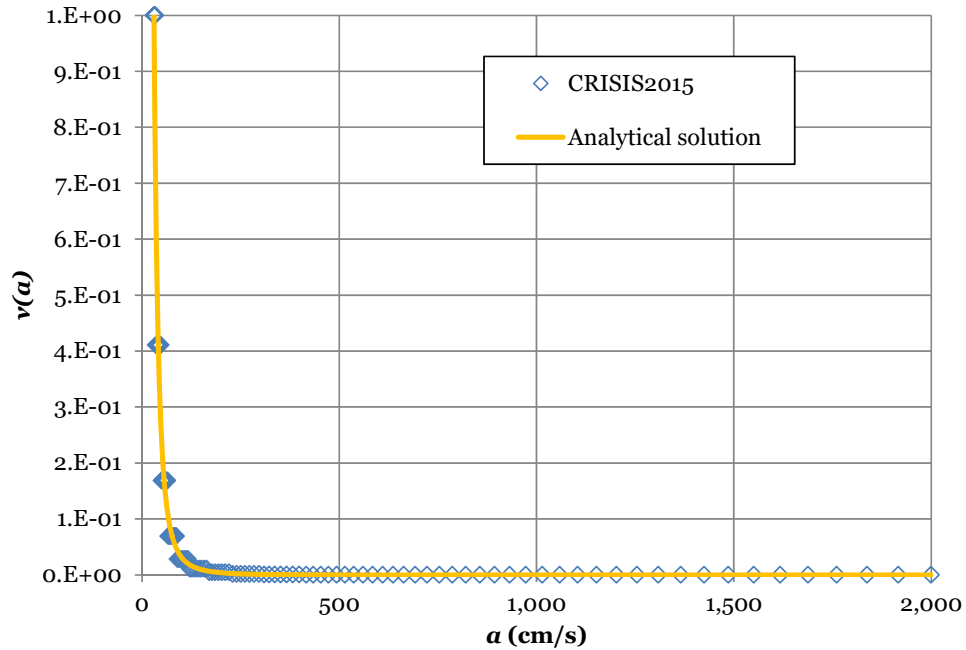


Figure 4-59 Comparison of analytical and numerical solutions for Case 1 of Ordaz (2004)

4.4.2 Case 2: Point source with probabilistic GMPM

This case is similar as the previous one with the difference that now the uncertainty in the GMPM is accounted for during the calculation process. For this purpose, different values of σ are used (0.3, 0.5 and 0.7). Figures 4-60 to 4-62 show the comparison between the analytical and the numerical solutions for this case considering different sigma values.

Note: no truncation has been considered in this case.

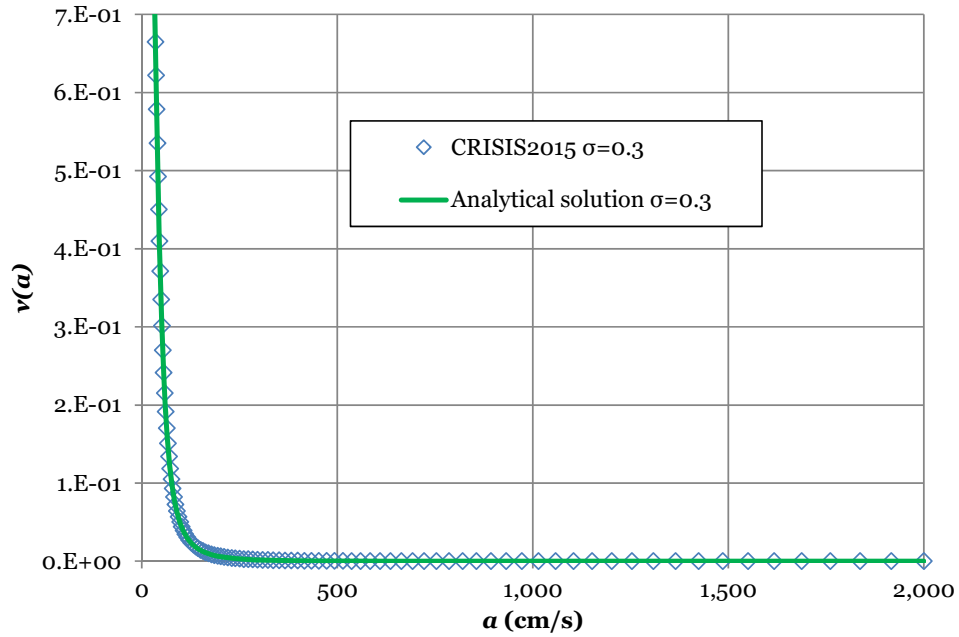


Figure 4-60 Comparison of analytical and numerical solutions for Case 2 of Ordaz (2004); $\sigma=0.3$

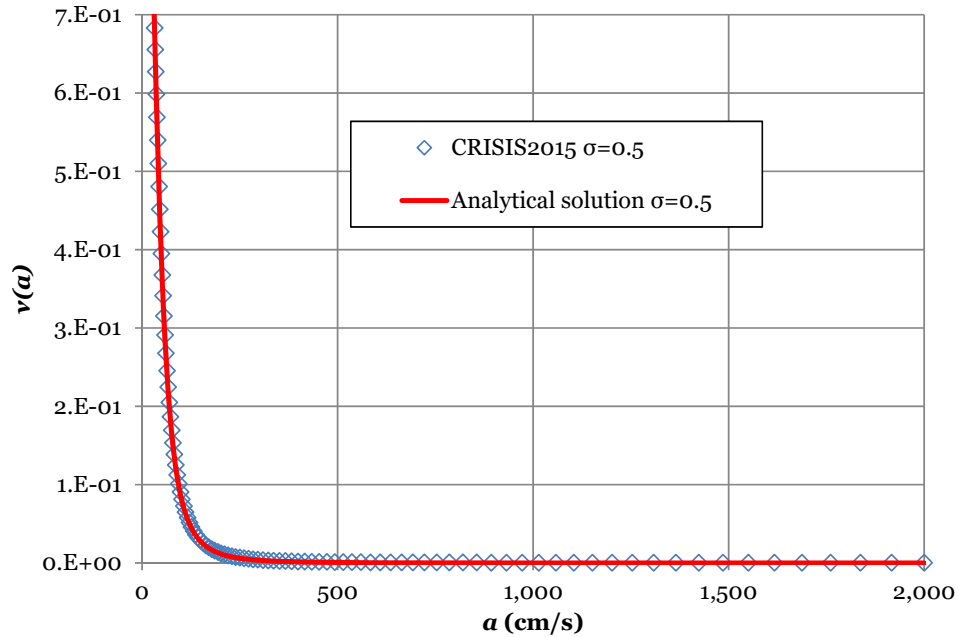


Figure 4-61 Comparison of analytical and numerical solutions for Case 2 of Ordaz (2004); $\sigma=0.5$

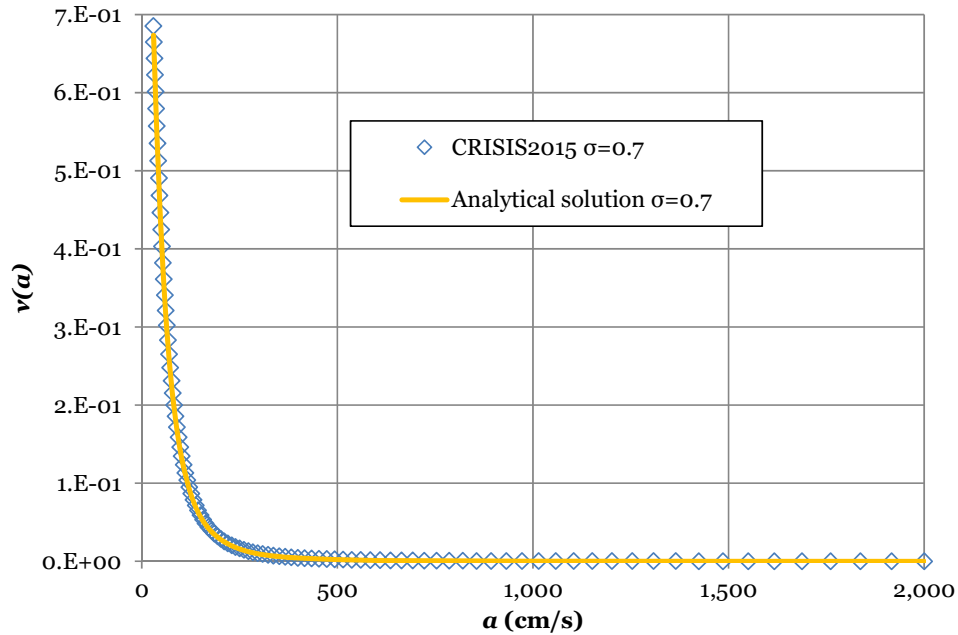


Figure 4-62 Comparison of analytical and numerical solutions for Case 2 of Ordaz (2004); $\sigma=0.7$

4.4.3 Case 3: Area source with probabilistic GMPM

For this case which corresponds to an area source, the latter is represented by means of a disc with uniform seismicity with a radius of 50 km, located at a depth equal to 10 km. The GMPM with $\sigma=0.7$ is used herein. Figure 4-63 shows the comparison between the analytical and numerical solutions.

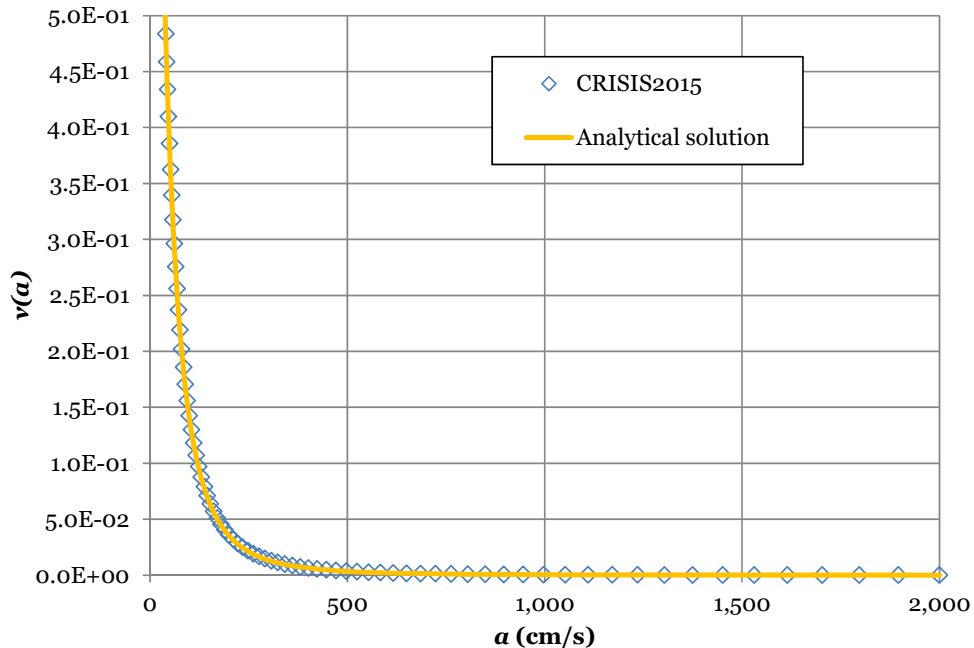


Figure 4-63 Comparison of analytical and numerical solutions for Case 3 of Ordaz (2004)

4.5 GMPM validation tests

Some of the built-in GMPM available in R-CRISIS have been validated (see Table 2-20) by means of different procedures based on the raw data availability for performing comparisons, verifications and validations. Those range from direct comparison against data published by the GMPM developers, direct contact with the authors in order to access to some information and graphical comparisons with the figures published in the dissemination reports and/or academic journals. Also, some authors of R-CRISIS have participated in the development of GMPM included in the built-in set and for those cases, even if no formal validation process has been applied, they are assumed to be properly implemented in the program.

The following sections summarize this process considering the different selected approaches with the aim of showing in a transparent way how said procedure has been developed.

4.5.1 Comparison against published raw data

For some of the GMPM developed under the NGA-West2 framework, the raw data for different magnitudes, distances, spectral ordinates and other characteristics (e.g. dip, V_{s30} , etc.) was published by the authors. Using those and the results obtained after the implementation of said GMPM as built-in models in R-CRISIS, different comparisons were performed to validate the latter.

Abrahamson et al. (2014)

Figures 4-64 and 4-65 show the comparison between the authors' values (median and percentile 84 respectively) and those obtained in R-CRISIS for the Abrahamson et al. (2014) GMPM with:

- $M=7$
- $R_{RUP}=10$ km
- $V_{s30}=760$ m/s
- $F_{TV}=1$
- $FHW=1$
- $Dip=90^\circ$

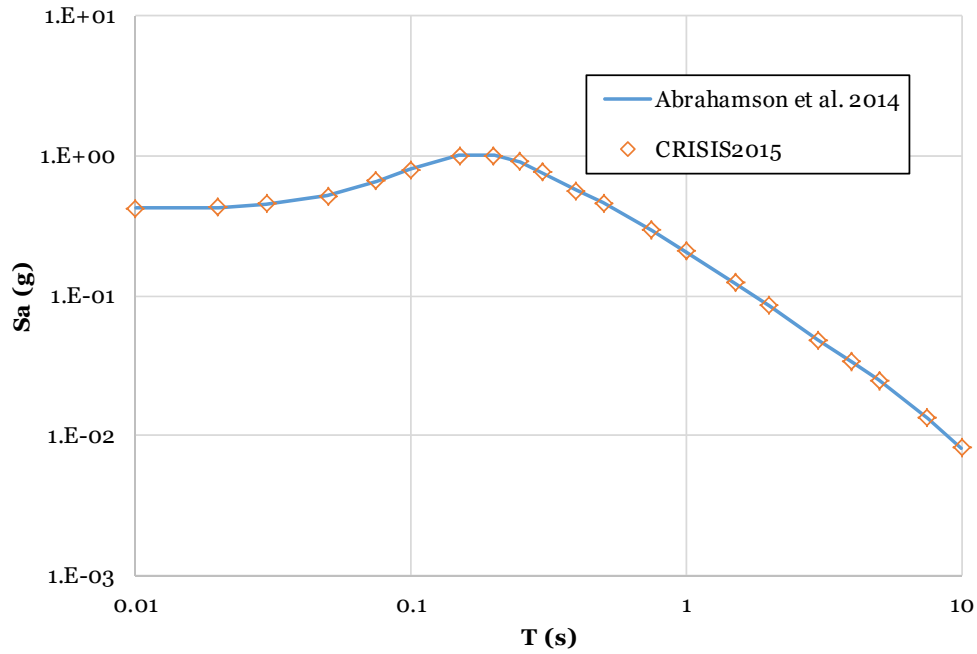


Figure 4-64 Comparison of median values between original and built-in Abrahamson et al. (2014) GMPM

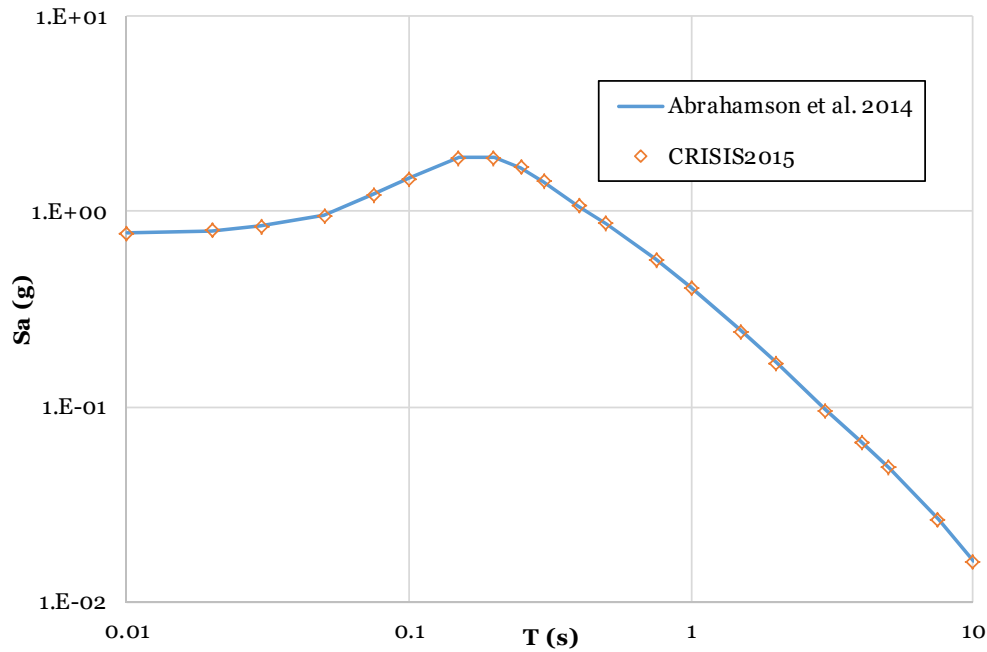


Figure 4-65 Comparison of percentile 84 values between original and built-in Abrahamson et al. (2014) GMPM

From both figures, the total congruence along the spectral range can be found. Results of the same type were obtained for other magnitude, V_{s30} , dip and distance values.

Chiou and Youngs (2014)

Figures 4-66 and 4-67 show the comparison between the author’s values (median) and those obtained in R-CRISIS for the Chiou and Youngs (2014) GMPM for four magnitudes (5.5, 6.5, 7.5 and 8.5) with $R_x=1$ and $R_x=10$ km respectively. From both figures, the total congruence along the spectral range can be found.

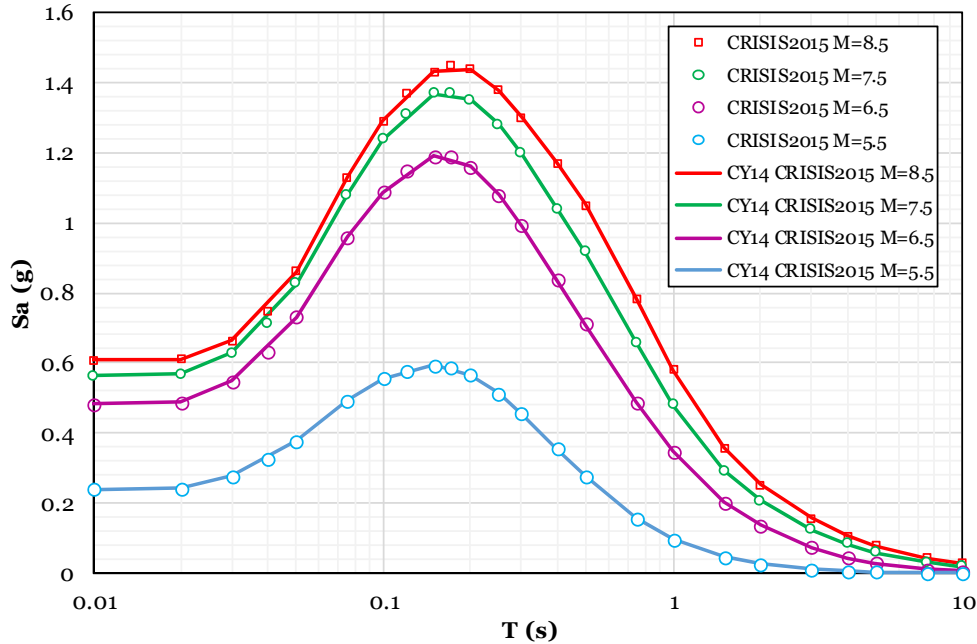


Figure 4-66 Comparison of median values between original and built-in Chiou and Youngs (2014) GMPM with $R_x=1$ km

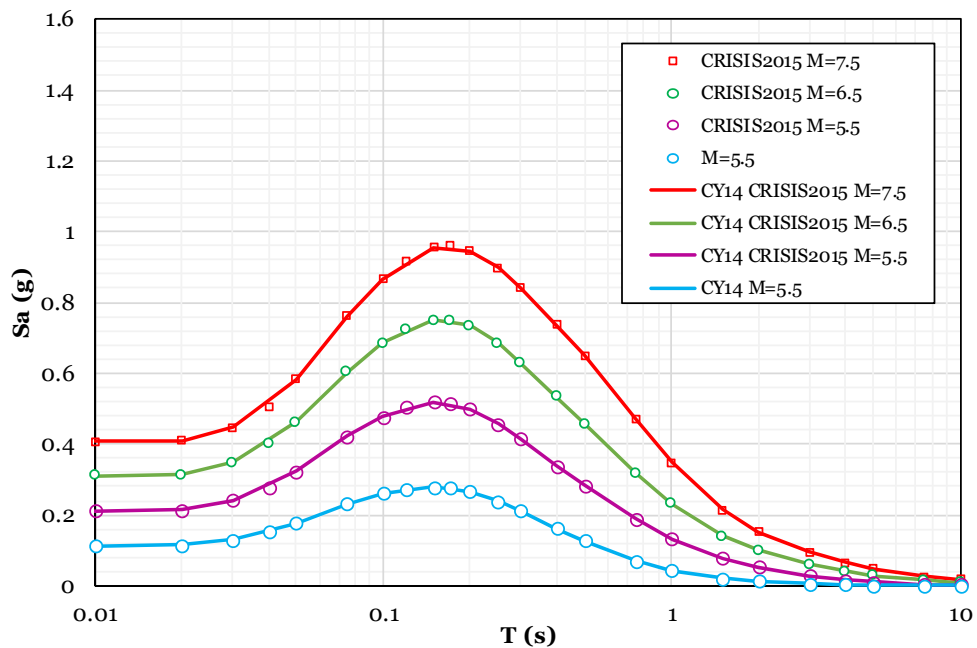


Figure 4-67 Comparison of median values between original and built-in Chiou and Youngs (2014) GMPM with $R_x=10$ km

Campbell and Bozorgnia (2014)

The validation of the built-in GMPM has been done for the Campbell and Bozorgnia (2014) case by means of five cases which characteristics are summarized in Table 4-62.

Table 4-62 Characteristics of the 5 validation cases of the Campbell-Bozorgnia (2014) GMPM

Case	1	2	3	4	5
Mechanism	Strike Slip	Strike Slip	Normal	Normal	Strike Slip
Region	California	California	California	California	California
Vs30	760	760	760	400	760
Z2.5	0.61	2.00	2.00	2.00	2.00
M	7.0	7.0	7.0	7.0	7.0
Rrup	5.0	100.1	5.0	5.0	5.0
Ztor	5.0	5.0	5.0	5.0	5.0
RJB	0	100	0	0	0
Rx	0	100	0	0	0
Rfoc	5.0	100.1	5.0	5.0	5.0
Dip	90	45	45	45	45
Frv	0	0	0	0	0
Fnm	0	0	1	1	0
FHW	1	1	1	1	0

Figures 4-68 to 4-70 show the graphical comparison of the author’s values (median) and those obtained in R-CRISIS.

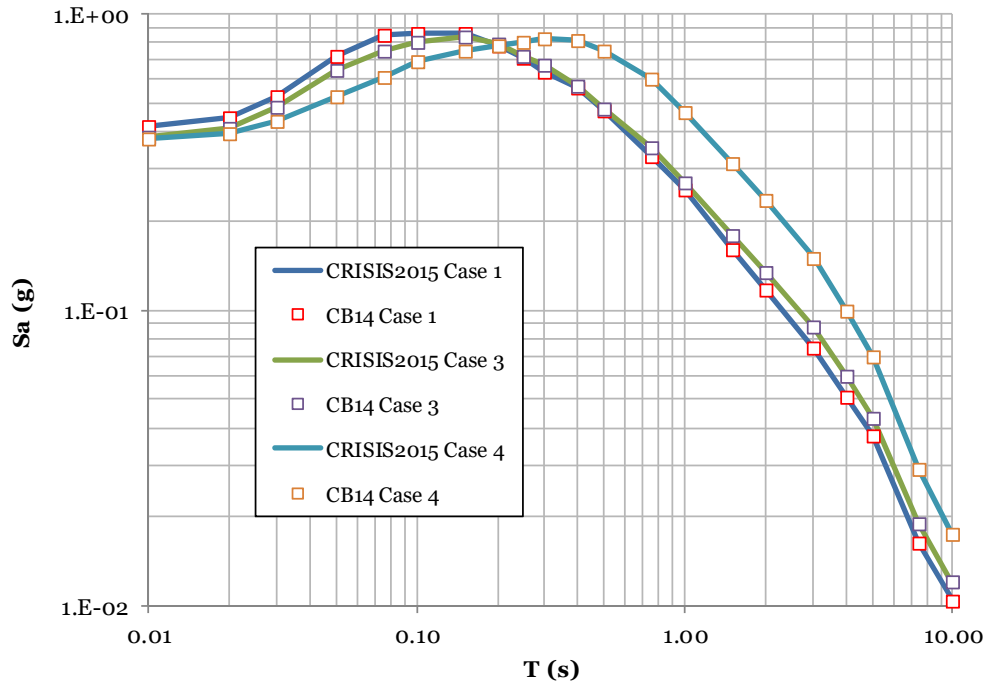


Figure 4-68 Comparison of median values between original and built-in Campbell and Bozorgnia (2014) GMPM. Cases 1, 3 and 4

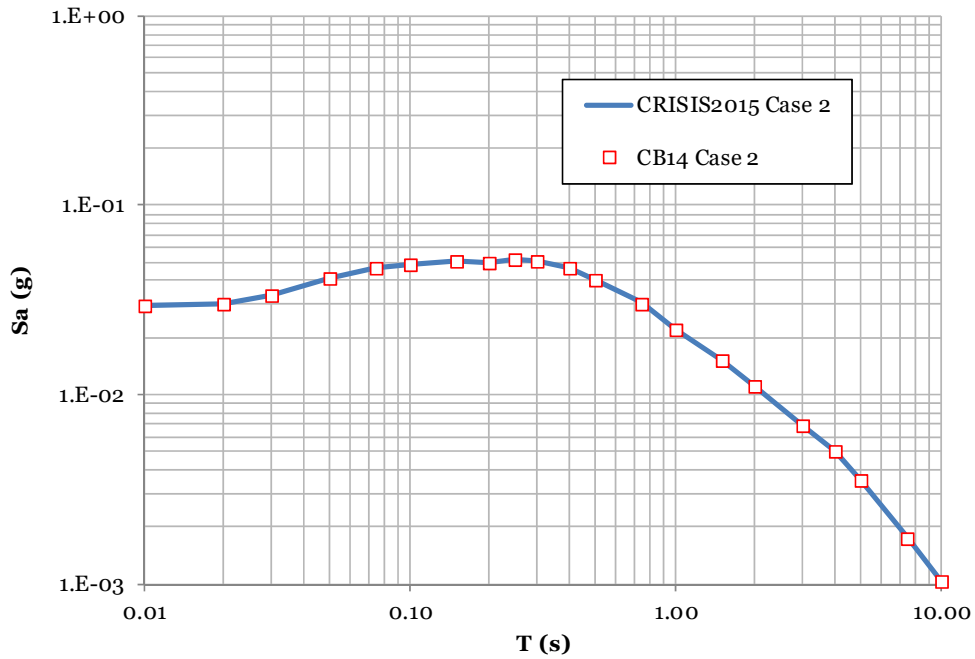


Figure 4-69 Comparison of median values between original and built-in Campbell and Bozorgnia (2014) GMPM. Case 2

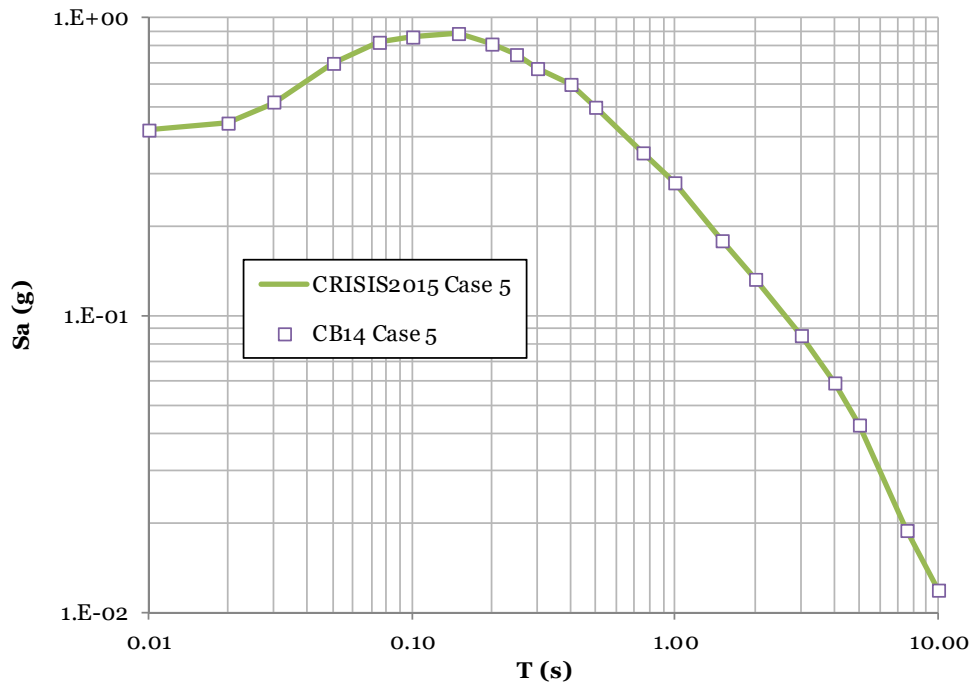


Figure 4-70 Comparison of median values between original and built-in Campbell and Bozorgnia (2014) GMPM. Case5

Akkar et al. (2014)

Figures 4-71 to 4-73 show the comparison of the attenuation plots obtained using the supplemental material from the Akkar et al. (2014) GMPM and those obtained from CRISIS. In all cases there is an exact agreement between the provided and programmed results.

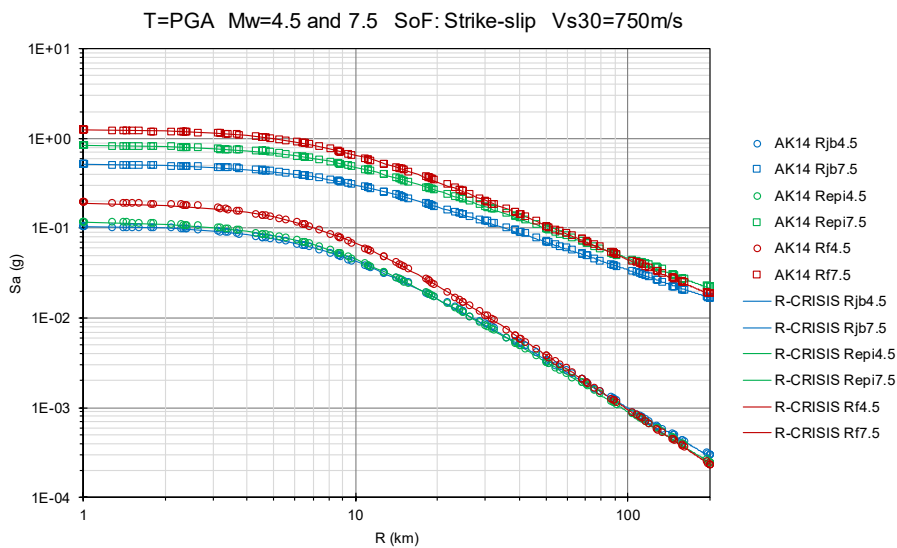


Figure 4-71 Comparison of distance scaling of the Akkar et al. (2014) model for different magnitudes and distances

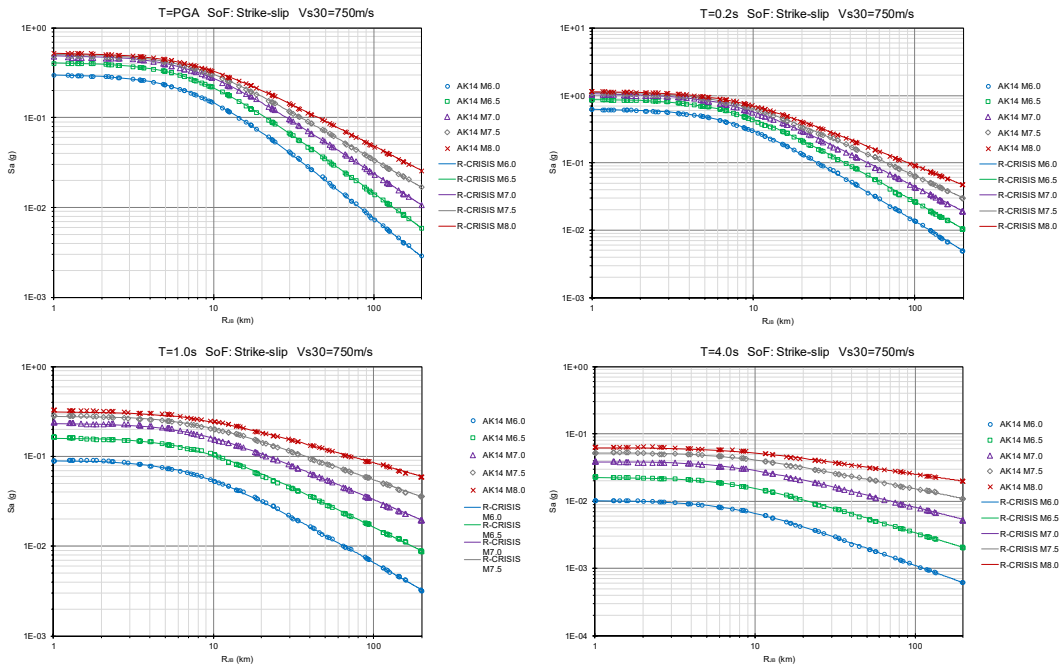


Figure 4-72 Comparison of distance scaling of R_{JB} model for different spectral ordinates. Top left: PGA; top right: 0.2s; bottom left: 1.0s; bottom right: 4.0s

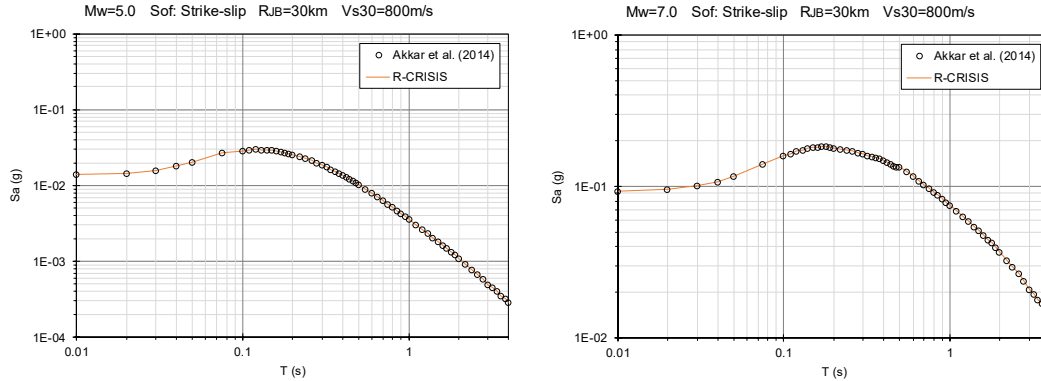


Figure 4-73 Comparison of median estimations of the predicted spectra for strike-slip mechanism, $R_{JB}=30\text{km}$, $V_{s30}=800\text{m/s}$ and $M_w=5$ (left) and $M_w=7$ (right)

4.5.2 Graphical comparisons

For the GMPM included in this section, a graphical comparison was performed between the figures included in the original publications of the authors and the built-in GMPM in R-CRISIS. This process required the scale adjustments of both, ordinates and abscises in order to guarantee consistency in the plots.

Zhao et al. (2006)

The graphical comparison for the Zhao et al. (2006) GMPM was made against the figures included in the original paper published in the Bulletin of the Seismological Society of America. Figure 4-74 shows the comparison using the data of Figure 3 (PGA) of the original publication from where it can be seen a total congruency between the original and the built-in models.

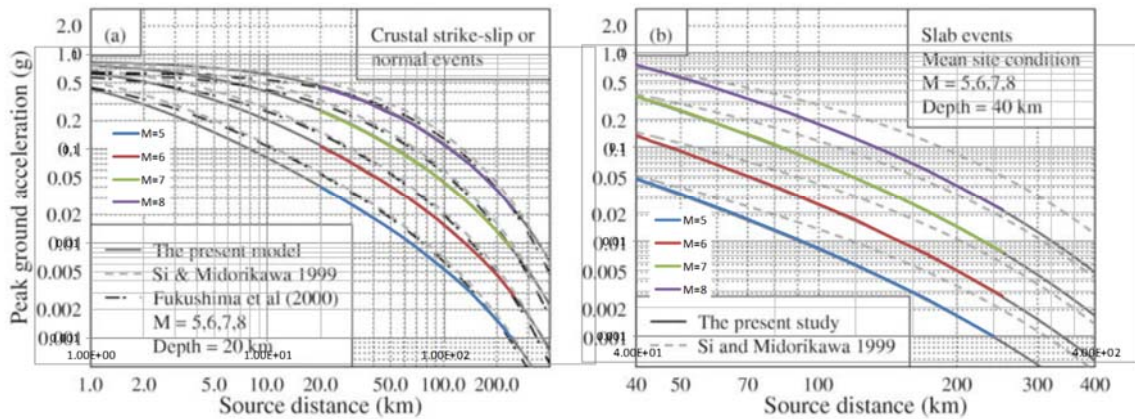


Figure 4-74 Comparison of median values between original and built-in Zhao et al. (2006) data. PGA and 4 magnitudes

Figure 4-75 shows the comparison for the complete spectral range for M=7, source distance=30 km, focal depth=20km and the four site classes. The base plot corresponds to Figure 6b of the original publication.

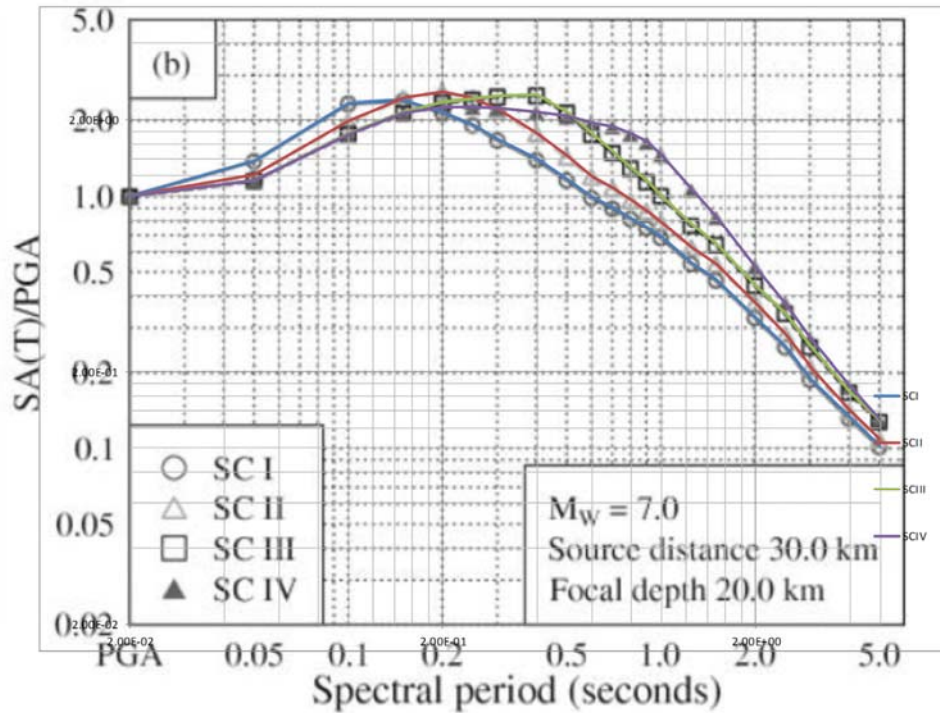


Figure 4-75 Comparison of median values between original and built-in Zhao et al. (2006) data. Full spectral range and 4 site classes

Figure 4-76 shows the comparison again for the complete spectral range, now in terms of pseudo-velocity (cm/s) for $M=7$, source distance=40 km, focal depth=20 km, site class II and crustal, interface and slab depths of 20 and 40 km. The base plot corresponds to Figure 7a of the original publication.

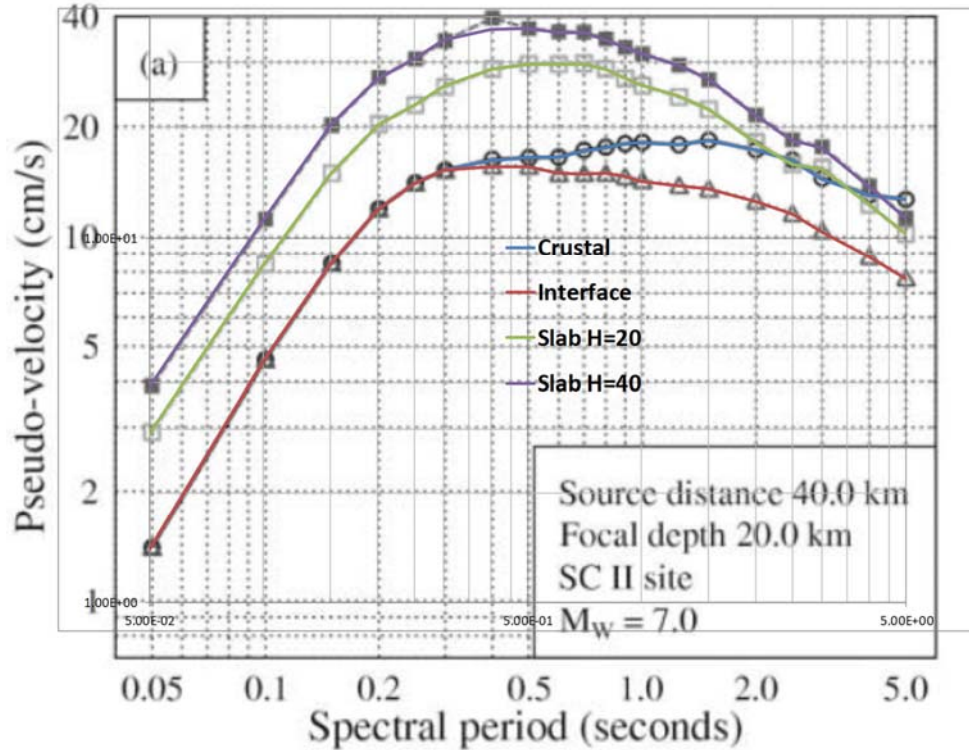


Figure 4-76 Comparison of median values between original and built-in Zhao et al. (2006) data. Full spectral range and pseudo-velocity. Source distance=40 km

Finally, Figure 4-77 shows the comparison for a similar case as the previous one but now using a source distance of 60 km. The base plot corresponds to Figure 7b of the original publication.

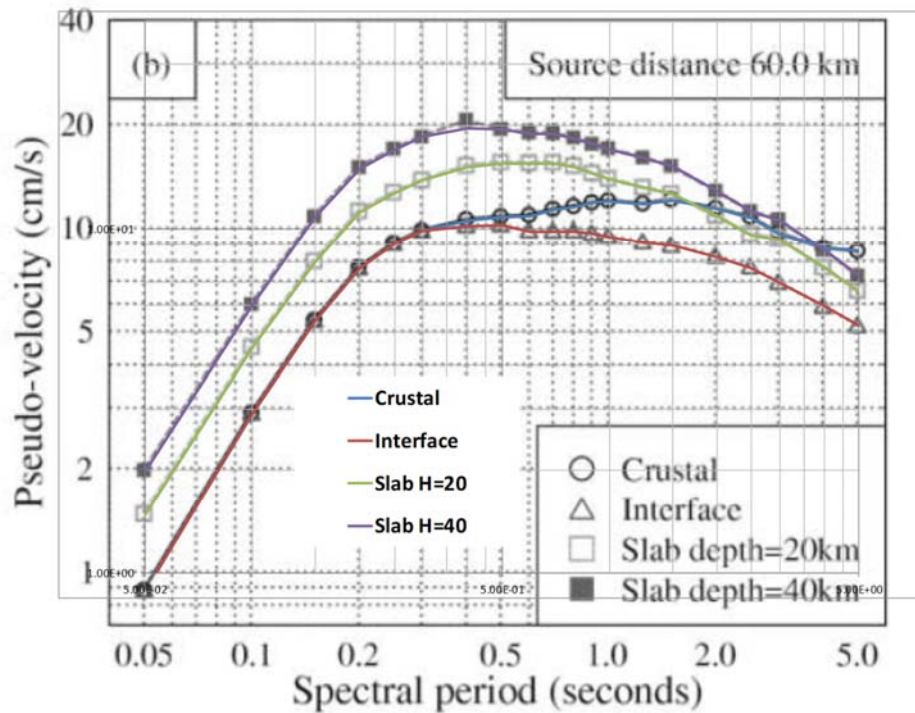


Figure 4-77 Comparison of median values between original and built-in Zhao et al. (2006) data. Full spectral range and pseudo-velocity. Source distance=60 km

For the Zhao et al. (2006) case, in all the comparisons total congruency is found between the author's values and those obtained by means of the built-in GMPM included in R-CRISIS.

Abrahamson and Silva (1997)

For this GMPM, the graphical comparison was made in terms of PGA for different mechanisms as shown in Figure 4-78 (for $M=7$ and rock) and for the full spectral range considering different magnitudes and soil conditions as shown in Figure 4-79. This last figure corresponds to Figure 9 of the original reference.

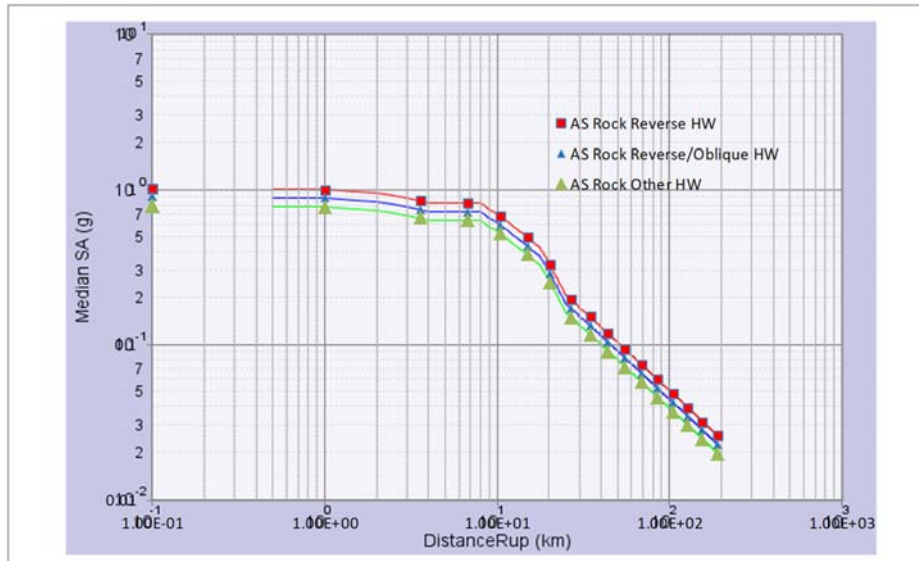


Figure 4-78 Comparison of median values between original and built-in Abrahamson and Silva (1997) GMPM. M=7, PGA, rock and different mechanisms

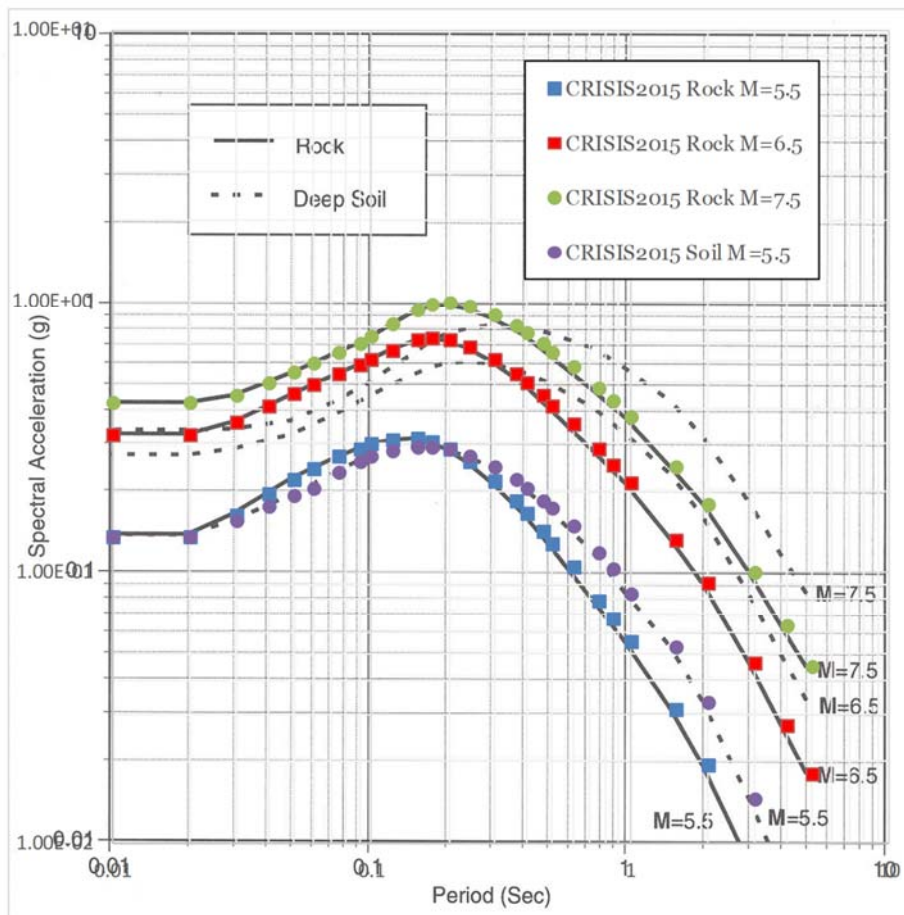


Figure 4-79 Comparison of median values between original and built-in Abrahamson and Silva (1997) GMPM. Strike-slip earthquake at a rupture distance of 10km. Average horizontal component

Chiou and Youngs (2008)

The validation of the Chiou and Youngs (2008) GMPM was made by means of the graphical comparison shown in Figure 4-80 which base data corresponds to Figure 14 of the Chiou and Youngs (2014) publication. This comparison is made for different magnitudes (3.5, 4.5, 5.5 and 8.5) in terms of the attenuation plots using $V_{s30}=760$ m/s, average Z_{TOR} and $\Delta DPP=0$. The comparison was made for $Sa=0.01s$ and $3.0s$.

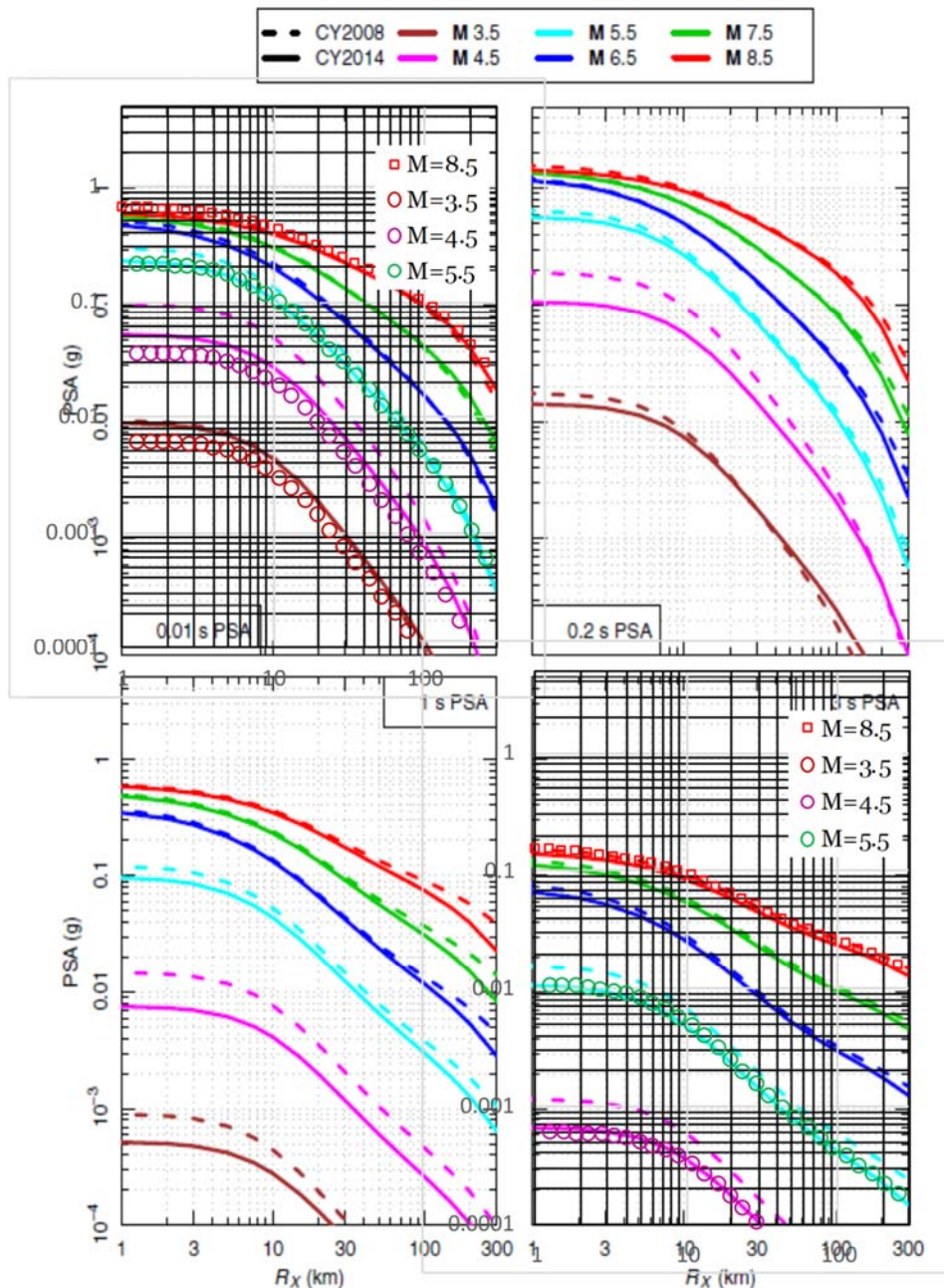


Figure 4-80 Comparison of median values between original and built-in Chiou and Youngs (2008) GMPM. 0.01s and 3.0s

Akkar and Bommer (2010)

The graphical comparison for the Akkar and Bommer (2010) GMPM was made, as shown in Figure 4-81, using as base data Figure 9 of the original publication in Seismological Research Letters. This comparison is made in terms of pseudo-spectral accelerations for rock sites at 10km. The mechanism corresponds to strike slip and three different magnitudes (5.0, 6.3 and 7.6) are used.

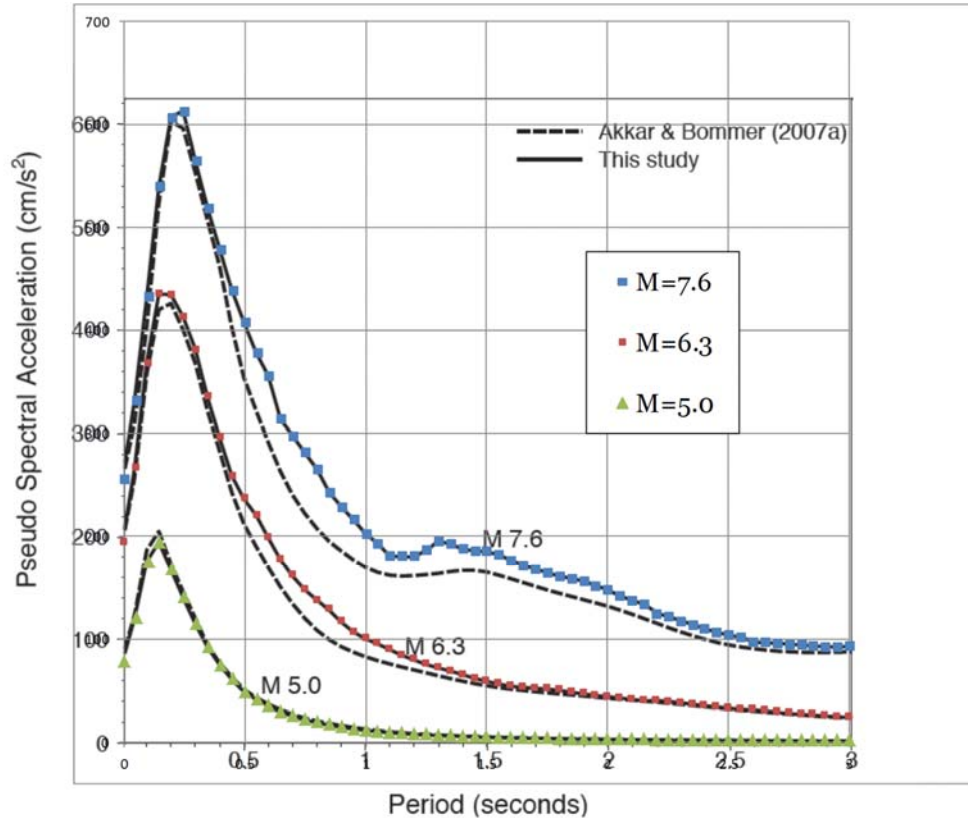


Figure 4-81 Comparison of pseudo spectral accelerations between original and built-in Akkar and Bommer (2010) GMPM

Cauzzi et al. (2017)

The validation of the built-in GMPM has been done for the Cauzzi et al. (2017) case by making graphical comparisons against the original figures provided in the article by the authors as shown in Figures 4-82 and 4-83.

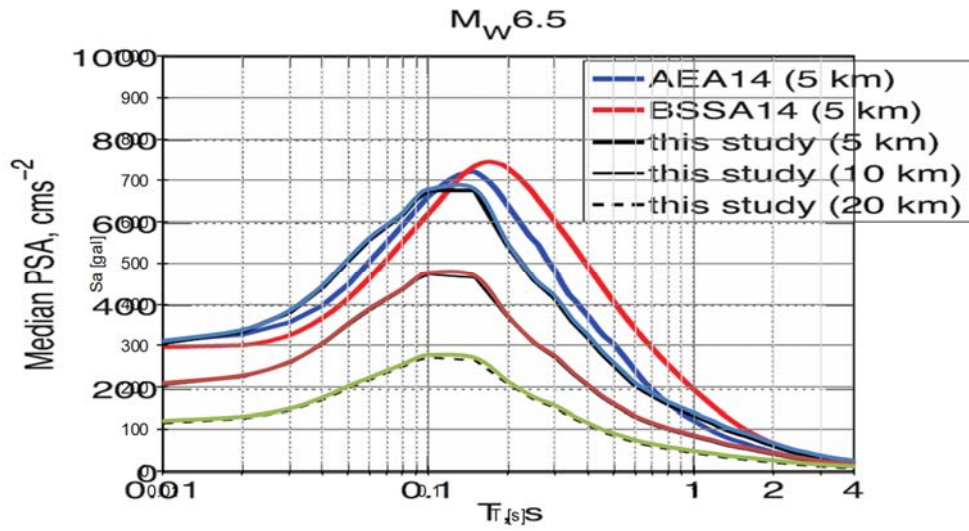


Figure 4-82 Comparison in terms of median PSA spectra at rock sites among the predictive equations of Cauzzi et al. (2017) for Mw 6.5

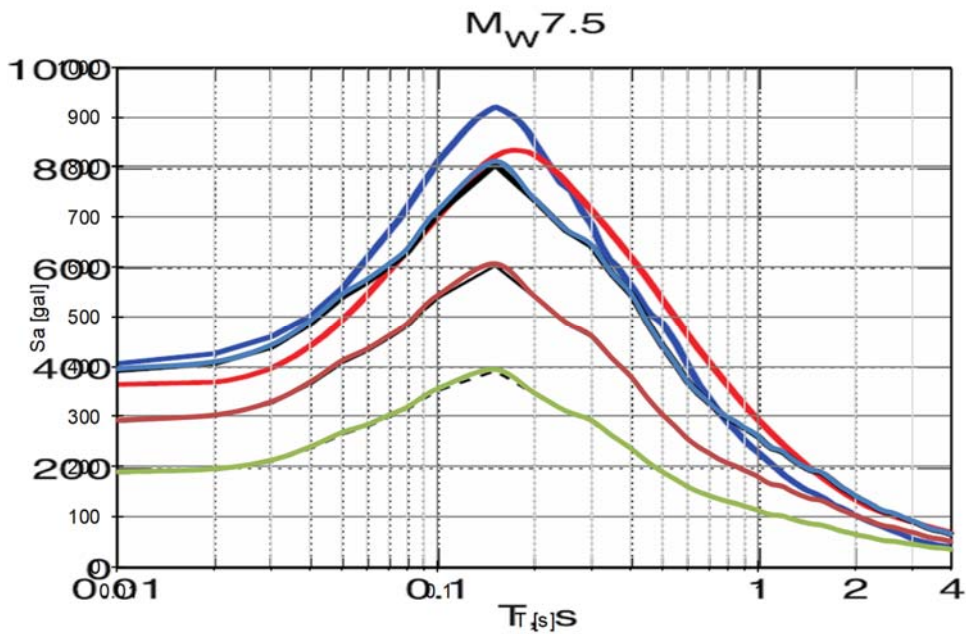


Figure 4-83 Comparison in terms of median PSA spectra at rock sites among the predictive equations of Cauzzi et al. (2017) for Mw 6.5

Montalva et al. (2017)

The validation of the built-in GMPM has been done for the Montalva et al. (2017) case by making graphical comparisons against the original figures provided in the article by the authors as shown in Figures 4-84 to 4-91.

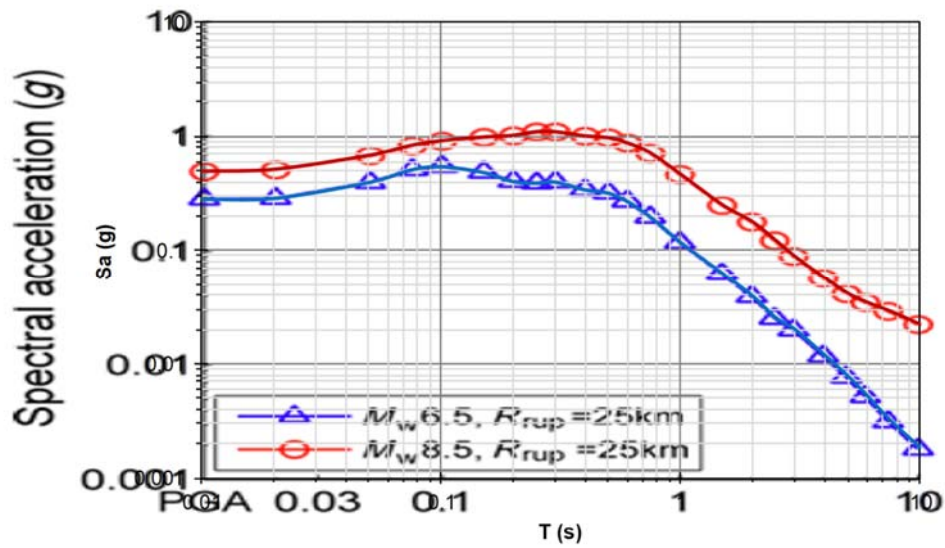


Figure 4-84 Comparison of response spectra for a fore-arc with $V_{s30}=300$ m/s for intraplate earthquake with Montalva et al. 2017 GMPM. $M_w=6.5$ and 8.5 ; $R_{RUP}=25$ km

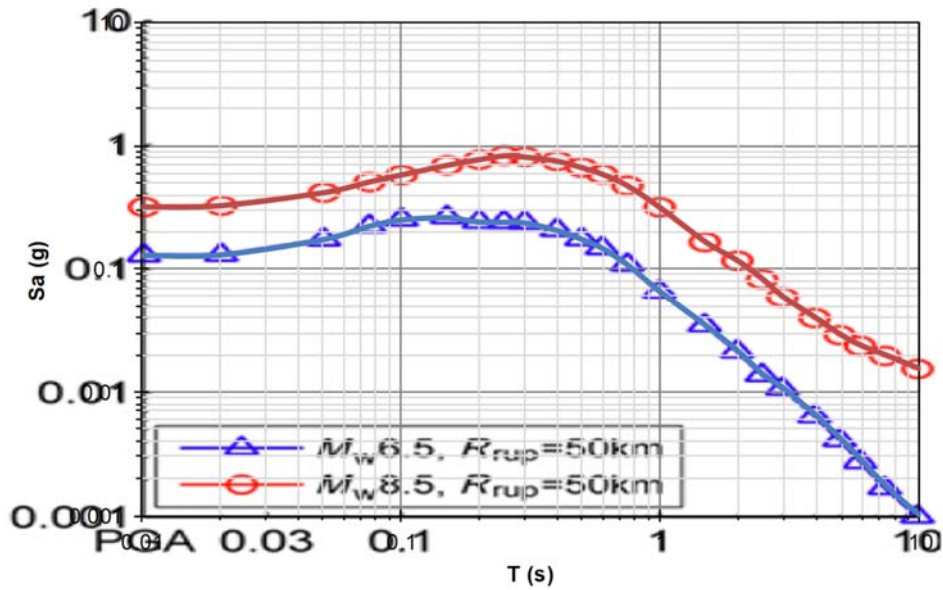


Figure 4-85 Comparison of response spectra for a fore-arc with $V_{s30}=300$ m/s for intraplate earthquake with Montalva et al. 2017 GMPM. $M_w=6.5$ and 8.5 ; $R_{RUP}=50$ km

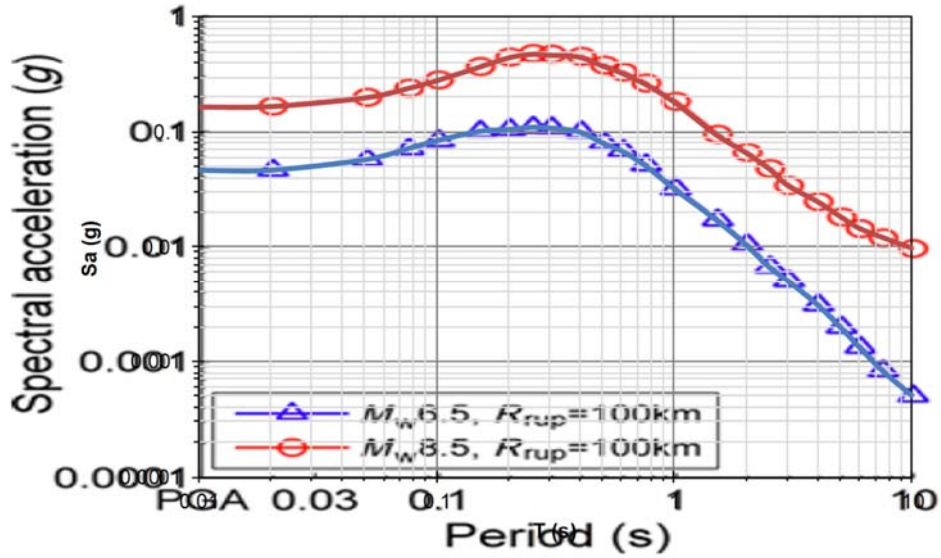


Figure 4-86 Comparison of response spectra for a fore-arc with $V_{s30}=300$ m/s for intraplate earthquake with Montalva et al. 2017 GMPM. $M_w=6.5$ and 8.5 ; $R_{RUP}=100$ km

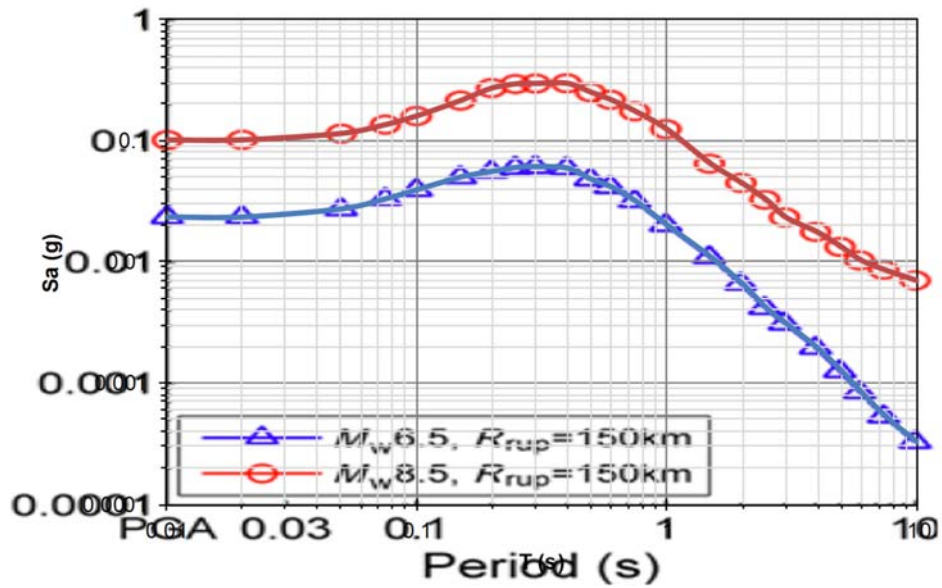


Figure 4-87 Comparison of response spectra for a fore-arc with $V_{s30}=300$ m/s for intraplate earthquake with Montalva et al. 2017 GMPM. $M_w=6.5$ and 8.5 ; $R_{RUP}=150$ km

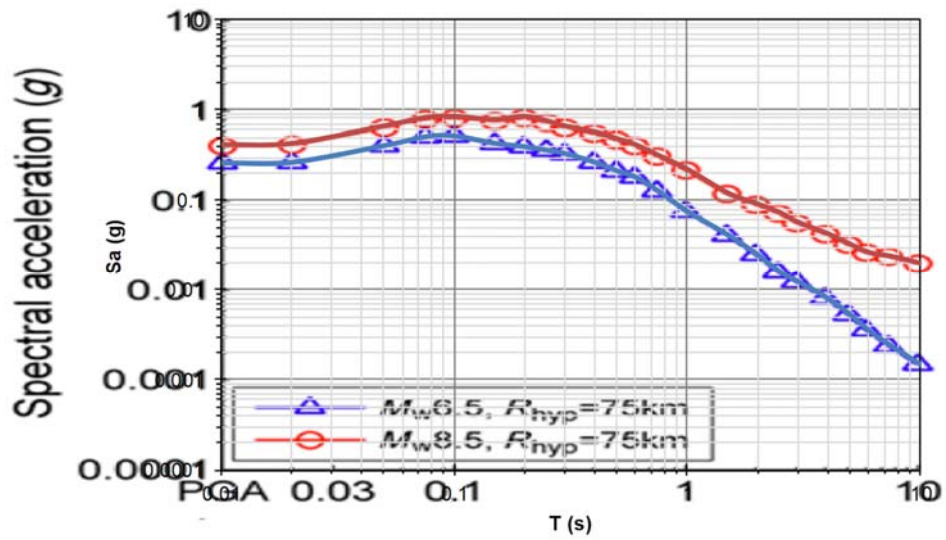


Figure 4-88 Comparison of response spectra for a fore-arc with $V_{s30}=300$ m/s for in-slab earthquake with Montalva et al. 2017 GMPM. $M_w=6.5$ and 8.5 ; $R_F=75$ km

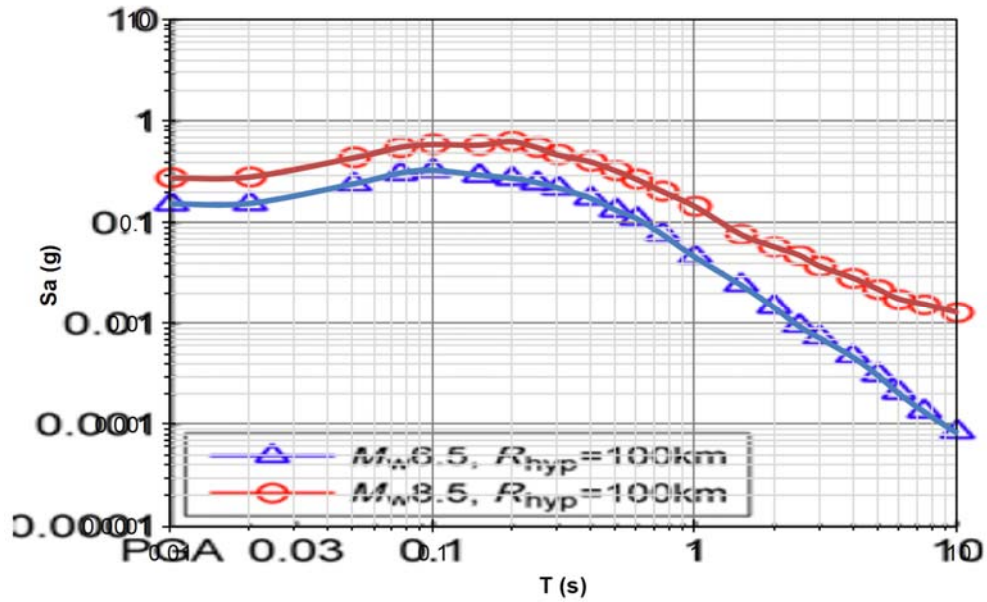


Figure 4-89 Comparison of response spectra for a fore-arc with $V_{s30}=300$ m/s for in-slab earthquake with Montalva et al. 2017 GMPM. $M_w=6.5$ and 8.5 ; $R_F=100$ km

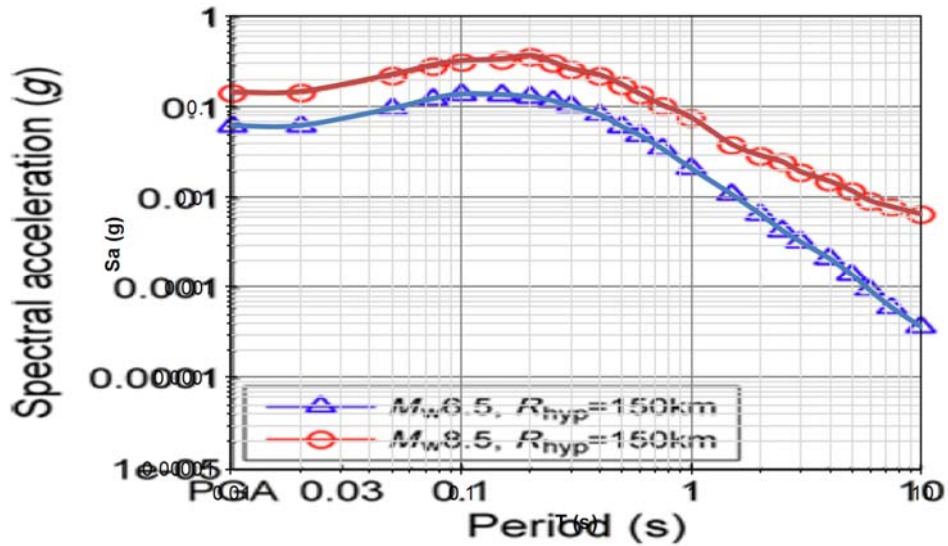


Figure 4-90 Comparison of response spectra for a fore-arc with $V_{s30}=300$ m/s for in-slab earthquake with Montalva et al. 2017 GMPM. $M_w=6.5$ and 8.5 ; $R_r=150$ km

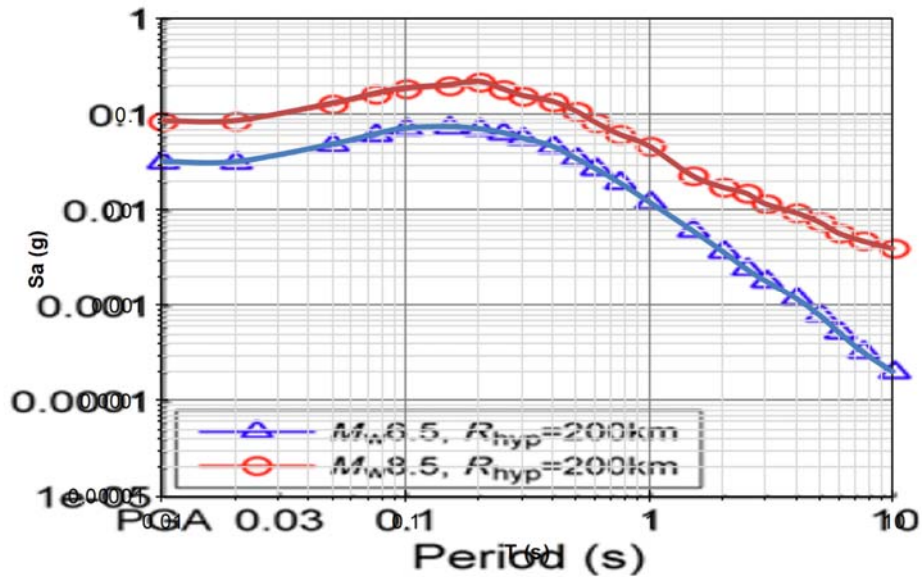


Figure 4-91 Comparison of response spectra for a fore-arc with $V_{s30}=300$ m/s for in-slab earthquake with Montalva et al. 2017 GMPM. $M_w=6.5$ and 8.5 ; $R_r=200$ km

Bindi et al. (2017)

The validation of the built-in GMPM has been done for the Bindi et al. (2017) case by making graphical comparisons against the original figures provided in the article by the authors as shown in Figures 4-92 to 4-94.

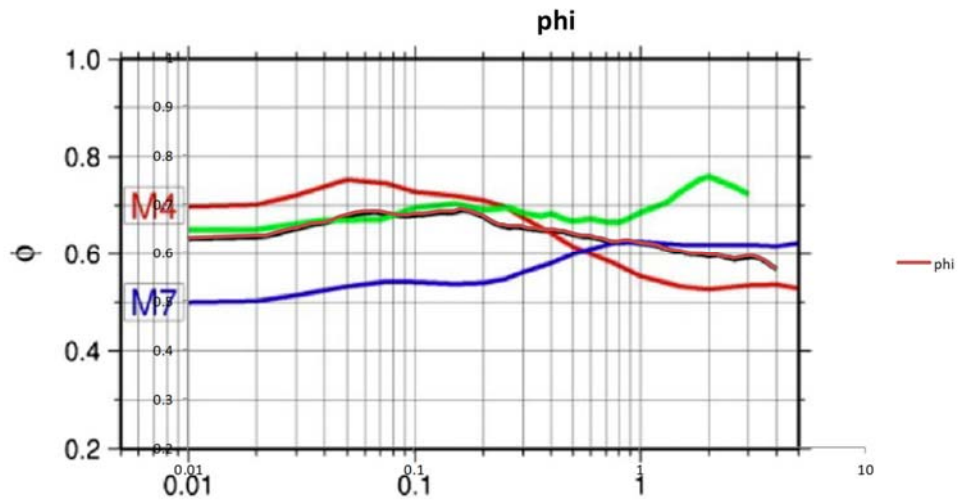


Figure 4-92 Within event standard deviation versus periods for Bindi et al. (2017) GMPM

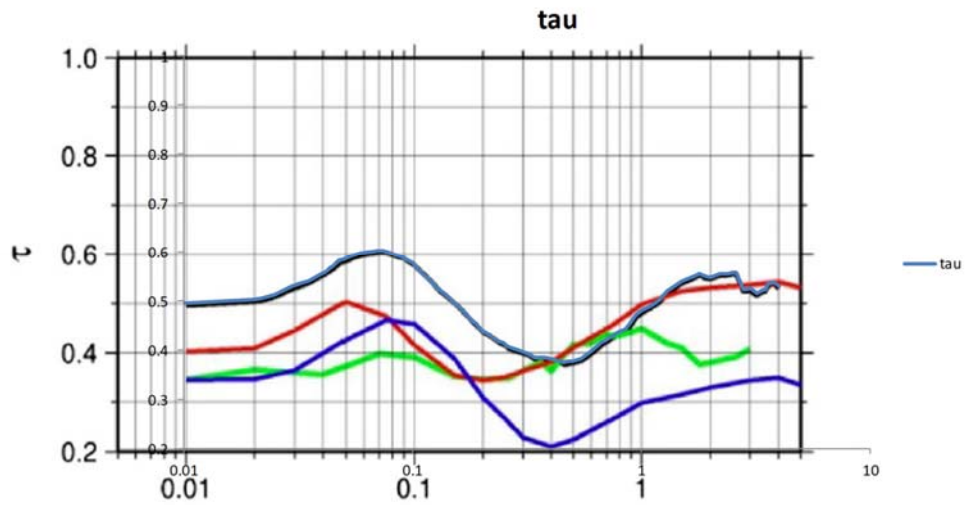


Figure 4-93 Between event standard deviation versus periods for Bindi et al. (2017) GMPM

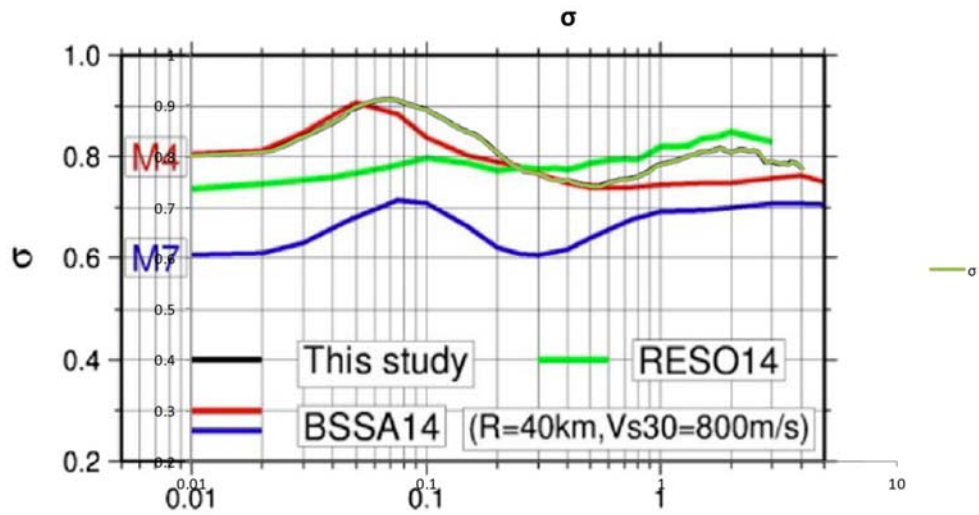


Figure 4-94 Total standard deviation versus periods for Bindi et al. (2017) GMPM

Derras et al. (2014)

The validation of the built-in GMPM has been done for the Derras et al. (2014) case by making graphical comparisons. Figures 4-95 to 4-100 show these comparison in terms of pseudo-spectral accelerations for different magnitude and Vs30 values.

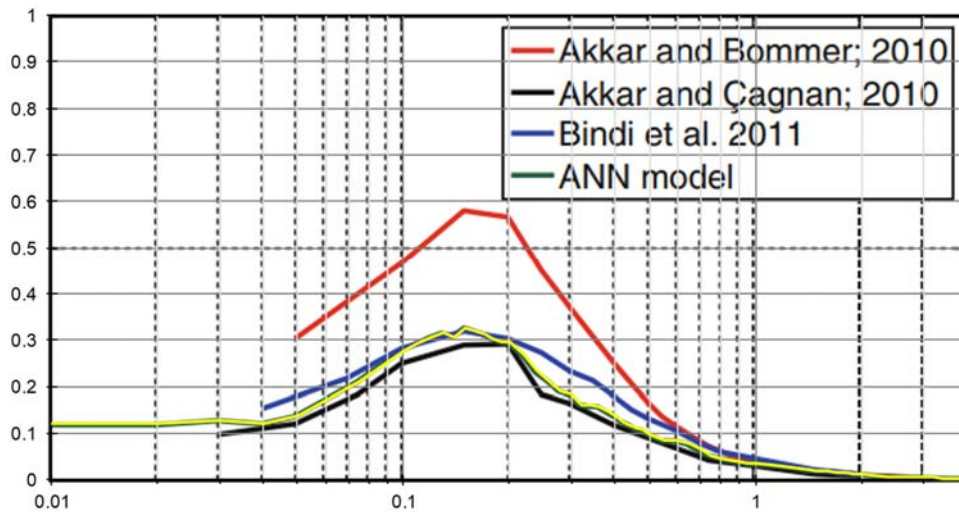


Figure 4-95 Comparison of the period-dependence of median pseudo spectral accelerations derived from Derras et al. (2014) with those proposed in other European GMPEs. Mw=5, Vs30=800m/s

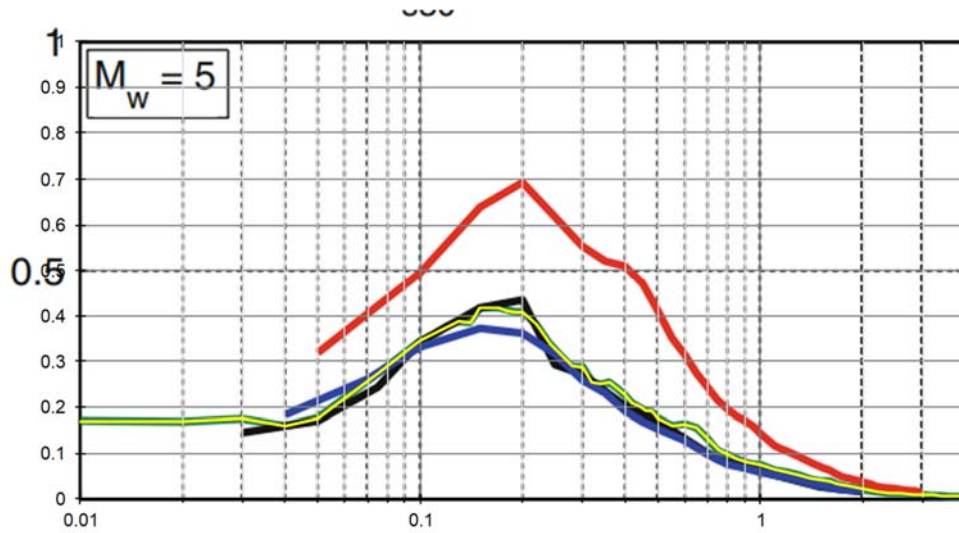


Figure 4-96 Comparison of the period-dependence of median pseudo spectral accelerations derived from Derras et al. (2014) with those proposed in other European GMPEs. $M_w=5$, $V_{s30}=300\text{m/s}$

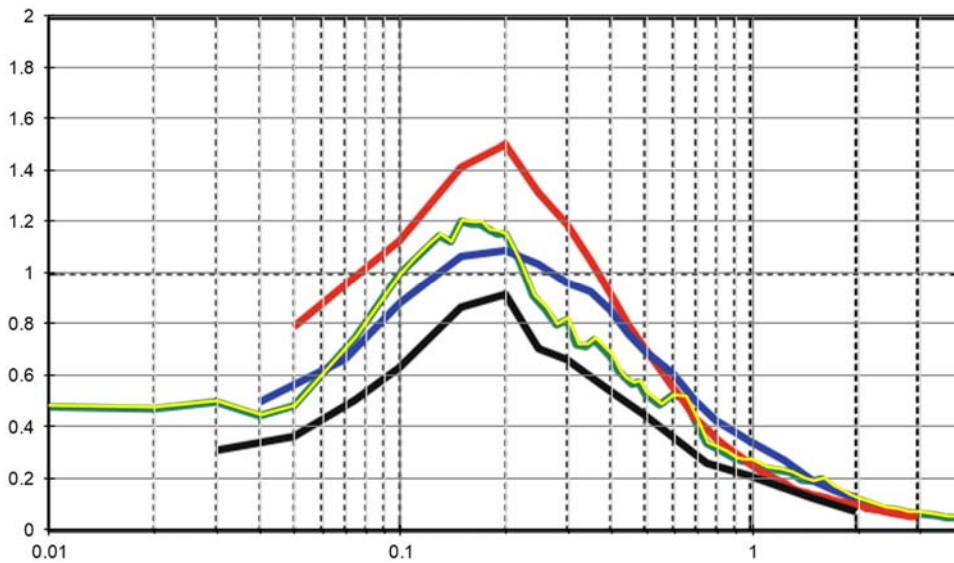


Figure 4-97 Comparison of the period-dependence of median pseudo spectral accelerations derived from Derras et al. (2014) with those proposed in other European GMPEs. $M_w=6$, $V_{s30}=800\text{m/s}$

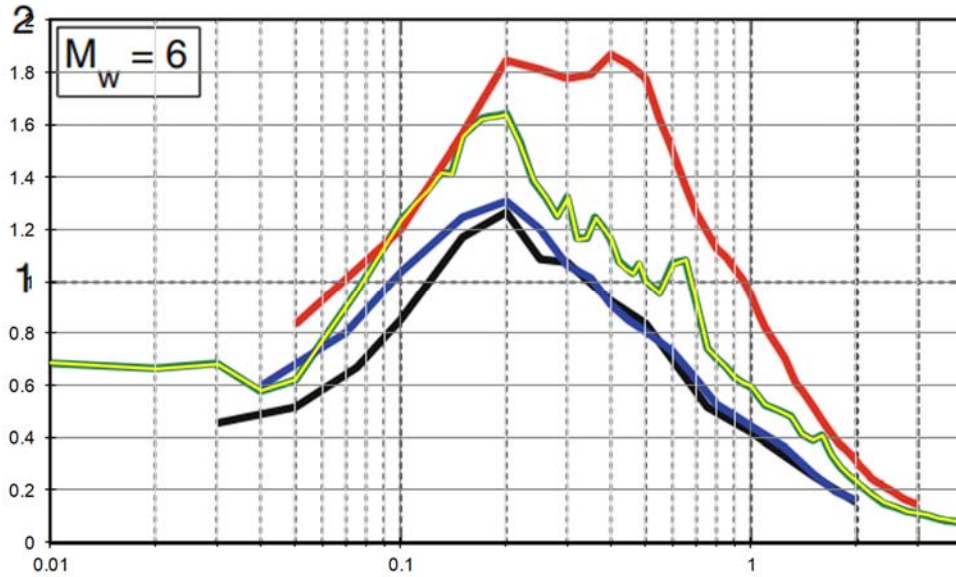


Figure 4-98 Comparison of the period-dependence of median pseudo spectral accelerations derived from Derras et al. (2014) with those proposed in other European GMPEs. $M_w=6$, $V_{s30}=300\text{m/s}$

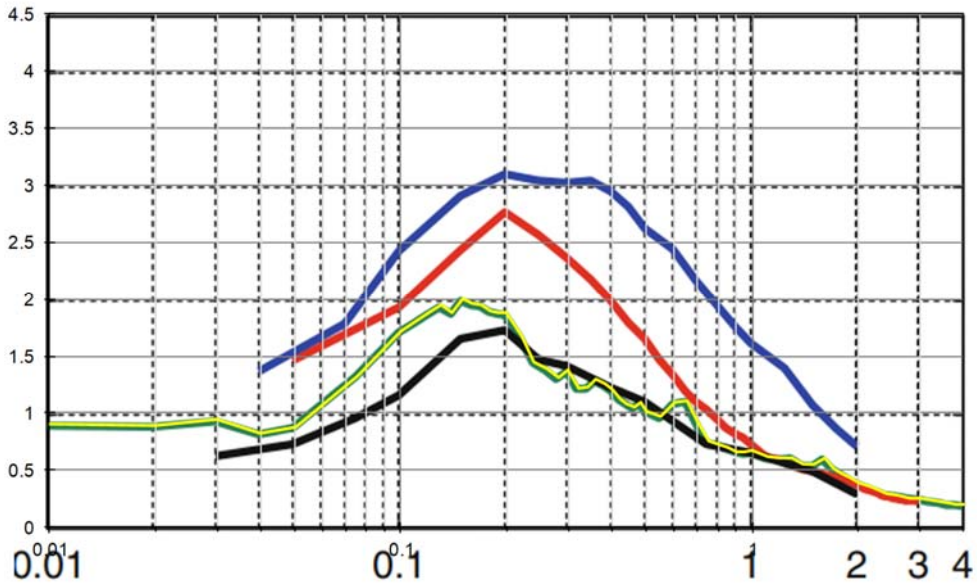


Figure 4-99 Comparison of the period-dependence of median pseudo spectral accelerations derived from Derras et al. (2014) with those proposed in other European GMPEs. $M_w=7$, $V_{s30}=800\text{m/s}$

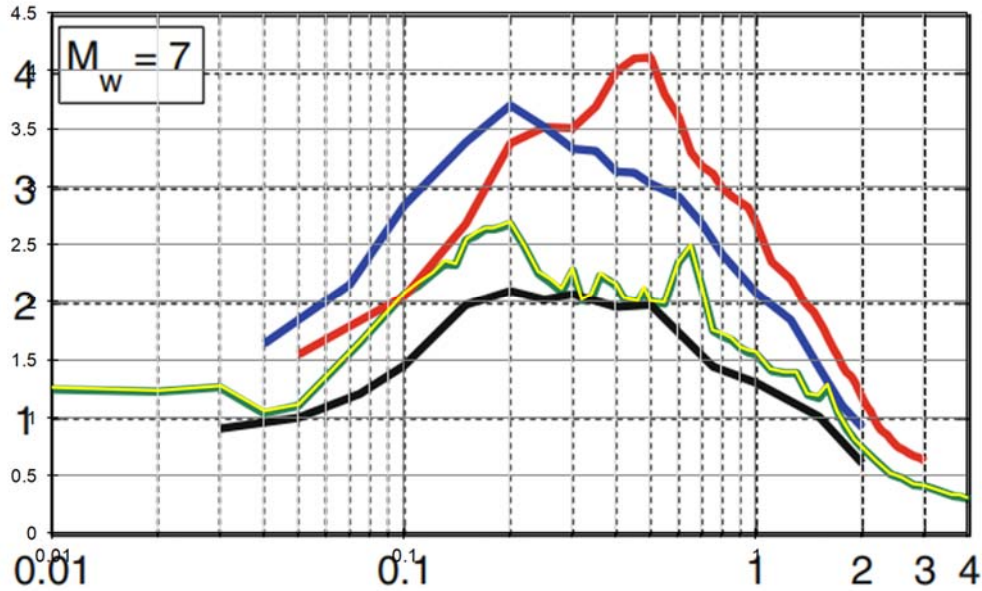


Figure 4-100 Comparison of the period-dependence of median pseudo spectral accelerations derived from Derras et al. (2014) with those proposed in other European GMPEs. $M_w=5$, $V_{s30}=300\text{m/s}$

Pankow and Pechmann (2004)

The validation of the built-in GMPM has been done for the Pankow and Pechmann (2004) case by making graphical comparisons, as shown in Figure 4-101, in terms of peak horizontal velocity as the data provided in the original reference.

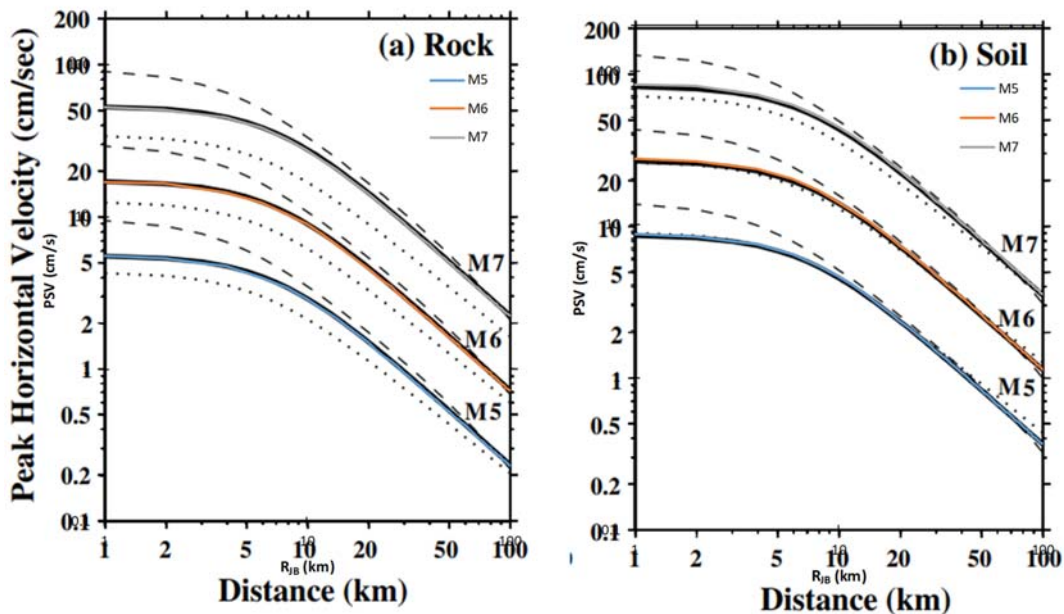


Figure 4-101 Validation of the predictions for peak horizontal velocities for M_w 5.0, 6.0 and 7.0. Left: rock; right: soil

Derras et al. (2016)

The validation of the built-in GMPM has been done for the Derras et al. (2016) case by making graphical comparisons. Figure 4-102 shows the comparison of median spectra for different magnitudes (3.5-7.5) at a stiff site and 30km distance, whereas Figure 4-103 shows the comparison for the total aleatory variability for two magnitudes (4.0 and 7.0) and two site conditions ($V_{s30}=270$ m/s and $V_{s30}=600$ m/s).

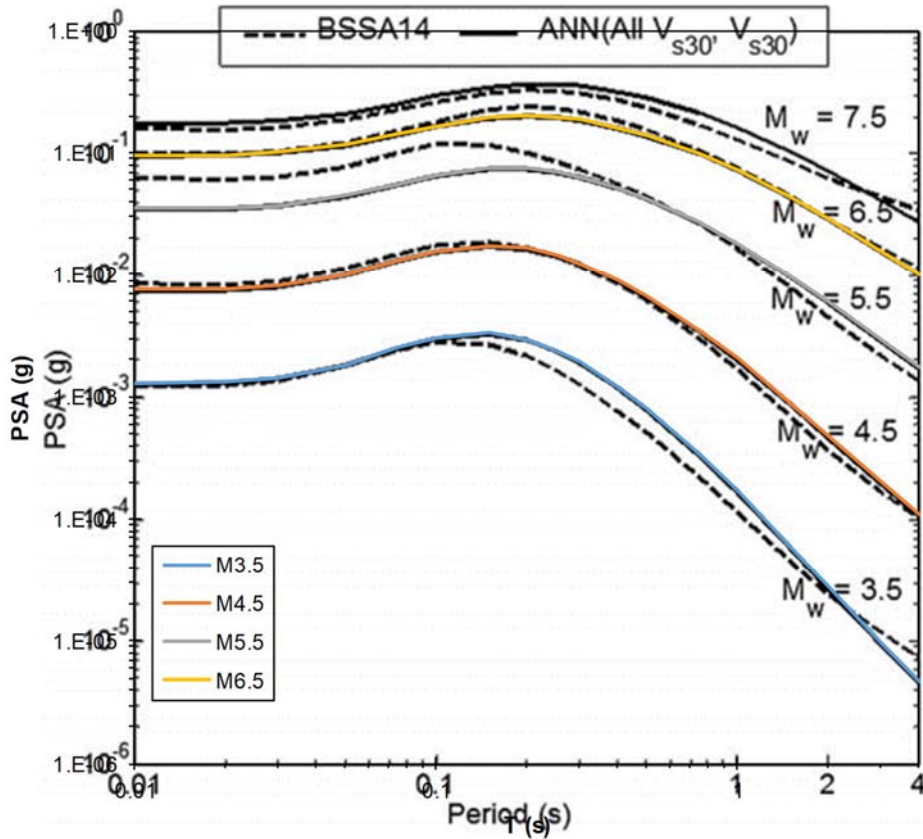


Figure 4-102 Validation of the median spectra predicted for increasing magnitudes at stiff site and 30km distance

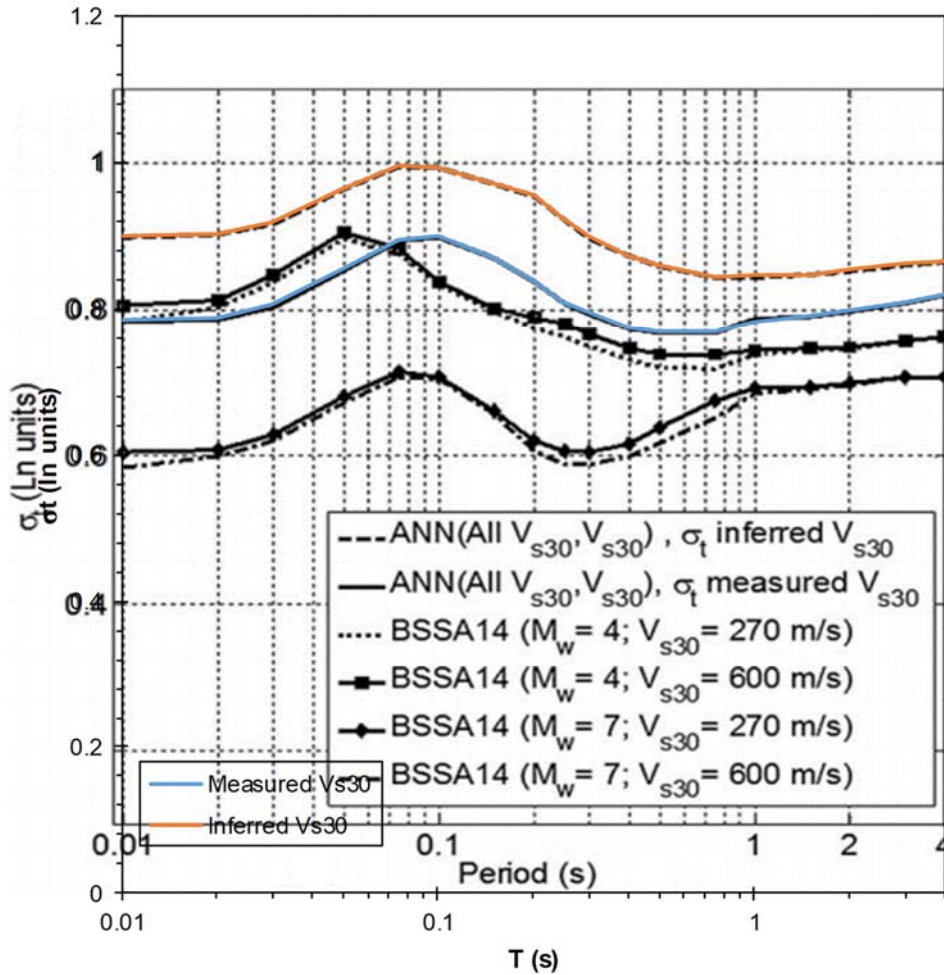


Figure 4-103 Validation of the total aleatory variability for two magnitudes (4.0 and 6.0) and soft and stiff soil conditions

Pezeshk et al. (2018)

The validation of the built-in GMPM has been done for the Pezeshk et al. (2018) in terms of graphical comparisons. Figures 4-104 to 4-106 show these comparisons which are made in terms of the response spectra predicted by the model for different distances and magnitudes using the stochastic and empirical scaling approaches together with the PGA and pseudo-acceleration response spectral values for four spectral ordinates.

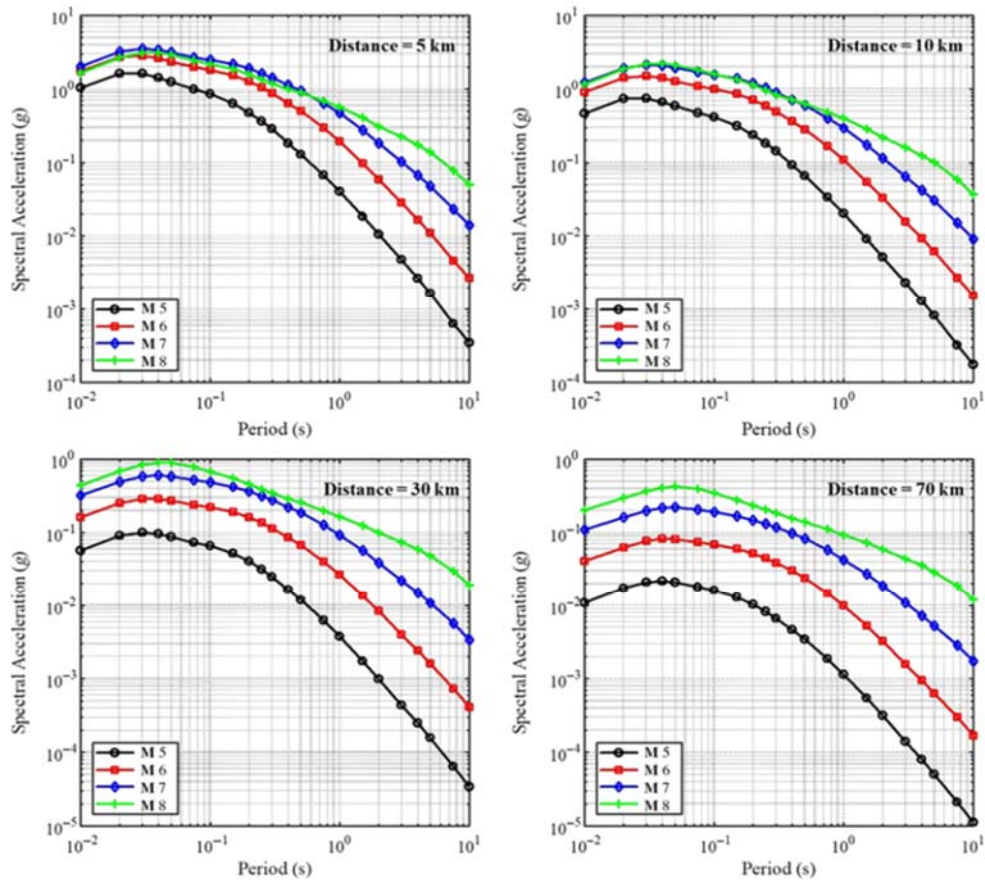


Figure 4-104 Validation of the response spectra predicted by the Pezeshk et al. (2018) GMPM based on the stochastic-scaling approach

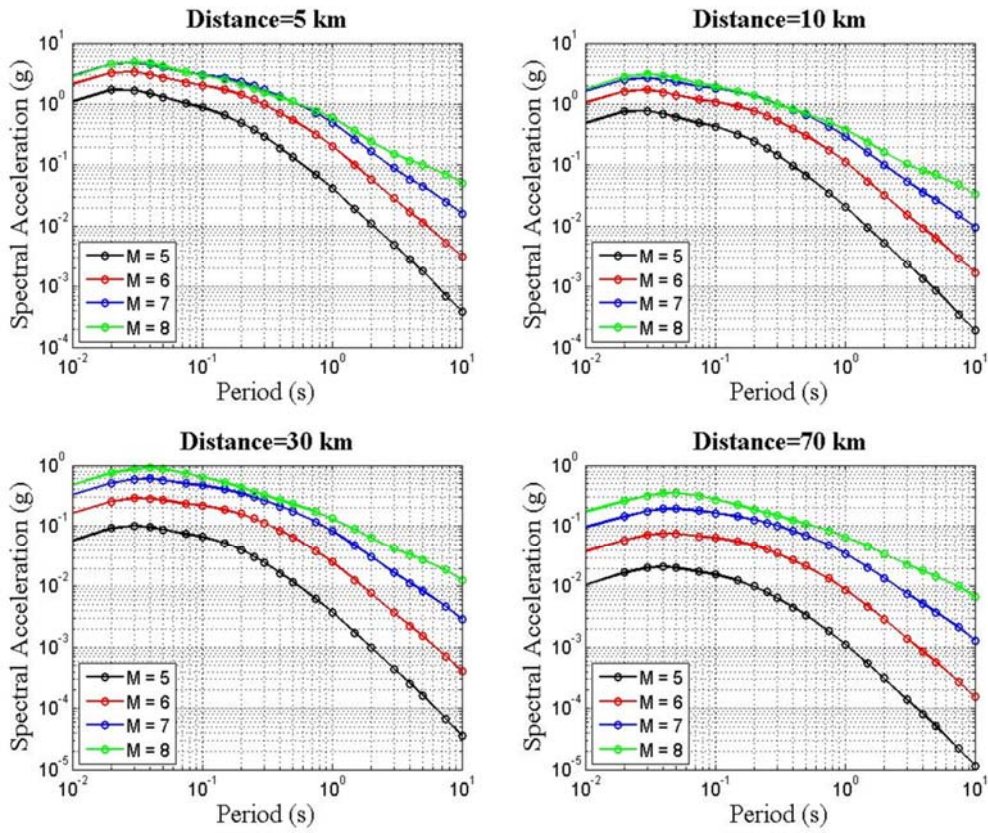


Figure 4-105 Validation of the response spectra predicted by the Pezeshk et al. (2018) GMPM based on the empirical-scaling approach

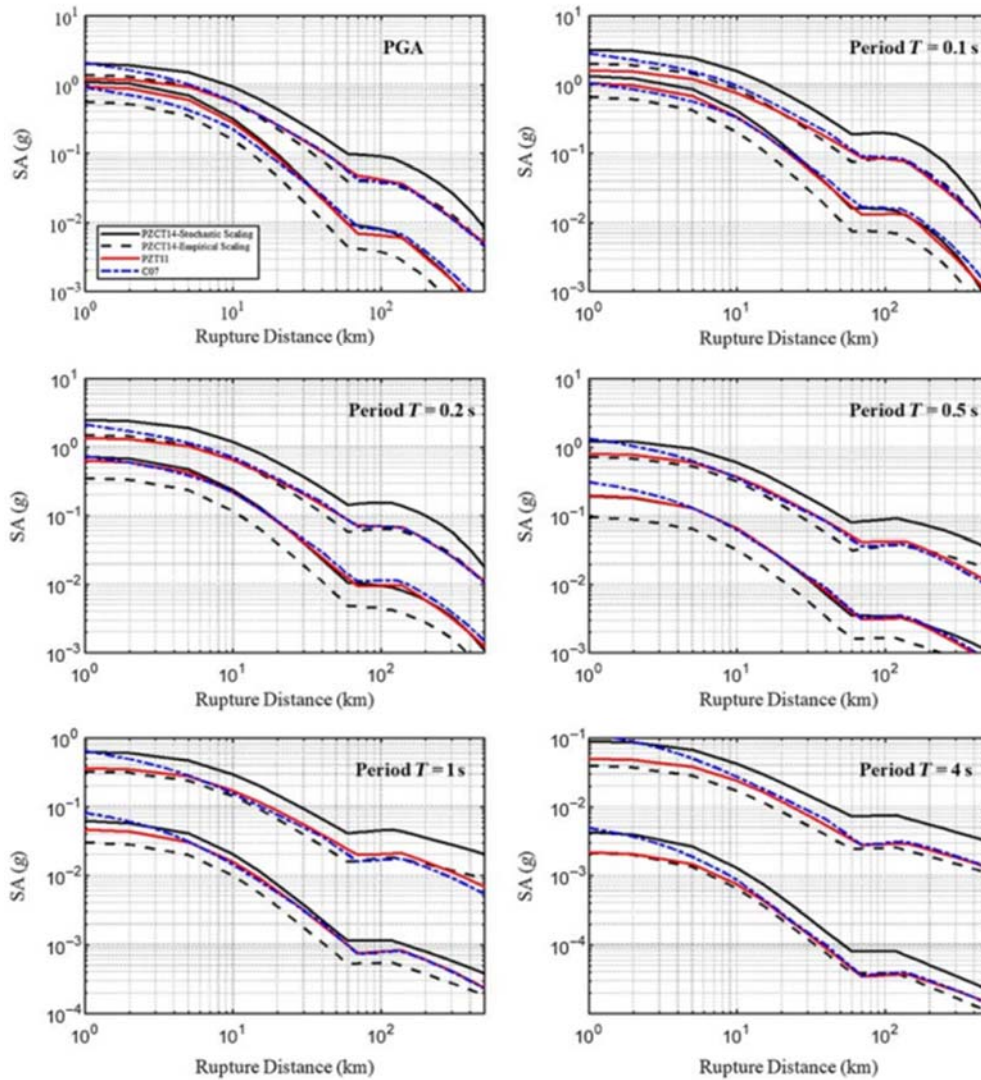


Figure 4-106 Validation of the PGA and PSA for four spectral ordinates

Yenier and Atkinson (2015)

The validation of the Yenier and Atkinson (2015) GMPM has been done for the two regions for which parameters are provided in the article: Central and Eastern North America (CENA) and California. Given that this can be considered as a “plug-and-play” GMPM, CRISIS allows incorporating in a simple manner the calibrated parameters for other regions so that its use can be expanded. Figure 4-107 shows the pseudospectral acceleration for the CENA region for different magnitudes, $d=10\text{km}$ and $V_{s30}=760\text{ m/s}$.

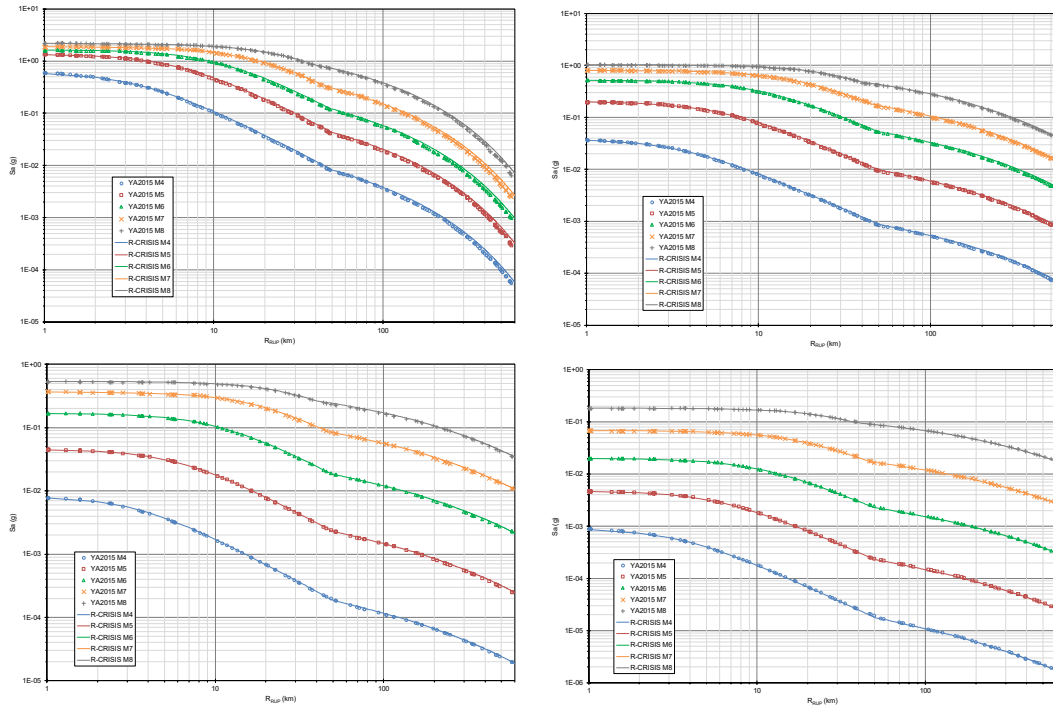


Figure 4-107 Validation of the CENA-adjusted GMPM for T=0.1s (top left), T=0.5s (top right), T=1.0s (bottom left) and T=3.0s (bottom right)

Figure 4-108 shows the validation for the response spectra for CENA and California regions using different D_{RUP} values (10 and 100km).

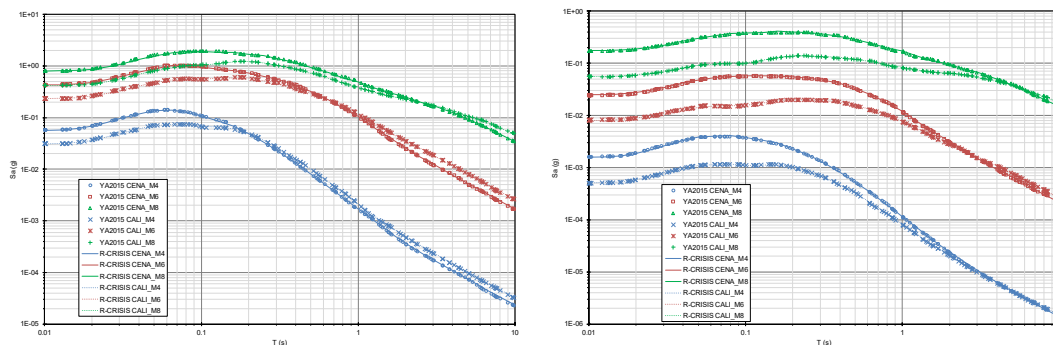


Figure 4-108 Validation of the CENA and California adjusted response spectra for $D_{RUP}=10\text{km}$ (left) and $D_{RUP}=100\text{km}$ (right)

Darzi et al. (2019)

The validation of the Darzi et al. (2019) GMPM has been done in a graphical manner considering the regional and global models. Figure 4-109 shows the PGA values for Mw 5.5 and 7.0, whereas Figure 4-10 shows the pseudo-accelerations for the same magnitudes and T=1.0s.

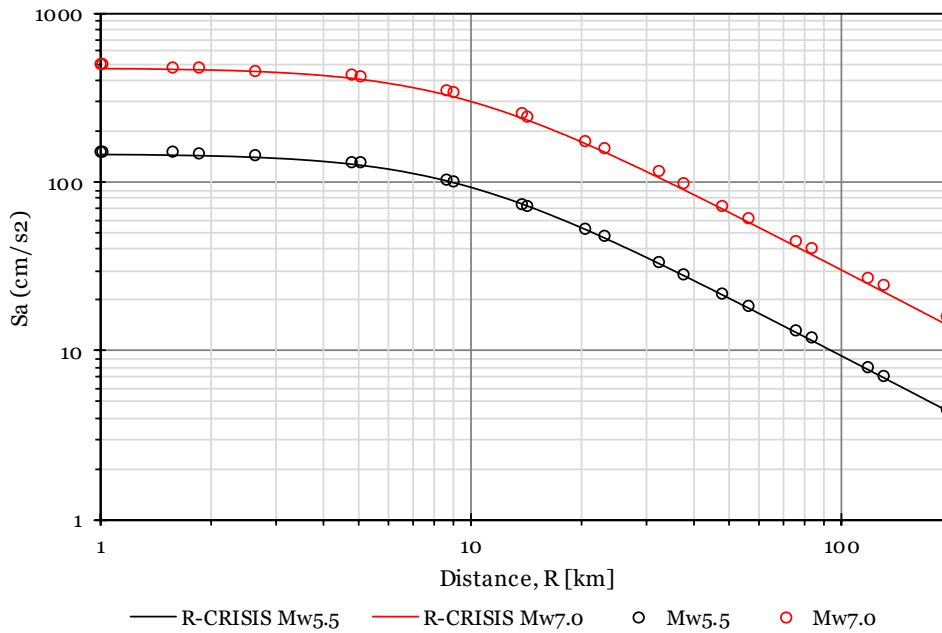


Figure 4-109 Validation of the PGA predictions of the Darzi et al. (2019) model for Mw 5.5 and 7.0

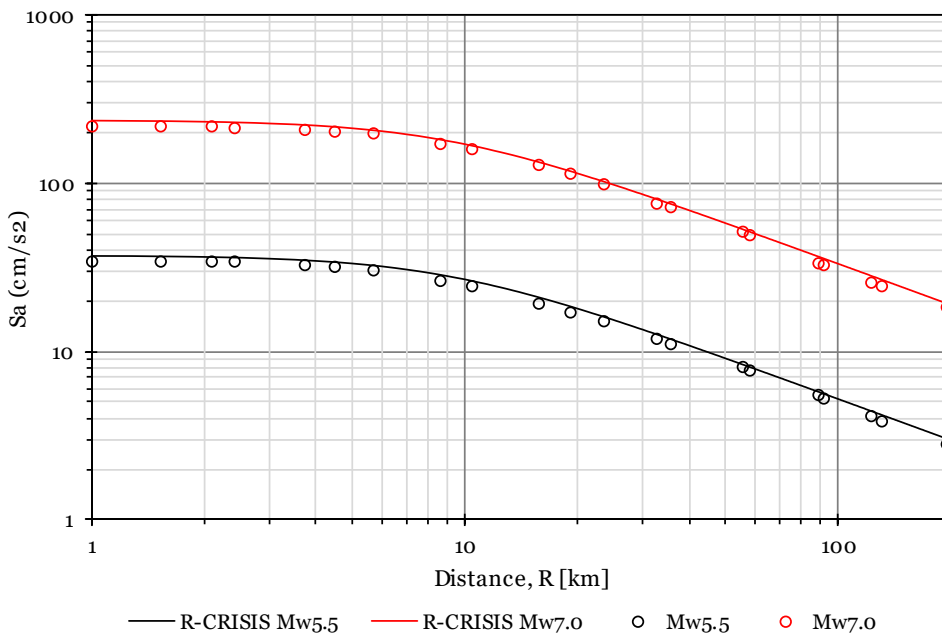


Figure 4-110 Validation of the T=1.0s predictions of the Darzi et al. (2019) model for Mw 5.5 and 7.0

Additionally, the validation of the consideration of different soil conditions was performed, as shown in Figure 4-111 where the median pseudo-acceleration for soil classes I, II and III are shown for $R_{JB}=5\text{km}$ and M_W 5, 6 and 7.

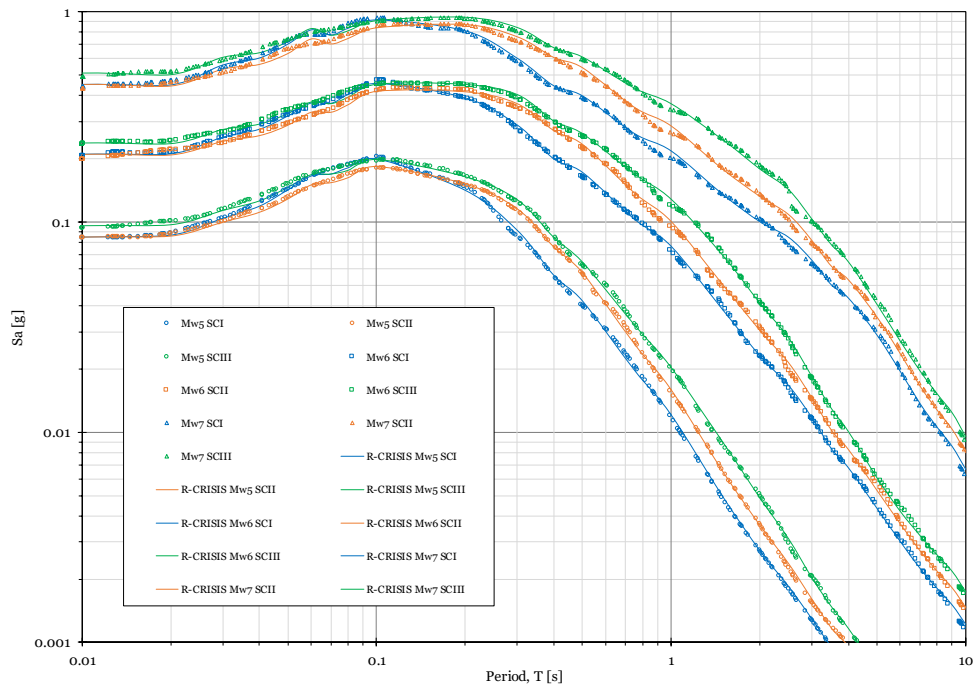


Figure 4-111 Validation of predicted median pseudo-acceleration of the Darzi et al. (2019) model for different soil classes. $R_{JB}=5\text{km}$

Lanzano et al. (2019)

The validation of the Lanzano et al. (2019) GMPM, denoted in the following plots as ITA18, has been performed in a graphical manner. Figure 4-112 shows the predictions of the model for $T=1.0\text{s}$ for Mw 4.0 and 6.8, normal faulting and $V_{s30}=600\text{ m/s}$ whereas Figure 4-113 shows the comparisons for the same spectral ordinate and magnitude values for strike-slip faulting mechanism and $V_{s30}=300\text{ m/s}$.

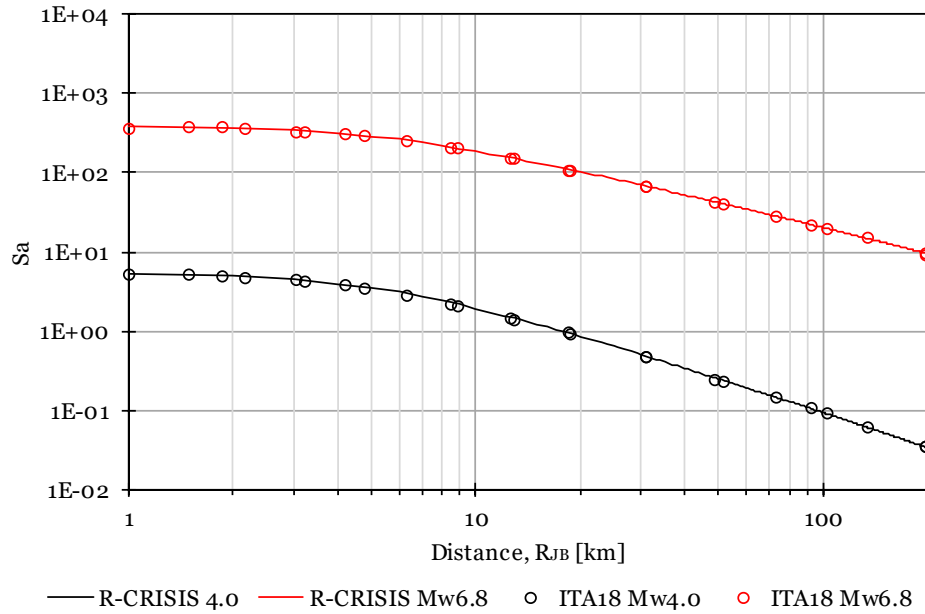


Figure 4-112 Validation of the T=1.0s predictions of the Lanzano et al. (2019) model for Mw 4.0 and 6.8, Vs30=600 m/s and normal faulting mechanism

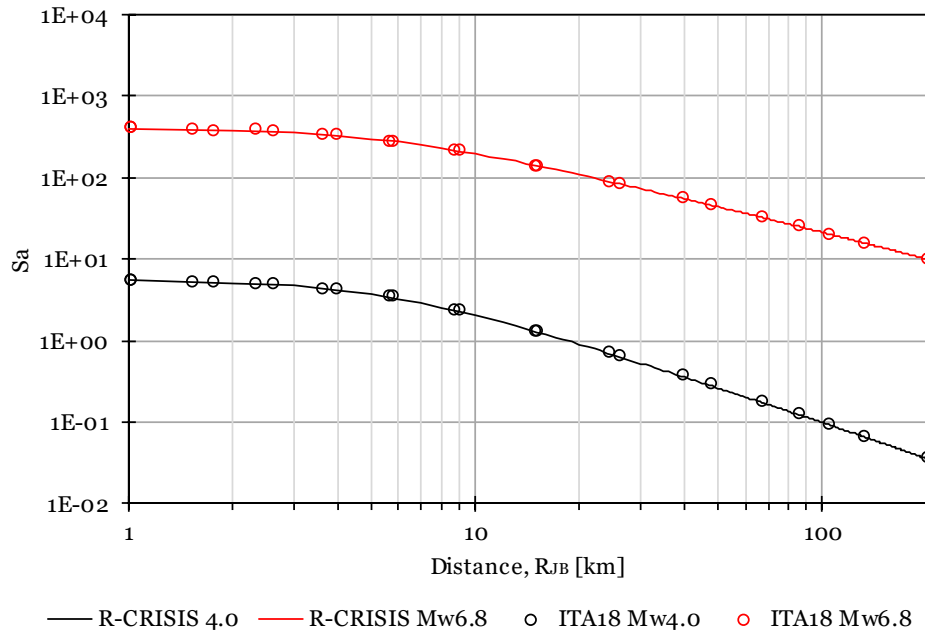


Figure 4-113 Validation of the T=1.0s predictions of the Lanzano et al. (2019) model for Mw 4.0 and 6.8, Vs30=300 m/s and strike-slip faulting mechanism

4.5.3 GMPM where R-CRISIS developers are authors

Since in some of the built-in GMPM the CRISIS developers are authors, those are assumed to have been validated and therefore, well implemented in the program. The GMPM within this category are listed next:

- Arroyo et al. (2010)
- García et al. (2005)
- Jaimes et al. (2006)

4.5.4 GMPM data provided directly by the authors

For some cases, the source code for the GMPM included as built-in models in R-CRISIS has been provided directly by their authors. That is the case of Cauzzi and Faccioli (2008) and Faccioli et al. (2010). In these cases, the GMPM are considered as validated.

4.6 Additional validation tests

4.6.1 Hybrid GMPM vs. Logic trees calculations

The comparison of both approaches has been tested in R-CRISIS using the PEER benchmark -Set 2, case 5b- (Thomas et al., 2014; Hale et al., 2018) in which a particular case among the hybrid GMPM is used. That case corresponds to a *composite model* which in summary is a weighted combination of GMPM with the same mean but different sigma (i.e. unimodal). The following table shows the comparison of the hazard intensity annual exceedance probabilities²² between the results obtained in R-CRISIS after (1): using logic-trees and (2) using a hybrid GMPM – mixture model). From Table 4-63 it can be seen that both approaches yield in the same results.

Table 4-63 Comparison of annual exceedance probabilities with logic-trees and hybrid GMPM approaches

²² This is done in terms of exceedance probabilities for the reasons well explained in Ordaz and Arroyo (2016)

Amax	Annual exceedance probability	
	1	2
1.00E-03	1.590E-02	1.591E-02
1.00E-02	1.590E-02	1.590E-02
5.00E-02	1.410E-02	1.413E-02
1.00E-01	8.880E-03	8.880E-03
2.00E-01	2.740E-03	2.743E-03
4.00E-01	4.380E-04	4.384E-04
6.00E-01	1.210E-04	1.214E-04
8.00E-01	4.380E-05	4.381E-05
1.00E+00	1.850E-05	1.846E-05
1.25E+00	7.240E-06	7.244E-06
1.50E+00	3.190E-06	3.193E-06
2.00E+00	7.910E-07	7.910E-07
2.50E+00	2.450E-07	2.453E-07
3.00E+00	8.900E-08	8.898E-08
4.00E+00	1.620E-08	1.615E-08
5.00E+00	3.930E-09	3.930E-09
6.00E+00	1.170E-09	1.168E-09
7.00E+00	4.020E-10	4.019E-10

Note: when performing these calculations, results compared in terms of exceedance rates may change for the reasons explained in Ordaz and Arroyo (2016).

4.6.2 Verification of the handling of the non-Poissonian occurrence probabilities

The way of computing hazard based on occurrence probabilities of events and probabilities of exceedance of intensity values and not anymore on exceedance rates is checked through a test in which Poissonian probabilities are treated in a non-Poissonian way.

The geometry of the source is very simple: a point source located at a depth of 15km. In spite of this simplicity, the test is general enough since, internally, R-CRISIS performs all the arithmetic related to exceedance probability calculations with discrete point sources. For this example, the computation site is located on the surface of the Earth, 0.2° west and south of the point source.

The seismicity is described by means of a modified G-R relation with $\lambda_0=0.07/\text{year}$, $\beta=2$ (treated as deterministic), $M_0=5$ and $M_U=8$ (treated as deterministic). Once these seismicity parameters are known, it is possible to compute, under the Poissonian assumption, the discrete probabilities of having 0, 1,....., N events in given time frames. These probabilities were externally computed and later provided to R-CRISIS as if they were probabilities obtained from a non-Poissonian model of unspecified type. Results are compared with those obtained providing R-CRISIS the same seismicity parameters in the form of a Poissonian source. Figures 4-114 to 4-116 show these comparisons, for time frames of 20, 50 and 100

years, respectively. In each case, the hazard plots are coincident, which means that the non-Poissonian occurrence probabilities are correctly handled by the R-CRISIS code.

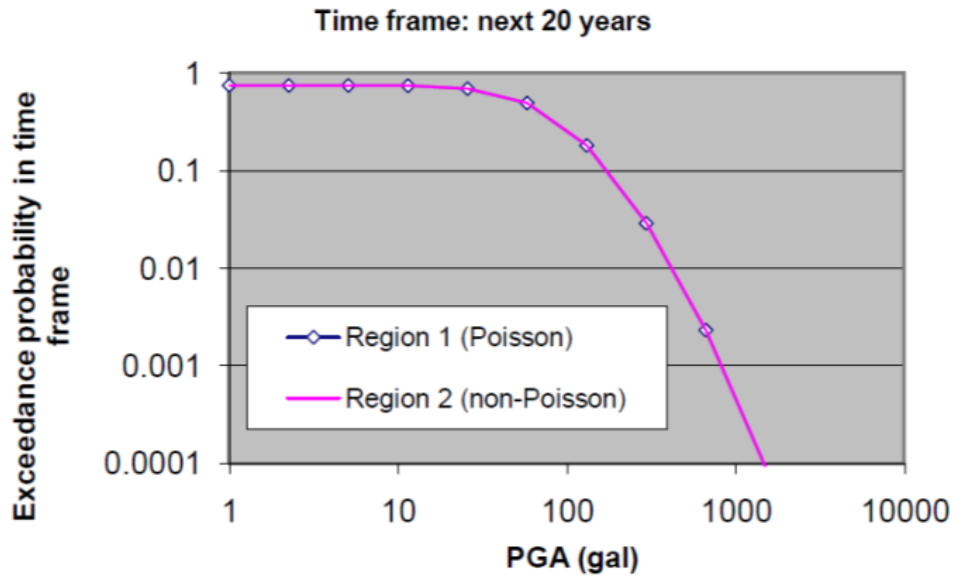


Figure 4-114 Comparison of the results obtained with Poissonian and non-Poissonian sources for 20 years timeframe

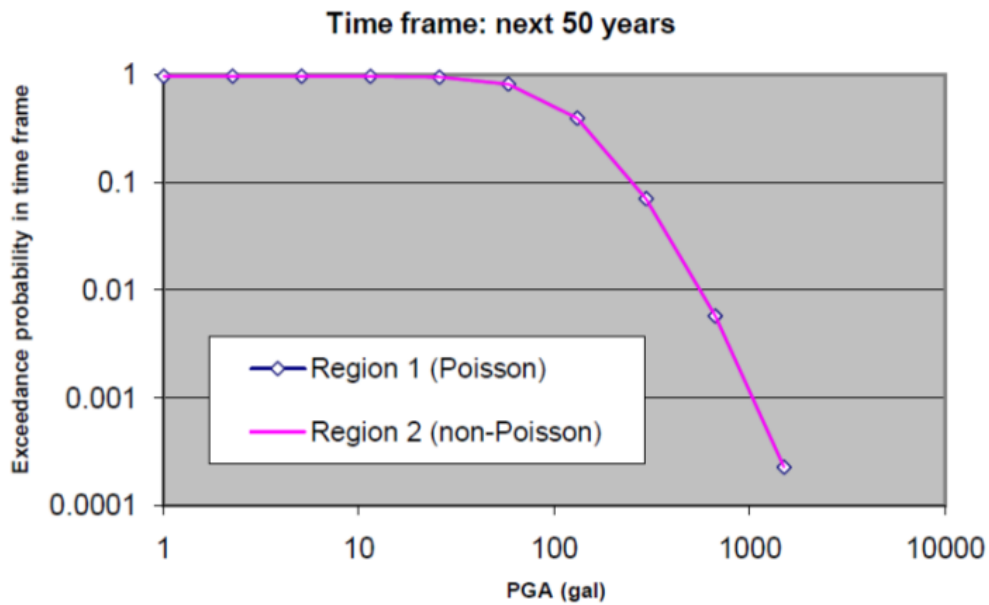


Figure 4-115 Comparison of the results obtained with Poissonian and non-Poissonian sources for 50 years timeframe

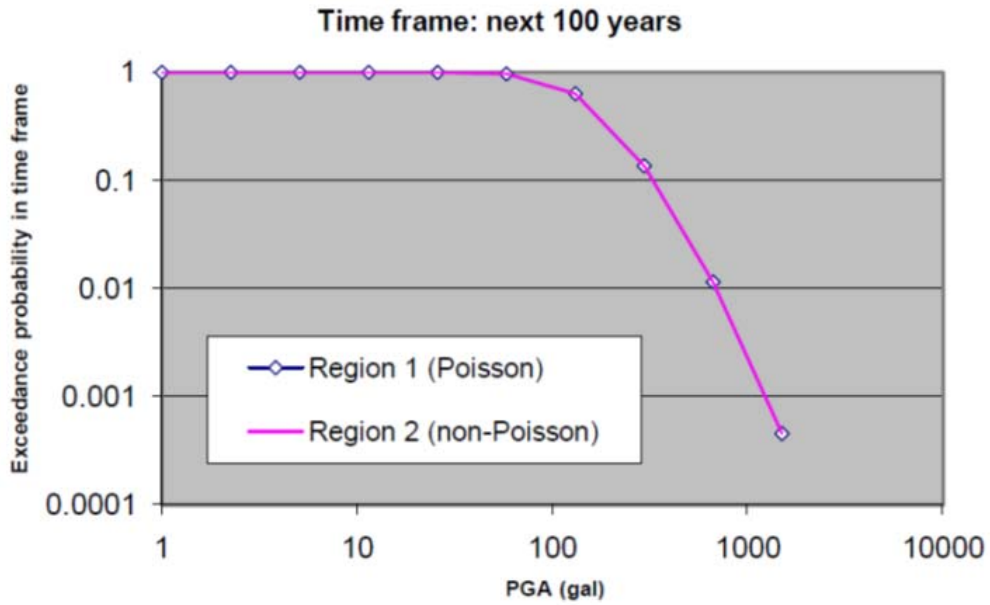


Figure 4-116 Comparison of the results obtained with Poissonian and non-Poissonian sources for 100 years timeframe

5 References

- Abrahamson N.A. and Silva W.J. (1997). Empirical response spectral attenuation relationships for shallow crustal earthquakes. *Seismological Research Letters*. 68:94-127.
- Abrahamson N.A., Silva W.J., and Kamai R. (2014). Summary of the ASK14 Ground Motion Relation for Active Crustal Regions. *Earthquake Spectra*. 30:1025-1055.
- Abrahamson N.A., Gregor N. and Addo K. (2016). B.C. Hydro ground motion prediction equations for subduction earthquakes. *Earthquake Spectra*. 32(1):23-44.
- Akkar S. and Bommer J.J. (2007). Empirical prediction equations for peak ground velocity derived from strong-motions records from Europe and the Middle East. *Bulletin of the Seismological Society of America*. 97:511-530.
- Akkar S. and Bommer J.J. (2010). Empirical equations for the prediction of PGA, PGV and spectral accelerations in Europe, the Mediterranean region and the Middle East. *Seismological Research Letters*. 81:195-206.
- Akkar S., Sandikkaya M.A. and Bommer J.J. (2014). Empirical ground-motion models for point- and extended-source crustal earthquake scenarios in Europe and the Middle East. *Bulletin of Earthquake Engineering*. 12:359-387.
- Ambraseys N.N., Smit P. Douglas J., Margaris B., Sigbjornsson R., Olafsson S., Suhadolc P. and Costa G. (2004). Internet site for European Strong-motion Data. *Bolletino di Geofisica Applicata*. 45(3):113-129.
- Arroyo D., García D., Ordaz M., Mora M.A. and Singh S.K. (2010). Strong ground-motion relations for Mexican interplate earthquakes. *Journal of Seismology*. 14:769-785.
- Atkinson G.M. and Boore D.M. (2003). Empirical ground-motion relations for the subduction-zone earthquakes and their application to Cascadia and other regions. *Bulletin of the Seismological Society of America*. 93:1703-1729.
- Atkinson G.M. and Boore D.M. (2006). Earthquake ground-motion prediction equations for Eastern North America. *Bulletin of the Seismological Society of America*. 96:2181-2205.
- Atkinson G.M. (2008). Ground-motion prediction equations for Eastern North America from a referenced empirical approach: implications for epistemic uncertainty. *Bulletin of the Seismological Society of America*. 98:1304-1318.
- Bajer J.W. and Jayaram N. (2008). Correlation of spectral acceleration values from NGA ground motion models. *Earthquake Spectra*. 24(1):299-317.
- Berge-Thierry C., Cushing E., Scotti O. and Bonilla F. (2004). Determination of the seismic input in France for the Nuclear Power Plants Safety: regulatory context, hypothesis and

uncertainties treatment. Proceedings of the CSNI Workshop on seismic input motions, incorporating recent geological studies. Tsukuba, Japan.

Bindi D., Pacor F., Luzi L., Puglia R., Massa M., Ameri G. and Paolucci R. (2011). Ground-motion prediction equations derived from the Italian strong motion database. *Bulletin of Earthquake Engineering*. 9:1899-1920.

Bindi D., Cotton F., Kotha S.R., Bosse C., Stromeyer D. and Grunthal G. (2017). Application-driven ground motion prediction equation for seismic hazard assessments in non-cratonic moderate-seismicity areas. *Journal of Seismology*. 21(5):1201-1218.

Bommer J.J., Scherbaum F., Bungum H., Cotton F., Sabetta F. And Abrahamson N.A. (2005). On the use of logic trees for ground-motion prediction equations in seismic-hazard analysis. *Bulletin of the Seismological Society of America*. 95(2):377-389.

Boore D.M. and Atkinson G.M. (2008). Ground-motion prediction equations for the average horizontal component of PGA, PGV and 5%-damped PSA at spectral periods between 0.01 s and 10.0 s. *Earthquake Spectra*. 24:99-138.

Boore D.M., Stewart J.O., Seyhan E. and Atkinson G.M. (2014). NGA-West2 Equations for Predicting PGA, PGV, and 5% Damped PSA for Shallow Crustal Earthquakes. *Earthquake Spectra*. 30:1057-1085.

Brune J.N. (1970). Tectonic stress and the spectra of seismic shear waves from earthquakes. *Journal of Geophysical Research*. 75(26):4997-5009.

Campbell K.W. (2003). Prediction of strong ground motion using the hybrid empirical method and its use in the development of ground-motion (attenuation) relations in Eastern North America. *Bulletin of the Seismological Society of America*. 93:1012-1033.

Campbell K.W. and Bozorgnia Y. (2003). Updated near-source ground motion (attenuation) relations for the horizontal and vertical components of peak ground acceleration and acceleration response spectra. *Bulletin of the Seismological Society of America*. 93:315-331.

Campbell, K.W. and Bozorgnia, Y. (2008). NGA ground motion model for the geometric mean horizontal component of PGA, PGV, PGD and 5% damped linear elastic response spectra for periods ranging from 0.1 to 10s. *Earthquake Spectra*. 24:139-171.

Campbell K.W. and Bozorgnia Y. (2014). NGA-West2 Ground Motion Model for the Average Horizontal Components of PGA, PGV and 5% Damped Linear Acceleration Response Spectra. *Earthquake Spectra*. 30:1087-1115.

Cauzzi C. and Faccioli E. (2008). Broadband (0.05 to 20 s) prediction of displacement response spectra based on worldwide digital records. *Journal of Seismology*. 12:453-475.

- Cauzzi C., Faccioli E., Vanini M. and Bianchini A. (2015). Updated predictive equations for broadband (0.01-10 s) horizontal response spectra and peak ground motions, based on a global dataset of digital acceleration records. *Bulletin of Earthquake Engineering*. 13(6): 1587-1612.
- Chávez J.A. (2006). Attenuation relationships for spectral acceleration in Peru. National University of Engineering, Faculty of Civil Engineering. Lima, Peru.
- Chiou B. and Youngs R. (2008). An NGA model for the average horizontal component of peak ground motion and response spectra. *Earthquake Spectra*. 24:173-215.
- Chiou B. and Youngs R. (2014). Update of the Chiou and Youngs NGA Model for the Average Horizontal Component of Peak Ground Motion and Response Spectra. *Earthquake Spectra*. 30:1117-1153.
- Climent A., Taylor W., Ciudad Real M., Strauch W., Villagran M., Dahle A. and Bungum H. (1994). Spectral strong motion attenuation in Central America. NORSAR Technical Report No. 2-17.
- Contreras V. and Boroschek R. (2012). Strong ground motion attenuation relations for Chilean Subduction Zone Interface Earthquakes. *Proceedings of the 15th World Conference on Earthquake Engineering*. Lisbon, Portugal.
- Cornell C.A. (1968). Engineering seismic risk analysis. *Bulletin of the Seismological Society of America*. 58(5):1583-1606.
- Cornell, C. A., and Vanmarke E. H. (1969). The major influences on seismic risk, in *Proceedings of the 3rd World Conference on Earthquake Engineering*, Santiago, Chile.
- Darzi A., Zolfaghari M.R., Cauzzi C. and Fah D. (2019). An empirical ground-motion model for horizontal PGV, PGA and 5% damped elastic response spectra (0.01-10 s) in Iran. *Bulletin of the Seismological Society of America*. In press. DOI: 10.1785/0120180196.
- Department of Defense (1997). *World Geodetic System 1984, Its definition and relationships with local geodetic systems*. NIMA Technical Report TR8350.2, Third Edition. USA.
- Derras B., Bard P.Y. and Cotton F. (2014). Towards fully data driven ground-motion prediction models for Europe. *Bulletin of Earthquake Engineering*. 12(1):495-516.
- Derras B., Bard P.Y. and Cotton F. (2016). Site-condition proxies, ground motion variability, and data-driven GMPEs: Insights from the NGA-West2 and RESOURCE data sets. *Earthquake Spectra*. 32(4):2027-2056.
- EPRI – Electrical Power Research Institute (2006). Program on technology innovation: use of the cumulative absolute velocity (CAV) in determining effects of small magnitude earthquakes on seismic hazard analyses. Report No. 1014099. California, USA.

- Esteva L. (1970). Regionalización sísmica de México para fines de ingeniería. Instituto de Ingeniería. Universidad Nacional Autónoma de México.
- Faccioli E., Bianchini A. and Villani M. (2010). New ground motion prediction equations for $T > 1s$ and their influence on seismic hazard assessment. Proceedings of the University of Tokyo Symposium on Long-Period Ground Motion and Urban Disaster Mitigation. Tokyo, Japan.
- García D., Singh S.K., Herráiz M., Ordaz M. and Pacheco J.F. (2005). Inslab earthquakes of Central Mexico: Peak ground-motion parameters and response spectra. Bulletin of the Seismological Society of America. 95:2272-2282.
- Gómez A.A. (2017). Macroseismic intensity attenuation model for Italy and Colombia. Istituto Nazionale di Geofisica e Vulcanologia, sezione di Milano.
- Hale C., Abrahamson N. and Bozorgnia Y. (2018). Probabilistic seismic hazard analysis code verification. PEER Report 2018/03. Pacific Earthquake Engineering Research Center. Berkeley, California, USA.
- Hanks T.C. and Kanamori H. (1979). A moment magnitude scale. Journal of Geophysical Research: Solid Earth. 84(B5):2348-2350.
- Idriss, I. (2008). An NGA Empirical Model for Estimating the Horizontal Spectral Values Generated By Shallow Crustal Earthquakes. Earthquake Spectra. 24:217-242.
- Idriss I. (2014). An NGA-West2 Empirical Model for Estimating the Horizontal Spectral Values Generated by Shallow Crustal Earthakes. Earthquake Spectra. 30:1155-1177.
- IRSN (2005). Propositions pour la sélection et la génération d'accélérogrammes intégrant la variabilité des indicateurs du mouvement sismique. Rapport DEI/SART/2005-022.
- Jaimes M., Reinoso E., Ordaz M. (2006). Comparison of methods to predict response spectra at instrumented sites given the magnitude and distance of an Earthquake. Journal of Earthquake Engineering. 10:887-902.
- Jaimes M.A., Ramírez-Gaytán A. and Reinoso E. (2015). Ground-motion prediction model from intermediate-depth intraslab earthquakes at the hill and lake-bed zones of Mexico City. Journal of Earthquake Engineering. 19(8):1260-1278.
- Jaimes M.A. and Candia G. (2019). Interperiod correlation model for Mexican interface earthquakes. Earthquake Spectra. 35(3):1351-1365.
- Kanno T., Narita A., Moriwawa N., Fujiwara H. and Fukushima Y. (2006). A new attenuation relation for strong ground motion in Japan based on recorded data. Bulletin of the Seismological Society of America. 96:879-897.

- Kostov M. (2005). Site specific estimation of cumulative absolute velocity. Proceedings of the 18th international conference on structural mechanics in reactor technology. Beijing, China.
- Ku C.S., Juang C.H., Chang C.W. and Ching J. (2012). Probabilistic version of the Robertson and Wride method for liquefaction evaluation: development and application. Canadian Geotechnical Journal. 49(1):27-44.
- Lanzano G., Luzi L., Pacor F., Felicetta C., Puglia R., Sgobba S. and D'Amico M. (2019). A revised ground-motion prediction model for shallow crustal earthquakes in Italy. Bulletin of the Seismological Society of America. 109(2):525-540.
- Lin P-S., and Lee C-T. (2008). Ground-motion attenuation relationships for subduction-zone earthquakes in Northeastern Taiwan. Bulletin of the Seismological Society of America. 98:220-240.
- Lin T., Harmsen S.C., Baker J.W. and Luco N. (2013). Conditional spectrum computation incorporating multiple causal earthquakes and ground-motion prediction models. Bulletin of the Seismological Society of America. 103(2A):1103-1116.
- McGuire R.K. (2004). Seismic hazard and risk analysis. Earthquake Engineering Research Institute. Oakland, California, USA.
- McVerry G.H., Zhao J.X., Abrahamson N.A. and Somerville P.G. (2006). New Zealand acceleration response spectrum attenuation relations for crustal and subduction zone earthquakes. Bulletin of the New Zealand National Society for Earthquake Engineering. 39:1-58.
- Montalva G.A., Bastías N. and Rodríguez-Marek A. (2017). Ground-motion prediction equation for the Chilean Subduction Zone. Bulletin of the Seismological Society of America. 107(2): 901-911.
- Newmark N.M and Rosenblueth E. (1971). Fundamentals of earthquake engineering. Prentice-Hall. Englewood Cliffs, New Jersey, United States of America.
- Ordaz M. (1991). CRISIS. Brief description of program CRISIS, Internal report. Institute of Solid Earth Physics. University of Bergen, Norway, 16pp.
- Ordaz M. (1999). User's manual for program CRISIS1999. Technical report. Universidad Nacional Autónoma de México. Mexico City, Mexico.
- Ordaz M. (2004). Some integrals useful in probabilistic seismic hazard analysis. Bulletin of the Seismological Society of America. 94(4):1510-1516.
- Ordaz M., Jara J.M. and Singh S.K. (1989). Seismic risk and design spectra for the State of Guerrero. Report 8782. Instituto de Ingeniería. Universidad Nacional Autónoma de México. Mexico City, Mexico.

- Ordaz M. and Aguilar A. (2015). Validation of R-CRISIS code. Technical Report. Instituto de Ingeniería, Universidad Nacional Autónoma de México. Mexico City, Mexico.
- Ordaz M. and Arroyo D. (2016). On uncertainties in PSHA. *Earthquake Spectra*. 32(3):1405-1418.
- Pankow K.L. and Pechmann J.C. (2004). The SEA99 Ground-motion predictive relations for extensional tectonic regimes: revisions and a new peak ground velocity relation. *Bulletin of the Seismological Society of America*. 94(1):341-348.
- Pasolini C., Albarello D., Gasperini P., D'Amico V. and Lolli B. (2008). The attenuation of seismic intensity in Italy, Part II: Modeling and validation. *Bulletin of the Seismological Society of America*. 98:692-708.
- Peruzza L., Azzaro R., Gee R., D'Amico S., Langer H., Lombardo G., Pace B., Pagani M., Panzera F., Ordaz M., Suárez M.L. and Tusa G. (2017). When probabilistic seismic Hazard climbs volcanoes: the Mt Etna case, Italy – Part 2: computational implementation and first results. *Natural Hazards and Earth Systems Science*. 17:1999-2015.
- Pezeshk S. and Zandieh A. (2011). Hybrid empirical ground-motion prediction equations for Eastern North America using NGA models and updated seismological parameters. *Bulletin of the Seismological Society of America*. 101(4):1859-1870.
- Pezeshk S., Zandieh A., Campbell K.W. and Tavakoli B. (2018). Ground-motion prediction equations for Central and Eastern North America using the hybrid empirical method and NGA-West2 empirical ground-motion models. *Bulletin of the Seismological Society of America*. In press.
- Reyes C. (1998). El estado límite de servicio en el diseño sísmico de edificios. Ph. D. Thesis. Universidad Nacional Autónoma de México. Mexico City, Mexico.
- Rosenblueth E. (1976). Optimum design for infrequent disturbances. *Journal of the Structural Division ASCE*. ST9:1807-1825.
- Sabetta F. and Pugliese A. (1996). Estimation of response spectra and simulation of nonstationary earthquake ground motions. *Bulletin of the Seismological Society of America*. 86:337-352.
- Sadigh K., Chang C.Y., Egaj J.A., Makdisi F.I. and Youngs R.R. (1997). Attenuation relationships for shallow crustal earthquakes based on California strong motion data. *Seismological Research Letters*. 68:190-189.
- Scordilis E.M. (2006). Empirical global relations converting M_s and m_b to moment magnitude. *Journal of Seismology*. 10(2):225-236.

- Scherbaum F., Bommer J.J., Bungum H., Cotton F. and Abrahamson N.A. (2005). Composite ground-motion models and logic trees: methodology, sensitivities and uncertainties. *Bulletin of the Seismological Society of America*. 95(5):1575-1593.
- Sharma M.L., Douglas J., Bungum H. and Kotadia J. (2009). Ground-motion prediction equations based on data from the Himalayan and Zagros Regions. *Journal of Earthquake Engineering*. 13(8):1191-1210.
- Singh S.K., Bazan E. and Esteva L. (1980). Expected earthquake magnitude from a fault. *Bulletin of the Seismological Society of America*. 70(3):903-914.
- Spudich P., Joyner W.B., Lindh A.G., Boore D.M. Margaris B.M. and Fletcher J.B. (1999). SEA99: A revised ground motion prediction relation for use in extensional tectonic regimes. *Bulletin of the Seismological Society of America*. 89:1156-1170.
- Tavakoli B. and Pezeshk S. (2005). Empirical-stochastic ground-motion prediction for Eastern North America. *Bulletin of the Seismological Society of America*. 95:2283-2296.
- Thomas P., Wong I. and Abrahamson N. (2010). Verification of probabilistic seismic hazard analysis computer programs. Pacific Earthquake Engineering Research Center. PEER 2010/106 Report. California, USA.
- Toro G.R., Abrahamson N.A. and Schneider J.F. (1997). A model of strong ground motions from earthquakes in Central and Eastern North America: Best estimates and uncertainties. *Seismological Research Letters*. 68:41-57.
- Villani M., Faccioli E. and Ordaz M. (2010). Verification of CRISIS2008 code. Technical Report.
- Villani M., Faccioli E., Ordaz M. and Stupazzini M. (2014). High-resolution seismic hazard analysis in a complex geological configuration: the case of the Sulmona Basin in Central Italy. *Earthquake Spectra*. 30(4):1801-1824.
- Wells D.L. and Coppersmith K.J. (1994). New empirical relationships among magnitude, rupture length, rupture width, rupture area and surface displacement. *Bulletin of the Seismological Society of America*. 84(4):974-1002.
- Whitman R.V. and Cornell C.A. (1976). Design. In: *Seismic Risk and Engineering Decisions*. Lomnitz and Rosenblueth (eds.). Elsevier.
- Woo, G. (1996). Kernel Estimation Methods for Seismic Hazard Area Source Modeling. *Bulletin of the Seismological Society of America*. 68(2):353-362.
- Yenier E. and Atkinson G.M. (2015). Regionally adjustable generic ground-motion prediction equation based on equivalent point-source simulations: application to Central and Eastern North America. *Bulletin of the Seismological Society of America*. 105(4): 1989-2009.



- Youngs R.R. and Coppersmith K. (1985). Implications of fault slip rates and earthquake recurrence models to probabilistic seismic hazard estimates. *Bulletin of the Seismological Society of America*. 58:939-964.
- Youngs R.R., Chiou S.J., Silva W.J. and Humphrey J.R. (1997). Strong ground motion attenuation relationships for subduction zone earthquakes. *Seismological Research Letters*. 68:58-73.
- Zhao, J. X.; Zhang, J.; Asano, A.; Ohno, Y.; Oouchi, T.; Takahashi, T.; Ogawa, H.; Irikura, K.; Thio, H.K.; Somerville, P.G. and Fukushima, Y. (2006). Attenuation relations of strong ground motion in Japan using site classification based on predominant period. *Bulletin of the Seismological Society of America*, 96:898-913.

Annex 1: Triangulation algorithm (for sub-sources division)

This annex includes the copy of the R-CRISIS source code routine used for the recursive division of the seismic sources with the geometry provided by the user into triangular sub-sources. Texts in green denote the comments included in the original source code (those in Spanish are translated to English in brackets).

A schematic explanation of this procedure can be found in Section 2.6.1 of this document.

```
Private Function AcomodaTriangulos(ByVal Plan As Short, ByVal xy(.) As Double, ByVal ixy3(.) As Short) As Triangulo()
```

```
Dim I As Integer
Dim Ntri As Integer = Me.Nver - 2
Dim Tri(Ntri) As Triangulo
Dim V1, V2, V3 As New PointType
```

```
For I = 1 To Ntri
```

```
  Select Case Plan
```

```
    Case 1
```

```
      'Vertice 1 (Vertex 1)
      V1.x = xy(1, ixy3(1, I))
      V1.y = xy(2, ixy3(1, I))
      V1.z = xy(3, ixy3(1, I))
      'Vertice 2 (Vertex 2)
      V2.x = xy(1, ixy3(2, I))
      V2.y = xy(2, ixy3(2, I))
      V2.z = xy(3, ixy3(2, I))
      'Vertice 3 (Vertex 3)
      V3.x = xy(1, ixy3(3, I))
      V3.y = xy(2, ixy3(3, I))
      V3.z = xy(3, ixy3(3, I))
```

```
    Case 2
```

```
      'Vertice 1 (Vertex 1)
      V1.x = xy(1, ixy3(1, I))
      V1.z = xy(2, ixy3(1, I))
      V1.y = xy(3, ixy3(1, I))
      'Vertice 2 (Vertex 2)
      V2.x = xy(1, ixy3(2, I))
      V2.z = xy(2, ixy3(2, I))
      V2.y = xy(3, ixy3(2, I))
      'Vertice 3 (Vertex 3)
      V3.x = xy(1, ixy3(3, I))
      V3.z = xy(2, ixy3(3, I))
      V3.y = xy(3, ixy3(3, I))
```

```
    Case 3
```

```
      'Vertice 1 (Vertex 1)
      V1.y = xy(1, ixy3(1, I))
      V1.z = xy(2, ixy3(1, I))
      V1.x = xy(3, ixy3(1, I))
      'Vertice 2 (Vertex 2)
      V2.y = xy(1, ixy3(2, I))
      V2.z = xy(2, ixy3(2, I))
```




```
V2.x = xy(3, ixy3(2, I))  
'Vertice 3 (Vertex 3)  
V3.y = xy(1, ixy3(3, I))  
V3.z = xy(2, ixy3(3, I))  
V3.x = xy(3, ixy3(3, I))
```

End Select

```
Tri(I) = New Triangulo()  
Tri(I) = Triangulo.LlenaConVertices(V1, V2, V3)
```

Next I

Return Tri

End Function

Function Triangulate(ByRef errMsg As ArrayList, Optional ByRef Plano As Short = 0) As Triangulo()

```
errMsg = New ArrayList  
Plano = 0
```

```
If Me.Nver < 3 Then  
  errMsg.Add("Polygon has too few vertex")  
  Return Nothing  
End If
```

```
Dim ms As String = ""  
Dim Tr() As Triangulo
```

```
Tr = Me.TriangulateInPlane(1, ms)  
If Not IsNothing(Tr) Then  
  errMsg.Clear()  
  Plano = 1  
  Return Tr  
Else  
  errMsg.Add("In plane XY: " & ms)  
End If
```

```
Tr = Me.TriangulateInPlane(2, ms)  
If Not IsNothing(Tr) Then  
  errMsg.Clear()  
  Plano = 2  
  Return Tr  
Else  
  errMsg.Add("In plane XZ: " & ms)  
End If
```

```
Tr = Me.TriangulateInPlane(3, ms)  
If Not IsNothing(Tr) Then  
  errMsg.Clear()  
  Plano = 3  
  Return Tr  
Else  
  errMsg.Add("In plane YZ: " & ms)  
  Plano = 0  
  Return Nothing  
End If
```

End Function



```
Private Function TriangulateInPlane(ByVal IPlano As Short, ByRef errMsg As String) As Triangulo()  
  
    errMsg = ""  
  
    'Muy pocos vértices (Too few vertexes)  
    If Me.Nver < 3 Then  
        errMsg = "Polygon has too few vertex"  
        Return Nothing  
    End If  
  
    Dim PolProv As New Poligono(Me.Nver)  
    PolProv.IgualaCon(Me)  
    For i As Integer = 1 To Me.Nver  
        Dim xx, yy, zz As Double  
        Select Case IPlano  
            Case 1  
                'Plano X-Y (X-Y plane)  
                xx = PolProv.mvarVertice(i).x  
                yy = PolProv.mvarVertice(i).y  
                zz = PolProv.mvarVertice(i).z  
            Case 2  
                'Cambiamos al plano X-Z (Change to X-Z plane)  
                xx = PolProv.mvarVertice(i).x  
                yy = PolProv.mvarVertice(i).z  
                zz = PolProv.mvarVertice(i).y  
            Case 3  
                'Cambiamos al plano Y-Z (Change to X-Z plane)  
                xx = PolProv.mvarVertice(i).y  
                yy = PolProv.mvarVertice(i).z  
                zz = PolProv.mvarVertice(i).x  
        End Select  
        PolProv.SetVertex(i, New PointType(xx, yy, zz))  
    Next i  
  
    'Verificamos que los bordes no se crucen (Verification that borders do not cross among them)  
    If PolProv.IsComplex(errMsg, 0, False) Then Return Nothing  
  
    'Si no se cruzan, Ponemos el orden correcto (If they do not cross are arranged in the proper order)  
    PolProv.PonSentido(TipoSentido.CounterClockWise)  
  
    'Verificamos que no sean colineales en este plano (Verification that vertexes are not colinear in this plane)  
    'Simplemente calculamos el área: (Its area is calculated)  
    Dim Am As Double = PolProv.Area(False)  
    'La comparamos con el área de su boundingBox (It is compared with the area of its boundingBox)  
    Dim AmBB As Double = PolProv.AreaXYOfBounds  
  
    If AmBB > 0 Then  
        If Am / AmBB <= 0.00000001 Then  
            errMsg = "Polygon has null area in this plane"  
            Return Nothing  
        End If  
    Else  
        errMsg = "Polygon has null area in this plane"  
        Return Nothing  
    End If  
  
    'Divide en triángulos (Division into triangles)  
    Dim Xy(3, Me.Nver) As Double  
    Dim Ixy(Me.Nver) As Short
```



```
Dim Ixy3(3, Me.Nver) As Short
For i As Short = 1 To CShort(Me.Nver)
    Xy(1, i) = PolProv.Vertice(i).x
    Xy(2, i) = PolProv.Vertice(i).y
    Xy(3, i) = PolProv.Vertice(i).z
    Ixy(i) = i
Next i
Dim M As Integer
Call Deldivide(CShort(Me.Nver), Ixy, Xy, M, Ixy3)
Return Me.AcomodaTriangulos(IPlano, Xy, Ixy3)
```

End Function

```
''' <summary>
''' Determines if a polygon is complex or not
''' </summary>
''' <param name="errMsg">Input: nothing; output: contains the reasons why a given polygon is complex</param>
''' <param name="Tolerance">Parameter that indicates how close two points have to be in order to be considered
the same. The distance is Tolerance*Polygon Perimeter</param>
''' <returns>True if the polygon is complex, False if the polygon is simple</returns>
''' <remarks></remarks>
Public Function IsComplex(ByRef errMsg As String, Optional Tolerance As Double = 0, Optional checkAlsoZ As
Boolean = False) As Boolean
```

```
    errMsg = ""
    Dim Tol As Double = Tolerance * Me.Perimetro
    'Tol = 0
    'checkAlsoZ = False

    'Verificamos que no haya vértices iguales (Verification that there are not equal vertexes)
    For I As Integer = 1 To Me.Nver
        For J As Integer = I + 1 To Me.Nver
            Dim Delta As PointType = Me.Vertice(I) - Me.Vertice(J)
            Dim Dx As Double = Math.Abs(Delta.x)
            Dim Dy As Double = Math.Abs(Delta.y)
            Dim Dz As Double = Math.Abs(Delta.z)
            If checkAlsoZ Then
                If Dx <= Tol And Dy <= Tol And Dz <= Tol Then errMsg = errMsg & "Vertex " & I & " and " & J & " are the same"
                & vbCrLf
            Else
                If Dx <= Tol And Dy <= Tol Then errMsg = errMsg & "Vertex " & I & " and " & J & " are the same" & vbCrLf
            End If
        Next
    Next I
    If errMsg <> "" Then Return True

    'Creamos segmentos (Segments are created)
    Dim NSeg As Integer = Me.Nver
    Dim Seg(NSeg) As Segmento
    For I As Integer = 1 To Me.Nver
        Dim J As Integer = I + 1
        If J > Me.Nver Then J = 1
        Seg(I) = New Segmento(Me.Vertice(I), Me.Vertice(J))
    Next I

    'Barremos segmentos (Segments are transited)
    For I As Integer = 1 To NSeg
        For J As Integer = I + 1 To NSeg
            If Segmento.TheseSegmentsCross(Seg(I), Seg(J)) Then errMsg = errMsg & "Segments " & I & " and " & J & "
intersect" & vbCrLf
```



Next J
Next I

```
If errMsg = "" Then  
    Return False  
Else  
    Return True  
End If
```

End Function

```
Public Sub Circum(ByRef x1 As Double, ByRef y1 As Double, ByRef x2 As Double, ByRef y2 As Double, ByRef x3 As  
Double, ByRef y3 As Double, _  
    ByRef x0 As Double, ByRef y0 As Double, ByRef rsq As Double)
```

```
    Dim sx13, sy13 As Double  
    Dim dx13, dy13 As Double  
    Dim sx12, sy12 As Double  
    Dim dx12, dy12 As Double  
    Dim Den As Double  
    Dim xfac1, xfac2 As Double  
    Dim yfac1, yfac2 As Double  
    Dim xnum, ynum As Double  
    Dim dx20, dx10, dx30 As Double  
    Dim dy20, dy10, dy30 As Double  
    Dim rsq2, rsq1, rsq3 As Double
```

```
    x0 = -999.0  
    y0 = -999.0  
    rsq = -999.0  
    sx13 = (x1 + x3) / 2  
    sy13 = (y1 + y3) / 2  
    dx13 = (x3 - x1)  
    dy13 = (y3 - y1)  
    sx12 = (x1 + x2) / 2  
    sy12 = (y1 + y2) / 2  
    dx12 = (x2 - x1)  
    dy12 = (y2 - y1)  
    Den = (dx13 * dy12) - (dx12 * dy13)
```

```
'No puede cuando los puntos son colineales (It is not possible if vertexes are colineal)  
If (Den = 0) Then Exit Sub
```

```
    xfac1 = (sy13 * dy13) + (sx13 * dx13)  
    xfac2 = (sy12 * dy12) + (sx12 * dx12)  
    yfac1 = (sx13 * dx13) + (sy13 * dy13)  
    yfac2 = (sx12 * dx12) + (sy12 * dy12)  
    xnum = (xfac1 * dy12) - (xfac2 * dy13)  
    ynum = (yfac1 * dx12) - (yfac2 * dx13)
```

```
    x0 = xnum / Den  
    y0 = -ynum / Den  
    dx10 = x1 - x0  
    dx20 = x2 - x0  
    dx30 = x3 - x0  
    dy10 = y1 - y0  
    dy20 = y2 - y0  
    dy30 = y3 - y0  
    rsq1 = (dx10 * dx10) + (dy10 * dy10)
```



```
rsq2 = (dx20 * dx20) + (dy20 * dy20)
rsq3 = (dx30 * dx30) + (dy30 * dy30)
rsq = rsq1
```

End Sub

```
Friend Sub Delaunay(ByRef N As Integer, ByRef Ixy() As Short, ByRef xy(,) As Double, ByRef j1 As Short, ByRef j2
As Short, _
ByRef j3 As Short, ByRef idel As Short)
```

```
Dim xj2, xj1, xj3 As Double
Dim yj2, yj1, yj3 As Double
Dim dx31, dx23, dx12 As Double
Dim sx31, sx23, sx12 As Double
Dim dy31, dy23, dy12 As Double
Dim sy31, sy23, sy12 As Double
Dim term2, term1, term3 As Double
Dim yo, Area, xo, rsq As Double
Dim k, kj As Integer
Dim dY, dX, r2 As Double
```

```
xj1 = xy(1, j1)
xj2 = xy(1, j2)
xj3 = xy(1, j3)
yj1 = xy(2, j1)
yj2 = xy(2, j2)
yj3 = xy(2, j3)
```

```
dx23 = xj3 - xj2
dx31 = xj1 - xj3
dx12 = xj2 - xj1
sx23 = xj3 + xj2
sx31 = xj1 + xj3
sx12 = xj2 + xj1
```

```
dy23 = yj3 - yj2
dy31 = yj1 - yj3
dy12 = yj2 - yj1
sy23 = yj3 + yj2
sy31 = yj1 + yj3
sy12 = yj2 + yj1
```

```
term1 = (dx23 * sy23) - (dy23 * sx23)
term2 = (dx31 * sy31) - (dy31 * sx31)
term3 = (dx12 * sy12) - (dy12 * sx12)
```

```
Area = -(term1 + term2 + term3) / 4
```

```
If (Area < 0) Then idel = 5
If (Area = 0) Then idel = 4
If (Area > 0) Then idel = 3
```

```
Call Circum(xj1, yj1, xj2, yj2, xj3, yj3, xo, yo, rsq)
```

```
If (idel > 3) Then Exit Sub
```

```
If (rsq = -999) Then GoTo 30
```

```
For k = 1 To N
```



```
kj = Ixy(k)
If (xy(1, kj) = xy(1, j1) And xy(2, kj) = xy(2, j1)) Then GoTo 10
If (xy(1, kj) = xy(1, j2) And xy(2, kj) = xy(2, j2)) Then GoTo 10
If (xy(1, kj) = xy(1, j3) And xy(2, kj) = xy(2, j3)) Then GoTo 10
dX = xy(1, kj) - xo
dY = xy(2, kj) - yo
r2 = (dX * dX) + (dY * dY)

If (r2 - rsq) < -0.00001 Then GoTo 30
If (r2 = rsq) Then
    idel = 2
End If
10:
Next k

idel = 1
Exit Sub

30:
idel = 3
Exit Sub

End Sub

Public Sub Deldivide(ByRef N As Short, ByRef Ixy() As Short, ByRef xy(.) As Double, ByRef m As Integer, ByRef
ixy3(.) As Short)

    Dim i, ii As Integer

    m = 0
    For i = N To 3 Step -1
        ii = i
        m = m + 1
        Call Delsplit(ii, Ixy, xy, ixy3, m)
    Next i

End Sub

Friend Sub Delsplit(ByRef N As Integer, ByRef Ixy() As Short, ByRef xy(.) As Double, ByRef ixy3(.) As Short, ByRef
Ncol As Integer)

    Dim j3, j1, j2, j As Integer
    Dim ixyj1 As Short
    Dim ixyj2 As Short
    Dim ixyj3 As Short
    Dim ielim1 As Short
    Dim ielim2 As Short
    Dim ielim3 As Short
    Dim idel As Short

    If (N = 3) Then

        ixy3(1, Ncol) = Ixy(1)
        ixy3(2, Ncol) = Ixy(2)
        ixy3(3, Ncol) = Ixy(3)
        Ixy(1) = 0
        Ixy(2) = 0
        Ixy(3) = 0
        N = 0
```

Else

```
For j2 = 1 To N
  j1 = j2 - 1
  If (j1 <= 0) Then j1 = j1 + N
  j3 = j2 + 1
  If (j3 > N) Then j3 = j3 - N
  ixyj1 = Ixy(j1)
  ixyj2 = Ixy(j2)
  ixyj3 = Ixy(j3)
  Call Delaunay(N, Ixy, xy, ixyj1, ixyj2, ixyj3, idel)
  If (idel = 1 Or idel = 2) Then
    ielim1 = Ixy(j1)
    ielim2 = Ixy(j2)
    ielim3 = Ixy(j3)
    ixy3(1, Ncol) = Ixy(j1)
    ixy3(2, Ncol) = Ixy(j2)
    ixy3(3, Ncol) = Ixy(j3)
    For j = j2 To N - 1
      Ixy(j) = Ixy(j + 1)
    Next j
    Ixy(N) = 0
    N = N - 1
  Exit Sub
End If
Next j2

End If

End Sub
```

Annex 2: Supplementary information and datasets

The following files are included in the electronic supplement from which the seismic hazard model developed in Chapter 3 can be reconstructed:

- Reference map: Island_Contour.shp
- Reference cities: Cities.asc
- Digital elevation model: Capra Island DEM.grd
- Seismic microzonation: Microzonation.grd and Microzonation.ft
- Spectral ordinates: Spectral_ordinates.xlsx
- Seismicity parameters: Seismicity_parameters.xlsx
- Gridded seismicity parameters:
 - Lo.grd
 - EB.grd
 - MU.grd
- Geometry of seismic sources: Sources_geometry.xlsx
- Output files:
 - *.res: Capra Island.res
 - *.gra: Capra Island.gra
 - *.fue: Capra Island_cities.fue
 - *.map: Capra Island_cities.map
 - *.des: Capra Island_cities.des